

<h1 style="text-align: center;">REPORT DOCUMENTATION PAGE</h1>			<i>Form Approved</i> OMB No. 0704-0188	
<small>Public reporting burden for this collection of information is estimated to average 1 hour per response, including the time for reviewing instructions, searching existing data sources, gathering and maintaining the data needed, and completing and reviewing the collection of information. Send comments regarding this burden estimate or any other aspect of this collection of information, including suggestions for reducing this burden, to Washington Headquarters Services, Directorate for Information Operations and Reports, 1215 Jefferson Davis Highway, Suite 1204, Arlington, VA 22202-4302, and to the Office of Management and Budget, Paperwork Reduction Project (0704-0188), Washington, DC 20503.</small>				
1. Agency Use Only (Leave blank).		2. Report Date. September 1998		3. Report Type and Dates Covered. Final
4. Title and Subtitle. Coastal Benthic Boundary Layer (CBBL) Research Program: Final Report				5. Funding Numbers. <i>Program Element No.</i> 0601153N <i>Project No.</i> R3103 <i>Task No.</i> 000 <i>Accession No.</i> DN252025 <i>Work Unit No</i> 74-5258-08.
6. Author(s) Michael D. Richardson				
7. Performing Organization Name(s) and Address(es). Naval Research Laboratory Seafloor Geosciences Division Stennis Space Center, MS 39529-5004				8. Performing Organization Report Number NRL/MR/7430--98-8213
9. Sponsoring/Monitoring Agency Name(s) and Address(es). Office of Naval Research Dr. Fred Saafeld, Code 01 Ballston Centre Tower One 800 N. Quincy Street Arlington, VA 22217-5660				10. Sponsoring/Monitoring Agency Report Number.
11. Supplementary Notes.				
12a. Distribution/Availability Statement. Approved for public release; distribution unlimited				12b. Distribution Code.
13. Abstract (Maximum 200 words). The Coastal Benthic Boundary Layer (CBBL) Special Research Program is a 5-year Office of Naval Research study that addressed the physical characterization and modeling of benthic boundary layer processes and the impact these processes have on seafloor structure, properties and behavior. This final report is a summary of the results compiled and published from FY92 through FY98. Quantitative physical models of the benthic boundary layer were tested in a series of experiments at coastal locations where differing environmental processes determine sediment structure. The sites were Eckernförde Bay, Baltic Sea; the West Florida Sand Sheet off Panama City, Florida; the lower Florida Keys; and the shallow continental shelf off Northern California. Predictive models developed through this program should enhance MCM technological capabilities in several important areas including acoustic and magnetic detection, classification, and neutralization of proud and buried mines; shock wave propagation; prediction of mine burial; and sediment classification. This report includes an introduction to the program, a summary of the results of those experiments, a list of publications that have resulted from CBBL research, and final reports from 24 of the 30 groups supported by the CBBL.				
14. Subject Terms. Sediments, Acoustics, Mines				15. Number of Pages. 386
				16. Price Code.
17. Security Classification of Report UNCLASSIFIED	18. Security Classification of This Page. UNCLASSIFIED	19. Security Classification of Abstract. UNCLASSIFIED	20. Limitation of Abstract.	

CONTENTS

1.0 INTRODUCTION

1.1 DESCRIPTION OF THE ECKERNFÖRDE BAY EXPERIMENTS

1.2 DESCRIPTION OF THE WEST FLORIDA SAND SHEET EXPERIMENTS

1.4 DESCRIPTION OF THE NORTHERN CALIFORNIA EXPERIMENTS

1.5 ACKNOWLEDGMENTS

1.6 REFERENCES

2.0 FINAL PROJECT REPORTS

2.1 Discrete element simulation of the microstructure of marine cohesive sediments. A. Anandarajah, D.L. Lavoie, P.J. Burkett and M.D. Richardson

2.2 Measurement and description of upper seafloor sub-decimeter heterogeneity for macrostructure geoaoustic modeling. A. Anderson, T.H. Orsi, A.P. Lyons, M.E. Duncan, J.A. Hawkins, R.A. Weitz, L. Buzi, and F. Abegg

2.3 High-frequency scattering from sediment roughness and sediment volume inhomogeneities. K.B. Briggs, M.D. Richardson and P.D. Jackson.

2.4 Effects of carbonate dissolution and precipitation on sediment physical properties and structure in the Key West area: microfossils component. C.A. Brunner

2.5 Processes of macro scale volume inhomogeneity in the benthic boundary layer. W.R. Bryant and N.C. Slowey

2.6 Acoustic penetration and backscatter at the water-sediment interface. N.P. Chotiros

2.7 New geophysical technologies applied to the quantitative evaluation of seabed properties relate to mine burial prediction. A.M. Davis, D. Huws, J. Pyrah and R. Haynes

2.8 Analysis of the rheological properties of nearbed (fluid mud) suspensions occurring in coastal environments. R.W. Fass

2.9 Early diagenesis of the shallow water sediments in the vicinity of Dry Tortugas, Florida. Y. Furukawa

2.10 Measurement of high frequency acoustic scattering from coastal sediments. D.R. Jackson and K.L. Williams

2.11 Structural analysis of marine sediment microfabric. J.J. Kollé, A.C. Mueller and J. Dvorkin

- 2.12 Quantification of high frequency acoustic response to seafloor micromorphology in shallow water. D.N. Lambert and D.J. Walter
- 2.13 Measurement of shear modulus in-situ and in the laboratory. D.L. Lavoie and Y. Furukawa
- 2.14 Quantification of gas bubble and dissolved gas sources and concentrations in organic-rich, muddy sediments. C.S. Martens and D.B. Albert
- 2.15 Physical and biological mechanisms influencing the development and evolution of sedimentary structure. C.A. Nittrouer and G.R. Lopez
- 2.16 Contact micromechanics for constitutive acoustic modeling of marine sediments. M.H. Sadd and J. Dvorkin
- 2.17 The detection of continuous impedance structures using full spectrum sonar. S. Schock
- 2.18 Effects of carbonate dissolution and precipitation on sediment physical properties and structure—Pore water flux component. A. Shiller
- 2.19 Geomechanical and geoacoustical behavior of nearshore sediments – CBBL SRP. A.J. Silva, G.E. Veyera, M.H. Sadd and H.G. Brandes
- 2.20 Experimental and theoretical studies of near-bottom sediments to determine geoacoustic and geotechnical properties. R.D. Stoll, R. Flood and E.O. Bautista
- 2.21 Modeling surficial roughness and sub-bottom inhomogeneities from acoustic data analysis. D. Tang and G.V. Frisk
- 2.22 Backscatter characteristics from different sea floor types. T.F. Wever, G. Fechner, H.M. Fiedler and I.H. Stender
- 2.23 Mobility' of gas in muddy sediments. T.F. Wever and H.M. Fiedler
- 2.24 Acoustic lance: In situ acoustic seabed velocity and attenuation. R.H. Wilkens, L.N. Frazer, T.J. Gorgas and S.S. Fu
- 2.25 Physical transport processes influencing shelf sedimentary structure. L.D. Wright and C.T. Friedrichs
- 2.26 The relationship between high-frequency acoustic scattering and seafloor structure. L.Zhang and R.R. Goodman

3.0 LIST OF CBBL PUBLICATIONS

COASTAL BENTHIC BOUNDARY LAYER:
A FINAL REVIEW OF THE PROGRAM

NRL MEMORANDUM REPORT
1 September 1998

Michael D. Richardson
Chief Scientist, CBBL
Marine Geosciences Division
Naval Research Laboratory

ABSTRACT

The Coastal Benthic Boundary Layer (CBBL) Special Research Program is a 5-year Office of Naval Research study that addressed the physical characterization and modeling of benthic boundary layer processes and the impact these processes have on seafloor structure, properties and behavior. This final report is a summary of the results compiled and published from FY92 through FY98. Quantitative physical models of the benthic boundary layer were tested in a series of experiments at coastal locations where differing environmental processes determine sediment structure. The sites were Eckernförde Bay, Baltic Sea; the West Florida Sand Sheet off Panama City, Florida; the lower Florida Keys; and the shallow continental shelf off Northern California. Predictive models developed through this program should enhance MCM technological capabilities in several important areas including acoustic and magnetic detection, classification, and neutralization of proud and buried mines; shock wave propagation; prediction of mine burial; and sediment classification. This report includes an introduction to the program, a summary of the results of those experiments, a list of publications that have resulted from CBBL research, and final reports from 24 of the 30 groups supported by the CBBL.

COASTAL BENTHIC BOUNDARY LAYER (CBBL) RESEARCH PROGRAM:

FINAL REVIEW

1.0 INTRODUCTION

The Coastal Benthic Boundary Layer (CBBL) Research Program is a 5-year Office of Naval Research (ONR) program that addressed physical characterization and modeling of benthic boundary layer processes and the impact these processes have on seafloor properties that affect shallow-water naval operations. Four workshops were convened between November 1991 and February 1992 to establish program direction (Richardson, 1992). Based on workshop recommendations, research was focused on modeling the effects benthic boundary layer processes have on sediment structure, properties and behavior (Figure 1).

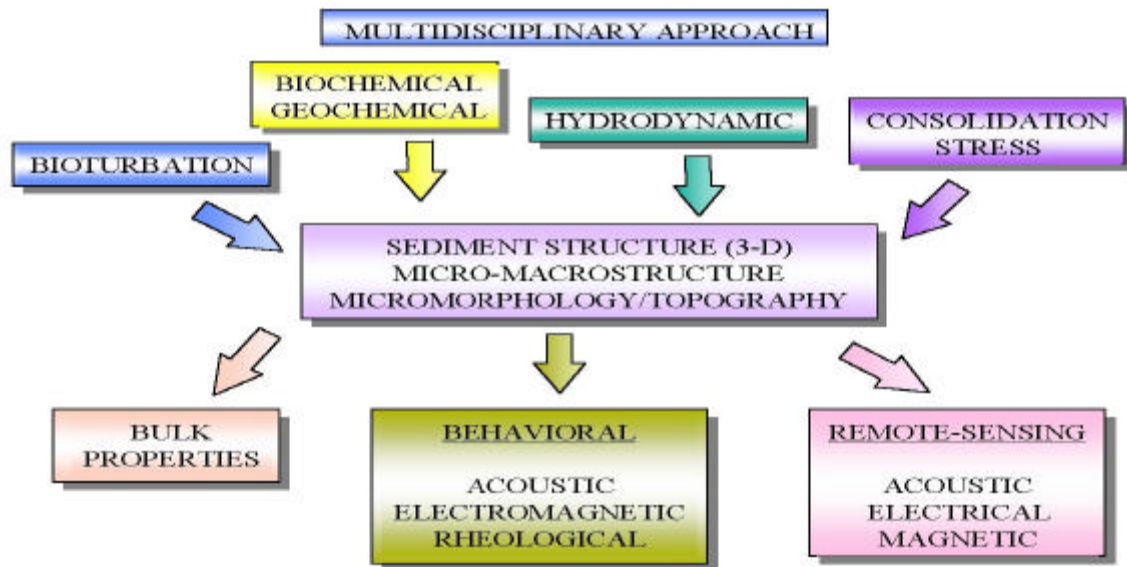


Figure 1. Schematic depiction of the Coastal Benthic Boundary Layer Special Research Program scientific direction.

Sediment physical structure provided the common perspective to: a) quantitatively model relationships among sediment physical, acoustic, electrical, and rheological (mechanical) properties; b) quantify the effects of environmental processes on the spatial and temporal distribution of sediment properties; and c) model sediment behavior (acoustic, electrical, and mechanical) under direct and remote stress.

Basic understanding of the physical relationships among processes and properties will contribute to the development of realistic models of: sediment strength, stability, and transport; sediment stress-strain relationships in cohesive and non cohesive sediments; dynamic seabed-structure interactions; animal-sediment interactions; high-frequency acoustic scattering phenomena; and propagation of high-frequency acoustic energy into and through poro-elastic media. Predictive

models developed through this program should enhance MCM technological capabilities in several important areas including acoustic and magnetic detection, classification, and neutralization of proud and buried mines; shock wave propagation; prediction of mine burial; and sediment classification.

Quantitative physical models were tested by a series of field experiments at coastal locations where differing environmental processes determine sediment structure (Richardson, 1994a, 1995; Tooma and Richardson, 1995; Richardson and Bryant, 1997; Lavoie, Richardson and Holmes, 1997; and Richardson and Davis, in press). The first experiment was a joint United States and German study of the gas-rich mud of Eckernförde Bay in the Baltic Sea. At this site biogeochemical processes were responsible for the formation of subsurface methane gas bubbles that significantly affected sediment structure, behavior, and properties. The second experiment was conducted on the West Florida Sand Sheet, southeast of Panama City, Florida. Sediments consisted of a mixture of clastic sands and shells that were reworked by wave-current action (hydrodynamic processes) and biological processes (bioturbation). Experiments were conducted in a carbonate environment in the Florida Keys where biogeochemical diagenetic processes, such as sediment mineralization, dissolution and cementation, as well as sediment mixing by bioturbation control sediment structure. Scientists supported by the CBBL also participated in the STRATAFORM experiments (Nittrouer and Kravitz, 1997) conducted on the shallow continental shelf off northern California. Sediment structure at this site is controlled by combination of sediment deposition from the Eel River, high energy reworking of sediments by waves and bottom current generated by storms, and mixing (bioturbation) by benthic fauna. The goal of the CBBL was to provide physical models that predict sediment structure and behavior from knowledge of environmental processes for each environment. The CBBL program supported 28 projects during its five year duration (Table 1)

The following sections (1.1 through 1.4) describe CBBL results from the four experimental sites. The descriptions of the Eckernförde Bay and West Florida Sand Sheet experiments were edited from introductory articles in special issues of Geo-Marine Letters and Continental Shelf Research (Richardson and Bryant, 1996, Richardson and Davis, in press). The description of the Key West Campaign was edited from an introductory article in GeoMarine Letters (Lavoie and Ricahrdson and Holmes, 1996). References are deleted from this presentation and can be found in the original articles.

1.1 DESCRIPTION OF THE ECKERNFÖRDE BAY EXPERIMENTS

1.1.1 Background and motivation

Most gas in surficial, shallow-water sediments is biogenic and originates from the generation of methane as a by-product of metabolism by methanogenic bacteria. Areas of rapidly accumulating fine-grained muddy sediment rich in organic matter (e.g. Eckernförde Bay) provide ideal environments for the formation of this biogenic methane. Such areas are not uncommon, occurring widely around coastal fringes and in surrounding shallow water seas (Figure 2).



Figure 2. Worldwide distribution of shallow-water sediments that contain free-gas. Most sites were located based on seismo-acoustic survey techniques. The actual distribution of gassy sediments is probably much greater, especially in the poorly surveyed Southern Hemisphere. The numbers correspond to references in Fleischer and are available from the first author.

Once incorporated in the sediment body, methane may exist in various states: as free gas in bubble form (in the pore space), as dissolved gas in solution, or in special circumstances as gas hydrate. Gas concentration, temperature, salinity, and pressure control the state of methane and free bubbles can form when methane concentration exceeds saturation. Methane hydrate forms under specific ranges of temperature (low) and pressure (relatively high). The presence and quantity of methane, together with its state of occurrence, influence the sediment's bulk properties and behavior, and can have such diverse effects as impacting sonar performance, influencing sea floor stability, and even contributing to global climatic change.

Qualitatively, geographical distributions of gassy sediments can be arrived at using conventional seismo-acoustic surveying methodologies. At seismo-acoustic frequencies, typically a few hundred hertz to a few tens of kHz, acoustic propagation in sediments is severely affected by the presence of free gas; bubble layers act as scatterers of acoustic energy, giving rise to clearly recognizable seismic "textures" on sub-bottom profiler records. Traditionally, spatial distribution maps have been produced on the basis of delineating areas of "acoustic turbidity". While this effect provides a useful means of investigating lateral spatial distribution, rapid attenuation combined with scattering prevents analysis of depth distribution of gas, as sub-bottom penetration is severely restricted. Sidescan sonar has also proved useful for routine remote investigations of gassy sediment environments. Surface expressions of gas seeping to the seabed surface are readily recognizable on sidescan records, e.g. pockmarks and domes and these time-lapse phenomena can be monitored on the basis of repeated surveys.

While seismo-acoustics provides an ideal tool for field recognition of gassy sediments, the acousticians goal of providing estimates of gas volume and bubble size distribution on the basis of field seismo-acoustic signature remains. Indirect seismic evidence (large scale) of gas bubbles in sediments has recently been accompanied by finer scale direct evidence of the presence of free gas through headspace analysis of sediment cores, compositional analysis of sediment pore waters by gas chromatography and mass spectroscopy, and observation of bubbles by SEM, x-radiography, and x-ray computer tomographic (CT) techniques. Seismic techniques are primarily restricted to determination of the presence or absence of gas charged sediments; whereas, headspace analysis, chemical analysis, and x-radiographic techniques allow a characterization of percent gas volume.

Laboratory investigations have contributed to significant advances in modeling the frequency dependent behavior (propagation and scattering) of high-frequency energy in gas-rich sediments. For fine-grained sediments, where the bubble size is often considered large compared to the particle size, bubble interactions with the sediment particle frame are known to play an important role in controlling bubble resonance, sound speed, and damping thus greatly influencing sonar performance. In situ validation of these model predictions has suffered from the lack of concurrent in situ measurement of acoustic properties and methane bubble volume, size, shape, and spatial distribution. Models of geotechnical behavior of gassy sediment have been developed based on the relatively few concurrent measurements of sediment structure, physical properties, and strength of sediment retained at in situ pressure in pressurized corers and on sediment created under laboratory conditions. Although not validated by in situ experiments, model predictions are consistent with behavior observed in situ. In soft sediments the presence of gas can either increase or decrease undrained sediment strength, depending on the consolidation history and ambient pore pressure. Gas in sediments also increases sediment compressibility greatly increasing the likelihood of sediment liquefaction, especially in sands. Models of acoustic and geotechnical behavior must account for the relationship of bubbles to sediment pore space. Common bubble-matrix relationships include interstitial bubbles, such as in sands where bubble size is small compared to pore space; sediment displacing bubbles, such as Eckernförde Bay mud where bubble size is large compared to pore space; and gas reservoirs, where gas volume is high and particles are included within the bubble volume.

Gas in marine sediments originates from either bacterial or thermogenic reduction of organic matter. Most gas in surficial, shallow-water sediments is biogenic and originates from the generation of methane as a by-product of metabolism by methanogenic bacteria. Thermogenic methane gas, formed at high temperature and pressure (> 1000-m), can migrate to the sediment surface forming another source of trapped shallow gas accumulations. Carbon and hydrogen isotopic analysis of the gas can be used to determine origin. In mud with high organic content, aerobic respiration is usually restricted to the upper few centimeters of the seafloor. Below that zone, sulfur bacteria produce black, odorous sediment rich in hydrogen sulfide. After all of the sulfate is used as a terminal electron acceptor, methanogenic bacteria further reduce simple organic compounds producing methane. Pore water methane concentrations increase until they exceed saturation levels and free methane bubbles form in the sediment. The kinetics of these biochemical reaction are well known, but the prediction of the volume or even the presence or absence of free methane gas that is needed to determine sediment acoustic and geotechnical properties has not been possible.

The defense and petroleum industries will undoubtedly benefit from an improved understanding and predictability of gassy sediment environments. Interest lies both in the performance of higher frequency naval detection and classification sonars and lower frequency seismo-acoustic systems used to prospect for oil and gas. In addition accurate models of the behavior of gassy sea floor sediments are essential for the prediction of object burial and foundation stability. Gas in sediments also has implications for engineering and environmental studies. Free gas in the sediment void space significantly affects the sediment's engineering properties: it is highly compressible and even small quantities of undissolved gas will increase the sediment's compressibility and reduce its undrained shear strength. Sea floor stability problems associated with trapped or migrating gas have also been reported in the literature.

Methane is one of the most important radiatively active (greenhouse) gases in the atmosphere. Its global warming potential is 3.7 times that of carbon dioxide and up to 12% of greenhouse forcing is the result of atmospheric methane. It is therefore important to have an accurate inventory of sources and sinks of methane and to understand the dynamics of shallow-water methane generation, consumption, transport, and subsequent emission into the atmosphere. Hovland and Judd estimate that 30% of the world's shallow water area produces methane bubbles and that 8 to 65 Tg CH₄ per year is transported into the atmosphere. These emission volume estimates, which account for up to 20% of the total atmospheric contributions of methane, are based on very limited data. Accurate estimates of gas volume, bubble size, and transport dynamics are required to predict the contribution of shallow-water methane to climatic cycles. Also of interest to the environmentalists is the evidence for enhanced biomass of meiofauna and macrofauna at some seep sites as a direct consequence of methane escaping to the seabed.

1.1.2 Eckernförde Bay: early investigations

Some of the earliest evidence for the presence of gassy sediments in Eckernförde Bay was presented by Schüler who noted a reduction of the penetration of acoustic energy into shallow basin sediments in the Baltic Sea. The associated acoustic texture, referred to locally as the "Becken Effekt" and internationally recognized as "acoustic turbidity", was presumed to be the result of gas interacting with acoustic energy. Seabed depressions (later referred to as pockmarks) were also evident in these early acoustic records. By the mid-70's chemical analyses of sediments collected with piston cores and by in situ pore water and gas samplers demonstrated that the acoustic turbidity was the result of free gas in sediments oversaturated with methane. The biochemical origin of methane and delineation of zones of aerobic respiration, sulfate reduction, and methanogenesis were described by Michael Whiticar in a series of papers in the 70's and early 80's. The origin and maintenance of pockmarks in Eckernförde Bay has incited considerable debate. Early explanations include erosion, military or fishing activity, or methane gas ebullition but the current hypothesis primarily attributes pockmarks to submarine freshwater seepage from groundwater aquifers.

Scientists at the University of Kiel championed much of the early research relating to oceanographic conditions, biology and chemistry of the water column and sediments, and geological processes in Eckernförde Bay. Many of these studies were part of two, six-year interdisciplinary programs (1971-1982) designed to develop models of water column - seafloor interaction in the southwestern Baltic Sea. Although the goal of developing quantitative models

linking all aspects of water column - seafloor interaction were never met, scientists supported by this program provided much of the early knowledge of conditions and processes in Eckernförde Bay. During this period, the physical and biological processes that control annual cycles of plankton primary and secondary productivity were quantified. Organic flux to the seafloor in the southwestern Baltic was found to be highest in late spring and autumn separated by long periods of low flux to the seafloor. The high input of organic matter that occurs during the spring phytoplankton bloom, and lack of water column mixing can create anoxic conditions that destroy benthic communities in the deeper parts of Eckernförde Bay. Benthic fauna that do exist in central Eckernförde Bay consists of small opportunist species restricted to near surface sediments that do little to mix the sediment. The high organic flux to the seafloor combined with the restricted benthic activity provides an ample source of energy to drive the biochemical processes that eventually produce methane in near surface sediments of central Eckernförde Bay.

Kiel Bay is an area where oceanic waters from the North Sea mix with fresh waters of the eastern Baltic. Horizontal mixing is driven by a Baltic-wide seiche. The stratification of less dense fresh water over the denser higher salinity water of the North Sea is intensified during the formation of a summer (April to October) thermocline. Tidal range is minimal and vertical mixing occurs primarily during winter major storms. Sediment transport is therefore primarily dependent on storm-induced wave action and topography.

Siebold studied the marine geology of Kiel Bay (including Eckernförde Bay) and designated this part of the southern Baltic a large fjord comprising a system of subglacial channels; Eckernförde Bay forms one semi-enclosed basin within this large fjord system. Water depth and oceanographic conditions control sediment distribution in the southwestern Baltic Sea. Coarse-grained sediments (morainal tills, coarse and medium sands) are found on topographic highs at depths shallower than 12 m. Grain size generally decreases with depth and basins, at depths greater than 20 m, are filled with muddy sediments. Eckernförde Bay is partially cut off from the rest of Kiel Bay by a glacial moraine (Mittelgrund) located at the head of the Bay. The central basin, where near bottom energy levels are at a minimum, effectively acts as a sediment sink, i.e., an area of net sediment accumulation. Sediment is derived mainly from cliff erosion, and although accumulation rates show some fluctuation, it has been concluded that the average accumulation rate is high. Milkert attributes some of the fluctuation in sediment accumulation to storm activity. Strong currents generated from easterly winds erode sediments from the shallower regions of Eckernförde Bay and deposit them in the central basin. Preservation of these storm deposits is possible as their thickness often exceeds the depths of biological mixing.

The combination of high organic flux to the seafloor, high rates of sedimentation, slow bottom currents, depositional nature of the environment, occasional anoxic conditions, and the shallow depth of bioturbation, create conditions ideal for methane formation.

1.1.3 Summary of the Eckernförde Bay experiments (1993-1995)

Based on the considerable knowledge base existing on the gas-rich sediments of Eckernförde Bay, a site in the central basin of the Bay was chosen to study the relationships among the environmental processes responsible for methane bubble formation, and the resultant sediment structure, properties, and behavior. A strong emphasis was placed on acoustic bubble interactions and the possible use of acoustics to characterize these gassy sediments.

Eckernförde Bay, a semi-enclosed, fjord-like bay located in the southwestern Baltic Sea (Figure 3).

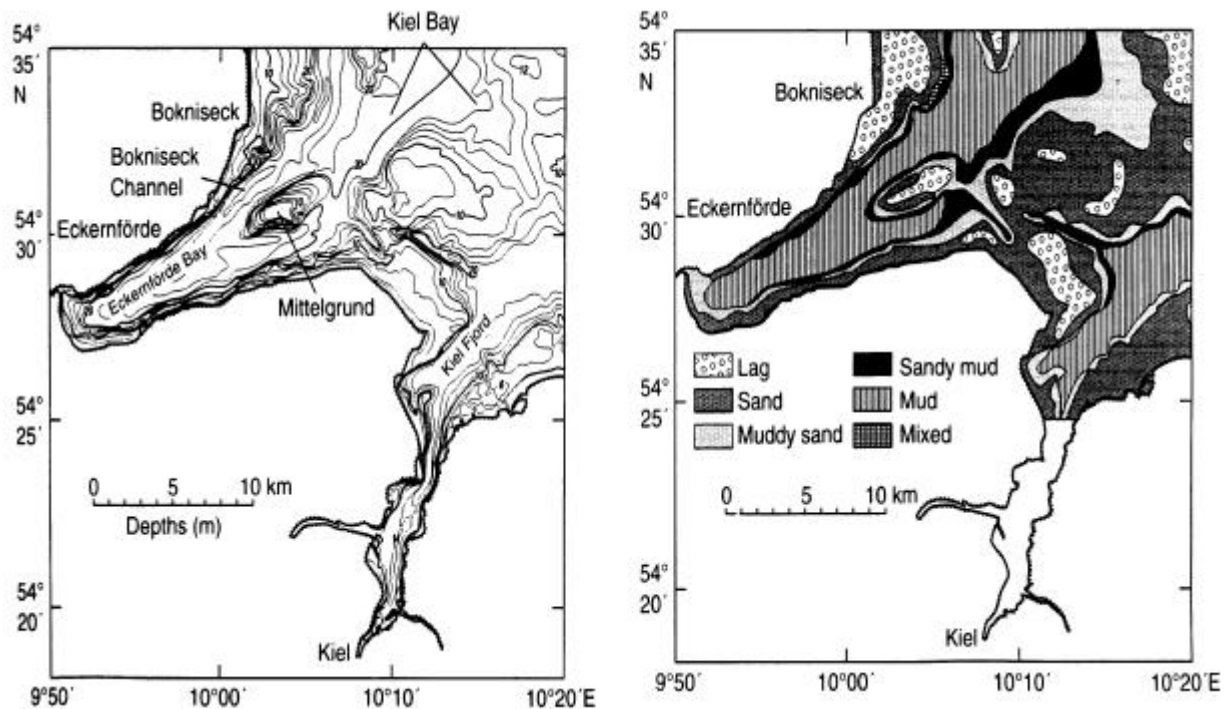


Figure 3. The Morphology of Eckernförde Bay including bathymetry (A) and sediment distribution (B). Hausgarten and NRL (this study) are the location of extensive interdisciplinary research efforts.

is a depression that was formed when glaciers receded during the last ice age (13,000-yr. BP). Sediments accumulating in the central basin formed a relatively flat (~26 m) basin that rises abruptly to the surrounding shorelines. The east entrance to the bay is partially blocked by a morainal sill (Mittelgrund) which divides water flow between a larger northern channel (Bocknis Eck) and a smaller southern channel. The water column is stratified especially during summer and bottom waters of the bay often experience hypoxia with occasional anoxia. Tidal range is slight and wind, storm surges, and baroclinic seiches control fluctuations in sea level. Oscillations in bottom currents correlate in time but not magnitude with the 26-28 hour barotropic Baltic-wide seiche. This weak barotropic seiche creates near resonance internal waves in the stratified Eckernförde Bay, which in turn generate the stronger baroclinic currents. In the deep central basin, however, bottom currents resulting from these baroclinic currents or from local wind or storm driven currents are insufficient to erode sediments. The central basin therefore acts as a trap for sediment advected into the bay by bottom currents or eroded from nearby shorelines and shallow subtidal areas during storms.

Sediments in the central basin of Eckernförde Bay are soft, organic-rich, silty clays with evidence of considerable near-surface biological activity. During subbottom oxide conditions, the uppermost sediments consist of a 2- to 3-cm layer of brown, oxidized mud, which overlies soft, black sediment with a distinct hydrogen-sulfide odor. These surface sediments are heavily

colonized by tube-dwelling, surface deposit-feeding spionid polychaetes (*Polydora ciliata*) and surface deposit-feeding bivalves (*Abra alba*). Radiochemical profiles of excess ^{234}Th and bioturbation experiments with fluorescence tracer particles demonstrate that most biological mixing is restricted to the top 5-10 mm of the sediment. Ventilation of surface sediment with oxygenated bottom water by the small, head-down, deposit-feeding polychaetes (*Heteromastus filiformis* and *Capitella* sp.) and tubificid oligochaetes probably controls the depth of the brown, oxidized layer and affects rates of near-surface biochemical processes. Functional group characteristics, young age, small organism size, low diversity, and shallow particle mixing are all consistent with the hypothesis that this benthic community is controlled by regular disturbance which maintains the community at a low level of complexity (i.e., a pioneering community). In spite of the limited depth of mixing, the benthic community effectively pelletizes most of the sediment reaching the surface. Sediment accumulation rate, determined by ^{210}Pb geochronology, ranges between 3-10 mm y^{-1} . Laminated bedding, preserved in the sedimentary record, results from alternating deposition of thin (< 1 cm) storm-suspended sediments (non-pelletal, often graded bedding) eroded from adjacent shallow-water areas and a fair-weather deposition of thicker (> 10 cm) layers organic-rich suspended material (pelletal, anisotropic fabric). This record is preserved as a result of relatively high sediment accumulation rates in a predominantly depositional environment and the absence of significant physical or biological mixing.

Eckernförde has long been characterized by acoustic turbidity, masking deeper sediments from acoustic characterization. This acoustically turbid zone was evident in acoustic records covering the frequency range of 0.5 to 50 kHz. Although a persistent feature in Eckernförde Bay, the areal extent, intensity, and depth of acoustic turbidity varies with season. These seasonal variations correlate with sediment temperature and are controlled by methane solubility rather than changes in rates of methane production or bubble formation. X-ray Computer aided Tomographic (CT) scans of sediment core samples retained at ambient pressure and temperature revealed only occasional methane gas bubbles from the upper 50 cm depth in the sediment, while below that depth, numerous clusters of small methane bubbles were found. These bubbles occurred in distinct horizons rather than in a continuous distribution. Bubble radii range from 0.4 mm (the smallest radius resolvable by this technique) to as large as 5.0 mm. Larger gas bubbles appear non-spherical and have two long and one short axes (disk-shaped). Gas bubble concentrations ranged from 0 to 2% by volume within the main experimental site and reached as high as 8% in the seafloor within a nearby pockmark. It is apparent that the pockmarks included in these studies are considerably different than the pockmarks near Mittelgrund where acoustic turbidity is absent. These CT techniques represent the first quantitative characterization of bubble size, shape, and distribution in marine sediments and provide a unique opportunity to test models of acoustic propagation and scattering.

Biogeochemical studies demonstrate that methane concentrations in this organic-rich, anoxic sediment reach saturation within less than a meter of the sediment-water interface. Aerobic metabolism is generally restricted to the upper 1-2 cm of sediment with sulfate reducing sediments (50-100 cm thick) found between the zones of aerobic respiration and methane production. Martens, Albert and Alperin developed a kinetic model of the complex biochemical interaction of bacterial methane production, methane consumption at the base of the hydrogen sulfide reduced horizon, advective and diffusive transport processes, organic supply, and sedimentation rates in methane-rich sediments. They demonstrated that predicted methane distribution is most sensitive to the flux and degradation rate of reactive organic matter. Albert

and Martens successfully used this model to predict methane and sulfate concentration profiles, rates of biogeochemical reactions, and methane gas volumes in the sediments of Eckernförde Bay. Differences in the depth of methane bubbles at three sites were, in part, controlled by rate of vertical pore water advection from freshwater aquifers. Higher rates of flux of reactive organic matter to local topographic depressions such as pockmarks resulted in a decrease of depth and increase in volume of free methane gas. Bussmann and Suess demonstrate that high ground water flow increases the concentration of methane in bottom waters near the pockmarks of Eckernförde Bay, increasing flux of methane to the atmosphere. Possible ebullition of methane bubbles was also detected acoustically.

High sedimentation rates, high organic contents, near surface anoxic conditions, and restricted biological activity in sediment from the central basin result in surficial sediments with very high water content and low bulk density. These bubble free sediments are easily compressed and have very little strength, therefore exhibiting low values of shear strength, compressional wave speed and attenuation, shear wave speed and shear modulus. Characterization of in situ sediment physical, acoustical and geotechnical properties of the deeper gassy sediments presented a considerable technical challenge. Laboratory measurements on depressurized sediments are suspect, as ebullition of gas when sediments are depressurize tends to disrupt sediment structure. In situ measurements or measurements on cores retained at ambient pressure and temperature are preferred. With the exception of sharp gradients in bulk density and water content in the upper 5-10 cm, sediment physical properties such as water content, bulk density, mean grain size, and organic content varied little within the upper few meters. The high sediment organic content, high sedimentation rate, pelletized nature of the sediment, and presence of free gas may limit consolidation by self-weight. Shear strength although very low, increased with depth in the sediment. A comparison of in situ and laboratory shear strengths suggests a slight reduction in shear strength due to gas bubbles. Shear wave speed, another measure of sediment strength or rigidity, was the lowest ever reported for marine sediments based on in situ measurements. The presence of gas bubbles appeared to have little affect on this frame borne property, which is in agreement with predictions from current propagation models. Values of sediment permeability were higher than expected for silty-clay sediments, as the pellitized nature of the sediment creates microchannels that allow increased fluid flow.

In addition to standard laboratory methods, sediment macrostructure was measured by x-radiographic and micro-resistivity imaging of sediment cores. Employed together, these techniques elucidate not only spatial correlation lengths but allow determination of sediment tortuosity, a rarely measured parameter for modeling conductivity and fluid flow in porous media. Image-based texture analysis of x-radiographs and resistivity images of near surface sediments indicates that density structure is highly anisotropic with shorter correlation lengths in the vertical (graded or laminated bedding) than the horizontal direction. Graded and laminated bedding, as well as burrows and occasional shells are evident in x-radiographs of the upper 30-cm of surface sediments. These laminae correspond to the well-pelletized layers deposited in quiescent periods and the non-pellitized graded beds deposited as a result of storm events described by Nittrouer and by Milkert. Sediment microstructure, determined using transmission electron micrographs (TEM) of the upper 2 meters of the sediment column, is characterized by dense aggregates of silt and clay-sized particles separated by relatively large, fluid-filled canals. This pattern may reflect the dominant preservation of surficial zones pelletized by deposit-feeding invertebrates. High sediment permeability, for muds, is probably related to the very loose

sediment microstructure, lack of consolidation, and existence of channels between remnants of fecal pellets. Weak sediment fabric may also explain high values of sediment compressibility, whereas physico-chemical strengthening of interparticle bonding may account for the high apparent overconsolidation of near-surface Eckernförde mud. Discrete element simulations based on microfabric images appear to have promise in the prediction of acoustic (wave speeds) and finite (compressibility, strength, apparent overconsolidation) behavior in bubble-free fine-grained sediments from Eckernförde Bay.

Analysis of high-frequency (40 kHz) acoustic backscattering data demonstrated that scattering originates from a layer of free methane gas 0.5 to 1.0 meters below the seafloor rather than from the sediment-water interface. Spatial and temporal variability, including migrations and differences in concentrations of free methane gas, probably account for the high spatial variability and temporal decorrelation of backscatter images. Event-like changes in acoustic scattering in the water column were attributed to ebullition of gas bubbles from the seafloor. These events did not correlate with bottom stress due to bottom currents, temperature changes, or refraction due to stratification but were strongly correlated with changes in bottom pressure. These observations are consistent with gas ebullition due to pressure release. The flux of methane to the water column is estimated at between $3 - 20 \text{ mol m}^{-2} \text{ d}^{-1}$, based on estimated bubble radius and a comparison between measured and predicted scattering strengths. These data support observations of a significant flux of methane from the seafloor to the water column reported by Bussman and Suess, and suggest a direct flux to the atmosphere. Knowledge of bubble volume, size, shape, distribution provided by Anderson and Abegg has allowed quantitative modeling of high-frequency acoustic scattering heretofore impossible. The effects of non-spherical bubbles shapes, multiple scattering, bistatic have been quantified. Volume scattering, based on normal incident acoustic profiles obtained by sediment classifiers (15-30 kHz), has been effectively modeled for the first time given sediment properties and the bubble distribution and characteristics provided by this program.

Initial measurements of the speed and attenuation of compressional and shear waves in Eckernförde Bay sediments were in general agreement with model predictions and laboratory studies. In situ shear wave speeds were the lowest ever reported for marine sediments. These low shear speeds and near surface gradients were, however, in agreement with physical and empirical models developed for gas-free sediments. It is apparent that the small volume of free gas (< 2%) found in most Eckernförde sediments has very little effect of sediment rigidity. On the other hand, the small volume of gas in Eckernförde sediments greatly affected compressional wave speed and attenuation. Attenuation of compressional waves was very high as a result of scattering from individual bubbles at high frequency, damping near bubble resonance and scattering from bubble clouds at low frequency. Sound speeds were greatly reduced below bubble resonance and speeds were near that of bubble-free sediments at higher frequencies. This unique set of data, including bubble size, shape, and distribution; sediment, pore water, and gas physical properties; and in situ acoustic measurements over the frequency range of 5-400 kHz, provided the first opportunity to test propagation models developed for gassy sediments. The agreement between measurement and theory convinced both Richardson and Lyons that measurements of acoustic propagation within and scattering from the seafloor can be used to determine bubble volume, size, and distribution in fine-grained gassy sediments.

1.1.4 Modeling

The primary objectives of the interdisciplinary studies of gassy sediments of Eckernförde Bay were to characterize and model benthic boundary layer processes and the impact these processes have on seafloor structure, properties and behavior. Measurements made during these experiments have considerably increased our knowledge of the characteristics of these gas-rich sediments. CT scans of sediment retained at ambient pressure and temperature have provided the first quantitative characterization of in situ bubble populations including estimates of bubble shape, size, and distribution. Questions still exist as to the possible contributions of bubbles with radii smaller than 0.4 mm and the importance of scales of spatial and temporal heterogeneity found for these bubble populations. Processes controlling bubble formation, size distribution, and migration are still unknown.

The quantitative bubble population data combined with a unique set of in situ acoustic and physical property measurements have allowed us to validate acoustic propagation and scattering models. Accurate predictions of frequency dependent sound speed, attenuation due to bubble damping and scattering, and volume scattering suggest that acoustic techniques can be used for in situ characterization of bubble volume, size and distribution. Acoustic perturbation models that account for surface roughness and volume heterogeneity do not adequately predict high frequency scattering from the seafloor in gassy sediment. New empirical models that treat bubbles (oblate spheroids) as discrete single or multiple scatters were developed to predict acoustic scattering from gas-rich layers.

Detailed biological and oceanographic measurements have allowed models of sediment transport, erosion, deposition, and sediment physical and biological reworking to be developed. Models of strata preservation based on depths and rates of biological and physical mixing, sedimentation rates, frequency of storms, and source of particles are in agreement with the observed stratigraphic record. A kinetic model of the complex biochemical interactions of bacterial methane production and consumption, advective and diffusive transport processes, organic supply, and sedimentation rates has successfully been used to predict methane and sulfate concentration profiles, rates of biogeochemical reactions, and gas volumes. The spatial distribution and strength of acoustic turbidity is accurately predicted by these biochemical models, whereas the seasonal migration of the acoustic turbidity horizon correlates with changes in sediment temperature and is modeled using methane solubility. Accurate prediction of the rate of input of reactive organic matter to the sediment, rates of methane production and consumption, and groundwater advection are generally not available thus restricting the use of these static kinetic biochemical models. Historical changes in rates of sedimentation and organic flux to the seafloor, seasonal changes in sediment temperature and salinity and short-term changes in bottom pressure and the hydraulic flow from subbottom aquifers all dictate the need for time dependent kinetic biochemical and solubility models. Studies that combine acoustic characterization of temporal changes, migration, and ebullition of methane bubble populations with biochemical studies may help in the development and validation of those models.

1.2 DESCRIPTION OF THE WEST FLORIDA SAND SHEET EXPERIMENTS

1.2.1 Geological Background

The West Florida Sand Sheet experimental site is located 23 nm southeast of Panama City, Florida on an otherwise fine-grained, sand-wave field (Cape San Blas Sand Facies) of the inner continental shelf. The shelf of the northeastern Gulf of Mexico is currently sediment-starved with most material deposited by the Apalachicola River during lower sea stands. Hydrodynamic processes, especially major storms, control recent large-scale seafloor morphology. Silt- and clay-sized particles are occasionally deposited over the sand sheet during severe storms. These finer sediments can be either worked into the predominantly sandy surface sediments by biological activity or winnowed out of the sediments by minor storms. Small ripples form at coarse sand sites in response to the passage of winter fronts, and may persist for months. Hurricanes and other major storms also change bottom relief forming 2-10 m megaripples as a result of strong bottom currents. Megaripples formed after the passage of hurricanes Elena (September- October, 1985) and Kate (November, 1985) decayed after two years, presumably a result of active bioturbation during quiescent periods

Acoustic surveys of a 20-km²-area, using side-scan sonar, chirp sonar and 3.5 kHz echo sounding, allowed experimenters to delineate a 600-by-625 m primary experimental site which had uniformly high acoustic reflectivity (Figure 4).

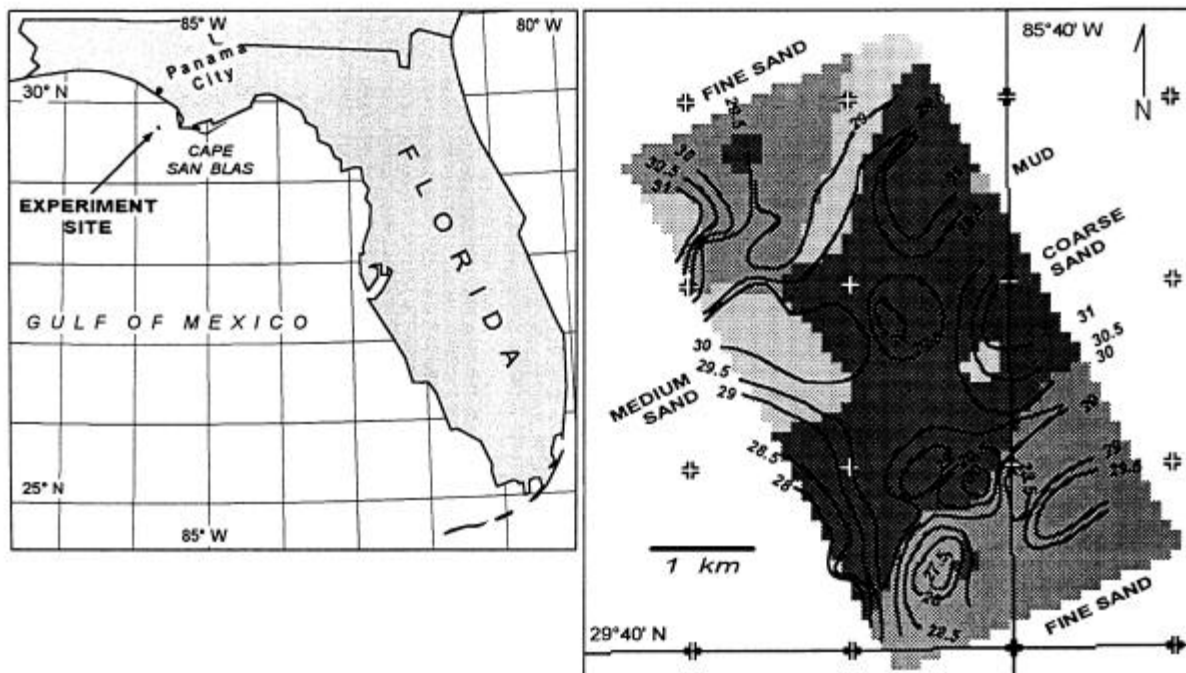


Figure 4. Bathymetry (meter isobaths) and sediment types of the West Florida Sand Sheet experimental site (adapted from K.S. Davis et. al. 1996 and Fleischer et. al. 1996)

Acoustic backscattering strength in the larger area was highly correlated with sediment mean grain size and carbonate content. Sediments in the highly reflective area were coarse-grained sands (mean phi: 0.84 phi) mixed with shell hash, coralline algae fragments and numerous large mollusk shells. Sediments outside the experimental site were comprised of lower reflective, medium- and fine-grained sands (mean: 2.39 phi) with little shell hash and occasional muddy layers or inclusions. Values of porosity (mean: 40.3 %), density (mean: 2.01 g cm⁻³),

compressional wave velocity (mean: 1711 m s^{-1}), attenuation (mean: 30.4 dB m^{-1} at 58 kHz) and shear wave velocity (mean: 118 m s^{-1}) varied little between sediment types. CT-scans of sediment core samples from the highly reflective area reveal thousands of shell and shell fragments per cubic meter. The suggestion, based on acoustic measurements, that this sediment contains small amounts of free gas was not supported by geochemical evidence or groundwater flow.

1.2.2 Acoustic Modeling and Experiments

Acoustic scattering experiments and time-lapse monitoring of environmental conditions were restricted to the highly reflective sediment. Temporal decorrelation of successive acoustic scans of the seafloor was an order of magnitude greater than at the Eckernförde site. Rapid decorrelation of acoustic scans collected during experimental manipulations of the bottom by divers suggests that the short-term acoustic decorrelation noted in the long-term acoustic record were the result of changes in fine-scale topography. The near-bed hydrodynamic regime was dominated by reversing tidal currents with typical speeds of 10-cm s^{-1} or less. Maximum bed shear stresses remained too low to resuspend or transport the sediments. The high temporal variability in acoustic scattering strengths must, therefore, be related to biologically induced changes in bottom micro-roughness. Therefore hydrodynamic processes, especially major storms, dominate kilometer-scale decadal sediment characteristics of this site, whereas meter-scale, seasonal-to-daily bottom characteristics are controlled by minor storms and biological activity.

Acoustic model simulations by Anderson and Lyons, based on the distribution of shells from CT-scans of core samples, suggests that at 40 kHz acoustic backscattering strength from the sea floor is controlled by seafloor roughness above a grazing angle of about 10 degrees, while sediment volume scattering controls backscattering strength for lower grazing angles. Jackson and Williams, on the other hand, demonstrated that surface roughness accounts for most of the modeled backscattering strength over grazing angles of $5\text{-}60$ degrees. Their acoustic model predictions based on perturbation theory and the extensive environmental characterization available from this site (sediment physical properties, seafloor roughness, and spatial heterogeneity) is in agreement with measured backscattering strengths over the range of 5 to 20 degrees. In either case roughness and volume heterogeneity are both dominated by the distribution of shells within an otherwise homogeneous sand-sized sediment. Biological and hydrodynamic processes, which control this spatial heterogeneity, must be understood in order to predict the frequency dependent nature of seafloor scattering and its temporal variations. It was also shown, by frequency dependent target strength measurements, that the larger shells alone can provide the same order of magnitude of acoustic backscattering strength as was measured from the sea floor in these field experiments. The importance of discrete scattering from shells at or near the surface should therefore be included in bottom scattering models as well as the aforementioned roughness and volume scattering mechanisms.

Measurements of the penetration of high-frequency acoustic energy into the sediments at Panama City, Florida were inconsistent with sediment modeled as fluid with flat interface where a critical grazing angle is predicted below which there will be no appreciable acoustic penetration. These anomalous results together with other field and laboratory studies have lead to an Office of Naval Research (ONR) Departmental Research Initiative (DRI) to study these phenomena. Experiments are planned for the continental shelf off Panama City during the summer of 1999.

At present, three mechanisms are hypothesized to contribute to this subcritical acoustic penetration. First, the porous nature of the sediment leads to a "slow" wave with a speed less than the speed of sound in water; thus no critical angle for that converted wave exists. Second, seafloor roughness diffracts energy into the sediment. Third, sediment volume heterogeneity scatters the evanescent wave energy that propagates along the seafloor interface into the sediment. Measurement of normal incident reflection loss in these sandy sediments was also found to be inconsistent with models that approximate the sediment as a fluid. Chotiros and Boyle used modifications of the Biot theory to model these data. Their assumptions, including values of grain and skeletal moduli have generated much controversy and will require additional well-controlled experiments.

1.3 DESCRIPTION OF THE KEY WEST CAMPAIGN

1.3.1 Introduction

The third major experimental site was in the vicinity of the Marquesas Keys and the Dry Tortugas in the Lower Florida Keys where bioturbation and biogeochemical processes were believed to control sediment structure (Tooma and Richardson, 1995). The area surrounding the Florida Keys provide the only environment in continental US waters which is analogous to shallow-water tropical carbonate settings that are becoming increasingly important to naval interest. During February 1995, four research vessels (WFS PLANET, R/V SEWARD JOHNSON, R/V PELICAN and R/V SEAWARD EXPLORER) and 115 scientists and technicians from five nations mounted a major cooperative scientific effort that became known as the Key West Campaign. (Figure 5).

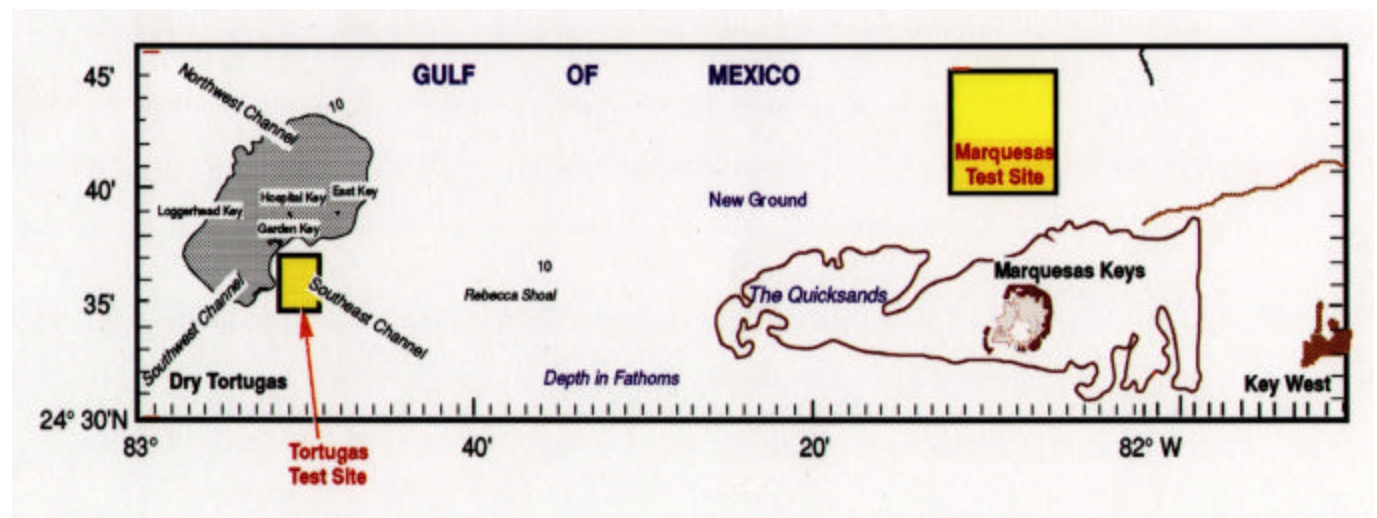


Figure 5. Map of two major experiment sites during the Key West Campaign.

1.3.2 Geological Background

The Florida platform is constructed of approximately 10 km of Cretaceous to Holocene carbonates and evaporates resting on a patchwork basement of Precambrian to Jurassic igneous, metamorphic and sedimentary rocks. Based on the analyses of samples and approximately 2500 km of high-resolution, single channel seismic data, Holmes defined 26 facies on the southern most Florida Platform. These facies were divided into four categories: (1) hardground and outcrops; (2) areas of recent sediment movement; (3) periplatform deposits; and (4) the "inner shelf" deposits. The nature origin, and distribution of the units classed as hardgrounds and outcrops (the Miocene terrace, the shelf-edge reef complexes, the central reef trend, and the southern banks) are keys to the geological history of the area. The second category, areas of recent sediment movement, characterizes the sedimentary processes presently active on the shelf. The third category, the periplatform deposits show evidence of past sedimentary processes responsible for the shelf accretion in their morphology and bedding. The inner shelf deposits are the result of longshore processes and sediment trapping landward of the hardgrounds.

The areas of concentration for the CBBL program encompass two of the categories; category two, an area of present sedimentary activity immediately seaward (facing the Florida Straits) and the fourth category, those sediments deposited in the lee of a hardground. The area selected for the most intense investigation was the region of present sedimentation, adjacent and east of the complex of islands dominated by Garden Key (Fort Jefferson). In this region, the nearly circular Dry Tortugas Platform is indented, possibly due to the fracture pattern in the bedrock. This indentation forms a sediment trap, a region of lower energy, which contains sediment washed by the winds and tides from the adjacent platforms to the west and north. These sediments appear to be coarse attesting to their origin and the high physical energy in the environment of deposition.

The secondary area of study is located on the eastern edge of the sedimentary basin, north of the sands that extend west from the Marquesas Keys. The adjacent platform, known as the quicksands due to the rapidly migrating sand waves, which wash across it, forms a barrier to large physical activity from the south. The basin is also deeper than the shelf to the north. As a result, the basin is a sediment trap, which contains finer components than the other areas. This sedimentary body is characterized by a high organic content attested to by the rich shrimping grounds in this part of the Gulf of Mexico. These two sites, in close proximity, with contrasting sediment types and differing physical and chemical settings, made this location ideal for the CBBL program in a carbonate environment.

1.3.3 Description of the Key West Campaign experiments

Acoustic surveys utilizing the Acoustic Sediment Classification System (ASCS), a chirp subbottom profiler, a sidescan sonar system, and seismic sled (Magic Carpet) towed along the bottom characterized the distribution of sediment properties in the Lower Florida Keys. Based on data from these efforts, a protected area appropriate for the many planned experiments in the Southeast Channel of the Dry Tortugas (Figure. 5) was chosen for intensive study. Within this experimental site, high-frequency acoustic scattering measurements were made from the R/V SEWARD EXPLORER using the Applied Physics Laboratory Benthic Acoustic Measurement System tower and from the R/V SEAWARD JOHNSON using a remotely-operated vehicle designed by Applied Research Laboratory/University of Texas.

Shallow sediments were sampled using box cores, gravity cores, and diver coring for radiological, geotechnical, biological, biogeochemical, physical, and geoacoustic studies. The resultant data provide an understanding of the environmental processes that affect sediment structure, a quantification of sediment structure from the micron to cm scale, and a measure of sediment behavior under various stress-strain conditions. Hydrodynamic data were collected with an instrumented tetrapod fielded by the Virginia Institute of Marine Science and, in conjunction with the sediment data, are being used to improve our understanding of scattering mechanisms and to validate or develop new acoustic scattering models.

The original framework established by the CBBL illustrates how the interrelationship between prevailing processes and sediment properties and behavior operates in the Key West environment (Figure 6).

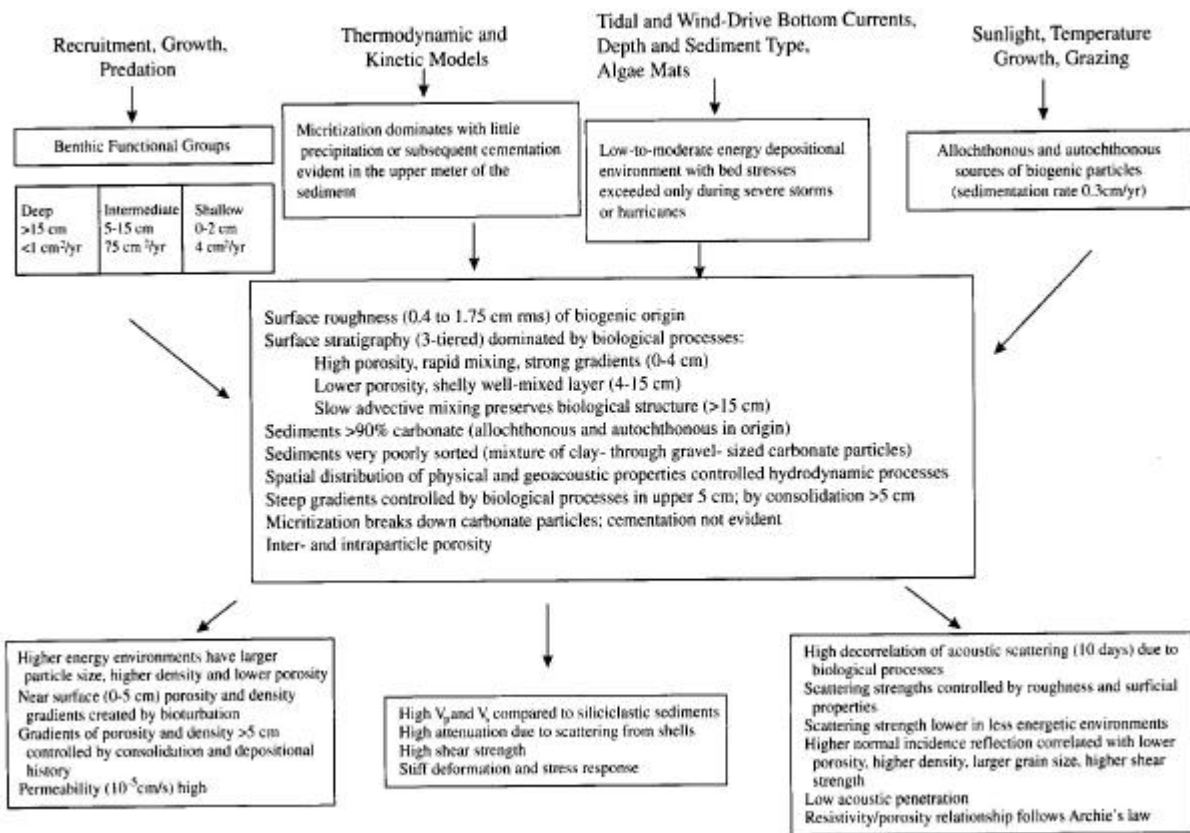


Figure 6. Schematic summary of the major environmental processes and sediment structure, properties and behavior.

Benthic fauna at the Dry Tortugas site are vertically tiered and can be divided into three functional groups: a shallow fauna, surface deposit and suspension feeders, which thoroughly mix the upper 4-5 cm in days to weeks; an intermediate fauna, carnivores/scavengers, deep deposit feeders, and head-down deposit feeders, which intensely mix sediment to depths of 15 cm over time scales of 10-20 years; and a deeper fauna, gallery-creating callianassid shrimp, which only partially mix sediments. Rates and depths of sediment mixing, rates of deposition and

the depth and frequency of erosion can be used to model the preservation potential of sediment layers and structure generated by both physical and biogenic processes.

Shallow-water carbonates normally undergo extensive post-depositional biogeochemical diagenesis that includes dissolution, precipitation, and subsequent cementation. Significant changes in surficial carbonate fabric result from subaerial exposure, exposure to fresh-water, micritization, bioturbation, and pore water chemical changes due to the breakdown of organic matter. Although pore waters supersaturated with carbonate, no significant precipitation was noted in the upper meter of sediment at the Dry Tortugas. Current thermodynamic or kinetic models are unable to explain this lack of precipitation or cementation, which is common in other carbonate environments. Advection of water rich in oxygen by bioirrigation to depths as great as 15 cm may explain these model discrepancies. Foraminifera tests show only a slight evidence of the weak reducing conditions found in subsurface sediments. The dissolution features, minor precipitation of calcium carbonate and formation of occasional pyrite framboids may result from the presence of micro-chemical habits within the tests. The dominant processes affecting sediment structure appear to be mechanical and chemical breakdown of carbonate particles, effectively converting sand- and silt-sized carbonate particles to clay-sized matrix material.

Benthic biological processes act in complex concert with physical processes to control sediment transport and seafloor microtopography. The benthic boundary layer at the Dry Tortugas is characterized by low to moderate energy. Bed stresses, primarily due to tidal currents, only occasionally exceed the threshold for sediment transport. Sediment microtopography is biologically dominated, in part a result of surface algal mats that bind sediments increasing sediment critical skin friction. Thus, the Dry Tortugas site is a low-energy sediment sink with most sediment being derived from erosion of the Dry Tortugas Bank just to the north. Severe winter storms and hurricanes can redistribute sediments locally.

Sediments in the Dry Tortugas originate primarily from the breakdown and subsequent transport of biogenic carbonate material from nearby reefs and other hardgrounds (allochthonous) rather than through in situ (autochthonous) production. Sedimentation rates are approximately 0.3 cm/yr. The result is a carbonate sediment (>90%) consisting primarily of aragonite plates and needles derived from the breakdown of plates of aragonitic green algae (*Halimeda*, *Penicillus*, and *Udeota*), molluscan shells, benthic and planktonic foraminifera, echinoid spines, sponge and coral fragments, diatoms, and less than 5% particles of siliciclastic origin. Microroughness (0.5- to 1.75-cm rms) is primarily biogenic in origin. Sediment is tiered with a thin (0-4 cm) high porosity, homogenous layer covering a more heterogeneous (4-15 cm) shell layer. Bioturbation creates the strong depth gradients in porosity, bulk density and sediment geoacoustic properties. A combination of biogenic mixing and storm-generated stress creates inhomogeneities such as fine laminae and shell lag deposits. Below 15 cm, biogenic heterogeneity dominates the sediment. The vertical gradients and variability of sediment physical, geotechnical, electrical and geoacoustic properties reflect the tiered nature of these sediments. Pore water is distributed as both intra- and inter-particulate porosity.

The distribution of sediment characteristics is primarily controlled by the biological processes that generate carbonate skeletal material and by hydrodynamic processes that erode, fragment and redistribute those particles. Post-depositional biogeochemical processes appear to have little effect on surficial sediment physical and geoacoustic properties in the lower Florida Keys. The distribution of geoacoustic properties correlates with the areal distribution of surficial sediment

physical properties including grain size, porosity and sediment bulk density. Higher sound speeds are found in more energetic environments where coarser-sized particles dominate and lower values of sediment porosity and density are found. Empirical relationships between sediment physical and geoacoustic properties for these carbonate sediments are significantly different than for siliciclastic sediments. Higher shear and compressional wave speeds relate to the high percentage of interparticle porosity, the higher grain bulk modulus, and the very poorly sorted nature of these carbonate sediments compared to siliciclastic sediments. High attenuation in carbonate sediments is probably the result of increased scattering from abundant gravel- and sand-size shells rather than differences in intrinsic attenuation. Empirical relationships among porosity, density, resistivity and shear wave speed have also been established for carbonate sediments. The stiff deformation and stress responses of the sediments do not reflect cementation but may be caused by interlocking of angular particles.

Surface backscattering strengths (at 40 kHz) and bistatic scattering strengths can accurately be predicted from bottom roughness and values of surficial sediment density, velocity and attenuation, only if the sediment properties are based on an average of the upper few centimeters. Scattering strengths appear to be dominated by surface roughness scattering. Subsequent acoustic modeling must include the effects of the steep gradients in sediment bulk density and sound speed. High frequency bottom scattering rapidly decorrelates with time probably as a result of near-surface biological activity.

1.4 DESCRIPTION OF THE NORTHERN CALIFORNIA EXPERIMENTS

Several teams of CBBL investigators participated in the STRATA FORMation on Margins (STRATAFORM) experiments on the Northern California continental shelf during the summer of 1996. STRATAFORM is an ONR-sponsored program designed to unravel the effects of past and present shallow-water benthic boundary layer processes on sediment fine-scale stratigraphy (Nittrouer and Kravitz, 1996). The strength of the STRATAFORM program is the interaction of marine geologists who study active benthic processes and relate these processes to strata being created and marine geophysicists who document stratigraphic relationships through seismic records and attempt to interpret the history of formative processes (Nittrouer and Kravitz, 1996).

The (CBBL) objectives were to determine and model the effects of current benthic processes on the spatial variability of physical, geoacoustic and mechanical properties in surficial sediments. We also planned to characterize the sediment structure of the upper 2 meters of the sediment column to determine which benthic processes dominate the recent stratigraphic record. Data on the spatial variability of sediment physical and geoacoustic properties and bottom roughness collected by CBBL scientists will also be used as input to and test of high-frequency acoustic bottom scattering models. Concurrent and long-term measurement of high-frequency (40 kHz) acoustic backscattering and bistatic scattering were obtained as part of the STRATAFORM program at site S-60 by Jackson and Williams (APL-University of Washington). The effects and rates of environmental benthic boundary layers processes (hydrodynamic bottom stress, rates and depths of bioturbation, and rates of sediment deposition) were quantified at S-60 by other STRATAFORM scientists. These data are analogous to the concurrent environmental, sediment property, and high-frequency scattering data collected during CBBL experiments at Eckernförde Bay, Panama City and Key West and will greatly expand our comparative database.

A combination of high-frequency acoustic remote sensing, in-situ measurements, and laboratory sediment analysis techniques were employed to quantify the spatial (horizontal and vertical) variability of sediment strength, stability, geacoustic properties, sediment reflectivity, and sediment impedance. Sediment distribution at the study site, located in 30-100 meters water depth off the northern California coast, is controlled by complex interactions among benthic boundary layer processes including: sediment deposition from floods from the Eel River, erosion and deposition due to intense winter storms, and sediment mixing by benthic fauna. Measurements were made along two transects; one normal to the coast (S-line) about 30-km north of the mouth of the Eel River, and the second parallel to the coast along the 70-m isobath. The central axis of recent deposition from Eel River floods occurs along the 70-m isobath. An emphasis was placed in determination of vertical and horizontal variability of sediment properties at the S-60.

Sediments at the shallow-most sites (10-40 meters water depth) were low-porosity, high-density sands. Strong bottom currents and wind-wave resuspension apparently winnowed out most fine-grained sediment and transported particles in both northward and offshore directions. Values of in-situ surficial sediment compressional wave speeds (1580-1647 m/s) and shear wave speeds (60-112 m/s) were high and within-station variability of these sediment properties was relatively low. The mid-shelf sediment (80-100 meters water depth) was primarily a fine-grained, high-porosity, low-density mud. Values of in-situ compressional wave speed (1458-1480 m/s) and shear wave speeds (30-42 m/s) were significantly lower than at the shallower sandy sites but also exhibited low horizontal and vertical variability. This region is primarily depositional and sediment mixing is dominated by bioturbation. Sediment at the intermediate location between 45 and 65 meters water depth was a mixture of sand-sized and fine-grained clay particles. The high values of vertical and horizontal variability in sediment grain size were reflected in the high variability in other sediment properties such as compressional and shear wave speeds, porosity, sediment density, and shear strength. The highly variable structure was also evident in x-radiographs from the mid-depth sites.

The surficial in-situ measurements of sediment geacoustic properties were complemented by direct measurements of low frequency seismic shear wave propagation (Magic Carpet) within the upper meter of sediment. The seismic techniques provided detailed vertical and horizontal gradients of shear wave speeds within water depths of 40 to 70 meters. The agreement between high-frequency in-situ shear wave speeds and shear wave speeds from these lower frequency seismic techniques is remarkable. The good correlation between seismic shear wave speed and sediment porosity and void ratio demonstrate the value of these techniques in estimating gradients and spatial variability of seafloor physical properties.

A dominance of wind-wave-current effects in shallow-water stations is manifested in a low variability in values of geacoustic and physical properties. Hydrodynamic stress affects the sediment structure by mobilizing the surficial sediment and creating relatively homogeneous, low variability sands. In deeper water (70-100 m), only exceptional waves can effect the movement of water near the sea floor and the lack of significant hydrodynamic stress on the sediment results in little or no resuspension or migration of sediments. Biological activity of benthic infauna at the deeper sites affects the sediment structure by mixing the surficial sediment and creating relatively homogeneous clayey silts and silty clays. Structure (layers) created by changes in sediment deposition is destroyed by active surficial bioturbation. At intermediate water depths (45-60 m), interaction between biological and hydrodynamic processes creates

great variability in acoustic and physical properties. Interplay between processes creates a complicated structure reflecting flood deposition, erosion and redeposition by storm events, and mixing by bioturbation. When one process dominates over the other, the tendency is toward uniformity in acoustic and physical properties.

This interplay among benthic process and the variability of seafloor physical properties and sediment mechanical and geoacoustic behavior was evident at deeper depths within the sediment. The record of past benthic boundary layer processes was preserved and observed in sediments collected with gravity corers, direct in-situ low-frequency seismic studies, and also reflected in remote high-frequency (15-30 kHz) seismo-acoustic profiling. Conditions during the experiments were less than ideal for remote acoustic data acquisition, and the resolution of the acoustic records was degraded by heavy seas. In spite of these difficulties it is obvious that similar environmental processes have acted over the last several thousand years, and traces of that record are preserved in the sedimentary record.

Laboratory tests on the contractive/dilative behavior of shallow water sand suggests that sand sediment along the California coast (30 to 40 meters water depth) is too compact to liquefy under seismic or ocean wave stresses. Object burial by liquefaction is therefore unlikely in this high-energy environment.

1.5 ACKNOWLEDGMENTS

The primary financial support for the CBBL was provided by the Office of Naval Research (ONR) with contributing support from the Naval Research Laboratory (NRL) and by Forschungsantalt der Bundeswehr für Wasserschall- und Geophysik (FWG). Dr. Fred E. Saalfeld, Deputy Chief of Naval Research and Technical Director of ONR, provided the original program direction. All CBBL scientists thank Dr. Saalfeld for his unwavering support of their research during the 6-year existence of the program. Prof. Peter Wille (Technical Director, FWG) and Dr. Timothy Coffey (Director of Research, NRL) were both strong supporters of the CBBL contributing both encouragement as well as program financial support. John Cornette (ONR) provided friendship and useful insights during the development and execution of the program. The contributions of the CBBL review panels, which include J.E. Andrews, M.R. Barker, D.L. Bradley, W.K. Ching, H.C. Eppert, J.M. Harding, J.D. Grembi, D. Inman, J.H. Kravitz, C.M. McKinney, G. Pollitt, C. Stuart, D.G. Todoroff, P.R. Vogt, J.T. Warfield and B. Winokur, are gratefully acknowledged. Workshops for planning the direction of the CBBL were hosted by R. H. Bennett, C.S. Clay, W.A. Dunlap, G.D. Gilbert, D.R. Jackson, P.A. Jumars, H.J. Lee, and T.G. Muir.

Operational support for the many experiments was provided by Forschungsantalt der Bundeswehr für Wasserschall- und Geophysik (FWG), Wehrtechnische Dienststelle-71, University of Kiel, Naval Air Station Key West, US Park Service, Florida Keys National Marine Sanctuary, Texas A&M, Naval Research Laboratory, US Coast Guard, and Air National Guard. Ships used during these investigations included the *GYRE*, *HELMSAND*, *HIEV*, *KRONSORT*, *PELICAN*, *PLANET*, *WILHELM PULLWER*, *SEWARD JOHNSON*, *SEAWARD EXPLORER* and *WECOMA*. The captains and crew of these ships are to be commended for job well done.

The Coastal Benthic Boundary Layer (CBBL) program research team included M.D. Richardson (chief scientist) and the following principal investigators, technicians, and graduate students: A. Ag, D.B. Albert, M.J. Alperin, R. Anandrajah, A.L. Anderson, R.A. Altenburg, R.J. Baerwald, E.O. Bautista, P. Beaujean, J.D. Bennell, S.J. Bentley, R.H. Bennett, F.A. Boyle, H.G. Brandes, K.B. Briggs, D.R. Brogen, G.R. Brooks, C.A. Brunner, W.A. Bryant, P.J. Burkett, L. Buzi, W.-A. Chiou, N.P. Chotiros, D. Chu, J.C. Cranford, N.I. Craig, A.F. D'Andra, A.M. Davis, K.S. Davis, D.L. DeBruin, M.E. Duncan, J.J. Dvorkin, R. Elder, R.W. Faas, A. Falster, K.M. Fischer, P. Fleischer, R.C. Flint, R. Flood, N.L. Frazer, V. Freyermuth, C.T. Friedrichs, G.V. Frisk, S.S. Fu, Y. Furukawa, R.A. Gammish, S. Gibson, K.E. Gilbert, G. Jin, R.R. Goodman, T.J. Gorgas, S.R. Griffin, T.L. Hebert, R. Haynes, J.A. Hawkins, D.A. Hepworth, C.A. Holmes, R.J. Holyer, M.H. Hulbert, D.G. Huws, D.R. Jackson, P.D. Jackson, J.J. Kolle, D.N. Lambert, D.L. Lavoie, D.M. Lavoie, L.R. LeBlanc, Y. Lee, G.R. Lopez, A.P. Lyons, T. Lu, C.S. Martens, D.F. McCammon, A.C. Mueller, M. M. Meyer, E.C. Mozely, C.A. Nittrouer, T.H. Orsi, J. Piper, R. Priebe, H.A. Pittenger, J. Pyrah, R.I. Ray, A. Reed, A.K. Rutledge, M.H. Sadd, J.C. Sandidge, W.A. Sawyer, S.G. Schock, A.M. Schiller, A.J. Silva, N.C. Slowey, C.K. Sommerfield, S. Stanic, T.K. Stanton, K.P. Stephens, R.D. Stoll, G. Sykora, D.J. Tang, K.R. Thornton, G.E. Veyera, D.J. Walter, R.A. Weitz, K.L. Williams, R.H. Wilkens, W.A. Wood, L.D. Wright, J. Yuan, M. Yao, D.C. Young, D.K. Young, L. Zhang and J. L. Zhang. Numerous other technicians and graduate students also contributed to the CBBL experiments. I apologize for any omissions in the long list of CBBL participants. Other significant contributors to the CBBL program included I.H. Stender, Th.F. Wever, G. Fechner, R. Thiele and H.M. Fiedler of FWG; R. Grotirian of WTD-71; F. Abegg, D. Milkert, F. Theilen, and F. Werner of the University of Kiel; M. Schlüter, I. Bussman, and E. Suess of GEOMAR; D. Mallinson, S. Locker, M. Hafen, D. Naar, A. Hine, from University of South Florida; and Sam Tooma and Dan Lott from the Naval Research Laboratory. Leona Cole, Lori Stockstill and Dinah Kennedy were responsible for completion of this report. The NRL contribution number is NRL/MR/7430--98-8213.

1.6 REFERENCES

- Lavoie, D.L. and M.D. Richardson (Editors) (1997) Proceedings of the Coastal Benthic Boundary Layer Key West Workshop. Naval Research Laboratory Memorandum Report NRL/MR/7431--97-8044, 222 pps.
- Lavoie, D.L., M.D. Richardson and C. Holmes (1997) Benthic boundary layer processes in the Lower Florida Keys. *Geo-Marine Letters* **17**:232-236.
- Nittrouer, C.A. and J.H. Kravitz (1996) STRATAFORM: A program to study the creation and interpretation of sedimentary strata on continental margins. *Oceanography* **9**:146-152.
- Richardson MD (Editor) (1992) The Coastal Benthic Boundary Layer Special Research Program: Program Direction and Workshop Recommendations. Naval Oceanographic and Atmospheric Research Laboratory Special Report NOARL SP 017:361:92, 149 pp.
- Richardson, M.D. (1994a) Investigating the Coastal Benthic Boundary Layer. *Eos Transactions, American Geophysical Union* **75**: 201-206

- Richardson, M.D. (Editor) (1994b) Coastal Benthic Boundary Layer Special Research Program: A Review of the First Year. Naval Research Laboratory Memorandum Report. NRL/MR/7431--94-7099:323pp.
- Richardson, M.D. (Editor) (1995) Coastal Benthic Boundary Layer Special Research Program: A Review of the Second Year. Naval Research Laboratory Memorandum Report. NRL/MR/7431--95-7595:276 pp.
- Richardson, M.D. (Editor) (1996) Coastal Benthic Boundary Layer Research Program: A Review of the Third Year. Naval Research Laboratory Memorandum Report. NRL/MR/7431--96-8001:236 pp.
- Richardson, M.D. (Editor) (1998) Coastal Benthic Boundary Layer Research Program: A Review of the Fourth Year. Naval Research Laboratory Memorandum Report. NRL/MR/7431--98- pp.
- Richardson, M.D. and W.R. Bryant (1996) Benthic boundary layer processes in coastal environments: An introduction. *Geo-Marine Letters* **16**:133-139.
- Richardson, M.D. and A.M. Davis (In press) Modeling gassy sediments from Eckernförde Bay: an introduction. *Continental Shelf Research*
- Tooma, S.J. and M.D. Richardson MD (1995) University, government laboratory, international effort focuses on coastal benthic boundary layer, combining basic, applied programs. *Sea Technology* **36**: 17-25.
- Wever, T.F. (Editor) (1994) Proceedings of the Gassy Mud Workshop held at the FWG, Kiel, 11-12 July, 1994. FWG Report 14: 114 pps.
- Wever, T.F. (Editor) (1995) Proceedings of the Workshop: Modelling Methane-Rich Sediments of Eckernförde Bay held at Eckernförde, 26-30 June, 1995.

TABLE 1. RESEARCH PROJECTS SUPPORTED BY THE COASTAL BENTHIC BOUNDARY LAYER PROGRAM (FY93-97)

Discrete element simulation of the microstructure of marine cohesive sediments (Johns Hopkins) • *Rajah Anandrajah*

Measurement and description of the upper seafloor sub-decimeter heterogeneity for macrostructure geoacoustic modeling (Texas A&M) • *A.L. Anderson*

Sediment properties from grain and macrofabric measurement (NRL, University of New Orleans, and Resource Dynamics) • *R.H. Bennett, Dennis Lavoie, P.J. Burkett, R.J. Baerwald, and M.H. Hulbert*

High-frequency acoustic scattering from sediment roughness and sediment volume inhomogeneities (NRL) • *K.B. Briggs and M.D. Richardson*

Effects of carbonate dissolution and precipitation on sediment physical properties and structure: microfossils component (University of Southern Mississippi) • *C.A. Brunner*

Processes of macro scale volume inhomogeneity in the benthic boundary layer (Texas A&M) • *W.A. Bryant and N.C. Slowey*

Analysis of data from in-situ acoustic scattering experiments (University of Texas) • *N.P. Chotiros*

New geophysical technologies applied to the quantitative evaluation of seabed properties related to mine burial prediction (UCNW) • *A.M. Davis*

Analysis of the rheological properties of nearbed (fluid mud) suspensions occurring in coastal environments (Lafayette College) • *R.W. Faas*

Statistical characterization of the benthic boundary for broadband acoustic scattering (Penn State) • *K.E. Gilbert, T.J. Kulbago*

The chemical dynamics of the South Florida carbonate test site (USGS and Eckerd College) • *C.A. Holmes and G.R. Brooks*

Measurement of high-frequency acoustic scattering from coastal sediments (University of Washington) • *D.R. Jackson and K.L. Williams*

Electrical resistivity imaging of unconsolidated sediments (BGS) • *P.D. Jackson*

Structural analysis of marine sediment microfabric (Quest Integrated, Inc.) • *J.J. Kolle and A.C. Mueller*

Qualification of high frequency acoustic response to seafloor micromorphology in shallow water (NRL) • *D.N. Lambert, D.J. Walter and J.A. Hawkins*

Measurement of shear modulus in-situ and in the laboratory (NRL) • *Dawn Lavoie, Y. Furukawa and A. Pittenger*

Quantification of gas bubbles and dissolved gas sources and concentrations in organic-rich, muddy sediments (University of North Carolina at Chapel Hill) • *C.S. Martens and D. Albert*

Physical and biological mechanisms influencing the development and evolution of sediment structure (State University of New York and Virginia Institute of Marines Science) • *C.A. Nittrouer, L.D. Wright, G. Lopez and C. Friedrichs*

Contact micromechanics for constitutive acoustic modeling of marine sediment (University of Rhode Island and Stanford University) • *M.H. Sadd and J. Dvorkin*

The detection of continuous impedance structures using full spectrum sonars (Florida Atlantic University) • *S.G. Schock and L.R. LeBlanc*

Variability of seabed sediment microstructure and stress-strain-time behavior in relation to acoustic characterization (University of Rhode Island) • *A.J. Silva, M. Sadd, G.E. Veyera and H. Brandes*

Effects of carbonate dissolution and precipitation on sediment physical properties and structure: pore water flux component (University of Southern Mississippi) • *A.M. Shiller*

High-resolution bottom backscattering measurements (NRL) • *S. Stanic*

Experimental and theoretical studies of near-bottom sediments to determine geoacoustic and geotechnical properties (Lamont-Doherty) • *R.D. Stoll*

Characterization of surficial roughness and subbottom inhomogeneities from seismic data analysis (Woods Hole Oceanographic Institution) • *D.J. Tang, G.V. Frisk and T.K. Stanton*

Image analysis of acoustic texture: A rapid predictor of physical and acoustic properties of unconsolidated marine sediments and processes affecting their relationships (NRL) • *D.K. Young, R.J. Holyer and J.C. Sandidge*

Acoustic Lance studies *R.H. Wilkens and S.S. Fu and L.N. Frazer*

The relationship between high-frequency acoustic scattering and seafloor structure (University of Southern Mississippi) • *Li Zhang and Ralph Goodman*

DISCRETE ELEMENT SIMULATION OF THE MICROSTRUCTURE OF MARINE COHESIVE SEDIMENTS

A. Anandarajah

The Johns Hopkins University

D. L. Lavoie, P. J. Burkett and M. D. Richardson

Naval Research Laboratory

ABSTRACT

The objective of this project is to investigate, for the Baltic sea sediments, the relationship between microstructure and macroscopic geotechnical properties. The goal is to be achieved using a numerical simulation technique known as the discrete element method (DEM), which allows load-deformation experiments to be carried out numerically, just as experiments are performed in laboratories. The primary soil type in the Eckernförde Bay where most of the CBBL experiments were conducted is clay and the DEM analysis used in the study accounts for the special characteristics of clayey sediments. Using the numerical procedure, a systematic study is conducted to simulate the compressibility of the sediments as follows. With the aid of an image processing software, representative TEM micrographs of Eckernförde Bay sediments are digitized for obtaining quantitative data concerning clay fabric and used in developing an initial numerical specimen. The effect of organic matters is simulated by introducing interparticle contact cementation, although the exact values of stiffness and strength of cemented contacts can not be determined. Another variable that is difficult to quantify is particle thickness. From the knowledge of clay mineral types and from micrographs, a possible range of values can be estimated for the particle thickness. In view of these difficulties of parameter determination, a systematic parametric study is performed with respect to the degree of cementation and particle thickness. The study sheds some light into such important aspects as the apparent overconsolidation and microstructure collapse resulting in large compressibility. It is also shown that upon using a reasonable set of values for these parameters, the numerical compressibility relationship becomes close to laboratory experimental data.

ORIGINAL AND REVISED OBJECTIVES

The original objectives of the study were to model the microstructure of Baltic sea cohesive sediments, including gas bubbles and organic matters (Richardson, 1994), for investigating the relationship between the microscopic variables of the sediments and macroscopic geotechnical properties. Due to time limitations, the influence of gas bubbles could not be considered, but the influence of organic matters has been considered by introducing cementation on the interparticle mechanical force-displacement relations. The geotechnical property investigated is compressibility, and other properties such as wave propagation characteristics will be studied in the future. One of the tasks to be performed was parallelization of the computer code, which has been achieved. However, due to unexpectedly high CPU and clock times, most of the analyzes were performed on a workstation, but a few parallel runs were made to verify the accuracy of small scale runs performed on workstations.

BACKGROUND

Due to the particulate nature, a microscopic approach to constitutive modeling is more desirable for soils than a phenomenological approach, and this is particularly true for soils with a complex microstructure such as a marine cohesive sediment. One such approach is a numerical simulation technique known as the discrete element method (DEM), developed for granular materials by Cundall and Strack (1979). DEM offers the possibility of performing microscopic experiments on a numerical specimen of the desired particulate material, observe the behavior in terms of microscopic and macroscopic quantities, and develop understanding necessary for constructing predictive models. In the past, DEM has been applied mostly to study the behavior of granular materials such as a sand. Anandarajah and his co-workers have pursued this technique for application to cohesive materials such as a clay. The method is applied here to study the compressibility of Baltic sea sediments.

DESCRIPTION OF NUMERICAL TECHNIQUE

In many respects, the discrete element method (Cundall and Strack, 1979) is similar to the classical molecular dynamics, which has for decades been used in physics and physical science. The molecular dynamics is used to numerically simulate the behavior of an assembly of molecules, whereas the discrete element method (DEM) is used to study the behavior of an assembly of discrete bodies.

Basically, DEM allows a load-deformation experiment to be numerically carried out on numerical specimens, just as laboratory experiments are performed on real samples. In a two-dimensional analysis, numerical specimens are formed by placing discrete particles within a confined region, such as, a rectangular box. Each particle must be in equilibrium under the forces acting on it, which typically include the forces between this particle and its neighbors (i.e., interparticle forces), and in some cases, the gravity, electromagnetic and other similar body forces. If the forces or the moment do not sum up to zero, the particle gains an inertia, and is set in motion in accordance with the Newton's law. A suitable time integration scheme can be used to trace its motion until it comes to rest, which occurs when the forces and the moment sum up to zero. Once such an assembly is created, a boundary load, just as the one applied in the laboratory on a triaxial sample, can be applied. This is done by moving the boundaries inward or outward and following the manner in which this disturbance propagates, again with the aid of the Newton's law. Once particles reach a state of static equilibrium, the applied external load is in equilibrium with internal interparticle forces. In contrast to a real experiment, in a numerical experiment, all internal forces and fabric details are available for further examination. The disadvantage, of course, is that a numerical study is performed on ideal particles and assumed internal laws.

Past studies have used DEM to study the behavior of granular materials (e.g., sands), where the interparticle interaction is purely mechanical. Analysis of cohesive soils such as clays requires consideration of, in addition to the mechanical interparticle forces, physico-chemical interparticle forces. Two most important physico-chemical forces are the double-layer repulsive force and the van der Waals attractive force. In some cases, forces such as the solvation forces also are important, which are not considered in the present study. In addition, clay particles are plate like and slender, requiring

consideration of particle bending. During the past several years, fundamental theories and techniques needed to account for these unique aspects in a DEM study has been developed (Anandarajah and Chen, 1994, Anandarajah and Chen, 1995, Anandarajah and Chen, 1997, Chen and Anandarajah, 1996, Anandarajah and Lu, 1991a, Anandarajah and Lu, 1991b).

Some preliminary results were published in Anandarajah (1994), which established the feasibility of applying DEM to analyze cohesive particles. Some aspects of the DEM analysis results have been verified using experimental data; for example, the variation of fabric anisotropy computed from numerical results has been shown to be consistent with that measured in the laboratory using an electrical technique (Anandarajah and Kuganenthira, 1995; Anandarajah et al., 1996; and Kuganenthira et al., 1996). At the start of this project, Anandarajah and his co-workers had a computer code developed for analyzing a two-dimensional assembly of plate-like particles, with consideration to the mechanical and double-layer repulsive interparticle forces. The program did not have capability to consider the van der Waals attractive force in the analysis, although theories had already been developed for this purpose. As part of the current project, these theories have been implemented into the computer code. In addition, the serial computer code had to be parallelized for analyzing a larger number of particles than it was possible in a workstation, and this task has also been successfully completed. In regard to the parallel analysis, however, the CPU and the clock times turned out unexpectedly high and thus most of the analyzes were performed on workstations. However, a few runs were made on a parallel supercomputer, which revealed that the small scale runs made on the workstations are accurate enough to make most of the conclusions reported in this report, although some aspects require larger specimens, and such studies will be conducted in the future.

INPUT PARAMETERS FOR NUMERICAL MODELING

The discrete element method of analysis requires the following compositional parameters: fluid's static dielectric constant ϵ , temperature T , cations' concentration n_0 and valence v , Hamaker constant A , particles' thickness h_p , and electric potential of the negative charge on the clay mineral surface ψ_0 . In addition, the analysis requires the definition of initial fabric; i.e., the manner in which the particles/domains are arranged. As described in the subsequent sections, specific values for the compositional and fabric parameters have been determined for the Eckernförde Bay sediment, and used in the analyses reported here.

COMPOSITIONAL PARAMETERS

The value of water's static dielectric constant is about 80.0. Room temperature of about 20° C may be assumed in simulating a laboratory loading process, as is the intent of the work presented in this report. As per the ionic type and concentration, the sea water is in general dominated by NaCl. Clegg and Whitfield (1995) report that a given seawater has the following composition at 35 ppt salinity; Cations: Na^+ - 0.48525 M, Mg^{2+} - 0.05519 M, Ca^{2+} - 0.01064 M, K^+ - 0.01058 M, Sr^{2+} - 0.00009 M, and Anions: Cl^- - 0.56579 M, SO_4^{2-} - 0.02927 M, Br^- - 0.00087 M, F^- - 0.00006 M, and HCO_3^- - 0.00241 M. The concentration of ions in Baltic sea is considered to be higher than that of a typical seawater reported here. For the purpose of performing numerical analysis, the

seawater may be assumed to consist of 1.0 M NaCl; the influence of other ions on the double-layer repulsive force is considered to be minimal.

In addition to fluid's composition, the numerical analysis requires clay mineral composition. From the TEM images, the mineral type is identified to be predominantly smectite, which on an average has a CEC value of about 100 meq/100g (Grim, 1968, van Olphen, 1963). The theoretical value of the specific surface, S , of smectite is about 800 m²/g. With CEC=100 meq/100g, $S=800$ m²/g, $n_0 = 1.0$ M and $v=1$, the surface potential may be calculated to be approximately 46 mv (Anandarajah, 1997); for convenience, the relevant equations are listed in Appendix I.

The van der Waals attractive force is controlled by a parameter known as the Hamaker constant, which for a smectite-water system is computed to be 0.87×10^{-20} Joules (Anandarajah and Chen, 1997; Chen, 1996).

INTERPARTICLE FORCE-DISPLACEMENT LAWS AND THE PARAMETERS

The first task in DEM analysis is defining the interparticle force-displacement laws. The double-layer repulsive force is computed using the simplified procedure presented in Anandarajah and Chen (1994). The van der Waals attractive force is calculated using the closed-form equations developed in Anandarajah and Chen (1997) for a system of a plate placed next to a wall. Certain approximations have to be made in adopting the procedures presented in the above references to account for the fact that particles are arbitrarily oriented in a many-particle assembly to be analyzed here.

In regard to the mechanical contact laws, linear-elastic, perfectly-plastic, force-displacement laws were used in the preliminary study presented in Anandarajah (1994). These laws are modified here to approximately simulate the effect of cementation on the force-displacement relations. The modification basically involves introduction of bending stiffness, along with normal and shear stiffness, with the force or the moment limited to specified values, representing the “strength of cementation”. Also, in the normal direction, the contact is assumed to be capable carrying a tensile force, depending on the strength of cementation. Once one of the forces (normal force, shear force or moment) reaches its respective limit, the cementation is assumed to be broken, and the contact type reverts to the “regular” type (one that is incapable of carrying moment or tensile force, and whose shear strength is controlled by a simple Coulomb's friction law).

Denoting the maximum values of normal force, shear force and moment of cemented contacts by F_n^p , F_s^p , and M^p , it is assumed that (1) $F_n^p = F_s^p = F^p$, (2) F^p in compression and tension are equal to each other, and (3) $M^p / F^p = 0.01m$ (derived from a plastically-deformed beam subjected to a bending/axial force). When the cementation breaks at a contact, the properties of the contact are changed to that of the “regular” contact.

A particle is in general subjected to all three interparticle force types (repulsive, attractive and mechanical) and the net force controls its behavior. At very small separation distances, the attractive force becomes infinity (Anandarajah and Chen, 1997) and the repulsive force becomes very large (Anandarajah and Chen, 1994), both of which are unrealistic. The mechanical contact force (which represents the integrated effect of Born repulsion) begins to act not when the separation between particles is exactly zero, but at a specific non-zero value of particle separation, which is referred to here as the “cut-off distance”. To make the interparticle net force versus separation relation realistic,

(1) the double-layer repulsive force and the van der Waals attractive force are assumed to remain unchanged for separations less than the cut-off distance, and (2) the mechanical interparticle normal force is assumed to linearly increase with decreasing separation starting from a value of zero at the cut-off distance. A value is (arbitrarily) chosen for the cut-off distance such that for all values of possible particle orientations, the maximum value of the attractive force is about as large as the maximum value of the repulsive force (arbitrarily selected rule).

The various components of the interparticle force-separation distance relations, including the one associated with the net force (which is arithmetic sum of repulsive, attractive and mechanical forces), is shown in Fig. 1 for a system of two parallel clay platelets, each 0.125 μm long. The system variables used in computing the results presented in Fig. 1 are: fluid's static dielectric constant $\epsilon=80$, temperature $T=293^\circ\text{K}$, concentration $n_0=1.0\text{M}$, valence of cations in the fluid $v=1$, Hamaker constant $A=0.87 \times 10^{-20}$ Joules, particle thickness $h_p=0.02 \mu\text{m}$ (to be further discussed below), and surface electric potential of clay mineral $\psi=46\text{mv}$.

Fig. 1b presents the net force-separation distance relations for three different interparticle angles: 0° (parallel), 90° (perpendicular) and 45° . Note that both the repulsive force and the attractive force decrease with increasing interparticle angle. Also note that the interparticle attractive force is larger for the interparticle angle 45° than 90° ; the reader is referred to Anandarajah and Chen (1997) for complete explanation of this.

GENERATION OF INITIAL FABRIC

DEM analysis requires an initial “numerical” specimen. Particles must be arranged in such a way that each particle exists in a state of static equilibrium; i.e., mechanical, repulsive and attractive forces exerted on to the particle by its neighbors must sum up to zero. The only viable method of obtaining such an initial fabric is as follows: (a) Use a suitable method to generate an assembly that is kinematically admissible (particles do not cross each other, particles do not cross the boundaries, etc.), and (b) perform an internal loading until the assembly (implying each particle in the assembly) reaches a static equilibrium state. For further details, the reader is referred to Anandarajah (1994). For the Eckernförde Bay sediments, the fabric details have been extracted from TEM pictures as follows.

Quantification of Fabric from TEM Micrographs

The Eckernförde Bay sediments consist of silt- and clay-sized particles (including some that are pelletized), biogenic materials, methane gas, and other organic materials. The study reported here is limited to the analysis of the part of the sediment that consists only of clay-sized particles and organic materials.

From representative TEM pictures, the microstructure has been found to consist of the following three types of pore spaces: (1) space between (almost) parallel particles within a domain (referred to here as intra-domain void space), and (2) space between domains within an aggregate (referred to here as intra-aggregate void space), and (3) space between aggregates of domains (referred to here as the inter-aggregate void space). As previously noted by Bennett et al. (1996) and Lavoie et al. (1996), onion-skin arrangement of clay particles is prevalent around the large circular inter-aggregate void spaces.

With the assumption that the particles are arranged parallel to each other within each domain, for the purpose of numerical modeling, the following microstructural geometrical parameters are needed: (1) size of domains, (2) number of particles within domains, (3) spacing between particles within a domain (intra-domain pore space), (4) size of individual particles, and (5) size of small and large inter- and intra-aggregate pore spaces. The above parameters are statistical quantities, and are randomly distributed within specific ranges.

From the size of individual particles, the clay mineral types are identified to be predominantly smectite, with a small amount of illite. For simplicity, particle thickness is kept a constant within a given numerical specimen. The theoretical value of a basic smectite unit is about 1.0nm (using a value of 800 m²/g for the specific surface, one computes a value of 0.925nm for the thickness). However, from the TEM images, it has been found that the thickness of individual particles is more than one nano meter, implying that each particle consists of several unit layers.

Stepkowska (1990) shows by computing the specific surface of a Na-bentonite from water sorption at given relative humidity that values of specific surface are in the range $65.8 < S < 395 \text{ m}^2/\text{g}$, corresponding to particles consisting of 12 to 2 unit (1nm thick) layers. For another type of bentonite, the number of unit layers within a particle is reported to be as many as 20, which corresponds to an effective particle thickness of about 20 nm. The analyzes reported here have been performed by varying the particle thickness between 2nm and 20nm.

Image processing techniques are used to develop a statistical distribution of the length (or diameter) and thickness of particle domains. When TEM images are produced from ultra thin sections, black areas in the image represent, for the most part, edges of particles and domains, though some amount of wedge effect is always to be expected. The wedge effect results in black areas that are larger than the area of domain (or particle) edges.

From a representative TEM picture, the domains are first visually identified and hand-sketched. When identifying domains manually, the wedge effect can be to a large extent accounted for, and the hand-sketch used for further analyzes are believed to be free from wedge effects. For the purpose of DEM analysis, it is assumed that statistical distribution of domain size can be developed from the hand-sketch.

First, the hand-sketch is scanned and digitized. With the aid of an image processing software, the length and width of the domains are computed and the results plotted, as shown in Fig. 2. It may be noted that, on an average, the width increases with length. The domain length (l_d) and width (h_d) are in the range $0.01 < l_d < 0.72 \text{ }\mu\text{m}$ and $0.01 < h_d < 0.27 \text{ }\mu\text{m}$.

Table 1: Approximate Representation of Domain Size

No.	Interval				centroid			$A_i = \sum \ell_{ki} h_{ki}$	$n_i = \frac{A_i}{\ell_i h_i}$	% $\frac{100A_i}{\sum A_i}$	$\frac{100n_i}{\sum n_i}$
	ℓ_{min}	ℓ_{max}	h_{min}	h_{max}	ℓ_i	h_i	m_i				
1	0.040	0.196	0.01	0.13	0.118	0.07	22	1.237	16.5	51	18
2	0.196	0.376	0.03	0.15	0.286	0.09	38	0.743	25.6	30	28
3	0.376	0.624	0.08	0.24	0.500	0.37	64	0.413	50.0	18	54

To develop statistics of particle length, individual particles that could be visually identified are hand-sketched. The sketch is then scanned and the grain size distribution shown in Fig. 3 (the dotted line) is developed.

The size distribution data is further categorized as follows: As shown in Fig. 2, three rectangular regions are defined, which, collectively, incorporate almost all of the points in the figure; note that out of a total of 131 points, 7 points are outside these rectangular areas. Representative values of width and length are taken for each of the rectangular regions to be those at the centroid of the areas. An equivalent number of particles with these values of width and length are then calculated as:

$$n_i = \frac{1}{\ell_i h_i} \sum_{k=1}^{k=m_i} \ell_{ki} h_{ki}$$

where n_i is the equivalent number of particles for rectangular area with an average length of ℓ_i and width of h_i , and ℓ_{ki} and h_{ki} are length and width respectively at k th data point for rectangle i . There are m_i points within the i th rectangular area. The results are summarized in Table 1. The percent fraction of types 1, 2 and 3 are calculated both on the basis of the number of particles ($=100n_i/S n_i$) and of the particle area ($=100A_i/S A_i$).

Development of Initial Fabric for DEM Analysis

One of the challenging tasks in the present work is to create a fabric that resembles that of the Eckernförde Bay sediments, as per the parameters reported in the preceding section (Table 1); i.e., one involving domains with individual particles arranged parallel to each other, large inter-domain void spaces, and aggregates of domains. This is achieved here as follows. Within a rectangular box confined within four walls, a number of “blocks”, rectangular in shape and capped with semi-circles at the ends, are placed at random locations and at random orientations. The blocks have variable values of thickness and length. Using the same DEM computer program, but using only the mechanical interparticle forces, the assembly is densified by moving all four of the walls inward (i.e., isotropic compression), until forces just begin to develop on the walls. The assembly at this stage is shown in Fig. 4.

The blocks are to represent domains of clay particles and the large inter-domain void space, and an attempt is made to preserve the domain size distribution reported in Table 1. The eight thickest blocks seen in Fig. 3 are to represent the large inter-domain pore spaces. The thickest blocks are removed and the remaining blocks are filled with individual particles in a certain manner. The assembly using particles of thickness 20nm is shown in Fig. 5.

Each particle is divided into a number of discrete elements of a constant length, 0.125 μm . The longest particle in the assembly is made up of 4 discrete elements, and thus has a length of 0.5 μm . The face-to-face spacing between particles is 0.006 μm . To make the assembly even more realistic, void space is introduced between particles in the length direction as well.

The size and number of blocks in Fig. 1 has to be chosen to satisfy the geometrical constraints (grain size distribution, domain statistics, particle thickness, interparticle spacing within domains, etc.) in an optimal sense. In addition, a limit (700) has to be

placed on the total number of discrete elements to use in the analysis in order to fit the problem in the memory of a workstation that is used for most of the runs reported here. To verify whether the limit of 700 on the number of discrete element adversely affected the results, one of the problems is repeated using 1257 elements in a parallel supercomputer T3E and it is found that the results are reasonably close; the results will be presented later in this report.

The grain size distribution associated with the assembly (the solid line) is compared with the intended one (the dotted line) in Fig. 3. When the total number of elements is limited to 700, it is not possible to match the curves exactly, however, the difference is not substantial.

The initial void ratio of the assembly in Fig. 2 is computed as follows: Total volume of specimen, $V = 2.18 \times 2.18 \text{ m}^2 = 4.7524 \text{ m}^2$, volume of solids, $V_s = 700 \times 0.125 \times 0.02 \text{ m}^2 = 1.75 \text{ m}^2$, and thus the void ratio, $e = V/V_s - 1 = 1.71$.

While the assembly of blocks shown in Fig. 4 is in a state of static equilibrium, the one shown in Fig. 5 is not, and an internal loading needs to be applied in order to obtain one that is in equilibrium.

DETAILS OF ONE-DIMENSIONAL COMPRESSION ANALYSIS

The Eckernförde Bay sediment is found to have a high percentage of organic materials (on an average, about 12%). In addition, there are other forms of biogenic materials at domain-to-domain and particle-to-particle contacts. It is suspected that these organic materials must provide some stability to the in situ fabric, which exists at an unusually high void ratio ($e=4$ to $7!$). To simulate the associated mechanics, it is assumed here that the increased stability provided by the organics may be simulated by introducing a certain degree of interparticle cementation. There is no definite way of quantifying the strength of the cementation; it is, however, estimated to be small.

To develop an understanding of the role of cementation on the stability of the microstructure shown in Fig. 5, 4 different runs are made, one without any interparticle cementation, and the other three with different degrees of cementation strength F^p : $1.0 \times 10^7 \text{ N}$, $5.0 \times 10^7 \text{ N}$, and $100.0 \times 10^7 \text{ N}$. The ratio M^p/F^p is kept the same at $0.01 \mu\text{m}$ in all three runs. This particular parametric study is performed on the assembly shown in Fig. 5, which consists of $0.02 \mu\text{m}$ thick particles.

Contacts are designated to be cemented as follows: At the beginning and before applying any forms of loading, all contacts where the distance between a free node and a discrete element (center-to-center) is less than $1.5 \times h_p$ are cemented (i.e., a cemented contact type is assigned). The assembly is then subjected to an internal loading, which involves turning on internal physico-chemical forces, and allowing particles to move around (as dictated by the Newton's law) to reach a state of static equilibrium. During this internal loading phase, new contacts formed are also designated to be cemented contacts. At this stage, the assembly should be in a state of static equilibrium and all of the existing interparticle contacts are to be cemented types. The particle-to-wall contacts are, however, always assumed to be non-cemented.

In the run with no cementation, the same initial internal loading process is followed, with the following differences: (a) initial and new contacts are formed when the distance between a free node and a discrete element is less than $1.0 \times h_p$ (instead of $1.5 \times h_p$) to

allow for the fact that there is no “cementation material” between particles, and (b) all contacts, interparticle and particle-to-wall, are assumed to be of the non-cemented types.

While both in cemented as well as in non-cemented assemblies, the initial internal loading will lead to certain amount of collapse of the initial microstructure shown in Fig. 5; a greater collapse takes place within the non-cemented assembly than within cemented assemblies.

The assemblies are then loaded under one-dimensional condition, by moving the two horizontal walls inward (so as to apply a compression) at equal loading rates. The initial assembly, which has a void ratio of 1.71, may not yet be dense enough to resist the wall movements and to build up forces on them (exerted by the particles). In fact, in the case of the assembly with no cementation, the void ratio has to be decreased to 1.47 before forces develop between the walls and the particles; the assembly at this stage is shown for this case in Fig. 6.

During the one-dimensional compression loading, when a cemented contact breaks, it is set back to a non-cemented contact type, and no new cemented contacts are created. This is due to the fact that the intent of the loading is to simulate a laboratory loading process and no cementation forms during a laboratory loading process; it is only broken.

It may be seen from Fig. 6 that some of the domains have experienced certain level of collapse. The collapse is smaller (not shown) for assemblies with greater degree of cementation.

The one-dimensional loading is continued until the vertical stress increases to sufficiently high values. Presented in Fig. 7 is relationship between the void ratio e and the vertical stress σ_v , with σ_v computed as the average between the stresses on the bottom and top horizontal walls. Results from the four runs are shown together in Fig. 7.

It is to be noted that the results are numerical, and the accuracy of computed quantities (e.g., wall stress) will depend on how close to static equilibrium the specimen is, which in turn will depend on the number of “free vibration” analysis steps that have been performed; free vibration analysis with a suitable damping dissipates inertial energy. There is another consideration that influences the accuracy: computer time. The analysis is very computer CPU intensive; each of the four runs presented in Fig. 7 takes on an average about 4 days of CPU time. Several trial runs also had to be made before making a few final runs. To control the computer CPU time, the number of free vibration steps had to be limited. When the specimen is judged to have reached a state close to a static equilibrium, the next loading is continued.

The following observation provides an indication of the accuracy of results presented here: the stress on one of the horizontal walls is computed to be within 2% of that on the second horizontal wall (They are to be equal to each other.) at higher stress values (> 20 kPa), and within 10% at lower stress values.

The points marked by “stars” in Fig. 7 are from the analysis performed in a parallel supercomputer using 1257 elements. The results are to be compared with those from the run performed on the workstation involving 700 elements and moderately-cemented interparticle contacts ($F^p = 1.0 \times 10^{-7}$ N); The details are almost the same in these runs except for the number of discrete elements. It is seen that the results from the two analyzes are reasonable close.

DISCUSSION OF RESULTS

Strain-Softening Like Numerical Behavior

A number of observations of fundamental significance may be made from the results. The e versus σ_v curves presented in Fig. 7 may be seen to be somewhat irregular, with strain-softening like hooks on some of them; e.g., points A, B and C. These hooks are due to sudden loss of stiffness. The ones at points B and C are found to be due to sudden loss of cemented load-carrying columns, and the one at point A due to collapse of unstable microstructure (the unique microstructure with large, circular-shaped inter-domain void spaces). Such hooks are almost never reported in the literature on one-dimensional compression behavior of clays. The discrepancy seen here is suspected to be due to one or more of the following reasons: (a) Most laboratory consolidation tests are performed in a load-controlled mode, which is incapable of capturing softening behavior, whereas the numerical loading reported here has been performed in a displacement-controlled mode, and (b) the numerical specimen used in the present study does not have sufficient number of particles to “smooth” out the softening resulting from collapse of some of the load-carrying particle columns. The results from the parallel analysis appear to support the second possible reason, however, a detailed study is deemed necessary before reaching conclusions on this.

Apparent Overconsolidation

As a result of the numerical convergence problems discussed earlier, the results are somewhat crude at very low stress levels, especially, when σ_v is less than about 0.5 kPa. By examining the results for $\sigma_v > 0.5$ kPa in Fig. 7, it is evident that the specimens behave like “overconsolidated” specimens. This is clearly established for all three of the cemented specimens, and further runs (with the walls moved very slowly and with the accelerations in the specimen controlled to be smaller), are required to establish this with certainty for the non-cemented specimen, though there is indication that the trend shown in Fig. 7 is representative.

In view of the fact that all of the numerical specimens are normally consolidated, the apparent overconsolidation seen in Fig. 7a for cemented specimens can only be attributed to the cementation. As the strength of cementation F^p increases, the apparent overconsolidation ratio increases.

The laboratory tests conducted by Ag (Ag, 1994; Silva et al., 1996; Brandes et al., 1996) show overconsolidation, some mild and others strong, and it was described as “apparent overconsolidation”. Results obtained on two of the Eckernförde Bay samples (Nos. 035-BS-BC and 029-BS-BC), one from a depth of 26cm and the other from 377cm, are re-plotted from Ag (1994) in Fig. 8. The one from 26cm depth has a preconsolidation pressure, overconsolidation ratio and compression index of $\sigma_c = 4.1$ kPa, OCR=6.7, and $C_c = 4.1$ respectively, and the respective values for the sample from 277cm depth are $\sigma_c = 11.1$ kPa, OCR=1.7, and $C_c = 4.3$ respectively. Note the unusually high compression index values of these samples. Soils without active minerals have a compression index of around 1.0. For example, Silva and Jordan (1984) report that illite-rich clays found in the North Central Pacific have C_c values less than 1.1, whereas clays with significant smectite contents, which are apparently found at the same location below 5m depth, have C_c values between 1.5 and 3.0.

Silva and Jordan (1984) states that the “apparent overconsolidation” has been observed at many locations around the world. The hypothesis presented in the past as to the cause of this “apparent overconsolidation” is that it is caused by interparticle bonds due to physico-chemical means, and interparticle cementation. These are all certainly possible causes, and the study presented here supports the second cause (cementation) with certainty and suggests that even the first one (that highly porous microstructure where the particle/domains are held together by physico-chemical interparticle forces, especially, the attractive force) is plausible. According to Silva et al. (1996), for the Eckernförde Bay sediments of interest here, the stress state approaches a normally consolidated condition below a depth of 2.5 meters, at which depth the vertical stress is little under 5 kPa. This implies that the cementation or the interparticle physico-chemical force that is responsible for the apparent overconsolidation must be a weak one since its effect seems to be erased at such a small stress as 5 kPa. It may be noted from Fig. 7 that the curves associated with moderate cementation and no cementation do show a tendency to merge with each other after a certain vertical stress.

Degradation of Cementation/Collapse of Microstructure

The next observation made here has to do with the manner in which the interparticle contacts evolve during the consolidation, with special focus on cementation degradation and collapse of microstructure. As the loading progresses, the following events take place: cementation disintegrates, microstructure collapses, number of non-cemented contacts increases, and in the cases with low degree of cementation, the domains themselves collapse.

The rate at which the cementation disintegrates with increasing stress decreases with increasing strength of cementation; note from Fig. 7b that N_{cem}^{pp} decreases faster with stress for specimens with smaller cementation strength. As the cementation breaks, the cemented contacts revert to normal contacts, and N_{reg}^{pp} increases (Fig. 7c).

For the case with no cementation ($F^p = 0$ N), Fig. 6 presents the assembly at an early stage (i.e., the stage where the vertical stress begins to develop) and Fig. 9 at an intermediate stage during the loading (i.e., when $e = 0.727$, $\sigma_v = 46$ kPa). By comparing the assemblies shown in Fig. 6 and 9, it is evident that one-dimensional compression causes significant collapse of the initial microstructure.

The assembly for the case with high cementation ($F^p = 5.0 \times 10^{-7}$ N) is shown at an intermediate stage $e=0.926$, $\sigma_v = 951$ kPa) in Fig. 10. The assembly for this case at $e = 1.47$ is very close to that for the case of no cementation (Fig. 6). The collapse is found to be equally intense regardless of the degree of cementation for the four cases considered.

To examine this point further, the highly-cemented specimen ($F^p = 5.0 \times 10^{-7}$ N) is further analyzed at its final void ratio considered ($e=0.926$). Defining a force cut-off line at mid-way between the average and maximum forces ($F=0.5 (F_{ave} + F_{max})$), the locations of cemented and non-cemented contacts for above and below this cut-off line are marked in Fig. 11, along with the centroidal axes of particles. First, while most contacts are still cemented (compare Figs. 11a and 11c with 11b and 11d), most of the cemented-contacts are intra-domain (Fig. 11d) and carry very little load (note that there are no points marked in Fig. 11b). The contacts that carry high level of forces are non-cemented and inter-domain (Fig. 11a). That is, the intensity of forces at the inter-domain contacts are high, leading to early degradation of cementation at these locations, whereas the intensity

is low at intra-domain contacts, which help preserve the integrity of domains until the consolidation pressure reaches high values.

While the microstructure collapse appears to be about the same regardless of the degree of cementation, there is one significant difference between the deformations; compare Fig. 9 with Fig. 10. Comparing the domains that are still intact in Fig. 9 (and there are several such domains) with those in Fig. 10, it is seen that in Fig. 9 (a) the particles within domains are closer to each other, with domains becoming denser and (b) the inter-domain pore space is larger. Additionally, note that the shape of domains in Fig. 9 is different from that in Fig. 10; the particles in Fig. 9 have experienced significant sliding along the length direction (like a “pack of cards”), whereas this sliding is small in Fig. 10; i.e., the original shape and size of most of the domains seen in Fig. 5 are still preserved in Fig. 10.

The explanation of the observed behavior requires consideration of the net interparticle force shown in Fig. 1. When two parallel particles fall within the attractive valley seen in Fig. 1, they get “locked” up and it is not easy to pull them apart from each other; a force of about 2.0×10^{-7} N needs to be applied in the direction normal to particles to separate them from each other. In this sense, the van der Waals attraction acts like “cementation” of strength 2.0×10^{-7} N. However, the attractive force acts only in the direction normal to the particles, and offers no resistance in the length direction. The mechanical normal force is almost zero when the particles are in the valley, and thus the shear resistance, which is proportional to the mechanical normal force, is also very nearly zero, leading to the type of domain distortion seen in Fig. 9.

Effect of Particle Thickness

Thinner particles in general lead to larger void ratios, and a detailed discussion on this may be found in Anandarajah (1997). Consider, for example, the model used by Bolt (1956) to represent the soil in a one-dimensional compression cylinder in his one-dimensional theory of consolidation. In Bolt's model, the particles are assumed to be parallel to each other with their faces perpendicular to the direction of consolidation, and an applied vertical consolidation stress is assumed to be supported purely by the double-layer repulsive forces between these parallel particles. The void ratio of such an assembly is given by s/h_p , where s is the face-to-face spacing and h_p is the particle thickness. Comparing two systems where the only difference between the two is particle thickness (repulsive force is the same for the same face-to-face particle spacing), the void ratio of a system with $h_p = 0.01 \mu\text{m}$ is twice as large as that with $h_p = 0.02 \mu\text{m}$ at the same externally-applied vertical pressure.

The model of the soil described above, of course, is an unrealistic one: In a real soil, particularly in Eckernförde Bay sediments, particles are not parallel to each other, and, in addition to interparticle double-layer repulsive forces, there are interparticle attractive and mechanical forces; these factors are considered in a DEM analysis. (Another approximate analysis method which considers the above factors may be found in Anandarajah, 1997.)

Two additional analyses are performed, one using $0.01 \mu\text{m}$ thick particles and another using $0.002 \mu\text{m}$ thick particles. In both analyses, the contacts have been assumed to be moderately-cemented specimen ($F^p = 1.0 \times 10^{-7}$ N). It has been found that the numerical void ratio at a given vertical stress increases with decreasing particle thickness.

The e versus σ_v relations computed from the DEM results for the case with $h_p = 0.002 \mu\text{m}$ is shown in Fig. 12. Also superimposed in the figure are the experimental data presented in Fig. 8 (Ag, 1994; Silva et al., 1996; Brandes, et al., 1996).

It may be observed that the DEM results are very close to the experimental results. Note that there is significant irregularity in the numerical e versus σ_v curve, indicating that a larger number of particles must be used in the DEM analysis in this case. However, the qualitative conclusion derived from the analysis (that smaller particle thickness leads to larger void ratio values) is expected to hold even in analysis using larger number of particles.

Three-Dimensional Effects

A three-dimensional numerical specimen will definitely behave differently from a comparable (in terms of compositional variables and some aspects of the fabric variables) two-dimensional specimen. While such a discrepancy is likely to be caused by a number of inter-woven, complex factors, the following two elements are considered to be significantly more important than others. At comparable average interparticle spacing, (1) due to geometric constraints, a three-dimensional assembly is likely to have a larger void ratio than a two-dimensional assembly, and (2) due to three-dimensional orientation of particles, the external force that can be carried by a three-dimensional assembly (i.e., one that will be in a state of static equilibrium with the internal physico-chemical and mechanical forces) will be different from that which can be carried by a two-dimensional assembly. (It is not clear whether it will be smaller or larger at this point.)

Only way of examining the second cause is to develop a three-dimensional DEM code and use it to perform the analyses; this is deferred to a future study. To examine the first cause in an approximate manner, a computer code is written that can generate a three-dimensional assembly purely on the basis of kinematic constraints. The domains are assumed to be of the shape of a disk. Using the same domain size distribution and a box size ($3 \times 3 \mu\text{m}$ for the 2D assembly, and $3 \times 3 \times 3 \mu\text{m}$ for the 3D assembly), two-dimensional and three-dimensional programs are used to obtain the densest possible assemblies. The thickest particles, as explained earlier, are to be removed to simulate the large, circular (or spherical, in the case of three-dimensional assembly) inter-domain void spaces. Accounting for all of these, the void ratio of the two-dimensional assembly (e_{2D}) and three-dimensional (e_{3D}) assemblies are computed to be 3.196 and 5.4 respectively. This indicates that on this basis alone, void ratios of three-dimensional assemblies could be as high as $5.4/3.196=1.7$ times those of two-dimensional assemblies.

ACCOMPLISHMENTS

To the authors' knowledge, this is the first time the behavior of a marine sediment involving clay minerals has been numerically simulated from a microscopic viewpoint. While a number of difficulties have become apparent, which would provide directions for further research, a fair amount of fundamental understanding has been developed, and the feasibility of conducting microscopic studies of the kind addressed in the research has been established. The researchers involved are now confident that microscopic data gathered by image processing of micrographs, along with other relevant compositional parameters, can indeed be used to construct a numerical specimen to approximately

represent a real specimen. It is believed that this line of research would lead to physically-based theories, and more reliable in situ methodologies.

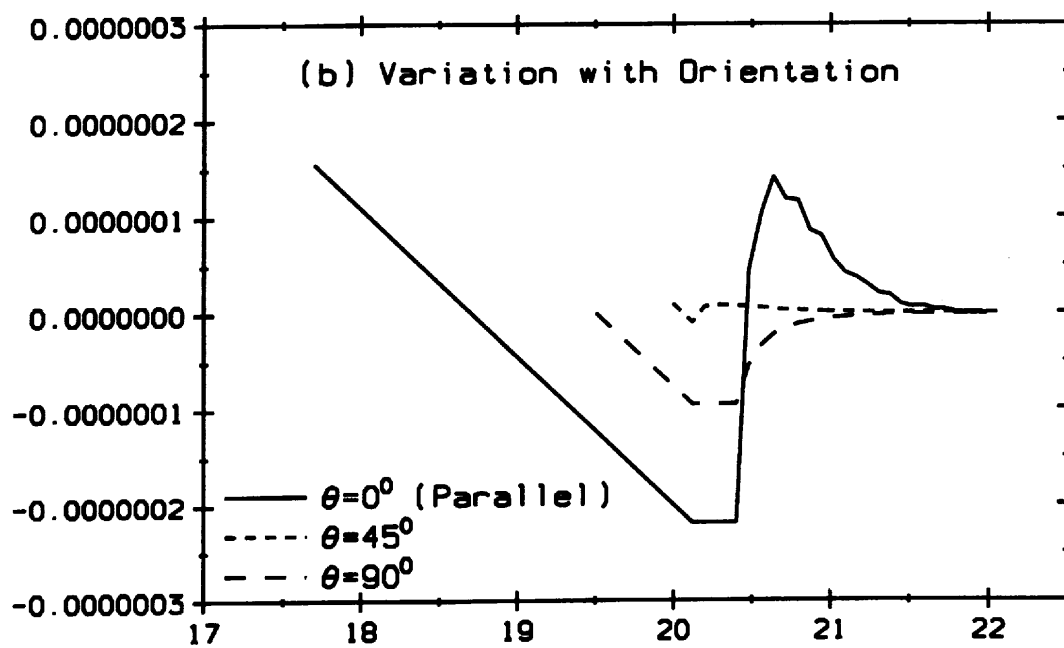
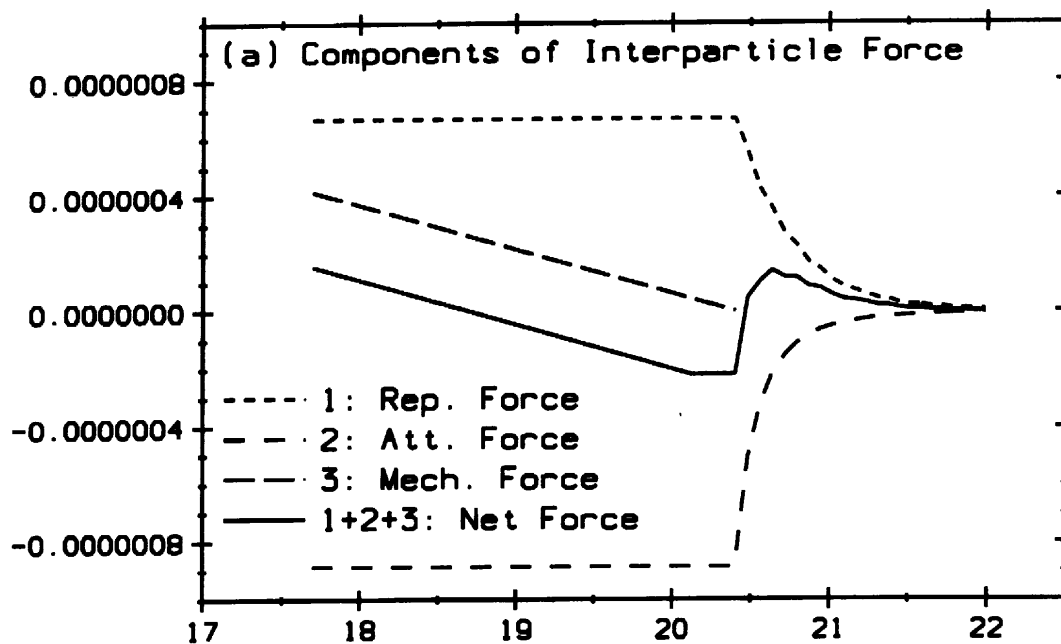


Fig. 1. Interparticle Physico-Chemical, Mechanical and Net Forces.

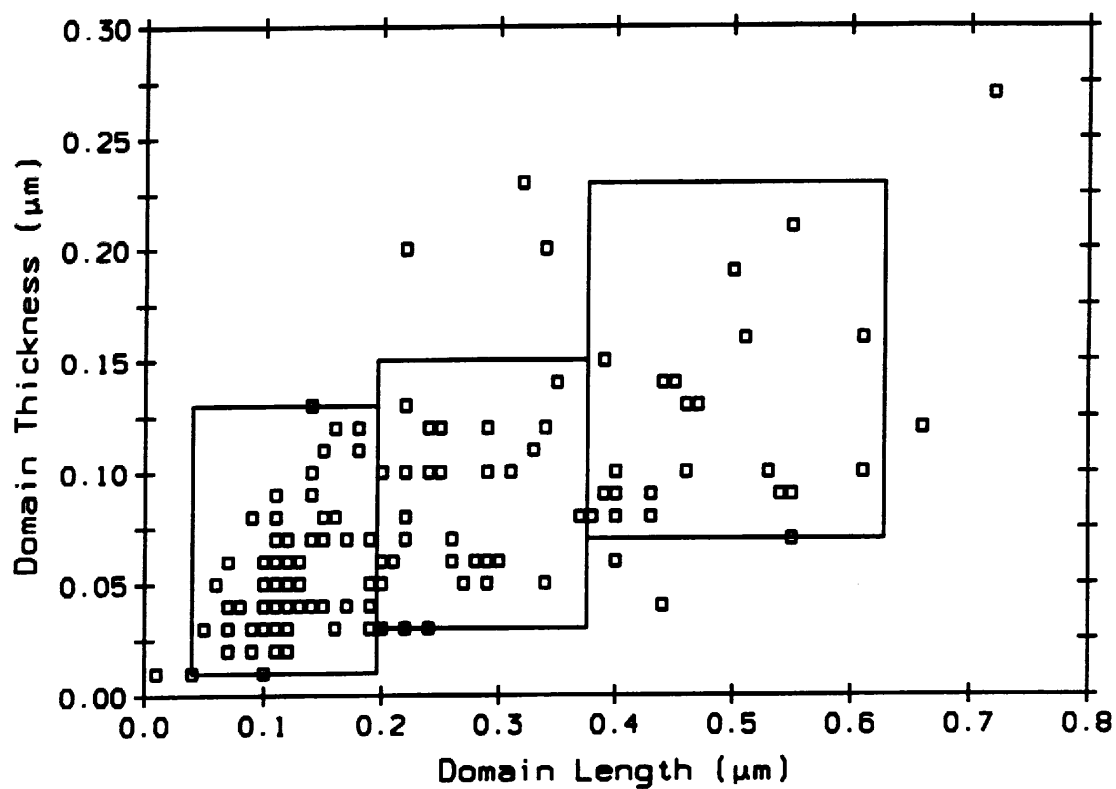


Fig. 2. Domain Size Distribution Determined by Image Processing of Domains Hand-Sketched from TEM Micrograph, and Partitioning of Domain Size Data.

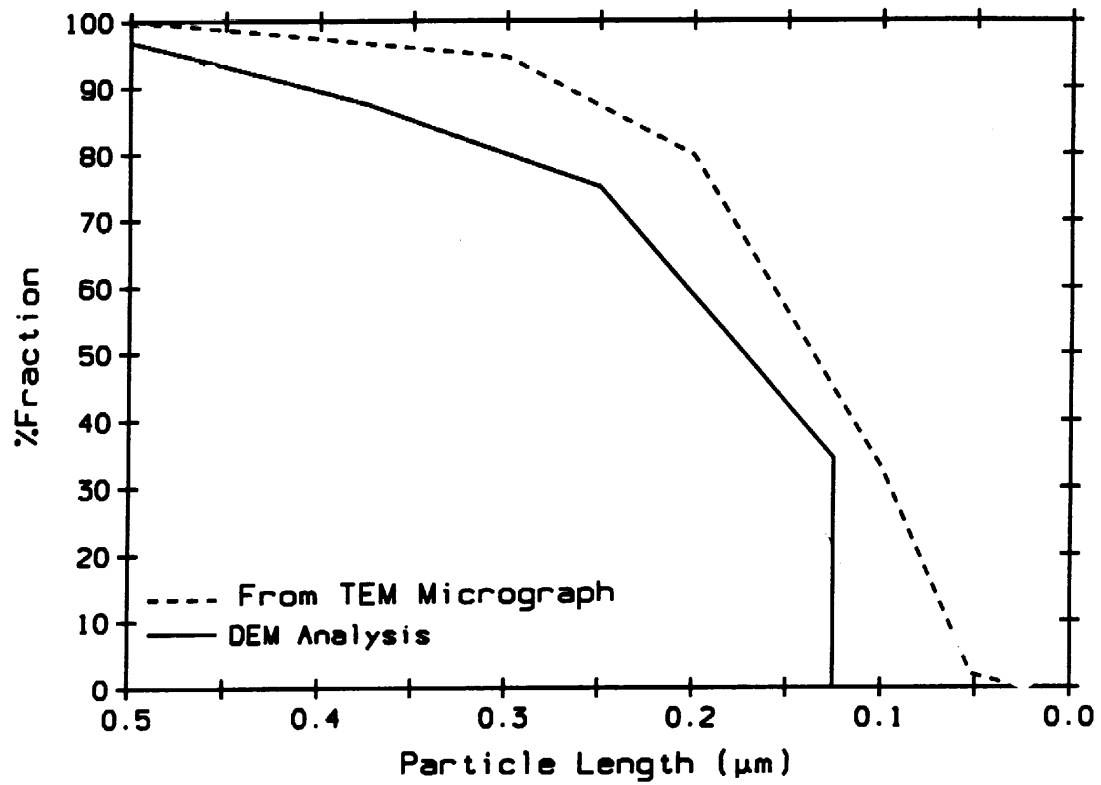


Fig. 3. Comparison of Grain Size Distribution Used in DEM Analysis with that Determined from TEM Micrograph.

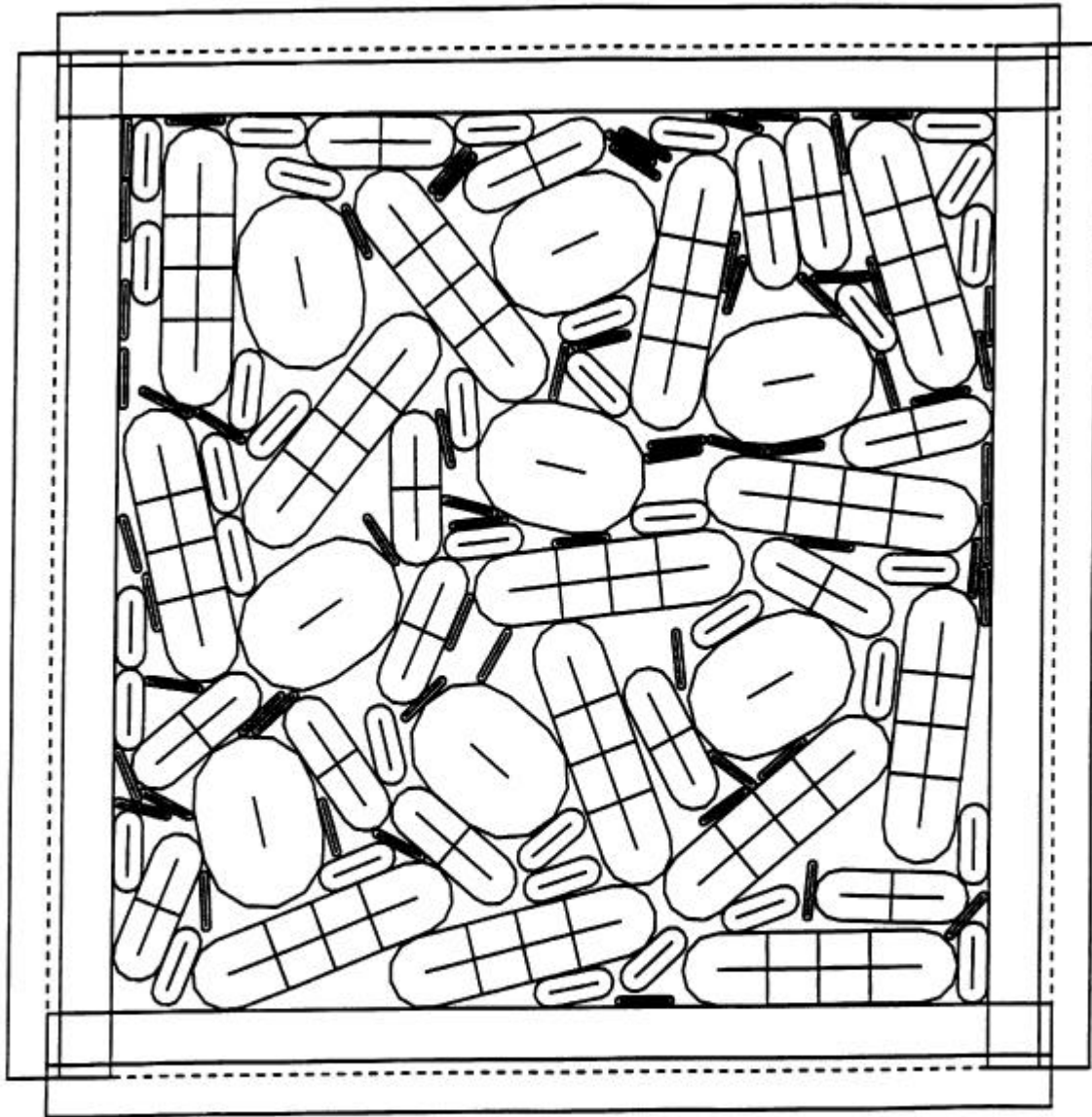


Fig. 4. Densified Assembly of Blocks to be Used to Generate Initial Fabric for DEM Analysis.

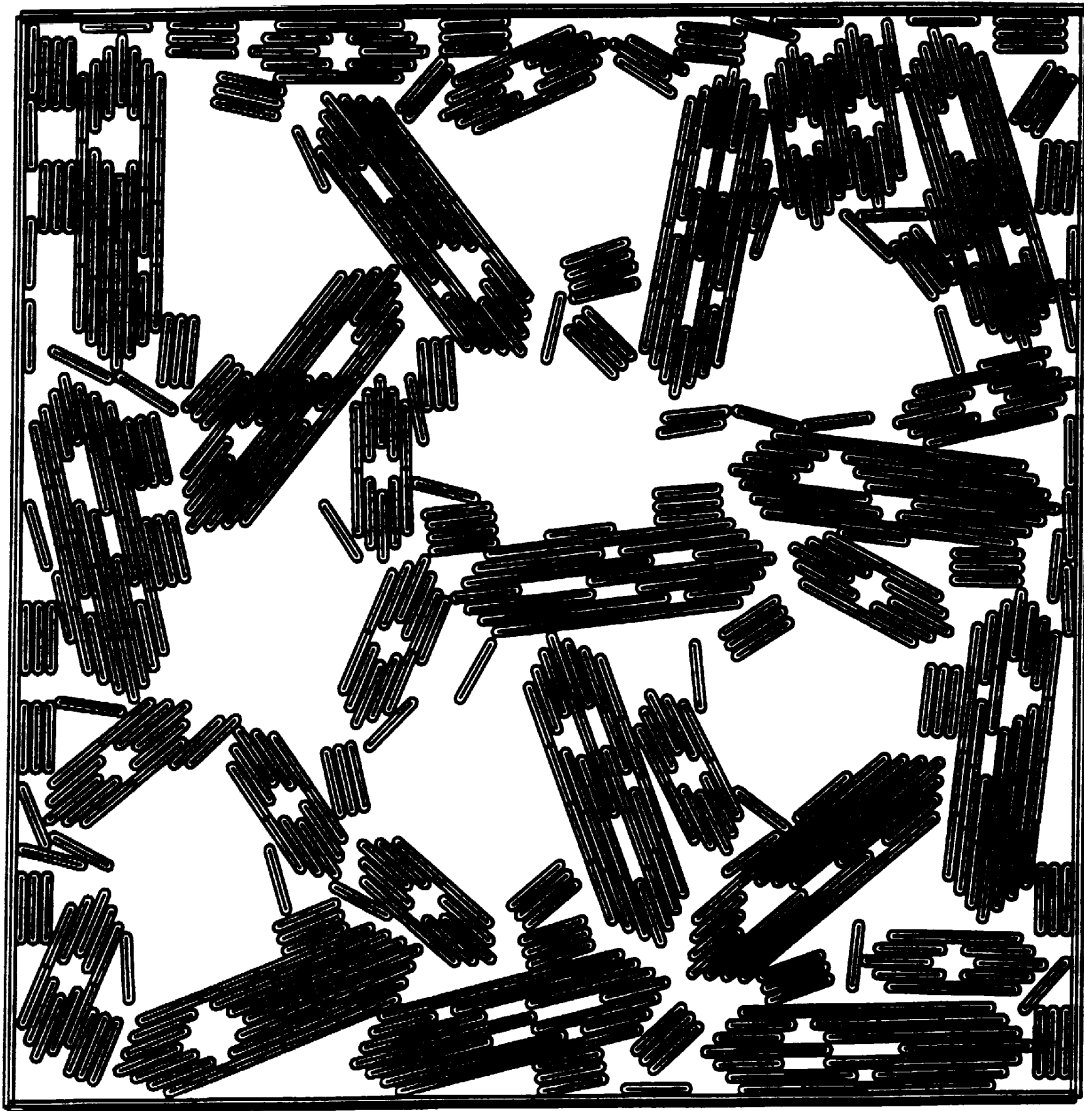


Fig. 5. Initial Fabric for DEM Analysis Consisting of 0.02 μm Thick Particles.

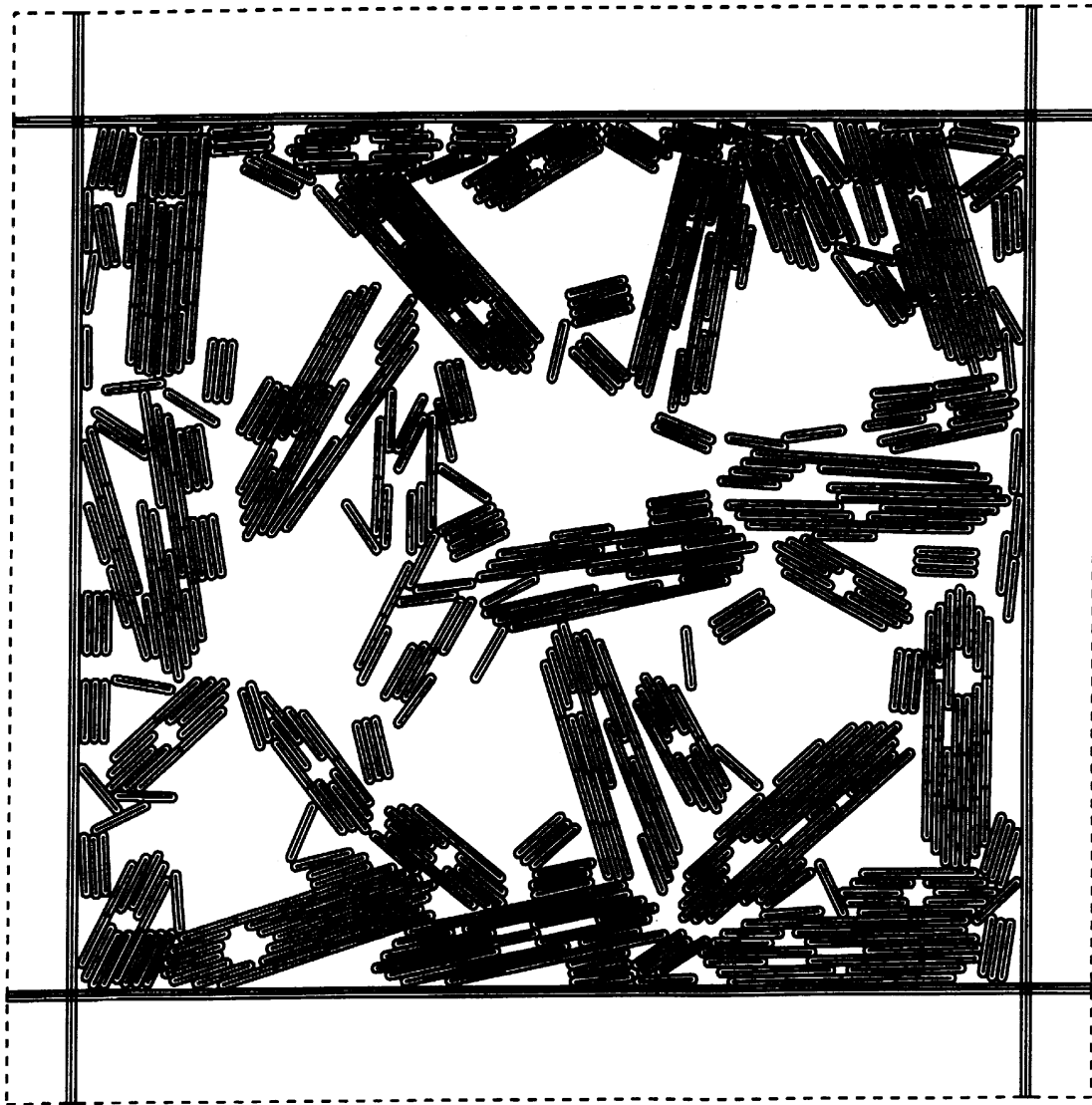


Fig. 6. Assembly with No Cementation ($F^p=0$) at $e=1.47$.
 $\sigma_v=0.001$ kPa, $h_p=0.02$ μm , Number of Elements = 700.

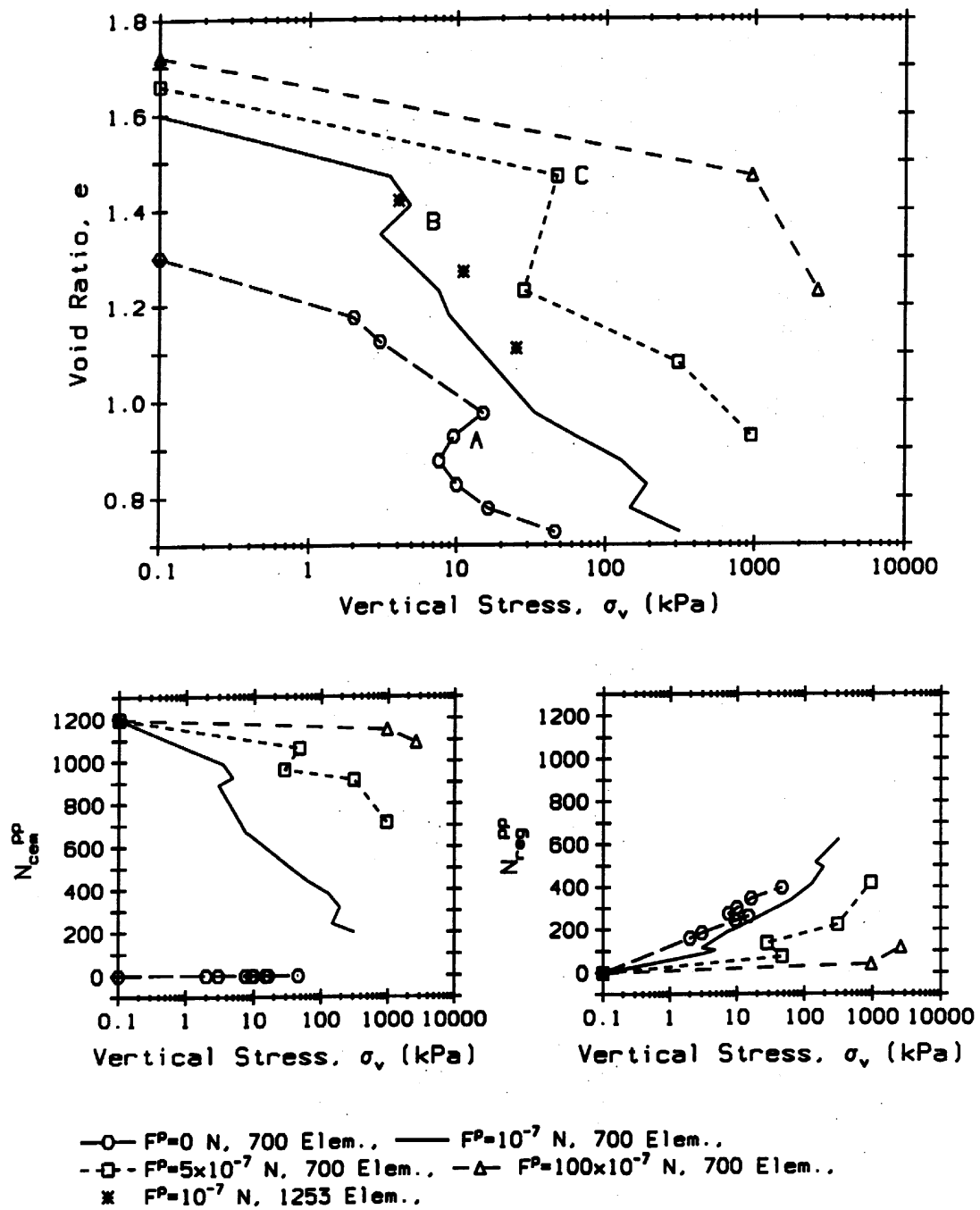


Fig. 7. One-Dimensional Behavior of Numerical Specimens of 0.02 μm Thick Particles for Different Degree of Cementation.

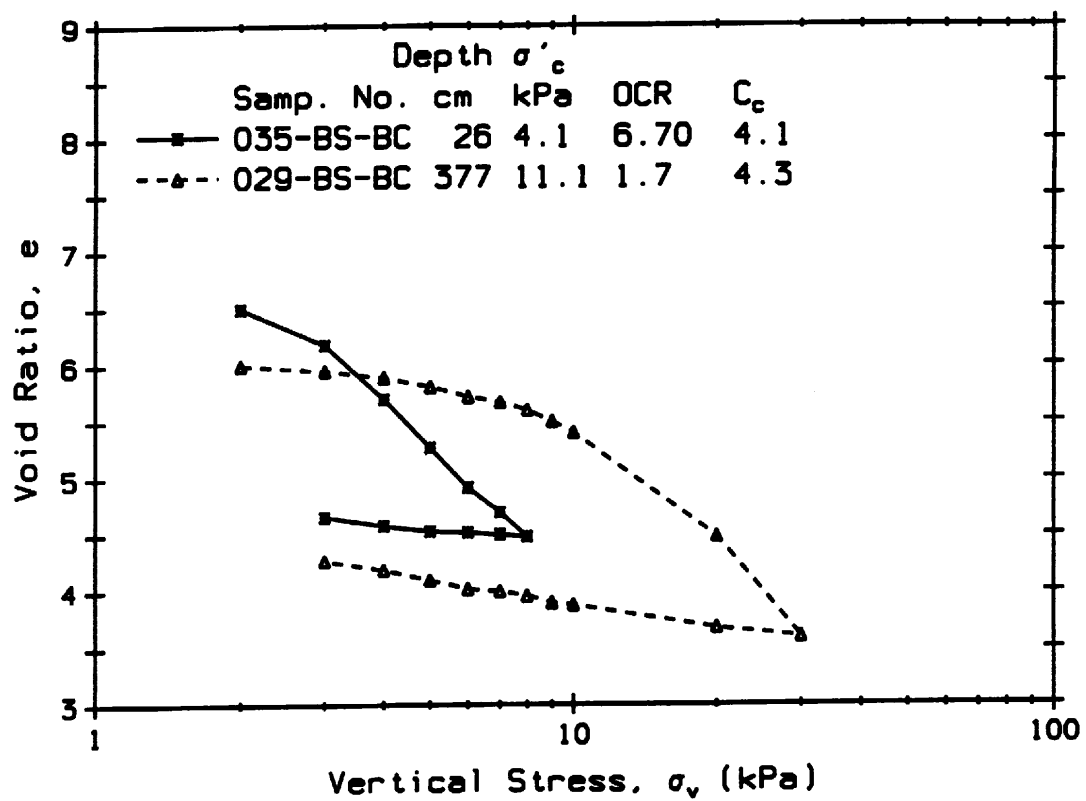


Fig. 8. One-Dimensional Compression Behavior of Eckernförde Bay Sediments Determined in the Laboratory by Silva et al., 1996; Ag, 1994.

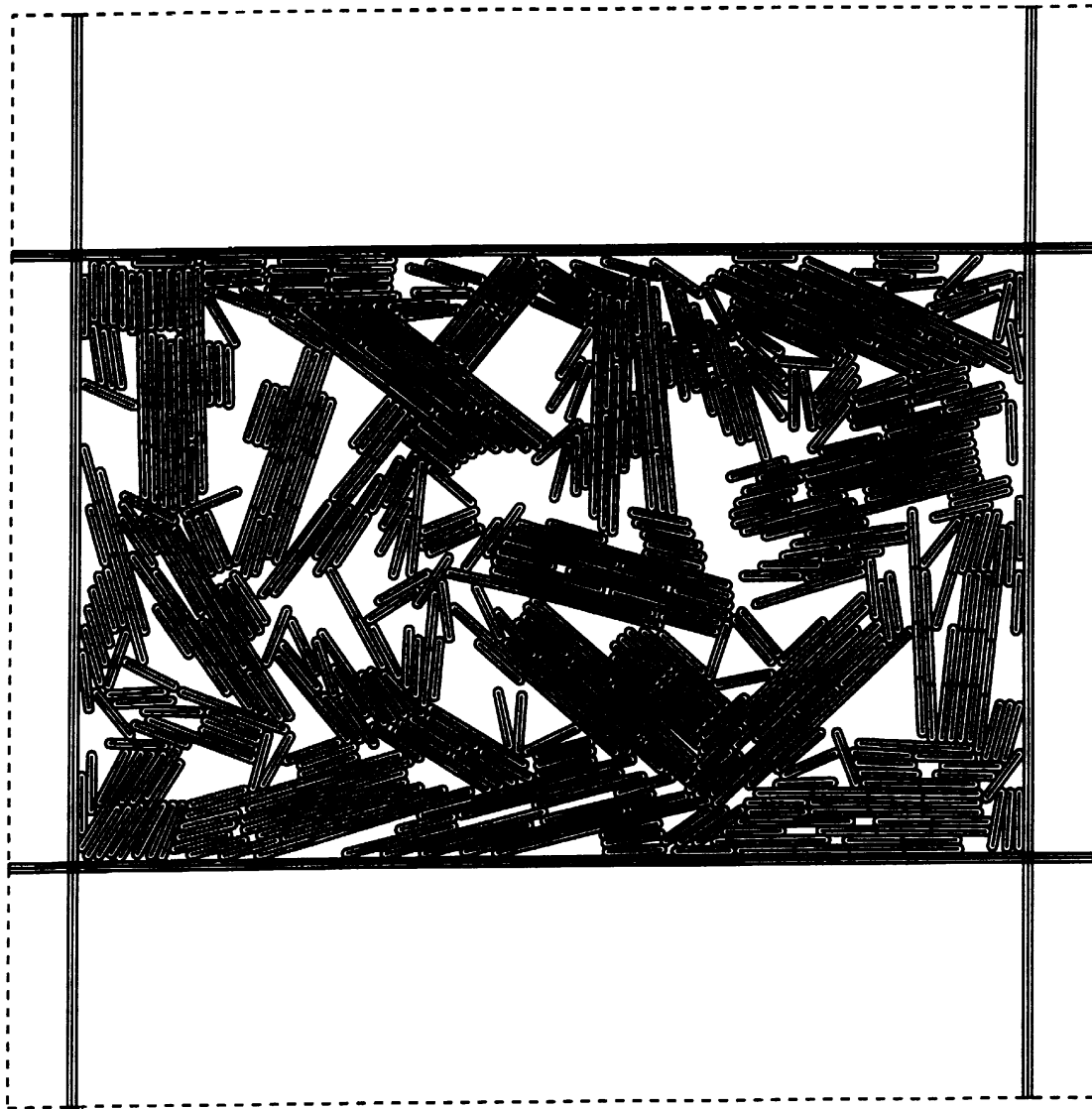


Fig. 9. Assembly with No Cementation ($F^p=0$) at $e=0.727$.
 $\sigma_v=46$ kPa, $h_p=0.02$ μm , Number of Elements = 700.

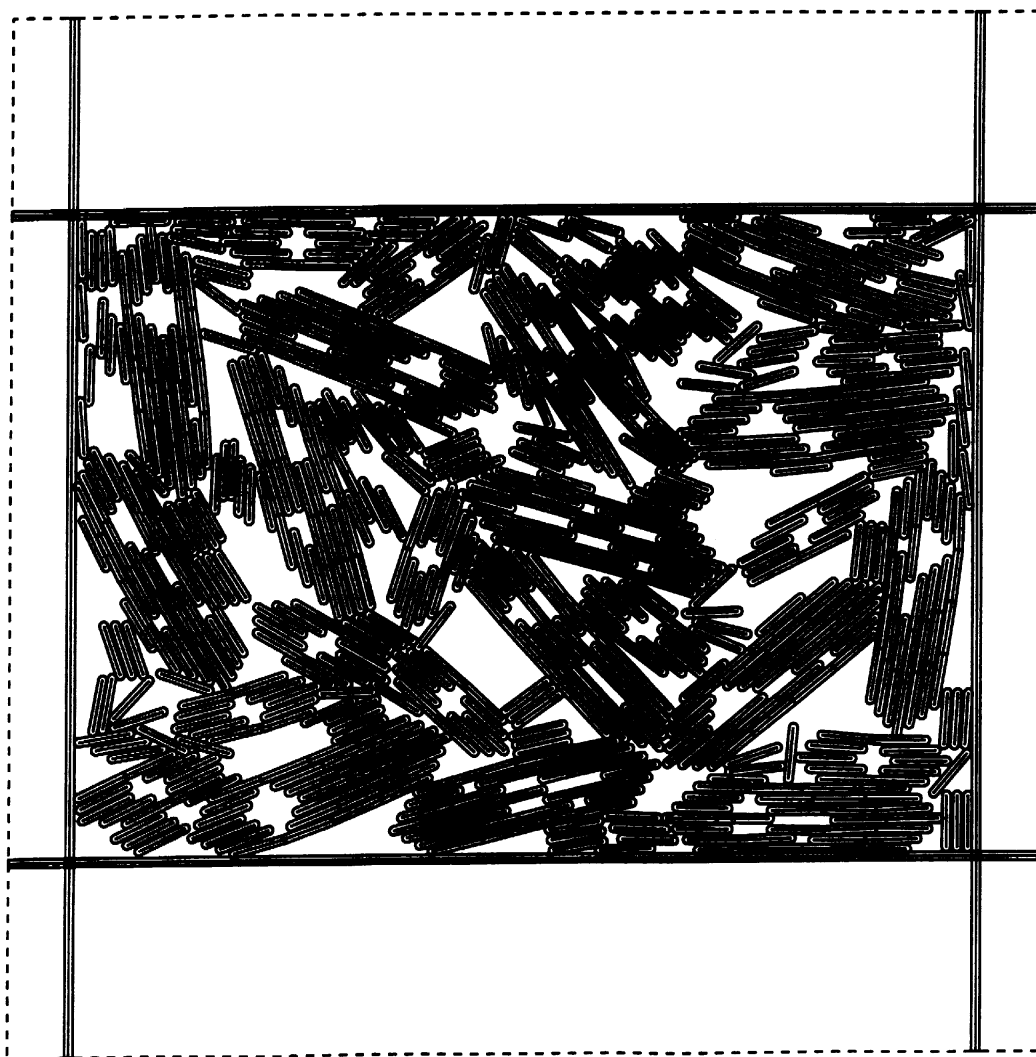
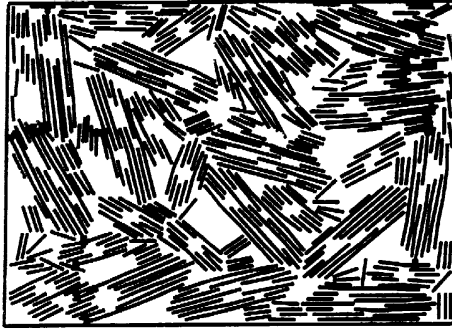
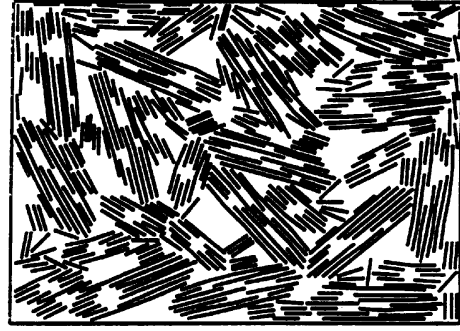


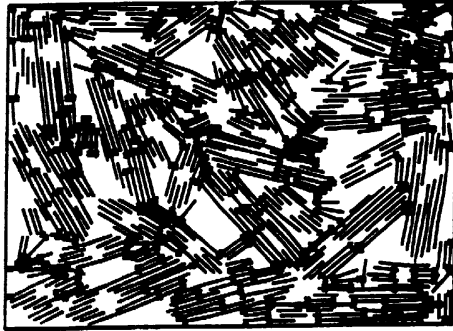
Fig. 10. Assembly with High Cementation ($F^p=5 \times 10^{-7} \text{N}$) at $e=0.926$
 $\sigma_v=951 \text{ kPa}$, $h_p=0.02 \text{ }\mu\text{m}$, Number of Elements = 700.



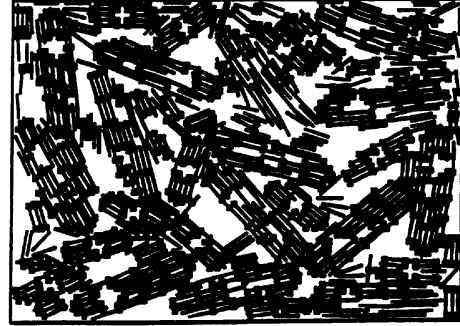
(a) Regular Contacts
 $F > 0.5(F_{\max} + F_{\text{ave}})$



(b) Cemented Contacts
 $F > 0.5(F_{\max} + F_{\text{ave}})$



(c) Regular Contacts
 $F < 0.5(F_{\max} + F_{\text{ave}})$



(d) Cemented Contacts
 $F < 0.5(F_{\max} + F_{\text{ave}})$

Fig. 11. Evolution of Interparticle Contacts During One-Dimens Compression for High Cementation ($F^p = 5 \times 10^{-7} \text{N}$) at $e = 0.926$.
 $\sigma_v = 951 \text{ kPa}$, $h_p = 0.02 \mu\text{m}$, Number of Elements = 700.

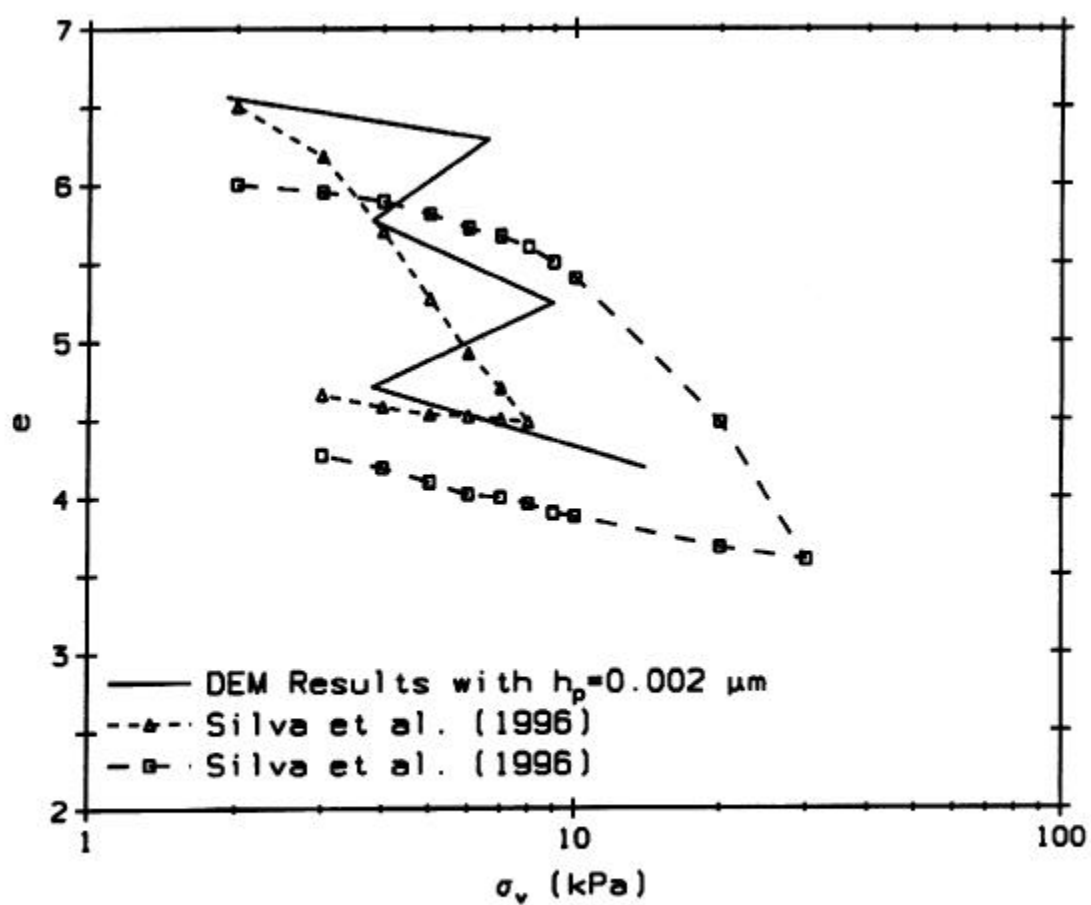


Fig. 12. Comparison of Experimental Results with DEM Results for $h_p = 0.002 \mu\text{m}$.

Publications Resulting from the Study Symposium Proceedings

1. Anandarajah A, and Yao M (1997) Parallel algorithm for the discrete element analysis of clays. Proc. Sym. Mech. of. Granular. Materials, Joint ASCE/ASME Summer meeting, Northwestern University, June 29-July 2.
2. Anandarajah A, and Yao M (1997) Discrete element analysis of clays on a parallel computer. Proc. ASCE Fourth Congress on Computing in Civil Engineering, Philadelphia, June 16-18.
3. Anandarajah A (1998) Discrete element modeling of marine sediments. Proc. 12th. Engr. Mech. Conf., La Jolla, California, May 17-20.
4. Anandarajah A (1998) Computational difficulties in discrete element analysis of colloidal suspensions. Proc. 12th. Engr. Mech. Conf., La Jolla, California, May 17-20.
5. Anandarajah A (1998) Mechanics and physics of clean and contaminated clays. Proc. 35th. Annual Technical Meeting, Society of Engineering Science, Pullman, Washington, September 27-30.
6. Anandarajah A and Chen J (1998) Influence of pore fluid composition on volume of sediments in kaolinite suspensions. Clays and Clay Minerals, Vol. 46 (in print).

Peer Reviewed

1. Anandarajah A and Chen J (1998) Influence of pore fluid composition on volume of sediments in kaolinite suspensions. Clays and Clay Minerals, Vol. 46 (in print).
2. Anandarajah A (1998) A microscopic study of one-dimensional compression of clays. Geotechnique (in preparation).
3. Anandarajah A, Lavoie DL, Burkett, PJ and Richardson MD (1998) Discrete element simulation of the microstructure of marine cohesive sediments. Marine Geology (in preparation).

SUMMARY AND CONCLUSIONS

A series of two-dimensional discrete element analyses are performed on numerical specimens prepared on the basis of system parameters representing the Eckernförde Bay sediments. The details of the microstructure representing the Eckernförde Bay sediments are extracted from representative TEM pictures with the aid of an image processing software. The results indicate that (1) interparticle bonding due to interparticle cementation and/or the van der Waals attractive force can attribute to the apparent overconsolidation observed in the laboratory behavior, (2) unusually high observed compressibility of the soil is due to the highly porous initial microstructure, and (3)

large change in void ratio during compression is largely due to large inter-domain movements, rather than collapse of the domain themselves. The numerical void ratio values at a given vertical stress significantly depends on the assumed value for the particle thickness. As the particle thickness is decreased, the numerical void ratio increases, and when the particles are assumed to consist of two basic montmorillonite sheets, the numerical void ratio values become close to the experimental values. An approximate analysis indicates that a three-dimensional analysis is likely to lead, at a given vertical stress values, to larger numerical void ratio than a comparable two-dimensional analysis. In addition, there are other factors, not considered in the study presented here (e.g., gas bubbles, sands, silts, etc.), which could also contribute to the discrepancy between the theoretical and experimental compressibility results.

ACKNOWLEDGEMENT

The study has been supported by the CBBL-SRP program, directed by the chief scientists Dr. Michael D. Richardson. The financial support is gratefully acknowledged. The quantification of the microfabric from TEM pictures was performed by Manchun Yao of Johns Hopkins University, Nancy Carnaggio of NRL, and Allen Reed of USM. In addition, Dr. Richard H. Bennett of Seaprobe, Inc., provided valuable advise in understanding the microstructure of the Eckernförde Bay sediment.

- [1] Ag A (1994) Consolidation and permeability behavior of high porosity Baltic sea sediments. MS thesis. University of Rhode Island, Narragansett, Rhode Island. 131pp.
- [2] Anandarajah A (1994) Discrete element method for simulating behavior of cohesive soils. J. Geotech. Eng. Div., ASCE, 120:1593-1615.
- [3] Anandarajah A (1997) Influence of particle-orientation on one-dimensional compression of montmorillonite. J. Colloid Interface Sci. 194:44-52.
- [4] Anandarajah A and Chen J (1994) Double-layer repulsive force between two inclined platy particles according to Gouy-Chapman theory. J. Colloid Interface Sci. 168:111-117.
- [5] Anandarajah A and Chen J (1995) Single correction function for retarded van der Waals attraction. J. Colloid Interface Sci. 176:293-300.
- [6] Anandarajah A and Chen J (1997) Van der Waals attractive force between clay particles in water and contaminant. Soils and Foundations, JSSMFE. 37:27-37.
- [7] Anandarajah A and Kuganenthira N (1995) Some aspects of fabric anisotropy of soils. Geotechnique 45:69-81.
- [8] Anandarajah A and Lu N (1991a) Structural analysis by the distinct element method. J. Geotech. Eng. Div., ASCE, 117:2156-2159.

- [9] Anandarajah A and Lu N (1991b) Numerical study of the electrical double-layer repulsion between non-parallel clay particles of finite length. *Int. J. Numer. Anal. Meth. Geomech.* 15:683-702.
- [10] Anandarajah A, Kuganenthira N and Zhao D (1996) Variation of fabric anisotropy of kaolinite in triaxial loading. *J. Geotech. Eng. Div., ASCE*, 122:633-640.
- [11] Brandes HG, Silva AJ, Ag A and Veyera GE (1996) Consolidation and permeability characteristics of high-porosity surficial sediments in Eckernförde bay. *Geo-Marine Letters*, 16:175-181.
- [12] Chen J (1996) Physico-chemical analysis of contaminated clays. Doctoral thesis, The Johns Hopkins University.
- [13] Clegg SL and Whitfield M (1995) A chemical model of sea water including dissolved ammonia and the stoichiometric dissociation constant of ammonia in estuarine water and seawater from -2 to 40° C. *Grochimica et Cosmochimica Acta.* 59:2403.
- [14] Cundall PA and Strack ODL (1979) A discrete numerical model for granular assemblies. *Geotechnique* 29:47-65.
- [15] Grim RE (1968) *Clay mineralogy*. 2nd Edition, New York, McGraw Hill Co.
- [16] Kuganenthira N, Zhao D and Anandarajah A (1996) Measurement of fabric anisotropy in triaxial shearing. *Geotechnique* 46:657-670.
- [17] Lavoie DM, Lavoie DL, Pittenger, HA and Bennett RH (1996) Bulk sediment properties interpreted in light of qualitative and quantitative microfabric analysis. *Geo-Marine Letters*, 16:226-231.
- [18] Richardson MD (1994) Investigating the coastal benthic boundary layer. *EOS, Trans. Amer. Geophys. Union* 75:17.
- [19] Silva AJ and Jordan SA (1984) Consolidation properties and stress history of some deep sea sediments. In: Denness (Ed.), *Seabed Mechanics, Proc. IUTAM and IUGG Symposium*, pp. 25-40.
- [20] Silva AJ, Brandes HG and Veyera GE (1996) Geotechnical characterization of surficial high-porosity sediments in Eckernförde bay. *Geo-Marine Letters*, 16:167-174.
- [21] Stepkowska ET (1990) Problems of particle delamination and of stepwise aggregation in clay swelling. In: *Microstructure of Fine-Grained Sediments: from Mud to Shale*, eds. R. H. Bennett, W. R. Bryant and M. H. Hulbert (Eds.) Springer-Verlag, 1990, 382 pages.

[22] van Olphen H (1963) An introduction to clay colloid chemistry. Wiley Interscience, New York.

[23] Verwey EJW and Overbeek JTG (1948) Theory of the stability of lyophobic colloids. Elsevier Publishing Company.

Appendix I: Equations to Compute Surface Potential, Double-Layer Thickness and Particle thickness

Assuming values for the “cation exchange capacity” (CEC) and specific surface (S), a value is computed for the surface charge density ρ (van Olphen 1963). With the aid of the Gouy-Chapmann one-dimensional theory, the charge density is then related to f_0 (normalized surface potential) in terms of n_0 , $\epsilon\hat{I}$, and T . y_0 is computed from f_0 . A value is computed for the thickness of particles h from the value of S. Specific equations to compute the relevant parameters are as follows. Given CEC (meq/100g), S (m^2/g), n_0 (moles/liter), \hat{I} , v , G_s (specific gravity) and T ($^\circ\text{K}$), the parameters h , ρ , f_0 , y_0 and Z (double-layer thickness or the Debye length) are calculated using

$$h = \frac{2000}{SG_s} \text{ nm} \quad (2)$$

$$r = 29000 \frac{\text{CEC}}{S} \frac{\text{esu}}{\text{cm}^2} \quad (3)$$

$$f_0 = 2 \sinh^{-1} \left[\frac{r}{230 \sqrt{n_0 \epsilon T}} \right] \quad (4)$$

$$y_0 = 0.08614 \left[\frac{T f_0}{u} \right] \text{ mv} \quad (5)$$

$$Z = 0.002 \sqrt{\frac{\epsilon T}{n_0 u^2}} \text{ nm} \quad (6)$$

Measurement and Description of Upper Seafloor Sub-Decimeter
Heterogeneity for Macrostructure Geoacoustic Modeling

Aubrey L. Anderson

Professor of Oceanography
Department of Oceanography
Texas A&M University
College Station, Texas 77843-3146, U.S.A.

including the work of

Thomas H. Orsi, Anthony P. Lyons, Michael E. Duncan,
James A. Hawkins, Richard A. Weitz and Larry Buzi

and substantial collaboration with

Friedrich Abegg
Geologisch-Paläontologisch Institut der Universität Kiel, Kiel, Germany

Abstract:

Acoustic interaction with the seafloor involves many processes including reflection and scattering from interfaces and volume heterogeneities. Internal volume scattering of the sediment is one of the most difficult parameters to predict. One reason for this is the difficulty of obtaining appropriate information to geoacoustically characterize the sediment interior. The purpose of this project has been to examine and develop methods for measuring and characterizing the internal volume heterogeneity of sediments and to apply these methods at the CBBL field sites.

The scale of these measurements is within the CBBL designation of macroscale. Measurements were made on core samples with a nominal diameter of 1 decimeter. The core length was typically of the order of 1 m and resolution of the measurements typically approximated 1 mm³. The primary measurement mode was x-ray CT scanning of the undisturbed core sample. Calibration procedures developed in the study have allowed interpretation of the 3-dimensional digital data base from the sequential CT scans as bulk density distribution of the cored sediment. This has allowed estimation of heterogeneity parameters needed for perturbation calculation of volume scattering.

A method for recovering samples of gassy sediments retained under *in situ* conditions has allowed both unambiguous confirmation of the presence of bubbles of free gas in the seafloor and quantitative characterization of the bubble populations. Also contributing to this capability was methods developed for CT scanning the samples while they are retained at seafloor pressure and software for extracting bubble population data from the CT digital data base.

Distribution of gas bubbles in the floor of Eckernförde Bay was found to be highly heterogeneous, even in the 'gassy' zones. Bubbles identified by the techniques used here ranged

in size from about 0.4 mm to almost 1 cm equivalent radius. Gas concentrations were typically less than 2% in most of the bay floor but with maxima approximating 9% in a pockmark floor.

Models were developed and tested for calculating the volume scattering strength resulting from perturbations of the bulk sediment geoacoustic properties (density and compressibility) for non-gassy sediment. Other models were generated to calculate a depth distributed impulse response for bubbly seafloor depth intervals. Simulations of system response based on such calculations have provided encouraging indications that the models should be useful for further studies.

Original Objectives:

The workshops that were used to define and prioritize CBBL basic research objectives identified the importance of investigating the relative contributions of sediment interface and volume scattering to the total field returned when an acoustic wave interacts with the seafloor. These workshops also indicated the potential importance of gas bubbles to seafloor acoustic interaction and defined sediment macrostructure as a range of sediment property variation spanning from millimeter to 10's of centimeters scale.

The original objectives of this project were designed to address sediment geoacoustic properties on this scale. Specifically, sediment core samples from the CBBL field sites - typically of about a decimeter in size (diameter) - were to be measured by techniques allowing description of internal seafloor heterogeneity for the upper meter or so of the seafloor with a resolution of about a millimeter. Heterogeneity of sediment bulk density was the primary goal for description though the causes of this heterogeneity were also of interest. In the special case of the presence of bubbles of free gas in the sediment, identification and detailed description of the bubble population was to be carried out. The significance of the sediment macrostructure heterogeneity to geoacoustic modeling was to be investigated, especially in regard to internal volume scattering.

Although work had been carried out by the principal investigator and associates in a variety of areas relevant to these objectives, none of the techniques were to the stage of a finished tool that simply required application to the CBBL studies. Instead, sampling, measurement, geoacoustic description and acoustic modeling capabilities all required further research and development for their use in this study.

Approach:

This multi-faceted project involved several types of activities. The primary method for determining upper seafloor heterogeneity was measurements on samples recovered from the seafloor at CBBL field sites. Samples were obtained by: subsampling material retrieved by other investigators with box corers, 'unprotected' (not pressure-retaining) diver cores and pressure-retaining cores obtained either by divers or with gravity corers.

Two methods of measurement were used for the recovered sediment material. Almost all of the core samples for this project were measured by X-ray CT scanning. This scanning was done at Kiel, Germany for most of the samples from the nearby Eckernförde Bay field site, while samples from the two field sites in Florida (near Panama City and Key West), and the remaining Eckernförde Bay samples, were scanned in Texas. After the CT scanning, many of these core samples were also subjected to very high resolution physical sub-sampling both to provide a higher-than-normal resolution series of physical bulk density determinations and to serve as a calibration allowing interpretation of the CT data as bulk density (Orsi dissertation 1994 P).

Several types of analysis were carried out with these data. First, imagery generated from the CT measurements provided qualitative representation of the sediment heterogeneity. Images from individual CT scans allowed useful interpretation of the heterogeneity at a given depth within the core sample. Images generated from the full three-dimensional CT data base for a given core provided visualization of the full spatial distribution, including depth distribution, of heterogeneity and the relationship between density layering, shells, burrows and other features such as gas bubbles. (Abegg and Anderson, 1997 P)

Quantitative analysis extended the usefulness of these data beyond the qualitative imagery. First, calibration of the CT data allowed interpretation of the recorded CT values in terms of bulk density. This allowed generation of profiles of density versus depth in much the same manner that such profiles might be generated from the usual physical sampling but at much higher resolution. These data were then used to extract geoacoustic parameter values, especially those required for volume scattering calculations. The data were supplemented in some cases by measurements of sound speed and density with a p-wave logger. (Orsi, *et al.*, 1996 P)

For samples of gassy sediments, software was written to identify bubbles of free gas in CT scan data from pressure-retained cores. This software allowed generation of continuous depth profiles of free gas concentration, bubble size, shape and location and other derived characteristics such as size distribution of the bubble population. (Anderson, *et al.*, in press, P)

In the absence of gas bubbles, modeling the sediment volume scattering strength was performed using an extended version of a previously developed model that treats density and compressibility within the seafloor as perturbations of the sediments mean properties (Lyons, *et al.*, 1994; Lyons dissertation 1995 P). For bubbly sediment, a much earlier model for calculating bulk properties of the sediment (Anderson and Hampton, 1980) was extended to allow treatment of non-spherical bubbles and to generate volume scattering strength estimates. This capability was then incorporated into a multiple layered model of the gassy seafloor, including extinction losses for each layer and forward scattering contributions to a propagating acoustic wave. Simulations of returns from the seafloor for a given acoustic profiling system were generated by convolving the system's pulse waveform with the model generated, spatially (temporally) distributed impulse response of the bubbly seafloor. (Lyons, *et al.*, 1996 P)

Results:

In addition to new techniques and modeling developed as part of this CBBL project, some techniques that were begun in a previous ONR supported study of gassy sediment were refined and applied. One technique involved calibration of x-ray CT scan data from seafloor cores to allow interpretation of the recorded CT data as bulk density values (CT density). This was accomplished either by scanning known density samples during a core scanning session or by high resolution, physical subsampling of cores after they were CT scanned then physically measuring the actual bulk density of the subsamples (Orsi dissertation 1994 P). An example of one application of the results of such calibration is shown in Figure 1.

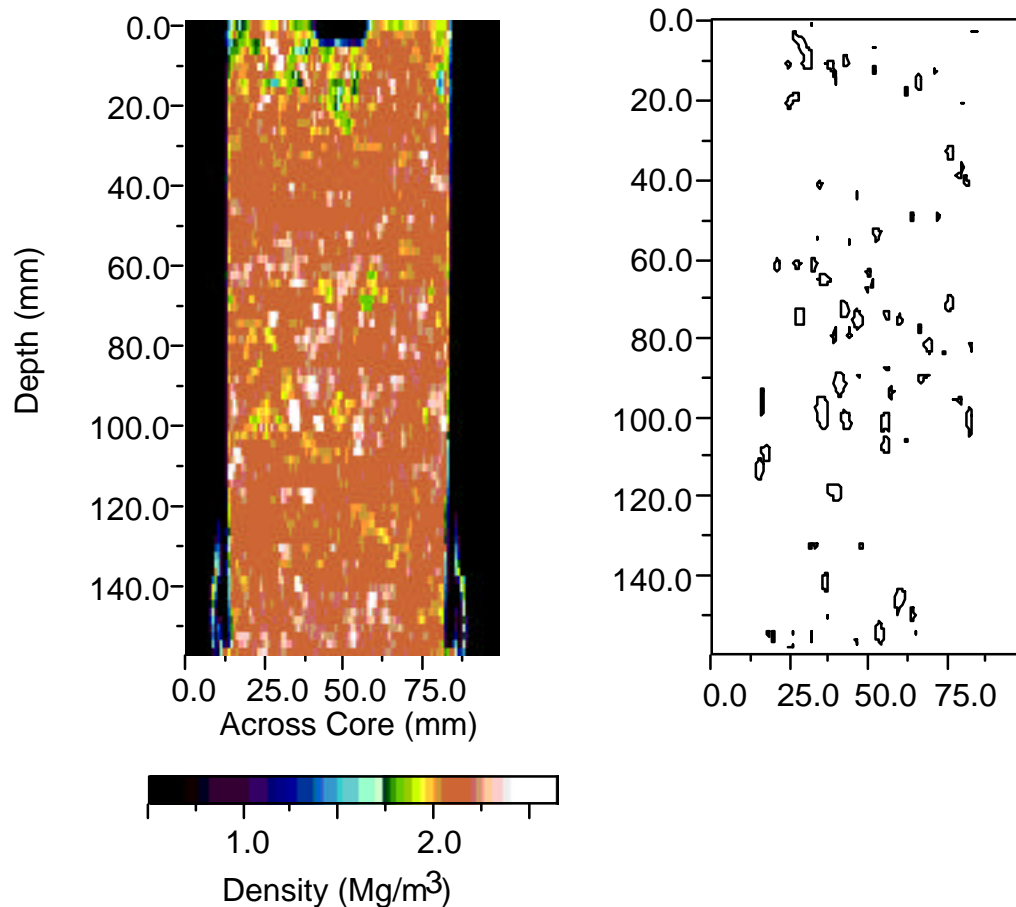


Figure 1 Imagery from CT data for core 413-PC-DC

Core 413 is one of three diver cores collected at the Panama City CBBL site for CT study. The left panel of Fig. 1 is a false color image of a slice through the 3D CT number data base in a direction that would be vertical for the *in situ* orientation of the core. The CT values have been converted linearly to bulk density by the calibration procedure described above. Typical of all three cores studied from this site, this shallow portion of the seafloor consists of a large number of shell pieces distributed through a sand sediment. The bulk density difference between shell material and the sand aggregate allows using a density threshold to identify the shell pieces. The right panel of Fig. 1 shows the outlines of shell pieces 'cut' by this vertical slice through the CT

data. These outlines are simply contours of a bulk density value midway between that for the sand aggregate and the shell pieces. Volume scattering simulations for this shell hash sediment were carried out using a model for scattering from a distribution of non-resonant spheres in a matrix. Size distribution information for the calculation was determined by stereological examination of several vertical sections, as shown in Fig. 1, of core 413 CT data. These simulations suggested that, at 40 kHz, roughness of the seafloor-seawater interface dominated seafloor backscattering for grazing angles above about 10 degrees, while volume scattering controlled the seafloor backscattering strength for lower grazing angles. The simulated values agreed well with CBBL backscattering measured at this frequency (Lyons dissertation 1995 P).

Other seafloor backscattering simulations for non-gassy areas of the CBBL sites were made using a continuum model that treats the seafloor volume heterogeneity as perturbations of the density and sound speed of the sediment bulk properties. The model used was an extension of one reported by Lyons *et al.* (1994). This model requires values for the correlation length of the depth profile of these characteristics. Studies indicate that the continuum scattering is

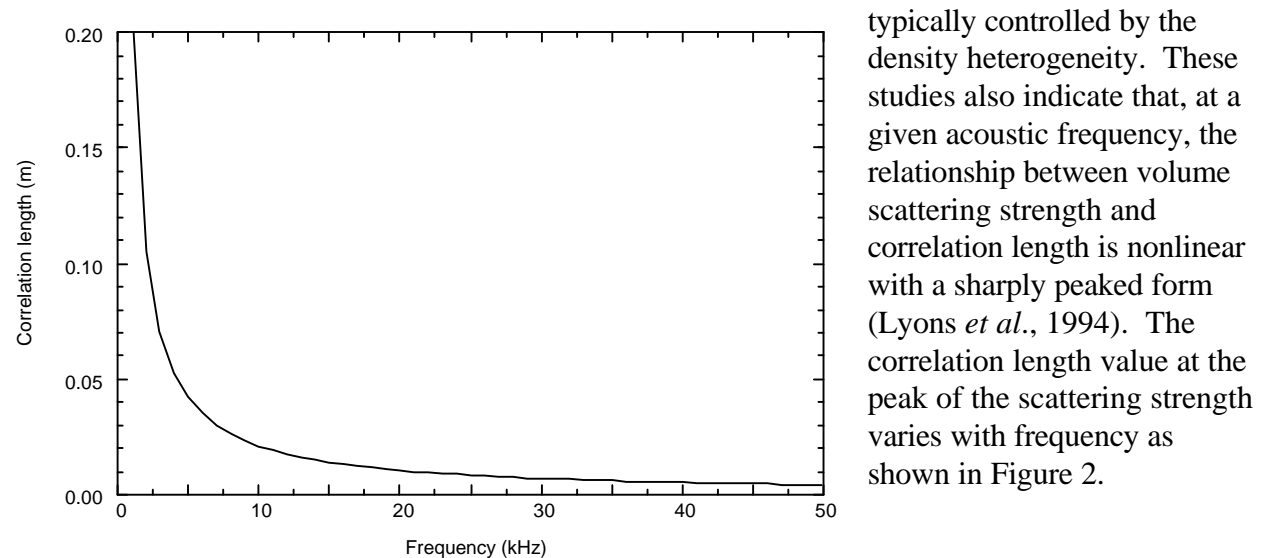


Figure 2 Correlation length at the maximum of the continuum scattering cross section versus frequency

Correlation length values, determined from core data for each of the three CBBL field sites, are about: 1 cm for Panama City, 2 cm for Eckernförde Bay and 4 cm for Key West (Marquesas Keys). These values could not be determined from most normal physical sampling profiles for sediment core physical properties and the smaller lengths would not be available even from high resolution sampling. Only a technique such as CT density profiling can provide the required resolution for the determination. The continuum volume scattering model also requires values for the normalized variance of density and compressibility within the sediment volume. Based on the CT data profiles and other information, these values were determined to be on the order of 10^{-3} for each of the CBBL sites. These small values result in a usually modest contribution to overall seafloor backscattering except for some ranges of grazing angles and frequencies.

Availability of multiple bulk density profiles versus depth from the CT scan information allowed forming a model description of the profile. This vertical tiered model, with a surficial mixed layer and a deep historical layer joined by an intervening transitional layer, not only is

applicable to all three of the CBBL sites but also is consistent with density observations in other environments (Orsi and Anderson, in press P). This density profile information also has been cast in a functional form allowing determination of the impact on seafloor reflectivity of observed near surface density gradients (Lyons and Orsi, submitted P).

In contrast with often modest volume scattering from continuum heterogeneity, when free gas bubbles are present, large volume scattering cross sections may exist and other geoacoustic properties of the seafloor may be altered. Thus the portions of Eckernförde Bay with gassy sediments represent a special case. In addition to the special acoustical characteristics of gassy sediments, these sediments also present unique sampling challenges. One result of the CBBL study is a technique for recovery and retention of gassy sediment samples at near *in situ* conditions. This is accomplished by the use of pressure transfer chambers and diver processing of the cores. Either diver retrieved cores up to 2 m in length or gravity cores up to 5 m in length are sectioned into 1 m lengths and capped at the seafloor. Also at the seafloor, these 1 m core sections are each placed into individual pressure-tight aluminum pressure transfer chambers (APTCs), which are then raised to the sea surface and brought on board ship. These pressure retained core sections, maintained under refrigeration in warm weather, are then transported to a nearby radiology laboratory for CT scanning in the evening. The smooth-walled aluminum chambers allow CT scanning while the samples remain pressure tight. On several occasions, rescanning of short depth intervals of the cores after pressure-release indicates that new gas bubbles are formed and existing bubbles are enlarged. Thus confirming the necessity for maintaining the cores under pressure for accurate determination of the *in situ* characteristics of the free gas bubble population of the samples.

Over a three year period, pressure-retained cores were taken with this technique primarily from two areas. One was the primary CBBL field site and near the location, in the summer of 1993, of bottom standing towers for measurement of acoustic scattering. The other area was within one of several pockmarks, this one near the edge of the flat, central portion of Eckernförde Bay. Figure 3 is an example of imagery developed from the 3D data base of CT scan data for visualizing the distribution of free gas bubbles in the seafloor.

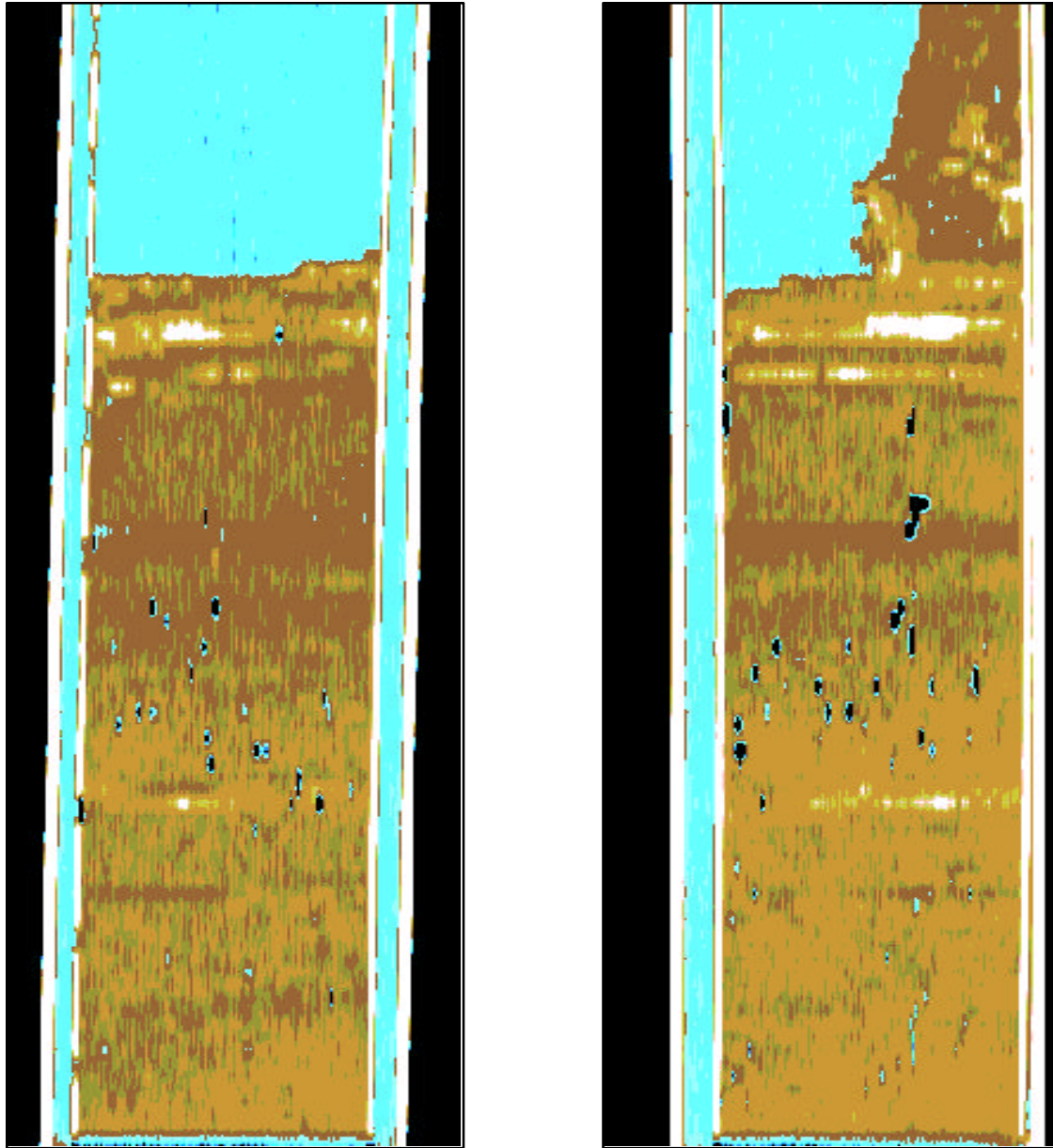
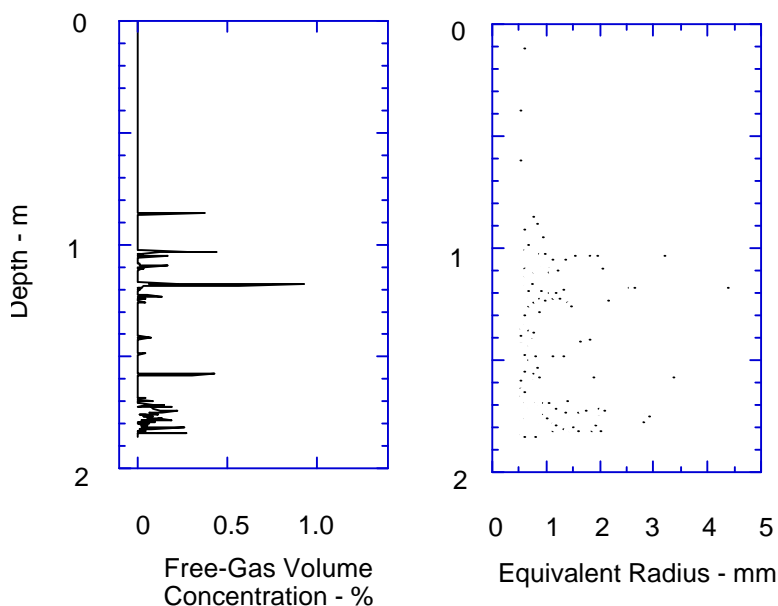


Figure 3 Imagery from CT data for pockmark core 339-BS-DC

The two panels of Fig. 3 are vertical sections of CT density generated from the CT data base for this core from the pockmark location. The two vertical sections are mutually orthogonal and the sediment extending upward at the edge of the right panel is sediment material that slumped inside the core liner after the core was removed from the seafloor. This points out one of the problems in early core retrievals in the APTCs. For these first cores, the top of the sediment sample was stabilized by a sponge inserted into the open top of the core liner by the divers. This method was later supplanted by a diver inserted piston that preserved the very top of the core material and allowed more complete definition of the near surface layering and bubbles. In Fig. 3, bubbles are the dark objects distributed through the sediment, especially at mid-depth in the core. Within the floor of the pockmark, the largest bubbles (up to volumes equal to a sphere

with radius of almost 1 cm) and highest gas concentrations (up to volume concentrations of almost 9% within a single image - i.e., 2.5 mm thick interval) were observed. The free gas concentration profiles of pockmark cores indicate that gas bubbles begin almost immediately below the water-sediment interface and extend almost continuously with depth into the upper seafloor.

Abegg and Anderson (1997 P) present additional imagery plus gas concentration profiles for 339 and other cores from the gassy floor of Eckernförde Bay. These results indicate several differences between the bubble populations in the floor of the pockmark and in the gassy muds in



the central (backscattering tower) portion of the bay. At the tower site, significant numbers of gas bubbles do not begin immediately beneath the water-sediment interface but rather at a greater depth of several decimeters. Both the largest gas bubbles and the free-gas volume concentrations are smaller at the tower site. Maximum bubble sizes are 4 to 5 mm equivalent radius. Free-gas concentrations are essentially zero over the first few decimeters into the seafloor. Average concentrations are of the order .02% from 80 cm to 1.5 m depth and ~ .1% from 1.5 to 3 m.

Figure 4 Bubble population data for Core 707-BS-DC (P2)

Maximum gas volume concentrations in any depth at the tower site are less than 2%. An example concentration profile is shown in the left panel of Figure 4. The non-continuous nature of gas bubble occurrence over a vertical section is evident in this profile.

Anderson *et al.* (in the press P) provide similar gas concentration profiles for three additional cores obtained along a horizontal line including the location of 707-BS-DC with a total horizontal span of about 4.25 m. These authors show that the gas bubble occurrence is also variable in the horizontal although there is a tendency for greater spatial correlation of bubble occurrence in horizontal. This variable bubble concentration occurs in a seafloor region chosen for study because of the relative uniformity of returns generated by acoustic profiling systems operated over the region (Richardson 1994).

Simulations of acoustic returns from a gassy seafloor require more information than the gas concentration profile - for example, bubble distribution. One type of bubble distribution that was found to be useful in such simulations is shown in the right panel of Fig. 4 which shows the equivalent radius and center-of-gravity depth for each bubble of this core.

Several modeling steps were taken to allow these simulations. A model originally put forward by Anderson and Hampton (1980) has been found over the years to have five errors. These errors were corrected and the model was extended. One extension was to incorporate a

method to take into account some of the consequences of non-sphericity of the bubbles. This is done by incorporating each bubble's surface area ratio (sar: ratio of actual bubble surface area to that of an equivalent volume sphere). Software developed on this project not only identified each bubble but also determined bubble depth, volume, equivalent radius and sar. Another model extension was to incorporate the corrected Anderson and Hampton model, with sar capability, into an algorithm for calculation of bubble scattering strength (the original model was written to calculate sound speed and attenuation through a bubbly sediment). Finally, this scattering strength computation was made for each of a sequence of thin sublayers extending over the bubbly depth interval of the seafloor. The energy propagating downward through each sublayer was attenuated by the scattering extinction in the layer and the forward scattered energy was 'added back' into the propagating wave. This same set of energetics partitioning was taken into account for energy propagating upward from a deeper scattering layer. The resulting calculation determines the spatially (temporally) distributed impulse response of the bubbly interval of sediment - thus allowing simulation of the seafloor volume backscattered return versus time for an arbitrary acoustic waveform. This model is more fully described by Lyons *et al.* (1996 P) and by Anderson *et al.* (in press P). These authors also illustrate some results of the simulation. An example of a simulation compared with acoustic profiler returns is shown in Figure 5. The measured data are from the pockmark area and the simulations are based on core 339. Because of the large footprint of the acoustic profiler, one would not expect perfect agreement from a simulation based on one core from the seafloor. Nevertheless, the degree of comparability between the information in the two panels of Fig. 5 is encouraging. Additional studies with

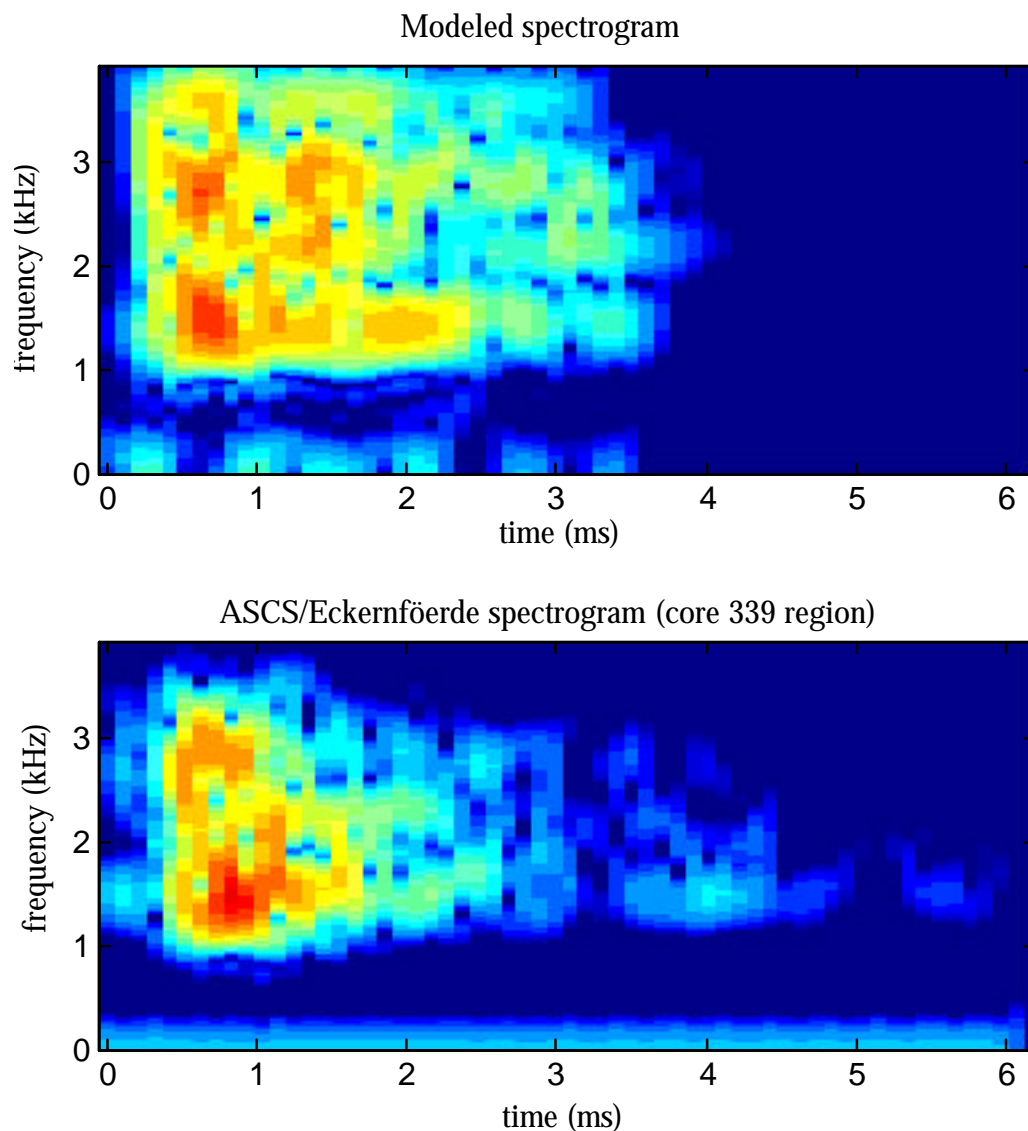


Figure 5 Measured and modeled acoustic returns for the pockmark floor

Monte Carlo realizations of core 339-guided bubble populations would be useful. An important observation from Fig. 5 is that both the measured and simulated results indicate a variation of the strength of the acoustic return with both frequency of the acoustic wave and depth into the seafloor that is generating the backscattering. Thus, narrowband profiling systems of different frequencies may produce differing representations of the buried bubbly depth interval. The depth variation of bubble population characteristics has already been noted and is illustration in Fig. 4. Abegg and Anderson (1997 P) noted a difference in the depth of initial indication of acoustic turbidity in Eckernförde Bay and the shallower depth at which measured total methane concentration exceeds methane saturation values. They suggest that the bubbles initially forming at the shallower depths are smaller than resonant size for the 3.5 kHz profiler producing the indications of turbidity. Profilers of other frequencies may indicate different depths of initiation of the turbidity.

Accomplishments:

Methods for calibration of CT scan digital data allowing interpretation as sediment density were improved and extended. This capability allows description of sediment bulk density in three dimensions and with unprecedented spatial resolution. Application of these methods to CBBL seafloor samples has allowed estimation of the variance and correlation scale of sediment internal density variation thus allowing quantitative estimation of volume scattering. These parameters could not have been determined for the CBBL samples from more conventional measurement methods because of limitations of spatial resolution of the information. Also, from the CT bulk density profiles, a tiered model of the vertical structure of density at the CBBL sites was developed and related to natural causes.

Techniques were developed for recovery of seafloor samples retained at *in situ* conditions of pressure and temperature and allowing x-ray CT scanning under these conditions. Data resulting from application of these techniques provided new information about the presence and distribution of free gas in the seafloor. Although a variety of types of evidence previously had been interpreted as indicative of *in situ* free gas bubbles in the seafloor, sampling and measurements carried out in this project unambiguously confirmed the existence of these bubbles.

Software was generated for identification of free gas bubbles in CT scan data for the pressure-retained cores. Application of this capability allowed detailed, quantitative description of the *in situ* bubble population including gas concentration profiles; location, size and shape of each bubble; and distribution statistics. Gas bubbles in the floor of Eckernförde Bay were found not to be uniformly distributed in the gassy regions, even for a region selected for study because of the uniformity of its seafloor acoustic response.

Several types of new modeling capability were produced for calculations of acoustic interaction with a bubbly sediment. Several errors were corrected in a model used for two decades to calculate bulk geoacoustic properties (sound speed and attenuation) in a bubbly sediment. This model was also extended to allow treatment of non-spherical bubbles and to calculate acoustic scattering cross-sections. Also developed was a model for treating thick layers of bubbly sediment. This last model correctly accounts for acoustic field/bubble energetics by including extinction losses and forward scattering additions to acoustic fields traversing each bubble layer. The resulting spatially (temporally) distributed impulse response allows simulation of the returns for acoustic systems profiling bubbly sediment zones.

References:

(if a 'P' follows a reference date in the text, the reference citation is given in the list of publications for this project that is provided below)

Anderson, A.L. and L.D. Hampton 1980 Acoustics of gas-bearing sediments I. Background and II. Measurements and models. *Journal of the Acoustical Society of America*, 67, 1865-1903.

Lyons, A.P., A.L. Anderson and F.S. Dwan 1994 Acoustic scattering from the seafloor: Modeling and data comparison. *Journal of the Acoustical Society of America*, 95, 2441-2451.

Richardson, M.D. 1994 Investigating the Coastal Benthic Boundary Layer. *EOS*, 75(17), 201-206.

Publications:

Peer Reviewed

Orsi, T.H. and A.L. Anderson 1994 Bubble characteristics in gassy sediments. *Transactions, Gulf Coast Association of Geological Societies*, 44, 533-540.

Lyons, A.P., M.E. Duncan, A.L. Anderson and J.A. Hawkins 1996 Predictions of the acoustic scattering response of free-methane bubbles in muddy sediments. *Journal of the Acoustical Society of America*, 95, 163-172.

Orsi, T.H., A.L. Anderson and A.P. Lyons 1996 X-ray tomographic analysis of sediment macrostructure and physical property variability in Eckernförde Bay, Western Baltic Sea. *Geo-Marine Letters*, 16(3), 232-239.

Orsi, T.H., F. Werner, D. Milkert, A.L. Anderson and W.R. Bryant 1996 Environmental overview of Eckernförde Bay, Northern Germany. *Geo-Marine Letters*, 16(3), 140-147.

Abegg, F. and A.L. Anderson 1997 The acoustic turbid layer in muddy sediments of Eckernförde Bay, Western Baltic: methane concentration, saturation and bubble characteristics. *Marine Geology* 137, 137-147.

Anderson, A.L., F. Abegg, J.A. Hawkins, M.E. Duncan and A.P. Lyons (in press) Bubble populations and acoustic interaction with the gassy seafloor of Eckernförde Bay. *Continental Shelf Research*.

Orsi, T.H. and A.L. Anderson (in press) Vertical tiering of sediment bulk density in Eckernförde Bay: a conceptual model using x-ray CT. *Continental Shelf Research*.

Orsi, T.H., A.L. Anderson, W.R. Bryant, K.S. Davis and A.K. Rutledge (in press) Computed tomography of carbonate macrostructure: Marquesas Keys and Dry Tortugas (south Florida). *Geo-Marine Letters*.

Lyons, A.P. and T.H. Orsi (submitted) The effect of a layer of varying density on high-frequency reflection, forward loss and backscatter. *IEEE Journal of Oceanic Engineering*.

Symposium proceedings

Abegg, F. and A.L. Anderson 1994 The acoustic turbid layer in soft mud: methane concentration, saturation and bubble characteristics. Examples from Eckernförde Bay, Germany. *Proceedings, Third International Conference on Gas in Marine Sediments*, Texel, The Netherlands.

Abegg, F., A.L. Anderson, L. Buzi, A.P. Lyons and T.H. Orsi 1994 Free methane concentration and bubble characteristics in Eckernförde Bay, Germany. in: T.F. Wever (ed.) *Proceedings of the Gassy Mud Workshop held at FWG, Keil, FWG Report 14*, Keil, 84-89.

Anderson, A.L., A.P. Lyons, L. Buzi, F. Abegg and T.H. Orsi 1994 Modeling acoustic interaction with a gassy seafloor including examples from Eckernförde Bay. in: T.F. Wever (ed.) *Proceedings of the Gassy Mud Workshop held at FWG, Keil, FWG Report 14*, Keil, 90-94.

Lyons, A.P., A.L. Anderson and T.H. Orsi 1994 Modeling acoustic volume backscatter from two shallow-water marine environments by side-scan sonar. *Proceedings, IEEE-OES OCEANS 94*. Brest, France, Vol. I, 862-865.

Orsi, T.H., A.L. Anderson and A.P. Lyons 1994 Geoacoustic characterization of shallow-water marine sediments for high-frequency applications. *Proceedings, IEEE-OES OCEANS 94*. Brest, France, Vol. I, 866-871.

Anderson, A.L., F. Abegg and R.A. Weitz 1995 Gas concentration and bubble distribution in the floor of Eckernförde Bay: ground truth from core sample measurements. in: T.F. Wever (ed.) *Proceedings of the Workshop on Modelling Methane-Rich Sediments of Eckernförde Bay, FWG Report 22*, Keil, 70-72.

Anderson, A.L., A.P. Lyons, F. Abegg, M.E. Duncan, J.A. Hawkins and R.A. Weitz 1995 Modeling acoustic volume scattering by a bubbly mud seafloor with examples from Eckernförde Bay. in: T.F. Wever (ed.) *Proceedings of the Workshop on Modelling Methane-Rich Sediments of Eckernförde Bay, FWG Report 22*, Keil, 243-247.

Hawkins, J.A., D.N. Lambert, D.J. Walter, A.P. Lyons, M.E. Duncan and A.L. Anderson 1995 Spectral characterization of bubbly sediments using high frequency, short duration acoustic pulses. in: T.F. Wever (ed.) *Proceedings of the Workshop on Modelling Methane-Rich Sediments of Eckernförde Bay, FWG Report 22*, Keil, 65-69.

Orsi, T.H., M.E. Duncan, A.P. Lyons, K.B. Briggs, M.D. Richardson and A.L. Anderson 1997 High-resolution characterization of seafloor sediments for modeling acoustic backscatter. in: N.G. Pace, E. Pouliquen, O. Bergem and A.P. Lyons *High Frequency Acoustics in Shallow Water*, SACLANTCEN Conference Proceedings Series CP-45, 409-415.

Orsi, T.H., K.B. Briggs, M.D. Richardson and A.L. Anderson (in press) CT analysis of physical property variability in carbonate sediments. in: D. Lavoie (ed.) *Proceedings, Key West Workshop*, Naval Research Laboratory, Stennis Space Center, MS.

Published abstracts

Anderson, A.L. and F. Abegg 1994 Measurement of gas bubble concentration and distribution in the seafloor of Eckernförde Bay, Germany. *EOS Supplement*, 75(3) 159.

Fischer, K.M. and T.H. Orsi 1994 Porosity gradients in Eckernfoerde Bay (Baltic Sea). *EOS Supplement*, 75(3) 220.

Lyons, A.P., A.L. Anderson and T.H. Orsi 1994 Estimates of volume scattering cross section and related parameters due to property variability in Eckernförde Bay. *EOS Supplement*, 75(3) 203.

Lyons, A.P., M.E. Duncan, J.A. Hawkins and A.L. Anderson 1994 Predictions of the acoustic response of free methane bubbles in muddy sediments. *Journal of the Acoustical Society of America*, 96(2, pt. 2), 3217.

Orsi, T.H. and A.L. Anderson 1994 Macroscale heterogeneity of sediments from Eckernförde Bay (Western Baltic Sea). *EOS Supplement*, 75(3) 220.

Richardson, M.D., S.R. Griffin, K.B. Briggs, A.L. Anderson and A.P. Lyons 1994 The effects of free methane bubbles on the propagation and scattering of compressional and shear wave energy in muddy sediments. *Journal of the Acoustical Society of America*, 96(2, pt. 2), 3218.

Orsi, T.H. and A.L. Anderson 1995 X-ray computed tomography of macroscale variability in sediment physical properties, offshore Louisiana. *AAPG Bulletin*, 79(10), 1565.

Orsi, T.H., A.L. Anderson, W.R. Bryant, K. Davis, R. Rezak, K.M. Fischer and C. Brunner 1995 Computed tomography of physical property heterogeneity of carbonate muds from Marquesas Keys and Dry Tortugas, South Florida. *SEPM Congress on Sedimentary Geology, St. Pete Beach, Florida*, 1, 96.

Other Presentations

Lyons, A.P. and T.H. Orsi 1994 Characterization of seafloor property variability and estimates of volume scattering cross section in Eckernförde Bay, Germany. 6th Annual Student Symposium, College of Geosciences and Maritime Studies/Ocean Drilling Program, Texas A&M University, College Station, TX.

Orsi, T.H. 1994 Computed tomography of macrostructure and physical property heterogeneity in surface sediments of Eckernförde Bay (Western Baltic Sea). 6th Annual Student Symposium, College of Geosciences and Maritime Studies/Ocean Drilling Program, Texas A&M University, College Station, TX.

Orsi, T.H. 1994 A method for quantifying bubble characteristics in gassy aqueous sediments. 6th Annual Student Symposium, College of Geosciences and Maritime Studies/Ocean Drilling Program, Texas A&M University, College Station, TX.

Anderson, A.L. 1995 Indications of seafloor free gas, the interaction of underwater sound and bubbly sediment. Workshop on Modelling Methane-Rich Sediments of Eckernförde Bay, Eckernförde, Germany.

Dissertations

Orsi, T.H. 1994 Computed tomography of macrostructure and physical property variability of seafloor sediments. Ph.D. dissertation, Texas A&M University.

Lyons, A.P. 1995 Acoustic volume scattering from the seafloor and the small scale structure of heterogeneous sediments. Ph.D. dissertation, Texas A&M University.

High-Frequency Scattering from Sediment Roughness and Sediment Volume Inhomogeneities

K.B. BRIGGS, M.D. RICHARDSON, and P.D. JACKSON*

Seafloor Sciences Branch
Naval Research Laboratory
Stennis Space Center, MS 39529 USA

and
*British Geological Survey
Kingsley Dunham Centre
Keyworth, Nottingham UK NG12 5GG

Abstract: High-quality, high-resolution environmental data were collected by divers from four sediment types for use in testing high-frequency scattering models. Environmental measurements of sediment compressional wave velocity, porosity and density were collected in conjunction with measurements of acoustic scattering in order to accurately test contributions from sediment volume scattering. The surface roughness power spectrum calculated from seafloor microtopography was used as a model parameter, thus providing predictions of backscattering without fitting of the model to data. Autocorrelation functions calculated from vertical profiles of sediment sound velocity and density provided correlation lengths, which were used as model parameters. In addition to these direct assays of acoustic and physical properties in vertical profile, image processing of sediment X-radiographs and sediment micro-resistivity was used to determine correlation lengths of density fluctuations in horizontal as well as vertical profile.

Comparison of environmental data with acoustic data over the four sediment types was instructive in identifying relative contributions to high-frequency bottom backscattering from interface and volume scattering. Data from the Eckernförde experiment site indicated that high scattering strengths could be found in sediment with small surface roughness, low water-sediment impedance contrast, and low variability in sediment sound velocity and density, provided that near-surface biogenic gas was present. Conversely, data from the Panama City experiment site indicated that sediment consisting of coarse shell fragments and coarse sand provides intense interface scattering that overwhelms scattering contributions from an inhomogeneous sediment volume. Variations in acoustic scattering at the Panama City site were due to changes in orientation and/or distribution of surficial shell hash by megafaunal activity. At the Dry Tortugas experimental site, areas of rapidly changing sediment surface roughness and volume inhomogeneity were shown to be directly related to changes in scattering strength. Also at the Dry Tortugas site, roughness spectral slope and intercept was directly correlated with anthropogenic manipulation of surface roughness, but changes in roughness were not correlated with scattering strength. An additional experimental site off the Eel River in northern California provided data on scattering from sediments with small surface roughness, low water-sediment impedance contrast, but high variability in sediment sound velocity and density due to flood layering. In this regime of sediment variability generated by both hydrodynamic and biological processes, bottom backscattering strength was expected to be relatively high and variable.

Original Objectives: By establishing the autocorrelation functions of sediment density/porosity and compressional wave velocity fluctuations as parameters for modeling of sediment inhomogeneities, we will determine sediment structure in order to unravel relationships among sediment properties. By measuring and predicting biological and hydrodynamic processes that control sediment surface roughness and volume inhomogeneities, we will quantify the effects of

environmental processes on sediment properties. By employing X-radiography and electrical resistivity to elucidate three-dimensional macrostructure and spatial variability of sediments, we will demonstrate new methods to measure and quantify sediment three-dimensional structure. By using high-quality, high-resolution, environmental and acoustic data to test the extant high-frequency scattering models, we will determine effects of environmental processes on sediment properties to extend acoustic predictions to other environments.

Approach: Investigators will characterize inhomogeneities within the sediment volume in order to better understand geoaoustic variability at the Eckernförde, Panama City, Dry Tortugas, and Eel River experiment sites. At the same time, seafloor interface roughness will be measured photogrammetrically to complement the measurements of the sediment volume. Sediment properties to be measured from all sites in order to correspond to acoustic scattering model inputs are sediment compressional wave velocity and attenuation (at 400 kHz), sediment porosity, sediment density, and sediment surface roughness. In addition, sediment density to x-rays and electrical resistivity will be measured at the experiment sites. Other sediment parameters, such as grain size distribution, shear strength, and permeability, will be measured in order to correlate acoustic and physical property fluctuations with hydrodynamic, biological, and sedimentological processes (Briggs and Richardson, 1996; Briggs *et al.*, 1998). X-radiographs and CT scans will be used to look at multi-dimensional, high-resolution, sediment density fluctuations with the intention of generating autocorrelation functions from which correlation lengths can be determined.

Of particular importance to this approach is the lateral variability of sediment sound velocity and porosity within a site or along a transect over which sediment classification sonars have collected data. These measures of velocity and porosity are obtained through standard "ear-muff" transducers through core liners and through water content assays, respectively (Richardson, 1986; Richardson and Briggs, 1993). X-radiography, CT scans, and an electrical micro-resistivity core scanner developed by Peter Jackson are used for fine-scale sediment density measurements (Hoyer *et al.*, 1996; Orsi *et al.*, 1996; Jackson *et al.*, 1996). Emphasis is placed on the careful and consistent collection of diver cores, with the desired result being regularly spaced measurements of nearly undisturbed sediments. The high quality of the measurements is demonstrated through comparison with in-situ measurements made at the same locations (Richardson and Briggs, 1996).

Results: Values of sediment parameters required for the composite roughness model and the volume scattering model of Hines measured at the four experiment sites are presented in Table 1.

Table 1. Average values of sediment parameters: compressional wave velocity (V_p) ratio, water sound velocity (V_{pw}), compressional wave attenuation (α), density correlation length (l_r), density () ratio, roughness spectral exponent (g_l), roughness spectral strength (w_l), sound velocity variance (σ_v^2), and porosity variance (σ_p^2).

Site	V_p Ratio	V_{pw} m/s	α dB/m	l_p cm	Ratio	γ_l cm ⁴	w_l $\times 10^{-3}$ cm ³	σ_v^2 m ² /s ²	σ_p^2
Eckernförde Bay	0.991	1448	2.69	2.11	1.18	-2.42	0.3028	3.62	0.00015
Panama City	1.126	1532	19.91	1.66	1.97	-2.12	1.983	406.45	0.00024
Dry Tortugas	1.020	1525	12.20	2.81	1.72	-2.29	2.092	78.24	0.00199
Eel River (S60)	1.022	1480	4.29	2.03	1.75	na	na	783.98	0.00252

Compressional wave velocity ratio, water sound velocity, compressional wave attenuation, density correlation length, density ratio, roughness spectral exponent, and roughness spectral strength constitute the input parameters for the composite roughness model. Variance of the values of sediment sound velocity and porosity are required for the sediment volume scattering model of Hines (Hines, 1990). Values of compressional wave velocity and attenuation are reported as measurements made with the in-situ sediment acoustic measurement system at 38 kHz (Richardson *et al.*, 1996).

Backscattering strength as a function of grazing angle is predicted from the composite roughness model of Jackson *et al.* (1996) for the four experiment sites in Figure 1. The predictions are for 40 kHz and we assume that the roughness spectrum for the Eel River S60 site conforms to default values for silty sediment, in lieu of data yet to be analyzed. Scattering from the sediment volume contributes greatly to the predicted scattering at the Dry Tortugas site and contributes nearly as much to the scattering at the Eel River site due to the high sediment density variance. Confirming this similarity requires the use of the measured roughness spectrum parameters from the Eel River site rather than the default values. Comparison of the predictions from Dry Tortugas with Panama City indicates that the contribution from the sediment volume above 13° grazing angle at Dry Tortugas is exceeded by the contribution from the strong impedance contrast and greater interface roughness at Panama City.

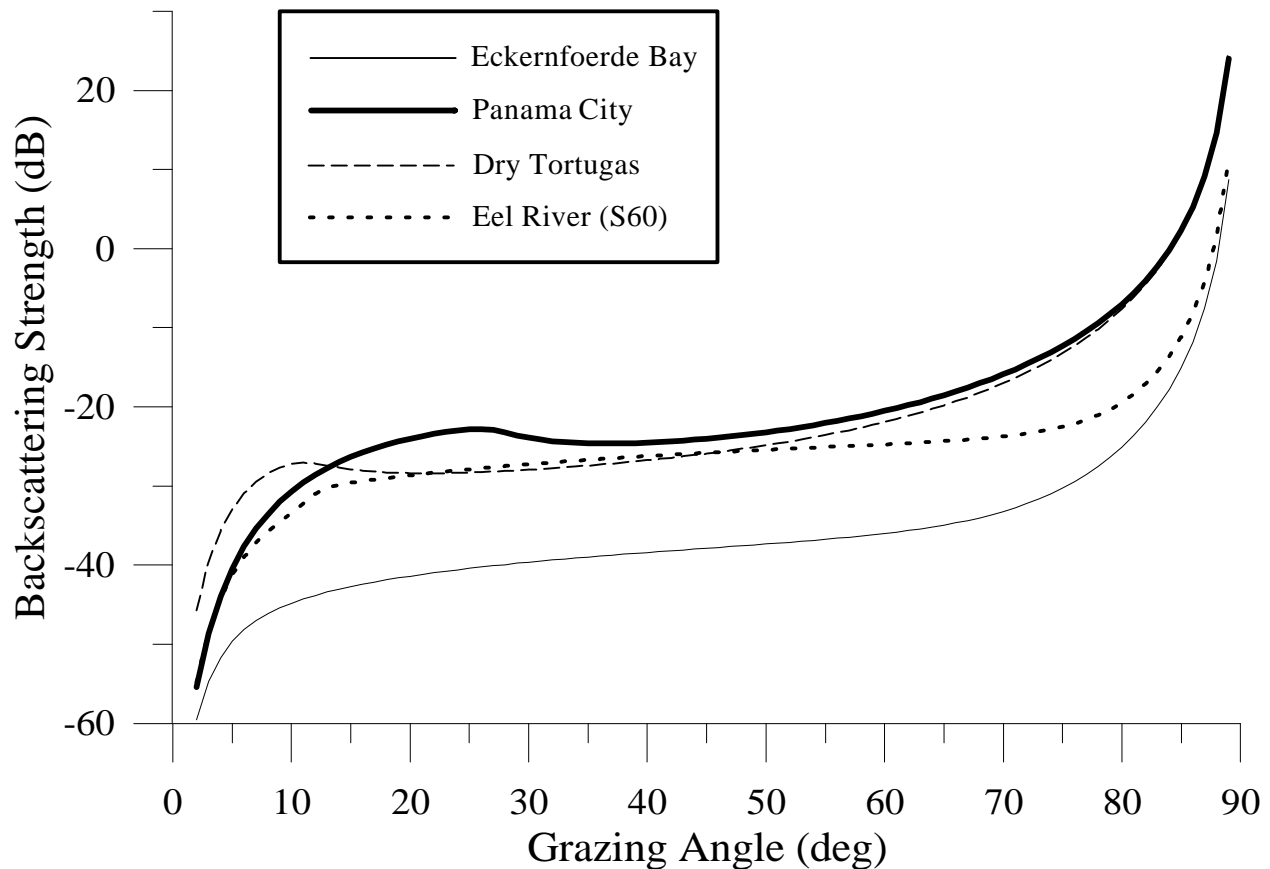


Figure 1. Predictions of backscattering strength vs. grazing angle from the composite roughness model using input parameters from Table 1.

Accomplishments: Central to the success of our proposed research was the development of the capability to assess the variability of the sediment properties that are responsible for creating scattering of high-frequency acoustic energy penetrating the sediment-water interface. We were able to measure fluctuations of sediment sound velocity at a 1-cm vertical resolution with 400-kHz “ear muff” transducers. Calculation of autocorrelation functions from these data using Burg’s algorithm yielded vertical correlation lengths on the order of 1-2 times the sampling frequency (Briggs and Percival, 1997). Although lacking in information on horizontal fluctuations, these measurements are probably the best small-scale assessment of sediment sound velocity fluctuations to date. Two-dimensional tomographic techniques can provide the additional dimension of velocity fluctuations, but can not provide any greater resolution.

Use of conventional techniques for assessing sediment density fluctuations involves sectioning cores at 2-cm intervals and autocorrelation functions calculated from these data indicated that there might be aliasing in the calculation of correlation lengths, as well as a lack of information on horizontal density fluctuations. Therefore, we developed some new techniques to assess sediment density fluctuations in two and three dimensions as well as at a greater resolution. Firstly, we employed X-radiography to assess two-dimensional sediment density in rectangular cores specially designed to minimize disturbance upon insertion into the sediment. These X-radiograph images were digitized and then manipulated with image processing techniques to yield vertical and horizontal autocorrelation functions of sediment (X-ray) density fluctuations (Briggs *et al.*, 1998). Secondly, we employed electrical micro-resistivity to measure porosity (which is directly proportional to density) on the same cores. X-radiography and micro-resistivity measurements indicated conclusively that anisotropy exists in sediment density fluctuations, with greater correlation lengths in the horizontal dimension than in the vertical dimension. The magnitude of the correlation length estimates indicated that conventional techniques were undersampling the fluctuations. Finally, we employed CT scanning of cylindrical cores to achieve very-high resolution (2-mm) measurements of sediment density that avoided any ambiguity due to superimposing of sediment features on the X-ray image. Also, this technique can be used to assess small-scale horizontal fluctuations, though somewhat limited in extent (Orsi *et al.*, 1996). This technique has allowed the estimation of correlation lengths of small-scale vertical density fluctuations that are similar in magnitude (*c.* 2-3 cm) to those estimated from conventional methods. These data perhaps indicated that, in most cases, sampling sediment density at 1-cm intervals might be satisfactory for acoustic modeling purposes.

A unique tool into sediment fabric characteristics from the Eckernförde Bay sediments was developed through a combined interpretation of X-radiographic and micro-resistivity imaging data (Briggs *et al.*, 1998). The combination of formation factor (through electrical micro-resistivity) and porosity (through X-ray attenuation) enabled Archie’s m parameter to be calculated. Values of this parameter were extremely sensitive to sediment microstructure and were diagnostic of the pelletized sediments and storm laminae found in the bay. The two microstructure types (pelletized sediment and coarse laminae) exhibited different tortuosities, as calculated from the flow of electrical current. Thus, electrical tortuosity is analogous to the sediment tortuosity that is an input for predicting sediment compressional wave propagation with the Biot model. Figure 2 depicts an estimate of tortuosity indicating a silty fine-sand storm layer with high resistivity and high tortuosity amongst pelletized sediments of lower resistivity, higher porosity, and lower tortuosity. The lower tortuosity is achieved through the better connected

pores created by the regularly sized, oblong-spherical pellets as compared to the poorly sorted, angular silt and sand particles.

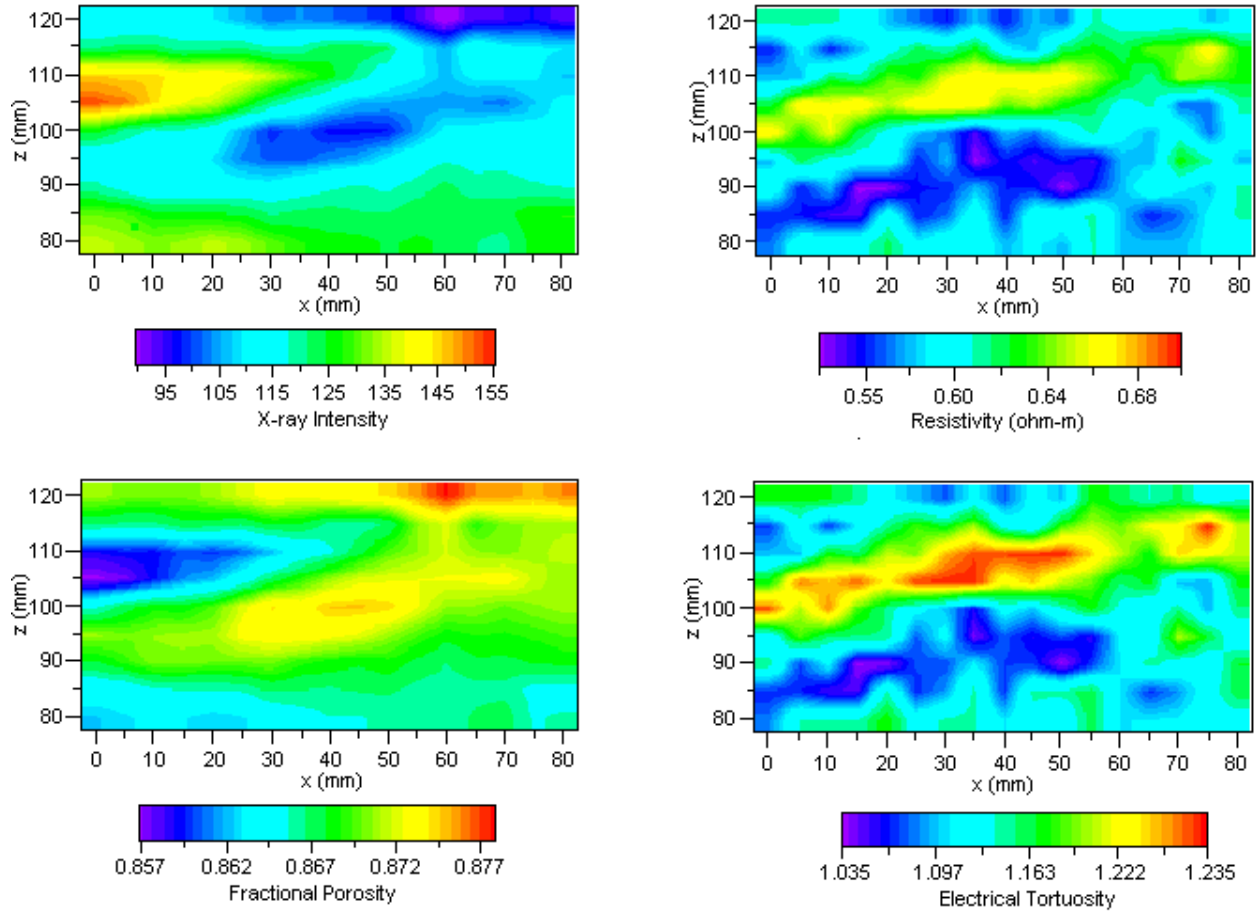


Figure 2. Combined interpretation of X-ray and micro-resistivity data provides an estimate of sediment tortuosity. A silt-and-fine-sand storm layer is indicated at the 100 to 110 mm depths.

The measurements of sediment physical and acoustic properties from the Dry Tortugas experiment site indicated a much different sediment structure than that of the Eckernförde Bay site, resulting in a more complex pattern of sediment volume heterogeneity. Whereas the Eckernförde Bay sediment had an anisotropy in density fluctuations due to horizontal to sub-horizontal laminae embedded in a highly pelletized (from bivalve mollusks) matrix, the Dry Tortugas sediment exhibited greater variability with density fluctuations distributed in more dimensions. Such fluctuations in sediment density dictated the use of a different technique in assessing variability in the sediment volume. Using a grid of resistivity electrodes placed on the sediment-water interface within a box core sample, we were able to measure sediment micro-resistivity throughout a 20×28×6-cm volume by inductive techniques (Fig. 3). In Fig. 4, sediment heterogeneity at the Dry Tortugas site is displayed in three dimensions, with a range-separated plot of the sediment volume indicating the distribution of sediment micro-resistivity in x, y, and z dimensions. These data have yet to be processed to yield sediment formation factor, porosity, and density in order to calculate the correlation lengths for density fluctuations in the x, y, and z dimensions.

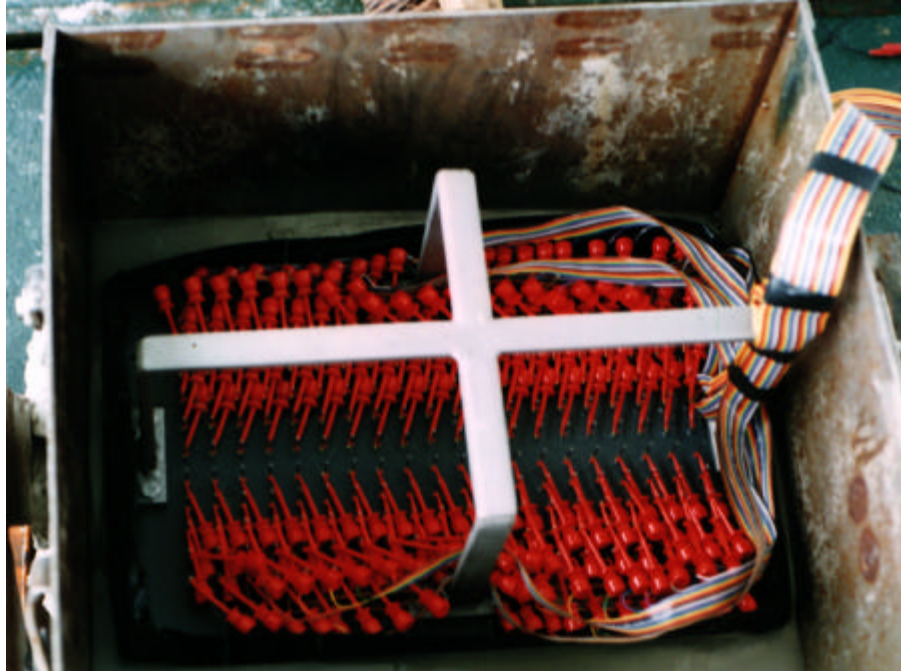


Figure 3. Photograph of the electrical micro-resistivity array used to image the 3-D heterogeneity within the 50- \times -50-cm box core.

Unlike the Eckernförde Bay sediment, the Dry Tortugas sediment was subject to biological activity (burrowing) below the top 2-3 cm of sediment. X-radiograph cores, diver cores, and diver observations indicated that patchily distributed decapods and heart urchins were responsible for creating networks of burrows through which fine sediment was ejected and subsequently wafted away by currents (Briggs and Richardson, 1997). Intensely bioturbated sediment was coarser and denser than sediment without evidence of faunal disturbance at the Dry Tortugas. Reworking of the sediment by burrowing infauna may have facilitated de-watering of the sediment on scales longer than the period of monitoring by the Applied Physics Laboratory scanning sonar tower. That is to say, the patterns of “hot spots” and “cold spots” observed in the decorrelation imagery from the sonar did not change appreciably during the term of the experiment (2 weeks).

A comparison of results from the Dry Tortugas and Marquesas Keys sites of the Key West Campaign illustrated an important concept concerning spatial and temporal variability in sediment properties. Measurements of physical and acoustic properties within the top 40 cm of sediment indicated that there were three classes of parameter variability relevant to acoustic bottom scattering at the Dry Tortugas and Marquesas Keys sites. Bioturbation created strong depth gradients in the top 5 cm of sediment. The gradient variability in sediment porosity, sound velocity, and sound attenuation was long term and widespread. A combination of biogenic mixing and storm-generated hydrodynamic stress created inhomogeneities such as fine laminae and shell lag deposits. The laminae at the Marquesas site were short-term features, but widespread within that site. The shell layer variability was a long-term and widespread feature, but restricted to the Marquesas site. Biogenic mixing was also responsible for creating short-term, localized variability in surficial sediments that was identified by the “hot spots”.

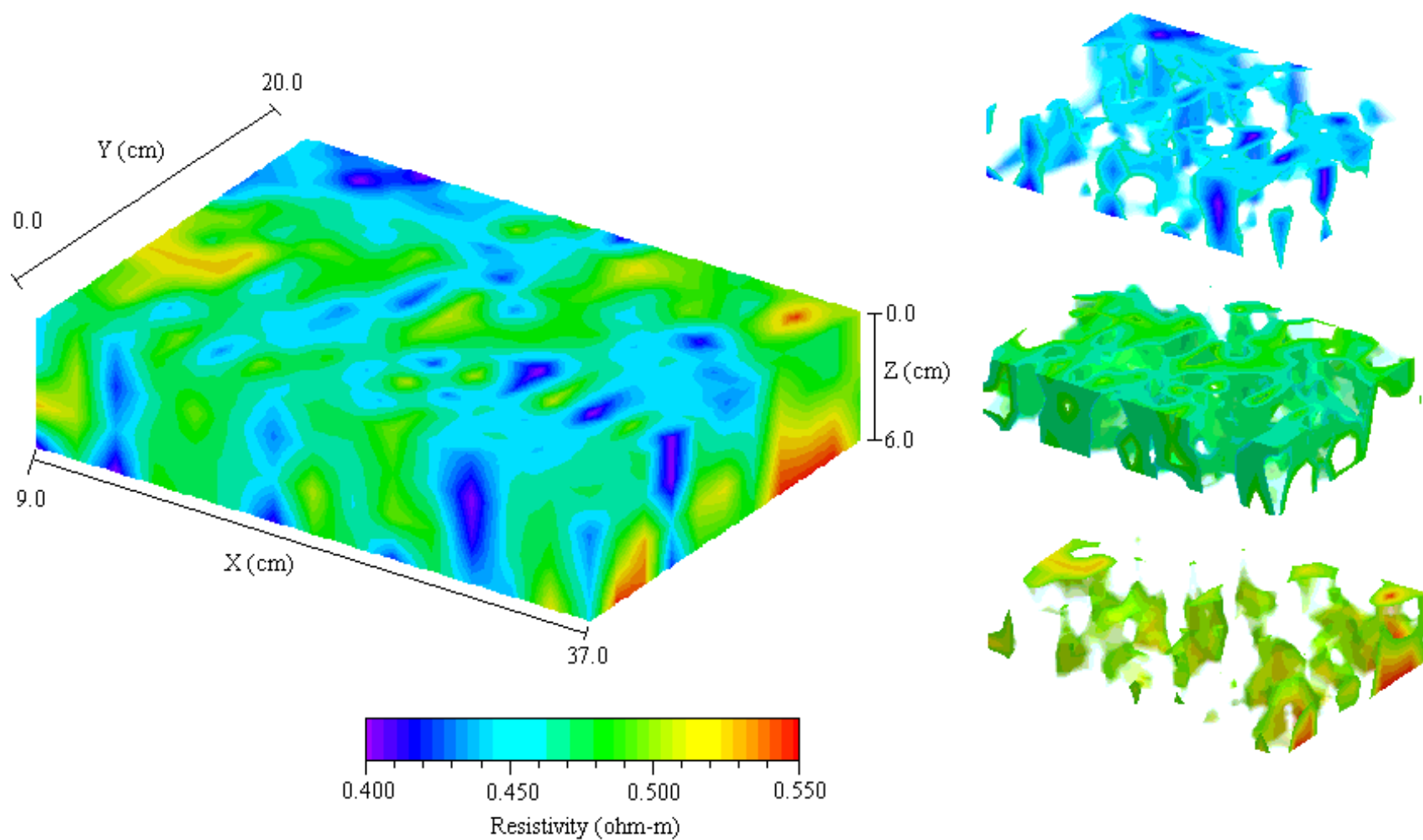


Figure 4. Sediment heterogeneity investigated using 3-D micro-resistivity measurements in box core KW-PL-BC-200 from the Dry Tortugas experiment site. A range-separated plot of the 3-D volume is displayed on the right.

Ongoing research: With the conclusion of the CBBL program, there remain several aspects of research that demand attention and are worth pursuing. We are investigating the three-dimensional assessment of sediment density through micro-resistivity measurements at the Dry Tortugas site. We plan to develop CT scanning as a tool for very-fine-scale, 1-, 2-, and 3-dimensional sediment density assessment. We are examining permeability as a salient parameter in explaining sediment diagenesis and sedimentary history in the Eel River sediments. Analysis of the interface roughness data from the Eel River S60 site will allow a rigorous evaluation of the acoustic scattering predictions in conjunction with the predictions made with environmental data from the other three sites. Finally, we are continuing to use the Applied Physics Laboratory's sonar tripod together with the environmental measurements to develop the sensitivity of acoustic models to various sediment volume parameters.

References:

- Briggs, K.B. and M.D. Richardson. 1996. Variability in in-situ shear strength of gassy muds. *Geo-Mar. Ltrs.*, 16: 189-195.
- Briggs, K.B. and M.D. Richardson. 1997. Small-scale fluctuations in acoustic and physical properties in surficial carbonate sediments and their relationship to bioturbation. *Geo-Mar. Ltrs.*, 17: 306-315.
- Briggs, K.B. and D.B. Percival. 1997. Vertical porosity and velocity fluctuations in shallow-water surficial sediments and their use in modeling volume scattering. In, N.G. Pace, E. Pouliquen, O. Bergem, and A.P. Lyons (eds.), *High Frequency Acoustics in Shallow Water*, NATO SACLANT Undersea Res. Ctr., La Spezia, Italy, pp. 65-73.
- Briggs, K.B., M.D. Richardson and S.J. Bentley. 1998. Permeability of successive flood deposits off the Eel River, Northern California: effects of bioturbation. *EOS*, 79: O34-35.
- Briggs, K.B., P.D. Jackson, R.J. Holyer, R.C. Flint, J.C. Sandidge, and D.K. Young. (1998) Two-dimensional variability in porosity, density, and electrical resistivity in Eckernförde Bay sediment. *Contin. Shelf Res.*, in press.
- Hines, P.C. 1990. Theoretical model of acoustic backscattering from a smooth seabed. *J. Acoust. Soc. Amer.* 88: 325-334.
- Holyer, R.J., D.K. Young, J.C. Sandidge, and K.B. Briggs. 1996. Sediment density structure derived from textural analysis of cross-sectional x-radiographs. *Geo-Mar. Ltrs.*, 16: 204-211.
- Jackson, D.R., K.B. Briggs, K.L. Williams, and M.D. Richardson. 1996. Tests of models for high-frequency sea-floor backscatter. *IEEE J. Oceanic Engin.*, 21: 458-470.
- Jackson, P.D., K.B. Briggs, and R.C. Flint. 1996. Evaluation of sediment heterogeneity using micro-resistivity imaging and X-radiography. *Geo-Mar. Ltrs.*, 16: 219-226.
- Orsi, T.H., A.L. Anderson, and A.P. Lyons. 1996. X-ray tomographic analysis of sediment macrostructure in Eckernförde Bay, western Baltic Sea. *Geo-Mar. Ltrs.*, 16: 232-239.
- Richardson, M.D. 1986. Spatial variability of surficial shallow water sediment properties. In, T. Akal and J.M. Berkson (eds.), *Ocean Seismo-Acoustics*, Plenum Press, London, pp. 527-536.
- Richardson, M.D. and K.B. Briggs. 1993. On the use of acoustic impedance values to determine sediment properties. In, N.G. Pace and D.N. Langhorne (eds.), *Acoustic Classification and Mapping of the Seabed*, Institute of Acoustics, University of Bath, pp. 15-25.
- Richardson, M.D. and K.B. Briggs. 1996. In-situ and laboratory geoacoustic measurements in soft mud and hard-packed sand sediments. *Geo-Mar. Ltrs.*, 16: 196-203.

Richardson, M.D., S.R. Griffin, and F.B. Grosz. 1996. ISSAMS: An in-situ sediment acoustic measurement system. In, *Proc. Int. Conf. on Underwater Acoustics*, Australian Acoustical Soc., Univ. of So. Wales, Sydney, pp. 104-106.

Publications:

Peer-reviewed

- Briggs, K.B. and M.D. Richardson. 1996. Variability in in-situ shear strength of gassy muds. *Geo-Mar. Ltrs.*, 16: 189-195.
- Briggs, K.B. and M.D. Richardson. 1997. Small-scale fluctuations in acoustic and physical properties in surficial carbonate sediments and their relationship to bioturbation. *Geo-Mar. Ltrs.*, 17: 306-315.
- Briggs, K.B., P.D. Jackson, R.J. Holyer, R.C. Flint, J.C. Sandidge, and D.K. Young. (1998) Two-dimensional variability in porosity, density, and electrical resistivity in Eckernförde Bay sediment. *Contin. Shelf Res.*, in press.
- Bennett, R.H., M.H. Hulbert, M.M. Meyer, D.M. Lavoie, K.B. Briggs, D.L. Lavoie, R.J. Baerwald, and W.-A. Chiou. 1996. Fundamental response of pore water pressure to microfabric and permeability characteristics: Eckernförde Bay. *Geo-Mar. Ltrs.*, 16: 182-188.
- Holyer, R.J., D.K. Young, J.C. Sandidge, and K.B. Briggs. 1996. Sediment density structure derived from textural analysis of cross-sectional x-radiographs. *Geo-Mar. Ltrs.*, 16: 204-211.
- Jackson, D.R., K.B. Briggs, K.L. Williams, and M.D. Richardson. 1996. Tests of models for high-frequency sea-floor backscatter. *IEEE J. Oceanic Engin.*, 21: 458-470.
- Jackson, D.R., K.L. Williams, and K.B. Briggs. 1996. High-frequency acoustic observations of benthic spatial and temporal variability. *Geo-Mar. Ltrs.*, 16: 212-218.
- Jackson, P.D., K.B. Briggs, and R.C. Flint. 1996. Evaluation of sediment heterogeneity using micro-resistivity imaging and X-radiography. *Geo-Mar. Ltrs.*, 16: 219-226.
- Richardson, M.D. and K.B. Briggs. 1996. In-situ and laboratory geoacoustic measurements in soft mud and hard-packed sand sediments. *Geo-Mar. Ltrs.*, 16: 196-203.
- Richardson, M.D., D.L. Lavoie and K.B. Briggs. 1997. Geoacoustic and physical properties of carbonate sediments of the Lower Florida Keys. *Geo-Marine Ltrs.*, 17: 316-324.
- Stanic, S., R. Goodman, K.B. Briggs, N. Chotiros and E. Kennedy. (in review). Shallow-water bottom reverberation measurements. *IEEE J. Oceanic Engin.*

Symposium Proceedings

- Briggs, K.B. and M.D. Richardson. 1994. Geoacoustic and physical properties of near-surface sediments in Eckernförde Bay. In, Wever, T.F. (ed.), *Proc. Gassy Mud Workshop FWG, Kiel, 11-12 July, 1994*, pp. 39-46.
- Briggs, K.B. and M.D. Richardson. 1995. Physical property variability in sediments in and proximal to Eckernförde Bay. In, Wever, T.F. (ed.), *Proc. of the Workshop Modelling Methane-Rich Sediments of Eckernförde Bay*. Eckernförde, Germany, 26-30 June 1995, pp. 208-214.
- Briggs, K.B. and D.B. Percival. 1997. Vertical porosity and velocity fluctuations in shallow-water surficial sediments and their use in modeling volume scattering. In, N.G. Pace, E. Pouliquen, O. Bergem, and A.P. Lyons (eds.), *High Frequency Acoustics in Shallow Water*, NATO SACLANT Undersea Res. Ctr., La Spezia, Italy, pp. 65-73.

- Briggs, K.B. and R.I. Ray. 1998. Seafloor roughness power spectra: trends and implications for high-frequency acoustic modeling. *Proc. Inter. Conf. Shallow-Water Acoustics*, Beijing, China, 21-25 April 1997, in press.
- Jackson, P.D. and K.B. Briggs. 1995. Evaluation of heterogeneity within gas-rich sediments using micro-resistivity imaging and x-radiography. In, Wever, T.F. (ed.), *Proceedings of the Workshop Modelling Methane-Rich Sediments at Eckernförde Bay*. Eckernförde, Germany, 26-30 June 1995, pp. 215-216.
- Richardson, M.D. and K.B. Briggs. 1995. The effects of methane gas bubbles on sediment geoaoustic properties in Eckernförde Bay. In, Wever, T.F. (ed.), *Proceedings of the Workshop Modelling Methane-Rich Sediments of Eckernförde Bay*. Eckernförde, Germany, 26-30 June 1995, pp. 199-206.

Reports

- Briggs, K.B. 1994. *High-frequency acoustic scattering from sediment interface roughness and volume inhomogeneities*. Naval Research Laboratory, Stennis Space Center, MS. NRL Form. Rep. 7431-94-9617, 154p.
- Briggs, K.B., D. L. Lavoie, K. Stephens, M. D. Richardson and Y. Furukawa. 1996. *Physical and geoaoustic properties of sediments collected for the Key West Campaign, February 1995: A data report*. Naval Research Laboratory, Stennis Space Center, MS. NRL/MR/7431--96-8002, 395p.
- Orsi, T.H., K.B. Briggs, and M.D. Richardson. 1996. *Computed tomography of marine sediments: I. STRATAFORM, Eel River Study 1996*. Planning Systems Inc., Slidell, LA. Technical Report S250, 6p + 3 App.
- Stephens, K.P., D.L. Lavoie, K.B. Briggs, Y. Furukawa and M.D. Richardson. 1997. *Geotechnical and geoaoustic properties of sediments off south Florida: Boca Raton, Indian Rocks Beach, lower Tampa Bay, and the lower Florida Keys*. Naval Research Laboratory, Stennis Space Center, MS. NRL/MR/7431--97-8042, 310p.

Published Abstracts

- Briggs, K.B. 1994. Correlation functions for sediment acoustic properties. *J. Acoust. Soc. Am.*, 96: 3245-3246.
- Briggs, K.B., M.D. Richardson and D.R. Jackson. 1994. High-frequency bottom backscattering volume scattering from gassy mud. *J. Acoust. Soc. Am.*, 96: 3218.
- Briggs, K.B., M.D. Richardson and D.B. Percival. 1994. Correlation functions estimated from vertical profiles of sediment porosity and compressional wave velocity fluctuations. *EOS*, 75: 202.
- Briggs, K.B. and M.D. Richardson. 1995. Geoaoustic and physical properties of carbonate sediments from the Key West Campaign. *SEPM Congress on Sedimentary Geology*, St. Petersburg, FL, 13-16 Aug. 1995, p. 33.
- Briggs, K.B. and M.D. Richardson. 1996. Small-scale fluctuations in acoustic and physical properties in surficial carbonate sediments. *EOS*, 76: OS172.
- Briggs, K.B. and M.D. Richardson. 1996. Preservation of surficial gradients of sediment porosity and shear strength in successive flood deposits off the Eel River, northern California. *EOS*, 77: F316-317.
- Briggs, K.B., M.D. Richardson and S.J. Bentley. 1998. Permeability of successive flood deposits off the Eel River, Northern California: effects of bioturbation. *EOS*, 79: O34-35.

- Briggs, K.B. and R.I. Ray. 1998. Seafloor roughness power spectra: trends and implications for high-frequency acoustic modeling. *Proc. Inter. Conf. Shallow-Water Acoustics*, Beijing, China, 21-25 April 1997, (*in press*)
- Briggs, K.B. and S. Stanic. 1998. High-frequency bottom backscattering from a homogeneous seabed. *J. Acoust. Soc. Am. Suppl. 1*, 103: (*in press*)
- Holyer, R.J., D.K. Young, J.R. Chase and K.B. Briggs. 1994. Sediment density structure inferred by textural analysis of cross-sectional x-radiographs and electron microscopy images. *EOS*, 75: 202.
- Jackson, P.D., K.B. Briggs, R.F. Flint, M.A. Lovell and P.K. Harvey. 1994. Evaluation of the porosity structure of coastal benthic boundary layer sediments using micro-resistivity imaging. *EOS*, 75: 201.
- Jackson, P.D., K.B. Briggs, R.F. Flint, M.A. Lovell and P.K. Harvey. 1994. The investigation of millimeter scale heterogeneity in Coastal Benthic Boundary Layer sediments using microresistivity and x-ray imaging of "diver" cores. *J. Acoust. Soc. Am.*, 96: 3245.
- Richardson, M.D., S. Griffin and K.B. Briggs. 1994. In-situ sediment geoacoustic properties: a comparison of soft mud and hard packed sand sediments. *EOS*, 75: 220.
- Richardson, M.D., D.N. Lambert, K.B. Briggs and D.J. Walter. 1994. Comparison of acoustic seafloor classification (ASCS) and in-situ geoacoustic (ISSAMS) data collected from a variety of sediment types in Kiel Bay, Germany. *International Conference on Underwater Acoustics*. University of New South Wales, Sydney, pp. 89-90. Australian Acoustic Society, Darlinghurst, Australia.
- Richardson, M.D., K.B. Briggs, and A.M. Davis. 1996. Geoacoustic properties of carbonate sediments. *EOS*, OS172.
- Richardson, M.D., K.B. Briggs, L.D. Wright, and C.T. Friedrichs. 1996. The effects of biological and physical processes on near-surface sediment geoacoustic properties. *EOS*, 77: F317.
- Stephens, K., D.L. Lavoie, Y. Furukawa and K.B. Briggs. 1995. Variability of physical properties from the Dry Tortugas and Marquesas Keys. *SEPM Congress on Sedimentary Geology*, St. Petersburg, FL, 13-16 Aug 1995, p. 117.

Dissertations

- Briggs, K.B. 1994. *High-frequency acoustic scattering from sediment interface roughness and volume inhomogeneities*. Ph.D. Dissertation, Univ. of Miami, Coral Gables, FL, 143p.

Effects of Carbonate Dissolution and Precipitation on Sediment Physical Properties and Structure in the Key West Area: Microfossils Component

CHARLOTTE A. BRUNNER

**Associate Professor of Marine Science
Department of Marine Science
Institute of Marine Sciences
The University of Southern Mississippi
John C. Stennis Space Center, MS 39529, U.S.A.**

Abstract:

Early diagenesis of organic matter in sediments affects not only the chemistry of sediment pore waters, but also modifies the solid constituents. The two approaches in combination, analysis of pore waters and observation of solid constituents, provide an effective approach to monitoring the reducing condition of the sediment. This study examined the effects of early diagenesis on benthonic foraminifers, a common constituent of sediments from the Key West area, and compared the results with the pore water profiles analyzed by A. Shiller. Some foraminifers showed evidence of reducing conditions in test interiors indicated by dissolution features, minor precipitation of calcium carbonate, and formation of pyrite framboids, which required reduction of sulfate. However, pore waters showed evidence of only mildly reducing conditions, where sulfate reduction was not reached. Evidently, the foraminifer tests successfully formed micro-chemical habitats in which more strongly reducing conditions were occasionally achieved. Interestingly, the distribution of tests with diagenetic modifications bears little relationship to the diagenetic zones defined from the pore water chemistry, which is entirely consistent with intense bioturbation.

Other accomplishments achieved as a by-product of the proposed work included depositional histories of the Dry Tortugas and Marquesas test sites, and an estimate of depth of bioturbational mixing of sand-size particles.

Original Objectives:

Benthic foraminifers are important constituents of sediments in the backreef environment. They form a significant proportion of the sediments in the Dry Tortugas region, comprising about 12% of the particles in the sand-size fraction (Orsi et al., unpub. rep., 1995). The large proportion is consistent with data on foraminifer productivity, which shows that carbonate production by large foraminifers (Hallock et al., 1986) is on the same order of magnitude as that of green algae, like *Halimeda* (Hudson, 1985), which are widely regarded as a principal source of the carbonate in the platform/reef environment. For example, *Archaias angulatus*, a large miliolid foraminifer, produces 60 g of $\text{CaCO}_3/\text{m}^2/\text{y}$ in Key Largo Sound of the Florida Keys, and large rotaliine foraminifers

produce up to 2,800 g of $\text{CaCO}_3/\text{m}^2/\text{y}$ in the reef flats of Palau (Hallock, 1981, 1984, 1986).

Oxidation of organic matter is an important process in surface sediments of the Tortugas region, based on preliminary data (Shiller et al., 1995). Early diagenesis of organic matter proceeds through a sequence of reducing reactions described by Froelich et al. (1979). The reactions include bacterial reduction of oxygen, followed by manganese oxide, nitrate, iron oxides, and sulfate. Some of these reactions produce protons, which promotes the dissolution of a carbonate, and other reactions consume protons, which promotes carbonate precipitation. The resultant dissolution and cementation could significantly affect the acoustic properties of sediment, and so study of early diagenesis is relevant to the CBBL project.

Solid products of organic carbon diagenesis

Foraminifer tests may play an interesting and important role in early diagenesis of carbonate sediment for two reasons. (1) The chambered tests enclose a chemical micro-environment that is isolated from surrounding pore waters and matrix except for restricted access through narrow apertures, canals, and small pores. The test interiors of the diverse fauna (7 of 10 extant suborders and more than 155 species) offer a variety of shapes and different-sized spaces, which may promote dissolution or precipitation of carbonate and other solid products of oxidation and reduction, such as manganese oxide and iron sulfide. (2) Tests of different suborders are made of different forms of calcium carbonate, including high and low magnesian calcite and aragonite. These different phases have different solubilities, and their surfaces may affect precipitation in different ways.

This work examines the following questions. 1) *Do foraminiferal tests harbor indications of early diagenesis due to oxidation of organic matter in a pattern consistent with the pore water chemistry?* 2) *Does the reduction sequence in the sediment column occur in test interiors sooner (e.g., at a shallower depth) than in the matrix hosting the tests due to formation of chemical micro-habitats in test interiors?* 3) *Does test composition promote or retard precipitation?*

Paleoenvironmental analysis and depth of mixing

In the original proposal, I hoped to develop a proxy of paleo-reduction intensity by comparing the ratio of epifaunal to infaunal species in gravity cores. However, many epifaunal species appear to have been transported to the Dry Tortugas test site, so it was not possible to develop such a proxy. However, analysis of the fauna from gravity cores produced several useful results. First, successions of depositional environments were clearly defined and detailed based on a census of foraminiferal species. Second, the depth of mixing estimated by Pb-210 was corroborated by faunal assessment.

Approach: The Role Of Foraminifers In Early Diagenesis Of Carbon

Box core KW-PL-BC-185 from the Southeast Channel of the Dry Tortugas, was selected for detailed analysis because the surface layer was apparently recovered intact, the core was relatively long (>20 cm), and pore water profiles of various chemical tracers of organic matter respiration and carbonate precipitation/cementation were available. The box core was divided into 1-cm thick slabs from 0 to 11 cm below sea floor (bsf) and 2-

cm thick slabs from 11 to 17 cm bsf. A 20-cc subsample was removed from each slab and washed on a 63 μm screen to remove clay- and silt-size particles. Ten to 15 specimens of each of two species were hand picked from the $>150\ \mu\text{m}$ fraction of the sand-size residue, mounted in low viscosity SPURR resin, sectioned, polished and prepared for scanning electron microscopy using backscattered electrons.

The species selected were *Parasorites orbitiloides* and *Nonionella grateloupe*, which differ from each other in several relevant qualities. The former is made of high-magnesian calcite, and its interior is subdivided into a labyrinth of hundreds of small chamberlets that average 40 to 50 μm in diameter (Murray, 1991). The protist is epiphytic and was likely swept from the shallow banks of the Dry Tortugas and transported to the test site. In contrast, the latter protist is made of low-magnesian calcite, and its interior is subdivided into ~15 chambers that increase in size from about 40 μm to 300 μm in length. The protist is infaunal and likely lived *in situ* (Murray, 1991).

Each sectioned test was completely inspected at 1000x magnification, and a census was made of features indicative of carbonate dissolution, carbonate precipitation, and presence of solid products of early diagenesis, such as pyrite, phosphorite, and manganese oxide.

The box core was subdivided into chemical zones that characterized oxidation state based on pore water concentrations of Mn, Mo, U, and PO_4 (Shiller, pers. comm., 1998). A suboxic zone from 1.5 to 8.5 cm bsf was delineated based on an increase in pore water concentrations of Mn. More oxic intervals characterized the surficial layer from 0 to 1.5 cm bsf and the basal layer from 12 cm bsf to bottom of the core. A zone of heightened oxygenation was noted from about 8.5 to 12 cm bsf, based on elevated concentrations of Mo and U and depleted concentrations of Mn and PO_4 . The heightened oxygenation suggests the recent passage of a burrowing organism, which entrained oxygenated bottom water into its burrow.

Results: Early Diagenesis

Carbonate was dissolved from tests by two separate processes: (1) chemical dissolution and (2) boring by endolithic micro-organisms, principally algae (Golubic et al., 1984; Perry, 1998). Endolithic micro-organisms excavated elongate holes 4 to 8 μm in diameter that originate at inner or outer test surfaces and extend in curved or straight form into interiors of test walls (Perkins and Tsentas, 1976; Golubec et al., 1975). The interior sculpture could be used to determine the taxa of the borers, but this question was not pursued in this study (Golubic et al., 1970). Among the high-magnesian calcite tests, nearly half of all the specimens examined were heavily bored, and virtually no test was left untouched (Plate 1). Boring likely occurred in the photic zone during transport from the banks to the site, and during residence on the sediment surface before burial. By contrast, the infaunal, low-magnesian calcite tests were only lightly bored, with on average 9% of the tests scarred by less than a dozen holes (Fig. 1). Since this species is infaunal, boring likely occurred only when tests were brought to the lighted surface during bioturbation.

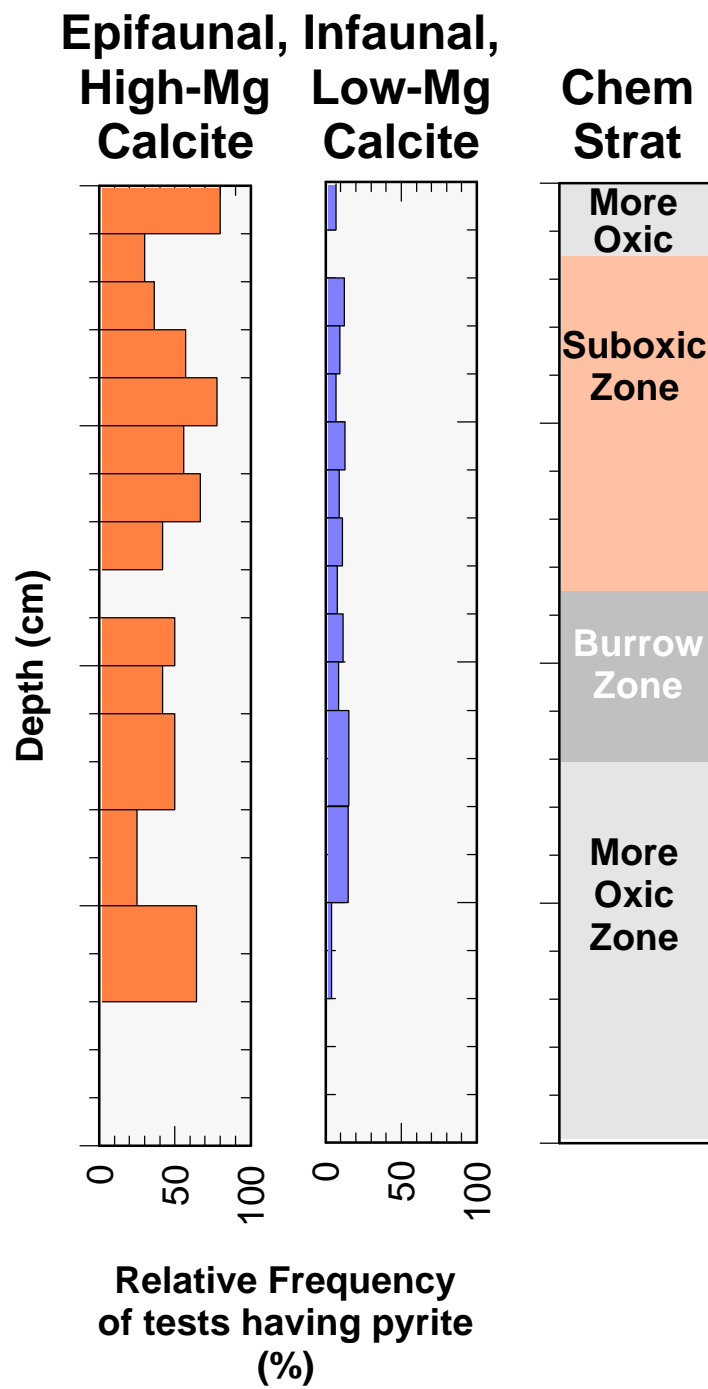


Figure 1. Relative frequency of tests that show heavy boring due to endolithic microorganisms.

Chemical dissolution was evidenced in both high and low magnesian calcite tests. Dissolution was marked in high magnesian calcite tests by thinning of chamberlet walls and delamination of whorls (Plate 2). Dissolution manifested itself in low magnesian calcite tests by widening of natural pores that pierce the test walls, roughening of inner chamber walls, and in severe cases, roughening of outer test walls (Plate 2).

The census of dissolution features shows that the proportion of both low- and high-magnesian calcite tests with dissolution features is small in the upper interval of the box core within the upper, more oxic interval and increases at depth beginning in the upper to middle suboxic zone (Fig. 2). The increases to more frequently damaged tests is clear and consistent among the low-magnesian calcite tests, averaging 81% below 3 cm bsf. This species lives *in situ* at the site, and its dissolution history is affected solely by processes in the core. By contrast, the frequency of dissolved tests is much more variable among the high-magnesian calcite tests, which average only 45% damaged forms below 5 cm bsf. This species was probably transported to the site from the banks surrounding Long and Middle Keys, so its dissolution history is controlled by processes that, in part, occurred outside the core.

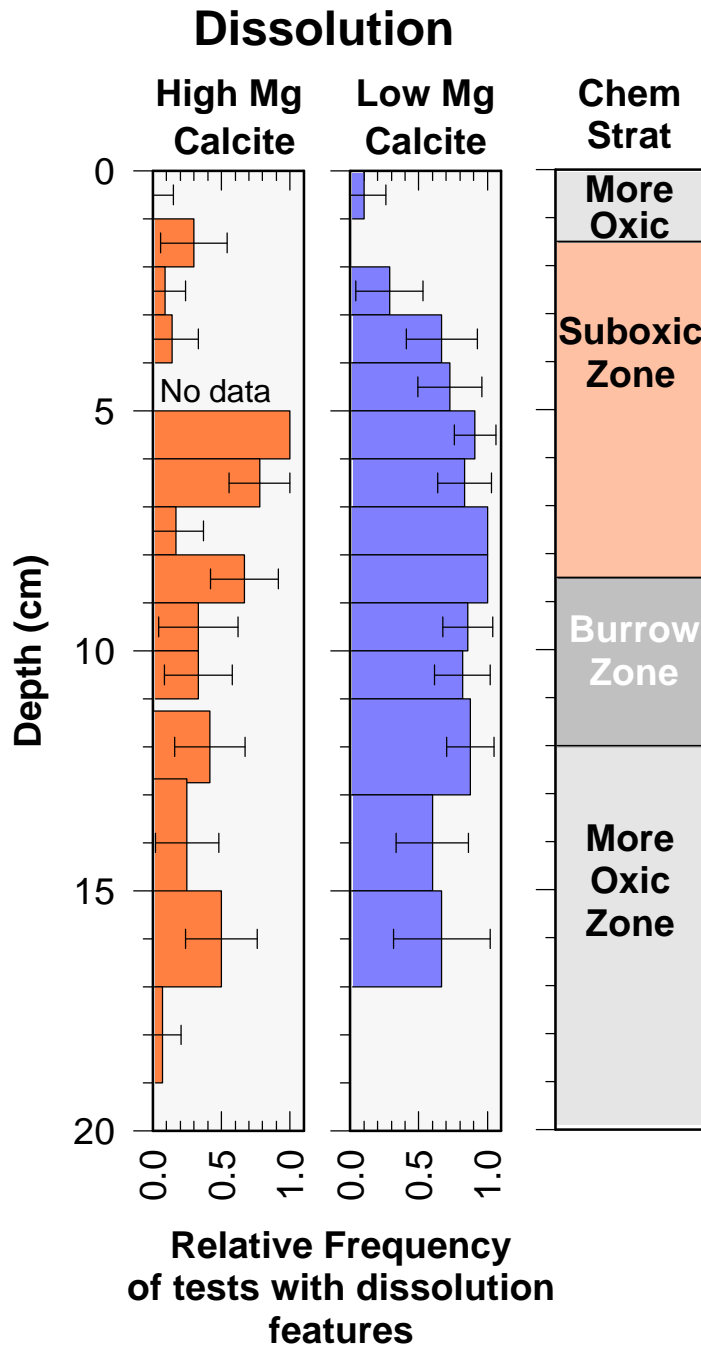
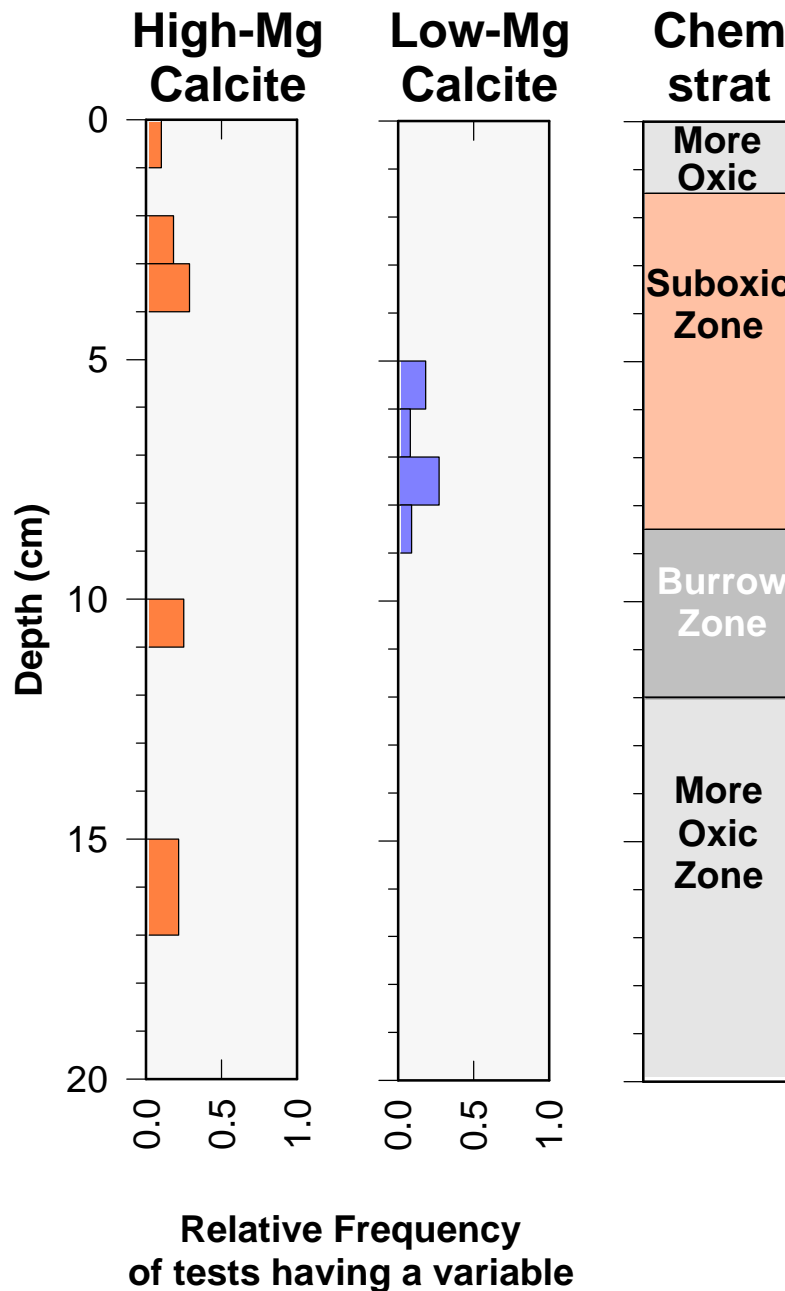


Figure 2. Relative frequency of tests damaged by dissolution.

Calcium carbonate precipitation occurred in two forms: (1) as masses of radiating crystals (aragonite?) about 10 to 15 μm in diameter in micrite both inside and outside

tests, and (2) as microcrystalline filling and rinds in the chamberlets of the high-magnesian calcite tests (Plate 3). Only a few tests of either high- or low-magnesian calcite contain precipitated carbonate, and the amount in any one test is very small, filling no more than $60\text{-}\mu\text{m}^2$. Precipitation on high-magnesian calcite tests occurred in every chemical zone, whereas precipitation on low-magnesian calcite tests was limited to the lower suboxic zone (Fig. 3). However, there were so few instances of precipitation, and it occurred in such small amounts that the apparent trends should be interpreted with



caution.

Figure 3. Relative frequency of tests containing a trace of calcium carbonate precipitation.

Pyrite forms during reduction of sulfate, for example, during bacterial respiration when iron is available (Plate 4). Pyrite framboids approximately 10 μm in diameter occur in tests sporadically with depth and in all chemical zones of the box core (Fig. 4). However, the number of framboids is typically one per test and seldom exceeds three per

test. Hence, the total amount of pyrite found in the tests is extremely small. Pyrite apparently formed in chemical microhabitats within tests that became significantly more reducing than pore waters external to framboid-bearing tests.

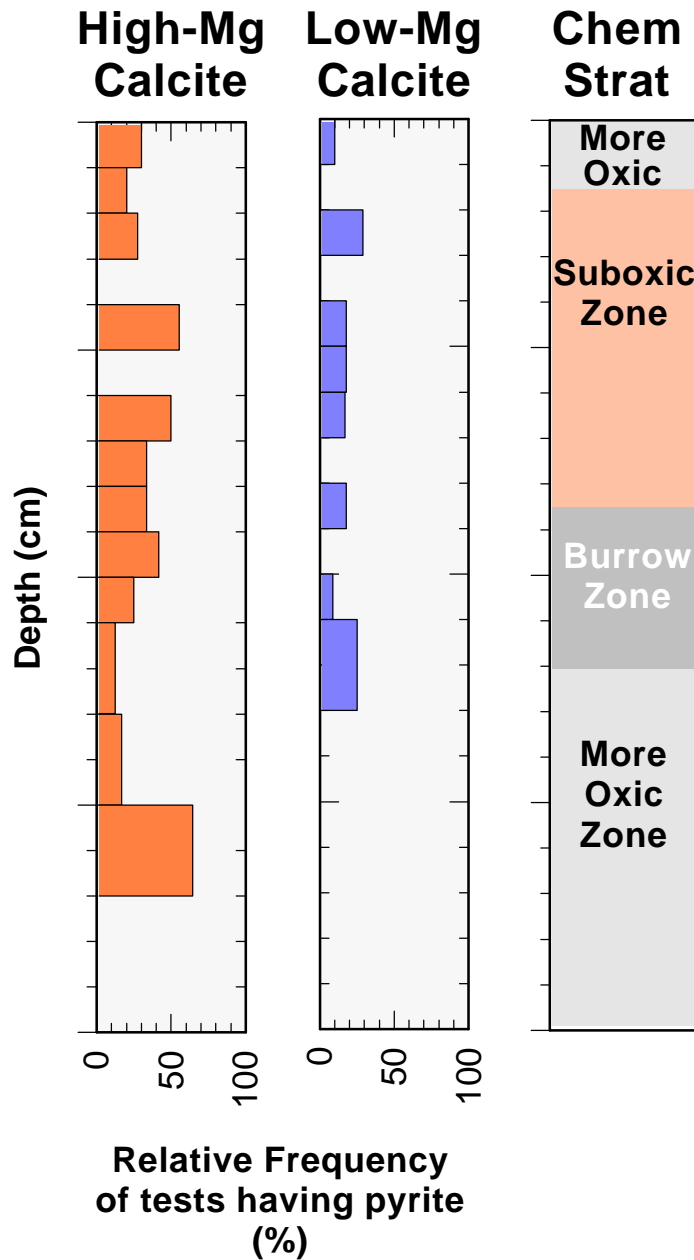


Figure 4. Relative frequency of tests with one or more framboids of pyrite.

Accomplishments: Early Diagenesis

Do foraminiferal tests harbor indications of early diagenesis due to oxidation of organic matter in a pattern consistent with the pore water chemistry? The results show that foraminifer tests do harbor indications of early diagenesis. Specifically, some tests bear framboids of pyrite, many tests are scarred by mild dissolution, and some tests harbor trace amounts of carbonate precipitation. However, the pattern of occurrences of these indicators does not clearly follow that expected based on the model of organic matter oxidation of Froelich et al. (1979). The distribution of affected tests is haphazard throughout the box core, and most effects occur in every zone defined by the pore water zonation of Shiller (pers. comm., 1998).

Shiller (1998) concluded that the pore water chemistry of box cores from the Dry Tortugas test area was profoundly affected by strong bioturbation by the resident callianassid shrimp faunal association (D'Andrea and Lopez, 1997; Lopez, pers. comm., 1998). The result is to circulate oxygenated pore waters into the biotic mixed zone so rapidly that the energetic electron acceptors are refreshed and sulfate reducing bacteria never dominate except in discrete microhabitats. In fact, the process is so vigorous that manganese reduction ceases below 8.5 cm bsf and does not dominate again until more than 150 cm bsf (Shiller, 1998). The tests themselves are stirred through the mixed zone into and out of the various pore water regimes. The effects of organic matter oxidation, however, once imprinted on the tests, persist even though the tests may be removed from the particular pore water environment that produced the effect. Hence, a haphazard distribution of solid effects is produced relative to chemical zonation.

It was not possible to determine if the effects of organic matter oxidation in test interiors preceded those occurring in the matrix, because the distributions were dominated by bioturbation and the reduction gradient was not well developed in the sense of Froelich et al. (1979). It was not possible to show whether high- or low-magnesian calcite tests promoted precipitation, because too little precipitation was observed to make a statistically valid test of the question.

Approach: Paleoenvironment And Depth Of Bioturbation

Two gravity cores were chosen for study. Gravity core KW-PE-GC-225 was selected in preference to others from the Southeast Channel of the Dry Tortugas because it recovered and well represented all of the lithostratigraphic horizons described by Stephens et al. (1997). Gravity core KW-PE-GC-235 was selected from others of the Marquesas study area because of its great length. Additionally, 3 samples, 0-1, 1-2, and 2-3 cm bsf, were selected from the surficial mixed zone (D'Andrea and Lopez, 1997; Bentley and Nittrouer, 1997) of box core KW-PL-BC-185.

The gravity cores were described and sampled at 10-cm intervals. A 20-cc subsample was extracted from the freshly split gravity cores and the box core and washed on a 63 μm screen to remove clay- and silt-size particles. The samples were sieved when dry using a 150 μm screen, and the volume of the residue was reduced to a random subsample of 300 to 400 foraminifers using a microsplitter. The foraminifers were hand-picked from the subsamples, and a census of species was tabulated. Identifications were verified by comparisons to the type material of Cushman (1922), Poag (1981), and Bock

et al. (1971) at the Smithsonian Institution. Grain size data are from Stephens et al. (1997).

Q-mode cluster analysis was used to group together samples with similar relative species frequencies. The clustering method used a simple Euclidean distance coefficient and a within group amalgamation protocol displayed graphically as a dendrogram (Norusis, 1988).

Results: Paleoenvironment

The foraminifer assemblages from the Dry Tortugas and Marquesas Keys are very diverse containing seven suborders and more than 155 species. Inspection of plots of species frequencies versus depth shows several major changes in assemblages at the two sites. At the Dry Tortugas test area, the basal assemblage is dominated by rotalid species characteristic of a shallow marsh environment, including *Criboelphidium poeyanum* and *Ammonia tepida* (Fig. 5). The fauna consists of more than 55% infaunal taxa, and the sediment itself is equal parts silt- and clay-size particles with minor amounts of sand. By contrast, the overlying assemblage is dominated by miliolid and textularid species, and has a much more equitable species distribution. 60 to 75% of the fauna is epifaunal, preferring either hard or phytal substrates to life in the sediment. The sediment is distinctly more sand- and silt-rich than the underlying marsh facies. The faunal sequence suggests environmental succession from a marsh to a backreef, consistent with the Holocene rise in sealevel. It is possible that many of the epiphytic species and those that live on hard substrates have been transported to the site from the adjacent shallow banks because no plants or hard substrates occur in the test site at this time.

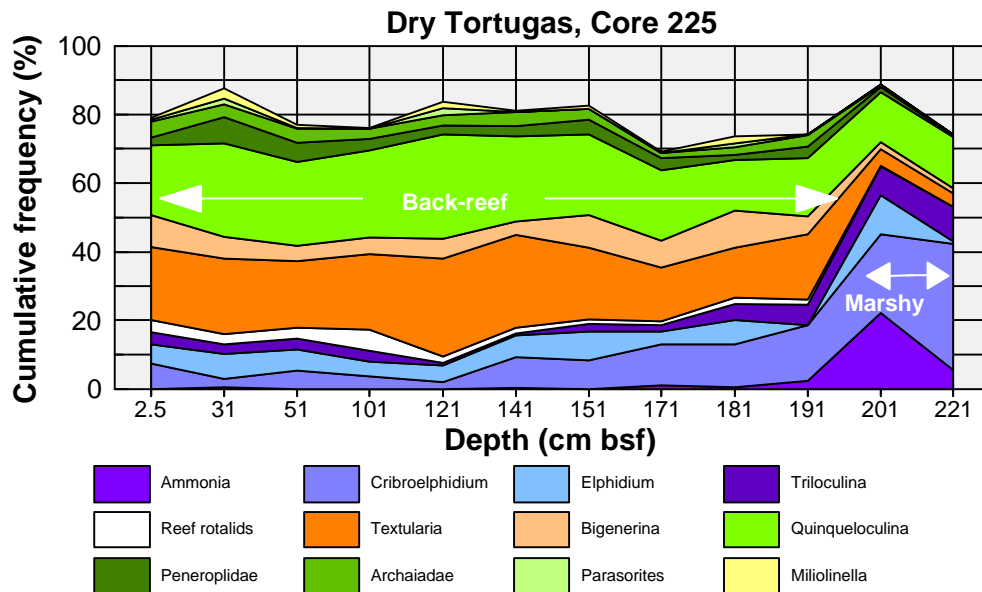


Figure 5. Cumulative frequency of principal taxonomic groups of foraminifers in gravity core KW-PE-GC-225 showing a marsh assemblage at the base of the core and a backreef assemblage in the upper sequence.

At the Marquesas site, the mid-core assemblage is dominated by *Ammonia* and other rotalid species characteristic of a shallow marsh environment (Fig. 6). The fauna consists of more than 80% infaunal taxa, and the sediment itself is a clayey silt with minor amounts of sand. In contrast, samples at the base and top of the core are typical of a carbonate platform environment. Species frequencies are comparatively equitable, with about 40% epifaunal taxa and 60% infaunal taxa. The sediment is sandier and more gravel-rich than that from the middle of the core. The succession of assemblages suggests the passage of a shallow mud bank across the site after the Holocene flooding of the carbonate platform.

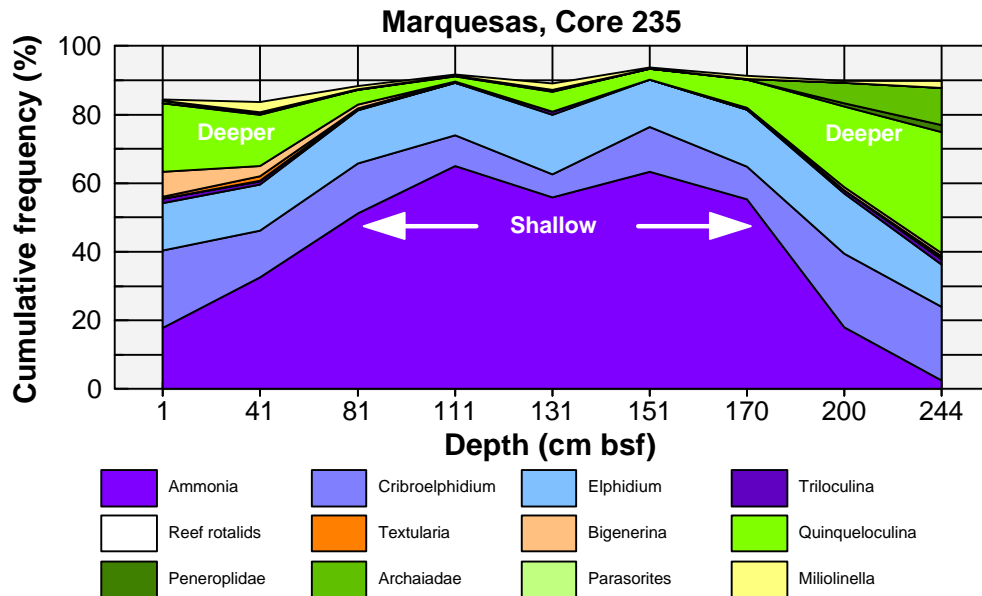


Figure 6. Cumulative frequency of principal taxonomic groups of foraminifera in gravity core KW-PE-GC-235 showing a shallow marshy assemblage between 81 and 170 cm bsf and a carbonate platform assemblage above and below the shallow assemblage.

Results: Depth of bioturbation

The foraminifer assemblage at the Dry Tortugas site can be used to estimate the depth of mixing of sand-size particles as an independent verification of the Pb-210 estimates of Nittrouer and Bentley (1997). A cluster analysis was done on the fauna from the gravity core from Southeast Channel. Included in the analysis were three samples each 1-cm thick from the top 3 cm of the box core, KW-PE-BC-185. I assume that the three samples represent the species currently being mixed in the biotic mixed layer (D'Andrea and Lopez, 1997; Bentley and Nittrouer, 1997). Two clusters emerged from the cluster analysis (Fig. 7). One cluster consisted of the three samples from the top of box core KW-PE-BC-185, three samples from 2.5, 15, and 30 cm bsf and two samples from 180 and 190 cm bsf of gravity core KW-PE-GC-225. The second cluster grouped together samples from 50 to 170 cm bsf in gravity core KW-PE-GC-225.

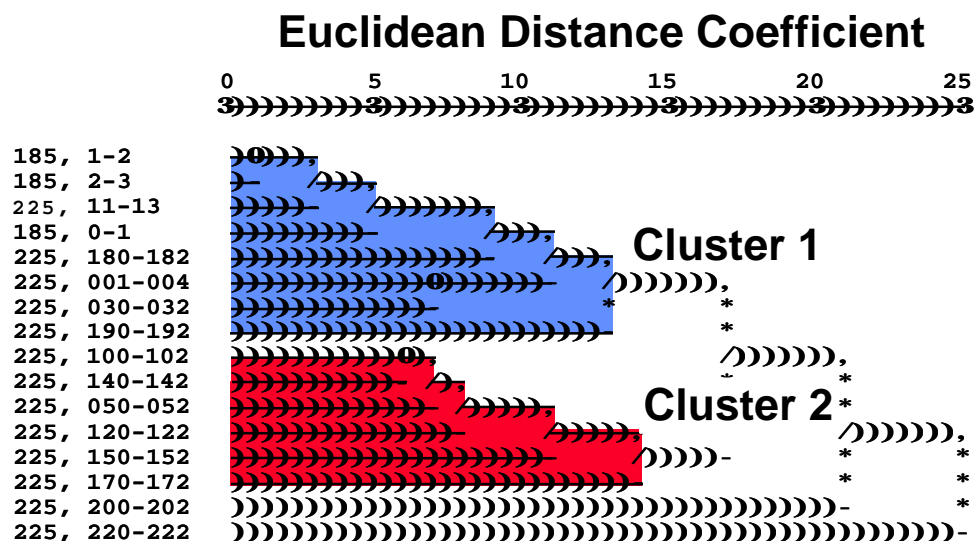


Figure 7. Dendrogram of samples from the mixed layer of box core KW-PL-BC-185 grouped with the samples from gravity core KW-PE-GC-225. Notice that the samples from the upper 30 cm bsf of the gravity core cluster with the samples from the mixed layer.

Cluster 1 is interpreted to be an assemblage of the bioturbated mixed zone of the present-day, because it contains samples that are undoubtedly from the mixed zone of the box core. In contrast, cluster 2 groups together samples containing an assemblage that is significantly different. The implication is that sand-size particles between 30 and 50 cm are no longer moved very much, so that the foraminiferal assemblage is essentially fixed into the permanent record by this depth. The assemblage in the upper mixed zone drifts in species composition from the permanent record because climate continues to change.

Accomplishments: Paleoenvironment And Depth Of Bioturbation

It is important to understand the nature of bioturbational mixing in the Dry Tortugas area. D'Andrea and Lopez (1997) observed two layers of mixing, a shallow zone and a deep zone. The shallow zone from 0 to 4 cm is dominated by surface deposit feeding polychaetes and burrowing bivalves that mix the sediment in days to weeks. The result is vsupported by the activity of Th-234 with depth (Bentley and Nittrouer, 1997). The deep zone may extend to 40 to 60 cm bsf and includes deep deposit feeders such as *Callianassa* sp. and *Notomastus* sp., which recycle sediment at rates that diminish with increasing depth (Lopez, pers. comm., 1998; D'Andrea and Lopez, 1997; Bentley and Nittrouer, 1997). Deep deposit feeders, like callianassid shrimp, feed in deep burrows with inhalent and exhalent burrows. Water, organic particles, and small sediment grains are entrained in the inhalent tube, and small grains are expelled through the exhalent tube. The shrimp build elaborate burrows with chambers and galleries for various purposes. The excavated silt and finest sand is expelled (recycled) to the surface, and coarse grains are stacked in chambers, which are filled and abandoned.

The activities leave a distinctive lithologic signature described by Tudhope and Scoffin (1984) and consistent with the succession of lithologic units described throughout

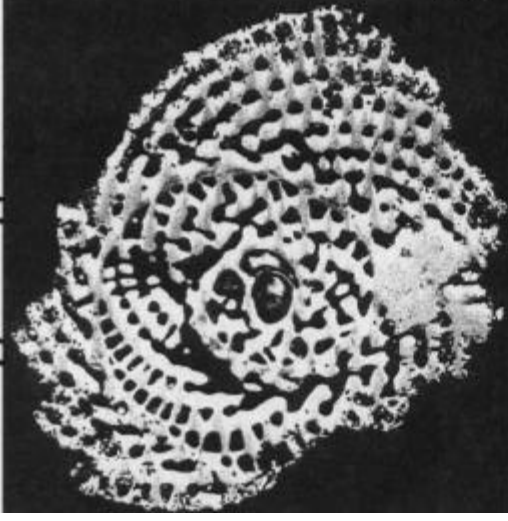
the Dry Tortugas test site (Stephens et al., 1997). The texture of such a sequence is silty at the top where *Callianassa* pile expelled sediment, and grades at depth to sand with concentrations of shells in poorly sorted sand at depth (Tudhope and Scoffin, 1984). Gravel-size particles are probably moved the least because they are sequestered in storage chambers by the shrimp, though the gravel-size shells could have originated at any depth overlying the shrimp or along its excavated burrow system. The silt and finest sediment is most susceptible to repeated recycling, in which it is excavated from depth, piled at the surface, and subsequently remobilized down the inhalent tube for another cycle of movement. Sand-size debris, like foraminifers, likely has a fate that falls between that of silt and gravel. These results suggest this middle course for the fate of sand-size debris because the foraminiferal fauna has taken on a permanent aspect between 30 and 50 cm bsf, above the shallowest concentration of shell debris in the core (90 cm bsf) and perhaps above or similar to the depth of habitation of the callianassid shrimp.

There is a period of time before a permanent record is deposited, and the mixed layer, including the tests that it contains, holds a mixture of specimens that lived throughout the time interval before permanent deposition. The minimum duration to deposit 35 cm is about 117 years, based on the maximum possible accumulation rate estimated from excess Pb-210 gradients (Bentley and Nittrouer, 1997). A reasonable maximum duration to deposit 35 cm is about 1750 years calculated by assuming a sedimentation rate equal to the net Holocene rate (~20 cm/ky).

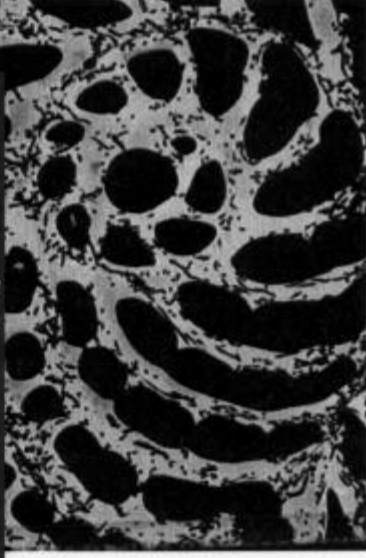
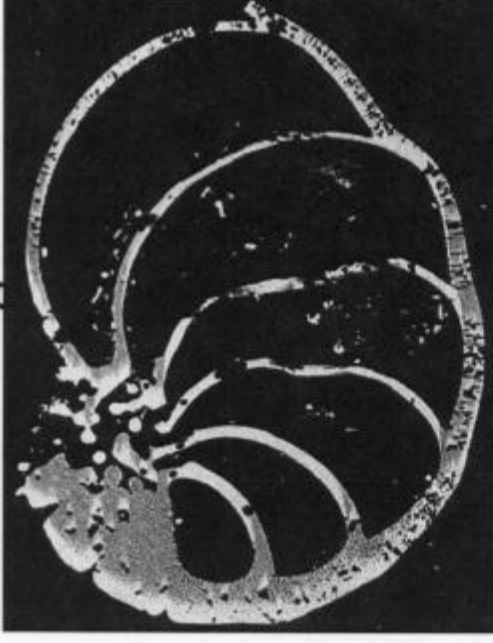
Summary Of Principal Accomplishments:

- 1) Scanning electron microscopic examination of foraminifer tests revealed only trace effects due to oxidation of organic matter. There was some dissolution, minor amounts of aragonite(?) precipitation, and very minor amounts of pyrite formation.
- 2) The effects due to oxidation of organic matter, especially formation of pyrite, apparently occurred in microhabitats found, for example, within foraminiferal tests. Results from pore water chemistry (see Shiller publications listed in references) suggest that sediments at the Dry Tortugas test site are suboxic within millimeters of the sediment surface, but never reach levels strong enough to reduce sulfate in the general mass of sediment.
- 3) The sequences at the Dry Tortugas test site include a basal marsh deposit overlain by coarser backreef sediments extensively reworked by deep deposit feeders. The sequence is consistent with deposition during the Holocene rise in sea level. The sequence at the Marquesas test site consists of a shallow mud-bank deposit that is under- and overlain by typical carbonate platform sediments. The sequence is consistent with migration of a mudwave across the site after inundation by the Holocene rise in sea level.
- 4) The depth where mixing of sand-size foraminifers affectively ceases and the permanent record begins lies between 30 and 50 cm bsf. This depth of mixing is consistent with results from excess Pb-210 (Bentley and Nittrouer, 1997).

High-Mg calcite



Low-Mg calcite



Bore holes

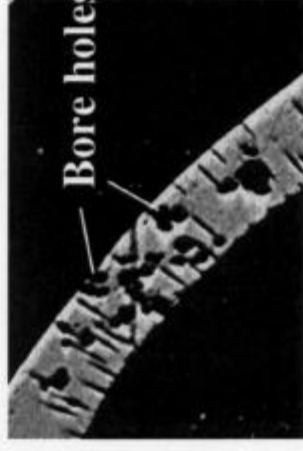
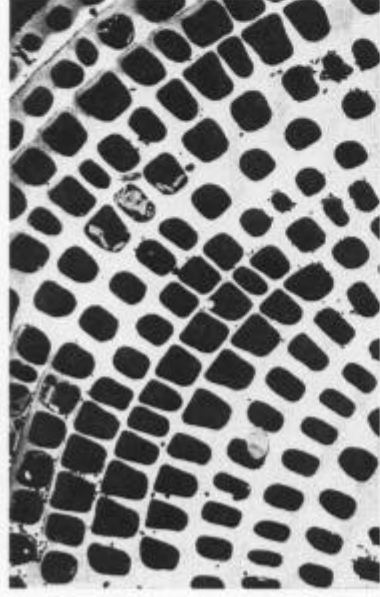


Plate 2.

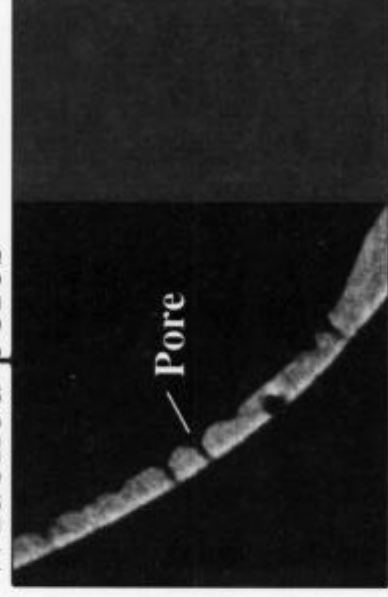
High-Mg calcite

Thinned walls

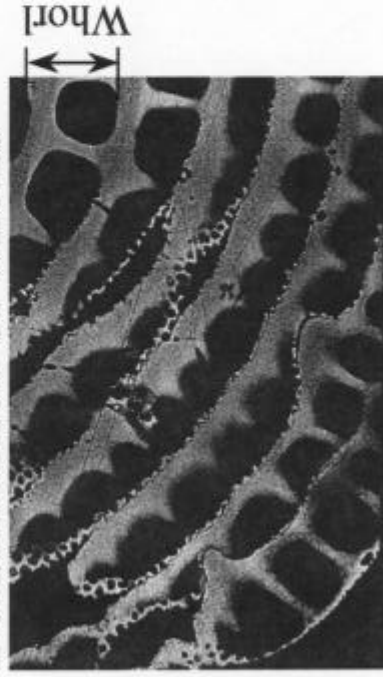


Low-Mg calcite

Widened pores



Delamination of whorls



Normal pores

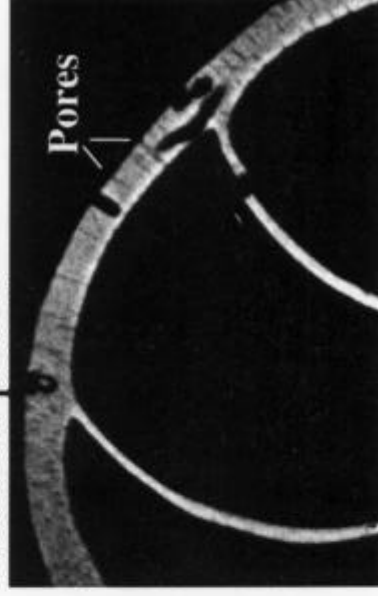
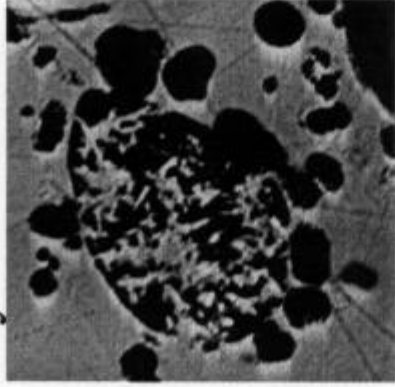
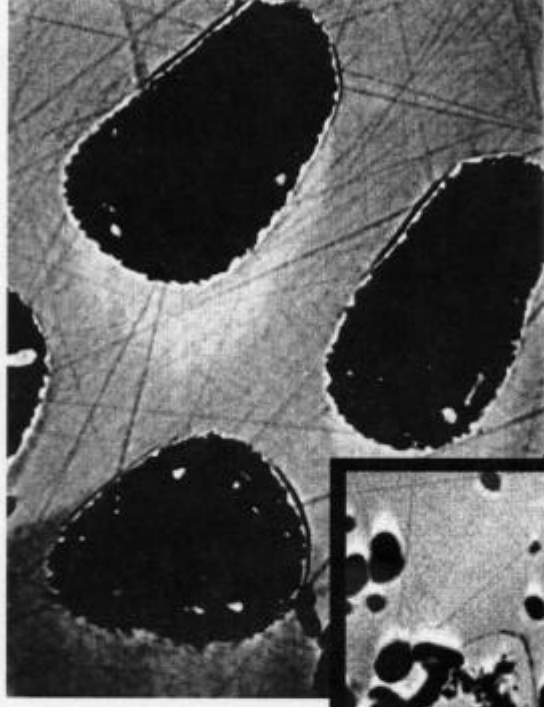


Plate 3.

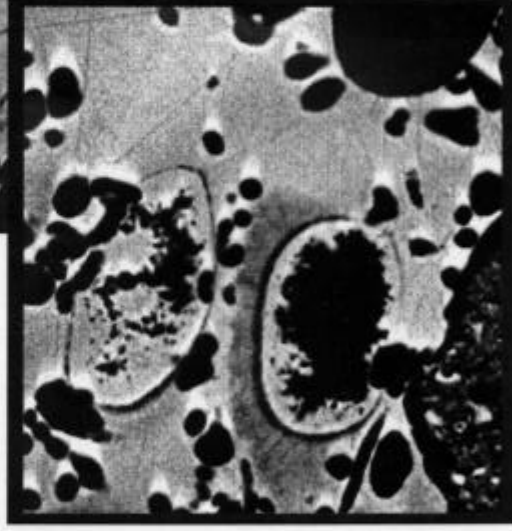
Crystals in chamberlet



Rinds in chamberlets



Rinds

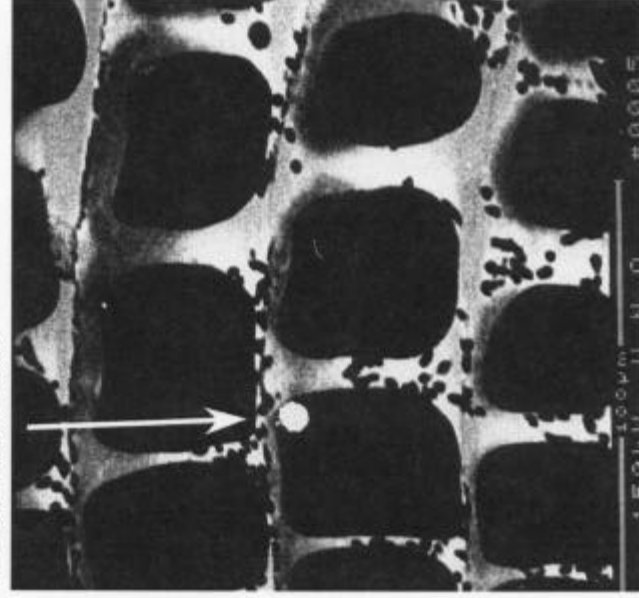


Crystal mass

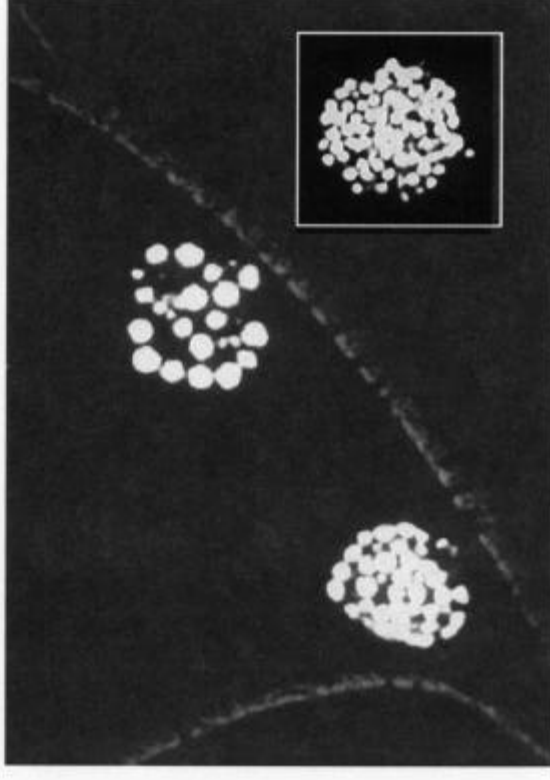


Plate 4.

Framboid



Framboids



References:

- Bentley, S. J., and Nittrouer, C. A., 1997. Environmental influences on the formation of sedimentary fabric in a fine-grained carbonate-shelf environment: Dry Tortugas, Florida Keys. *Geo-Marine Letters*, 17:268-275.
- Bock, W. D., Hay, W. W., Jones, J. I., Lyntz, G. W., Smith, S. L., and Wright, R. C., 1971. A Symposium of Recent South Florida Foraminifera, Miami Geological Society Memoir 1, 245p.
- Cushman, Joseph A., 1922. Shallow-water foraminifera of the Tortugas Region, Carnegie Institution of Washington No. 133, 97p.
- D'Andrea, A. F., and Lopez, G. R., 1997. Benthic macrofauna in a shallow water carbonate sediment: major bioturbators at the Dry Tortugas. *Geo-Marine Letters*, 17:276-282.
- Froelich, P. N., Klinkhammer, G. P., Bender, M. L., Luedtke, N. A., Heath, G. Ross, Cullen, Doug, and Dauphin, Paul, 1979. Early oxidation of organic matter in pelagic sediments of the eastern equatorial Atlantic: suboxic diagenesis. *Geochimica et Cosmochimica Acta*, 43:1075-1090.
- Golubec, S., Perkins, R. D., and Lukas, K. J., 1975. Boring microorganisms and microborings in carbonate substrates. In: Frey, R. W., (ed.), *The Study of Trace Fossils*, Springer-Verlag, New York, p. 229-260.
- Golubec, S., Campbell, S. E., Drobne, K., Cameron, B., Balsam, W. L., Cimerman, F., and DuBois, L., 1984. *J. Paleontology*, 58(2):351-361.
- Golubic, S., Brent, G., and Le Campion, T., 1970. Scanning electron microscopy of endolithic algae and fungi using a multipurpose casting embedding technique. *Lethaia*, 3:203-209.
- Hallock, Pamela, Cottey, Theresa L., Forward, Linda B., and Halas, John, 1986. Population biology and sediment production of *Archaias angulatus* (Foraminiferida) in Largo Sound, Florida, *Journal of Foraminiferal Research*, 16(1):1-8.
- Hudson, J. Harold, 1985. Growth rate and carbonate production in *Halimeda opuntia*: Marquesas Keys, Florida. In: D. F. Toomey and M. H. Nitecki, eds., *Paleoalgology: Contemporary Research and Application*, p. 257-263.
- Mullins, Hank T., Thompson, J.B., McDougall, Kristin, and Vercoutere, T.L., 1985. Oxygen-minimum zone edge effects: evidence from the central California coastal upwelling system. *Geology*, 13:491-494.

Murray, John W., 1991. Ecology and Palaeoecology of Benthic Foraminifera, John Wiley & Sons, Inc., New York, 397p.

Norusis, M.J., 1988. SPSS/PC+Advanced Statistics TM V2.0 for the IBM PC/XT/AT and PS/2: Chicago(SPSS Inc.).

Orsi, Thomas, H., Anderson, A.L., Davis, K. S., Bryant, W. R., Rezak, R., Rutledge, A. K., Fischer, K., Falster, A., and Brunner, C., (in prep.), Computed tomography and geoacoustic properties of carbonate muds from Marquesas Keys and Dry Tortugas, South Florida (Coastal Benthic Boundary Layer Special Research Project), NRL Report. Perry, C. T., 1998. Grain susceptibility to the effects of microboring: implications for the preservation of skeletal carbonates. *Sedimentology*, 45:39-51.

Poag, C. Wylie, 1981. Ecologic Atlas of Benthic Foraminifera of the Gulf of Mexico. Marine Science International, Woods Hole, MA, 174 p.

Shiller, Alan, M., Brunner, Charlotte A., Furukawa, Yoko, Hebert, Tracy, and Yuan, Jinchun, 1998. Early Diagenesis of carbonate sediments in the Dry Tortugas and Marquesas Keys, Florida, USA. . *Journal of the Mississippi Academy of Sciences*, 43(1):52.

Shiller, A. M., Hebert, T. L., Thornton, K. R., and Brunner, C. A., 1995. Sediment chemistry and pore water fluxes in the vicinity of the Dry Tortugas, The 1st SEPM Congress on Sedimentary Geology, Congress Program and Abstracts, v. 1, p. 113.

Stephens, Kevin P., Fleischer, Peter, Lavoie, Dawn, and Brunner, Charlotte, 1997. Scale-dependent physical and geoacoustic property variability of shallow-water carbonate sediments from the Dry Tortugas, Florida. *Geo-Marine Letters*, 17(4):299-305.

Stephens, K. P., Lavoie, D. L., Briggs, K.B., Richardson, M. D., and Furukawa, Y., 1997. Geotechnical and geoacoustic properties of sediments off south Florida: Boca Raton, Indian Rocks Beach, Lower Tampa Bay, and the Lower Florida Keys. Stennis Space Center, MS, Naval Research Laboratory, NRL/MR/7431-97-8042. 310p.

Publications:

Peer Reviewed:

Brunner, C. A., (in prep.). Paleoenvironment at Marquesas Keys and Dry Tortugas CBBL Sites, Florida. *Marine Geology*.

Brunner, C. A., (in prep.). Affect of early diagenesis on foraminifer tests from a backreef environment. *Journal of Foraminiferal Research*.

Shiller, A., and Brunner, C. A., (in prep.). Early diagenesis of carbonate sediments in the backreef environment of the Dry Tortugas, Florida. *Marine Geology*.

Symposium Proceedings:

Brunner, C. A., 1997. Paleoenvironment at Marquesas Keys and Dry Tortugas CBBL Sites, Florida, CBBL Workshop, Feb 4-7, 1997, Stennis Space Center, MS.

Published Abstracts:

Shiller, A. M., Hebert, T. L., Thornton, K. R., and Brunner, C. A., 1995. Sediment chemistry and pore water fluxes in the vicinity of the Dry Tortugas, The 1st SEPM Congress on Sedimentary Geology, Congress Program and Abstracts, v. 1, p. 113.

Brunner, C., Reed, A., Elder, R., Falster, A., and Shiller, A., 1996. Effects of organic carbon respiration on preservation of foraminifers from the Dry Tortugas, Florida. *Journal of the Mississippi Academy of Sciences*, 41(1): 54.

Shiller, Alan, M., Brunner, Charlotte A., Furukawa, Yoko, Hebert, Tracy, and Yuan, Jinchun, 1998. Early Diagenesis of carbonate sediments in the Dry Tortugas and Marquesas Keys, Florida, USA. *Journal of the Mississippi Academy of Sciences*, 43(1):52.

Thesis:

I served as major professor and chaired the thesis committee of Kevin P. Stephens.

Stephens, Kevin P., 1997. Scale-dependent physical and geoacoustic property variability of shallow-water carbonate sediments from the Dry Tortugas, Florida. University of Southern Mississippi, Masters Thesis, 87p.

Effects of Carbonate Dissolution and Precipitation on Sediment Physical Properties and Structure in the Key West Area: Microfossils Component

CHARLOTTE A. BRUNNER

**Associate Professor of Marine Science
Department of Marine Science
Institute of Marine Sciences
The University of Southern Mississippi
John C. Stennis Space Center, MS 39529, U.S.A.**

Abstract:

Early diagenesis of organic matter in sediments affects not only the chemistry of sediment pore waters, but also modifies the solid constituents. The two approaches in combination, analysis of pore waters and observation of solid constituents, provide an effective approach to monitoring the reducing condition of the sediment. This study examined the effects of early diagenesis on benthonic foraminifers, a common constituent of sediments from the Key West area, and compared the results with the pore water profiles analyzed by A. Shiller. Some foraminifers showed evidence of reducing conditions in test interiors indicated by dissolution features, minor precipitation of calcium carbonate, and formation of pyrite framboids, which required reduction of sulfate. However, pore waters showed evidence of only mildly reducing conditions, where sulfate reduction was not reached. Evidently, the foraminifer tests successfully formed micro-chemical habitats in which more strongly reducing conditions were occasionally achieved. Interestingly, the distribution of tests with diagenetic modifications bears little relationship to the diagenetic zones defined from the pore water chemistry, which is entirely consistent with intense bioturbation.

Other accomplishments achieved as a by-product of the proposed work included depositional histories of the Dry Tortugas and Marquesas test sites, and an estimate of depth of bioturbational mixing of sand-size particles.

Original Objectives:

Benthic foraminifers are important constituents of sediments in the backreef environment. They form a significant proportion of the sediments in the Dry Tortugas region, comprising about 12% of the particles in the sand-size fraction (Orsi et al., unpub. rep., 1995). The large proportion is consistent with data on foraminifer productivity, which shows that carbonate production by large foraminifers (Hallock et al., 1986) is on the same order of magnitude as that of green algae, like *Halimeda* (Hudson, 1985), which are widely regarded as a principal source of the carbonate in the platform/reef environment. For example, *Archaias angulatus*, a large miliolid foraminifer, produces 60 g of $\text{CaCO}_3/\text{m}^2/\text{y}$ in Key Largo Sound of the Florida Keys, and large rotaliine foraminifers

produce up to 2,800 g of $\text{CaCO}_3/\text{m}^2/\text{y}$ in the reef flats of Palau (Hallock, 1981, 1984, 1986).

Oxidation of organic matter is an important process in surface sediments of the Tortugas region, based on preliminary data (Shiller et al., 1995). Early diagenesis of organic matter proceeds through a sequence of reducing reactions described by Froelich et al. (1979). The reactions include bacterial reduction of oxygen, followed by manganese oxide, nitrate, iron oxides, and sulfate. Some of these reactions produce protons, which promotes the dissolution of a carbonate, and other reactions consume protons, which promotes carbonate precipitation. The resultant dissolution and cementation could significantly affect the acoustic properties of sediment, and so study of early diagenesis is relevant to the CBBL project.

Solid products of organic carbon diagenesis

Foraminifer tests may play an interesting and important role in early diagenesis of carbonate sediment for two reasons. (1) The chambered tests enclose a chemical micro-environment that is isolated from surrounding pore waters and matrix except for restricted access through narrow apertures, canals, and small pores. The test interiors of the diverse fauna (7 of 10 extant suborders and more than 155 species) offer a variety of shapes and different-sized spaces, which may promote dissolution or precipitation of carbonate and other solid products of oxidation and reduction, such as manganese oxide and iron sulfide. (2) Tests of different suborders are made of different forms of calcium carbonate, including high and low magnesian calcite and aragonite. These different phases have different solubilities, and their surfaces may affect precipitation in different ways.

This work examines the following questions. 1) *Do foraminiferal tests harbor indications of early diagenesis due to oxidation of organic matter in a pattern consistent with the pore water chemistry?* 2) *Does the reduction sequence in the sediment column occur in test interiors sooner (e.g., at a shallower depth) than in the matrix hosting the tests due to formation of chemical micro-habitats in test interiors?* 3) *Does test composition promote or retard precipitation?*

Paleoenvironmental analysis and depth of mixing

In the original proposal, I hoped to develop a proxy of paleo-reduction intensity by comparing the ratio of epifaunal to infaunal species in gravity cores. However, many epifaunal species appear to have been transported to the Dry Tortugas test site, so it was not possible to develop such a proxy. However, analysis of the fauna from gravity cores produced several useful results. First, successions of depositional environments were clearly defined and detailed based on a census of foraminiferal species. Second, the depth of mixing estimated by Pb-210 was corroborated by faunal assessment.

Approach: The Role Of Foraminifers In Early Diagenesis Of Carbon

Box core KW-PL-BC-185 from the Southeast Channel of the Dry Tortugas, was selected for detailed analysis because the surface layer was apparently recovered intact, the core was relatively long (>20 cm), and pore water profiles of various chemical tracers of organic matter respiration and carbonate precipitation/cementation were available. The box core was divided into 1-cm thick slabs from 0 to 11 cm below sea floor (bsf) and 2-

cm thick slabs from 11 to 17 cm bsf. A 20-cc subsample was removed from each slab and washed on a 63 μm screen to remove clay- and silt-size particles. Ten to 15 specimens of each of two species were hand picked from the $>150\ \mu\text{m}$ fraction of the sand-size residue, mounted in low viscosity SPURR resin, sectioned, polished and prepared for scanning electron microscopy using backscattered electrons.

The species selected were *Parasorites orbitiloides* and *Nonionella grateloupe*, which differ from each other in several relevant qualities. The former is made of high-magnesian calcite, and its interior is subdivided into a labyrinth of hundreds of small chamberlets that average 40 to 50 μm in diameter (Murray, 1991). The protist is epiphytic and was likely swept from the shallow banks of the Dry Tortugas and transported to the test site. In contrast, the latter protist is made of low-magnesian calcite, and its interior is subdivided into ~15 chambers that increase in size from about 40 μm to 300 μm in length. The protist is infaunal and likely lived *in situ* (Murray, 1991).

Each sectioned test was completely inspected at 1000x magnification, and a census was made of features indicative of carbonate dissolution, carbonate precipitation, and presence of solid products of early diagenesis, such as pyrite, phosphorite, and manganese oxide.

The box core was subdivided into chemical zones that characterized oxidation state based on pore water concentrations of Mn, Mo, U, and PO_4 (Shiller, pers. comm., 1998). A suboxic zone from 1.5 to 8.5 cm bsf was delineated based on an increase in pore water concentrations of Mn. More oxic intervals characterized the surficial layer from 0 to 1.5 cm bsf and the basal layer from 12 cm bsf to bottom of the core. A zone of heightened oxygenation was noted from about 8.5 to 12 cm bsf, based on elevated concentrations of Mo and U and depleted concentrations of Mn and PO_4 . The heightened oxygenation suggests the recent passage of a burrowing organism, which entrained oxygenated bottom water into its burrow.

Results: Early Diagenesis

Carbonate was dissolved from tests by two separate processes: (1) chemical dissolution and (2) boring by endolithic micro-organisms, principally algae (Golubic et al., 1984; Perry, 1998). Endolithic micro-organisms excavated elongate holes 4 to 8 μm in diameter that originate at inner or outer test surfaces and extend in curved or straight form into interiors of test walls (Perkins and Tsentas, 1976; Golubec et al., 1975). The interior sculpture could be used to determine the taxa of the borers, but this question was not pursued in this study (Golubic et al., 1970). Among the high-magnesian calcite tests, nearly half of all the specimens examined were heavily bored, and virtually no test was left untouched (Plate 1). Boring likely occurred in the photic zone during transport from the banks to the site, and during residence on the sediment surface before burial. By contrast, the infaunal, low-magnesian calcite tests were only lightly bored, with on average 9% of the tests scarred by less than a dozen holes (Fig. 1). Since this species is infaunal, boring likely occurred only when tests were brought to the lighted surface during bioturbation.

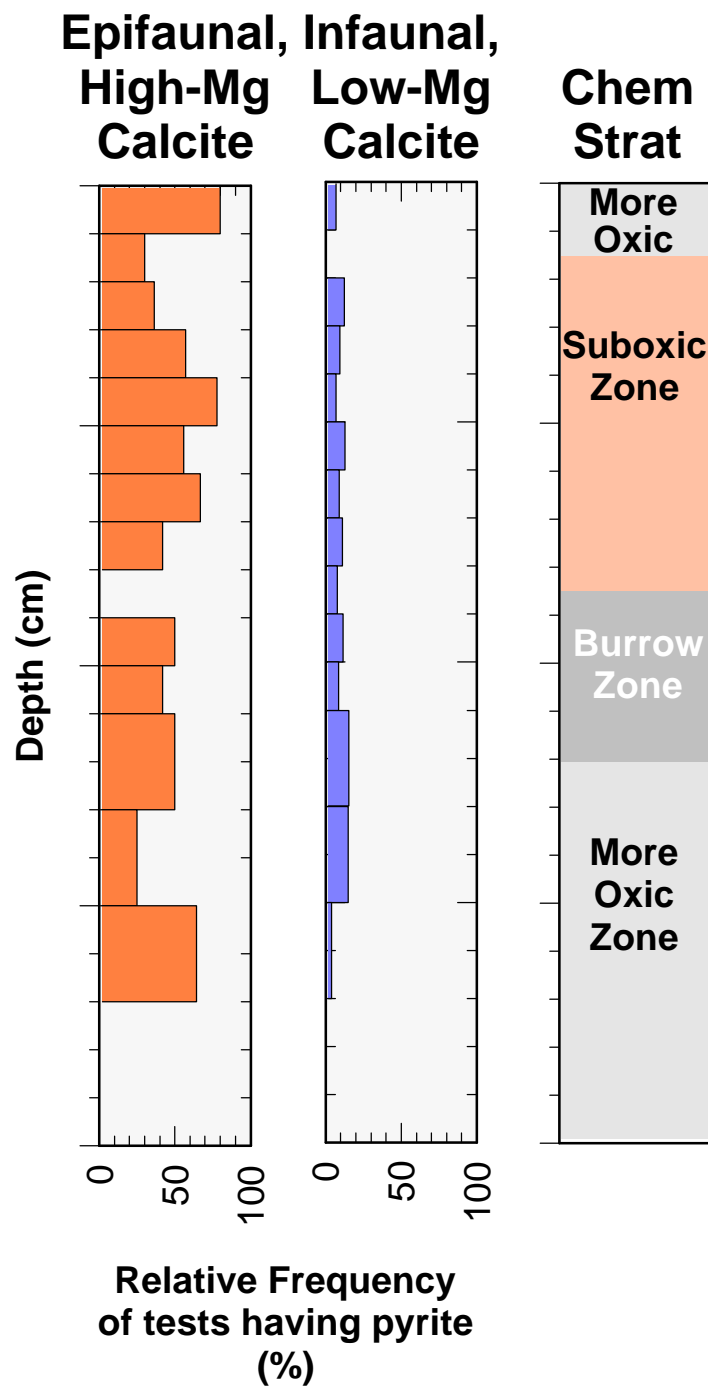


Figure 1. Relative frequency of tests that show heavy boring due to endolithic microorganisms.

Chemical dissolution was evidenced in both high and low magnesian calcite tests. Dissolution was marked in high magnesian calcite tests by thinning of chamberlet walls and delamination of whorls (Plate 2). Dissolution manifested itself in low magnesian calcite tests by widening of natural pores that pierce the test walls, roughening of inner chamber walls, and in severe cases, roughening of outer test walls (Plate 2).

The census of dissolution features shows that the proportion of both low- and high-magnesian calcite tests with dissolution features is small in the upper interval of the box core within the upper, more oxic interval and increases at depth beginning in the upper to middle suboxic zone (Fig. 2). The increases to more frequently damaged tests is clear and consistent among the low-magnesian calcite tests, averaging 81% below 3 cm bsf. This species lives *in situ* at the site, and its dissolution history is affected solely by processes in the core. By contrast, the frequency of dissolved tests is much more variable among the high-magnesian calcite tests, which average only 45% damaged forms below 5 cm bsf. This species was probably transported to the site from the banks surrounding Long and Middle Keys, so its dissolution history is controlled by processes that, in part, occurred outside the core.

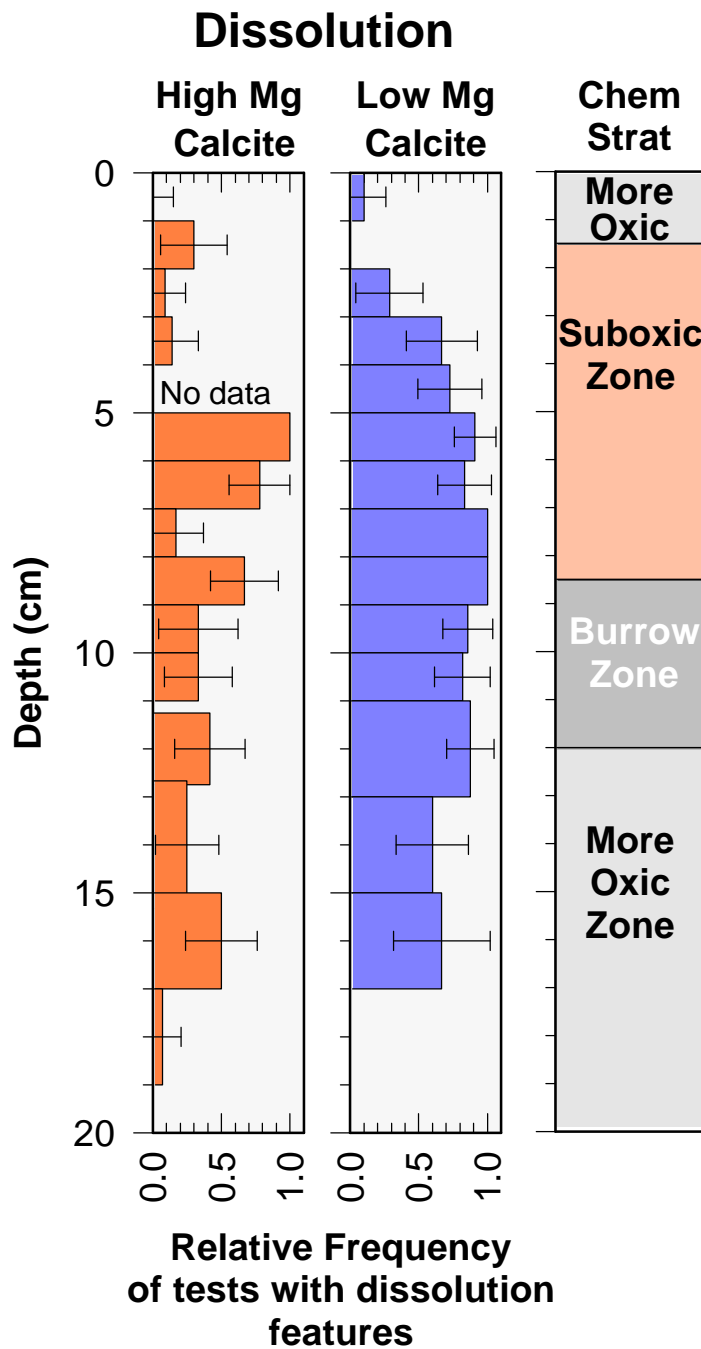
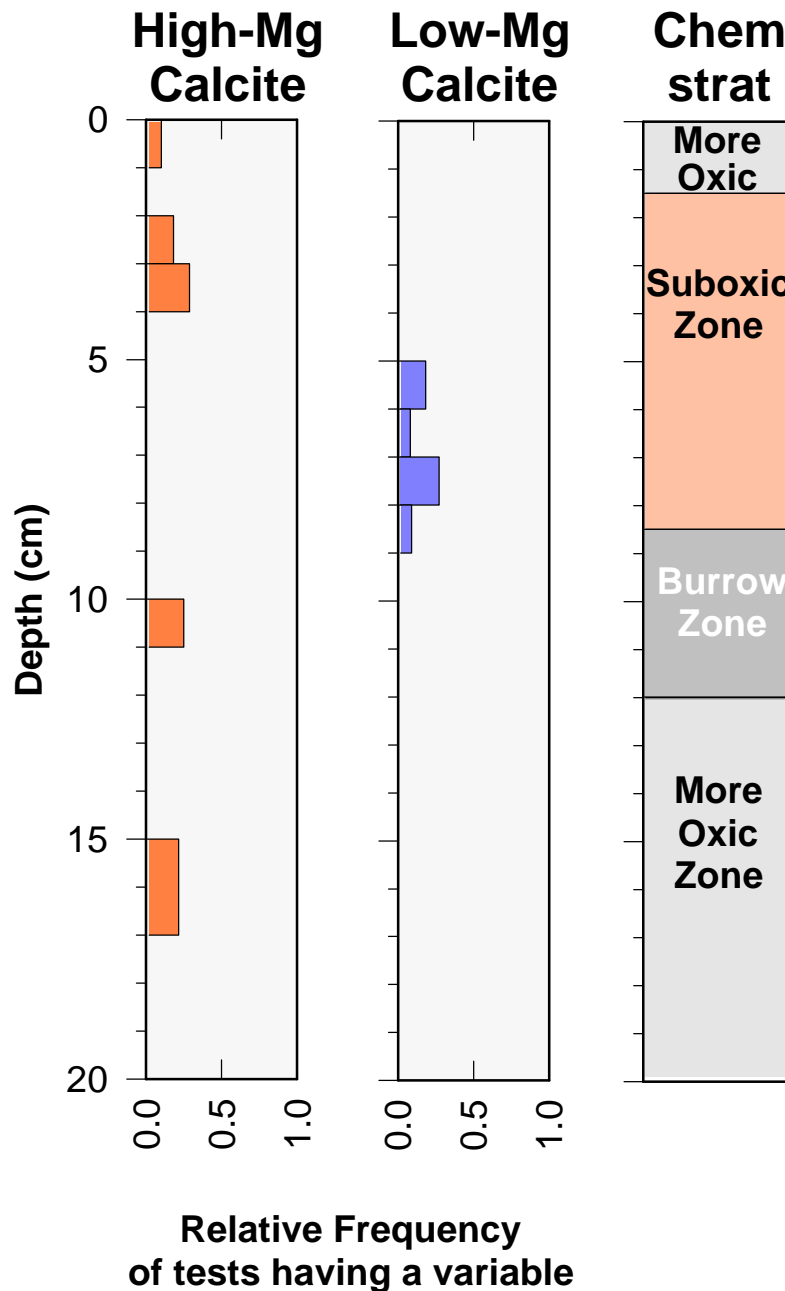


Figure 2. Relative frequency of tests damaged by dissolution.

Calcium carbonate precipitation occurred in two forms: (1) as masses of radiating crystals (aragonite?) about 10 to 15 μm in diameter in micrite both inside and outside

tests, and (2) as microcrystalline filling and rinds in the chamberlets of the high-magnesian calcite tests (Plate 3). Only a few tests of either high- or low-magnesian calcite contain precipitated carbonate, and the amount in any one test is very small, filling no more than $60\text{-}\mu\text{m}^2$. Precipitation on high-magnesian calcite tests occurred in every chemical zone, whereas precipitation on low-magnesian calcite tests was limited to the lower suboxic zone (Fig. 3). However, there were so few instances of precipitation, and it occurred in such small amounts that the apparent trends should be interpreted with



caution.

Figure 3. Relative frequency of tests containing a trace of calcium carbonate precipitation.

Pyrite forms during reduction of sulfate, for example, during bacterial respiration when iron is available (Plate 4). Pyrite framboids approximately 10 μm in diameter occur in tests sporadically with depth and in all chemical zones of the box core (Fig. 4). However, the number of framboids is typically one per test and seldom exceeds three per

test. Hence, the total amount of pyrite found in the tests is extremely small. Pyrite apparently formed in chemical microhabitats within tests that became significantly more reducing than pore waters external to framboid-bearing tests.

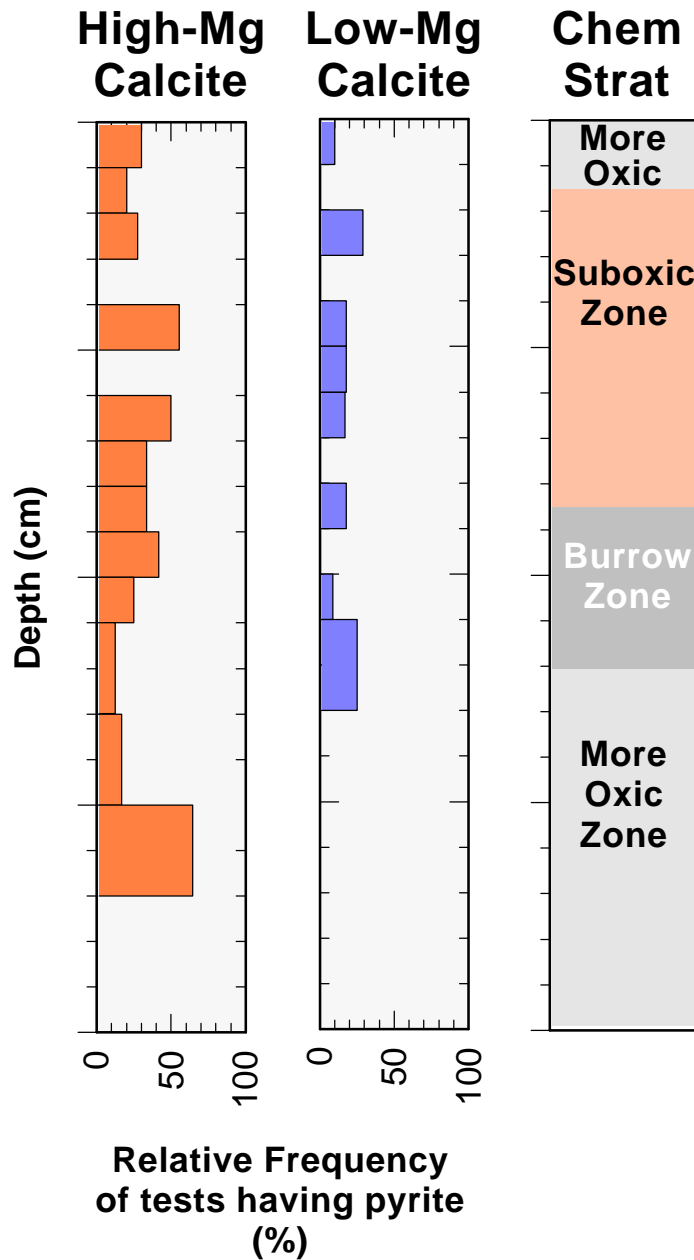


Figure 4. Relative frequency of tests with one or more framboids of pyrite.

Accomplishments: Early Diagenesis

Do foraminiferal tests harbor indications of early diagenesis due to oxidation of organic matter in a pattern consistent with the pore water chemistry? The results show that foraminifer tests do harbor indications of early diagenesis. Specifically, some tests bear framboids of pyrite, many tests are scarred by mild dissolution, and some tests harbor trace amounts of carbonate precipitation. However, the pattern of occurrences of these indicators does not clearly follow that expected based on the model of organic matter oxidation of Froelich et al. (1979). The distribution of affected tests is haphazard throughout the box core, and most effects occur in every zone defined by the pore water zonation of Shiller (pers. comm., 1998).

Shiller (1998) concluded that the pore water chemistry of box cores from the Dry Tortugas test area was profoundly affected by strong bioturbation by the resident callianassid shrimp faunal association (D'Andrea and Lopez, 1997; Lopez, pers. comm., 1998). The result is to circulate oxygenated pore waters into the biotic mixed zone so rapidly that the energetic electron acceptors are refreshed and sulfate reducing bacteria never dominate except in discrete microhabitats. In fact, the process is so vigorous that manganese reduction ceases below 8.5 cm bsf and does not dominate again until more than 150 cm bsf (Shiller, 1998). The tests themselves are stirred through the mixed zone into and out of the various pore water regimes. The affects of organic matter oxidation, however, once imprinted on the tests, persist even though the tests may be removed from the particular pore water environment that produced the effect. Hence, a haphazard distribution of solid effects is produced relative to chemical zonation.

It was not possible to determine if the effects of organic matter oxidation in test interiors preceded those occurring in the matrix, because the distributions were dominated by bioturbation and the reduction gradient was not well developed in the sense of Froelich et al. (1979). It was not possible to show whether high- or low-magnesian calcite tests promoted precipitation, because too little precipitation was observed to make a statistically valid test of the question.

Approach: Paleoenvironment And Depth Of Bioturbation

Two gravity cores were chosen for study. Gravity core KW-PE-GC-225 was selected in preference to others from the Southeast Channel of the Dry Tortugas because it recovered and well represented all of the lithostratigraphic horizons described by Stephens et al. (1997). Gravity core KW-PE-GC-235 was selected from others of the Marquesas study area because of its great length. Additionally, 3 samples, 0-1, 1-2, and 2-3 cm bsf, were selected from the surficial mixed zone (D'Andrea and Lopez, 1997; Bentley and Nittrouer, 1997) of box core KW-PL-BC-185.

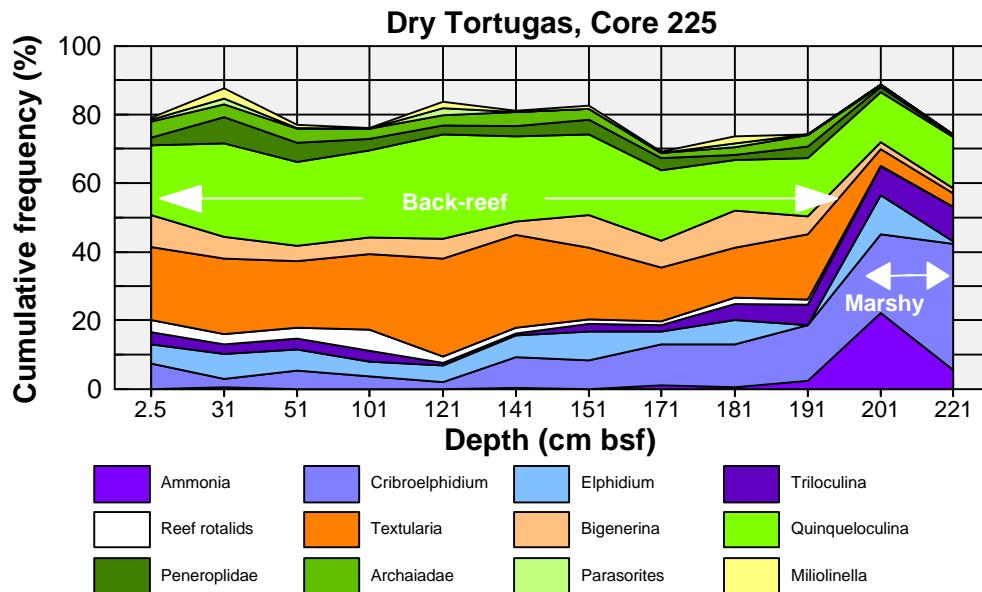
The gravity cores were described and sampled at 10-cm intervals. A 20-cc subsample was extracted from the freshly split gravity cores and the box core and washed on a 63 μm screen to remove clay- and silt-size particles. The samples were sieved when dry using a 150 μm screen, and the volume of the residue was reduced to a random subsample of 300 to 400 foraminifers using a microsplitter. The foraminifers were hand-picked from the subsamples, and a census of species was tabulated. Identifications were verified by comparisons to the type material of Cushman (1922), Poag (1981), and Bock

et al. (1971) at the Smithsonian Institution. Grain size data are from Stephens et al. (1997).

Q-mode cluster analysis was used to group together samples with similar relative species frequencies. The clustering method used a simple Euclidean distance coefficient and a within group amalgamation protocol displayed graphically as a dendrogram (Norusis, 1988).

Results: Paleoenvironment

The foraminifer assemblages from the Dry Tortugas and Marquesas Keys are very diverse containing seven suborders and more than 155 species. Inspection of plots of species frequencies versus depth shows several major changes in assemblages at the two sites. At the Dry Tortugas test area, the basal assemblage is dominated by rotalid species characteristic of a shallow marsh environment, including *Criboelphidium poeyanum* and *Ammonia tepida* (Fig. 5). The fauna consists of more than 55% infaunal taxa, and the sediment itself is equal parts silt- and clay-size particles with minor amounts of sand. By contrast, the overlying assemblage is dominated by miliolid and textularid species, and has a much more equitable species distribution. 60 to 75% of the fauna is epifaunal, preferring either hard or phytal substrates to life in the sediment. The sediment is distinctly more sand- and silt-rich than the underlying marsh facies. The faunal sequence suggests environmental succession from a marsh to a backreef, consistent with the Holocene rise in sealevel. It is possible that many of the epiphytic species and those that live on hard substrates have been transported to the site from the adjacent shallow banks because no plants or hard substrates occur in the test site at this time.



At the Marquesas site, the mid-core assemblage is dominated by *Ammonia* and other rotalid species characteristic of a shallow marsh environment (Fig. 6). The fauna consists of more than 80% infaunal taxa, and the sediment itself is a clayey silt with minor amounts of sand. In contrast, samples at the base and top of the core are typical of a carbonate platform environment. Species frequencies are comparatively equitable, with about 40% epifaunal taxa and 60% infaunal taxa. The sediment is sandier and more gravel-rich than that from the middle of the core. The succession of assemblages suggests the passage of a shallow mud bank across the site after the Holocene flooding of the carbonate platform.

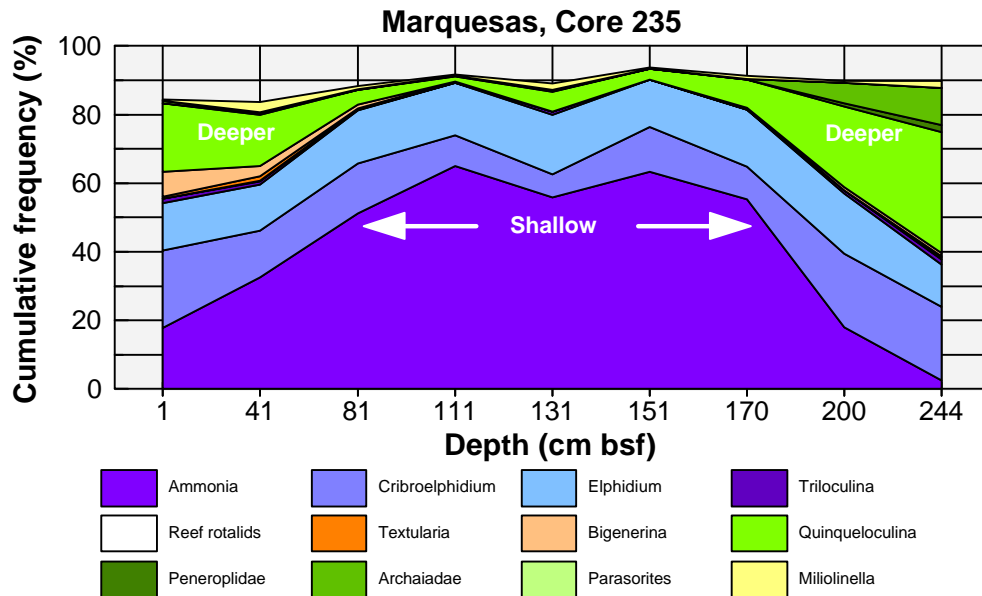


Figure 6. Cumulative frequency of principal taxonomic groups of foraminifera in gravity core KW-PE-GC-235 showing a shallow marshy assemblage between 81 and 170 cm bsf and a carbonate platform assemblage above and below the shallow assemblage.

Results: Depth of bioturbation

The foraminifer assemblage at the Dry Tortugas site can be used to estimate the depth of mixing of sand-size particles as an independent verification of the Pb-210 estimates of Nittrouer and Bentley (1997). A cluster analysis was done on the fauna from the gravity core from Southeast Channel. Included in the analysis were three samples each 1-cm thick from the top 3 cm of the box core, KW-PE-BC-185. I assume that the three samples represent the species currently being mixed in the biotic mixed layer (D'Andrea and Lopez, 1997; Bentley and Nittrouer, 1997). Two clusters emerged from the cluster analysis (Fig. 7). One cluster consisted of the three samples from the top of box core KW-PE-BC-185, three samples from 2.5, 15, and 30 cm bsf and two samples from 180 and 190 cm bsf of gravity core KW-PE-GC-225. The second cluster grouped together samples from 50 to 170 cm bsf in gravity core KW-PE-GC-225.

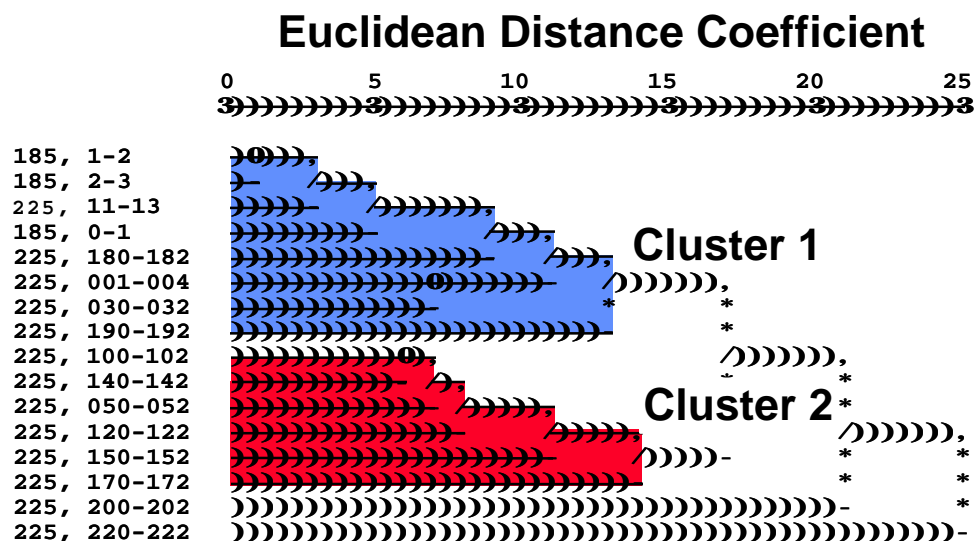


Figure 7. Dendrogram of samples from the mixed layer of box core KW-PL-BC-185 grouped with the samples from gravity core KW-PE-GC-225. Notice that the samples from the upper 30 cm bsf of the gravity core cluster with the samples from the mixed layer.

Cluster 1 is interpreted to be an assemblage of the bioturbated mixed zone of the present-day, because it contains samples that are undoubtedly from the mixed zone of the box core. In contrast, cluster 2 groups together samples containing an assemblage that is significantly different. The implication is that sand-size particles between 30 and 50 cm are no longer moved very much, so that the foraminiferal assemblage is essentially fixed into the permanent record by this depth. The assemblage in the upper mixed zone drifts in species composition from the permanent record because climate continues to change.

Accomplishments: Paleoenvironment And Depth Of Bioturbation

It is important to understand the nature of bioturbational mixing in the Dry Tortugas area. D'Andrea and Lopez (1997) observed two layers of mixing, a shallow zone and a deep zone. The shallow zone from 0 to 4 cm is dominated by surface deposit feeding polychaetes and burrowing bivalves that mix the sediment in days to weeks. The result is vsupported by the activity of Th-234 with depth (Bentley and Nittrouer, 1997). The deep zone may extend to 40 to 60 cm bsf and includes deep deposit feeders such as *Callianassa* sp. and *Notomastus* sp., which recycle sediment at rates that diminish with increasing depth (Lopez, pers. comm., 1998; D'Andrea and Lopez, 1997; Bentley and Nittrouer, 1997). Deep deposit feeders, like callianassid shrimp, feed in deep burrows with inhalent and exhalent burrows. Water, organic particles, and small sediment grains are entrained in the inhalent tube, and small grains are expelled through the exhalent tube. The shrimp build elaborate burrows with chambers and galleries for various purposes. The excavated silt and finest sand is expelled (recycled) to the surface, and coarse grains are stacked in chambers, which are filled and abandoned.

The activities leave a distinctive lithologic signature described by Tudhope and Scoffin (1984) and consistent with the succession of lithologic units described throughout

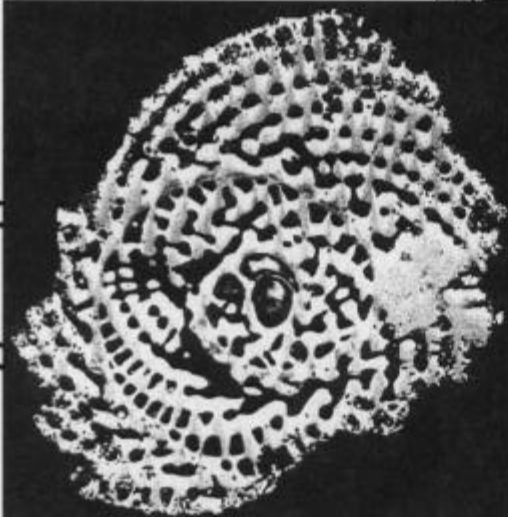
the Dry Tortugas test site (Stephens et al., 1997). The texture of such a sequence is silty at the top where *Callianassa* pile expelled sediment, and grades at depth to sand with concentrations of shells in poorly sorted sand at depth (Tudhope and Scoffin, 1984). Gravel-size particles are probably moved the least because they are sequestered in storage chambers by the shrimp, though the gravel-size shells could have originated at any depth overlying the shrimp or along its excavated burrow system. The silt and finest sediment is most susceptible to repeated recycling, in which it is excavated from depth, piled at the surface, and subsequently remobilized down the inhalent tube for another cycle of movement. Sand-size debris, like foraminifers, likely has a fate that falls between that of silt and gravel. These results suggest this middle course for the fate of sand-size debris because the foraminiferal fauna has taken on a permanent aspect between 30 and 50 cm bsf, above the shallowest concentration of shell debris in the core (90 cm bsf) and perhaps above or similar to the depth of habitation of the callianassid shrimp.

There is a period of time before a permanent record is deposited, and the mixed layer, including the tests that it contains, holds a mixture of specimens that lived throughout the time interval before permanent deposition. The minimum duration to deposit 35 cm is about 117 years, based on the maximum possible accumulation rate estimated from excess Pb-210 gradients (Bentley and Nittrouer, 1997). A reasonable maximum duration to deposit 35 cm is about 1750 years calculated by assuming a sedimentation rate equal to the net Holocene rate (~20 cm/ky).

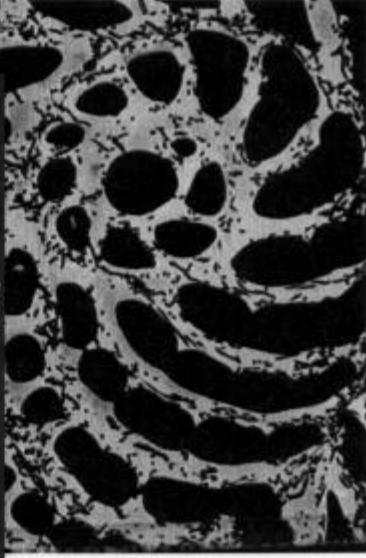
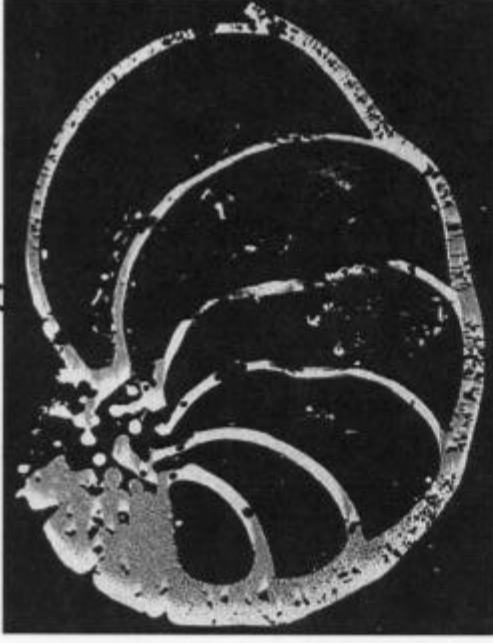
Summary Of Principal Accomplishments:

- 1) Scanning electron microscopic examination of foraminifer tests revealed only trace effects due to oxidation of organic matter. There was some dissolution, minor amounts of aragonite(?) precipitation, and very minor amounts of pyrite formation.
- 2) The effects due to oxidation of organic matter, especially formation of pyrite, apparently occurred in microhabitats found, for example, within foraminiferal tests. Results from pore water chemistry (see Shiller publications listed in references) suggest that sediments at the Dry Tortugas test site are suboxic within millimeters of the sediment surface, but never reach levels strong enough to reduce sulfate in the general mass of sediment.
- 3) The sequences at the Dry Tortugas test site include a basal marsh deposit overlain by coarser backreef sediments extensively reworked by deep deposit feeders. The sequence is consistent with deposition during the Holocene rise in sea level. The sequence at the Marquesas test site consists of a shallow mud-bank deposit that is under- and overlain by typical carbonate platform sediments. The sequence is consistent with migration of a mudwave across the site after inundation by the Holocene rise in sea level.
- 4) The depth where mixing of sand-size foraminifers affectively ceases and the permanent record begins lies between 30 and 50 cm bsf. This depth of mixing is consistent with results from excess Pb-210 (Bentley and Nittrouer, 1997).

High-Mg calcite



Low-Mg calcite



Bore holes

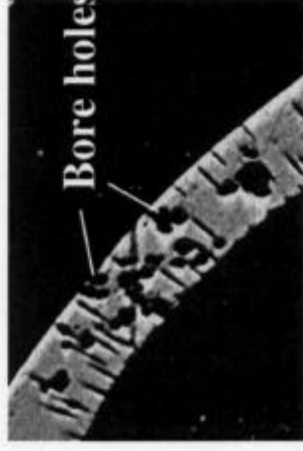
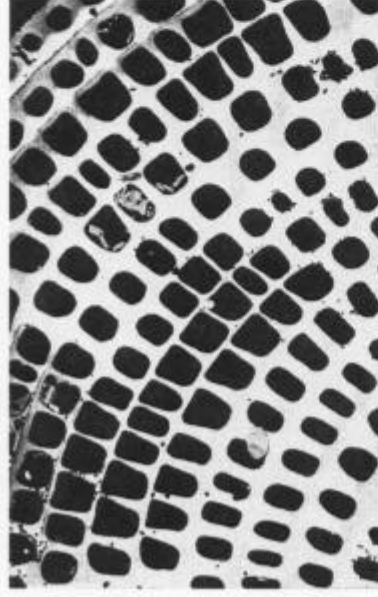


Plate 2.

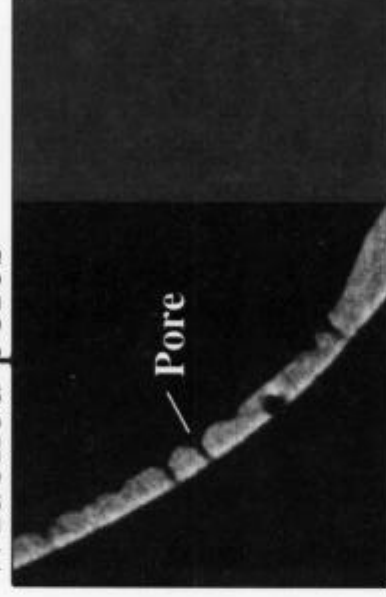
High-Mg calcite

Thinned walls

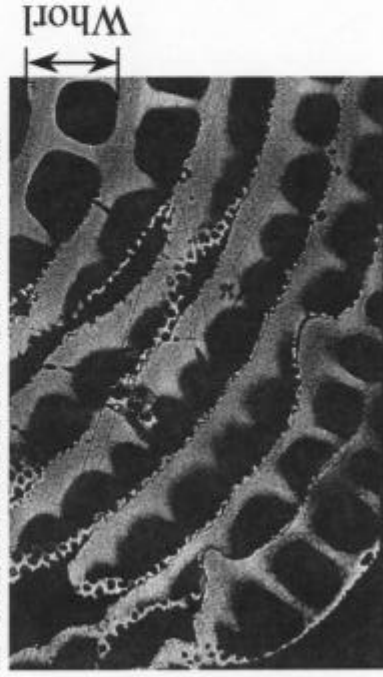


Low-Mg calcite

Widened pores



Delamination of whorls



Normal pores

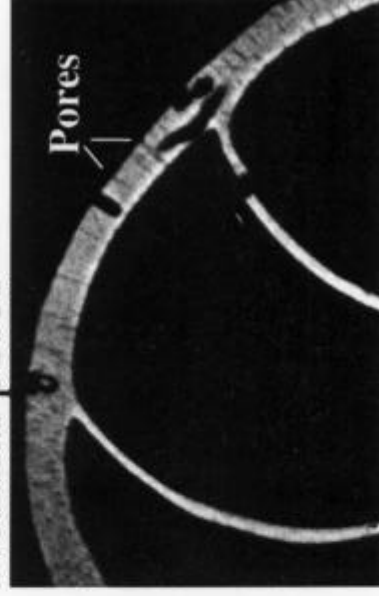
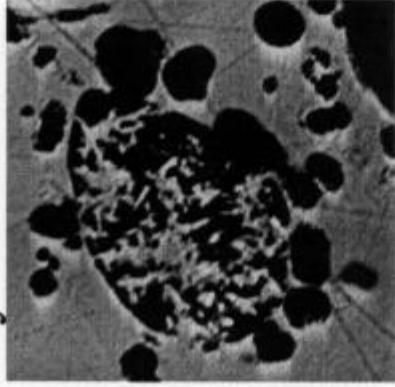
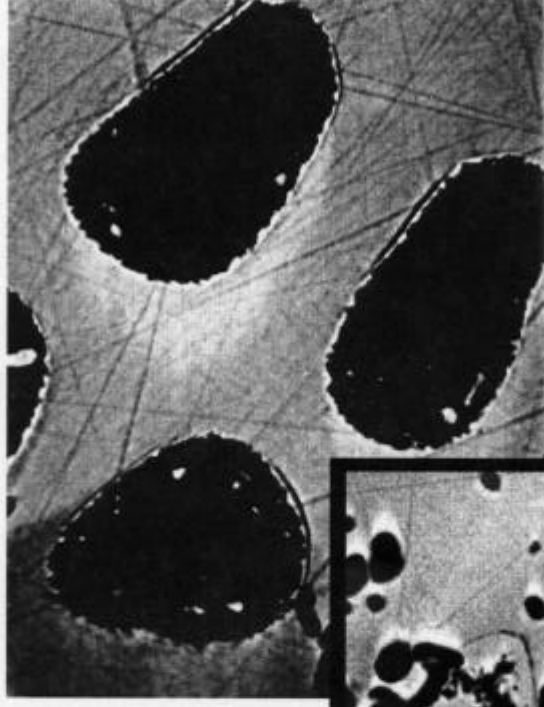


Plate 3.

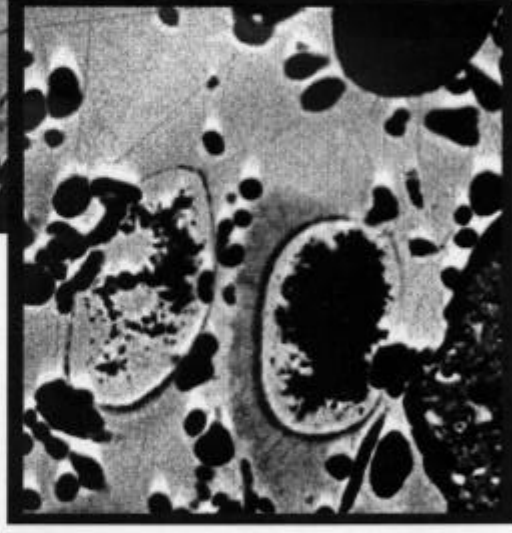
Crystals in chamberlet



Rinds in chamberlets



Rinds



Crystal mass

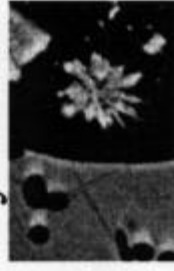
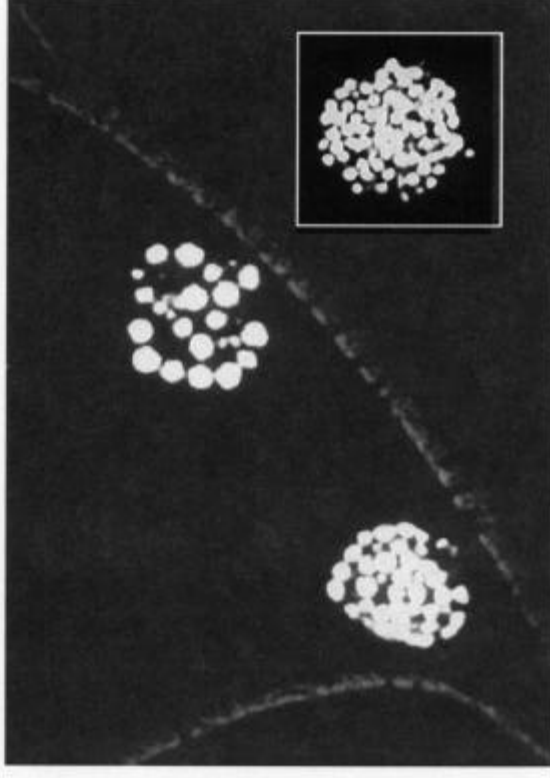
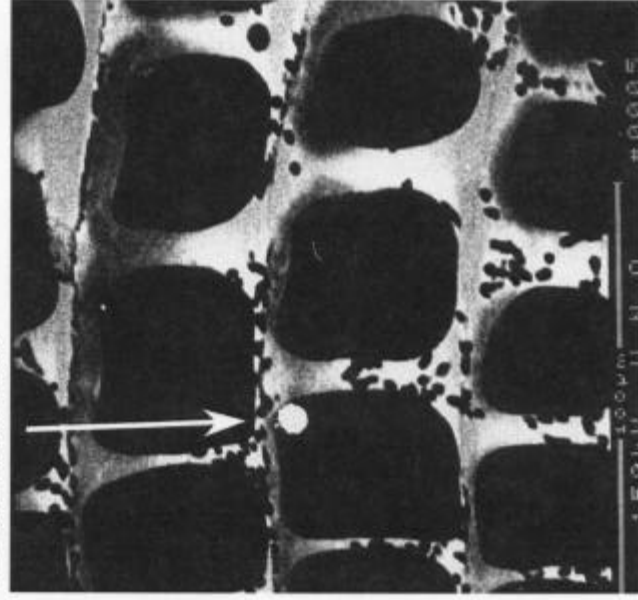


Plate 4.



References:

- Bentley, S. J., and Nittrouer, C. A., 1997. Environmental influences on the formation of sedimentary fabric in a fine-grained carbonate-shelf environment: Dry Tortugas, Florida Keys. *Geo-Marine Letters*, 17:268-275.
- Bock, W. D., Hay, W. W., Jones, J. I., Lyntz, G. W., Smith, S. L., and Wright, R. C., 1971. A Symposium of Recent South Florida Foraminifera, Miami Geological Society Memoir 1, 245p.
- Cushman, Joseph A., 1922. Shallow-water foraminifera of the Tortugas Region, Carnegie Institution of Washington No. 133, 97p.
- D'Andrea, A. F., and Lopez, G. R., 1997. Benthic macrofauna in a shallow water carbonate sediment: major bioturbators at the Dry Tortugas. *Geo-Marine Letters*, 17:276-282.
- Froelich, P. N., Klinkhammer, G. P., Bender, M. L., Luedtke, N. A., Heath, G. Ross, Cullen, Doug, and Dauphin, Paul, 1979. Early oxidation of organic matter in pelagic sediments of the eastern equatorial Atlantic: suboxic diagenesis. *Geochimica et Cosmochimica Acta*, 43:1075-1090.
- Golubec, S., Perkins, R. D., and Lukas, K. J., 1975. Boring microorganisms and microborings in carbonate substrates. In: Frey, R. W., (ed.), *The Study of Trace Fossils*, Springer-Verlag, New York, p. 229-260.
- Golubec, S., Campbell, S. E., Drobne, K., Cameron, B., Balsam, W. L., Cimerman, F., and DuBois, L., 1984. *J. Paleontology*, 58(2):351-361.
- Golubic, S., Brent, G., and Le Campion, T., 1970. Scanning electron microscopy of endolithic algae and fungi using a multipurpose casting embedding technique. *Lethaia*, 3:203-209.
- Hallock, Pamela, Cottey, Theresa L., Forward, Linda B., and Halas, John, 1986. Population biology and sediment production of *Archaias angulatus* (Foraminiferida) in Largo Sound, Florida, *Journal of Foraminiferal Research*, 16(1):1-8.
- Hudson, J. Harold, 1985. Growth rate and carbonate production in *Halimeda opuntia*: Marquesas Keys, Florida. In: D. F. Toomey and M. H. Nitecki, eds., *Paleoalgology: Contemporary Research and Application*, p. 257-263.
- Mullins, Hank T., Thompson, J.B., McDougall, Kristin, and Vercoutere, T.L., 1985. Oxygen-minimum zone edge effects: evidence from the central California coastal upwelling system. *Geology*, 13:491-494.

Murray, John W., 1991. Ecology and Palaeoecology of Benthic Foraminifera, John Wiley & Sons, Inc., New York, 397p.

Norusis, M.J., 1988. SPSS/PC+Advanced Statistics™ V2.0 for the IBM PC/XT/AT and PS/2: Chicago(SPSS Inc.).

Orsi, Thomas, H., Anderson, A.L., Davis, K. S., Bryant, W. R., Rezak, R., Rutledge, A. K., Fischer, K., Falster, A., and Brunner, C., (in prep.), Computed tomography and geoacoustic properties of carbonate muds from Marquesas Keys and Dry Tortugas, South Florida (Coastal Benthic Boundary Layer Special Research Project), NRL Report. Perry, C. T., 1998. Grain susceptibility to the effects of microboring: implications for the preservation of skeletal carbonates. *Sedimentology*, 45:39-51.

Poag, C. Wylie, 1981. Ecologic Atlas of Benthic Foraminifera of the Gulf of Mexico. Marine Science International, Woods Hole, MA, 174 p.

Shiller, Alan, M., Brunner, Charlotte A., Furukawa, Yoko, Hebert, Tracy, and Yuan, Jinchun, 1998. Early Diagenesis of carbonate sediments in the Dry Tortugas and Marquesas Keys, Florida, USA. . *Journal of the Mississippi Academy of Sciences*, 43(1):52.

Shiller, A. M., Hebert, T. L., Thornton, K. R., and Brunner, C. A., 1995. Sediment chemistry and pore water fluxes in the vicinity of the Dry Tortugas, The 1st SEPM Congress on Sedimentary Geology, Congress Program and Abstracts, v. 1, p. 113.

Stephens, Kevin P., Fleischer, Peter, Lavoie, Dawn, and Brunner, Charlotte, 1997. Scale-dependent physical and geoacoustic property variability of shallow-water carbonate sediments from the Dry Tortugas, Florida. *Geo-Marine Letters*, 17(4):299-305.

Stephens, K. P., Lavoie, D. L., Briggs, K.B., Richardson, M. D., and Furukawa, Y., 1997. Geotechnical and geoacoustic properties of sediments off south Florida: Boca Raton, Indian Rocks Beach, Lower Tampa Bay, and the Lower Florida Keys. Stennis Space Center, MS, Naval Research Laboratory, NRL/MR/7431-97-8042. 310p.

Publications:

Peer Reviewed:

Brunner, C. A., (in prep.). Paleoenvironment at Marquesas Keys and Dry Tortugas CBBL Sites, Florida. *Marine Geology*.

Brunner, C. A., (in prep.). Affect of early diagenesis on foraminifer tests from a backreef environment. *Journal of Foraminiferal Research*.

Shiller, A., and Brunner, C. A., (in prep.). Early diagenesis of carbonate sediments in the backreef environment of the Dry Tortugas, Florida. *Marine Geology*.

Symposium Proceedings:

Brunner, C. A., 1997. Paleoenvironment at Marquesas Keys and Dry Tortugas CBBL Sites, Florida, CBBL Workshop, Feb 4-7, 1997, Stennis Space Center, MS.

Published Abstracts:

Shiller, A. M., Hebert, T. L., Thornton, K. R., and Brunner, C. A., 1995. Sediment chemistry and pore water fluxes in the vicinity of the Dry Tortugas, The 1st SEPM Congress on Sedimentary Geology, Congress Program and Abstracts, v. 1, p. 113.

Brunner, C., Reed, A., Elder, R., Falster, A., and Shiller, A., 1996. Effects of organic carbon respiration on preservation of foraminifers from the Dry Tortugas, Florida. *Journal of the Mississippi Academy of Sciences*, 41(1): 54.

Shiller, Alan, M., Brunner, Charlotte A., Furukawa, Yoko, Hebert, Tracy, and Yuan, Jinchun, 1998. Early Diagenesis of carbonate sediments in the Dry Tortugas and Marquesas Keys, Florida, USA. *Journal of the Mississippi Academy of Sciences*, 43(1):52.

Thesis:

I served as major professor and chaired the thesis committee of Kevin P. Stephens.

Stephens, Kevin P., 1997. Scale-dependent physical and geoacoustic property variability of shallow-water carbonate sediments from the Dry Tortugas, Florida. University of Southern Mississippi, Masters Thesis, 87p.

COASTAL BENTHIC BOUNDARY LAYER SPECIAL RESEARCH PROGRAM

REF: NRL-DET BAA 92-3

FINAL REPORT

Processes Of Macro Scale Volume Inhomogeneity In
The Benthic Boundary Layer

William R. Bryant and Niall C. Slowey

Department of Oceanography

Texas A & M University

College Station, Texas 77843

Abstract:

The goals of our participation in the CBBL Research Program were to understand how and why the physical properties and the geology of the boundary layer vary in terms of time dependent physical, biological and chemical processes within various shallow water geological environments. Specifically, we investigated the geotechnical stratigraphy, which includes the density, compressional-wave velocity, shear strength (cohesion), porosity, saturation (gas) and sediment and biological component distribution and their three-dimensional structural arrangement, within the boundary layer in more detail than has previously been possible. These studies led to descriptions of boundary layer gradients of compressional wave velocity, density, porosity and cohesion and their relation to sediment type, structural arrangement, states of stress etc. In addition to sediments of a cohesive nature (clays and silts, clayey sands and sandy clays), fine-grained carbonate sediments were also investigated. The knowledge gained was used to deduce realistic measures of sediment micro and macrostructural volume inhomogeneity and to generate numerical models that predict physical and geoacoustic nature of the boundary layer. These results can be applied to geoacoustic problems and models which predict the penetration and stability of objects on the seafloor.

Original Objectives:

Our research is based on the premise that the fundamental properties which control both the mechanics of objects and the propagation of compressional waves at the seafloor include the bulk density, shear strength (cohesion), porosity, saturation (gas), macro and microfabric and compressibility of sediments. For this reason, the success of efforts to predict the location of objects and then acoustically detect them depends upon our understanding of the spatial and

temporal variability of these properties. The largest changes of the bulk density, shear strength and compressibility of sediments within most marine environments typically occur within the upper few meters of the seafloor (the boundary layer). We believe these changes are closely coupled with variations in the texture and structure, the fabric, of the sediments.

Based on this hypothesis, we proposed to investigate the spatial variability of the geotechnical, geoacoustic and geological properties, and the structure of sediments within the boundary layers of select marine environments. We had several specific goals: First, we wanted to characterize the variability (especially vertical gradients) of sediment properties in greater detail than before possible and to better understand how the variability of various properties are interrelated. Then, we wanted to use this understanding to develop predictive models of sediment properties for typical marine environments. Such knowledge is necessary for models used to predict the penetration and stability of objects on the seafloor, and it provides a realistic measure of sediment micro and macrostructural volume inhomogeneity that can be applied to geo- and seismo-acoustic modeling. Finally, wanted to relate the nature of sediment property variability to the character and origin/physical significance of reflections on high-resolution seismic profiles and side-scan sonar records. This knowledge contributes to our understanding of the factors that control acoustic scattering at and within the benthic boundary layer and it provides the ground-truthing for high-resolution seismic profiles and side-scan sonar records that can be generalized to various marine environments.

With the aid of other CBBL investigators, our general aim was to examine sediments from several different types of shallow water marine environments in order to typify and to better understand how and why variations in seafloor sediment characteristics arise from the dominant physical, biological and chemical processes within the benthic boundary layer. This report reviews our goals, efforts and accomplishments for the five year duration of the CBBL SRP.

Approach:

To investigate sediment property variability over a range of volumes and spatial scales in several different geologic environments, we employed the following strategy: Macro-scale variability (mm's to cm's) was examined two ways: 1) individual cores--with depth in each core and in grids spanning horizontal cross sections of each core, and 2) multiple cores--between gravity and piston cores from the same site as well as subcores from individual box cores. Micromorphologic scale variability (m's to 100 m's) was examined by collecting suites of regularly spaced cores from selected areas of the seafloor.

A Multi-Sensor Core Logger was used to determine the wet bulk density and compressional-wave velocity at down-core intervals of typically 1 cm on sediments recovered by box, gravity and piston cores from appropriate shallow-water locations. Cohesion was measured

at similar close intervals by the use of a Swedish Fall Cone and a motorized vane shear device. All gravity, piston and box cores were subsampled at regular intervals for other physical and geologic properties (grain size, mineralogy, water content, porosity, particle density, index properties and sedimentary structures). This approach yielded very detailed profiles of sediment properties for the upper 3 meters of surficial seafloor sediments. The three-dimensional macro-scale distribution of wet bulk density, cohesion and sediment components within selected sediment cores were investigated. The Multi-Sensor Core Logger determines the average density across a core section. Close-range x-ray stereophotogrammetric analysis and image processing of radiographs of successive sections of gravity, piston and box-cores was used to determine the macro-scale three dimensional arrangement of sediment and biological components. Tomographic x-ray techniques (CAT Scanning), at a resolution of 1 mm², was used to determine exactly how wet bulk densities vary within several core sections (upon which average densities are determined).

Statistical analyses were employed to yield a better understanding of the relationships among sediment properties and to develop predictive models for these properties. Working together with other CBBL investigators, we qualitatively and quantitatively compared changes of sediment properties with high-resolution vertical-incidence and side-scan sonar data. These comparisons yielded insight into how variability of sediment properties affects sound propagation within the benthic boundary layer.

Results:

We carried out field and laboratory investigations for our own research at the three CBBL study areas: Eckernförde Bay, Germany; the continental shelf off of Panama City, Florida; and the Marquesas Keys and the Dry Tortugas in southern Florida. We also facilitated the field and laboratory efforts of other CBBL investigators. It is impossible to adequately describe the results of these efforts in this short report; therefore, rather than attempt to do this, we have provided below brief descriptions of field efforts and examples of results obtained both in the field and laboratory.

Eckernförde Bay -- We collected a suite of approximately 47 gravity and box cores containing cohesive sediments (both gassy and non-gassy) from the Eckernförde Bay, Germany during February and May of 1993, and during June of 1994, and examined sediment property variability over both macro-scale and micro-morphologic spatial scales. We measured and described the sediment physical and geoacoustic properties and then investigated interrelationships among them using statistical techniques (see example in Figure 1). Certain cores were collected along at locations that fell on high-resolution seismic lines collected by other CBBL investigators (D. Lambert of NRL and S. Schock of FAU), so working together with

them, we investigated how sediment property variability affects compressional wave propagation and the origin of reflectors on high-resolution seismic profiles of Eckernförde Bay sediments (see example in Figure 2). To fully achieve our specific goals and broader CBBL aims, we also worked together with other CBBL investigators (tested and evaluated coring equipment on behalf of all investigators, helped geologically interpret the profiles collected during vertical incidence and side-scan sonar surveys, collected and sampled sediment cores, etc.), including groups led by A. Silva of URI, A. Anderson of TAMU, C. Martens of UNC, D. & D. Lavoie and M. Richardson of NRL, and R. Faas of Lafayette University.

Panama City Shelf Sands Study Site -- During the August-September 1994 cruise off of Panama City, members of our team obtained a suite of ~95 Shipek grab samples and short cores of surficial sediments for our own research needs. We determined the distribution patterns of the grain-size and carbonate content of the surficial sediments, and working with I. Stender and his group from FWG, investigated how their variations throughout the study site relate to side-scan sonar images and digital backscatter data (see example in Figure 3). Members of our group served the overall aims of the CBBL Research Program by helping to make arrangements for the use of RV GYRE and coring equipment for the cruise, we acted in the capacity of co-chief scientists to coordinate and satisfy the logistical needs of other investigators, and we contributed to NRL diving operations.

Marquesas Keys and the Dry Tortugas -- A member of our group participated on the 1994 site survey cruise to the Florida Keys in order to assist NRL investigators and to collect ~40 exploratory samples of surficial sediment for our research. Working with A. Silva and his group from URI, we recovered 70 gravity cores from the Marquesas and Dry Tortugas areas during the primary cruise in February, 1995. We also worked together with D. Lambert and his group from NRL to collect 9 vibracores of sandy sediment. These samples were analyzed using the same approach described above for samples collected at other localities. We suspect that the non-spherically shaped biogenic sediment grains may well become preferentially oriented at the seafloor, affecting their geoacoustic properties. We are therefore also investigating whether or not sediments exhibit compressional wave and bulk density anisotropy. This is being accomplished by measuring compressional wave velocities and density at 30 degree intervals around the circumference of each core (see example in Figure 4).

Accomplishments:

Throughout the course of this project, it has been our aim to characterize the variability of the properties of the sediments found in shallow-water marine environments and to examine their interrelationships. We wanted to use this understanding to develop predictive models of sediment properties for typical marine environments, and relate the nature of sediment property variability

to the character and origin/physical significance of reflections on high-resolution seismic profiles and side-scan sonar records. The following is a list of specific accomplishments resulting from our project that are consistent with these aims.

- Comparison and re-evaluation of shear strength measurements of fine-grained marine sediments obtained by miniature vane shear and fall cone tests.
- Development of a new method to measure bulk volume of small rock samples for determinations of porosity and mass accumulation rates.
- Examination of the general effects of gas expansion and core handling on measurements of the compressional-wave velocity of gassy marine sediments from the Santa Barbara Basin. Considered possible ways to minimize such effects during future ODP operations.
- Characterization of the bulk density, compressional-wave velocity and shear strength values of gassy and non-gassy marine sediments from Eckernförde Bay and the Baltic Sea.
- Determination of the character and origin of marine reflectors on high-resolution seismic profiles of gassy and non-gassy marine sediments.
- Development of an empirical model for estimating the dynamic shear modulus of fine-grained marine sediments in the benthic boundary layer from their void ratio and effective overburden and compared shear wave velocities calculated from the model with those measured in situ.
- Development of predictive regression equations describing how the compressional-wave velocity, shear wave velocity and shear strength of gassy and non-gassy fine-grained marine sediments depend upon other sediment properties.
- Characterization of first-order relationships between the properties of sandy marine sediments and acoustic-backscattering at the sediment-water interface of the northeast Gulf of Mexico shelf.
- Characterization of the variability and interrelationships among the geotechnical, geoacoustical and sedimentological properties of shallow-water carbonate sediments from the Dry Tortugas and Marquesas Keys.
- Determination of the extent and origin of the anisotropy of compressional-wave velocity in shallow-water carbonate sediments.

Publications:

Peer-reviewed publications:

1. Slowey, N. C. and W. R. Bryant, 1995, Effects of gas and core handling on measurements of compressional wave velocity in ODP Site 893 cores, *Proceedings of the Ocean Drilling Program, Scientific Results*, v. 146 (Part 2), p. 193-197.
2. Yeager, M. and N. C. Slowey, 1996, A new method for measuring the bulk volume of rock samples for porosity and mass accumulation determinations, *Journal of Sedimentary Research*, v. 66, p. 1036-1039.
3. Richardson, M. D. and W. R. Bryant, 1996, Benthic boundary layer processes in coastal environments: An introduction, *Geo-Marine Letters*, v. 16, p. 133-139.
4. Orsi, T. H., F. Werner, D. Milkert, A. L. Anderson, and W. R. Bryant, 1996, Environmental overview of Eckernförde Bay, northern Germany, *Geo-Marine Letters*, v. 16, p. 140-147.
5. Slowey, N. C., W. R. Bryant, and D. N. Lambert, 1996, Comparison of high-resolution seismic profiles and the geoacoustic properties of Eckernförde Bay sediments, *Geo-Marine Letters*, v. 16, p. 240-248.
6. Davis, K., N. Slowey, I. Stender, H. Fiedler, W. Bryant, and G. Fechner, 1996, Acoustic backscatter and sediment textural properties of inner shelf sands, northeastern Gulf of Mexico, *Geo-Marine Letters*, v. 16, p. 273-278.
7. Lu, T., and W. R. Bryant, 1997, Comparison of vane shear and fall cone strengths of soft marine clay, *Marine Georesources and Geotechnology*, v. 15, p. 67-82.
8. Lu, T., W. R. Bryant, and N. C. Slowey, 1998, An empirical model of dynamic shear modulus for surface marine sediments, *Marine Georesources and Geotechnology*, v. 16, p. 95-109.
9. Silva, A., H. G. Brandes, and N. C. Slowey, 1998, Geotechnical properties and behavior of high-porosity, organic-rich sediments in Eckernförde Bay, *Continental Shelf Research*, in press.
10. Lu, T., W. R. Bryant, and N. C. Slowey, Regression analysis of physical and geotechnical properties of surface marine sediments, *Marine Georesources and Geotechnology*, in press.
11. Lee, Y., W. R. Bryant, and N. C. Slowey, Geotechnical, geoacoustical and sedimentological properties of carbonate sediments from the Dry Tortugas and Marquesas Keys, in preparation.
12. Lee, Y., N. C. Slowey, and W. R. Bryant, Anisotropy of compressional wave in carbonate sediments from the Dry Tortugas and Marquesas Keys, in preparation.

Symposium proceedings and published reports:

1. Davis, K. S., W. R. Bryant, N. C. Slowey, and D. N. Lambert, 1994, Reflections on the geoacoustic and geotechnical characteristics in Eckernförde Bay sediments, *Proceedings of the*

Gassy Mud Workshop held at the Forschungsanstalt der Bundeswehr fur Wasserschall und Geophysik (FWG), Kiel, Germany, July 11-12, 1994, FWG Report 14, p. 47-53.

2. Bryant, W. R. and N. C. Slowey, 1994, Processes of macro scale volume inhomogeneity in the benthic boundary layer, Coastal Benthic Boundary Layer Special Research Program: A Review of the First Year, Naval Research Laboratory, Report No. NRL/MR/7431-94-7099, p. 59-82.

3. Slowey, N. C., W. R. Bryant, and D. N. Lambert, 1995, Geoacoustic properties of Eckernförde Bay sediments and the origin of reflectors of high-resolution seismic profiles, *Proceedings of the Modeling Methane-Rich Sediments of Eckernförde Bay Workshop held at the Forschungsanstalt der Bundeswehr fur Wasserschall und Geophysik (FWG), Kiel, Germany, June 26-30, 1995, FWG Report 22, p. 73-74.*

4. Bryant, W. R., N. C. Slowey, T. H. Orsi, and K. S. Davis, 1995, Processes of macroscale volume inhomogeneity in the benthic boundary layer, Eckernförde Bay, western Baltic Sea, *Proceedings of the Modeling Methane-Rich Sediments of Eckernförde Bay Workshop held at the Forschungsanstalt der Bundeswehr fur Wasserschall und Geophysik (FWG), Kiel, Germany, June 26-30, 1995, FWG Report 22, p. 217-224.*

Published Abstracts:

1. Orsi, T. H., A. L. Anderson, W. R. Bryant, and N. C. Slowey, 1992, Three-dimensional seafloor structure investigated using medical diagnostic imagery, EOS, Transactions of the American Geophysical Union, v. 73, p. 302.

2. Bryant, W. R. and N. C. Slowey, 1994, The geoacoustic and geotechnical properties of Eckernförde Bay, EOS, Transactions of the American Geophysical Union, v. 75, p. 220.

3. Davis, K. S., W. R. Bryant, N. C. Slowey, and D. N. Lambert, 1994, Reflections on the geoacoustic and geotechnical characteristics in Eckernförde Bay sediments, Proceedings of the Gassy Mud Workshop, Technical Abstracts, Forschungsanstalt der Bundeswehr fur Wasserschall und Geophysik (FWG), Kiel, Germany.

4. Slowey, N. C., W. R. Bryant, and D. N. Lambert, 1994, The geoacoustic and geotechnical properties of Eckernförde Bay, Third International Conference on Gas in Marine Sediments, Texel, The Netherlands.

5. Lambert, D. N., D. J. Walter, W. R. Bryant, N. C. Slowey, and J. C. Cranford, 1994, Acoustic prediction of sediment impedance, Acoustical Society of America Annual Meeting, Austin, Texas.

6. Bryant, W. R., N. C. Slowey, T. H. Orsi, and K. S. Davis, 1995, Processes of macroscale volume inhomogeneity in the benthic boundary layer, Eckernförde Bay, Western Baltic Sea,

Workshop on Modeling Methane-Rich Sediments of Eckernförde Bay, Forschungsanstalt der Bundeswehr für Wasserschall und Geophysik, Kiel, Germany.

7. Slowey, N. C., W. R. Bryant, and D. N. Lambert, 1995, Geoacoustic properties of Eckernförde Bay sediments and the origin of reflectors on high-resolution seismic profiles, Workshop on Modeling Methane-Rich Sediments of Eckernförde Bay, Forschungsanstalt der Bundeswehr für Wasserschall und Geophysik, Kiel, Germany.

8. Slowey, N. C., W. R. Bryant, K. S. Davis, D. N. Lambert, and D. J. Walter, 1995, Geoacoustic stratigraphy of the Marquesas Keys, SEPM Congress on Sedimentary Geology, Program and Abstracts, v. 1, p. 34.

Dissertations:

1. Lu, T., 1996, Statistical analysis and correlation of physical and geological properties of marine sediment in Eckernförde Bay, Baltic Sea. Dissertation. Texas A&M University, College Station, Texas. 149 pp.

2. Lee, E., Geotechnical and acoustical properties of carbonate sediments from the Dry Tortugas and Marquesas Keys. Dissertation. Texas A&M University, College Station, Texas. In preparation.

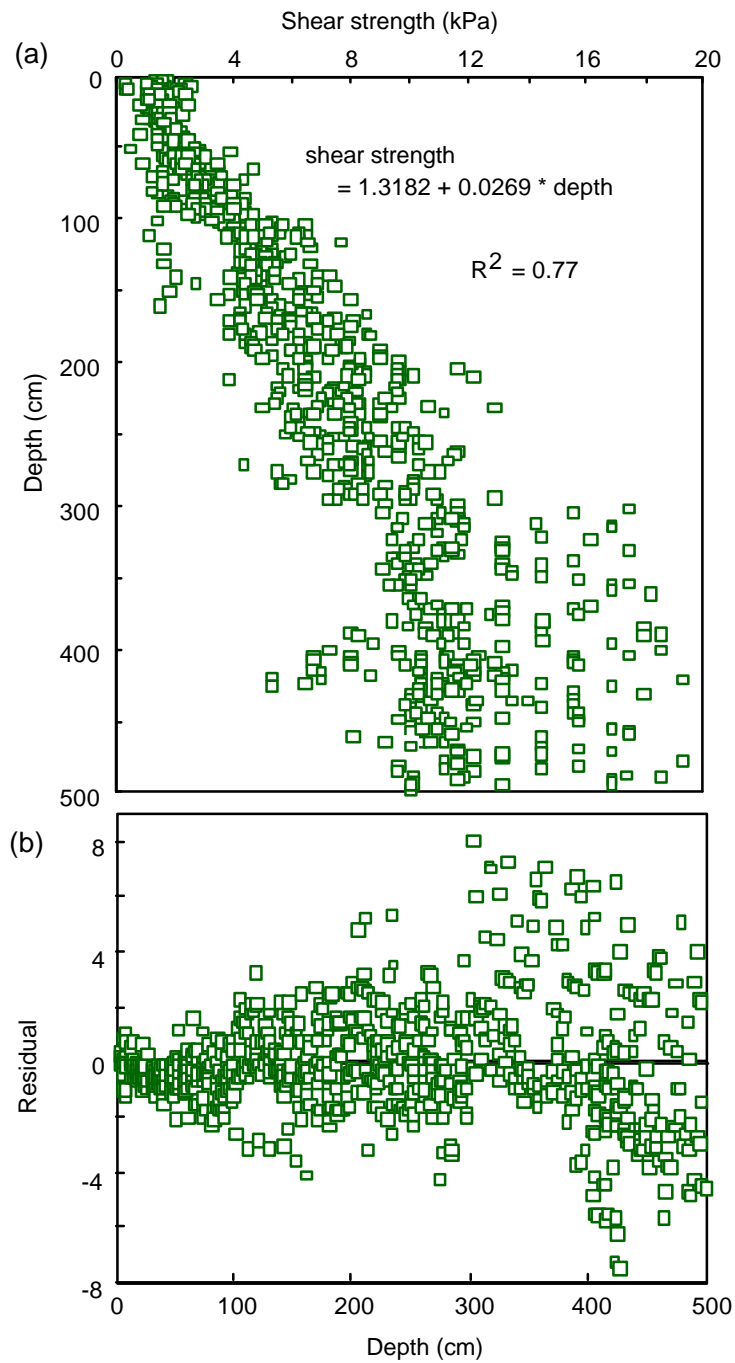


Figure 1. (a) In non-gassy sediments from Eckernförde Bay, undrained shear strength increases with depth. (b) A linear model describes this relationship well, as indicated by the lack of systematic patterns in the residual plot. When other independent variables are included in a regression model, they do not significantly improve the model (the increase of R^2 is small). Figure from Lu, Bryant and Slowey (in press).

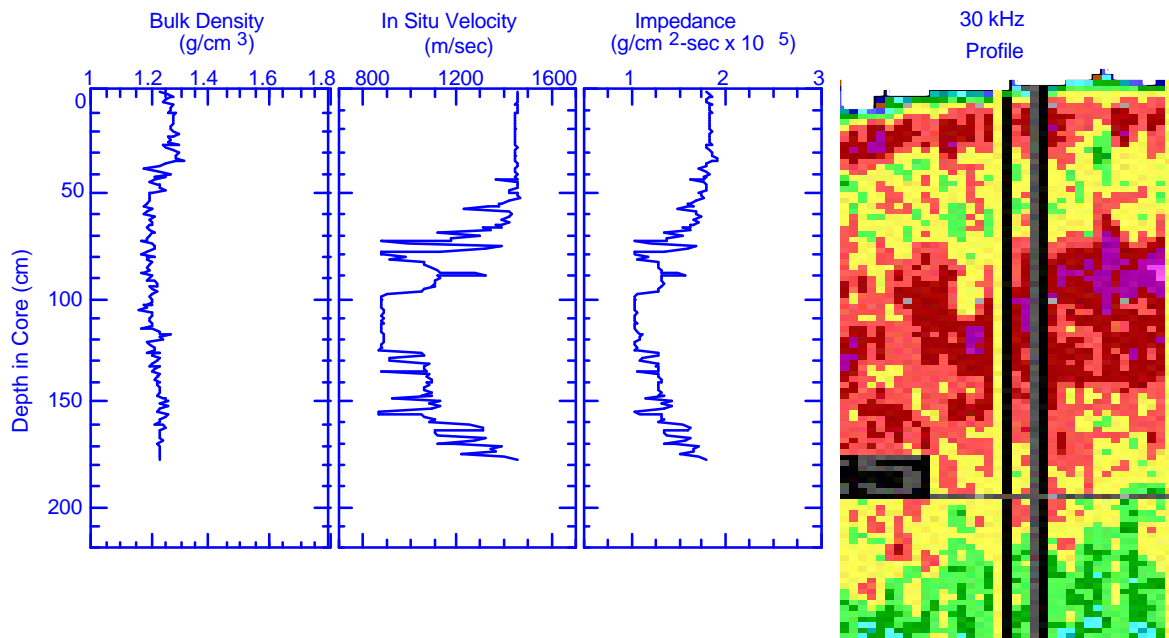


Figure 2. Down-core profiles of (a) saturated bulk density derived from Gamma-ray attenuation (lines) and measured water content (filled circles), (b) compressional wave velocity and (c) acoustic impedance for core 317, and together with (d) the 30 kHz profile of the location the core was collected in Eckernförde Bay. The upper 50 cm of sediments shows typical soft, fine-grained sediment velocities of about 1455 m/sec, but, the velocity of underlying sediments is sharply reduced. Over the depth range of about 50 to 70 cm, velocity decreases steadily, indicating the presence of free gas in the sediments. Measured velocity values of the sediments between 50 and 70 cm may be representative of actual velocities because studies suggest gassy sediments should have lower velocities than non-gassy sediments; however, the lowest velocities at >70 cm depths (1100 or 900 m/sec) are probably erroneously low due to the presence of high free gas concentrations. Consistent with the presence of free gas, high-resolution seismic profiles of the location where this core was collected display a strong acoustic reflector (red color) at about 50 to 70 cm depth below the seafloor and little compressional wave energy returns from the underlying sediments. Figure from Slowey, Bryant and Lambert (1996).

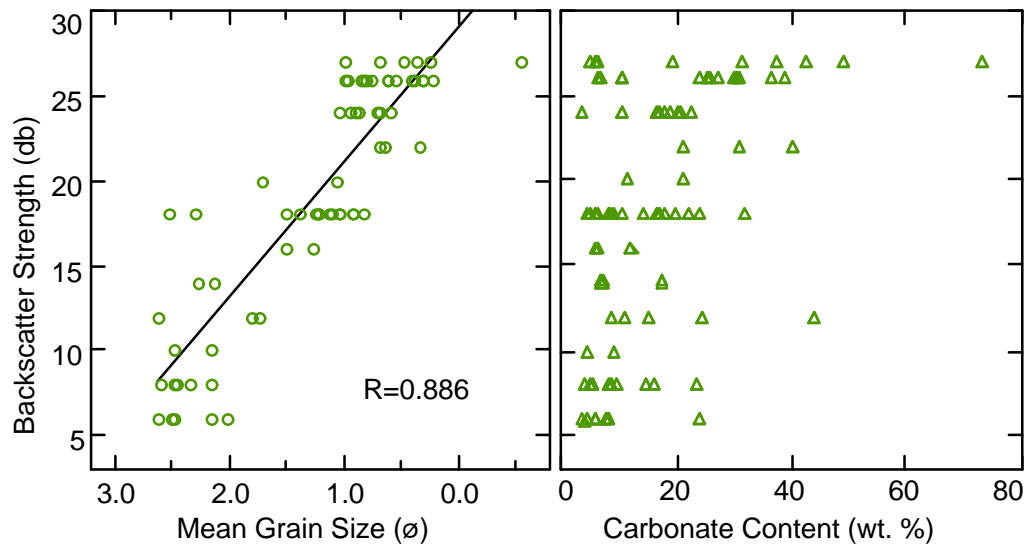


Figure 3. (a) Plot illustrating the strong correlation between mean grain size and relative backscattering strength. Consequently, in the region of the study site, we should be able to predict the sediment type based upon the observed relative backscattering strength, and in areas where backscattering strength is essentially constant, we should find laterally homogeneous sediment types. (b) Plot of carbonate content versus relative backscatter strength. Samples containing less than about 12-15% carbonate show an increase in relative backscattering strength while the carbonate content varies little, indicating something other than carbonate content is causing the change in backscattering strength. When backscattering strength is greater than 15 dB, carbonate content correlates fairly well ($R=0.67$) with relative backscattering strength. There are two possible reasons for this relationship: (1) increasing carbonate content results in an increase in mean grain size and so greater backscattering, and (2) the shape of the carbonate fragments, which have flat surfaces and many angles, makes them more effective at backscattering acoustic energy than more-spheroidal non-carbonate sediment grains. Figure from Davis, Slowey, Stender, Fiedler, Bryant, and Fechner (1996).

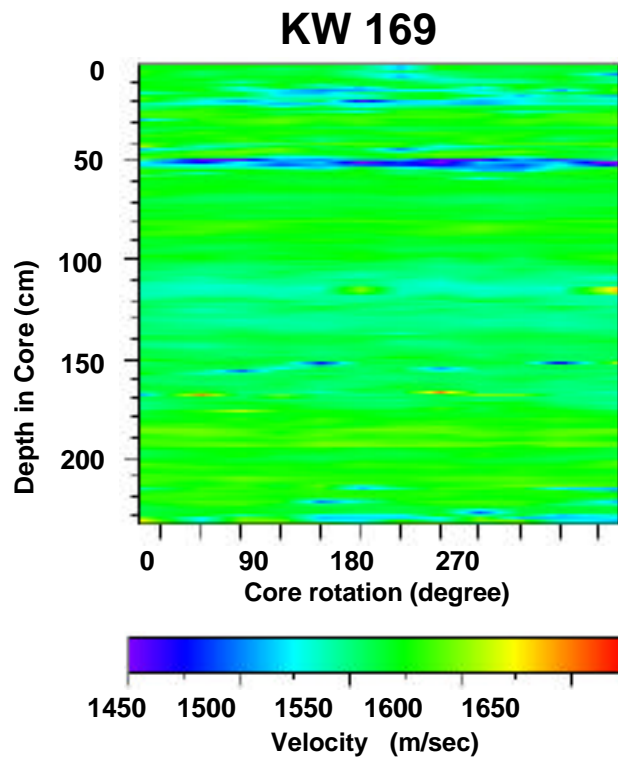


Figure 4. The compressional wave velocity across the diameter of gravity core 169 from Key West measured at 30 degree intervals. This plot graphically illustrates the extent of variability in velocity which depends of the particular horizontal direction compressional waves travel and also depth. Similar velocity and density data from the suite of Key West cores is being examined for the occurrence of significant anisotropy. Any areas within the core expressing anisotropy will be examined to determine the nature of the sediments in terms of size, composition, texture and, fabric which includes particle shape and orientation. Another valuable outcome of these type measurements was the fact that they showed that the core logger was recording, in some instances, the second cycle of the transmitted wave which results in an erroneous drop in velocity of approximately 50 m/sec. Figure from Lee, Bryant, and Slowey (in preparation).

Acoustic penetration and backscatter at the water-sediment interface

Final Report for “Bottom scattering strength measurement,” under Grant No. N00014-95-1-G906

by Nicholas P. Chotiros, Applied Research Laboratories, The University of Texas in Austin

Abstract:

Applied Research Laboratories, The University of Texas in Austin, (ARL:UT) participated in the Coastal Benthic Boundary Layer (CBBL) Special Research Program (SRP) from March 1993 to September 1996. The work was divided into two phases: (1) analysis of acoustic backscatter penetration of ocean sediments, using data collected by the Naval Research Laboratory, Stennis Space Center (NRL/SSC) from sites off Panama City, Florida and Eckernförde, Germany; and (2) to measure and analyze bottom backscattering data in the Key West Campaign, as part of a major effort to understand acoustic sediment interactions and develop relevant models. The detection of two acoustic sediment waves in sand indicated that Biot's theory is necessary to the proper understanding of sound propagation in the sediment, while soft muddy sediments may be approximated as a liquid for practical purposes. The apparent height dependence of backscattering strength over sand indicates a multiple scattering process.

Objectives:

The work contained two phases. In the first phase, the objective was to study the sound propagation from water into the sediment, in particular, to test the validity of Biot's theory at high frequencies.¹ Experiments were conducted by NRL/SSC in cooperation with ARL:UT to measure sound propagation into a muddy sediment in Eckernförde, Germany, and a sandy sediment off Panama City, Florida. In both sites, acoustic pulses at a number of frequencies were transmitted from a projector in the water towards a buried array of hydrophones buried in the sediment at a selection of discrete grazing angles. In

the second phase, high frequency reverberation data from shallow water sediments, particularly coral and mud sediments, were collected for measurement of spatial backscatter statistics, using sensors mounted on a remotely operated vehicle (ROV), in support of high frequency backscatter modeling, sonar imaging applications, and sediment classification.

Approach:

The approach to the first objective consisted of measuring acoustic signals that penetrated the water-sediment interface, using an array of buried receivers and the reflection coefficient. The signals were analyzed by an energy superposition method to give an ambiguity function in a direction and speed space in which one or more peaks are indicative of the presence of one or more waves at the indicated direction and speed coordinates.

The approach to the second objective was based on a direct measurement of acoustic backscatter, by insonifying the sediment with a sound pulse and recording the backscatter as a function of time. Given the height above bottom of the transducers, the grazing angle may be computed from the time delay, assuming that the scatterers act instantaneously and lay on the sediment surface. The signals were then processed to give plots of backscattering strength as a function of grazing angle.

Results:

The reflection loss of sandy sediments^{2,3} at normal incidence was found to be inconsistent with the models that approximate the sediment as a fluid. It could be explained by Biot's theory, but with modifications to the accepted assumption of the grain bulk modulus. An attempt was made to measure the grain bulk modulus,⁴ which resulted in the re-examination of the assumption that the skeletal frame is an isotropic, homogeneous elastic structure.⁵

In the sandy sediment, two acoustic waves were detected, one at a speed of 1700 m/s and the other at 1200 m/s, approximately. Both waves were present at a grazing angle of 30°, but only the slow wave was present at 10°. An example of the results, containing both waves, is shown in Fig. 1. The signal levels did not decay monotonically with depth in the 30° case, possibly due to interference between the two waves, making it difficult to estimate the attenuation coefficient. At 10° the slow wave was dominant and the signal levels were more consistent, although at 20 kHz the signal level at the deepest hydrophone was stronger than the signal level at shallower depths. Calculations were made of the attenuation coefficients where signal levels decreased with depth in a monotonic manner. The results fall near the top end of the range of reported values for ocean sediments⁶ and are consistent with values for sandy sediments.

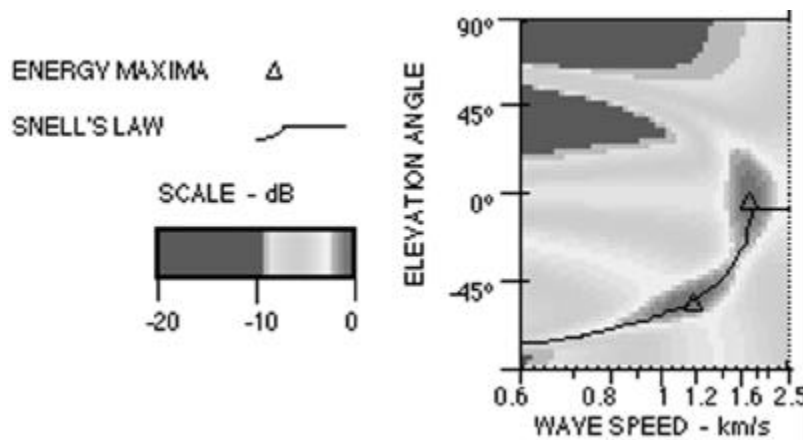


Figure 1

Example of sediment wave speed and direction ambiguity diagram at a grazing angle of 30° and 110 kHz in a sandy sediment.

In the muddy sediment, only one acoustic wave was detected, at a speed of approximately 1400 m/s, and was consistent with core measurements⁷ as shown in the example in Fig. 2. The signal levels appeared to increase with depth at the lower end of the frequency band, and decrease with depth at the high end, with a gradual transition in between. Calibration inaccuracies are the most likely cause, since the differences at the lower frequencies were small - only a few decibels. Where the signal levels decrease with increasing depth, calculations were made of the attenuation coefficient. The values are consistent with previously reported values for muddy sediments and are a factor of ten smaller than those of the sandy sediment.

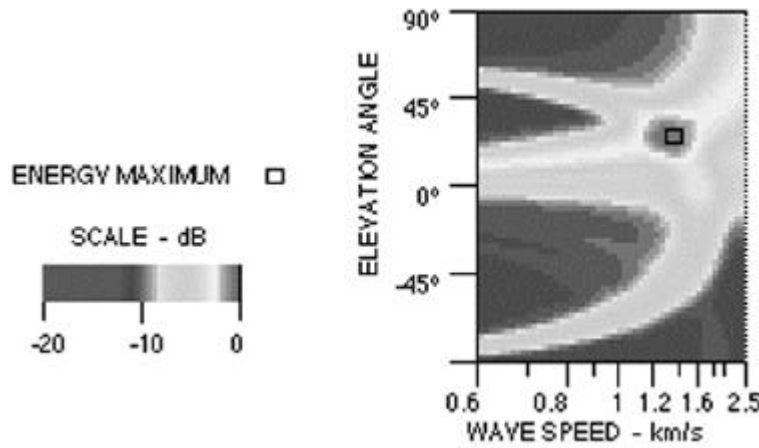


Figure 2

Example of wave sediment, wave speed, and direction ambiguity diagram at a grazing angle of 10° and 110 kHz in a muddy sediment.

In the second phase, high frequency reverberation data from shallow water sediments, particularly coral and mud sediments, were collected for measurement of spatial backscatter statistics using sensors mounted on a remotely operated vehicle (ROV), in support of high frequency backscatter modeling, sonar imaging applications, and sediment classification. The apparent dependence of backscattering strength on sonar height above bottom (HAB) was of particular interest, as shown in the example in Fig. 3. Apparent dependence on HAB was observed in the Eckernförde data, because the

scattering layer was not at the water-sediment interface but significantly deeper. In the Key West site, under the single scatter assumption, this was not expected to be the case because high acoustic attenuation in the sediment⁸ rules out the possibility of scattering from any depth greater than about 5 cm below the water-sediment interface. The apparent HAB dependence may be modeled in terms of a characteristic decay time of approximately 5 ms. In a granular medium such as sand, the most likely cause of a long decay time constant is multiple scattering. This involves acoustic interactions between two or more scatterers, in which acoustic energy is scattered from one scatterer to several others in a cascading fashion. Such a process may be approximated by diffusion theory.⁹

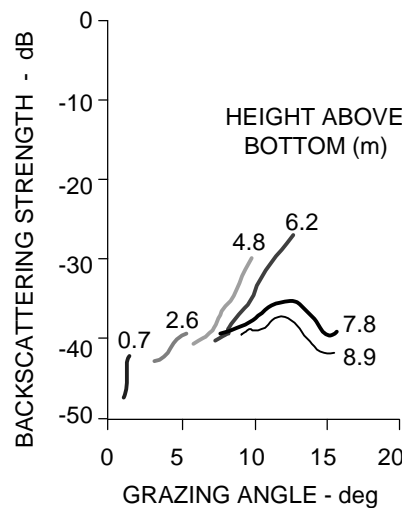


Figure 3

Example of backscattering strength versus grazing angle at various sonar heights above bottom at 200 kHz

Accomplishments:

The findings were very revealing of the nature of acoustic sediment interactions. The detection of two acoustic sediment waves in sand indicated that Biot's theory is necessary to the proper understanding of sound propagation in the sediment, while soft muddy sediments may be approximated as a liquid for practical purposes. The apparent height dependence of backscattering strength indicates that the scattering mechanism lay not at the water-sediment interface, but within the interior of the sediment. In view of the

high attenuation coefficient of the sandy sediment, the apparent height dependence indicated a decay time constant that was too long for a single scattering process, which lead to the conclusion that it should be treated as a multiple scattering process. The results provided valuable data for the development of a new model of bottom reflection and backscattering in a related 6.2 program.¹⁰

Publications:

Peer reviewed (published, in press, in preparation)

N. P. Chotiros, “Biot model of sound propagation in water saturated sand,” J. Acoust. Soc. Am., 97(1):199-244, 1995.

N. P. Chotiros, R. A. Altenburg, and J. Piper, “Analysis of acoustic backscatter in the vicinity of the Dry Tortugas,” Geomarine Letters, 17: 325-334, 1997.

Symposium proceedings:

N. P. Chotiros, "Ocean bottom acoustic interactions in MCM," Proceedings of IEEE-OES OCEANS 94, Brest, France, September 13-16, 1994, Vol. II:250-254.

N. P. Chotiros, "Inversion and sandy ocean sediments," NATO Conference on Full Field Inversion Methods, SACLANTCEN, Italy, 27 June - 1 July 1995.

N. P. Chotiros, "Acoustic sediment penetration measurement with a buried hydrophone array in Eckernförde Bay," (pps 89-96) in Proceedings of Modelling Methane-Rich Sediments at Eckernförde Bay, edited by T. F. Wever, held at Eckernförde, Germany, 26-30 June 1995. FWG Report 22.

N. P. Chotiros and S. Stanic, "Acoustic sediment penetration measurement with a buried hydrophone array in Eckernförde Bay," (pps 89-96) in Proceedings of Modelling Methane-Rich Sediments at Eckernförde Bay, edited by T. F. Wever, held at Eckernförde, Germany, 26-30 June 1995. FWG Report 22.

R. Priebe, N. P. Chotiros, D. J. Walter and D. N. Lambert, "Gas bubble recognition by wavelet analysis of echo-sounder signals," (pps 104-113) in Proceedings of Modelling Methane-Rich Sediments at Eckernförde Bay, edited by T. F. Wever, held at Eckernförde, Germany, 26-30 June 1995. FWG Report 22.

Reports:

N. P. Chotiros, "Analysis of sea test data I" Applied Research Laboratories, The University of Texas at Austin Technical Report No. 95-11 (TR-95-11), Applied Research Laboratories, The University of Texas at Austin, 1995.

Published abstracts:

N. P. Chotiros, R. A. Altenberg, and S. J. Stanic “High frequency acoustic penetration of ocean sediments,” J. Acoust. Soc. Am., 96(5):3265, 1994.

N. P. Chotiros, R. A. Altenburg, and F. A. Boyle, “Reflection coefficient of sandy ocean sediments in shallow water,” EOS, 75(3):181, 1994

R. Priebe, N. P. Chotiros, D. J. Walter, and D. N. Lambert “Sea floor classification by wavelet decomposition of fathometer echoes.” Abstract and presentation at OCEANS’95 MTS/IEEE, San Diego, CA 9-12 October 1995.

References:

1. N. P. Chotiros, S. J. Stanic, “Acoustic sediment penetration measurement with a buried hydrophone array in Eckernförde Bay,” Proc. Workshop on Modeling Methane-Rich Sediments of Eckernförder Bay, Eckernförder, 26-30 June 1995.
2. N. P. Chotiros, “Inversion and sandy ocean sediments,” in Full Field Inversion Methods in Ocean and Seismic Acoustics, NATO Conference Proceedings, Lerici, Italy (27 June - 1 July 1994). Published in Full Field Inversion Methods in Ocean and Seismic Acoustics, edited by Diachok, Caiti, Gerstoft, Schmidt, ISBN0-7923-3459-0, Kluwer Academic Press, 1995.
3. N. P. Chotiros, R. A. Altenburg, and F. A. Boyle, “Reflection coefficient of sandy ocean sediments in shallow water,” EOS, 75(3):181, 1994.
4. N. P. Chotiros, J. C. Molis, and J. L. Darrouzet, “A measurement of the bulk modulus of sand grains,” J. Acoust. Soc. Am., submitted February 1997.
5. N. P. Chotiros, “Reply to: Biot slow waves in sands near the seafloor, by R. D. Stoll,” J. Acoust. Soc. Am., in press 1998.
6. E. L. Hamilton, “Geoacoustic Modeling of the Sea Floor,” J. Acoust. Soc. Am. **68**, 1313-1340, 1980.

7. K. B. Briggs and M. D. Richardson, "Geoacoustic and physical properties of near surface sediments in Eckernförde Bay," 39 - 46, Proceedings of the Gassy Mud Workshop, FWG, Kiel, 11 - 12 July 1994.
8. K. B. Briggs et al, "Physical and Geoacoustic Properties of Sediments Collected for the Key West Campaign, February 1995: A Data Report," NRL/MR/7431 - 96-8002, Naval Research Laboratory, Stennis Space Center, MS 39529-5004, 10 May 1996.
9. N. P. Chotiros, A. M. Mautner, and J. Laughlin, "Backscatter Analysis from a Smooth Sand Surface: Diffusion Approximation," Applied Research Laboratories, The University of Texas at Austin Technical Report No. 95-30 (TR-95-30), Applied Research Laboratories, The University of Texas at Austin, 1 September 1995.
10. F. A. Boyle and N. P. Chotiros, "Bottom Grain Gas and Roughness Technique (BOGGART) Version 3.0: Bottom Backscatter Model User's Guide," Applied Research Laboratories, The University of Texas at Austin Technical Report No. 96-10 (TR-96-10), Applied Research Laboratories, The University of Texas at Austin, 4 June 1996.

New Geophysical Technologies Applied to the Quantitative Evaluation of Seabed Properties Related to Mine Burial Prediction

A.M.DAVIS, D.HUWS, J.PYRAH and R.HAYNES

Marine Geophysics Group
School of Ocean Sciences
University of Wales Bangor
Menai Bridge, LL59 5EY
Anglesey, Wales, UK

ABSTRACT

Within the Coastal Benthic Boundary Layer Project, a series of complementary geophysical experiments were undertaken with the primary objective of collecting data to assist the physical characterisation of sea floor sediments at the CBBL sites. It was envisaged that these experiments would lead to a strengthening of the physical knowledge base and result in an improved understanding of physical properties and process interactions. The research completed within this program has enabled UWB to provide valuable insights into the effects of geological, biochemical, and hydrodynamic processes on larger-scale sediment structure. Multi-channel digital seismic and electrical resistivity data were collected using surface- and bottom-towed arrays. At three of the CBBL sites - Eckernforde Bay, Key West, and the north Californian Shelf - profiling with a bottom-towed sled yielded shear wave velocities and electrical resistivity data indicative of the structural strength of the sediment and of the properties of the pore space. Processed digital sub-bottom profiler data acquired in Eckernforde Bay revealed significant variations in seismic character in the vicinity of seabed surface pockmarks and around "acoustic window" locations, leading to inferences on physical property variability and environmental process control. Representative shear wave velocities for the Eckernforde Bay soft gassy mud were, as expected, extremely low, ranging from <10 m/s at the surface to around 16 m/s at 2 m; the sediment shear wave velocity structure appeared unaffected by the known changes in gas saturation a few tens of centimeters below the sediment surface. Digital sub-bottom profiler data collected along closely-spaced lines in the Dry Tortugas area of the Florida Keys were combined and processed to produce contour maps of sea floor reflectivity strength and variance which were subsequently used to help identify and delineate the outcropping Pleistocene limestones and Holocene patch reefs. Higher than expected shear wave velocities were recorded from the soft carbonate silty muds. The experimental program for the north Californian Shelf was directed towards providing supporting information on the likely behaviour of the *in situ* sediment mass under a range of dynamic stress conditions. To this end a complementary series of specialist laboratory tests were undertaken on samples recovered from the site. These and associated experiments on a sediment sample taken from the Rebecca Shoals area of the Florida Keys, confirmed the usefulness of the seismic shear wave velocity as an index of liquefaction potential of uncemented sediments and lent support to the argument for using

a combined field and laboratory geophysical approach for *in situ* sediment behavioural prediction.

BACKGROUND

Within the published Program's Direction and Workshop Recommendations for the Coastal Benthic Boundary Layer Special Research Program, geophysical techniques were identified as being ideally suited to the remote sensing of seabed sediment properties; however, within the same document, it was also acknowledged that there was a need for additional basic research, both of a theoretical and practical nature, to further quantify the relationships between geotechnical properties and geophysical quantities. The University of Wales Bangor's (UWB) contribution to the CBBL Program arises from research carried out by the university's Geophysics Group over many years aimed specifically at improving the understanding of sea floor sediment geophysical-geotechnical property relationships.

OBJECTIVES

The initial objective of the project was to assess the extent to which UWB's newly developed geophysical technologies could be relied upon to provide quantitative information on the physical properties of a spatially heterogeneous sea floor. To this end a series of measurements were planned for selected trial sites in the southern Baltic as part of the CBBL's co-ordinated experiments in Eckernförde and Kiel bays. Following the successful completion of the Eckernförde Bay experiments, UWB's program objectives were revised and significantly extended. Further field geophysical experiments were planned with the express purpose of acquiring *in situ* data to assist the physical characterisation of the sea floor sediments at two other CBBL research sites: the Key West and northern Californian Shelf sites. Complementary and specialist laboratory tests to be undertaken on recovered sea floor samples from these two sites aimed at providing supporting information on the likely behaviour of the *in situ* sediment mass under a range of dynamic stress conditions. The laboratory experiments were expected to provide data of direct relevance to mine burial prediction.

APPROACH

In situ measurements:

In situ geophysical data to be used for sediment property prediction were acquired using one of two underway techniques. Information on sea floor sediment shear wave velocity and electrical resistivity variability was obtained using a bottom-towed geophysical sled device 'Magic Carpet' (Davis et al., 1989). Seismic shear wave records, which comprised a series of signal traces resulting from a single shot with a sled-mounted shear source,

were interpreted to provide information on the velocity structure in the upper 2-3 metres of sediment cover at each measurement location. Measurements of the sediment electrical resistivities were taken simultaneously with shear wave travel times using a focused electrode 'pad'; recorded values were converted to an equivalent formation factor through input of a seawater resistance. At all three of the investigated CBBL sites, measurements were performed at discrete intervals along predetermined survey tracks providing information on the geophysical property variability on the metre to kilometre scale.

At two of the CBBL sites - Eckernförde and Key West - high-resolution seismic reflection data were acquired in digital format ready for signal processing and geotechnical analysis. The subbottom profiling equipment used to acquire the high-resolution digital data was a combination of commercially available instruments and specialised equipment designed and built at UWB. An EG&G surface tow Uniboom was chosen for signal generation because of its highly repeatable source signature and its broad bandwidth, typically 400 Hz to 10kHz, which provides a vertical resolution to better than 30 cm. The reflection signals, received using either a single element hydrophone or a UWB-designed multichannel streamer, were recorded on DAT tape and post-processed using a commercial seismic software package (SierraSeis ISX) and specialized geotechnical software developed in-house within the university's geophysics laboratory. Processing of the Baltic Sea data set was directed towards data enhancement for seismic character recognition and concentrated on the investigation and analysis of anomalous features within the zones of gas-charged sediment in Eckernförde bay. Simple waveform analysis resulted in the production of attribute sections e.g. instantaneous phase, instantaneous frequency, or amplitude, making it possible to take a more quantitative approach to seismic character recognition. Processing of the Key West data set was directed towards providing information on the sea-floor reflectivity strength and its spatial variance (Haynes et al., 1997).

Laboratory studies:

Empirical relations between geophysical and geotechnical quantities for carbonate sediments are not particularly well developed. In an attempt to address this problem and provide data which might aid *in situ* property predictions, some preliminary geophysical/physical property measurements were performed in the laboratory on the sediment sample recovered from Rebecca Shoals. These measurements involved simultaneous monitoring of seismo-acoustic wave velocities (P and S), electrical resistivity and porosity (void ratio) during compaction (from loosest to densest packing state at ambient pressure).

Laboratory experiments to investigate the likely behaviour of sea floor sediments under dynamic stress conditions were centred around the definition of the state parameter, ψ . This parameter represents a quantitative measure of the consolidation state of a sediment and combines the effects of void ratio and effective stress in a unique way for a particular deposit. Sediments with a positive ψ tend to contract under shear giving rise to raised pore-pressures and a strain softening behaviour. Those with a negative ψ tend to dilate,

leading to lowered pore-pressures, and hence reducing the risk of liquefaction. Cyclic loading, such as that imposed by waves interacting with the seabed in shallow water, may also further modify sediment behaviour. Data from various laboratory testing programs have illustrated the applicability of this kind of approach both as an empirical normalising parameter and for the constitutive modelling of soil behaviour. Therefore the assessment of the *in situ* state parameter may be regarded as being of prime importance in mine burial prediction. These experiments aimed to capitalise and build on research recently completed at UWB (e.g. Pyrah, 1996) in which shear wave velocity was used as an index to liquefaction potential.

The bulk of the laboratory testing work was performed using a modified stepper-motor based triaxial apparatus. Principal modifications included the addition of shear wave 'bender' elements in re-designed end platens, and the development of purpose written software code which allowed both standard drained and undrained monotonic tests to be performed, in addition to one-way, stress controlled cyclic triaxial testing. Testing work centred around three sediments collected from two geographical areas: a carbonate sand recovered from Rebecca Shoals, Key West, and two samples recovered from the northern Californian shelf around Eureka. After suitable preparation, the sediments were subjected to an intensive testing program involving standard consolidated, undrained triaxial testing to determine steady state properties and, anisotropically consolidated undrained one-way cyclic triaxial tests to help determine the cyclic properties. During the consolidation phases of these tests a large number of shear wave velocity measurements were also made, allowing a general relationship between the shear wave velocity, void ratio, effective stress and overconsolidation ratio to be determined. Limited resonant column testing also further allowed the confirmation of these relationships. Integration of these laboratory relationships with the field data allowed the estimation of the *in-situ* state parameter.

RESULTS

Eckernforde Bay: *In situ* experiments

Analogue seismic subbottom profiler data have provided and will continue to provide important evidence on sea-floor and sub-surface sediment structure and stratigraphy. With the continued development of seismic processing software, advances in the understanding of the significance of seismic reflection signatures are to be expected, not least in the understanding of links between sediment physical property variability and reflection signature.

In Eckernforde Bay, seismic reflection attribute analysis provided a means of quantifying sediment property variability on a regional and localised scale. Within the Quaternary sediment cover, perhaps the most interesting seismo-acoustic features to comment on are the acoustic windows which interrupt the otherwise structurally featureless sections of acoustically turbid gas-charged material. An amplitude envelope section (instantaneous amplitude) for one such feature has been published in Davis et al. (1996). Within the

processed section the turbid zones associated with shallow gas appear as medium- to high-amplitude areas of incoherency and the underlying till surface appears as a high-amplitude coherent reflector. Clearly there are marked and significant changes in seismic character within the surface sediments around acoustic windows in the bay, and clearly there are processes operating in the bay that create the presented and other acoustic windows seen in the boomer records. Whatever the dominant process mechanisms, they will inevitably be strongly affected by the physical properties of the sediment. Based on the digital seismic data and other published evidence (e.g. Whiticar and Werner, 1981), it is perhaps not unreasonable to suggest that some of these windows represent points at which groundwater is circulating upwards from the underlying Pleistocene surface.

Shear wave tracks with the bottom-towed sled traversed a variety of surface lithologies (Davis et al., 1996). The interpreted velocity depth profile presented in Figure 1 below is representative of the typical velocity structure of the Eckernforde Bay mud. The interpretation of the shear wave velocity data confirms the expected low shear wave velocity at the surface (<10 m/s) for the soft muddy sediment and reveals the velocity gradient structure of the upper 2-3 m. These findings are in good agreement with those of other researchers working in the same area, notably Richardson and Griffin (1994), whose results are based on direct measurements with the ISSAMS probe, and Stoll (1994), whose interpretation is based on the analysis of surface wave arrivals. The surface velocity is as would be expected for a material of low stiffness, whilst the velocity gradient is controlled by the increasing vertical effective stress with depth. As reported by others (Briggs and Richardson, 1994), the shear wave velocity appears unaffected by the change in gas saturation known to occur a few tens of centimetres below the sediment surface (transition from fully water-saturated to gas-charged variable between approx. 30 and 100 cm.).

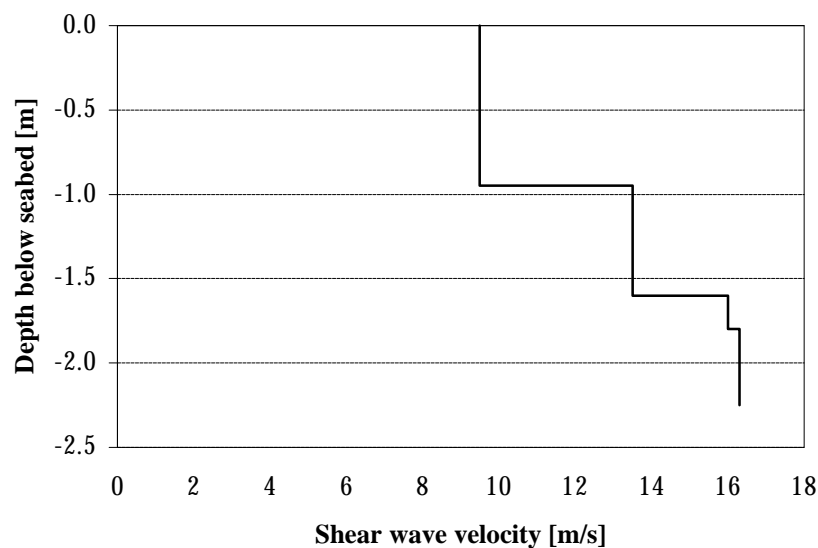


Figure 1. Interpreted velocity versus depth profile for the Eckernforde soft mud.

The sled measured electrical formation factor of the soft mud is characteristically low, approaching the value for seawater i.e. unity, and is typical of a very high porosity mud. A more in-depth discussion of the relations between sled measured geophysical quantities for the soft mud and other known properties can be found in Davis et al. (1996). Concerning measurements in other sedimentary environments, the sled data were, as expected, sensitive to changes in seabed surface lithology.

Key West: *In situ* experiments

Digital subbottom profiler data collected along closely spaced lines were processed to produce contour maps of sea-floor reflectivity strength and variance (Haynes et al., 1997). These were subsequently used to help map the spatial distribution of the Holocene sediment and to identify and delineate the outcropping Pleistocene limestones and Holocene patch reefs. This approach to subbottom profiler data interpretation provided for a more quantitative spatial mapping of the surficial sediment properties and/or characteristics. In particular, many of the surficial features identified from examination of individual subbottom profiler sections were subsequently able to be located and described more effectively.

The geophysical sled ‘magic carpet’ was bottom-towed for a total of 9.5 hours along 6 tracks near the Dry Tortugas, providing several hundred independent shear wave velocity measurements. Figures 2 & 3, containing a subset of the data collected along one line, illustrate the typical range of velocities recorded for the sediments in the vicinity of the APL experimental tower sites (for location map see Haynes et al., 1997). Higher than expected velocities (40-80 m/s in the upper 0.5 m) were recorded from these soft carbonate silty muds and most records indicated a marked increase in velocity with depth within the upper two meters of the sediment column. Although higher than expected, the velocities did show excellent agreement with those independently obtained by others using a remotely operated probe (ISSAMS, Richardson et al., 1996) in the same area.

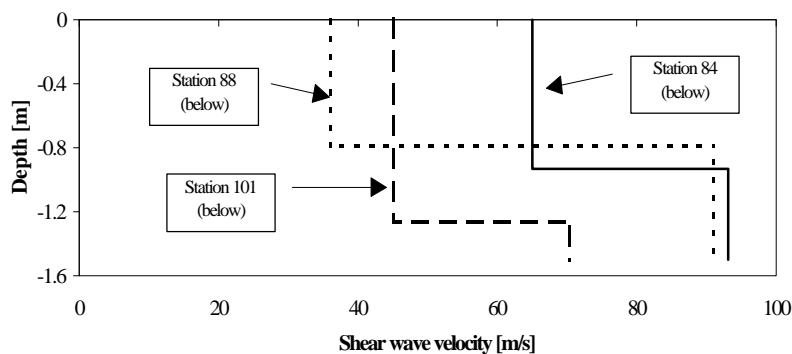


Figure 2. Discrete layer shear wave velocity versus depth models - Key West.

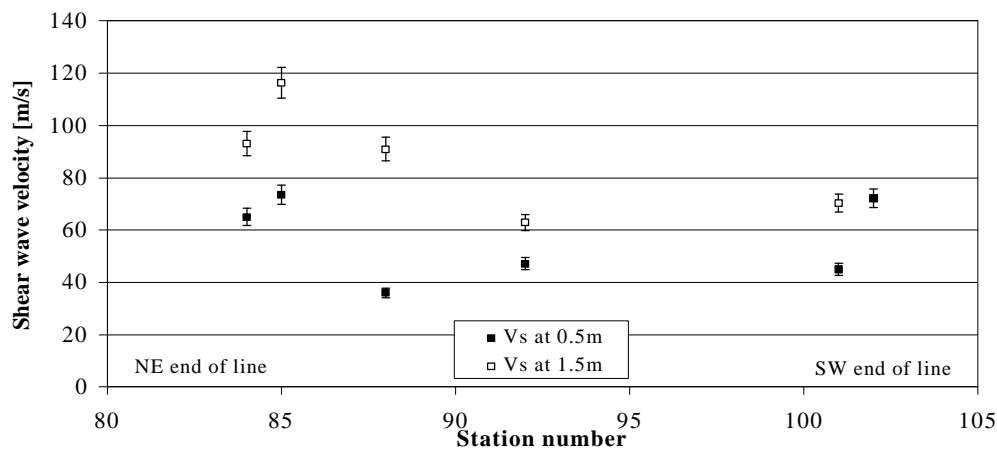


Figure 3. Spot measurements of shear wave velocity at 0.5 and 1.5m below seafloor, recorded along line 27.

One line (1.5 hours survey time) was run with the magic carpet in the Rebecca Shoals area to help characterise the physical properties of the more sandy carbonate material. As expected, the surface sediment shear wave velocities were much higher than within the carbonate muds (typically 120m/s). A sediment sample was recovered along the Rebecca Shoals line to provide the necessary material for future geophysical/geotechnical laboratory testing, with the primary objective to produce control data to aid the *in situ* interpretation.

Californian Shelf: *In situ* experiments

In situ shear wave data were acquired along a single track covering a bathymetric range of between 36 m and 70 m. Across the shelf the shear wave velocities were observed to correlate strongly with the changing grain size (Figure 4). Over the entire depth range covered by the survey, surface sediment velocities varied between c. 25 m/s and 85 m/s. At all locations the data indicated a velocity gradient structure in the upper few metres, and where coincident measurements were made, the sled measured velocities appeared to agree well with those obtained by Richardson using the NRL ISSAMS probe.

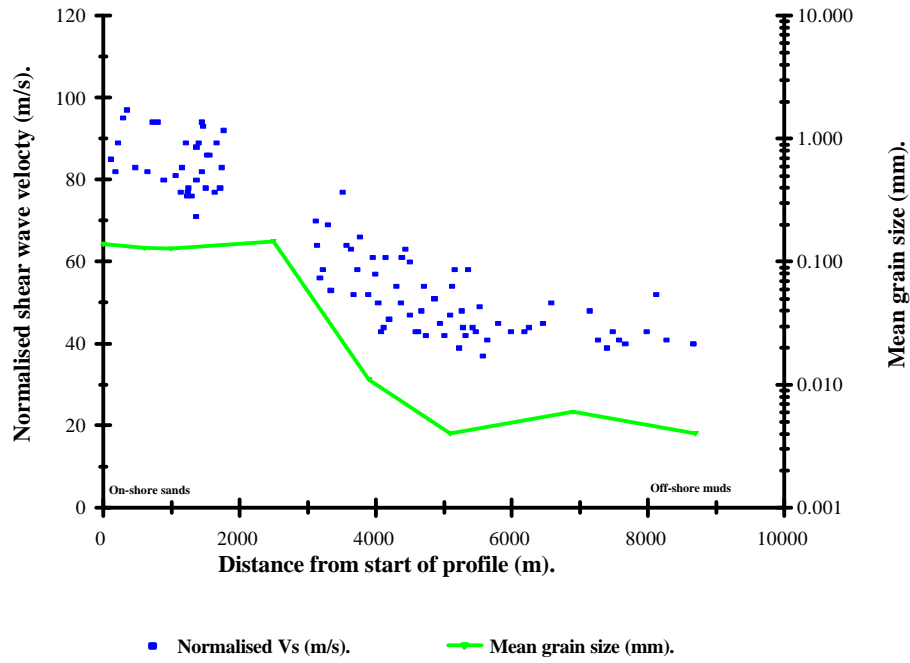


Figure 4. Variation of shear wave velocity (normalised to 30cm) across the ‘S-line’, Eel River, Northern California.

Post cruise analysis and interpretation of the magic carpet shear wave velocity data centred around estimating the *in situ* void ratio, based upon a knowledge of the *in situ* velocity measurements. It is widely accepted that the two most important parameters that can be used to simply model the variation in velocity are effective confining pressure and void ratio (e.g. Hardin and Richart, 1963; Bryan and Stoll, 1988). Both Bryan and Stoll (1988), and Richardson *et al.* (1991) have produced formulae relating shear wave velocity to void ratio and confining pressure (or burial depth):

$$V_s = (85/e) z^{0.30} \quad \text{Richardson } et al. (1991) \quad 1.$$

where V_s = shear wave velocity [m/s]
 z = depth [m]

Given that the magic carpet has provided *in situ* velocity-depth data, it would appear reasonable to estimate void ratio, e , by applying either of the published formulae. Figure 5 illustrates the measured velocity-depth trends and superimposed predicted void ratios (here plotted as porosity; porosity = $e/(1+e)$). However, there are quite large disparities between the models of Bryan and Stoll (1988), and Richardson *et al.* (1991), the differences being most accentuated at porosity values of 50% and at shallower depths. It should be noted that the former inter-relationship was derived in the laboratory, in the confining pressure range 24 to 700 kPa, somewhat higher than those encountered in the depth range sampled by the magic carpet system. Additionally, subsequent to the

formulation of the field data - derived inter-relationship by Richardson *et al.* (1991), velocity and void ratio information acquired in other siliclastic environments have confirmed the reliability of the predictions yielded (*pers. comm.*, Richardson 1996). It is thought, therefore, that the Richardson *et al.* (1991) equation is the most appropriate to apply in this case, and may therefore support the argument for using magic carpet velocity data to map the void ratio / porosity distribution over the entire survey track (Figure 6).

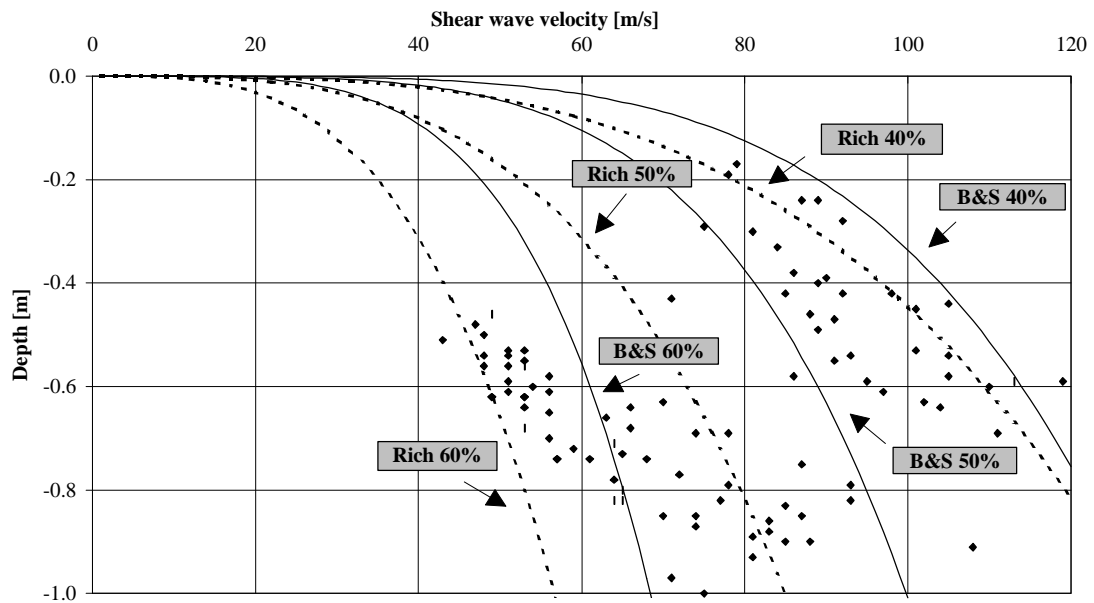


Figure 5. Measured velocity - depth trends and superimposed porosities. (B&S: Bryan and Stoll equation; Rich: Richardson equation).

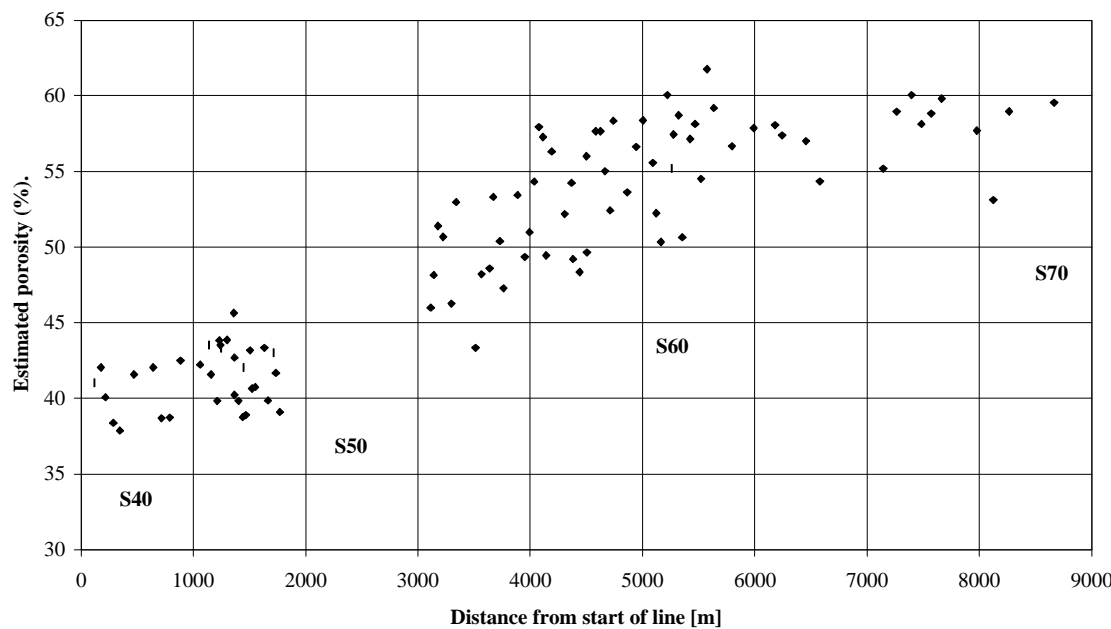


Figure 6. Estimated porosity distribution along the S-transect, Eel River.

Laboratory studies for *in situ* prediction

As mentioned above, the laboratory experiments performed during this study were principally focused around a series of undrained cyclic and monotonic triaxial tests on each sediment type, during which shear wave velocity observations were also made. Additional tests were also performed to further illustrate the relationship between shear wave velocity and void ratio.

The porosity cell devised by Jackson (1976) (and developed by Schultheiss, 1983) allows porosity to be altered and accurately measured, whilst at the same time enabling measurement of the shear wave velocity by means of time-of-flight measurements between two bender bimorph transducers. During the test procedure, the sample is initially settled via water pluviation, to achieve, effectively, a loose packing of high porosity. Velocity measurements are then performed, before the sample is mechanically settled by a known amount. This is repeated until no further settling can be induced by mechanical means. After correcting for the small change in confining pressure that results from the settling process, it is possible to derive the inter-relationship between shear wave velocity and porosity. Such tests were performed on those samples that were suitable for settlement by water pluviation i.e. the carbonate sand and the Californian Shelf siliclastic sand.

The laboratory data acquired for the carbonate sand showed that porosity ranges between 51% and 41% could be achieved in the cell, with shear wave velocities ranging from 65 m/s to 110 m/s respectively (at a confining pressure of 10 cms equivalent depth). These velocities are considerably higher than may be expected from siliclastic sediments over similar porosity ranges. Comparison with the velocities that would be predicted from the Richardson *et al.* (1991) inter-relationship are much lower (55 - 65%) than measured in the cell. For the siliclastic sands sampled on the Californian slope, porosity ranges from between 46% and 37%, with shear wave velocities ranging between 32 and 85 m/s. Considering the artificial nature of the 'loosest packing' state, these velocities agree well with the Richardson *et al.* relationship.

The laboratory triaxial testing program focused primarily upon the definition of the shear wave velocity behaviour, the steady state behaviour of the sediments and their behaviour under cyclic loading. The shear wave velocity behaviour was described in terms of the general equation listed below:

$$V_s = (m_1 - m_2 e) \cdot (p'/P_a)^c \cdot (OCR)^d \quad 2.$$

where, V_s = shear wave velocity, m_1 & m_2 , c and d are material constants, e = void ratio, p' = effective confining stress, P_a = 100kPa, OCR = overconsolidation ratio.

The key parameters in this equation for each sediment sample are tabulated below.

	m_1	m_2	c	d
Carbonate	459	254	0.31	0.06
S30	402	216	0.30	0.04
S40	347	168	0.31	0.06

Table 1. General shear wave relationship constants.

The steady state properties (Been & Jefferies, 1985) of a sand may be also defined in $e - \log p'$ and $q - p'$ space using the following relationships (Sladen et al, 1985):-

$$e'_{ss} = e_1 - C_{ss} \log p'_{ss} \quad 3.$$

$$q_{ss} = Mp'_{ss} \quad 4.$$

where, e'_{ss} = void ratio at steady state, e_1 = intercept at 1kPa, C_{ss} = slope of the steady state line in $e - \log p'$ space, p'_{ss} = effective confining stress at steady state, q'_{ss} = deviator stress at steady state, M = slope of the steady state line in $q - p'$ space.

The key parameters for these relationships are listed below:-

	e_1	C_{ss}	M	f'
Carbonate	1.064	0.030	1.47	36 ⁰
S30	1.028	0.054	1.26	31 ⁰
S40	1.028	0.060	1.30	33 ⁰

Table 2. Steady state parameters.

Refer to Pyrah et al. (1998) for a more complete description of these relationships and their derivations.

Under one-way undrained cyclic loading the sediments displayed two distinct failure modes. For dense samples (negative state parameter) the pore-pressure, after an initial rise, tended to stabilise around a mean value. For samples subjected to low stress ratios, the induced strain for each cycle slowly decreased, until eventually after a large number of cycles, the cyclic strain tended towards a limiting value. For sands subjected to larger stress ratios, pore-pressures again remained positive, but failure tended to occur at high strains in the form of a poorly defined shear plane. Loose sands tended to behave in a similar manner under both monotonic and cyclic loading conditions. In this case raised pore-pressures of a large magnitude were generated after only a small amount of strain, followed by the rapid collapse of the soil skeleton and rapid straining, to a steady state strength, characterised by constant volume, constant stress, and constant velocity (Poulos, 1981).

The laboratory data were then combined with the *in-situ* field data in an attempt to predict the likely large strain response of the surficial sediments (Figure 7). For the Eureka test site it was concluded that the expected sediment response would most likely be dilative in nature. This conclusion is not unexpected considering that the fairly high energy environment of the shelf is unlikely to favour accumulation of loose sediments. For the Rebecca Shoals area the results were less conclusive. Potential reasons for this uncertainty may arise from the complex particulate nature of the sediment, anisotropy, and unquantified cementation effects.

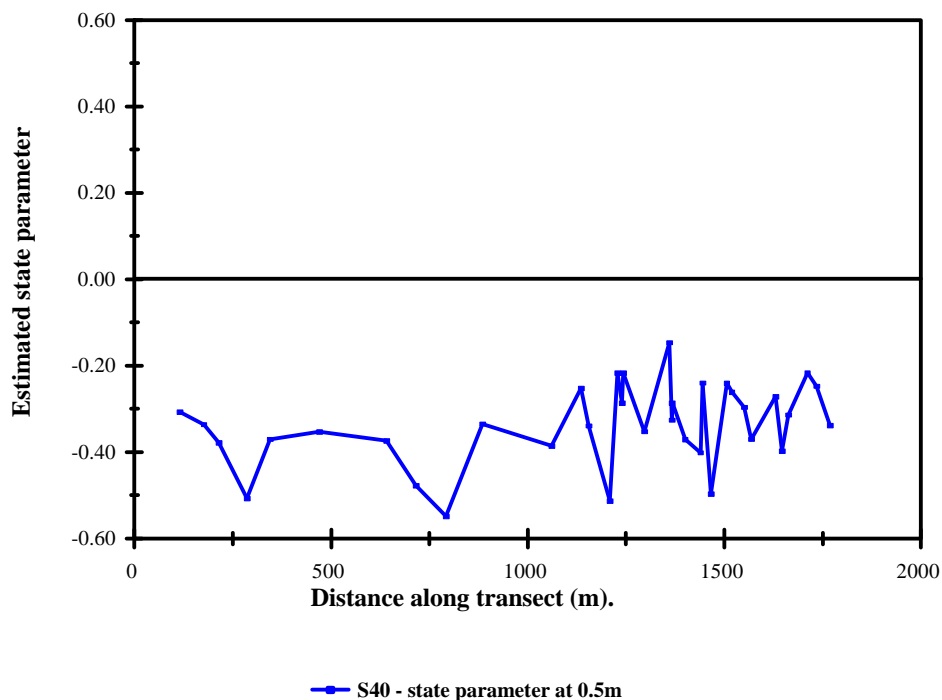


Figure 7. Estimated state parameter between sites S30 & S50, Eel River, Northern California.

CONCLUSIONS AND ACCOMPLISHMENTS

Concerning field methodologies, the CBBL program provided the UWB Geophysics Group with an ideal opportunity to assess its ability to provide a quantitative description of seabed sediment properties using newly developed and innovative underway geophysical techniques. Through field experimentation, in a range of sedimentary environments, it was demonstrated that geotechnically-significant geophysical quantities could be acquired routinely and in a cost effective manner, and that the acquired data could contribute important information at scales ranging from sub-metre to kilometre.

Profiling with the bottom-towed sled 'magic carpet' yielded shear wave velocities and electrical resistivity data indicative of the structural strength of the sediment and of the properties of the pore fluid. The sled data were, as expected, sensitive to changes in seabed surface lithology, which can be reasonably assumed to mirror changes in sediment physical properties. Additionally, shear wave velocity data yielded gradients in velocity indicative of an increase in sediment stiffness with depth, probably a combined response to overburden and biogeochemical effects in all cases. For all the sampled sites the sled measured shear wave velocities were in good agreement with velocities measured by others (e.g. Richardson et. al., 1996) over equivalent depth ranges despite the varying methods and scales of measurement. In the light of these findings and bearing in mind the systems' resolution, for studies of benthic boundary layer processes the magic carpet system would appear ideally suited to rapid reconnaissance surveys and to the spatial mapping of sediment variability, with finer detail being best provided through stationary sampling with apparatus such as NRL's ISSAMS.

Some significant progress was made towards predicting sediment void ratios on the basis of *in situ* sediment shear wave velocities obtained with the magic carpet. In this study predictions were made based on published empirical relations. Despite some disparities between the published predictor equations, it would appear on the basis of ground truth information that preliminary results are promising.

Through field experimentation it was demonstrated that high-resolution seismic reflection data recorded in digital format could be analysed for geotechnically-significant reflection attributes, and that given access to appropriate empirical relations and relevant control data, the geophysical attribute sections might be converted to equivalent physical property sections. Further it was demonstrated that given sufficient coverage, i.e. a dense grid of survey tracks, it becomes possible to produce maps of 'reflectivity features' allowing a more quantitative description of the surficial sediment spatial distribution. In terms of the CBBL program objectives, it can be concluded that the experiments involving digital high-resolution seismic sub-bottom profiler data acquisition and processing contributed crucial evidence on the physical characteristics and likely origin of the sea-floor and subsurface sediments of Eckernforde and Kiel bays, and of the carbonate sediments at the Key West experimental sites.

The combined laboratory and field studies aimed at investigating the physical characteristics and behaviour of the Rebecca Shoals carbonate sands and the north Californian Shelf siliclastic sediments, both confirmed the usefulness of shear wave velocity as an index to the liquefaction potential of uncemented sediments and provided information on the sediment behaviour under undrained cyclic loading. On the basis of the experimental work it was concluded that the state parameter of a laboratory prepared sand could be predicted with a reasonable degree of confidence from a knowledge of the shear wave velocity, the effective confining stress and the overconsolidation ratio. The cyclic testing part of the program further illustrated the effects of sediment density and cyclic stress ratio on the cyclic properties of sand. Interestingly, the research illustrated that for undrained one-way loading, positive pore-pressures were generated whether the sand had

a negative or positive state parameter; however, in these experiments only the loose sand actually liquefied. This effect clearly has implications concerning predictions of the burial of a mine resting on the sea floor.

REFERENCES

- Been, K. & Jefferies, M.G. 1985. A state parameter for sands. *Geotechnique*, 35(2), 239-249.
- Briggs, K.B & Richardson, M.D. 1994 Geoacoustic and physical properties of near surface sediments in Eckernförde Bay. In: Wever T (Ed), *Proceedings of Gassy Mud Workshop*, Report 14, Forschungsanstalt der Bundeswehr für Wasserschall- und Geophysik, Kiel, Germany. pp39-46
- Bryan, G. M., & Stoll, R. D. 1988. The dynamic shear modulus of marine sediments. *Journal of the Acoustical Society of America*, 83(6), 2159-2164.
- Davis, A. M., Bennell, J. D., Huws, D. G., & Thomas, D. 1989. Development of a seafloor geophysical sled. *Marine Geotechnology*, 8, 99-109.
- Davis, A.M, Huws, D.G. & Haynes, R. 1996 Geophysical ground-truthing experiments in Eckernförde Bay. *Geo-Marine Letters* 16, p160-166
- Hardin, B. O., & Richart, F. E. J. 1963. Elastic wave velocities in granular soils. *Journal of the Soil Mechanics and Foundation Division; Proceedings of the ASCE*, 89(SM1), 33-69.
- Haynes, R., Huws, D.G., Davis, A.M., & Bennell, J.D. 1997 Geophysical sea-floor sensing in a carbonate sediment regime. *Geo-Marine Letters*, 17: 253-259.
- Jackson P.D. 1975 An electrical resistivity method for evaluating the in situ porosity of clean sands. *Marine Geotechnology*, 1, 91- 115.
- Poulos, S. J. 1981. The steady state of deformation. *Journal of Geotechnical Engineering*, 107(GT5), 553-562.
- Pyrah, J.R. 1996. An integrated geotechnical - geophysical procedure for the prediction of liquefaction in uncemented sands. Ph.D thesis, University of Wales, Bangor.
- Pyrah, J.R, Huws, D, & Davis, A. 1998 Towards the prediction of in-situ state parameter. In press.
- Richardson, M.D., Muzi, E., Miaschi B. and Turgutcan F. 1991 Shear wave velocity gradients in near-surface marine sediments. In: *Shear waves in marine sediments*, Hovem J.M., Richardson, M.D. and Stoll R.D., Kluwer Academic Publications, Dordrecht, 295 - 304.
- Richardson, M.D. & Griffin, S.R. 1994 In-situ sediment geoacoustic properties. In: Richardson, MD (Ed), *Coastal Benthic Boundary Layer Special Research Program: A Review of the First Year*. NRL Special Report NRL/MR/7431-94-7099. pp146-148

Richardson, M.D., Briggs, K.B., & Davis, A.M. 1996 Geoacoustic properties of carbonate sediments. EoS 77(46):OS172

Schultheiss, P.J. 1983 The influence of packing structure and effective stress on Vs, Vp and the calculated dynamic and static moduli in sediments. In: Acoustics of the seabed, NG Pace (Ed.), Conf. Proc. Of the Inst. of Acoustics, Bath University Press, 19 - 28.

Sladen, J.A., D'Hollander, R.D., & Krahn, J. 1985. The liquefaction of sands; a collapse surface approach. Canadian Geotechnical Journal, 22, 564-578.

Stoll, R.D. 1994 Experimental and theoretical studies of near-bottom sediments to determine geoacoustic and geotechnical properties. In: Richardson MD (Ed), Coastal Benthic Boundary Layer Special Research Program : A Review of the First Year. NRL Special Report NRL/MR/7431-94-7099. pp275-293

Whiticar, M.J., & Werner, F. 1981 Pockmarks: Submarine vents of natural gas or freshwater seeps? Geo-Marine Letters 1:193-199

PUBLICATIONS

Peer reviewed papers:

Davis, A.M., Huws, D.G. and Haynes, R. 1996. Geophysical ground-truthing experiments in Eckernförde Bay. Geo-Marine Letters 16: 160-166.

Haynes, R., Huws, D.G., Davis, A.M. and Bennell, J.D. 1997. Geophysical sea-floor sensing in a carbonate sediment regime. Geo-Marine Letters 17: 253-259.

Pyrah, J., Huws, D.G., and Davis, A.M. 1998. Towards the prediction of *in situ* state parameter. In preparation. To be submitted to Geotechnique.

Richardson, M.D. and Davis A.M. 1998. Modelling methane-rich sediments of Eckernförde Bay. Continental Shelf Research Special Issue. In preparation.

Symposium Proceedings:

Davis, A.M., Haynes, R. and Huws, D.G. 1994. Geophysical approaches to determining the geotechnical characteristics of seafloor sediments: Acquisition and analysis of shear wave, electrical resistivity and digital seismic sub-bottom profiler data. In: Wever, T.F. (ed), Proceedings of the Gassy Mud Workshop held at FWG, Kiel, Germany, July 1994. FWG Report 14: 59-64.

Davis, A.M. and Richardson, M.D. 1995. Geophysical remote sensing of sea floor sediment properties. In: Proceedings of the 1st Meeting of Environmental and Engineering Geophysics, European Section, Torino, Italy, September. 176-179.

Haynes, R. and Davis, A.M. 1995. Using seismic reflection attributes to resolve subsurface sediment characteristics. In: Wever, T.F. (ed), Proceedings of Modelling Methane-Rich Sediments at Eckernfoerde Bay, held at Eckernfoerde, Germany, June 1995. FWG Report 22: 50-57.

Huws, D., Davis, A.M. and Pyrah, J. 1995. Using shear wave velocity and electrical resistivity to resolve the spatial variability of sea floor sediment properties in Eckernfoerde Bay. Wever, T.F. (ed), Proceedings of Modelling Methane-Rich Sediments at Eckernfoerde Bay, held at Eckernfoerde, Germany, June 1995. FWG Report 22: 189-193.

Huws, D., Davis, A.M. and Pyrah, J. 1997. Relating *in situ* shear wave velocity to void ratio and grain size for unconsolidated marine sediments. In: Pace, N.G. et al., (eds.), High Frequency Acoustics in Shallow Water, Saclantcen Conference Proceedings Series CP-45, NATO SACLANT Undersea Research Centre. 251-258.

Huws, D., Pyrah, J. and Davis, A. 1997. Geophysical and geotechnical characterization of carbonate sediments. In: Lavoie, D.L. and Richardson, M.D. (eds.), Proceedings of the Coastal Benthic Boundary Layer Key West Workshop held at Naval Research Laboratory, Stennis Space Center, MS, June 1997. 24-36.

Pyrah, J. Huws, D.G. & Davis, A.M. 1997. An innovative approach for determining sea-floor sediment behaviour under the influence of cyclic loading. In: Technology Transfer from Research to Industry. Seventh International Conference on Electronic Engineering in Oceanography, Southampton Oceanography Centre, UK.

Richardson, M.D. and Davis, A.M. 1995. Sea floor sensing of sediment shear wave properties. Proceedings of the 1st Meeting of Environmental and Engineering Geophysics, European Section, Torino, Italy, September 1995. 180-183.

Published Abstracts:

Davis, A.M., Huws, D.G. and Haynes, R. 1994. Geophysical ground-truthing experiments in Eckernfoerde Bay. J. Acoust. Soc. Am., 96 (5): 3218.

Davis, A.M., Huws, D.G., Haynes, R. and Bennell, J. 1995. Geophysical sea floor sensing in a carbonate sediment regime. SEPM Congress on Sedimentary Geology, held in St. Petersburg, Florida, August 1995. 1:43.

Richardson, M.D., Briggs, K.B. and Davis, A.M. 1996. Geoacoustic properties of carbonate sediments. EOS 76 (3):OS172.

Reports:

Haynes, R. 1995. Preliminary cruise and data report on the Eckernfoerde Bay sub-bottom reflection profiling cruises - June and November, 1994. AUGER Geophysical Services Report No. HDH 946111, University of Wales Bangor.

Haynes, R. 1995. Preliminary cruise and data report on the Key West sub-bottom reflection profiling cruise - February 1995. AUGER Geophysical Services Report No. HDH 95021, University of Wales Bangor.

Pyrah, J.R. 1996. The UWB instrumented monotonic and cyclic triaxial apparatus: year end report and user manual. AUGER Geophysical Services Report No. PBDH 96121, University of Wales Bangor.

ANALYSIS OF THE RHEOLOGICAL PROPERTIES OF NEARBED (FLUID MUD) SUSPENSIONS OCCURRING IN COASTAL ENVIRONMENTS

Submitted by
Richard W. Faas

Department of Geology
Lafayette College
Easton, PA 18042

Achievements, scientific advances, and conclusions

1. Demonstrated the effect of removal of organic matter on the rheological properties of the surficial fine-grained sediments in the Eckernförde (dramatic loss of yield stress and 'apparent' viscosity in the same sample).
2. Demonstrated the time-dependent relationships between 'apparent' viscosity, yield stress and sediment density. (resuspended sediment settles quite rapidly following the resuspension event and the rheological properties increase accordingly).
3. Demonstrated clear differences in rheological properties ('apparent' viscosity, yield stress, flow behavior) between similar sediments in Eckernförde Bay and the southern portion of Kiel Bay. These differences are attributed to relatively minor quantitative differences in the ratio between silt and clay as expressed by the silt/clay ratio. (there is a suggestion that flow behavior differences may be responsible for differences in the composition and abundance of the infaunal benthos between the two environments).

Original Objectives

1. Defining the role of particle shape, surface area, and surface texture in the flow process of fluid mud, e.g., what is the relationship of particle morphology and surface texture to the form of non-Newtonian flow behavior exhibited by the suspension. Why do some natural muds change flow behavior at specific densities while other natural muds do not under the same stress- strain rate conditions?
2. How does sediment resuspension really occur - is it by single particles and loose flocs which become reflocculated (coagulate) and settle back to the lutocline as turbulence decreases, or are clusters and clumps of particles torn from the lutocline and a) become disaggregated to primary particles which form new floccules, or b) settle back into the substrate essentially unchanged but perhaps slightly larger due to particle capture?

3. How does the fluid mud move as a coherent mass - why does it retain its integrity as a recognizable unit - what is happening to the microfabric of the particles within the mud layer as movement is taking place?
4. What is the effect of bacterial secretions on fluid mud behavior? Does this phenomenon contribute to the time-dependent effects (e.g., yield stress development, thixotropy) observed in tidal environments?

Modifications

It became obvious during the 1993 field season that fluid mud was not a significant component of the boundary layer. Indeed, no real fluid mud was observed, although divers reported that otterboard tracks were exposed on one day and observed to be covered on successive days. Nearbottom turbidity was minimal and when turbidity occurred, it appeared to be introduced from Kiel Bay rather than from bottom resuspension in Eckernförde Bay (Friedrichs and Wright, 1995). The potential for fluidization of the high water content muds does appear reasonable, particularly in areas of intense bioturbation and areas of disturbance due to trawling, pockmarks generated either through gas ebullition, or artesian pumping, and storm activity as documented by Milkert and Werner (1995). Several pockmarks showed localized areas of low density sediment within the crater which could be interpreted to be fluid mud. Consequently, sampling of the sediments concentrated on the upper centimeter of the box cores. This is the material which would constitute fluid mud if significant resuspension were to occur. Therefore the rheological properties of this material were evaluated.

Approach

It is often difficult to apply laboratory data on the behavior of dense suspensions directly to their actual behavior under natural shear stresses in the field. However, some indirect field observations, e.g., OBSS data, turbidity profiles measured in the water column over a tidal cycle, etc., can be interpreted to reflect the characteristics of the near bottom sediments and changes in those properties that may occur during an accelerating current velocity. For example, in some cases, resuspension may occur twice during a flood tide - the first occurring shortly after slack before flood, the second occurring shortly after maximum flood. This can be interpreted as a change in flow behavior, i.e., from shear thinning to shear thickening and again to shear thinning, as shear stress increases. Fine-sediment accumulation appears quite effective in some high energy environments. e.g., the Amazon inner continental shelf and macrotidal environments in some estuaries flowing into the Bay of Fundy. Sediments from these areas demonstrate time and density-dependent effects, e.g, high yield stress and shear thickening behavior that act to keep the sediment on the bottom and retard resuspension, even at high shear rates. One advantage in work of this kind is that sediment disturbance is not a problem. In fact, the sediment owes its existence as a fluid mud suspension specifically to the fact that it is alternately redispersed from the bottom and settles back to the bottom as a flocculent mass during each tidal cycle. Consequently, it appears possible to justify explaining

suspended sediment dynamics through the use of laboratory-derived behavioral characteristics.

Methods

Two samples (25 and 50 gm) of interfacial mud from each box core sampled were disaggregated with a blender and an ultrasonic transducer, placed in a 1 l settling tube with water of known salinity, mixed thoroughly with a plunger and allowed to flocculate and settle. A sharp flocculent interface (lutocline) formed within a short time (usually within a minute) which descended at a constant rate until the density of the material beneath the lutocline reached a density of 1.07 Mg/m³. Further settling followed a nonlinear path which became asymptotic with time as pore pressure dissipated and normal consolidation resumed. At the completion of the settling interval (usually 24 hours), the water was poured off and the slurry transferred into three beakers, providing a density gradient, generally ranging between 1.08 to 1.20 Mg/m³. These samples were analyzed for their rheological properties, e.g., 'apparent viscosity', yield stress, and flow behavior under shear stress. Analysis was accomplished with a Brookfield RVT 8-speed rotational viscometer using a concentric cylinder (couette-type) sensing element consisting of a stationary cylinder (cup) and a rotating cylindrical bob. The sample is sheared within the gap between the surface of the bob and the outer cylinder and the shear stress is recorded as torque on the instrument dial. A well-defined shear rate is a constant for each speed used, the rate dependent upon the dimensions of the cup and bob. For the analyses presented in this work, shear rates ranged from 0.61 s⁻¹ to 122.s⁻¹. The instrument has a history of use in sedimentological investigations (Faas, 1990) and has recently been used to study the effect of bacteria on the flow behavior of clay-seawater suspensions (Dade, et al, 1996).

As a component of the original proposal to CBBL, it was proposed to construct a settling tube (10 l capacity) to examine the hindered settling process in detail. The tube was to be equipped with sensitive pressure transducers which would measure the pore pressure changes that occur during the self-weight consolidation process. The tube was constructed to fit the Texas A&M core logger which would provide simultaneous data on sediment density and compressional wave velocities as the settling experiment proceeded to completion. The tube was also equipped with a pressure manifold which would allow a controlled quantity of gas or air into the settling suspension. Bubble size would be controlled through the use of different sizes of glass beads through which the gas/air would have to pass. Various experiments were planned which would analyze the before and after gas effects on the sediment density, p-wave velocity, and pore pressure development. The ultimate prize of this work would be the development of a technique which would sample the consolidating wet sediment at varying densities, pore pressures, and p-wave velocities, and, using the new JEOL 300 kV transmission microscope and the environmental cell at NRL, to determine the fabric configurations which are related to, and probably control the above parameters. It will be necessary to develop an appropriate in situ sampling technique which will minimize disturbance. Efforts are presently under way to solve this problem.

The settling column was constructed at Lafayette College during 1994-1995 but due to nonrenewal of the contract, no further progress was made until 1997 when the pressure transducers were purchased and installed. The tube is presently fully instrumented and it is planned to begin settling experiments within the next few weeks.

Results

1. The study examined the effect of organic matter on the rheological properties of the Eckernförde sediments. It is generally thought that organic matter increases the water holding capacity of the sediments and, consequently, weakens all the water dependent properties (Rashid and Brown; 1975; Keller, 1982). This research takes the problem a step higher and looks at the effect of organic matter on the viscous properties of a fluid mud (rather than the mechanical properties of a submarine soil). Several conclusions were drawn: 1) The yield stress of the natural sediment is several orders of magnitude greater than the yield stress of the sediment from which all organic matter has been removed. 2) Flow behavior of natural sediment shows tendencies toward shear thickening whereas extreme shear thinning flow behavior is found in the same sediment which has been cleaned. Thus, removal of organic matter tends to reduce the rheological properties, e.g., decreased yield stress and shear thinning flow behavior, whereas the non-treated suspension exhibited just the reverse. There may be significant problems of sediment management where treatment to change sediment properties to control behavior may be an important factor. There may be an application to nature where biological removal of organic matter by high populations of burrowing organisms may contribute to potential fluidization by loss of interparticle strength relationships.

2. Establishment of special indices which may be used to predict rheological behavior. For example, the silt/clay ratio seems useful in that $S/C < 1.0$ in Kiel Harbor sediments which exhibit exclusive shear thinning flow behavior whereas $S/C > 1.0$ usually exhibits an interval of shear thickening. This behavior may be responsible for the presence or absence of infaunal organisms in the Eckernförde and Kiel bays [burrowing organisms are found in the Eckernförde - Kiel Harbor muds appear to be barren]. Shear thickening may also result from the presence of fecal pellets in the Eckernförde sediments. These particles may act like fine sand or coarse silt grains and cause mechanical dilatancy (as opposed to rheological dilatancy). In the former, the grains move into a closer packing position which increases the density of the mass being sheared. Infaunal organisms utilize the shear strength of the sediment to facilitate burrowing. In the case of shear thinning, burrowing would cause weakening and possible fluidization with sediment failure and burrow collapse (Carney, 1981).

3. The identification of qualitative and quantitative relationships in fluid mud suspensions provide criteria which can be used in the construction and operation of process models. This is particularly important in sediment transport models when the sediment being modeled is a cohesive sediment, i.e., clay and clay-sized particles. Most such models consider the particles to react to stresses as if they were non-cohesive and

independent particles. For the most part the input parameters for such transport models include sediment shear strength, particle sizes and shapes, bottom roughness, and consolidation state, and the sediment bed is treated as if it were composed of noncohesive material. However, in highly turbid cohesive sediment environments, the estimates of shear strength, cohesion, roughness, and consolidation state are replaced by nonlinear time-dependent measurements of yield stress, shear thinning and shear thickening flow behavior, hindered settling rates, microfabric development, thixotropy and anti-thixotropy, all of which are overprinted by tidal (diurnal, semi-diurnal) and astronomical (spring-neap) tidal cycles. Modeling of boundary layer dynamics in such highly turbid, cohesive sedimentary environments has failed to incorporate rheological behavioral effects in their predictions primarily because such effects differ between environments, behavioral data vary in quantity and quality, and few secure relationships exist between governing parameters and environmental forcing factors for cohesive sediments (GESAMP, 1991).

References

Dade, W.B. and A. R. M. Nowell. 1991. Moving muds in the marine environment. Proc. Coastal Sediments '91, Am. Soc. Civ. Engrs, 1, 54-71.

Faas, R. W. 1990. A portable rotational viscometer for field and laboratory analysis of cohesive sediment suspensions. Jour. Coast. Res. 6 (3), 735-738.

Friedrichs, C. T. and L. D. Wright. 1995. Resonant internal waves and their role in transport and accumulation of fine sediment in Eckernförde Bay, Baltic Sea. Continental Shelf Research 15 (13) 1697-1721.

Keller, G. H. 1982. Organic matter and the geotechnical properties of submarine sediments. Geo-Marine Letters 2, 191-198.

Milkert, D. and F. Werner. 1995. Formation and distribution of storm layers in western Baltic Sea muds. The Baltic Yearbook (submitted).

Rashid, M. A. and J. D. Brown. 1975. Influence of marine organic compounds on the engineering properties of a remolded sediment. Engineering Geology 9, 141-154.

**Early Diagenesis of the Shallow Water Sediments in the Vicinity of Dry
Tortugas, Florida**

by

Yoko Furukawa

Institute of Marine Sciences
The University of Southern Mississippi
Stennis Space Center, MS 39529

CBBLSRP Final Technical Report

Submitted to

Naval Research Laboratory
Code 7431
Stennis Space Center, MS 39529

March 27, 1998

1. Introduction

Biogeochemical processes during early diagenesis significantly affect fabric and physical properties of shallow marine sediments. The change in pore water chemistry and activities of benthic macrofauna alter the sediment fabric that would otherwise be determined by physical settling and resuspension processes only. The change in sediment fabric due to biogeochemical processes causes the sediment to behave differently in response to compaction, shearing, and the application of acoustic waves.

Whereas one of the latest tools for the comprehensive study of early diagenesis is the reactive transport modeling, its use is still limited especially for shallow water sediments because of the temporal and spatial variability of fabric. This study uses dissolved O_2 to demonstrate the spatial variability of redox sequences in the sediments of Dry Tortugas area, and evaluates the effects of such variability on sediment geochemistry. This study is a first step toward the incorporation of spatial variability in reactive transport modeling.

2. Study Site and Methods

2.1. Field Site and Sampling Methods

The Dry Tortugas are located 110 km west of Key West, Florida, at the end of the Lower Florida Keys. The major constituents of the sediments are skeletal remains of *Halimeda* sp., an aragonitic green algae. The sediments also contain fragments of corals, mollusks, and foraminifers. Approximately 90 weight % of the dry bulk is composed of carbonate minerals, with aragonite constituting nearly 50 weight %, with the rest being composed of high-Mg and low-Mg calcite (Furukawa et al., 1997). A major source of sediment is *Halimeda* fragments transported from adjacent grass beds (Bentley and Nittrouer 1997). The general lithology of these unconsolidated Holocene carbonate sediments is described in Stephens et al. (1997). Active bioturbation of the sediment was apparent in the cores collected at North Key Harbor area in Dry Tortugas. Live bioturbating organisms, mostly spionid polychaetes, were observed down to approximately 15 cm below seafloor.

The data obtained for this study were collected during May-June 1997 on board R/V Pelican in the North Key Harbor area of the Dry Tortugas, where water depth is approximately 10 to 12 m. Fifteen cores were taken by SCUBA divers using clear Plexiglas liners. For O_2 micro-profiling and CT scanning, 8.5 cm diameter liners were used, whereas for other purposes 6 cm diameter liners were used. The diver cores penetrated approximately to 20 cm below seafloor. Eight bottom photographs were taken by SCUBA divers to cover approximately 1 m² within 10 m of the coring sites to quantify the burrow density. A slab core for X-radiography was collected to determine the burrow geometry. However, the slab core penetrated to only 5 cm into the sediments and thus the vertical extent of burrows could not be determined from the X-ray, rather it was estimated by visual inspection of all 15 cores and the CT scan image of one core.

Three 6 cm diameter diver cores were sealed and refrigerated for later analysis of porosity which took place within 3 months of sampling. Other 6 cm cores were visually inspected for the burrow characteristics, and some of them were subsampled for geochemical analyses by other participants. One 8.5 cm core was used for O_2 micro-profiling as described below, and the same core was later used to collect CT scan data. Two other 8.5 cm cores were stored as backups. All

fifteen cores were visually inspected to determine the burrow geometry and depth before storage or before and during slicing.

2.2. Oxygen microprofiling

Oxygen microprofiling was conducted under the supervision of A. Shiller of USM. Immediately after core retrieval on board the R/V Pelican, a Clarke-type oxygen microelectrode (Precision Measurement Engineering, Encinitas, CA) attached to a micro-manipulator was vertically inserted into the core, starting approximately 10 mm above the sediment-water interface, and profiling was accomplished by lowering the electrode in 0.2 mm increments and taking measurements. The electrode was lowered until the reading reached a steady minimum value. Eight profiles, approximately 1 cm apart from one another, were taken, and all profiles were completed within 7 hours of core collection. The electrode was calibrated immediately before use by using surface seawater whose oxygen concentration was determined by Winkler titration, and by assuming that the steady minimum reading below the sediment-water interface corresponds to $[O_2] = 0$.

2.3. Burrow characterization and porosity

The number of burrows were counted using the seafloor photographs taken by SCUBA divers. Holes of up to 1.5 cm in diameter and mounds of typically 1 to 4 cm in diameter were visible in the photographs. A closer visual inspection using diver cores and CT scan image revealed that the center of each mound was a burrow of typically 1 to 3 cm in diameter. The burrow depth was estimated by the visual inspection of all diver cores. Bulk porosity was determined for three cores at every 1 cm by measuring wet bulk density and dry density using a Quantachrome Pycnometer. These fabric and physical property analyses were conducted in collaboration with D. Lavoie of NRL.

3. Results

3.1. Oxygen microprofiles

The data from oxygen microprofiling are shown in Figure 1. All profiles show complete consumption of dissolved O_2 within the upper 4 mm of the sediments. The profiles indicate the existence of a diffusive boundary layer above the water-sediment interface (Jorgensen and Revsbech, 1985). The water-sediment interface is thus located below the depth at which the O_2 concentration first decreases. The approximate positions of the interface were determined to be where the exponential decay of the profiles initiates.

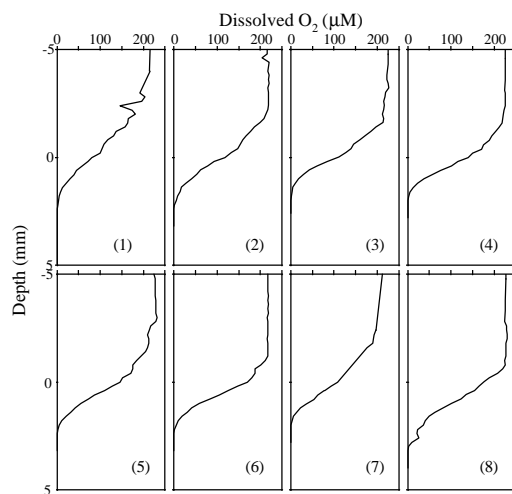


Figure 1. Dissolved O₂ profiles

3.2. Burrow distribution and geometry

The observed burrow density using the photographs at the study site is $705 (\pm 15)$ burrows per square meter of seabed. The diameter of all burrows visible in the visually inspected diver cores, CT scan images, and X-radiography ($n = 23$) fell between 1 and 3 mm, with 2 mm being the average. However, within 1.74 m^2 of the seabed surface inspected from the bottom photography, there were average 16 burrows per m^2 of seabed (2.3 % of the total number of burrows) whose diameters were larger than a few mm and up to a few cm. A full statistical description of the orientation and vertical extent of the burrows is not possible given the number of burrows for which a complete data set could be obtained. However, based on the visual inspection of visible burrows ($n=23$), we estimate that on average, the burrow have an orientation perpendicular to the water-sediment interface and a length of 15 cm. The CT scan image of the burrowed core is shown in Figure 2.

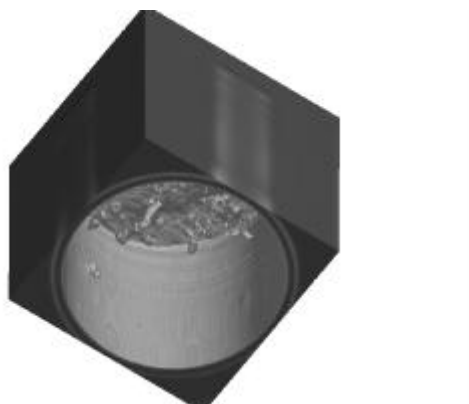


Figure 2. A CT scan image of a burrowed core. The image's point of view is "looking upward" at the water-sediment interface. The image is manipulated so that water is visible whereas bulk sediments appear transparent. Consequently, the interface and water-filled burrows are visible in this image. The diameter is 8.5 cm, and the height is 5 cm.

4. Horizontal Variability of Dissolved O_2

In this section, the effect of bioirrigation on the dissolved O_2 distribution is demonstrated using calculations based on Aller's idealized model of burrow irrigation (Aller, 1980). The computational steps involved are: (1) determination of the rate of O_2 consumption in the sediments; (2) incorporation of the rate term in the diffusion-reaction equation in cylindrical coordinates to calculate the O_2 concentration field; and (3) calculation of dissolved O_2 distribution in the sediments and horizontally-averaged O_2 depth profile.

4.1. Determination of the O_2 reaction term

The reaction rate for O_2 consumption in the North Key Harbor sediments is determined by matching a one-dimensional (1-D) steady-state diffusion-reaction model to O_2 microprofiles which are measured sufficiently far away from any burrow. Calculations presented later indicate that the effects of radial diffusion from burrows can be neglected when the microprofile is removed from the nearest burrow by a distance of at least 3 mm.

Because of the relatively low burrow density, the probability that a measured O_2 profile will be located outside the sphere of influence of radial diffusion from burrows is very high, on the order of 0.93. Thus, it is most likely that at least some of the microprofiles in Figure 1 are the result of a balance between O_2 consumption and vertical diffusion only. Furthermore, those profiles that are least affected by radial diffusion from burrows should display the steepest decreases of O_2 with depth. Several profiles in Figure 1 satisfy that requirement (e.g., profiles 3, 4, 6), while profile 1 shows a deeper average O_2 penetration depth. In what follows, profiles 3, 4, and 6 are used to constrain the O_2 consumption rate (R_0).

At steady state, when vertical diffusion is the only transport mechanism, the mass conservation equation describing the pore water profile of O_2 is,

$$D' \frac{d^2 C}{dx^2} + R = 0 \quad (1)$$

where D' is the molecular diffusion coefficient of O_2 corrected for sediment tortuosity, C is the O_2 concentration and R is the net reaction rate. For simplicity, we will assume that within the upper few mm of sediment the rate of consumption of O_2 remains constant. For boundary conditions

$$C(0) = C_0 \quad (2)$$

$$C(L) = 0 \quad (3)$$

The solution to equation (1) is (Cai and Sayles, 1996)

$$C(x) = C_0 - \left(\frac{C_0}{L} + \frac{R_0 L}{2D'} \right) x - \frac{R_0}{2D'} x^2 \quad (4)$$

where L is the oxygen penetration depth and R_0 is the constant rate of O_2 consumption. From equation (4) a simple expression for the rate term R_0 can be derived by imposing that at $x = L$ the flux of dissolved O_2 must be zero, that is,

$$\left. \frac{dC}{dx} \right|_{x=L} = 0 \quad (5)$$

We then obtain

$$R_0 = -\frac{2D' C_0}{L^2} \quad (6)$$

Equation (4) predicts depth profiles with an exponential curvature. An inspection of Figure 1 concludes this to be true for the lower portions of the measured profiles. Typically, however, a layer of finite thickness separates the upper boundary of the exponential portion of the profile from the uniform bottom water O_2 concentration. This probably indicates the presence of diffusive boundary layer above the water-sediment interface (Jorgensen and Revsbech, 1985). Thus, the concentration C_0 needed in equation (6) is not the bottom water concentration, but rather the concentration at the base of the boundary layer (Figure 3).

Values of C_0 and L are estimated graphically for a number of the microprofiles as shown in Table 1. These values are combined with an estimate of the sediment diffusion coefficient of O_2 at the measured porosity of 61.8 %. The rate of O_2 consumption is then calculated with equation (6), as shown in Table 1. In further calculations, we use an average consumption rate of $R_0 = 5.85$ mM/day.

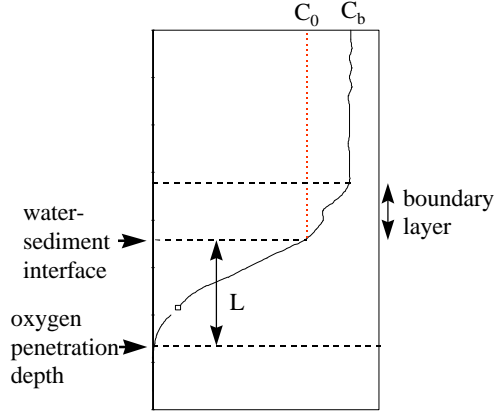


Figure 3. A Schematic interpretation of an O₂ microprofile.

Table 1. Graphically estimated values of C_0 and L , and calculated O₂ consumption rate R_0

profile	C_0 (μM)	L (mm)	R_0 (mM/day)
3	111.5	2.00	5.96
4	140.7	2.20	6.22
6	169.5	2.60	5.37
average	140.6	2.27	5.85

4.2. O₂ concentration distribution

In the tube model (Aller, 1980; Aller and Yingst, 1985; Boudreau and Marinelli, 1994), the time evolution of dissolved species concentrations can be expressed as the following diffusion-reaction equation in which vertical (x-direction) diffusion, radial (r-direction) diffusion, and reaction determine the concentration C :

$$\frac{\partial C}{\partial t} = D' \frac{\partial^2 C}{\partial x^2} + \frac{D'}{r} \frac{\partial}{\partial r} \left(r \frac{\partial C}{\partial r} \right) + R_0 \quad (7)$$

with the initial conditions for $C(x, r, t)$:

$$C(0, r, 0) = C(x, r_1, 0) = C_0 \quad (8)$$

$$C(x, r, 0) = 0 \quad (x \neq 0, r \neq r_1) \quad (9)$$

and the boundary conditions:

$$C(0, r, t) = C(x, r_1, t) = C_0 \quad (10)$$

where D' is the diffusion coefficient for the dissolved species after tortuosity correction, R_0 is the reaction term, and r_1 is the burrow radius (Figure 4). In this model, the sediments are divided into closely-packed vertical cylinders of the same geometry (Figure 4). At the center of each cylinder is a vertical void space that represents a burrow, and each cylinder is assigned the 2-dimensional coordinate system with vertical and radial axes. The amount of sediments that cannot be accounted for by the packed cylinders (9.5 volume % of total sediments) does not change the outcome of model calculation beyond its accuracy limit. Boundary conditions (10) is based on an assumption that the solute concentration is held at the steady value of C_0 at the sediment-water interface and at the burrow wall-water interface at all time.

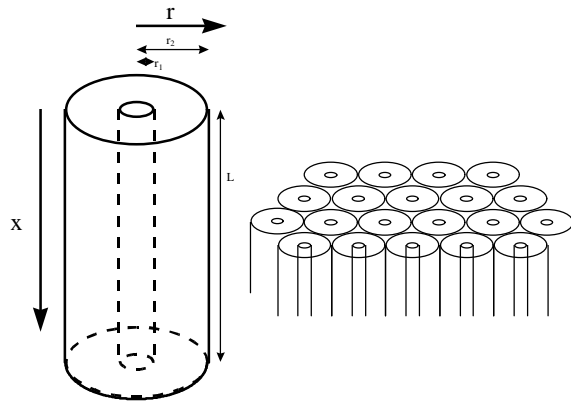


Figure 4. The tube model geometry (after Aller, 1980).

Although the analytical solutions of the steady state version of Equation (7) ($\partial C / \partial t = 0$) have successfully reproduced the depth profiles of ammonia, sulfate, and dissolved silica in many different sedimentary environment (Aller, 1980; Aller and Yingst, 1985), they are not appropriate for the modeling of dissolved O_2 . The consumption rate of O_2 is generally extremely fast as evident by the above derivation of R_0 , resulting in a significant part of the sediment having an O_2 concentration of zero. Consequently, because analytical solutions of diffusion-reaction equations such as Equations (1) and (10) only work when the concentration has a finite value, they cannot be implemented for all part of the sediments for the modeling of O_2 .

Thus, a numerical solution was implemented for this study. Equation (10) was first split into three 1-D equations using the Locally 1-D Method of Operator Splitting (Boudreau, 1997), and each separate differential equation was solved using the finite difference method. The Crank-Nicholson formula (Press et al., 1992) was used to implement the finite differencing because the highly negative R_0 value made other numerical formulas unstable. The grid sizes were set to be $dx = dr = 0.01$ cm, and the equation was solved as a time evolution problem (Press et al., 1992) with the time step of $dt = 10^{-4}$ day until steady state was reached. The steady state was reached after a

few thousand time steps (i.e., several hours). The burrow geometry parameters used in the calculations were from the results of burrow geometry and density measurements, and were $r_1 = 0.1$ (cm), $r_2 = 2.02$ (cm), and $L = 15$ (cm).

Figure 5 shows the distribution of O_2 concentration values as a contour map. Only the space near the water-sediment interface and burrow wall is shown. Note that high O_2 concentrations occur along the burrow wall as deep as the burrow depth, indicating that oxic respiration can occur at any given depth as long as burrows reach the depth. This horizontal variability in the redox condition significantly affects the use of reactive transport models in the study of early diagenesis, as all currently available models (Boudreau, 1996; Dhakar and Burdige, 1996; Soetaert et al., 1996; Van Cappellen and Wang, 1996) are based on the one-dimensional sequence of redox species.

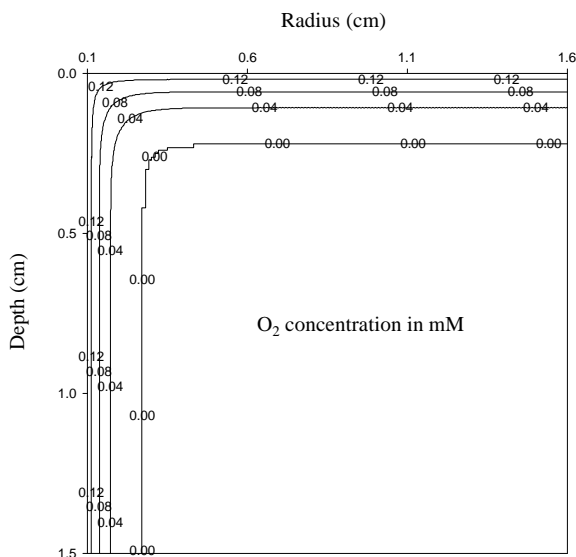


Figure 5. A contour map showing the calculated O_2 concentration distribution in the 2-D space.

4.3. Horizontally averaged O_2 profile

The horizontally averaged O_2 profile was calculated using the model by integrating the concentration values horizontally for each dr interval. The depth profile, shown in Figure 6, indicates that pore water O_2 exists as deep as the burrow depth, although the horizontally averaged value of dissolved pore water O_2 concentration at depths is only 0.4 % of the bottom water value.

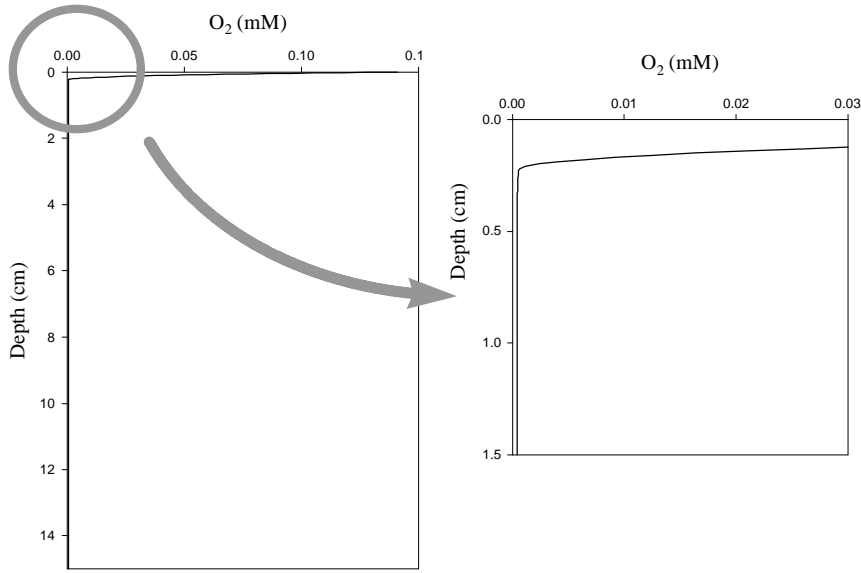


Figure 6. Horizontally averaged depth profiles of dissolved O_2 . The right figure shows a detail within the upper 1.5 cm.

5. Discussions and Geologic Implications

5.1. The rate of aerobic degradation of organic matter

The deep penetration of pore water O_2 due to bioirrigation promotes aerobic degradation of organic carbon (OC) at depths. The rate of aerobic OC degradation can be calculated using the Monod kinetics as follows (Boudreau, 1997):

$$\left(\frac{dG}{dt} \right)_{O_2} = -kG \frac{O_2}{K_{O_2} + O_2} \quad (11)$$

where G is the conventional symbol for the organic matter concentration, k is a rate constant, O_2 is the concentration of dissolved pore water O_2 , and K_{O_2} is a Monod-type saturation constant. This formulation means that the rate of aerobic OC degradation is nearly independent of the O_2 concentration when the value of O_2 is sufficiently high, whereas the rate decreases with the value of O_2 when the O_2 value is near or below the value of K_{O_2} . The depth dependence of the rate of aerobic OC degradation can now be calculated using the horizontally-averaged value of O_2 at each depth as calculated in Section 4.3., with the estimated value of $K_{O_2} = 0.008$ mM (Van Cappellen and Wang, 1996). The results are shown in Figure 7.

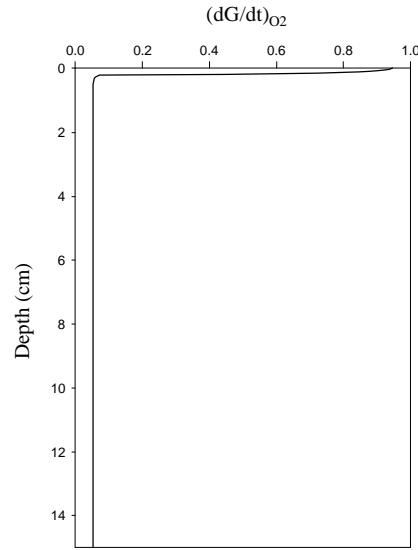


Figure 7. The depth profile of the relative reaction rate for aerobic organic matter degradation, normalized to the rate at water-sediment interface.

Through actual field measurements of pore water O_2 , aerobic degradation of OC in shallow water sediments is considered to be limited to the upper few to several mm of the sediments (e.g., Reimers et al., 1996). In the demonstrations of reactive transport models, the aerobic OC degradation is also considered to be limited to the upper several mm of the sediments, through the use of exchange coefficients for bioirrigation (Boudreau, 1996; Wang and Van Cappellen, 1996). However, the above calculation and Figure 7 indicate otherwise: in burrowed sediments, the deep penetration of dissolved O_2 promotes significant amount of aerobic OC degradation. Where as deep as 15 cm below water-sediment interface, the rate of aerobic degradation of OC is 5.6 % of the rate at the interface.

5.2. Significance of the biologically-enhanced O_2 penetration

It is easily suspected that an enhanced rate of aerobic OC degradation by bioirrigation as demonstrated as above will affect the amount of decayed and preserved OC in sediments and thus OC depth profiles.

A depth profile of reactive OC due to aerobic degradation can be calculated using a model equation:

$$\frac{\partial G}{\partial t} = D_B \frac{\partial^2 G}{\partial x^2} - w \frac{\partial G}{\partial x} - k_1 G \frac{O_2}{K_{O_2} + O_2}$$

where D_B is the diffusive mixing coefficient for bioturbation, w is the burial velocity, and k_1 is the rate constant for aerobic OC degradation. Figure 8 shows the depth profiles of reactive OC calculated from the above equation, using the horizontally averaged O_2 values calculated in the section 4.3. The depth profiles of reactive OC in the absence of O_2 irrigation, calculated using the O_2 values in the case of no irrigation calculated using Equation (1), are also shown. The parameter values used are: $k_1 = 1.0 \text{ (yr}^{-1}\text{)}$, $w = 0.3 \text{ (cm yr}^{-1}\text{)}$. The D_B values are changed between

1.0 and 100.0 ($\text{cm}^2 \text{yr}^{-1}$). It is seen that there is a significant difference in the calculated profiles between irrigation and no irrigation scenarios.

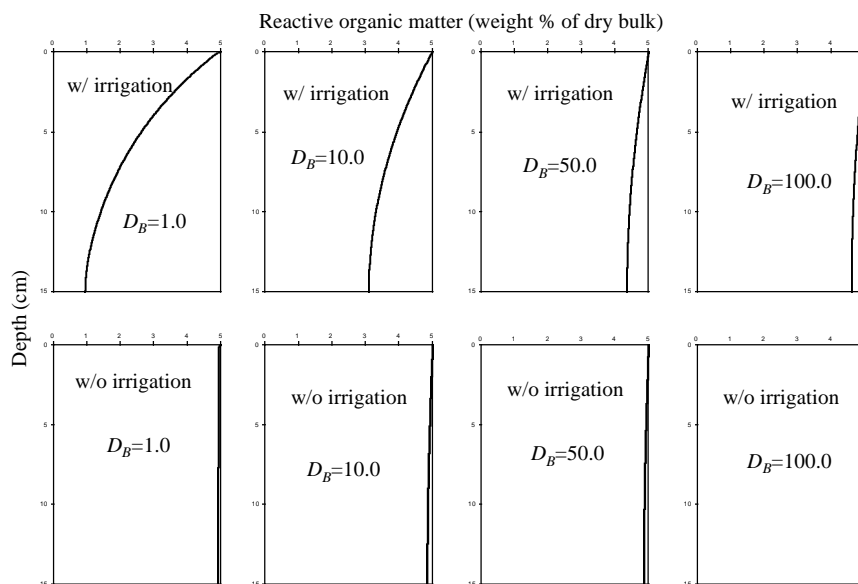


Figure 8. Depth profiles of reactive organic carbon calculated from the transport-reaction equation. The initial rain rate of reactive organic carbon is assumed to be 5 wt %. Note the deep oxygen penetration calculated for the study area sediments results in a significant amount of depth dependent decrease of reactive organic carbon especially at lower D_B values.

Acknowledgments --- A. Shiller provided instruments and training for the O_2 microprofiling, and porosity data are from D. Lavoie. We also acknowledge K. Mohanty for making CT scan equipment available to us, and K. Stephens, K. Briggs, and NRL Dive Team for their assistance in sampling and sample processing. The captain and crew of R/V Pelican were most helpful in making the on-board sampling and sample processing a success. Financial support was provided by the Office of Naval Research (N00014-95-1-G907) through a grant from Naval Research Laboratory (CBBLSRP).

References

- Aller, R. C. 1980. Quantifying solute distributions in the bioturbated zone of marine sediments by defining an average microenvironment. *Geochim. Cosmochim. Acta*, *44*, 1955-1965.
- Aller, R. C. and J. Y. Yingst. 1985. Effects of the marine deposit-feeders *Heteromastus filiformis* (Polychaeta), *Macoma balthica* (Bivalvia), and *Tellina texana* (Bivalvia) on averaged sedimentary solute transport, reaction rates, and microbial distributions. *J. Mar. Res.*, *43*, 615-645.
- Bentley, S. J. and C. A. Nittrouer. 1997. Biogenic influences on the formation of sedimentary fabric in a fine-grained carbonate-shelf environment: Dry Tortugas, Florida Keys. *Geo-Marine Letters*, *17*, 268-275.
- Boudreau, B. P. 1996. A method-of-lines code for carbon and nutrient diagenesis in aquatic sediments. *Computers & Geosciences* *22*, 179-196.
- Boudreau, B. P. 1997. *Diagenetic Models and Their Implementations*, Springer-Verlag, Berlin.

- Boudreau, B. P. and R. L. Marinelli. 1994. A modeling study of discontinuous biological irrigation. *J. Mar. Res.*, 52, 947-968.
- Cai, W.-J. and Sayles, F. L. 1996. Oxygen penetration depths and fluxes in marine sediments. *Mar. Chem.* 52, 123-131.
- Dhakar, S. P. and Burdige, D. J. 1996. A coupled, non-linear, steady-state model for early diagenetic processes in pelagic sediments. *Amer. J. Sci.* 296, 244-265.
- Furukawa, Y., D. Lavoie and K. Stephens. 1997. Effect of biogeochemical diagenesis on sediment fabric in shallow marine carbonate sediments near the Dry Tortugas, Florida. *Geo-Marine Letters*, 17, 283-290.
- Jorgensen, B. B. and N. P. Revsbech. 1985. Diffusive boundary layer and the oxygen uptake of sediments and detritus. *Limnol. Oceanogr.*, 30, 111-122.
- Press, W. H., S. A. Teukolsky, W. T. Vetterling and B. P. Flannery. 1992. *Numerical Recipes in FORTRAN*, Second Edition. Cambridge University Press.
- Reimers, C. E., Ruttenberg, K. C., Canfield, D. E., Christensen, M. B., and Martin, J. B. 1996. Porewater pH and authigenic phases formed in the uppermost sediments of the Santa Barbara Basin. *Geochim. Cosmochim. Acta* 60, 4037-4057.
- Soetaert, K., Herman, P. M. J. and Middleburg, J. J. 1996. A model for early diagenetic processes from the shelf to abyssal depths. *Geochim. Cosmochim. Acta* 60, 1019-1040.
- Stephens, K., P. Fleischer, D. L. Lavoie and C. Brunner. 1997. Scale-dependent physical and geoacoustic property variability of recent, shallow-water carbonate sediments from the Dry Tortugas Keys, Florida. *Geo-Marine Letters*, 17, in press.
- Van Cappellen, P. and Wang, Y. 1996. Cycling of iron and manganese in surface sediments: A general theory for the coupled transport and reaction of carbon, oxygen, nitrogen, sulfur, iron and manganese. *Amer. J. Sci.* 296, 197-243.
- Wang, Y. and P. Van Cappellen. 1996. A multicomponent reactive transport model of early diagenesis: Application to redox cycling in coastal marine sediments. *Geochim. Cosmochim. Acta*, 60, 2993-3014.

Appendix

Publications Under This Grant

Reviewed Articles

- Lavoie, D., Furukawa, Y., Lavoie, D., Burkett, P. J., and Urmos, J. (1998) Apparent underconsolidation in Eckernforde Bay sediments: A model based on physical, geochemical and microfabric properties. *Journal of Continental Shelf Research* (in review).
- Furukawa, Y., Lavoie, D. and Stephens, K. (1997) Effect of biogeochemical diagenesis on sediment fabric in shallow marine carbonate sediments near the Dry Tortugas, Florida. *Geo-Marine Letters*, 17, 283-290.

Abstracts and Reports

- Furukawa, Y., Lavoie, D. and Stephens, K. (1997) Early diagenesis of biologically reworked carbonate sediments near the Dry Tortugas, Florida. *Geological Society of America Abstracts with Program*, 29.

- Furukawa, Y., Lavoie, D. and Stephens, K. (1996) Carbonate sediment fabric as a tool to quantify early diagenesis. *American Geophysical Union 1996 Fall Meeting*.
- Furukawa, Y. and Lavoie, D. (1996) The impact of early diagenesis on sediment 3-D structure on shelf carbonate sediments near the Dry Tortugas, Florida. *American Geophysical Union 1996 Spring Meeting*.
- Furukawa, Y. and Lavoie, D. (1996) Mineralogy and microfabric of early diagenesis in shallow-water carbonate sediments from western Florida keys. *1996 Annual Meeting of the Mississippi Academy of Sciences*.
- Furukawa, Y. (1996) Form of Organic Matter in the Muddy Sediments Near Eckernfoerde Bay, Germany. NRL/CR/7431-96-0006, 11p.
- Briggs, K. B., Lavoie, D. L., Stephens, K., Richardson, M. S. and Furukawa, Y. (1996) Physical and geoacoustic properties of sediments collected from the Key West Campaign, February 1995: A data report. Naval Research Laboratory, Stennis Space Center, MS. NRL/MR/7431-96-8002, 393p.
- Furukawa, Y. and Lavoie, D. (1995) The use of mineralogy and microfabric as the indicators of early diagenesis in shallow-water carbonate sediments from western Florida Keys. *Geological Society of America Abstracts with Program*, **27**.
- Furukawa, Y., Lavoie, D. and Wiesenburg, D. (1995) Oxidation of aqueous sulfide in porewater as the possible cause for carbonate dissolution during early diagenesis. *The 1st SEPM Congress on Sedimentary Geology Congress Program and Abstracts*, **1**.
- Furukawa, Y. (1995) Mineralogical Study of the Seafloor Diagenesis of Carbonate Sediments Near Dry Tortugas, Gulf of Mexico, Using Rietveld Method of Crystal Structure Refinement. NRL/CR/7431-96-0001, 15p.
- Furukawa, Y. (1995) Evaluation of Early Diagenesis in Modern, Shallow-Water Carbonate Sediments by Mineralogy, Fabric and Porewater Geochemistry. NRL/CR/7431-95-0036, 10p.

Title: Measurement of High Frequency Acoustic Scattering from Coastal Sediments

Principal Investigators: Darrell R. Jackson, Kevin L. Williams

Organization: Applied Physics Laboratory, University of Washington

Abstract

The three CBBL field experiments included concurrent environmental measurements and acoustic measurement of scattering at 40 kHz. This allowed development and testing of scattering models where all the input parameters of the models had been measured. The Panama City sand site environment was the closest to the assumptions of the initial model tested and that model compares well with the scattering data when the measured environmental parameters are used. The Key West sand-silt-clay site was more complicated in that there was a significant gradient in acoustic parameters in the upper few centimeters. In spite of this, comparisons between model and scattering data show good agreement if the surficial values of the measured environmental parameters are used. The scattering at the Eckernförde gassy mud site was found to be primarily due to in-sediment bubble layers and required development of a model more specialized to this environment. When the measured bubble population densities were used in this “bubble scattering” model there is again good model/data agreement but with some indication that multiscattering effects not treated in the model may be important. In addition to scattering levels at the three sites, acoustic data were taken that allowed the examination of both spatial and temporal variability of scattering. The temporal correlation coefficients for the three sites show the most rapid benthic changes at the Panama City and the slowest at Eckernförde (the rate of change of the bottom at Eckernförde, as indicated by this measurement, is about 100 times slower than at Panama City). This difference in rate of change is most likely due to the fact that the significant scatterers at Eckernförde are well within the sediment whereas those at Panama City are surficial.

Original Objectives

The primary objective was to test hypotheses for high-frequency sound propagation and scattering in coastal sediments by making monostatic and bistatic scattering measurements at well characterized sites. These hypotheses were embodied in models in which widely used approximations (composite roughness, Kirchhoff, volume perturbation theory) are combined in models for backscattering and bistatic scattering. The scattering mechanisms of the models were roughly divided into two categories; scattering due to surface roughness and scattering due to volume inhomogeneities. Both categories assumed single scattering. The original proposal sought to examine several hypotheses:

- single scattering is an adequate approximation for describing scattering from ocean sediments in the 10 to 100 kHz range,

- the angular distribution of bistatic scattering reflects the type of scatterers that dominate the scattering process,

- sediment shear wave effects will be negligible for the types of sediments anticipated at the experimental sites,

volume scattering implies that sediment macrostructure is self-similar and fractal

A secondary objective was to employ the scattering data to examine spatial and temporal scales of change in the bottom due to biological and hydrodynamic activity.

Approach

The acoustic experiments on backscattering^{1-3,6,7} made use of the Benthic Acoustic Measurement System (BAMS) (Figure 1). BAMS operates at 40 kHz and acquires acoustic backscattering data from a circular region whose radius is set by surface reverberation. The system employs a planar transmitter/receiver array mounted on a rotator mechanism at the top of a 5-m-high tripod. A single BAMS scan covers a full 360° in 72 steps of 5°. The 5° step increment was chosen on the basis of the transmitting and receiving horizontal directivity patterns. For reception, the aperture is divided into upper and lower halves. Digitization and signal generation are controlled by a single clock. This makes it possible to make sensitive comparisons between echoes acquired in separate scans, even when the scans are weeks apart.

During the bistatic^{4,5,8,9} measurements, ship-mounted mobile, steerable arrays shown in Figure 1 were also deployed. The array on the BAMS tripod served as the transmitter, and the ship-deployed arrays served as receivers, steered by means of a hydraulically controlled rotator. The hydraulic controls were available during data acquisition, so different geometries could be obtained within a data acquisition cycle.

Concurrent with the acoustic measurements, environmental measurements were made by NRL-SSC that allowed determination of the parameters needed in the scattering models to be tested. Table 1 (reproduced from Ref. 3) show parameters of the backscattering and bistatic scattering models of Jackson as determined by environmental measurements. The numbers in parentheses in the Key West column are the surficial values for that site. Use of those numbers gave better model/data (see Key West discussion below) agreement.

Results

Only representative samples of the data acquired and the comparison with the acoustic models are presented here. The referenced publications as well as the final report by DJ Tang (in this compilation of reports) give further details.

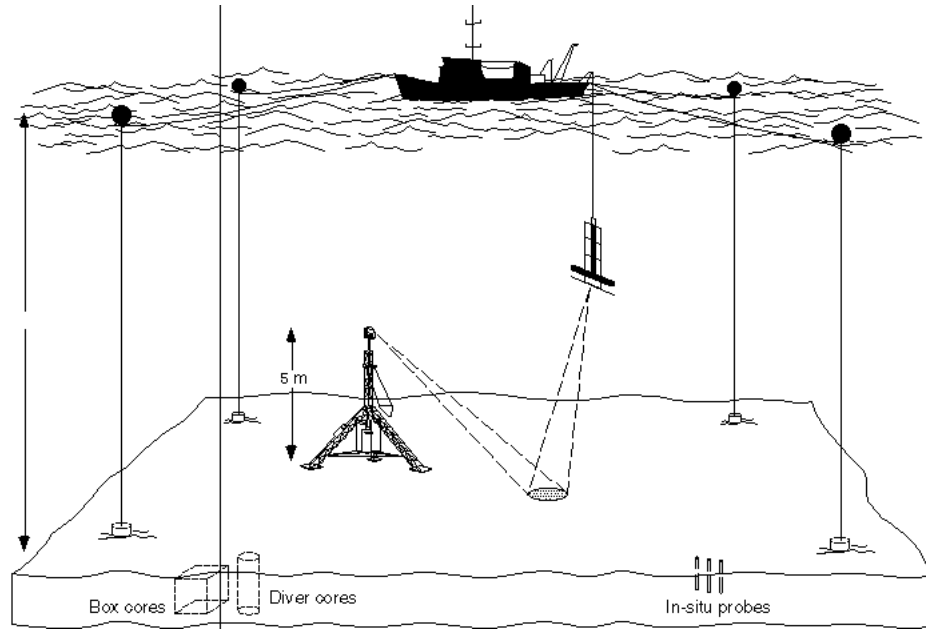


Figure 1. Illustrative diagram of experimental geometry for bistatic experiments carried out during the CBBL program. Bottom mounted tower also used for backscattering measurements.

Table 1.

Parameter	Eckernförde	Panama City	Key West
Compressional velocity ratio	0.991	1.126	1.020 (1.0)
Compressional loss parameter	0.00186	0.0166	0.00915
Shear velocity (m/s)	8.1	117.0	50.8
Density ratio	1.18	1.97	1.72 (1.45)
Density spectral exponent	4.0	4.0	4.0
Density spectral strength (cm ³)	3.52x10 ⁻⁶	1.61x10 ⁻⁵	2.41x10 ⁻⁵
Density correlation length (cm)	2.11	1.66	2.81
Compressibility fluctuation ratio	-0.69	-2.44	-1.31
Roughness spectral exponent	3.42	3.12	3.29
Roughness spectral strength (cm ⁴)	0.00231	0.00805	0.0122
Water sound speed (m/s)	1448	1532	1525

Gassy Mud - Eckernförde

The sediment had a very high water content, with a porosity of approximately 85%, and rather low acoustic attenuation (0.18 dB/kHz/m). Model parameters needed for this site are given in Table 1. As will be seen below, use of these parameters in that model leads to scattering strength predictions that are much lower than the data implies. This environment required development of a model that treated scattering by sub-surface bubbles. Indeed, the most striking acoustic feature at this site was a layer of free methane bubbles with an upper boundary 0.5 to 2.0 m below the sediment/water interface. The size distribution of these bubbles was measured by Anderson and Lyons using computer tomography, and estimates from these data indicate that volume-scattering strengths should be very high, between -10 and -20 dB/m. Tang et al.¹ have shown that these gas bubbles are the principal cause of backscattering at 40 kHz. This is due to the combination of low attenuation and high volume-scattering strength.

One of the primary results indicating scattering from subsurface bubbles is the depth of the scatterers derived from the backscattering data. The BAMS tower has split beam receivers so as to allow estimation of the height of the significant scatterers contributing to backscattering. Figure 2 plots altitude vs. Lambert parameter (a measure of scattering strength). The vertical scale indicates the mean altitude of the scatterers is about 124 cm below the seafloor. When these data are used to determine a correlation coefficient between altitude and Lambert parameter the results indicate that only about 10% of the variability of scattering strength is due to altitude changes, implying that most of the variation in scattering strength is due to variation in bubble concentration rather than layer depth.

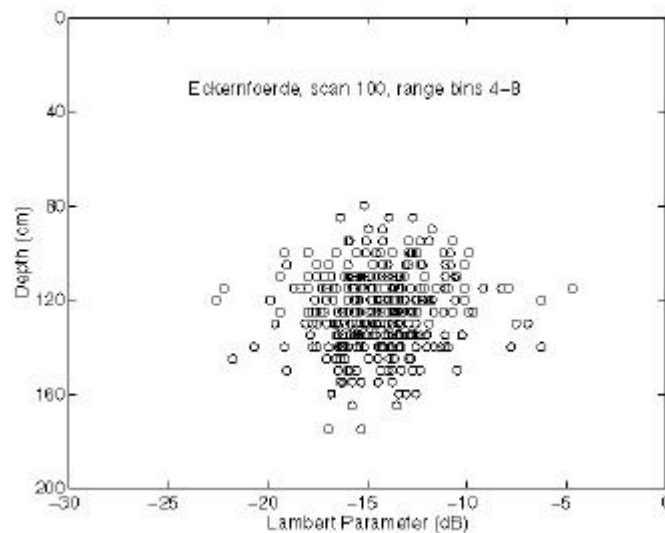


Figure 2. Scatterer depth vs. Lambert parameter.

Further evidence for bubble scattering is given in Figure 3. That figure shows that surface roughness scattering and volume perturbation scattering predictions using the data of Table 1 fall well below the data. The bubble scattering model curve, which is derived using a bubble layer scattering strength model, indicates bubble scattering as the primary scattering mechanism.

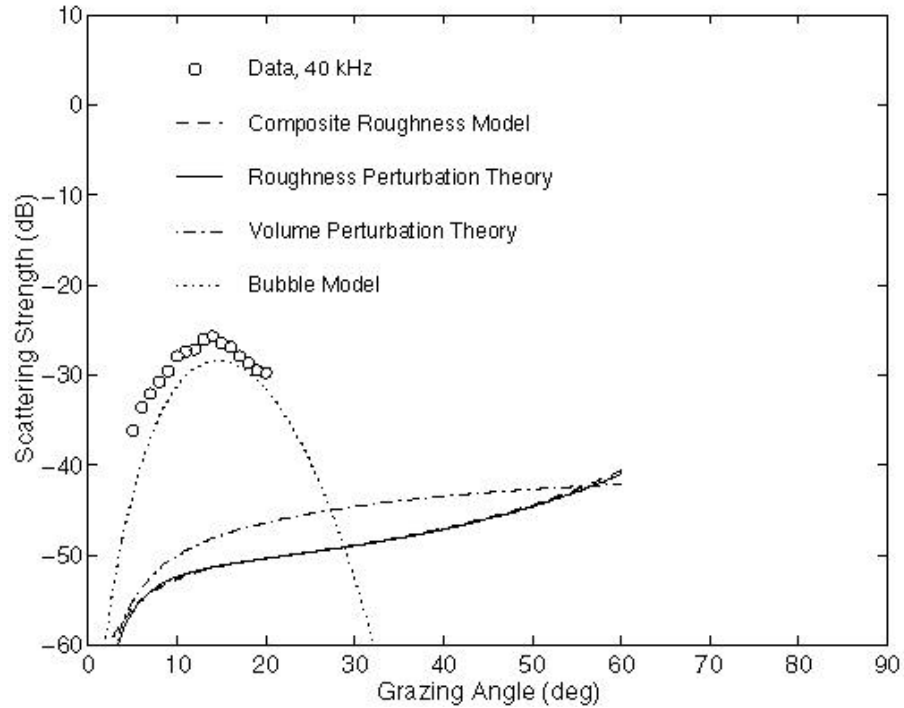


Figure 3. Backscattering data and model predictions for the gassy-mud site.

Changes in the structure of the gas layer happen much slower than changes affecting the Panama City sand site. This can be seen from Figure 4 where decorrelation of acoustic images from BAMS versus lag time is plotted for three sites. The Eckernförde Bay data show about a factor of 100 slower decorrelation times than Panama City. The much faster decorrelation times for Panama City have not been fully explained, however, it is known that surface roughness is the primary scattering mechanism at Panama City (see Panama City discussion below). As such, it is not surprising that the surface roughness changes over much shorter times scales than the subsurface bubble layer at Eckernförde.

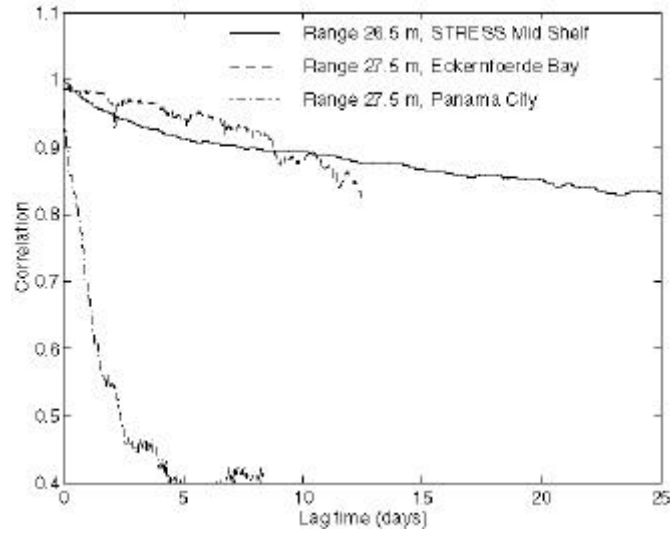


Figure 4. Acoustic correlation as a function of time lag, obtained by averaging over the BAMS correlation measurements at a fixed range.²

The bubble backscattering model was used as starting point for development of a bistatic model⁵. As seen in the bistatic scattering data/bubble model comparison in Figure 5 (from Ref. 4), the model (line) compares well with the data. However, if the model predictions are integrated over the entire solid angle of scattering they predict a violation of conservation of energy. The implication is that multiple scattering, which is not included in the model, is playing a role and will need to be taken into account in a more complete model of scattering in this environment.

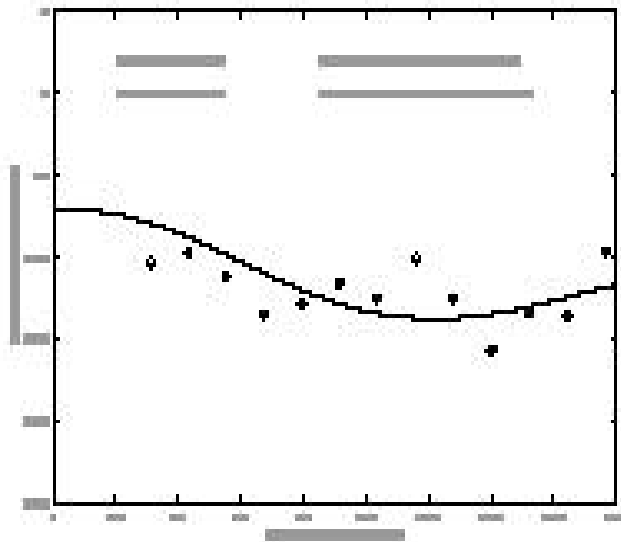


Figure 5. Subset of bistatic data acquired at Eckernförde compared with Chu et al bistatic scattering model.

Sand - Panama City

The environmental parameters of this coarse sand site are given in Table 1. This site comes closest to the assumptions of the scattering models. Both the backscattering model and the bistatic model compare well^{3,5} with data from the site when the parameters of Table 1 are used (Figures 6 and 7).

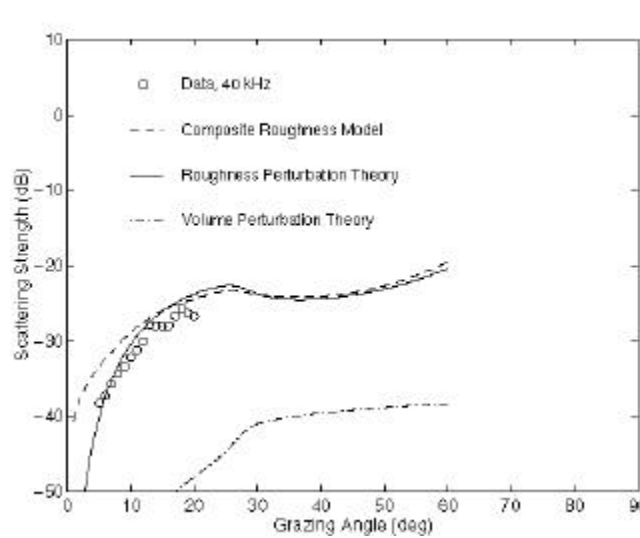


Figure 6. Backscattering data and model predictions for the sand site.

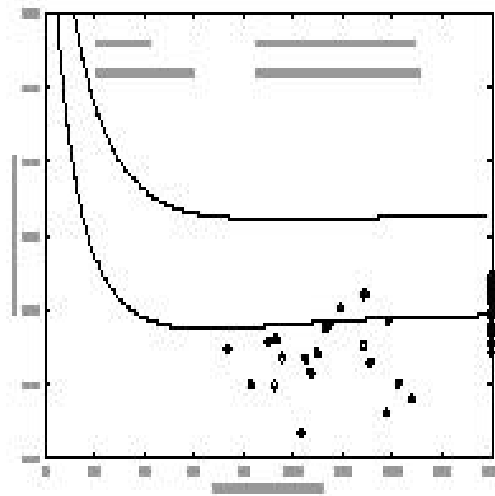


Figure 7. Subset of bistatic data acquired at Panama City compared with the bistatic scattering model.

Sand-Silt-Clay - Key West

The Key West site had a layer of soft sediment about 5 cm in depth over a harder sediment. Work is currently proceeding on whether inclusion of this gradient will lead to better data/model comparison. However, as a simpler alternative, when the surficial values of the compressional velocity ratio and density ratio are used good model/data agreement is found^{3,9} (Figures 8b and 9).

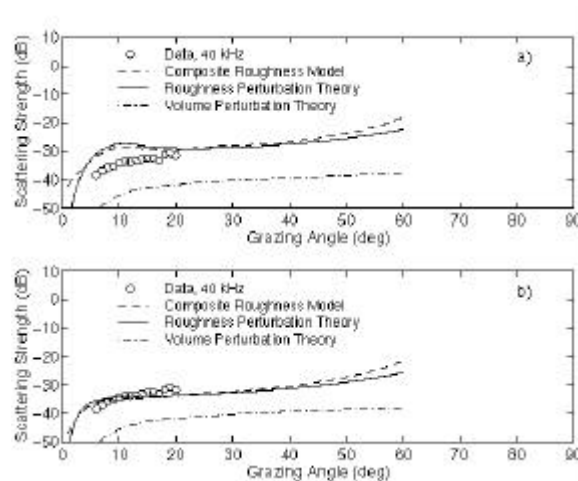


Figure 8. a) shows backscattering data/model comparison when environmental parameters derived from core averages are used, b) shows backscattering data/model comparison when surficial parameters from the site are used.

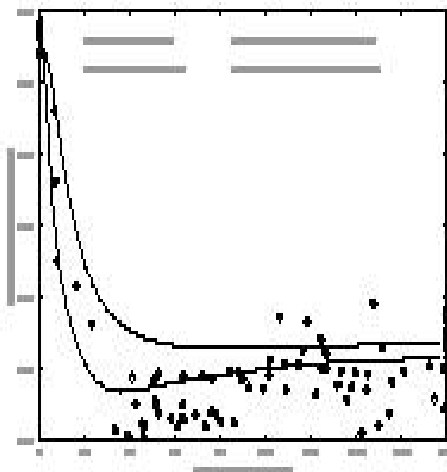


Figure 9. Subset of bistatic data acquired at Key West compared with the Jackson bistatic scattering model.

Geomarine Letters Vol. 16, 212-218 (1996).

3. D. R. Jackson, K. B. Briggs, K. L. Williams, M. D. Richardson, "Tests of Models for High-frequency Sea-Floor Backscatter," *IEEE J. Ocean Eng.*, **21**, 458-470 (1996)
4. D. Chu, K. L. Williams, D. Tang, D. R. Jackson, "High Frequency Bistatic Scattering by Sub-Acoust. Soc. Am., **102**, 806-14 (1997)
5. K. L. Williams, D. R. Jackson, "Bistatic Bottom Scattering: Model, Experiments, and Model/Data Comparison," *J. Acoust. Soc. Am.*, **103**, 169-181 (1998)

6. D. R. Jackson, K. L. Williams, T. F. Wever, C. T. Fredrichs, "Sonar Evidence for methane ebullition in Eckernförde Bay," submitted to Continental Shelf Research.

Symposium proceedings

7. K. L. Williams, D. R. Jackson (1995), "Acoustic scattering measurements at 40 kHz," Proceedings of the Workshop, Modeling Methane-Rich Sediments of Eckernförde Bay, T. Wever, Ed., FWG Report 22, 97-100.

8. K. L. Williams, D. R. Jackson, "High Frequency Bistatic Scattering By Ocean Sediments: *Proceedings of the Shallow Water Acoustics Conference*, Beijing, China, April 1997.

9. K. L. Williams, D. R. Jackson, "Bottom Bistatic Scattering: Experimental Results and Model Comparison for a Carbonate Sediment," *Proceedings of the High Frequency Acoustics in Shallow Water Conference*, Lerici, Italy, July 1997.

STRUCTURAL ANALYSIS OF MARINE SEDIMENT MICROFABRIC

CBBLSRP FINAL REPORT

February 26, 1998

Jack J. Kolle, Alan C. Mueller

Tempress Technologies Inc., 19308 – 68th Avenue South, Kent, WA 98032-1192

and Jack Dvorkin

Dept. of Geophysics, Stanford University, Stanford, CA 94305-2215

ABSTRACT

A finite element procedure for the general analysis of microstructured materials was applied to the acoustic modeling of three types of sediment – clean sand, gassy clay mud and soft clay mud. The analysis was compared with experimental results from the Coastal Benthic Boundary Layer Special Research Program. This work shows that a generic finite element analysis approach can predict the acoustic properties of a wide range of sediment types based on knowledge of constituent minerals and microfabric. Modeling of soft clay sediments identified a new mechanism for shear wave propagation involving differential pore pressures.

OBJECTIVES

The Coastal Benthic Boundary Layer Special Research Project (CBBL-SRP) represents a comprehensive study of geoacoustic and geotechnical properties in a variety of shallow marine environments (Richardson 1994). The first two field studies carried out under this program included a shallow muddy bottom in Eckernförde Bay near Kiel, Germany, and the West Florida sand sheet near Panama City, Florida. The studies included sampling of the bottom to determine the sediment structure on a microscopic scale; and in-situ measurements of compression and shear wave velocity.

Our objective was to link sediment microfabric with acoustic and geotechnical properties. In particular we wanted to evaluate the predictive capability of a finite element microstructure analysis code – MISTRA – by generating poroelastic constants for representative marine sediments and predict attenuation, dispersion and permeability relationships. We planned to model three sediment types studied in the first year of the CBBL program.

- Compact sand in the West Florida sand sheet
- Gassy clay sediment in Eckernförde Bay
- High porosity clay sediment in Eckernförde Bay

APPROACH

Modeling of elastic wave propagation in sediments has resulted in a wide variety of theories based on idealized mathematical descriptions. Wang and Nur (1992) list 14 theories of wave propagation which may be divided into 4 classes; effective medium models, wave propagation models, inclusion theories and contact theories. Effective medium models assume that the bulk elastic properties can be obtained through some average the properties of component moduli. The simplest example is Wood's equation which assumes that the bulk modulus of a fluid containing gas bubbles is the volume-weighted average of the fluid and gas moduli. Wave propagation theories provide elastic moduli based on the moduli of the solid phase, the solid framework and the fluid. These are represented by Gassmann's equation for static moduli and Biot theory for dynamic moduli. Inclusion and contact models provide framework moduli based on explicit descriptions of the sediment geometry. Examples include the Kuster-Toksoz (1974) and Berryman (1974) self-consistent models for dilute distributions of inclusions in a solid matrix. These models have found limited application since ellipsoidal inclusions are rarely found in nature. Contact models have evolved from evaluations of the moduli of regular packings of spheres to random packings, cementation effects, hydrodynamic effects at contacts and stress induced anisotropy (Stoll 1989). All of these efforts have focused on the limited problem of predicting velocities and dispersion in clean, well-sorted silt and sand.

The CBBL program included studies of a variety of bottom sediment environments which are not amenable to the explicit contact and inclusion theories described above. Our objective was to develop a uniform technique which is capable of determining geoacoustic properties of sediments from microfabric observations. We have applied a microstructure analysis technique (MISTRA) to obtain saturated and dry framework moduli of any sediment microfabric. MISTRA uses the finite element technique to carry out an analysis of a structural grid consisting of solid, water and gas phases (Mueller and Kolle 1991). Periodic, generalized plane strain boundary conditions appropriate for a representative unit cell embedded in an infinite medium are applied to a microstructure grid obtained from image analysis or using statistical structure generation routines. The properties of water or gas are parameterized with elastic moduli chosen to match the compressibility of water and very low shear modulus to calculate saturated and dry framework elastic moduli. These moduli can then be used to obtain low-frequency acoustic wave velocities and Biot dispersion in multi-phase materials. The power of this approach lies in the ability to deal with a broad range of sediment structures.

RESULTS

Compact Sand

Although a CBBL field experiment was carried out on the West Florida sand sheet in 1993, no data on the sediment microstructure or in-situ acoustic velocities was available in FY94. We therefore used a stochastic procedure to generate models of sand and compared this data with laboratory studies of acoustic velocity in sand. In this analysis we wanted to determine the limitations of an existing MISTRA code which uses structured finite element analysis grids. Structured, 20x20 stochastic sand grids with 22% and 39% porosity were generated by placing circular sand grains at a series of randomly selected points until the desired porosity is reached. The algorithm also allows for random variability in the grain diameter.

As porosity approaches a critical value of about 39%, sand changes from a framework structure to a suspension. Lower porosities imply a level of cementation among grains which is reflected in the analysis grid. The structured grid has a resolution scale which is limited by the grid size. As porosity increases the structure becomes dominated by grain contacts which cannot be well represented by the grid.

Both saturated and dry analyses were carried out for each structure. In the saturated case the pore space is filled with water and in the dry case the pores are empty. The finite element approach assumes that all phases are elastic solids so it is necessary to model water and void spaces as pseudo-elastic solids. The elastic properties used in the sand model are listed in Table 1. Water is modeled as a nearly incompressible elastomer with Poisson's ratio approaching 0.5. The void space is modeled as an elastic material with extremely low modulus. Sand grains are modeled with the elastic properties of quartz.

The MISTRA analysis generates orthotropic elastic moduli for the stochastic sand structures studied. We assume that the macroscopic sediment is isotropic and use a Reuss/Voigt average of the orthotropic moduli to calculate velocity of a random assemblage of elements with orthotropic properties (Christensen 1982).

Figure 1 shows the results of velocity simulations in ten stochastic sand models with porosities ranging from 1 to 39%. Both dry framework and saturated velocities are shown. These numerical data points are compared with the critical porosity model of Yin, Nur and Mavko (1993) which provides an upper bound (curves) to observations of velocity in clean sandstones and sand. The numerical simulations are all quite reasonable. Our previous results, had shown a problem with convergence and overestimates of moduli near the critical point. The new results reflect a more accurate, double precision solver which is capable of dealing with the singularity implicit in an elastic solution for an incompressible medium. MISTRA is capable of modeling the full range of sand behavior from a solid framework through a suspension with porosities greater than 39%.

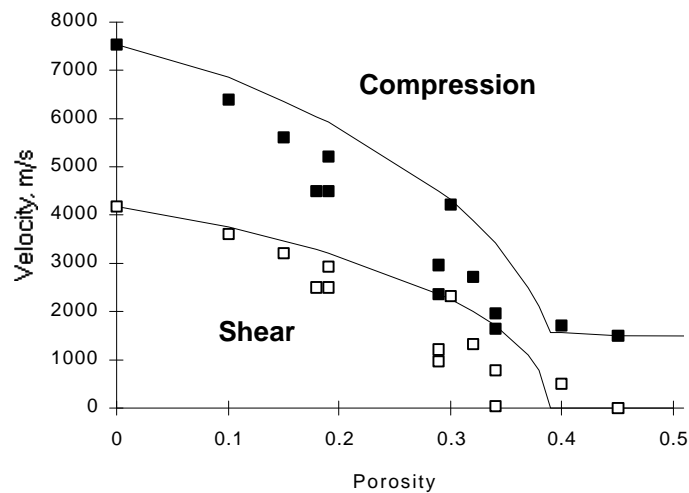
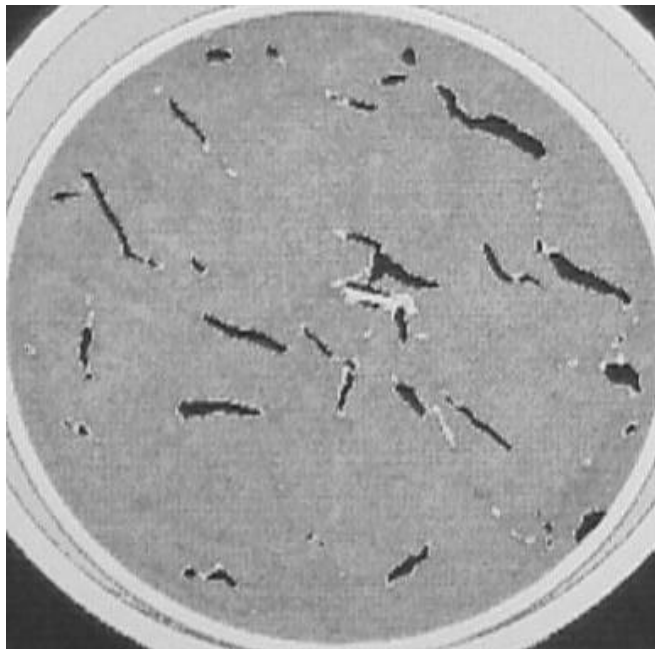


Figure 1. Compression and Shear Wave Velocities in Saturated Sand. MISTRA Results (square points) are Compared with Theoretical Upper Bound (curves).

Gassy Sediment

A structural modeling analysis of the effect of gas pockets on the acoustic properties of Eckernfoerde Bay mud was carried out using the finite element analysis method. We generated two dimensional structure models based on a CAT scan of a pressurized mud core containing a number of gas pockets (Figure 2, provided by Aubrey Anderson). High contrast image samples, were generated from the CAT scan image. The sample structures have porosities ranging from 3.1% to 9.5%. These high contrast images were used to generate structured finite element analysis grids. We also investigated the effects of square pores with a broad range of porosities on mud properties.



**Figure 2. CAT Scan of Eckernfoerde Core 339 - Pockmark Floor ~380 mm Depth.
(Image provided by Aubrey Anderson, Texas A&M University)**

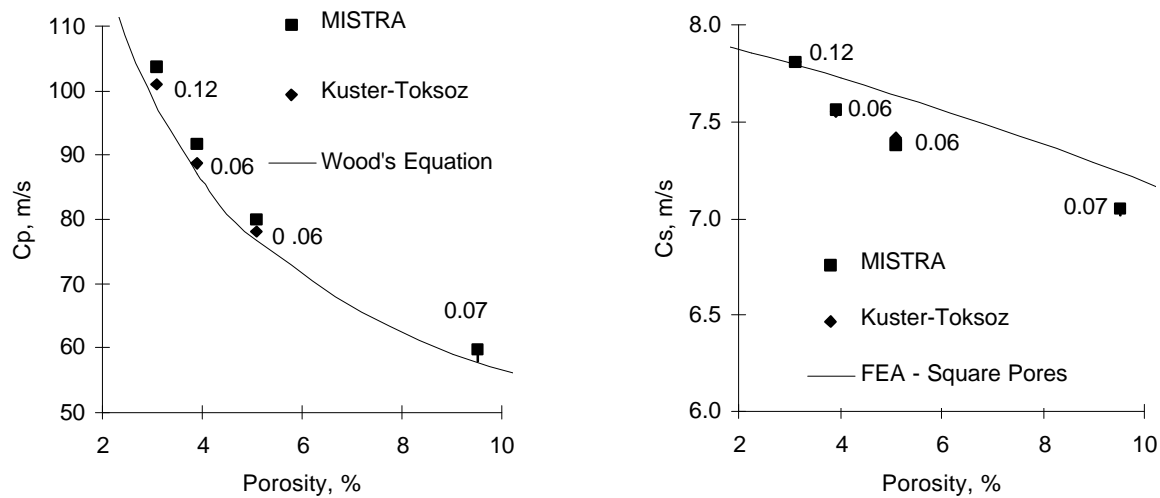
The gassy mud is modeled as a two-phase elastic composite. The elastic properties of the matrix (mud) phase were derived from the mean acoustic properties of the sediment in Eckernfoerde Bay as provided by Mike Richardson. Most of the near surface sediment sampled in the study do not contain gas pockets and the sediment density is consistent with this assumption. Elastic properties of the matrix were derived from the compression and shear wave velocities in the sediment. The gas pocket properties were derived from the properties of methane gas trapped at the ambient temperature of the mud using the ideal gas law gas law and pressure and temperature appropriate for Eckernfoerde Bay.

Note that this reverts to the relationship between incompressibility and acoustic wave velocity in a gas when $\nu = 0.5$; A Poisson's ratio of exactly 0.5 causes singularities in the stiffness matrix of the finite element solution for an elastic material, we therefore choose Poisson's ratio to be as close as possible to 0.5 consistent with the accuracy limitations of our computer. This results in a small but finite value for the shear wave velocity in the "gas". Mean Eckernfoerde sediment properties used in the simulations are listed in Table 1.

Table 1. Eckernfoerde Sediment Mean Properties

	r , kg/m ³	C_p , m/s	C_s , m/s	K , Pa	G , Pa	n	E , Pa
mud	1190	1428.6	8.00	2.43×10^9	7.62×10^4	0.49998432	2.28×10^5
“gas”	1.838	429.5	0.02	3.39×10^5	6.78×10^{-4}	$0.5 - 10^{-9}$	2.03×10^{-3}

We then modeled the geometries illustrated in Figure 2 using a structured grid. These results are shown as the four data points in Figure 3. The acoustic velocities given represent the low frequency limit for acoustic wavelengths larger than the scale of the void spaces. In this case, the voids are on the order of up to 10 mm in scale. The velocities are thus valid for compression wave frequencies under 1 kHz and shear wave frequencies under 100 Hz. The MISTRA model data are compared with the Kuster-Toksoz (KT) (1980) model for a dilute suspension of randomly oriented ellipsoids. Ellipse aspect ratios (shown alongside the KT points) were chosen to match the MISTRA data and are reasonable values for the voids shown in Figure 2. The MISTRA compression wave velocities are within 4% of the KT model and the shear velocities agree within 0.5%.

**Figure 3. Modeled Compression and Shear Wave Velocities in Gassy Eckernfoerde Sediments**

MISTRA was also used to calculate velocities in mud containing square pores to illustrate the influence of pore aspect ratio. There is little difference between predictions for compression wave velocity but a significant effect of pore aspect ratio on the shear wave velocity. The compression wave velocity may also be estimated using the isostress approximation for average compressibility of two fluids (Wood's equation). This relationship does not account for the finite shear modulus of the sediment, but as seen in Figure 3, the result provides a lower bound on velocity.

Clay Microfabric

Clay can be thought of as a collection of randomly oriented plates which, under weak electrostatic forces, are held together in a skeleton structure. The weak forces are a result of the opposite charges forming on the plate edges and the plate surfaces. Figure 4 shows a TEM image obtained from soft clay mud in Eckernforde Bay. The platelet skeleton structure is an interconnected maze through which the water may flow and this water can help to support the skeleton structure under hydrostatic loading.

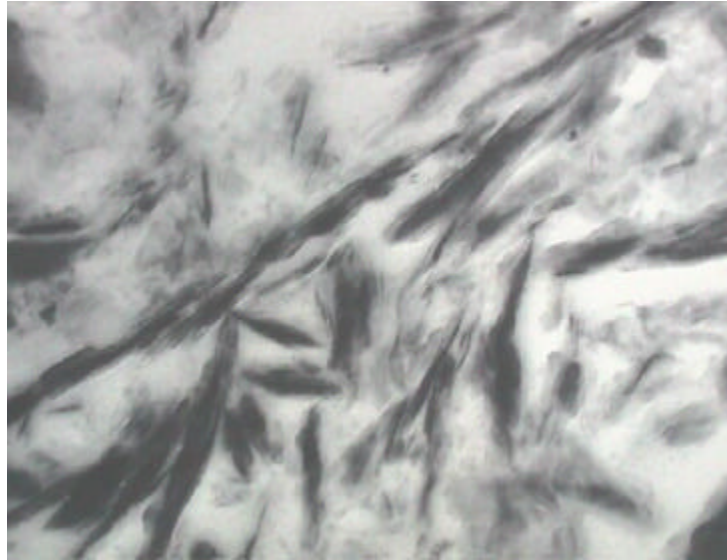


Figure 4. TEM Image of pressurized mud core from Eckernforde Bay, 145 cm below surface. Height of image is 2 μm . (Image provided by Dennis Lavoie, Naval Research Laboratory, Stennis Space Center)

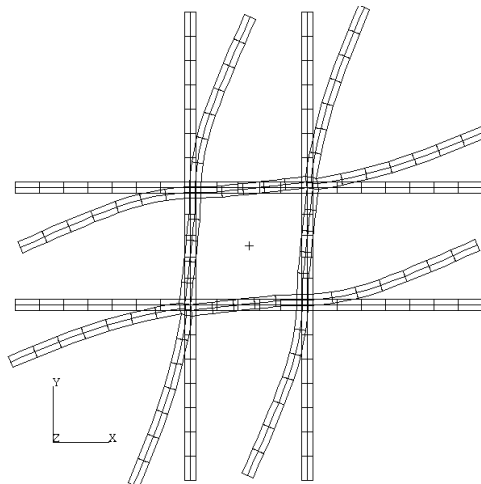


Figure 5. Regular Lattice Structure Showing Pure Shear Deformation of a Hinged/Cantilevered Model

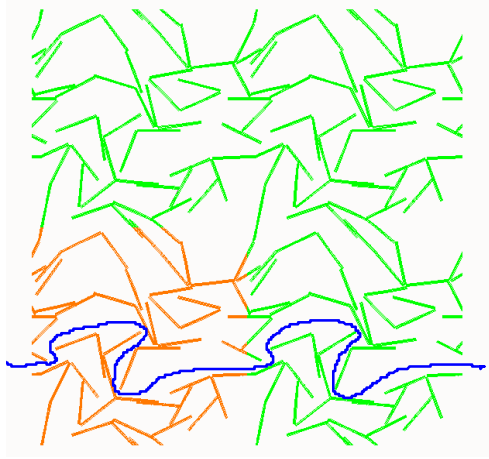
We first examined a very simple unit periodic framework structure shown in Figure 5. The widths of the plates have been chosen so that the porosity of this frame work is close to that of the Eckernfoerde mud of 90.4%. This model consists on nine individual, unconnected pores. To study the frame rigidity, the joints labeled A,B,C, and D have been considered hinged or cantilevered. The model identified as “Fully Cantilever” has all joints cantilevered, the modeled identified as “Fully Hinged” has all joints hinged and finally the model labeled Hinge-Cantilever has joints A and C cantilevered whereas B and D are hinged. All models were been subjected to macroscopic pure bulk strain and macroscopic pure shear strain load and the macroscopic bulk mean stress and shear stress are then computed as an average over all the elements in the model. Table 1 shows the elastic moduli and velocities used to model Illite, water and void spaces.

As one would expect the fully cantilevered model gave the strongest rigidity and the fully hinged model was the weakest. The fully hinged framework (void case) showed no shear rigidity because the platelets could pivot on the hinges. Furthermore, the water saturated fully hinged model showed no shear rigidity because the plates could pivot in such a way that the individual pores do not change volume. The fully cantilevered model behavior agrees with Gassmann’s equations in that the water saturated shear modulus is the same as the frame modulus. This is because the symmetry of the plate deformation is such that the individual pores do not change in volume under macroscopic shear. However, the hinged-cantilevered model shows that the saturated shear modulus is greater than the dry framework modulus. The increase shear rigidity is due entirely because the symmetry is broken and pore volume changes in pure shear. Hence some pores become compressed and others expand giving rise to a differential pore pressure.

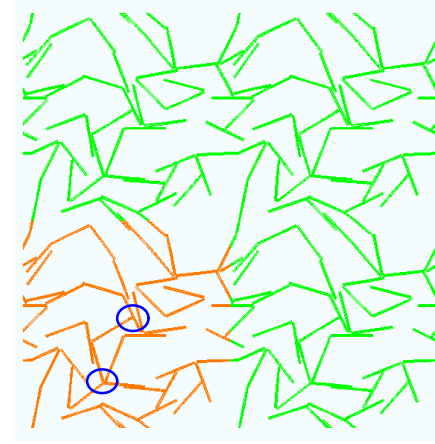
Table 2. Material Properties used in MISTRA Analysis of Clay Mud

Material	ρ	K	G	C_p	C_s
Illite	2790	5.19×10^{10}	3.09×10^{10}	5780	3330
water	1020	2.16×10^9	4.31	1454	0.065
void	1	1.67×10^2	3.33×10^{-7}	408	0.0

Not surprising all the simple frame models showed bulk and shear modulus which are larger than measures values of Eckernfoerde mud. To examine the role of the random structure we constructed two slightly different models of a random microstructure which, as before, have approximately 90.4% pore area fraction. The clay platelets were linked in an edge-face structure based on TEM images of Eckernfoerde mud. Structure “A”, shown in Figure 6 was generated by randomly placing randomly oriented clay platelets with an aspect ratio of 20:1. This model is permeable in the sense that a continuous pore space extends horizontally through the center of the model. No such pathway exists in any other directions, hence the model is somewhat anisotropic. This 2D model can not have any framework shear strength since it will slip along this line. For that manner, the modulus for loads acting approximated from top to bottom would not be resisted. To evaluate the influence of permeability we slightly modified the platelet structure in Model “B”, extending the platelets in order to close the flow and strengthen the framework.



Model A - Free Flow Geometry



Model B - Fully Connected

Figure 6. Stochastic Clay Platelet Structures Used for MISTRA Modeling

A series of tests were conducted on both structures assuming joints are fully cantilevered or fully hinged. As in the simple model, differential pressure developed in isolated, non-communicating pores. For example, even though the analysis indicated that framework of structure A-hinged, A-cantilevered, and B-hinged have no shear strength, the fully saturated models do possess some non-negligible strength. Only model B-cantilevered shows some framework shear resistance and yet even in this case, the addition of water tends to promote is shear modulus. Figure 7 shows the pressure in the pores under pure shear strain loading shows distinct pressure differentials among isolated (or nearly isolated) pores. To confirm that the differential pressure is responsible for the shear modulus and not the limitations of the pseudo-water assumptions of the analysis we plotted the shear stress in the pseudo-water filled pores and noted that the pseudo-water shear stress magnitude is much smaller than the macroscopic average shear stress.

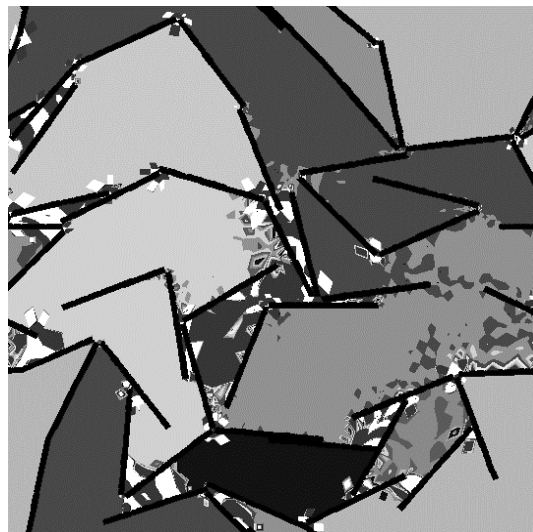


Figure 7. Pore Pressure Differentials in Clay Platelet Model Subject to Pure Shear Deformation. Grey In pore Space Indicates Pressure Level.

The hinged model predictions are compared to the measured properties of Eckernfoerde mud in Table 3. All the models do a good job predicting the bulk modulus. This is primarily due to the very weak dry bulk modulus of the platelet framework. The random model as expected predicts a much weaker modulus than the simple models. The very small shear modulus predicted by the random models are much closer to the experimentally observed values than the simple models. In fact the two hinged models bracket the observations of velocity in Eckernfoerde mud. The order of magnitude agreement to the measured values indicates that the framework shear modulus is quite weak and may be negligibly small. The models also points out that the rather small observed shear modulus in Eckernfoerde mud may not simply be the result of the framework, but a combination of the water and frame through the action of differential pressure in isolated pores.

Table 3. Comparison of MISTRA Analysis with CBBL Data

Property	A-Hinged	B-Hinged	Eck. Mud
K_s , Pa	2.38×10^9	2.38×10^9	2.43×10^9
K_d , Pa	0.0	0.0	N/A
G_s , Pa	2.77×10^4	3.81×10^5	6.72×10^4
G_d , Pa	0.0	0.0	N/A
C_p , m/s	1414	1414	1429
C_s , m/s	4.8	17.9	8.0

ACCOMPLISHMENTS

MISTRA was used to determine poroelastic moduli for three marine sediments encountered during the first two years of the CBBLSRP. A simple structured grid model of compact sand microfabric showed that saturated and dry framework moduli could be obtained from a finite formulation using pseudo-elastic moduli to simulate water and void space. MISTRA was also used to model gas pocket inclusions in gassy mud from Eckernfoerde Bay. Analyses were carried out on CAT scanned images of pressurized cores. Modeled compression and shear wave velocity anomalies agree well with analytical models of wave propagation in a medium containing ellipsoidal inclusions. Clay microfabric structural analysis results showed that the MISTRA approach was capable of modeling a clay platelet structure based on TEM imagery of mud from Eckernfoerde Bay. The clay structure models provide saturated moduli which bracket the observed properties. The shear modulus of the clay was shown to be due to differential pressures which arise in isolated pores as the clay framework is distorted. Thus the saturated clay structure can have a non-zero shear wave velocity even though the dry framework moduli are negligible.

This unified approach can be generally applied to sediment microfabric providing a significant advantage over the contact and inclusion theories currently available for sediment modeling.

REFERENCES

- Berryman J.G. (1980) "Long-wavelength propagation in composite elastic media II. Ellipsoidal inclusions," *J. Acoust. Soc. Am.*, **68** (6), 1820-1831.
- Christensen, N.I. (1982) "Seismic velocities," Handbook of Physical Properties of Rocks, Vol. II, ed. by R.S. Carmichael, 1-228, CRC Press, Boca Raton.
- Kuster, G.T. and M.N. Toksoz (1974) "Velocity and attenuation of seismic waves in two-phase media: Part I. Theoretical formulations," *Geophysics*, **39**, 587-606.
- Yin, H., A. Nur and G. Mavko (1993) "Critical porosity-a physical boundary in poroelasticity," *Int. J. Rock Mech. Min. Sci. & Geomech. Abstr.*, **30** (7), 805-808.
- Mueller, A. C and Kollé, J. J. (1991) "General approach to finite-element analysis of composite micromechanics," *Proceedings of the 8th International Conference on Composite Materials ICCM/8, Honolulu*, **3**, paper 29-E, Society for Advanced Material and Process Engineering, Covina, California.
- Richardson M.D. (1994) "Investigating the Coastal Benthic Boundary Layer," *EOS, Trans. Amer. Geophys Union.*, **75** (17).
- Stoll R.D. (1989) "Sediment Acoustics", *Lecture Notes in Earth Sciences*, **29**, ed. by S. Bhattacharji, G.M. Friedman, H.J. Neugebauer and A. Seilacher, Springer Verlag, New York.
- Wang Z. and A. Nur (1992) "Elastic wave velocities in porous media: A theoretical recipe," *Seismic and Acoustic Velocities of Reservoir Rocks, Vol. 2, Theoretical and Model Studies, Geophysics Reprint Series*, **10**, ed. by Z. Wang, A. Nur and F.K. Levin, Society of Exploration Geophysics, Tulsa.

PUBLICATIONS

Published abstracts:

- Kollé, J. J. (1994) "Structural analysis of marine sediment microfabric to derive Biot poroelasticity parameters," *Trans. Am. Geophys Union*, 4.
- Kollé, J. J., Mueller, A.C. and Dvorkin, J (1994) "Microstructural modeling of clay sediments in Eckernförde Bay," abstract of invited paper, *J. Acoust. Soc. Am.*, 96 (5), 3246.

Proceedings:

- Kollé, J.J., A.C. Mueller and J. Dvorkin (1995) "Microstructural Modeling of clay sediments in Eckerforde Bay," proceedings of the Workshop Modeling Methane-Rich Sediments of Eckernförde Bay, Eckernförde, June 26-30, FWG Report-22, pp. 233-240, FWG, Kiel, Germany.

Quantification of High Frequency Acoustic Response to Seafloor Micromorphology in Shallow Water

D.N. Lambert and D.J. Walter
Naval Research Laboratory, Code 7431
Stennis Space Center, MS 39529

Abstract: The Naval Research Laboratory has used a high resolution seafloor classification system designated the Acoustic Seafloor Classification System (ASCS) to characterize the sediment cover at several Coastal Benthic Boundary Layer (CBBL) study sites. The system uses empirical relationships to predict sediment properties after deriving acoustic impedance from single frequency, normal incident returns. Hardware and software improvements accomplished throughout the project have resulted in a system that can provide real-time, color-coded, navigation plots of predicted surficial sediment impedance. These 2-D maps can be used to develop a preliminary assessment of sediment properties in a study area that represent relative sediment type and distribution patterns. Additional mapping techniques were developed that used layered echostrength data to develop two-dimensional, color contoured, sediment property maps. This surface was draped over a 3-D bathymetric map to illustrate facies changes with co-registered bathymetry.

Correlation of the acoustic predictions and measured physical properties from a site in the southwest Baltic (a shallow glacial-marine environment) show reasonable agreement. Acoustic impedance predictions in a predominantly carbonate area (Dry Tortugas) required correction. Raw data from the carbonate site was processed after the sediment classification software was adjusted to the acoustic impedance calculated from single, ground truth core site. This data was then used to create a "core corrected" sediment facies map of the Dry Tortugas study site. Comparisons of the re-processed data to additional core locations at the study site show good agreement. A three-dimensional geologic fence model of this area was constructed from raw ASCS imagery obtained using a 3.5-kHz hull-mounted "transducer-of-opportunity" aboard the R/V Seward Johnson. This model provides a detailed geomorphic and volumetric view of the entire 6 X 6 km Dry Tortugas study site. A linearized least squares inversion has been used to invert real acoustic data from this site to derive estimates of acoustic impedance vs. time (depth). This technique shows promise for predicting an acoustic impedance profile in a real-time data acquisition mode.

The system was also used to delineate vertical and lateral distribution of gassy sediments at the Baltic site. Acoustic returns from these bubbly sediments show a frequency variation with depth. These effects occur over a wide range of frequencies and are roughly separated by the bubble resonance frequency, which is inversely proportional to bubble size.

Studies indicate that further refinement of empirical relationships between acoustic impedance and several physical and geotechnical properties is required especially in carbonate sediments. Also, incorporation of a deconvolution algorithm used with a high-frequency, narrow beam FM sweep has promise in providing the spatial and temporal resolution required for assessment of cm scale sedimentary structures and morphology.

Objectives: The objectives of this effort were (1) to investigate new methods of quantifying the effect of sediment micromorphologic structure on high frequency acoustic response in shallow water and its relationship to in situ acoustic and geotechnical properties and (2) to provide 3-D digital high resolution micromorphologic characterization of several CBBL program experimental sites. These objectives were meant to compliment other proposed collaborative efforts in this ONR/Special Research Program and other ongoing 6.2 and 6.3 programs, and thus, collectively provide the means to make significant improvements in remote sediment classification technology required for improved MIW and MCM system performance and performance prediction.

Approach: The project as originally proposed was to encompass three fiscal years, with a single field experiment planned for each of the first two years and data analysis and publications for the final and third year. The project lasted five years and included seven extensive site surveys. The first year effort consisted of: (1) an evaluation of the current method of sediment classification used by the ASCS; (2) the initiation of a theoretical and modeling study of potential sediment classification methods based primarily on recent technological advances in the field; and (3) a detailed acoustic characterization of the seafloor in the area of the CBBL experiment site in the Baltic Sea.

The initial evaluation of the ASCS sediment classification techniques utilized existing acoustic survey and ground truth core data from the Ship Island Testbed. This data was used to identify limitations in the original ASCS classification methodology such as estimating sediment column structural properties, detection of positive/negative impedance changes, and evaluating the relationship between sediment shear strength and acoustic impedance. This effort also provided insight into specific techniques that could be used to eliminate these limitations. Ultimately the task used data sets previously collected in the Ship Island Testbed and also the data collected during three field experiments in the Baltic Sea. These evaluations continued through the entirety of the project utilizing additional data obtained from the Chesapeake Bay, two additional surveys in the vicinity of Key West, and a final CBBL survey conducted in the Eel River flood deposition zone near Eureka, CA.

A theoretical study and modeling effort used the results of these evaluations to explore a number of signal processing techniques. A Post-Doctoral Investigator began working on this project in early 1993 utilizing MatLab™ signal processing software to assess the raw ASCS data. The approach was to evaluate the raw ASCS data obtained at several study areas and develop new algorithms for using this data to enhance present sediment classification techniques. Techniques investigated included the use of simultaneous multiple frequencies, high-frequency FM sweeps, parallel data processing, and the use of the broadband acoustic signals for sediment classification. The goal was to identify appropriate physical models or signal processing techniques that could be used with the acoustic data to accurately represent the micromorphological characteristics of the seafloor. These physics based models and techniques were expected to provide more quantitative values of geotechnical properties needed for mine burial prediction and system performance prediction. Concurrently, investigations were conducted to determine the feasibility of replacing or supplementing the empirical relationships typically used for sediment classification that relate any of several sediment properties to acoustic impedance (Hamilton 1980, Hamilton and Bachman 1982). The ASCS sediment classification

software utilizes these relationships, after deriving a value for sediment acoustic impedance, to predict sediment properties such as density, porosity and grain size.

The ASCS was used to provide geological site assessments of the sediment column in the CBBL experiment sites using a minimum of two frequencies (15 kHz and 30 kHz). Initially, the original Honeywell/ELAC hardware (Lambert 1988, Lambert and Fiedler 1991) which included a strip chart paper recorder with an associated digital signal processing set (EMG-2) were used to accomplish this task. Raw, six bit, echostrength data was transmitted via serial port to an 80386 personal computer that estimated sediment structure and acoustic impedance. The empirical relationship of acoustic impedance to a targeted sediment property value was used to predict the specific sediment property. An upgrade to this configuration that replaced the Honeywell/ELAC acquisition hardware with another personal computer and newly written acquisition software was tested during the initial Baltic sea trip (Lambert et al. 1993). This system utilized a new acoustic data acquisition board that provided analog to digital conversion at a 16 bit capacity and resulted in an increase in dynamic range to about 90 dB.

The ASCS system was used off Eureka, CA during the “Eel River” voyage to conduct a site survey of the Eel River storm depositional zone. Conditions during much of this trip were less than ideal for acoustic data acquisition due to the heavy seas encountered. However, real-time maps of surficial sediment impedance delineated a boundary between the nearshore sand blanket and an offshore, low impedance silty-sand zone (Figure 1). Acoustic data was obtained during the second leg using the 15-kHz ELAC transducer hanging over the side while the ship remained on station. Data obtained included the normal short pulse length single frequency data as well as long pulse length, high frequency FM sweeps. Unfortunately, this data suffered the same consequence of lower quality due to extensive ship motion. The approach for processing this data set was to use a calibrated wavelet to deconvolve the returned signal. The idea was to use a broad bandwidth pulse to achieve better vertical resolution in the upper 0.5 m of the sediment column. Specifically, the intent was to resolve microscale (cm scale) storm layer features that were deposited during and after excessive rainfall in the Eel River flood plain.

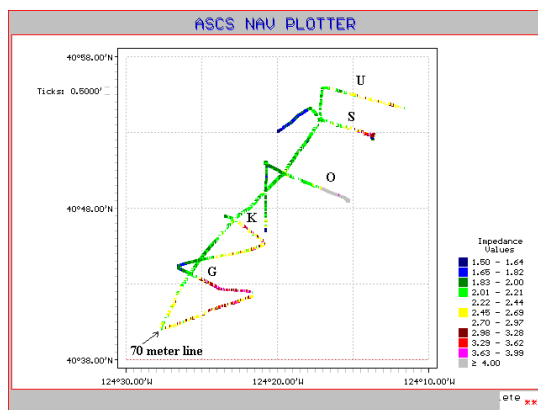


Figure 1. NRL/Acoustic Seafloor Classification System (ASCS) real time trackplot of acoustic impedance obtained using 15 kHz during Leg 1 of R/V WECOMA Cruise W9605B (Eel River). Grays are off scale and result from improper settings and should actually be in red color zone. Reds are coastal sands. Yellow and green colors indicate areas which transition from softer muddy sands to muds (or silts), respectively. Blues are indicative of very soft silts or muds.

Two separate systems were used aboard different vessels during the Key West Campaign, one on the *WFS Planet* and the other on the *R/V Seward Johnson*. Although each ASCS configuration was similar, a different transducer was used aboard each ship. The survey conducted aboard the Planet was done concomitantly with acquisition of both side scan sonar and 3.5-kHz subbottom profile data. Acquisition aboard the Seward Johnson utilized several transducer configurations including the towed ELAC 15-kHz transducer operating at both 15- and 30-kHz, and two of the ship's hull mounted transducers, one operating at 4-kHz and the other at 12-kHz. Trackline spacing was approximately 150 m for the *WFS Planet* survey to allow ample overlap of the side scan sonar data. *R/V Johnson* tracks were completed at a spacing of approximately 1 km. Data at three acoustic frequencies (15-, 30-, and 50-kHz) was also recorded on the *R/V Seward Johnson* at each core location. Other CBBL investigators (Slowey et al. 1995 and 1996, Stephens et al. 1997, Wever et al. 1997, Lyons et al. 1996, Hawkins et al. 1995, Anderson et al. 1995, and Anderson et al. in press 1998) have used considerable portions of this data.

Results: The new 16 bit ASCS data acquisition system provided a capability, heretofore unavailable, to record the raw, acoustic data on the acquisition computer prior to calculation of the sediment properties from the eight bit data on the second computer. In addition, this setup provided a high resolution color graphic scrolling screen display of the sub-seafloor for each acoustic shot that replaced the paper record (Figure 2).

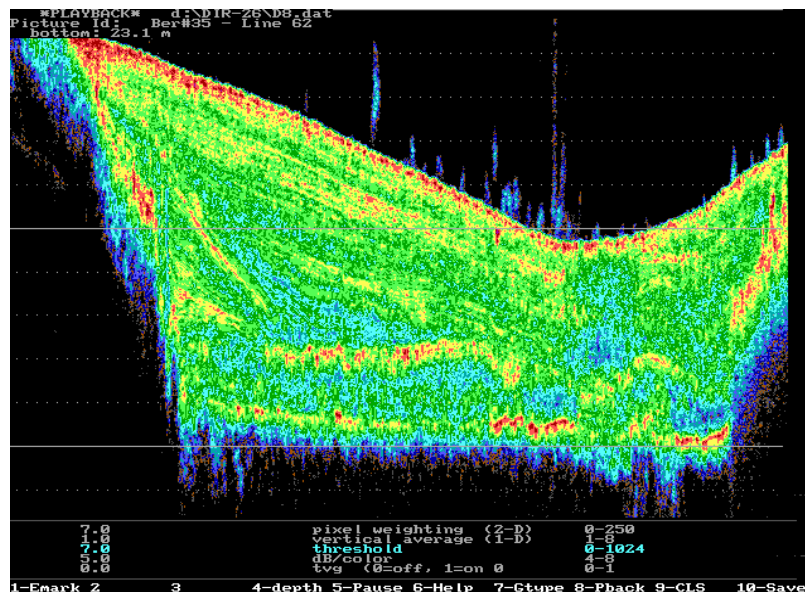


Figure 2. ASCS color seismic display recorded using 30 kHz @ 0.1 ms pulse length along Line V east of Bokniseck in the southwest Baltic north of Kiel Bay.

This enhancement resulted in a capability to record, display and process the raw high-resolution acoustic data and to save the imagery to disk as a separate file. The color display provides a full 90-dB dynamic range as compared to the paper record that provides a dynamic range of only about 30 dB. The complete outgoing pulse and return signal were also digitized and stored for reprocessing in the laboratory. This was not possible with the previous system.

Originally, the output from the ASCS was to be stored and used to develop a 3-D database of the experiment site utilizing Sierra GIS software. However, MatLab was used in lieu of Sierra and in conjunction with the Radian CPS-PC (™) mapping software to construct multiple (2-D) layer maps that delineate the distribution of shallow gas in the Eckernfoerder study site. Hawkins et al. (1994, Fig. 4) generated the first of these maps that illustrated the lateral and vertical distribution of high impedance sediments resulting from the presence of bubbles at the CBBL/JOBEX test site. Beginning with the 1994 fieldwork in the Baltic, the ASCS data was used to depict the study areas with a continuous 2-D impedance navigation map as each survey was conducted (Figure 3).

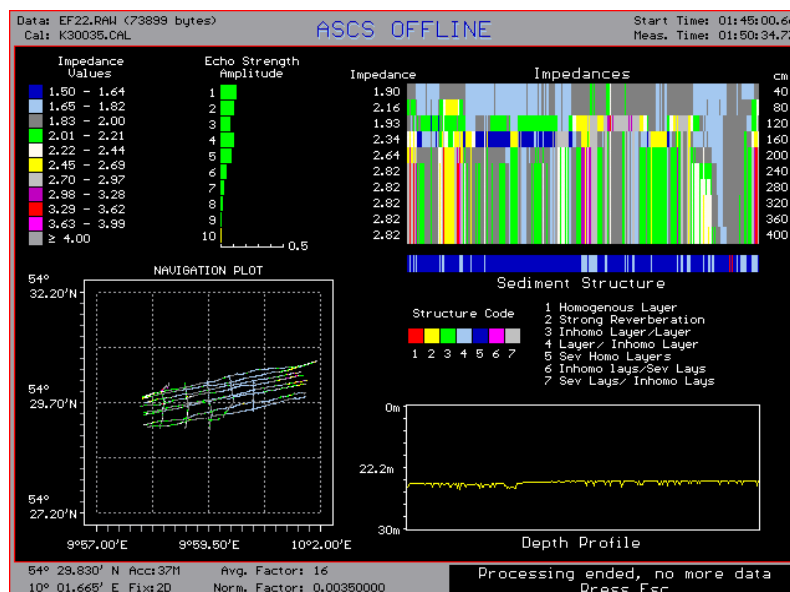


Figure 3. Color screen display from ASCS sediment classification computer showing scrolling impedance profile data (upper right), and surficial (0.0 – 0.4 m) sediment impedance along survey tracklines (lower left Navigation Plot) through the CBBL/JOBEX test area in Eckernfoerder.

This high resolution data set provided the first quantitative characterization of the micromorphologic sediment structure at this site, especially with respect to the distribution pattern of the biogenic gas that is predominant in this area. The ASCS also provided high-resolution imagery of unusual but prevalent “pockmark” features in the Eckernfoerder area. Figure 4 provides a very detailed perspective as the *WFS Planet* drifted across one of these features. These pockmarks usually contain high concentrations of methane gas that is delineated quite well by the high intensity red/purple return depicted in the center of the image just below the sediment/water interface. The bottoms of the pockmarks typically have irregular surfaces illustrated by the presence of small mounds of very low-density “fluff” material (light blue) at the sediment/water interface. Also observed in this image is the presence of gas bubbles in the water column, apparently escaping from the sediment surface at one of the mounds. Acoustic windows appear on either side of the pockmark revealing the underlying glacial till, indicating that these sediments have been degassed.

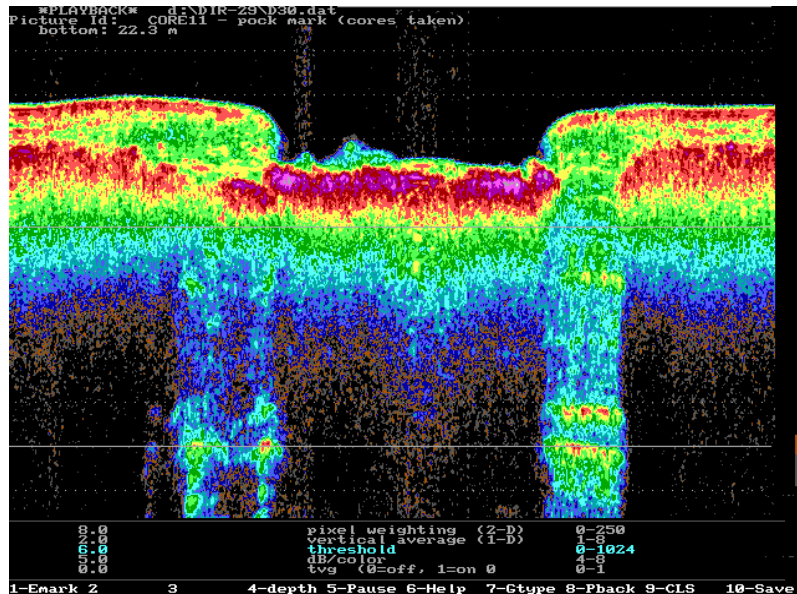


Figure 4. ASCS screen display on acquisition computer showing a crossing of a “pockmark” in Eckernförder Bay. Note the layer of highly reverberant gas (red and purple) below the sediment/water interface throughout the depression and two relatively gas free regions at the lateral boundaries of the feature where sublayers are detected 5.0 m below. Also note the presence of low impedance “fluff” at the left central portion of the feature (light blue and green) and the appearance of gas bubbles rising from the sediments into the water column.

ASCS data collected in real time within and near the CBBL test area indicates that the surficial sediments within the test area are softer and less acoustically reflective than in other areas adjacent to the test area. Figure 5a is a color 30 kHz seismic record obtained in the CBBL test area at Core Site 320. A comparison of ASCS predicted properties from this data to ground truth core data at the same location is shown in Figure 5b. Good correlation is shown in this plot for the upper 50 cm of the sediment column. Below 50 cm, the sediment acoustic response is dominated by the presence of methane gas bubbles in the sediment. These bubbles cause a stronger acoustic reflection than would be expected if the sediment did not contain the bubbles. Because of this, the ASCS tends to predict a higher value of acoustic impedance than it should in gassy sediments. Therefore, the ASCS predicts higher values of density and shear strength than it should. Similarly, impedance values determined from measurements on the core samples are low due to the slow compressional sound speeds (1000 - 1200 m/s) measured by the core scanner in the gassy sediments.

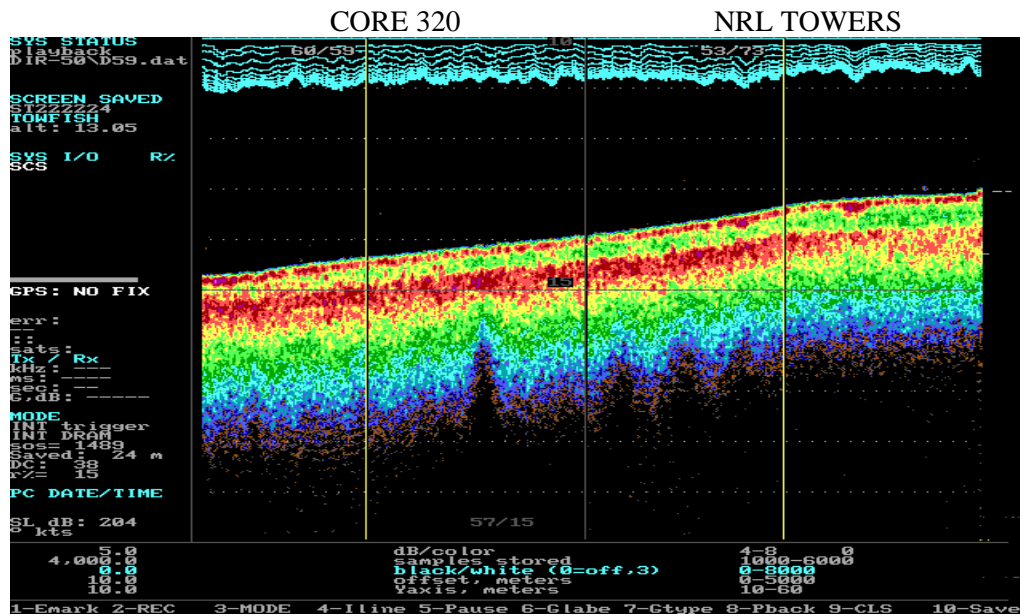


Figure 5a. 30 kHz ASCS trackline across the CBBL experiment site along Line I showing the location of Core 320 and NRL's backscatter and forwardscatter towers.

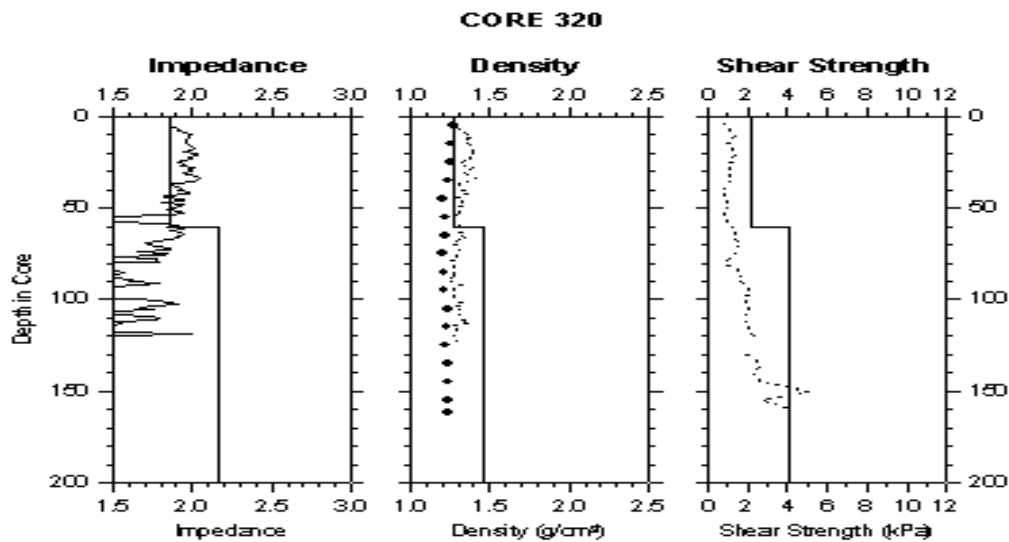
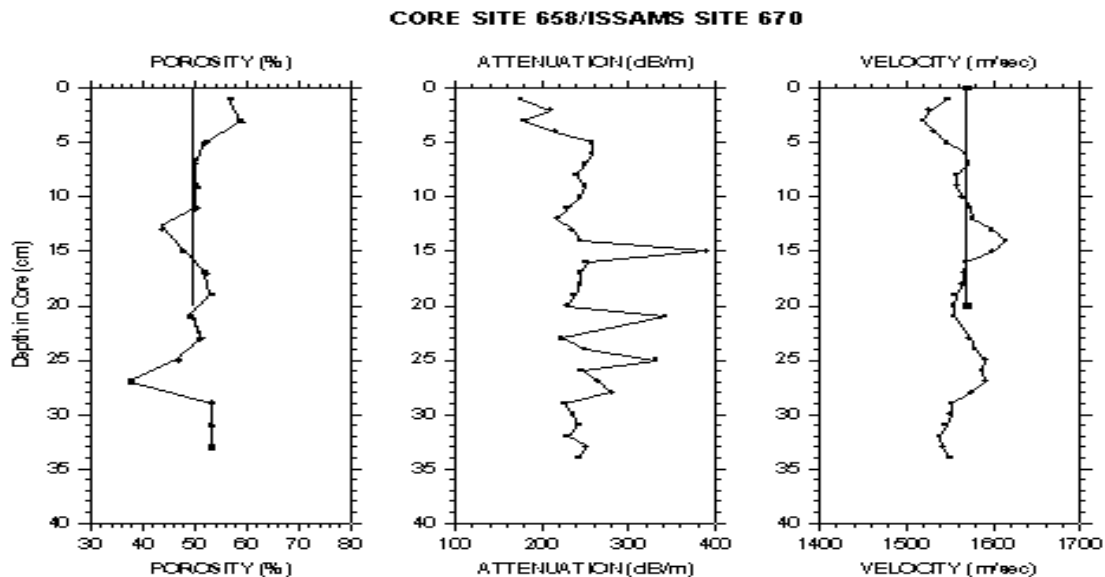


Figure 5b. Comparison of ASCS predicted sediment impedance, density, and shear strength (solid vertical lines) with ground truth, sediment core data (jagged and dotted lines) for core 320.

Figure 6a. ASCS 30 kHz seismic record across Line 47 showing the location of Core Site 658 and ISSAMS Site 670 in Eckernförder Bay, Germany.



Real-time correlation between the ASCS data and that obtained by the UCNW Magic Carpet and Uniboom systems was also observed (A. Davis and D. Huws, personal communication) during the coordinated tows where both systems were operated simultaneously.

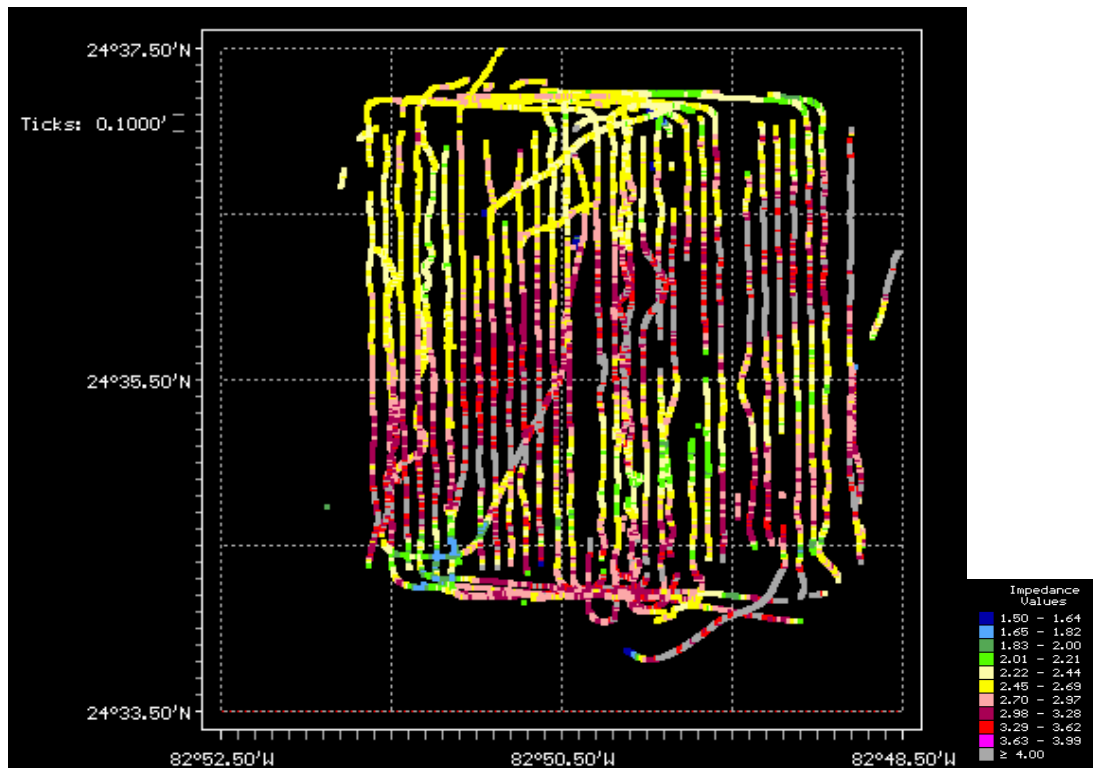
The investigation and testing of new signal processing techniques (e.g. reflectivity, deconvolution, inversion, bottom smoothing) continued throughout the history of this project. At this time, the deconvolution and a prior version of the bottom-smoothing algorithm are incorporated into the ASCS data acquisition software. Significant progress was made when Wood and Lindwall conducted an investigation under another basic research program but as a spin-off to the CBBL. They utilized ASCS data from the Dry Tortugas study site in conjunction with a single ground-truth core to evaluate two geophysical data processing methodologies for applicability with the ASCS data, a linear least squares inversion and simulated annealing (Wood and Lindwall 1996). Results of this study showed that Simulated Annealing (SA) provided a more accurate impedance profile but it is too computationally intensive to be used in real-time. The Linear Least Squares Inversion (LLSI) predicted the impedance profile with enough accuracy for most applications and it may be useable in real-time using a ping rate of one hertz or less.

An effort to develop a reliable method of remotely predicting sediment strength was initiated in FY94. This effort investigated both theoretical and empirical methods that appear to have reasonable applicability to the remote prediction of this very important parameter. Acoustic data and ground truth sediment core data from the Baltic experiment site and the Ship Island Testbed were used to test and verify this effort and to develop an initial empirical relationship between sediment shear strength and acoustic impedance. Another project conducted in coordination with the Naval Facilities Engineering Service Center provided data for this project. Seven field efforts supporting this project collected acoustic data with both expendable penetrometers and cone penetrometers. Final reports of the joint NRL/NFESC Project are being completed for publication. These reports will describe our present capability to remotely predict sediment shear strength using acoustic methods.

Another collaborative effort (MTEDS, funded out of the ONR 6.2 program) included utilization of the ASCS and sediment property prediction algorithms with an Impact Burial Prediction Model in the CBBL study area in the Dry Tortugas. This project developed methods that were shown to be applicable to MIW and MCM problems and that ultimately benefited the CBBL program by providing additional funding for further work on the acquisition software. This data has been used for several publications pertinent to the CBBL program (Walter et al. 1995, Walter et al. 1997a, Walter et al. 1997b).

In 1996 data from the Dry Tortugas study area was mapped in real-time (Figure 7) and later correlated with ground truth sediment core data to develop 2- and 3-D maps depicting the acoustic impedance of the surficial sediments and sediment column. These techniques provide a means for selecting appropriate locations where ground truth cores should be obtained as well as where additional geophysical and geotechnical sensors could be placed.

ASCS data obtained using a 3.5-kHz transducer operating at 4-kHz aboard the *Seward Johnson* also provided high-resolution imagery along tracklines that has been used to describe the morphology of the study site (Figure 8).



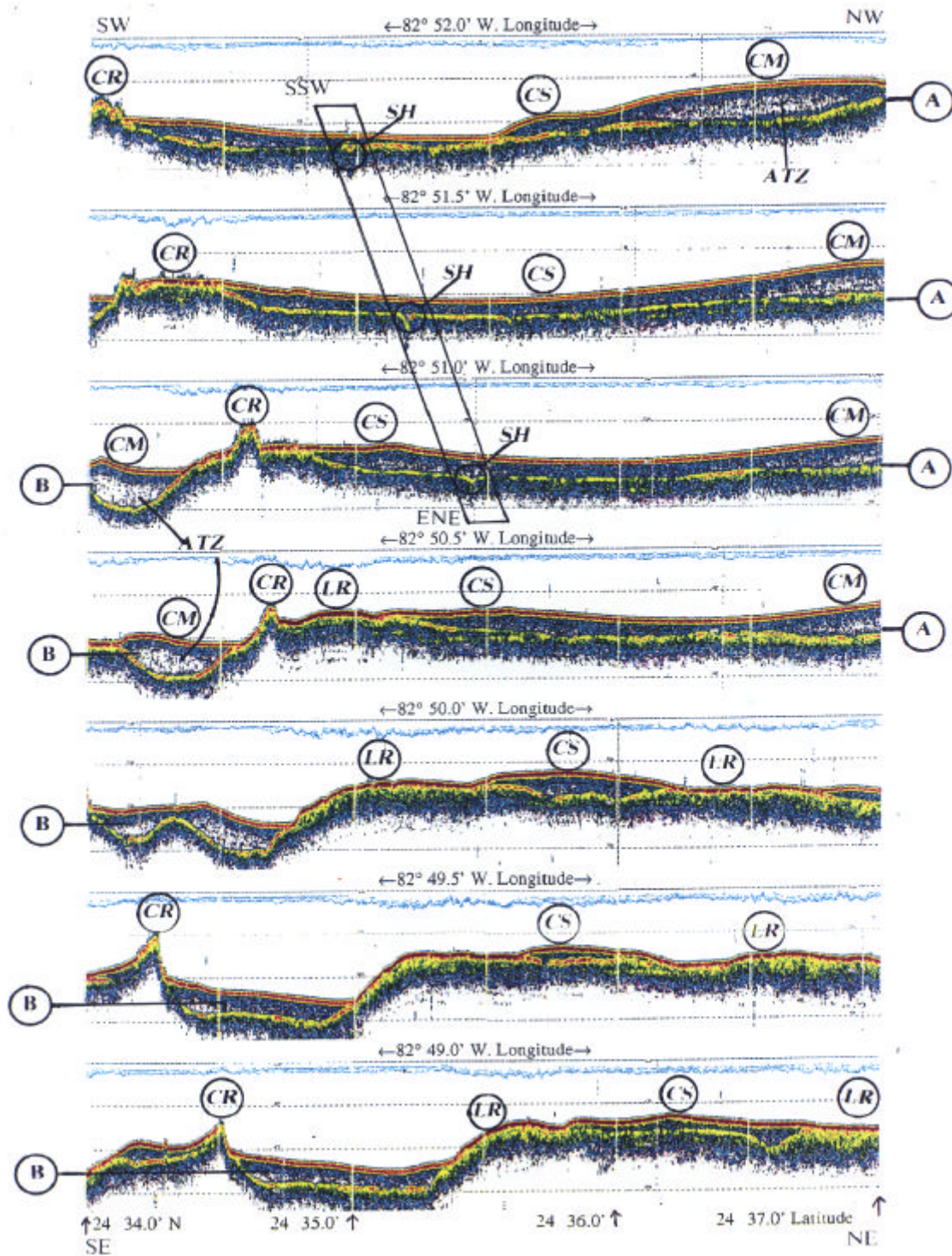
Color Key:

Interpretation of colorized tracklines using impedance/color scale below:

- Blue Low echo return (signal loss on steep slopes)
- Green Mud* (silt size) (sand:mud ratio <1:9)
- Yellow sandy Mud*(sand:mud ratio <1:1, may inc. shell)
- Pink muddy Sand*(sand:mud ratio >1:1, inc. shell)
- Red Sand* (sand:mud ratio >9:1)
- Gray Limestone rock or coral reef

* After Folk (1974, 1980)

Figure 7. Colorized trackplot of surficial (upper 0.4m) sediment acoustic impedance collected using the ASCS with 15-kHz transducer at hull depth aboard the *WFS Planet*. Trackline spacing is approximately 150 m.



*Legend: A = Key Largo limestone, B = Holocene sediment ponds, CR = coral reef, LR = limestone rock/lithified sand, CS = sand, CM = mud, SH = sink holes and paleochannel in bedrock.

Figure 8. Interpretation* of 4-kHz subbottom cross-sections along south (at left) to north (at right) tracks through the study area.

A portion of the 12-kHz ASCS impedance data obtained at a crossing of core site KW-PE-GC-167 was compared to averaged core measured values in the upper 0.4-m of the sediment column. ASCS system replay settings were then adjusted to match the ASCS impedance predictions with those of the averaged core values at that location. After this adjustment, the raw ASCS data was replayed to create a new file after correcting the data to the core values at one location. This new file was then used to construct a map of surficial sediment impedance (Figure 9).

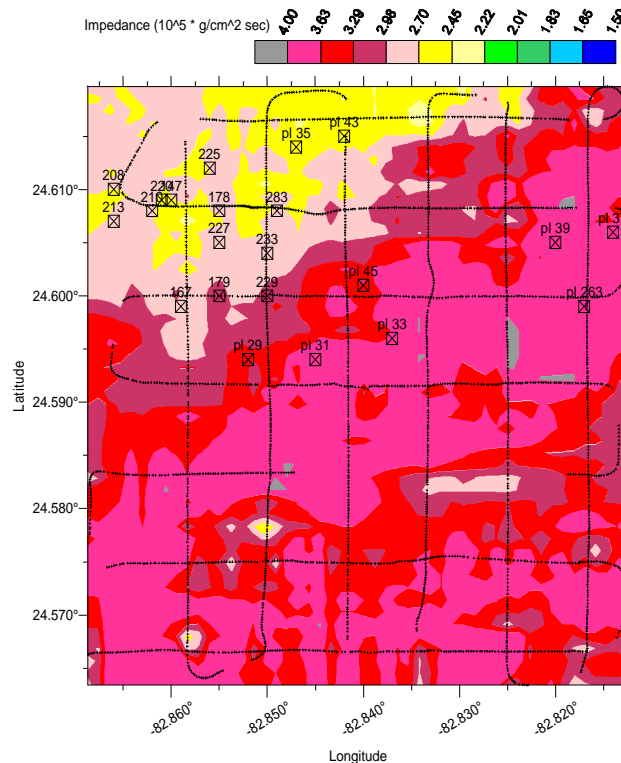


Figure 9. Two-dimensional surficial sediment (0.0 - 0.4 m) predicted acoustic impedance contour plot of reprocessed 12-kHz data obtained aboard *R/V Seward Johnson*. Sample locations are shown as an X within a box. Locations labeled (pl) denote grab sample sites in accordance with Wever et al. (1997).

This map provides an impedance model of the surficial sediment facies at the Dry Tortugas study site. Further analysis of this data correlated the core impedances with grain size measurements to select a descriptive term for the facies based on a combination of Wentworth (1922) and Folk (1974/1980) terminologies. Table 1 presents the impedance values from the core samples, the associated Wentworth and Folk terminologies and the impedance predictions obtained from both the trackline acoustic data as well as the color contour map. This work resulted in the construction of a sediment facies contour map that depicts the morphologic character and distribution of sediments in the Dry Tortugas study area (Figure 10).

Table 1. Wentworth and Folk terminology correlated with core calculated impedance, acoustic trackline predictions and predictions from impedance contour maps.

TERMINOLOGY				ASCS TRACK						CONTOUR MAP			
	(a) Wentworth size class	(b) Folk sand:mud ratio	calculated impedance	Real-time		Reprocessed		pred. imp.	pred. imp.	Reprocessed		pred. imp.	pred. imp.
				15-kHz color	15-kHz imp. range	15-kHz color	15-kHz imp. avg.3shots			12-kHz color	12-kHz imp. avg.3shots	15-kHz color	12-kHz color
Core #													
208	medium/fine silt	sM	2.73										yellow
220	medium silt	sM	2.64							lt. yel	2.22-2.44		yellow
210	medium/fine silt	sM	2.67							lt. yel	2.22-2.44		pink
213	medium/fine silt	sM	2.75										yellow
147	medium silt	mS	2.73	yellow	2.45-2.69	yel/pink	2.69		yel/red	3.11		yellow	yellow
225	medium silt	mS	2.78	yellow	2.45-2.69	red1	2.76					yel/pink	pink
178	medium silt	mS		lt. yel	2.22-2.44	pink	2.95					yel/pink	pink
227	medium silt	mS	2.8	yellow	2.45-2.69	yel/pink	2.67					pink	pink
179	medium silt		2.74	yellow	2.45-2.69	yel/pink	2.74					red1	red1
283			2.81	pink	2.7-2.97	pink/yel			lt. yel	2.22-2.44		pink	yel/pink
233			2.77	pink	2.7-2.97	pink	2.9		pink	2.71		pink	pink
229				red1	2.98-3.28	red1	2.86		red1	3.29		red1	red1
Calibration Site													
167	coarse silt	sM/mS	2.82	pink	2.7-2.97	pink/red	2.82		pink	2.88		pink	pink
** Empty cells denote lack of data													

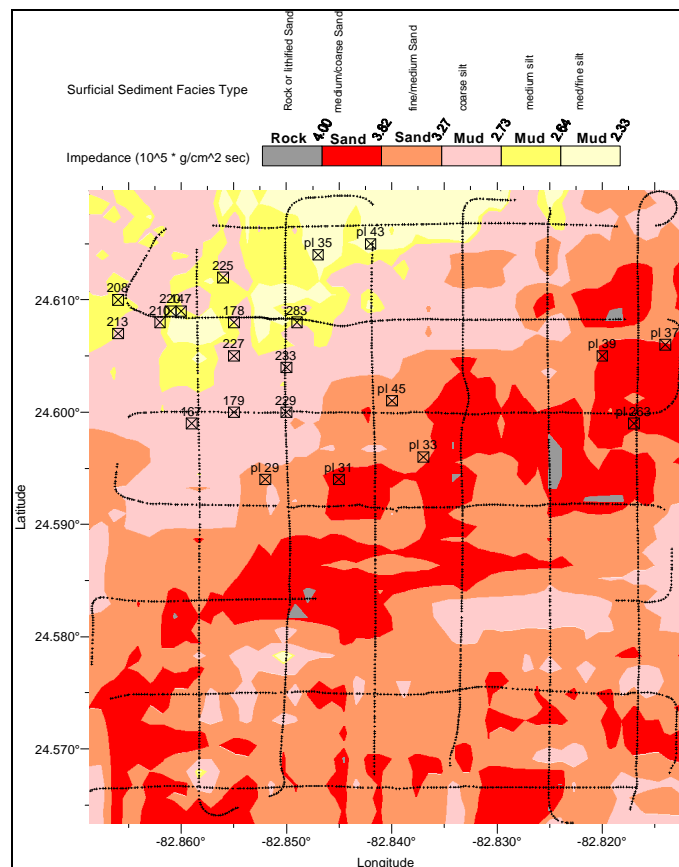


Figure 10. Acoustically predicted surficial sediment facies contour map with sample locations indicated. Contours are based on ASCS predicted acoustic impedance. Facies terminology in key at top was associated with pertinent impedance values and is based on correlation of core calculated impedance, mean grain size and sand to mud ratio after Wentworth (1922) and Folk (1974/1980).

Accomplishments: The following list summarizes the major accomplishment of this project.

- Upgraded ASCS hardware and software for use as a robust research tool, including a major change from paper chart to digital graphic color display.
- Developed capability to use the ASCS electronics and data acquisition hardware and software with a variety of transducers.
- Increased dynamic range from 6-bit/30 dB display to 16-bit/90 dB display.
- Increased digital sampling rate to 125-kHz (at 16 bits).
- Provided real-time site assessments in the form of color-coded trackline navigation maps for selection of ground truth and instrumentation locations in Eckernfoerder, Key West (Marquesas/Halfmoon Shoal/Dry Tortugas), and Eel River.
- Developed capability to construct 2-D and pseudo 3-D site maps of acoustic impedance and various sediment properties.
- Developed capability to delineate vertical and lateral distribution of gassy sediments in glacial marine and semi-enclosed/estuarine environments.
- Modeled acoustic response of sediment and developed techniques for calibration of acoustic system.
- Demonstrated the plausibility that acoustic returns from bubbly sediments show a frequency variation with depth, that these effects occur over a wide range of frequencies and that the effects are roughly separated by the bubble resonance frequency which is inversely proportional to bubble size.
- Identified two regions of high-energy acoustic return in Eckernfoerder sediments that have substantially different frequency content.
- Assisted in the development of a linearized least squares inversion technique to more accurately predict the impedance profile of the sediment column (Wood and Lindwall 1996) using ASCS data from Dry Tortugas study site.
- Determined that the ASCS delineated seafloor structure very accurately, matching sediment structure determined by detailed core analysis.
- Provided high-resolution data for several investigators working on the CBBL Program.
- Demonstrated that ASCS predictions of sediment shear strength and density could be used in real time to predict mine impact burial.
- Developed carbonate sediment facies map of Dry Tortugas study area based on acoustic impedance.
- Constructed 3-D physical fence model depicting geomorphology of Dry Tortugas study area using a hull mounted “transducer of opportunity” operating at 4-kHz.

References:

- Anderson, A. L., Abegg, F., Hawkins, J. A., Duncan, and Lyons, A. P. (in press). Bubble populations and acoustic interaction with the gassy seafloor of Eckernfoerder Bay. Continental Shelf Research.
- Anderson, A. L., Lyons, A. P., Abegg, F., Duncan, M. E., Hawkins, J. A., and Weitz, R. A. 1995. Modeling acoustic volume scattering by a bubbly mud seafloor with examples from Eckernfoerder Bay. In: Wever, T. F. (ed.) Proceedings of the Workshop on Modeling Methane-Rich Sediments of Eckernfoerder Bay, FWG Report 22, Kiel, p. 243-247.
- Folk, R.L., 1974/1980. Petrology of Sedimentary Rocks. Hemphills, Austin, Tex., 170 p.
- Hamilton, E.L., 1980. Geoacoustic Modeling of the Seafloor. J. Acoust. Soc. Amer. 68:1313-1340.
- Hamilton, E.L. and Bachman, R.T., 1982. Sound velocity and related properties of marine sediments. J. Acoust. Soc. Am. 72(6):1891-1904.
- Hawkins, J. A., Lambert, D.N., Walter, D. J., Lyons, A. P., Duncan, M. E., and Anderson, A. L., 1995. Spectral characterization of bubbly sediments using high frequency, short duration acoustic pulses. In: Wever, T. F. (ed.) Proceedings of the Workshop on Modeling Methane-Rich Sediments of Eckernfoerder Bay, FWG Report 22, Kiel, p.65-69.
- Lambert, D.N., 1988. An evaluation of the Honeywell ELAC computerized sediment classification system. NORDA Report 169, Stennis Space Center, MS, Naval Research Laboratory, 53 pp.
- Lambert, D.N. and Fiedler, H., 1991. Methods of High Resolution Remote Seafloor Characterization. Proceedings of the Marine Technology Society, MTS '91, New Orleans, LA, p. 1004-1011.
- Lambert, D.N., Cranford, J.C. and Walter, D.J., 1993. Development of a High Resolution Acoustic Seafloor Classification Survey System, Proceedings of the Institute of Acoustics, Bath, U.K. 15(2): 149-156.
- Lyons, A. P., Duncan, M. E., Anderson, A. L., and Hawkins, J. A., 1996. Predictions of the acoustic scattering response of free-methane bubbles in muddy sediments. J. Acoust. Soc. Am., 95, p. 163-172.
- Slowey, N. C., Bryant, W. R., and Lambert, D. N., 1996. Geoacoustic properties of Eckernfoerder Bay sediments and the origin of reflectors of high-resolution seismic profiles. Proceedings of the Modeling Methane-Rich Sediments of Eckernfoerder Bay Workshop, Kiel, Germany, FWG Report 22, p. 73-74.

- Slowey, N. C., Bryant, W. R., and Lambert, D. N., 1996. Comparison of high-resolution seismic profiles and the geoacoustic properties of Eckernfoerder Bay sediments, *GeoMarine Letters*, v. 16, p. 240-248.
- Stephens, K.P., Fleischer, P., Lavoie, D.L. and Brunner, C., 1997. Scale dependent physical and geoacoustic property variability of recent, shallow-water carbonate sediments from the Dry Tortugas Keys, Florida. *Geo-Marine Letters* 17:299-305.
- Walter, D. J. and D. N. Lambert 1995, A 3-D Acoustic View of the Seafloor in the CBBL Test Area Near Garden Key in Dry Tortugas, FL. Abstract and Poster SEPM Congress on Sedimentary Geology. St. Petersburg, FL, 13-16 August. 1995, 1:126.
- Walter, D. J., Lambert, D. .N., and Young, D.C. 1996 - Mine Burial Prediction Using Acoustic Techniques in a Shallow-Water Carbonate Environment. The Technical Cooperation Program (TTCP) Poster & Proceedings of the Symposium on Shallow Water Undersea Warfare/From Staging to Sustainment, Halifax, Nova Scotia, p 395-409.
- Walter, D. J., Lambert, D.N., Young, D.C. and Stephens, K.P., 1997a. Mapping sediment acoustic impedance using remote sensing acoustic techniques in a shallow-water carbonate environment. *Geo-Marine Letters* 17(4):260-267.
- Walter, D. J., Lavoie, D.M. and Stephens, K.P., 1997b. Southeast Channel Dry Tortugas, FL – geologic setting and comparison of acoustically predicted sediment properties with laboratory-measured core data. *J. Mississippi Acad. Sci.* 42:63.
- Wentworth, C.K., 1922. A scale of grade and class terms for clastic sediments. *J. Geol.*, 30:377-392.
- Wever, T.F., Fiedler, H.M., Fechner, G., Abegg, F. and Stender, I.H., 1997. Side-scan and acoustic subbottom characterization of the seafloor near the Dry Tortugas, Florida. *Geo-Marine Letters* 17(4):246-252.
- Wood, W. T. and D. A. Lindwall, 1996. Full Waveform Inversion of Field Sonar Returns for a Visco-Acoustic Earth; A Comparison of Linearized and Fully Nonlinear Methods. *IEEE Journal of Oceanic Engineering*, Vol. 21, No. 4.

Publications:

Peer Reviewed;

- Anderson, A. L., Abegg, F., Hawkins, J. A., Duncan, and Lyons, A. P. (in press). Bubble populations and acoustic interaction with the gassy seafloor of Eckernfoerder Bay. Continental Shelf Research.
- Davis, K. S., Bryant, W. R., Slowey, N. C., and Lambert, D. N., 1994. Reflections on the Geoacoustic and Geotechnical Characteristics of Eckernfoerder Bay Sediments. In: Wever, T.F. (ed.) Proceedings of Modeling Methane-Rich Sediments of Eckernfoerder Bay, Eckernfoerder, Germany, 26-30 June, 1995, FWG Report 22, p. 39-43.
- Lambert, D.N. and Anderson, A., 1996. Delineation of Methane-Rich Sediment Structures Using High Frequency Acoustics. Journal article in preparation to be submitted to Marine Geology.
- Lyons, A. P., Duncan, M. E., Anderson, A. L., and Hawkins, J. A., 1996. Predictions of the acoustic scattering response of free-methane bubbles in muddy sediments. J. Acoust. Soc. Am., 95, p. 163-172.
- Slowey, N. C., Bryant, W. R., and Lambert, D. N., 1996. Comparison of high-resolution seismic profiles and the geoacoustic properties of Eckernfoerder Bay sediments, GeoMarine Letters, v. 16, p. 240-248.
- Walter, D. J., Lambert, D.N., Young, D.C. and Stephens, K.P., 1997. Mapping sediment acoustic impedance using remote sensing acoustic techniques in a shallow-water carbonate environment. Geo-Marine Letters 17(4):260-267.

Patents and Invention Disclosures;

- Lambert, D.N., F.S. Carnaggio, and D.C. Young, 1994. Sediment Classification System, Patent Application and Award, Navy Case No. 75,520. Patent Issued September 24, 1996, Patent Number 5,559,754.
- Cranford, J.C., D.N. Lambert, and M. Crowe, 1994. Data Acquisition System and Method, Patent Application and Award, Navy Case No. 75,521. Patent pending.

Symposia proceedings;

- Anderson, A. L., Lyons, A. P., Abegg, F., Duncan, M. E., Hawkins, J. A., and Weitz, R. A. 1995. Modeling acoustic volume scattering by a bubbly mud seafloor with examples from Eckernfoerder Bay. In: Wever, T. F. (ed.) Proceedings of the Workshop on Modeling Methane-Rich Sediments of Eckernfoerder Bay, FWG Report 22, Kiel, p. 243-247.
- Davis, K. S., Bryant, W. R., Slowey, N. C., and Lambert, D. N., 1994. Reflections on the Geoacoustic and Geotechnical Characteristics of Eckernfoerder Bay Sediments. In: Wever, T. F. (ed.) Proceedings of the Gassy Mud Workshop, FWG Report 14, Kiel, p. 47-53.
- Hawkins, J. A., Lambert, D.N., Walter, D. J., Lyons, A. P., Duncan, M. E., and Anderson, A. L., 1995. Spectral characterization of bubbly sediments using high frequency, short duration acoustic pulses. In: Wever, T. F. (ed.) Proceedings of the Workshop on Modeling Methane-Rich Sediments of Eckernfoerder Bay, FWG Report 22, Kiel, p.65-69.
- Lambert, D.N., J.C. Cranford and D.J. Walter, 1993 Development of a High Resolution Acoustic Seafloor Classification Survey System, Proceeding of the Institute of Acoustics, Acoustic Classification and Mapping of the Seabed International Conference, Univ. of Bath, UK, p. 149-156.
- Lambert, D.N., D.J. Walter, D.C. Young, and M.D. Richardson, 1994. High Resolution Acoustic Seafloor Classification System for Mine Countermeasures Operations. Proc. of the International Conference on Underwater Acoustics, Univ. South Wales, Australia, p. 67-79. *Invited Paper*
- Lambert, D.N., M.D. Richardson, D.J. Walter, and J.A. Hawkins, 1995. Delineation of Shallow, Subbottom Gas Concentrations Using a Narrow Beam, High Frequency Acoustic System. In: Wever, T.F. (ed.) Proceedings of Modeling Methane-Rich Sediments of Eckernfoerder Bay, Eckernfoerder, Germany, 26-30 June, 1995, FWG Report 22, p. 39-43.
- Priebe, R., Chotiros, N. P., Walter, D. J., and Lambert, D. N., 1995a. Gas Bubble Recognition by Wavelet Analysis of Echo-Sounder Signals. In: Wever, T. F. (ed.) Proceedings of the Workshop on Modeling Methane-Rich Sediments of Eckernfoerder Bay, FWG Report 22, Kiel, p. 104-113.
- Priebe, R., N.P. Chotiros, D.J. Walter, and D.N. Lambert, 1995b. Sea Floor Classification by Wavelet Decomposition of Fathometer Echoes. Oceans '95 MTS/IEEE, San Diego, CA, 9-12 October 1995.
- Richardson, M.D., D.N. Lambert, K.B. Briggs, and D.J. Walter, 1994. Comparison of Acoustic Seafloor Classification (ASCS) and In-Situ Data Collected from a Variety of Sediment Types in Kiel Bay, Germany. Proc. of the International Conference on Underwater Acoustics, Univ. South Wales, Australia, p. 89-90. *Invited Paper*

Slowey, N.C., W.R. Bryant, and D.N. Lambert, 1994. The Geoacoustic and Geotechnical Properties of Eckernfoerder Bay. Proc. of the Third International Conference on Gas in Marine Sediments, Texel, Netherlands, Sept. 25-28.

Slowey, N. C., Bryant, W. R., and Lambert, D. N., 1995. Geoacoustic properties of Eckernfoerder Bay sediments and the origin of reflectors of high-resolution seismic profiles. Proceedings of the Modeling Methane-Rich Sediments of Eckernfoerder Bay Workshop, Kiel, Germany, FWG Report 22, p. 73-74.

Tooma, S., D. Lott, D.N. Lambert, J. Preston, G. Hearld, K. Murphy, R. Hurst, 1996. TTCP Sediment Classification Sea Trials off Key West, FL., 1-16 February 1995. Proceedings of The Technical Cooperative Program (TTCP), Subgroup G-Wide Symposium on Shallow Water UnderSea Warfare, Oct. 21-25, 1996, Halifax, Nova Scotia, Canada.

Walter, D.J., D.N. Lambert, and D.C. Young, 1996. Mine Burial Prediction Using Acoustic Techniques in a Shallow-Water Carbonate Environment. Proceedings of The Technical Cooperative Program (TTCP), Subgroup G-Wide Symposium on Shallow Water UnderSea Warfare, Oct. 21-25, 1996, Halifax, Nova Scotia, Canada.

Reports;

Lambert, D.N., S.R. Griffin, and K.C. Benjamin, 1998. The Constant Beam Width Transducer (CBT): Its Applicability for Sub-Bottom Profiling and Acoustic Sediment Classification, submitted as a NRL Formal Report.

Tooma, S., D. Lott, D.N. Lambert, J. Preston, G. Hearld, K. Murphy, R. Hurst, 1996. TTCP Sediment Classification Sea Trials off Key West, FL., 1-16 February 1995. NRL Memorandum Report, NRL/MR/7430--96-8020.

Lambert, D.N., et al., 1998. Six NFESC reports as a result of the Validation Project. These reports are scheduled to be published during the summer of 1998.

Published Abstracts;

Walter, D.J., D.N. Lambert, D.C. Young, and H. Herrmann, 1996. Acoustic Prediction of Seafloor Properties in a Shallow Water Carbonate Environment with Comparisons to Penetrometer and Core Data. Proc. Oceans '96 MTS/IEEE Conference, Ft Lauderdale, FL.

Walter, D.J. and D.N. Lambert, 1995. A 3-D Acoustic View of the Sea Floor Near Garden Key, Dry Tortugas, Florida. The 1st SEPM Congress on Sedimentary Geology "Linked Earth Systems", Aug. 13-16, 1995, St. Petersburg Beach, FL. Poster

- Bryant, W.B., N.C. Slowey, and D.N. Lambert, 1995. Geotechnical and Geoacoustic Stratigraphy of the Dry Tortugas. The 1st SEPM Congress on Sedimentary Geology "Linked Earth Systems", Aug. 13-16, 1995, St. Petersburg Beach, FL. Poster
- Priebe, R., N.P. Chotiros, D.J. Walter, and D.N. Lambert, 1995. Sea Floor Classification by Wavelet Decomposition of Fathometer Echoes. Abstract and presentation at OCEANS '95 MTS/IEEE, San Diego, CA, 9-12 October 1995.
- J.A. Hawkins, D.N. Lambert, D.J. Walter, and J.C. Cranford, 1994. Observations of Acoustic Reflectivity Associated with Near Surface (Shallow Subbottom) Gassy Sediments in Kiel and Eckernfoerder Bays. AGU Ocean Sciences 94 Conference, EOS, v. 75, n. 3, p.159.
- Lambert, D.N., J.C. Cranford, D.J. Walter, J.A. Hawkins, and R. Redell, 1994. Geological Characterization of Kiel and Eckernfoerder Bay Sediments Using a High Resolution Remote Acoustic Seafloor Classification System, AGU Ocean Sciences 94 Conference, EOS, v. 75, n. 3, p. 160.
- Bryant, W.B., N.S. Slowey, and D.N. Lambert, 1994. The Geoacoustic and Geotechnical Properties of Eckernfoerder Bay, AGU Ocean Sciences 94 Conference, EOS, v. 75, n. 3, p. 220.
- Lambert, D.N., D.J. Walter, W.R. Bryant, N.C. Slowey, and J.C. Cranford, 1994. Acoustic Prediction of Sediment Impedance, Acoustical Society of America Fall Meeting, Austin, TX, JASA, Vol. 96, No. 5, p. 3222. *Invited Paper*
- Lambert, D.N., D.J. Walter, D.C. Young, and J.C. Cranford, 1994. Use of a High Resolution, High Frequency, Normal Incident Seafloor Classification System for Mine Countermeasures Operations, Proceedings of the TTCP Subgroup G Symposium, Heriot-Watt University, Edinburgh, Scotland, July 11-15, 1994.
- Hawkins, J.A., W. Wood, D.N. Lambert, and D.J. Walter, 1994. The Characterization of Near-Surface Sediments with High Frequency Acoustic Pulses. Acoustical Society of America Fall Meeting, Austin, TX, JASA, Vol. 96, No. 5, p. 3223.
- Lambert, D.N., P.J. Valent, & R.Y. Lai, 1993. Use of High Frequency, Normal Incidence Acoustics for Sediment Classification and Shear Strength Estimation, Am. Soc. Civil Engineers, Civil Eng. in the Oceans Conference, College Station, TX.

Theses, dissertations:

- Walter, D. J., 1998. Sediment Facies Determination Using Acoustic Techniques in a Shallow-Water Carbonate Environment, Dry Tortugas, Florida. Master of Science Thesis, Geological Oceanography, Florida Institute of Technology, 118 pp.

Measurement of Shear Modulus In-situ and in the Laboratory

Dawn Lavoie

Naval Research Laboratory

Yoko Furukawa

University of Southern Mississippi

Original Objectives:

The long-term objectives of this effort over a three year period were to (1) investigate gradients of shear modulus in the field on the cm scale using a duomorph probe, (2) examine shear modulus as a function of direction (x and z planes) in the field, and in the laboratory in an instrumented triaxial cell where the shear wave velocity can be measured with the three principle stresses carefully controlled, and (3) relate in-situ shear modulus with geotechnical properties (particularly undrained shear strength) and other primitive sediment parameters (being investigated by other investigators under this SRP) as well as microfabric.

Because these properties are very much controlled by geochemical processes and physical reworking, especially in carbonate sediments such as the Key West environment, the initial objectives were modified to (4) develop and test a method to correlate the extent of submarine diagenesis to mineralogy, porewater chemistry and microfabric in carbonate sediments, and (5) correlate the extent of reworking to mineralogy, isotope data, porewater chemistry and microfabric. (See

companion year-end report submitted by Y. Furukawa and funded under this effort).

Approach:

In this multiyear project, the first year efforts were devoted to adapting the duomorph to an in-situ probe for use in the field. Once the instrumentation was satisfactorily tested, we participated in numerous field efforts including the Baltic Sea experiments and off Panama City, Florida in FY93; Eckernforde Bay and the Florida Keys in FY94; the Key West Campaign in FY95 where in situ measurements were made using DIAS and the shallow water ISSAMS systems. Significant laboratory analyses were completed after each field experiment to characterize the bottom sediments. In addition to physical and geotechnical properties analyses, geochemical analyses including mineralogy, pore water analyses and microfabric analyses were selectively performed in order to examine the effects of post-depositional alteration and predict properties of interest e.g., permeability. For more detail, see previous years' final reports.

Results:

Results of funded activities are summarized below. Actual data and significance of the results can be found in the published documentation.

In situ measurements	a) Probe development	-Lavoie et al., 1996
	b) environmental descriptions	- Lavoie & Richardson, 1996
Variability of geoacoustic &	Key West	- Briggs et al., 1996 - Walter et al., 1997

geotechnical properties		- Stephens et al., 1997 - Lavoie et al., 1997 - Mallinson et al., 199
Physical properties & microstructural relationships	Eckernfoerde Bay	- Bennett et al., 1996 - Lavoie et al., 1996
Diagenetic studies	Key West	- Furukawa & Lavoie, 1997 - Furukawa et al., 1997
Cruise/workshop reports	Key West	- Tooma et al., 1995 - Lavoie & Richardson, 1997

Accomplishments:

Instrumentation development

DIAS, the Duomorph In Situ Acquisition System, is an alternate technology requiring a single duomorph probe for measuring shear modulus in situ. The duomorph probe is a bending plate device which is vibrated and the resulting deflections measured using strain gauges. The ratio between the unconstrained bending of the duomorph in air and the constrained bending in sediment is a function of the sediment dynamic modulus. The theory underlying the DIAS system, the design of the system, the data reduction methods, and results from the initial deployment of the prototype system in Eckernfoerde Bay can be found in Lavoie et al., 1996.

Eckernförde Bay

Eckernförde Bay was chosen by the Coastal Benthic Boundary Layer Special Research Program as an ideal field laboratory to study biogeochemical processes. One of the distinct features of Eckernförde Bay sediments is the lack of dewatering, recognized in microfabric images as high porosity. We hypothesized that the physical and geoacoustic properties are controlled by microfabric and, therefore, the lack of dewatering can be explained by a model that includes microfabric properties. Two basic processes were considered: (1) the effect of the high organic content and migratory gas horizon (or gasturbation process), and (2) the impact of a high sedimentation rate on Eckernförde Bay sediments which are a mix of pellet and channel structure and less permeable, muddy storm cap layers. We concluded that gasturbation probably accounts for 10-12% of the observed apparent underconsolidation and the remainder results from the high sedimentation rate which prevents the sediment from dewatering normally.

Key West

Spatial variability of shallow-water carbonate sediments near the Dry Tortugas is scale dependent. Grain size is most variable, followed by porosity, wet bulk density, compressional wave velocity and grain density both vertically and laterally. Stephens empirically modeled variability by linear regression analysis to predict variability based on scale.

The same shallow marine sediments near the Dry Tortugas undergo extensive biogeochemical diagenesis upon deposition resulting in a post-depositional fabric comprised of micritic aggregates of clay-sized particles, a matrix of peloidal mud, and intraparticle cementation. Although Furukawa found the pore water to be supersaturated with carbonate, no significant precipitation was noted in the upper meter of sediment. Current thermodynamic and kinetic models are unable to

explain this lack of precipitation or cementation which is common in other carbonate environments. The dominant processes are the mechanical and chemical breakdown of carbonate particles, effectively converting sand and silt-size carbonate particles to clay-sized matrix material.

Publications

Lavoie, Dawn, Yoko Furukawa, Dennis Lavoie, Patti Jo Burkett. Apparent Underconsolidation in Eckernförde Bay Sediments: a Model based on Physical, Geochemical and Microfabric Properties. *Journal of Continental Research* (in review)

Furukawa, Y., D. Lavoie, S. Bentley, P. Van Cappellen and A. Shiller. Early Diagenesis Driven by Biologically-enhanced Oxygen Transport in North Key Harbor, Dry Tortugas National Park, Florida., *Marine Geology* (submitted)

Peer-reviewed

Lavoie, D.L., M.D. Richardson, and C. Holmes. 1997. Benthic Boundary Layer Processes in the Lower Florida Keys. *Geo-Marine Letters Special Issue*, v17, no. 4, pp. 432-436.

Furukawa, Y., D. Lavoie and K. Stephens. 1997. The effect of geochemical diagenesis on sediment structure and mineralogy in shallow marine carbonate sediments near the Dry Tortugas, Florida, *Geo-Marine Letters Special Issue*, v17, no. 4, pp. 283-290.

Stephens, K., D. Lavoie, and P. Fleischer. 1997. Physical and Geoacoustic Property Variability of Recent, Shallow-water Carbonate Sediments from the Dry

Tortugas Keys, Florida. Geo-Marine Letters Special Issue, v17, no. 4, pp. 299-305.

Mallinson, D., S. Locker, M. Hafen, D. Naar, A. Hine, D. Lavoie, S. Schock.

1997. A high resolution geological and geophysical investigation of the Dry Tortugas carbonate depositional environment. Geo-Marine Letters Special Issue, v17, no. 4, pp. 237-245.

Lavoie, Dawn, Sean Griffin, and Francis Grosz. 1996. DIAS - A Novel Technique for Measuring In-Situ Shear Modulus. Geomarine Letters, v. 16, p 254-260

Lavoie, Dennis, Dawn Lavoie, Alan Pittenger and Richard Bennett. 1996. Bulk Sediment Properties Interpreted in Light of Qualitative and Quantitative Microfabric Analysis. Geomarine Letters, v. 16:226-231

Bennett, R.H., M.H. Hulbert, M.M. Meyer, D.M. Lavoie, K.B. Briggs, D.L. Lavoie, R.J. Baerwald and W.A. Chiou. 1996. Fundamental Response of Pore-water Pressure to Microfabric and Permeability Characteristics: Eckernforde Bay. Geomarine Letters, v. 16:182-188

Symposium Proceedings

Lavoie, Dawn and M.D. Richardson, 1997. Proceedings of the Coastal Benthic Boundary Layer Key West Workshop, NRL Memorandum Report, NRL/MR/7431--97-8044, 222p.

Lavoie, Dawn, K. Stephens, Y. Furukawa, and D.M. Lavoie, 1997. Geotechnical Characteristics of Dry Tortugas and Marquesas Sediments, In: Lavoie and Richardson, eds. Proceedings of the Coastal Benthic Boundary Layer Key West Workshop, NRL/MR/7431--97-8044, pp. 170-180.

- Furukawa, Yoko and D. Lavoie, 1997. A Geochemical Investigation of Early Diagenetic Effects on Sedimentary Structures. In: Lavoie and Richardson, eds. Proceedings of the Coastal Benthic Boundary Layer Key West Workshop, NRL/MR/7431--97-8044, pp. 113-120
- Richardson, M.D., D.L. Lavoie, K.B. Briggs and K. Stephens, 1997. Geoacoustic and Physical Properties of Carbonate Sediments of the Lower Florida Keys. In: Lavoie and Richardson, eds. Proceedings of the Coastal Benthic Boundary Layer Key West Workshop, NRL/MR/7431--97-8044, pp. 121-134.
- Stephens, Kevin, P. Fleischer, D. Lavoie and C. Brunner, 1997. Scale-Dependence of Sediment Property Variability of the Dry Tortugas, Florida. In: Lavoie and Richardson, eds. Proceedings of the Coastal Benthic Boundary Layer Key West Workshop, NRL/MR/7431--97-8044, pp.149-157.
- Walter, D., D. Lavoie, D.N. Lambert, D.C. Young and K. Stephens, 1997. Southeast Channel, Dry Tortugas Geologic Setting and Comparison of Acoustically-predicted Sediment Properties with Laboratory-measured Core Data. In: Lavoie and Richardson, eds. Proceedings of the Coastal Benthic Boundary Layer Key West Workshop, NRL/MR/7431--97-8044, pp. 42-67.
- Lavoie, Dawn and M.D. Richardson. 1996. In Situ Geoacoustic Systems and Measurements in a Variety of Carbonate and Siliciclastic Environments. IEEE, pp 1467-1473.

Reports

- Fleischer, Peter and Dawn Lavoie, 1996. Ground-Truth Area Selection and Characterization for Mine Countermeasures Tactical Environmental Data System: Final Report, NRL/MR/7431--96--8000.
- Briggs, K.B., D.L. Lavoie, K. Stephens, M.S. Richardson and Y. Furukawa, 1996.

Physical and geoacoustic properties of sediments collected for the Key West Campaign, February 1995: A data report. Naval Research Laboratory, Stennis Space Center, MS. NRL/MR/--7431--96--8002.

Tooma, S., M. Richardson, Dawn Lavoie, D. Lott, K. Williams, and I. Stender, 1995. Collaborative Efforts within the Key West Campaign Sea Test, NRL/MR/7430--95-7694.

Theses/dissertations

Stephens, Kevin 1997. Scale-dependent Physical and Geoacoustic Property Variability of Shallow-water Carbonate Sediments from the Dry Tortugas, Florida. Thesis, University of Southern Mississippi, Hattiesburg, MS.

CBBL Final Report, March 1998

Title:

Quantification of Gas Bubble and Dissolved Gas Sources and Concentrations in Organic-Rich, Muddy Sediments

Principal Investigators:

Christopher S. Martens and Daniel B. Albert

Organization:

Dept. of Marine Sciences, University of North Carolina, Chapel Hill

Abstract:

High-frequency acoustic backscattering experiments in gassy sediments were a major component of the overall CBBL project. These required knowledge of sediment characteristics for interpretation of results. In particular, for Eckernförde Bay, the principal study site of the project, data on the methane gas distribution in the sediments was needed. The study objectives were all related to biogeochemistry of gas production, distribution and consumption via microbial processes in these organic-rich sediments. Analyses were designed to develop a detailed understanding of one site (NRL) where most of the other experiments took place, an acoustic window site and a pockmark were also sampled for comparative purposes. These comparisons led to the idea that upward percolation of fresh groundwater from underlying glacial till is a primary factor controlling variations in methane concentration profiles in Eckernförde Bay sediments and whether or not a gas phase is present. Exploration of this idea required the development and use of coupled advection/diffusion/reaction models for methane and sulfate to quantitatively assess the net result of competing effects. This model is the most complete and realistic one of its type that we are aware of. In development of this model it was also used for other gassy coastal sediment locations in North Carolina.

We also participated in one CBBL cruise studying the sandy shelf sediments off Panama City, Florida. It had been suggested that, on the basis of acoustic evidence, there could be gas in these sediments in the form of very tiny bubbles. No geochemical evidence of gas was found, nor was there any sign of fresh groundwater outflow, which would provide the most likely scenario for gas presence due to the shallow onset of methanogenesis. These results will not be discussed further.

We participated in a CBBL cruise to the Dry Tortugas to do a snapshot characterization of sulfate reduction rates and sulfide oxidation rates at the mooring site of the R/V Planet where most acoustic experimentation was done. The logic behind these measurements was that an active sulfur cycle could be involved in any carbonate dissolution/cementation taking place at the site that might be detected acoustically. The coarse carbonate sands of this site turned out to have barely detectable rates of these processes and no signs of cementation and will not be discussed further.

Specific Objectives:

- (1) Measurement of *in situ* depth vs. concentration profiles of biogenic methane and carbon dioxide and establish the depth of methane saturation in the sediments at representative sites within Eckernförde Bay.
- (2) Determine the stable isotopic composition (carbon and hydrogen) of methane and carbon dioxide in the sediment porewaters as tracers of the production and oxidation of methane.
- (3) Determine rates of sulfate reduction, methane production and oxidation in these sediments via radiotracer techniques.
- (4) Determine sedimentation rates using ^{210}Pb , ^{137}Cs and ^{14}C .
- (5) Develop models to describe the depth distribution biogenic methane and the processes which control it.

- (6) Look for evidence of gas bubbles in the sandy shelf sediments off Panama City, Florida where some of the other acoustic experiments took place.
- (7) Measure rates of sulfate reduction and sulfide oxidation in the high-energy, carbonate sand site occupied by the CBBL group in the Dry Tortugas. This was undertaken to determine if there was any carbonate dissolution/cementation chemistry occurring that was driven by sulfide oxidation.

Approach:

We wanted to obtain enough information on the biogeochemistry of the main study site in Eckernförde Bay to be able to construct a realistic advection/diffusion/reaction model describing the distribution of methane within the sediments. Because methane is both produced and consumed within anaerobic sediments this required the use of coupled models for methane and sulfate. Methane production is confined to sediment below the depth at which sulfate has all been consumed by sulfate reducing bacteria. Additionally, when methane diffuses upward into such sulfate reducing sediments, it is consumed. In spite of the lack of mechanistic understanding of the latter process, it is a well known phenomenon and can be mimicked in a model.

The model developed is based on physical and biogeochemical principles. It does not rely on statistical relationships. As such, it requires input of many different parameters, including sedimentation rate, input of metabolizable organic carbon, a rate constant for organic matter consumption and the advection rate of porewater. The latter is important in this system because Eckernförde Bay sediments lie atop very porous glacial till and there is flow of freshwater from these tills through the overlying sediment at rates that vary with location. We sought to obtain enough of this information to allow us to model methane concentration profiles in the bay.

Study Sites

The main study site for the CBBL Program in Eckernförde Bay, designated the NRL (Naval Research Lab) Site was in an area chosen, on the basis of acoustic surveys, to be representative of much of the Bay with respect to the depth of the gassy sediment horizon. In addition to gas-charged sediments the Bay contains other sedimentary features of particular interest. There are a significant number of "pockmarks" which, in general, are circular to elongate depressions in the seabed that vary widely in size, but appear to be formed and/or maintained by the discharge of gas or fluids. Those in Eckernförde Bay are tens to hundreds of meters in horizontal scale with ~1 m vertical relief. Within some pockmarks gas bubbles may be present very near the sediment-water interface compared to the rest of the bay.

In addition to the pockmarks there are areas of "acoustic windows" in which gassy layers are not present and acoustic signals penetrate to the underlying till layer. Unlike the pockmarks, acoustic windows are not necessarily distinguished by topographic variation. The pockmarks themselves often have a narrow rim of acoustic window surrounding them which then grades back into the more typical bay sediment with bubbles occurring at ~0.5-1 m depth.

Methane Sampling and Analysis

Sediments were collected using diver and gravity cores taken with five inch diameter thin-walled PVC pipe predrilled with 3 cm diameter holes covered with wide electrical tape. The tape allowed rapid sampling which minimized degassing artifacts. Methane concentrations were determined on 60 ml whole-sediment samples taken as horizontal subcores through the side walls of the core liners using cut-off syringes after removal of the tape with a razor knife. Each subcore was immediately expelled into a 250 ml jar and closed with a foam-sealed metal cap. After sealing samples were safe from additional degassing artifacts. The samples were allowed to warm to ambient temperature and degas, aided by shaking. The jars were then pierced using a septum-sealed jar piercer (Alltech). To establish accurate headspace volume at atmospheric pressure the headspace pressure built up due to degassing was allowed to displace the plunger of a 60 ml all-glass syringe. This plunger is displaceable with almost no resistance when lubricated with water. The displacement was measured in both the barrel-

pointing-up and barrel-pointing-down positions (to compensate for the weight of the glass plunger) and the average reading was added to the headspace volume in the jars for determination of methane content of the samples.

Methane concentrations were determined on the ship with a gas chromatograph equipped with a flame ionization detector. Hydrogen from a H_2 generator was used as both carrier and FID fuel gas. Air for the FID was supplied by a diaphragm pump. Headspace samples were withdrawn from the sample jars using displacement with water. Samples were injected into the GC by passing them through a small tube filled with Drierite and filling a fixed volume sample loop. The separation was performed on a 2 m HayeSep A column in series with a 2 m molseive 5A column at 60°C. Calibration gasses were premixed methane in air at several concentrations (Scott Specialty Gases). Concentrations were calculated assuming all methane was dissolved in the porewater (no gas phase).

Sulfate and Chloride Sampling and Analysis

Porewater samples for sulfate and chloride analysis were obtained using 'sippers'. These were 10 ml syringes attached to cylindrical porous polypropylene filters inserted horizontally through the holes in the wall of the core liner. Syringe plungers were then cocked open until a reasonable volume of sample was collected. Samples were then put through 0.4 micron syringe filters. Samples used for sulfate analysis (1 ml) were acidified with 10 μ l of 10% HCl and bubbled to drive off any dissolved sulfide as H_2S . Sulfate and chloride analyses were done by ion chromatography.

Methane and Carbon Dioxide Isotopic Signatures

Subsamples of the jar headspace from the methane analysis described above were used to displace water from immersed, inverted 10 ml serum vials. The vials were capped underwater, crimp sealed and refrigerated. Methane in these vials was purified and combusted using vacuum line technology. Briefly, the methane was flushed from the vial using flowing He. Water vapor and CO_2 were removed from the gas stream in cold traps and the methane was burned by passing over copper oxide wire/Pt catalyst packing in a furnace at 800°C. Combustion water, containing the H from the original methane and CO_2 were trapped in separate cryogenic traps and the He removed by vacuum. The open ends of the traps were sealed by melting the glass or quartz with a torch. The quartz water trap contained a zinc catalyst which, converted the water to H_2 and zinc oxide when heated in a 500°C oven. The gaseous contents of the traps were analyzed for stable carbon and hydrogen isotopic signatures using a Finnegan-MAT 252 isotope ratio mass spectrometer.

Anaerobic Methane Oxidation Rates

Small (3 ml) horizontal glass tube cores were filled with intact sediment by subsampling through taped holes in the walls of larger tube cores and stoppered with rubber stoppers containing a silicone plugged hole. These were injected with ^{14}C labeled CH_4 that had been cryogenically purified and was free of CO_2 and higher hydrocarbon contamination. Following incubation at the *in situ* temperature the samples were expelled into 60 ml serum vials with 1 ml 1M NaOH, crimp sealed and mixed to terminate activity. Radioactive methane was removed by stripping the sample with a stream of air which then passed over a bed of copper oxide wire at 800°C to burn the methane to CO_2 . The $^{14}CO_2$ was then trapped by bubbling the gas stream through 10 ml of a solution of β -phenethylamine, methanol and Scintiverse II (Fisher Scientific). Activity was quantified by direct scintillation counting of this mixture. After the methane was stripped the sample was acidified and $^{14}CO_2$ that had been produced by microbial methane oxidation was stripped from the vials, trapped and counted. Ambient methane concentrations in the syringe cores during incubation were determined by headspace analysis of the serum vials after the incubation was terminated, but prior to stripping for radioactivity counting. Rates were calculated based on the amount of label converted to CO_2 , the incubation time and the ambient methane concentrations.

Results:

Sulfate and Methane Concentration Profiles

Based on acoustic surveys revealing the depth of the gassy sediment horizon, the NRL site is probably representative of much of the bay below the 20 m isobath. Sulfate concentrations in the porewater dropped rapidly from 19 mM in the bottom water to an apparent lower threshold of 20 μ M by 30 cm depth (Fig. 1). Methane concentrations were low within the sulfate-containing sediments, but rose rapidly below 30 cm depth to reach saturation at 6.4 mM by 80 cm depth (Fig. 2). Below this there was a gradual decrease in concentrations to the deepest sample (~425 cm). Within the sulfate containing sediments above 40 cm depth, the methane profile was concave-upward, indicative of methane oxidation within these sediments

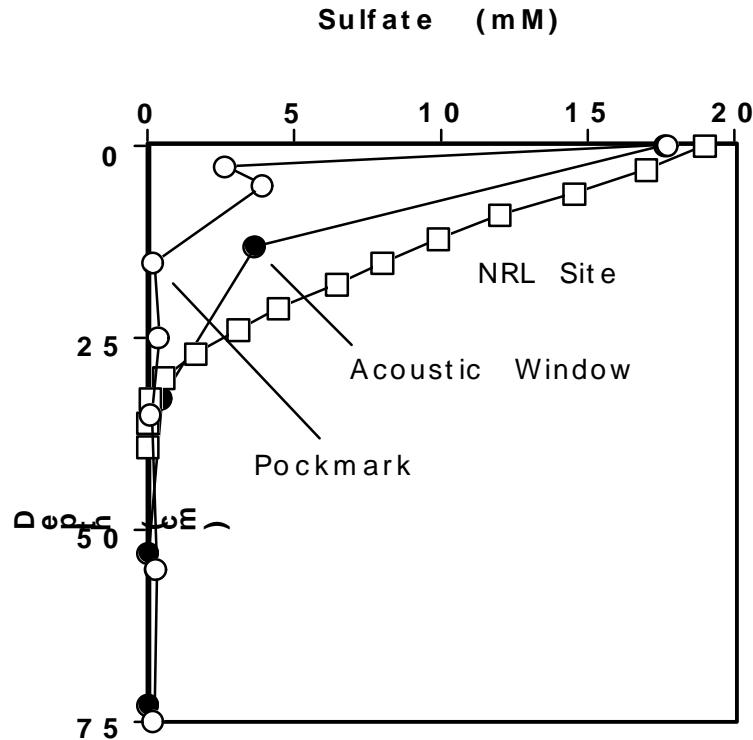


Figure 1. Porewater sulfate concentrations at three sites in Eckernförde Bay .

At the acoustic window site the sulfate concentration profile was not well defined because of the coarse sampling interval, but was steeper between the interface and 13 cm depth than the NRL site profile (Fig. 1). Methane concentrations were higher in the upper sediments than at the NRL site (Fig. 2) and the upward concavity in the profile was less pronounced, indicating that oxidation of the methane diffusing up from below was less complete. Below the depth of sulfate depletion (probably at about 20 cm depth) methane concentrations rose abruptly, but did not reach saturation. The maximum concentration was 5.2 mM at 142 cm depth. Below this, methane concentrations dropped and were concave-downward, reaching 0.91 mM at the bottom of the 422 cm core.

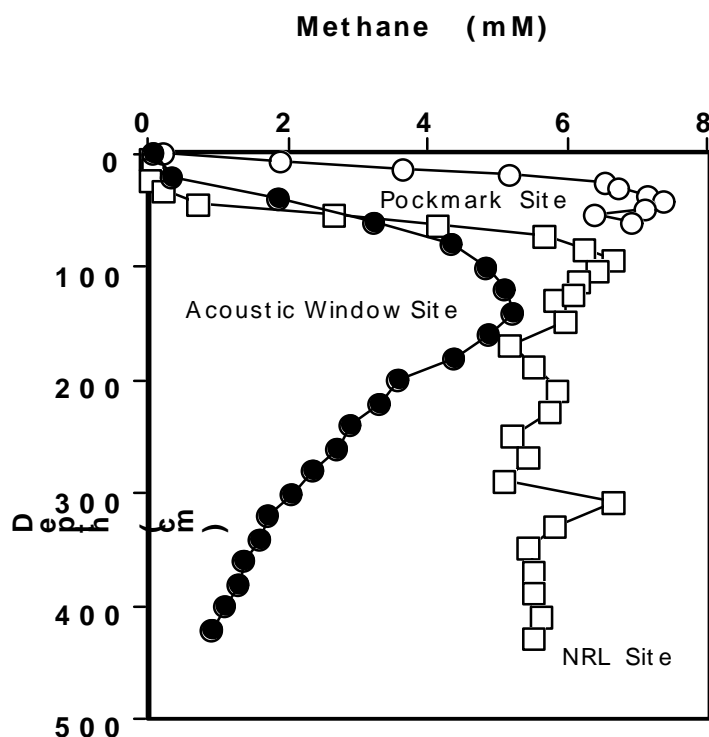


Figure 2. Porewater methane concentration profiles for three Eckernförde Bay sites.

In the pockmark core the sulfate concentration profile was also poorly defined by the relatively coarse sampling interval (Fig. 1). This was compounded by the fact that rapid expansion of the methane gas phase in the sediments caused self-extrusion of the cores before the porewater sampling was complete, making assignment of appropriate depths problematic. Sulfate dropped from 19 mM in the bottom water to 0.14 mM by 7.5 cm depth in one core and to 0.2 mM by 15 cm in the other core. The methane sampling was much faster than porewater sampling and less subject to the above problem. Methane concentrations rose rapidly beginning just below the sediment-water interface and reached saturation by about 25 cm depth (Fig. 2).

Chloride Concentration Profiles

All three sites showed a freshening of the porewater with depth (Fig. 3). This was least pronounced at the NRL site where chloride concentration decreased by ~50 mM over 425 cm. At the acoustic window Cl decreased ~350 mM over 422 cm with pronounced downward concavity, indicative of upward advection of fresher water from below. At the pockmark site this downward concavity was even more pronounced and the concentration decreased ~350 mM over only 155 cm.

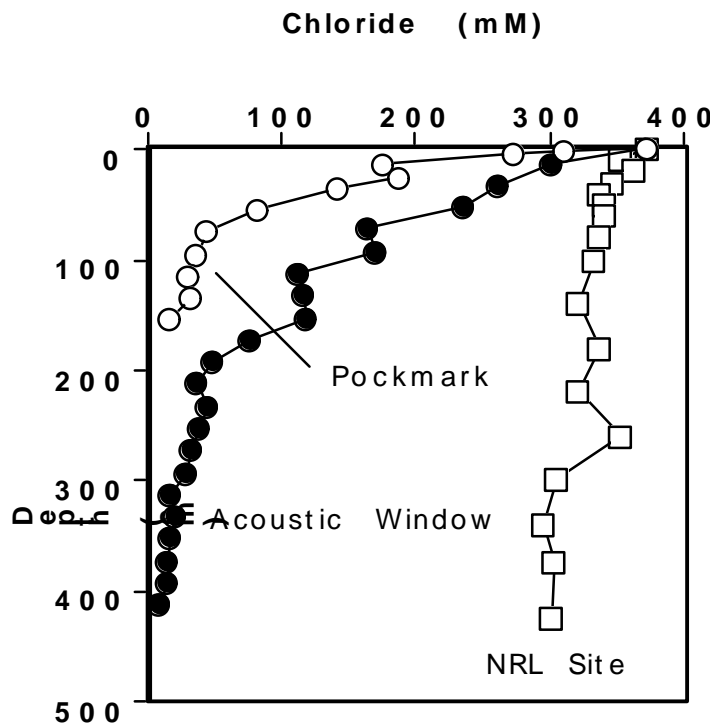


Figure 3. Porewater chloride concentrations at three Eckernförde Bay sites showing freshening with depth.

Methane Oxidation Rates and Methane and CO₂ Stable Isotopes

Methane oxidation rates in the sediments of the NRL site showed a sharp maximum of about $45 \mu\text{M}\cdot\text{d}^{-1}$ at 22 cm depth near the base of the sulfate reduction zone (Fig. 4B). This oxidation resulted in nearly quantitative removal of the methane diffusing upward at this site. Methane stable carbon and hydrogen isotopic compositions changed dramatically above the depth of the methane oxidation maximum (Fig. 4A). The carbon isotopic signature ($\delta^{13}\text{C}$) in the residual methane became heavier (enriched in the ^{13}C isotope) by about 10‰ and the hydrogen isotopic signature (δD) in methane became enriched in the heavier deuterium by about 140‰ as a result of isotopic fractionation during oxidation.

Below the depth of oxidation $\delta^{13}\text{C}$ of the methane tracked the signature of the ΣCO_2 pool from which much of the methane is derived, but was shifted about 70‰ lighter than the CO_2 due to fractionation during methane formation. The δD signature of methane below the oxidation maximum reflects fractionation from the signature of water the hydrogen is derived from and is thus very constant.

These measurements were repeated in 1994 and included methane isotopic signatures from the acoustic window and a pockmark sites (data not shown). As in 1993, the surficial sulfate-containing sediments at the NRL site had low methane concentrations, but below the depth of sulfate depletion they increased rapidly. The $\delta^{13}\text{C}$ and δD of the methane followed the same pattern as the 1993 data. $\delta^{13}\text{C}$ showed an even more dramatic oxidation signal within the sulfate reducing sediments shifting from -70‰ to as heavy as -47‰ . This was true of the δD data as well, showing an isotopic shift of 175‰ after oxidation.

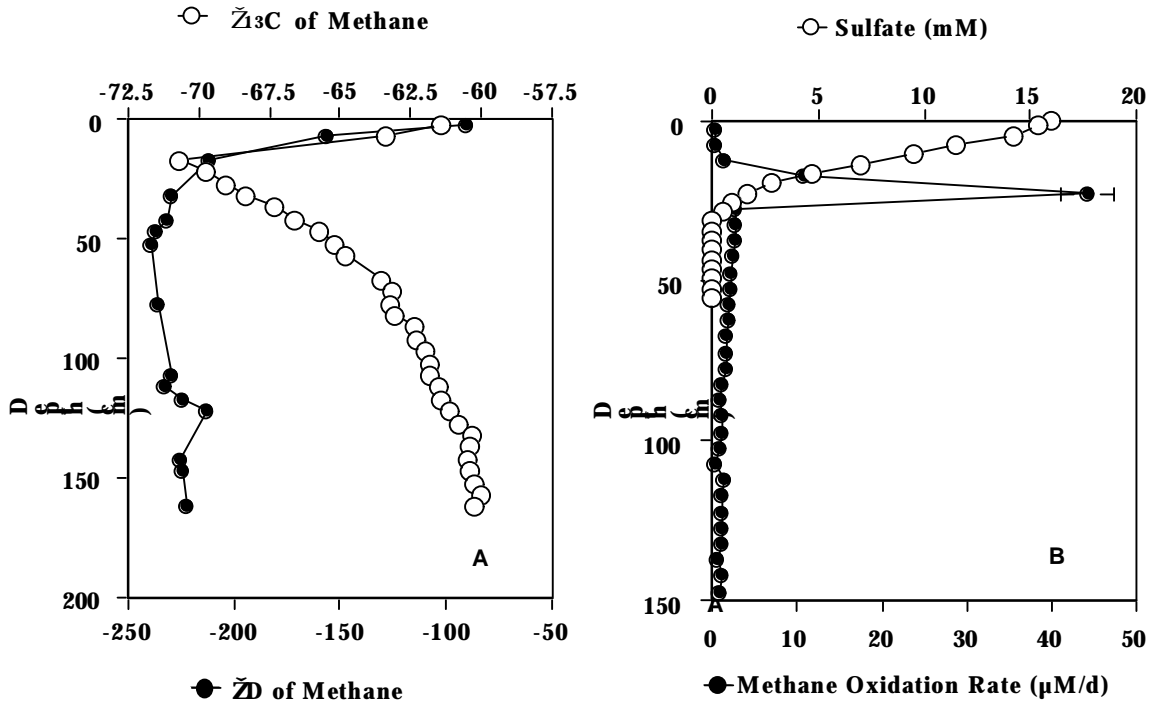


Figure 4 A. Stable Carbon and hydrogen isotopic composition of the methane at the NRL site in 1993. B. Rates of anaerobic methane oxidation and the sulfate concentration profile measured at the NRL site in 1993.

Groundwater Advection Rate Modeling

To model methane and sulfate concentrations at sites with any significant rates of porewater advection requires that these rates be known. The observed variations in salinity versus depth were used to determine the rates of vertical advection in the sediment porewaters at the three sites.

To determine the flow rate through the sediments at each site an advection/diffusion model based on a simple diagenetic equation was used. At steady-state, chloride concentrations (C) in sediment porewaters can be described by an equation that balances molecular diffusion of chloride into the sediment with advection out of the sediment:

$$\frac{d}{dz} \left(\phi D_s \frac{dC}{dz} \right) = -\phi \vartheta \frac{dC}{dz}$$

where:

- ϕ is the sediment porosity (vol. water/vol. wet sediment)
- D_s is the whole-sediment diffusion coefficient for Cl^- at the *in situ* temperature and salinity
- ϑ is the sum of the downward advection due to sedimentation and upward advection associated with groundwater flow in the porewaters.

Theoretical Cl^- profiles were calculated by varying the vertical advective velocity in the porewater to obtain the best fit to the data for each of the three sites. The best fit profiles are shown in Fig. 5. The very slight curvature in the profile at the NRL site is fit by an advection velocity of about 1 cm y^{-1} . The much more pronounced curvature at the acoustic window and the pockmark sites yield velocities of 3.5 and 10 cm y^{-1} , respectively.

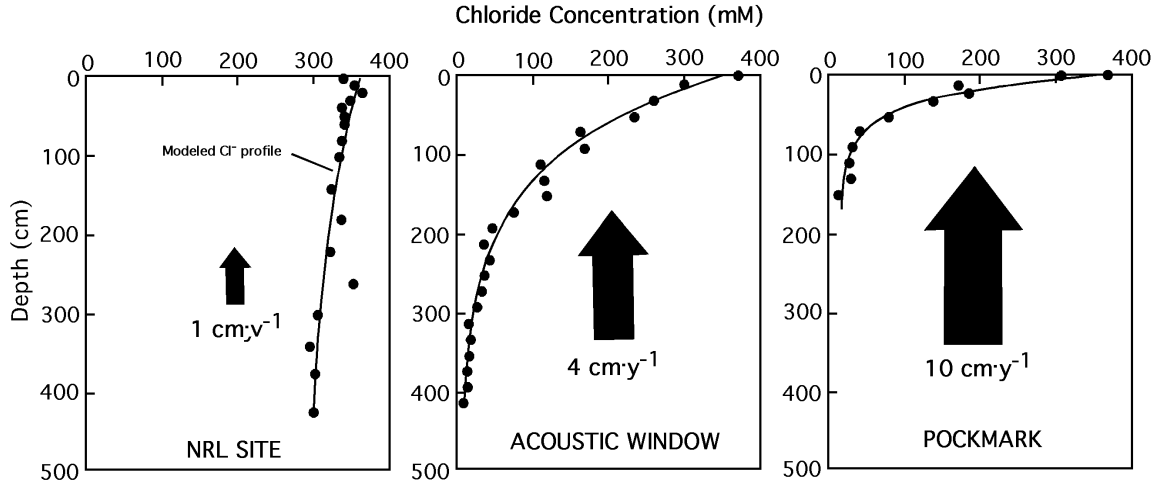


Figure 5. Modeled Cl^- profiles showing the best-fit chloride profiles (solid lines) in relation to the data (dots) for the specified vertical advection rates.

Methane and Sulfate Advection/Diffusion/Reaction Modeling

Diagenetic models consist of mass-conserving equations that simulate the balance of advective, diffusive and reactive processes which take place in sediments following deposition of reactive species (e.g. metabolizable organic carbon compounds). For sulfate (S) the steady-state diagenetic equation has a diffusive transport term for its input from the overlying seawater, an advective transport term to cover burial and the effect of the upward percolation of sulfate-free groundwater, and a reaction term to describe consumption of sulfate through bacterial sulfate reduction:

$$D_S \frac{d^2 S}{dz^2} - \vartheta \frac{dS}{dz} - f_1 \left[\frac{1}{2} k_G G + k_M M_{diss} \right] = 0$$

where D_S is the sediment diffusion coefficient for sulfate at the *in situ* temperature and salinity, ϑ is the sum of downward advection due to sedimentation and upward advection associated with groundwater flow (υ), k_M is the rate constant for methane oxidation and M_{diss} is the dissolved methane concentration. Sulfate reduction is represented by the term in brackets. Note that it has components for the oxidation of organic matter and dissolved methane. The coefficient (f_1) for the rate term is the error function (integrated Gaussian) which is used to simulate a smooth transition from sulfate reduction to methane production when the sulfate concentration falls below a threshold value (see Martens et al., in press, and Albert et. al., in press, for details).

The steady-state diagenetic equation for methane concentrations (M) is similar, but contains both a production term proportional to the overall carbon degradation rate at any depth and a consumption term to represent anaerobic methane oxidation via sulfate reduction:

$$D_M \frac{d^2 M_{diss}}{dz^2} - \vartheta \frac{dM_{diss}}{dz} + f_2 f_3 \left[\frac{1}{2} k_G G \right] - f_1 \left[k_M M_{diss} \right] + f_3 \left[k_D M_{gas} \right] = 0$$

where D_M is the sediment diffusion coefficient for methane at *in situ* temperature and salinity, k_D is the rate constant for dissolution of methane gas, and M_{gas} is the concentration of gaseous methane. Methane is the product of organic matter decomposition only when sulfate concentrations are below a threshold value and dissolved methane is only produced when methane concentrations are below *in situ* solubility. This is controlled by the coefficients f_2 and f_3 on the first rate term which are error function toggles allowing the smooth transitions required for numerical stability of the model. The coefficient f_1 is the error function toggle that allows methane oxidation (via sulfate reduction) only when sulfate concentrations are above the threshold.

Gaseous methane concentration is described by a steady-state diagenetic equation balancing sedimentation and methane production with gas bubble ebullition and dissolution.

$$-\omega \frac{dM_{gas}}{dz} + f_2 f_4 \left[\frac{1}{2} k_G G \right] - \left[k_B M_{gas} \right] - f_3 \left[k_D M_{gas} \right] = 0$$

where k_B is a rate constant for ebullition (i.e. ebullition is assumed to be a first order with respect to gas volume) and f_3 is the error function toggle that "turns on" gaseous methane production when dissolved methane concentrations exceed saturation (M^*).

The model results fit the dissolved sulfate and methane data for the NRL site very well (Fig. 6 A). The sulfate data are fit almost exactly. The upward concavity in the methane data due to methane oxidation and the peak concentrations between 1 and 1.5 m are also reproduced very closely. Methane gas bubbles are predicted between 80 and 120 cm by this run, with a peak gas concentration of only 0.3% by volume at 120 cm.

The concentration profiles derived from the model can be used to calculate depth distributions of sulfate reduction rate, methane production rate and methane oxidation rate. These model-generated profiles are shown in Fig. 6B. The sulfate reduction rate begins to drop below the interface on an exponential decay curve, but has a significant subsurface maximum due to the oxidation of methane that is both diffusing upward from below and being advected upward by groundwater flow (here at 1 cm y^{-1}). Under these conditions the integrated methane oxidation makes up 37% of the total sulfate reduction. See Albert et. al.(in press) for results of modeling at the other Eckernförde Bay sites and Martens et al. (in press) for application of the model to coastal sites in North Carolina.

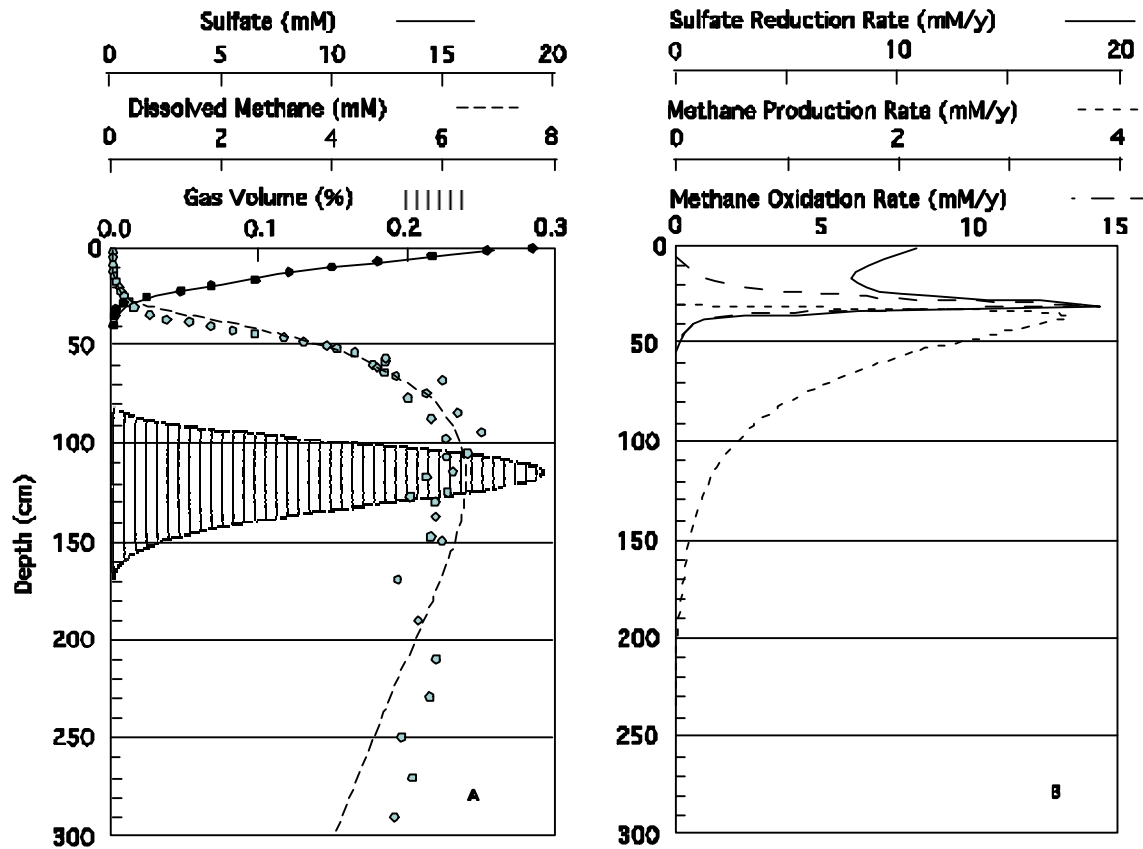


Figure 6. A. Model generated profiles of dissolved sulfate (solid line), methane (dashed line) and methane gas (shaded) at the NRL site. B. Model generated profiles of sulfate reduction, methane oxidation and methane

production rates. Note the subsurface maximum in sulfate reduction due to its assumed coupling to methane oxidation.

Accomplishments:

Understanding Methane Distributions within Eckernförde Bay

Methane gas distribution in the sediments of Eckernförde Bay has received considerable attention in the form of acoustic surveys and geochemical work, but given the variety of sites extant in the Bay we do not have a complete understanding of these distributions. This variety within a small area makes Eckernförde a unique place to study methane biogeochemistry because there are probably sites representative of many coastal locations as well as pockmark sites that are usually found in deeper waters. Our work there has contributed significantly to the understanding of these distributions in that it has become apparent that much of this variation over short spatial scales in Eckernförde is probably attributable to variations in groundwater flow that moves upward from the porous underlying till through the fine-grained recent sediments. Fresh groundwater flows and their effects on methane in the Bay sediments have been studied previously, but at sites near Mittlegrund where these flows are high enough to be termed seeps or springs. In these instances methane is actively stripped so concentrations are low and there is no gas phase present. Most of Eckernförde Bay is more similar to the sites we studied in that the groundwater movement is a very slow percolation through the porespace of the sediment and flows are on a scale of centimeters per year. Such seemingly trivial flows have significant geochemical consequences, however. Variations in these flows lead to the abrupt transitions from acoustically turbid, gassy sediments to acoustic windows and back again. They are also responsible, at least in part, for the formation and maintenance of gassy pockmarks in the Bay. While it is easy to logically deduce some of the geochemical consequences of these flows, the effects cannot be fully understood or quantified without modeling of the type we have done as part of this project.

Coupled Model of Sulfate and Methane Distributions in Sediments

The sediments of Eckernförde Bay yield an example of a case in which modeling is not an esoteric exercise, but is required to understand the complex interplay of competing factors which lead to the observed methane distributions. In the absence of groundwater advection, steady-state sedimentation leads to a situation in which, below the depth of sulfate depletion, methane concentrations rise until saturation is reached and further methane production below this depth builds up the gaseous methane inventory. Only in the presence of a vertical advective flow of water with lower concentrations from below will concentrations fall with depth as they do in these sediments. But this stripping of methane from below, which decreases the methane inventory, is in competition with another effect of these flows. The most metabolically active sediments are those near the sediment-water interface where the fresh organic materials arrive. This is generally sulfate reducing sediment since sulfate reducers are thermodynamically favored over methanogens which have to wait until the leftover metabolizable material is buried below the depth of sulfate depletion. Any process which leads to more rapid burial of this material or more rapid (shallower) sulfate depletion will enhance methane production and thus concentrations. Advection of porewater at a few cm/year is significant in countering the diffusive resupply of sulfate from overlying seawater and thus allowing the more rapid onset of methanogenesis. Modeling is required to quantify the net effect these competing processes have on the methane concentration profiles.

Modeling of methane and sulfate concentration profiles must be done with a coupling between the two since they are interdependent. Methane is only produced in significant quantity in the absence of sulfate and methane is consumed within sulfate reducing sediments, leading directly or indirectly to enhanced sulfate reduction. The coupling of these processes in the model developed in this study deals with this coupling in the most complete and realistic way so far developed.

In trying to achieve Eckernförde Bay-like methane and sulfate profiles with this model we encountered many unexpected results, which initially seemed counterintuitive, but on further investigation made sense. For instance, simulation of the addition of unrealistically large inputs of reactive organic carbon to the sediments may have little effect on the methane production/inventory if the reaction rate constant for its consumption is too high. It is all consumed at too shallow depths in the sediment via sulfate reduction and never gets into the methanogenic zone. Conversely, unrealistically low inputs of reactive carbon in these simulations can lead to the prediction of

huge methane inventories in the sediment if the reaction rate constant for the carbon is low. This allows burial to depths of methanogenesis with relatively little loss within the sulfate reducing zone. In the end the inputs and reaction rate constant utilized to achieve the fits shown above are plausible, but unproved. How to realistically parameterize overall organic carbon metabolism vs. time (over time scales that span one to hundreds of years), in spite of its apparent simplicity, remains the most important and interesting information we lack for realistic modeling of these processes in these, or any other, sediments.

Publications:**Peer-reviewed papers in press:**

Martens, C. S., D. B. Albert and M. J. Alperin. (in press) Biogeochemical processes controlling methane in gassy coastal sediments 1. A model coupling organic matter flux to gas production, oxidation and transport. *Cont. Shelf Res.*

Albert, D. B., C. S. Martens and M. J. Alperin. (in press) Biogeochemical processes controlling methane in gassy coastal sediments 2. Groundwater flow control of acoustic turbidity in Eckernförde Bay sediments. *Cont. Shelf Res.*

Peer-review-bound papers in prep:

Albert, D. B., C. S. Martens and M. J. Alperin. Stable carbon and hydrogen isotope tracing of methane production and consumption in Eckernförde Bay sediments.

Symposium proceedings:

Martens, C. S. and M. J. Alperin. 1997. Rates of biogeochemical processes in estuarine lagoonal sediments. *in* 5th International Symposium on Model Estuaries. May 25-29, 1997. p. 38. Rimouski, Quebec, Canada.

Martens, C. S. and D. B. Albert. 1995. Biogeochemical processes controlling concentrations and transport of biogenic methane in organic-rich coastal sediments. *in* Proceedings of the workshop modeling methane-rich sediments of Eckernförde Bay, Eckernförde, 26-30 June, 1995: pp. 10-17. Forschungsanstalt der Bundeswehr für Wasserschall und Geophysik, Kiel, Germany. Report 22.

Albert, D. B. and C. S. Martens. 1995. Stable isotope tracing of methane production and consumption in the gassy sediments of Eckernförde Bay, Germany. *in* Proceedings of the workshop modeling methane-rich sediments of Eckernförde Bay, Eckernförde, 26-30 June, 1995: pp. 114-120. Forschungsanstalt der Bundeswehr für Wasserschall und Geophysik, Kiel, Germany. Report 22.

Martens, C. S. and D. B. Albert. 1994. Biogeochemical processes controlling gas production, consumption and transport in organic-rich marine sediments. *in* Proceedings of the gassy mud workshop held at the FWG, Kiel, 11-12 July, 1994: pp. 101-107. Forschungsanstalt der Bundeswehr für Wasserschall und Geophysik, Kiel, Germany. Report 14.

Published abstracts:

Martens, C. S. and B. J. Ream. 1997. Distinguishing reactive organic matter in coastal sediments. Geological Society of America Annual Meeting. Abstract 13412.

Alperin, M. J., C. S. Martens and D. B. Albert. 1997. Biogeochemical processes controlling methane in gassy coastal sediments: A model for predicting the distribution of gaseous methane. Program and Abstracts, p. 82. American Society of Limnology and Oceanography Aquatic Sciences Meeting. Feb. 1997, Santa Fe, NM.

Albert, D. B., C. S. Martens and M. J. Alperin. 1997. Groundwater flow control over methane-induced acoustic turbidity in Eckernförde Bay Sediments. Program and Abstracts, p. 80. American Society of Limnology and Oceanography Aquatic Sciences Meeting. Feb. 1997, Santa Fe, NM.

Shank, G. C., W. Ussler and C. S. Martens. 1993. Physical factors controlling methane ebullition in Cape Lookout Bight, North Carolina. American Geophysical Union 1993 Spring Meeting, Baltimore, MD. Abstracts Book p. 179.

Physical and Biological Mechanisms Influencing the Development and Evolution of Sedimentary Structure

Charles A. Nittrouer and Glenn R. Lopez

Marine Sciences Research Center
State University of New York
Stony Brook, NY 11794-5000, USA

Original Objectives:

The general objective was "elucidation of the temporal and spatial development of sedimentary structure." Our research was accomplished in coordination with sediment-transport observations by the group at VIMS (Drs. D. Wright and C. Friedrichs). Our specific objectives are listed below.

- a) benthos measurements - to determine the distribution and abundance of functional groups of benthic macrofauna, and to assess particle bioturbation rates.
- b) particle bioturbation experiments - to provide data necessary to understand the dynamics of particle mixing.
- c) sedimentological observations - to obtain information about sedimentary structures on intermediate scales (mm-cm).
- d) radiochemical analyses - to measure the length and time scales of parameters needed to explain sedimentary structure and its variability.

Approach:

a) Field work - The two general study areas were in Eckernförde Bay and in the Florida Keys. The Central Basin in Eckernförde Bay (Fig. 1) was investigated during late winter and spring of 1993 and early summer of 1994. These periods include the energetic winter conditions, the productive spring bloom, and the onset summer hypoxia. The station locations were coordinated with the rest of the CBBL operations, and especially with the observations by Wright et al. and Jackson et al. Biological, sedimentological and radiochemical investigations examined seabed samples collected in box cores (length about 50 cm) and kasten cores (length 1-3 m).

Most box cores (Ocean Instruments) were collected in the Central Basin close to the tetrapod and acoustic-tower sites, in order to relate seabed properties directly to environmental observations. Additional box cores were collected to provide a regional perspective for the high-density sampling in the Central Basin. These other cores were located across a transect extending up the northern flank of Eckernförde Bay (to ~14 m water depth), and along the Bay axis: near the landward end, on the Mittelgrund sill, and in the north channel of the entrance (an area referred to as Hausgarten). At most stations, three or more replicate box cores were processed soon after collection to evaluate small-scale spatial variability. In addition, longer kasten cores were collected along the Bay axis to provide a historical perspective for sedimentary observations in the box cores.

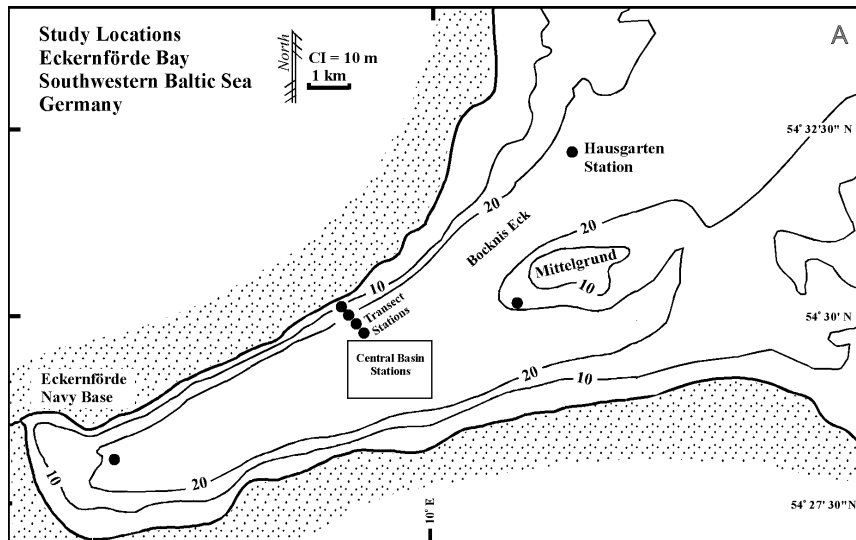


Figure 1. Station locations in Eckernförde Bay. Central Basin stations were the focus of the study. A transect of stations extends up the north flank of the bay. Other stations were distributed through the bay.

Three biological subcores (7-cm diameter) were taken from individual box cores. These subcores were sectioned (0-2, 2-10 cm), sieved (500 μ m), fixed, and stored. In addition, a bioturbation study was conducted for four stations (two from Central Basin; one on Mittelgrund; one at landward end of Bay) at each of which three replicate cores (12 cores total; 15-cm diameter) were obtained and incubated for three weeks in running seawater from Eckernförde Bay. Orange fluorescent particles were added at the beginning of the experiment to two replicate cores (15-cm diameter) from each station; the third replicate core was used as a control. A dozen small subcores (1.5-cm diameter) were obtained sequentially from each replicate over three weeks. They were sectioned and samples were saved.

Additional subsamples were removed from the box cores. Vertical slabs for x-radiography were obtained carefully with Plexiglas trays (2.5 cm x 12.5 cm cross section), fixed with formalin, and x-rayed aboard ship. Subcores (15-cm diameter) were obtained, extruded and sectioned to collect sediment for analysis of particle size and radiochemistry.

Similar studies were undertaken in the Dry Tortugas and Marquesas study areas in the Florida Keys during winter 1995, and subsequently during spring 1997. Most cores were located across a grid in Southeast Channel (Fig. 2), in order to study small-scale lateral variability in the vicinity of the tetrapod. Additional cores were obtained across a wide region encompassing the continental slope to the south, toward Rebecca Shoals to the east, and shallow water regions near Garden Key and East Key, in order to place the seabed of Southeast Channel in a regional perspective. Replicate cores (2-5) were taken at all stations, and DGPS was used for positioning. Four stations in Southeast Channel were sampled both at the beginning and end of the tetrapod deployment period. Cores were processed in a similar fashion to that described above for Eckernförde Bay, except that an in situ bioturbation study failed due to logistical difficulties. The focus of biological studies was near the tetrapod site, and cores were sectioned at 0-2 and 2-30 cm depths below the sediment surfaces.

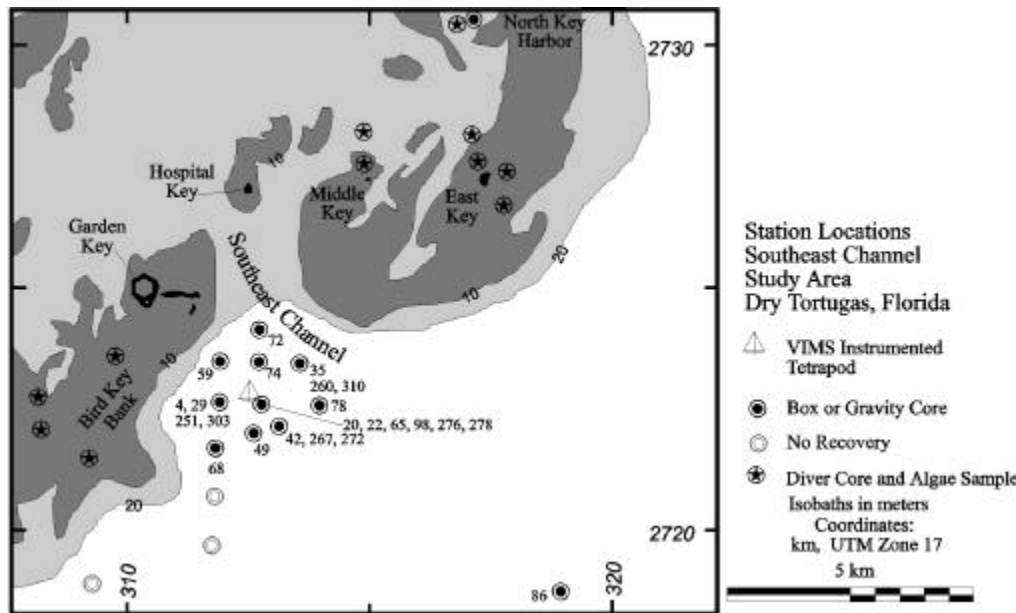


Figure 2.
Station
locations in
Southeast
Channel, Dry
Tortugas.

b) Laboratory work - Animals were collected by sieving biological subcores; fecal pellets also were saved in the Eckernförde study. The organisms were identified from microscopic examinations, assigned to a functional group, and their body sizes measured. The sizes and shapes of fecal pellets were examined from the across-Bay transect in Eckernförde and contrasted with pellets within the guts of animals from the same stations. Sediment saved from the Eckernförde bioturbation experiment was analyzed for fluorescence of tracer particles by drying and then extracting them in acetone. The fluorescence released was measured in a spectrofluorometer (Aminco).

X-ray slabs were carefully dissected to remove microfabric subsamples (2 cm x 4 cm x 0.5 cm), which were impregnated with a resin, thin-sectioned, and examined by petrographic techniques. Subsamples for grain-size analysis were disaggregated (using H₂O₂ and ultrasound) and analyzed with a Sedigraph 5100 (Micromeritics) for fine sediment, and an automated settling column for coarse sediment. ²³⁴Th (half-life 24.1 d) and ¹³⁷Cs (bomb produced) activities in dried sediment samples were measured by γ -spectroscopy (63-keV and 662-keV peaks, respectively) and ²¹⁰Pb activity (half-life 22.3 y) was measured by leaching sediment samples and analyzing by α -spectroscopy. Resulting profiles of radioisotopes were corrected for consolidation and interstitial salts, in order to calculate accumulation rates.

Results:

a) Eckernförde Bay - These results are summarized in Nittrouer et al. (in press). The macrobenthos observed in Eckernförde Bay represent a species-poor community dominated by small, and often juvenile, surface deposit feeders (D'Andrea et al., 1996). The spionid polychaete *Polydora ciliata* and the tellinid bivalve *Abra alba* represent 75-90% of individuals observed. These organisms feed and defecate at the surface, and have little effect on mixing of sediment particles. Bioturbation is largely controlled by capitellid polychaetes (*Heteromastus*

filiformis and *Capitella* sp.) and tubificid oligochaetes, which are head-down deposit feeders with body lengths indicating a mixing depth < 1 cm. The presence of few species, small size, young age, and shallow mixing are characteristics of a “pioneering” community, which indicates a recent or continuing disturbance that inhibits the ability of organisms to inhabit the seabed. The probable cause of the inhibition in this case is the stress caused by seasonal hypoxia affecting the Bay.

Eckernförde Bay demonstrates spatial and temporal variability in abundance and composition of benthic organisms (Fig. 3). The station on Mittelgrund is sandier and shallower than the other stations, and the benthic community is significantly higher in its fraction of suspension feeders and has larger subsurface deposit feeders. The station at the landward end has a benthic community similar to that of the Central Basin. Abundances of benthic organisms in the Central Basin dropped by an order of magnitude between spring (April 1993)

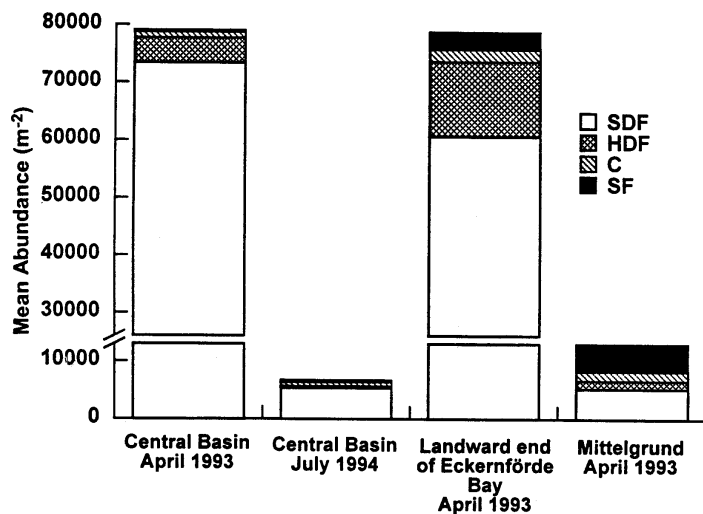


Figure 3. Absolute abundance of functional groupings for benthic organisms observed in Eckernförde Bay. SDF = surface deposit feeders; HDF = head-down deposit feeders; C = carnivores and scavengers; SF = suspension feeders. The Central Basin and landward end had similar community structure and abundance in April 1993. The substantial decrease in April 1993 for the Central Basin reflects the impact of summer hypoxia (from D'Andrea et al., 1996).

and summer (July 1994). The benthic community composition experienced a reduction in the fraction of surface deposit feeders and a proportional increase in carnivores. The effects of hypoxia are greater on deposit feeders and may explain these changes.

The depth into the seabed of biological reworking in the Central Basin was directly investigated by the incubation experiments during spring 1993. This is a period when benthic abundances are high (Fig. 3; i.e., before summer hypoxia) and benthic feeding activity is probably high also (due to the spring bloom). Therefore, biological mixing of particles in the seabed should be at an annual maximum. Labeled particles were carried to a depth of 1 cm, consistent with the character of organisms found in the Central Basin.

Despite the stresses caused by anoxia and despite the shallow depth of reworking, the benthos in Eckernförde Bay very effectively bioturbates the upper 1 cm, and production of robust ovoid pellets dominates the seabed (D'Andrea and Lopez, submitted). Based on the organisms present and the shape and rate of pellets they produce, the dominant organisms responsible for pelletization of the Eckernförde Bay seabed are *Abra alba*, capitellid polychaetes, and tubificid

oligochaetes. As water depth increases, the abundance and size of pellets increase, the abundance and size of producers decrease. At the base of the slope flanking the Central Basin (~ 25 m water depth), pellet concentrations reach a maximum, but the ambient benthic community is unable to produce the numbers and sizes of pellets observed. The size and density of the pellets cause them to be hydraulically equivalent to fine sand and coarse silt. The surplus pellets probably are resuspended in shallow water during storms and transported to deeper water with downwelling currents. In the Central Basin itself (i.e., beyond its flanks), the ambient benthos are sufficient in number and size to produce the pellets observed there. The oceanographic character of Eckernförde Bay leads to a pioneering community of benthic organisms, whose processing of seabed sediment is limited to the upper centimeter (or less) but is sufficient to cause most of the sediment to be packaged in robust fecal pellets (Fig. 4).

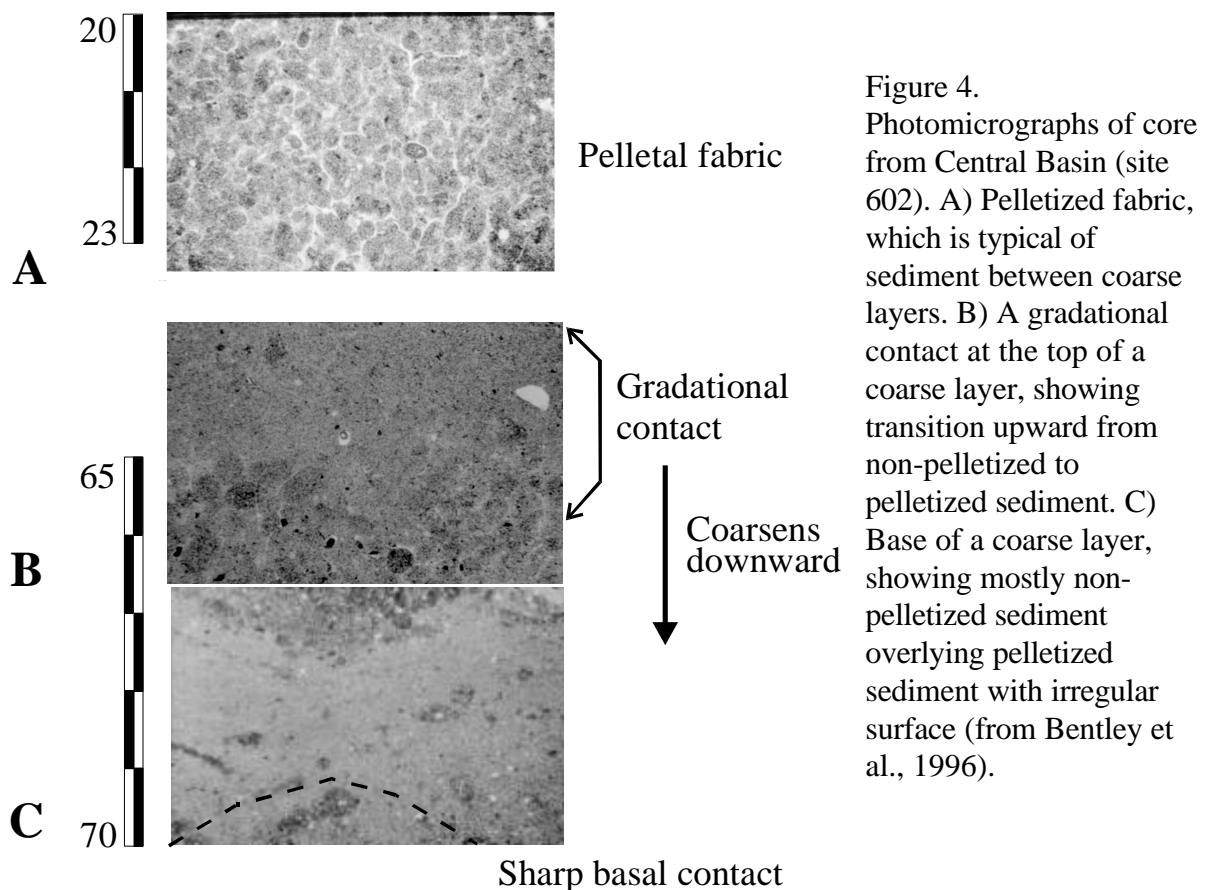


Figure 4.
Photomicrographs of core from Central Basin (site 602). A) Pelletized fabric, which is typical of sediment between coarse layers. B) A gradational contact at the top of a coarse layer, showing transition upward from non-pelletized to pelletized sediment. C) Base of a coarse layer, showing mostly non-pelletized sediment overlying pelletized sediment with irregular surface (from Bentley et al., 1996).

The sedimentary structure observed by x-radiography in Eckernförde Bay reveals a broad division into three characteristic regions (Bentley et al., 1996; Bentley and Nittrouer, submitted). In water depths < 25 m along the flanks of the Bay (e.g., the transect on the north side) and at the landward end, mud and sand are interbedded. Bivalve shells, coarse wood fragments, and mud clasts are found in sandy beds, which range in thickness from 5 cm at shallower locations (< 17 m) to 1-2 cm in deeper depths (~ 22 m). On Mittelgrund (at seaward end), the mud and sand are mottled and bedding is less distinct. The Central Basin and Hausgarten area (both > 25 m water

depth) reveal thick regions (> 1 cm) of homogeneous mud, separated by relatively thin laminations (mean thickness ~ 0.7 cm) of coarser sediment. Below about 30 cm depth in cores, x-radiographs reveal parting that implies the presence of gas.

The sedimentary fabric within the Central Basin was examined in finer detail (mm scale), and the thick homogeneous mud beds observed by x-radiography consisted predominantly of pelletized sediment (Fig. 4). The pellets are ovoid in shape, randomly oriented, 200-500 μm in length, and very resistant to disaggregation (i.e., H_2O_2 and ultrasound treatments were necessary to release component particles). The thin laminations are composed mostly of non-pelletized sediment. Typically the basal contacts of laminations are sharp and overlie a pelletized surface with irregular relief, whereas the upper contacts are gradational with overlying pelletized sediment. Where pellets are observed within laminations, they occur with their long axes parallel to layering.

Careful dissection of x-ray slabs from the Central Basin allowed for grain-size analysis of the pelletized beds and non-pelletized laminations. After disaggregation, pelletized sediment reveals a modal grain size of about 11.5ϕ ($0.41 \mu\text{m}$), which is clay-sized sediment. Additional particles are present in the $3-6 \phi$ range ($125-16 \mu\text{m}$), but these represent less than 10% by mass. The non-pelletized laminations are coarser, with the clay mode shifting to about 9.5ϕ ($1.38 \mu\text{m}$) and the sediment mass in the $3-6 \phi$ range increasing by several percent. Therefore, fine-scale stratigraphy in the Central Basin is characterized by thick beds (cm to > 10 cm) of pelletized clay, separated by thin laminations (< 1 cm) composed of non-pelletized coarser sediment.

Based on the time scale of interest (< 100 y), three radioisotopes were investigated (Bentley et al., 1996; Bentley and Nittrouer, submitted). ^{234}Th provides information about particle mixing in the seabed on scales of months. ^{210}Pb and ^{137}Cs give chronologic control for sediment accumulation over decades. Nine box cores were examined for ^{234}Th variation with depth in the seabed. These cores were collected from the Central Basin during various cruises, and the ^{234}Th profiles reflect characteristics of particle mixing for winter and spring conditions (January through June). Excess ^{234}Th always was restricted to the upper 1.5 cm, and usually to the upper 1.0 cm. A sampling interval of 0.25 cm, which was necessary to resolve mixing, was used only on the final cruise (June/July 1994) and indicated a bioturbation mixing coefficient of $0.7 \pm 0.3 \text{ cm}^2 \text{ y}^{-1}$ for spring conditions.

Profiles of ^{210}Pb were collected throughout Eckernförde Bay, but with an emphasis on the Central Basin. The ^{234}Th profiles indicate that biological mixing was negligible below the upper ~ 1 cm depth in the seabed. Therefore, an assumption of steady ^{210}Pb flux to the seabed allows for calculation of sediment accumulation rates unaffected by bioturbation. These values range from about 0.2 cm y^{-1} for Mittelgrund to 0.4 cm y^{-1} for the station at the landward end of the Bay. In the Central Basin, seven replicate profiles (Fig. 5) were obtained from box and kasten cores and the mean accumulation rate is $0.39 \pm 0.06 \text{ cm y}^{-1}$, which is consistent with observed penetration into the seabed of the bomb-produced isotope ^{137}Cs . ^{210}Pb activities reach supported levels within the upper ~ 50 cm of kasten cores, and box cores can be used for detailed analysis of excess ^{210}Pb profiles. The Hausgarten area reveals a tripartite profile in the upper ~ 30 cm, and the reproducibility of such trends is independently verified by previous studies in this area. The

combination of suppressed biological mixing depths (from ^{234}Th profiles) and substantial accumulation rates (from ^{210}Pb profiles) demonstrates that Eckernförde Bay has the potential to record a high-resolution record of oceanographic processes.

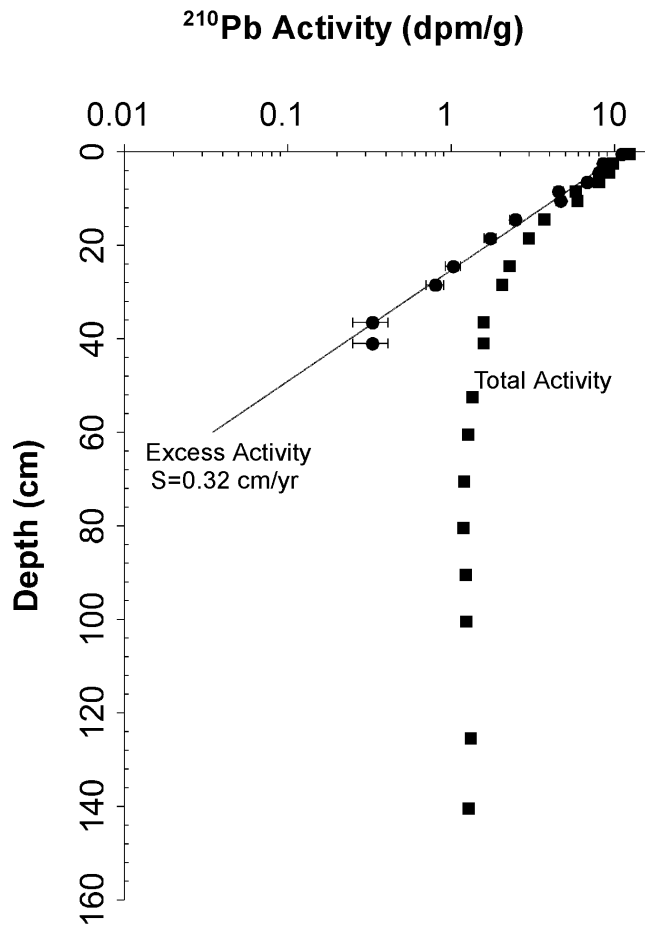


Figure 5. Profiles of ^{210}Pb activity from the Central Basin. Total and excess activity for a kasten core (site 94). At depth in the core, the total activity reaches a constant activity of about 1 dpm g^{-1} . The best fit for excess activity indicates an accumulation rate of 0.32 cm y^{-1} (from Bentley et al., 1996).

b) Florida Keys - Within Southeast Channel of the Dry Tortugas (Fig. 2), the benthic assemblage consisted of 40 species from 9 major taxa dominated by polychaetes (62.8%), bivalves (17.6%), and crustaceans (15.5%)(D'Andrea and Lopez, 1997). The benthic assemblage can essentially be divided into two parts. The first is primarily a surface deposit-feeding community dominated by the spionid polychaete *Prionospio cristata* (3052 m^{-2}) and the oweniid polychaete *Myriochele oculata* (539 m^{-2}), deposit-feeding bivalves, amphipods, and penaeid shrimp. This is a community dominated by surface deposit feeders and capable of mixing the top layer ($\sim 0\text{-}4 \text{ cm}$) of the sediment on short time scales (days to weeks) based on abundances, functional group, and animal size. The second community is a deep-dwelling community dominated by the large ($>6 \text{ cm}$ long) polychaete *Notomastus* (most likely *N. lobatus*), small buried or tube-associated caprellid amphipods, the polychaete *Lumbrineris verrilli*, penaeid shrimp, and a species of *Callianassa*, a deep borrowing thalassinid shrimp.

The mean abundance of the surface community is an order of magnitude greater than the deep community (one-way nested ANOVA, $F = 18.02$, $P < 0.001$) (Fig. 6A). The functional group composition is also distinctly different (one-way nested ANOVA, $F = 12.11$, $P < 0.001$)

between the two communities. The shallow community is dominated by surface deposit feeders and suspension feeders, whereas the deep community is dominated by carnivores, scavengers, deep deposit feeders, and head-down deposit feeders (Fig. 6B). The relatively high number of surface deposit feeders in the deeper community is a consequence of large numbers of tellinid bivalves and *Prionospio cristata*, which were in the 2- to 5-cm depth interval.

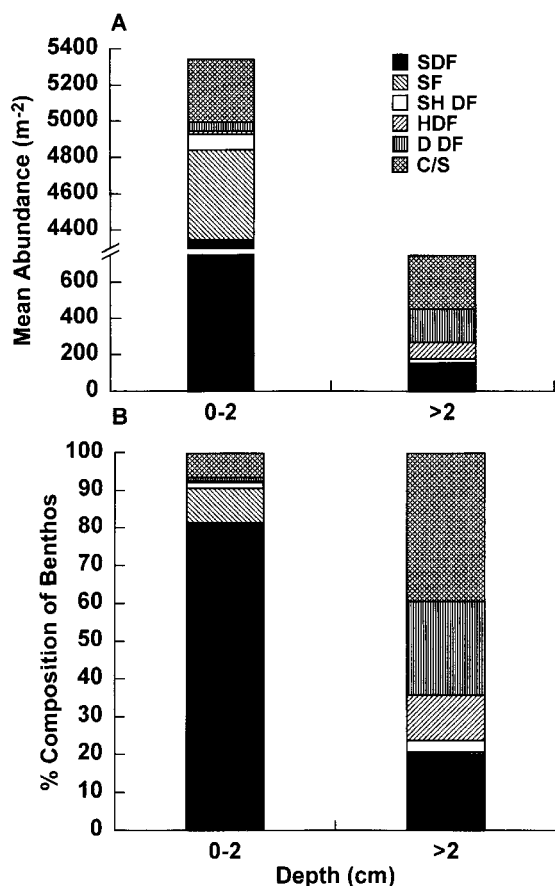


Figure 6. Mean abundances (A) and percent composition (B) of functional groups at Dry Tortugas tetrapod site separated into two depth intervals. SDF = surface deposit feeders; HDF = tubiculous head-down deposit feeders; SH DF = shallow deposit feeders; C/S = carnivores, omnivores, and scavengers; SF = suspension feeders; D DF = deep-burrowing deposit feeders.

X-radiographs of box cores from Southeast Channel reveal a low-density, variably bioturbated, muddy surface layer 1-5 cm thick overlying intensely bioturbated shelly muds (Bentley and Nittrouer, 1997). Some patchy physical stratification is evident in radiographs of the surface layer, but no preserved physical stratification is evident in deeper sediments, where fabric is dominated by centimeter-scale mottling associated with burrowing activity of ambient benthos.

Reoccupation of stations near the tetrapod site shows an increase of physical stratification in the shallow sediments (0-5 cm) between the first and second 1995 cruises. Faint millimeter-scale mottling is the prominent trait of the surface layer in all cores obtained on the first cruise and half of the cores taken on the second cruise. The remaining cores from the second cruise display patchy laminations in bioturbated surface sediment. In one core (core 260, Fig. 2), the X-ray subsample tray was inserted directly into a mound of sediment surrounding a *Callianassa* burrow, so the observed stratification probably results from deposition of material ejected from the burrow. In other cases, however, stratification does not appear to be associated with active burrows.

Fabric displayed in radiographs of deeper sediments is relatively uniform and completely biogenic over the entire study area. Specific types of biogenic structures include: thinly walled shafts (6-10 mm in diameter); unlined inclined burrows (2-4 mm in diameter; 7B) that are occasionally branched; helical burrows (4-8 mm diameter) coiled about a vertical axis that can be connected to uncoiled segments; and horizontal meniscate backfill (10-30 mm in diameter). The backfill is a subtle but ubiquitous aspect of biogenic fabric, evident in nearly all radiographs. Boundaries of the fill are gradational with surrounding sediment and are defined by imbricated fragments of mollusc shells. The core of the fill generally contains fewer shell fragments than do surrounding sediments. The coiled structures are clearly similar to the ichnogenus *Gyrolithes*.

Sediments in the study area are shelly carbonate muds. Analysis of particle size for this biogenic material is problematic because of the wide range of particle sizes and irregularity of particle shapes (spherical to platy to rod-like), roughness (smooth to very irregular), and effective density (owing to internal chambers, as in the case of foraminiferal tests)(Figs. 3 and 4). Nevertheless, merging of Sedigraph data with sieve data produces no obviously distorted results. Detailed analyses have been undertaken for a core from the tetrapod station over the upper 10 cm of the seabed at 1-cm intervals (two replicates per interval), and for selected intervals in two other cores from the same station. Mean grain sizes range between 4.75 and 5.75 ϕ (19 and 37 μm), and distributions are concentrated at about 5 ϕ (31 μm). Sediments coarsen with depth over the upper 8 cm, and the most pronounced gradient in mean grain size is across the upper 4 cm. This down-core increase (+40%) is much greater than variability between replicate analyses (<5%).

Microfabric in both the surface layer and deeper is characterized by coarse skeletal grains randomly oriented in a micritic matrix (Fig. 7A). Faintly graded bedding is evident in the upper 1 cm of some cores (Fig. 7A), produced by a downwardly increasing number of coarse skeletal particles (>100 μm). Thin, unlined, infilled burrows (1-2 mm diameter) occur in surface-layer sediments and are similar in scale to shallow, fine-scale mottling observed in X-radiographs. Burrow fill is very fine material, lacking skeletal particles larger than 20 μm , and thus differs from the surrounding sediments (Fig. 7B). Microfabric below 2-3 cm is similar to that in shallow sediments, but contains more and larger skeletal fragments, especially molluscan shell fragments. Other types of particles include fecal pellets, bryozoa, foraminifera, and coral fragments.

Excess ^{234}Th was restricted to the upper 2 cm of the seabed for both cores analyzed. Porosity was determined for each profile, and the distribution of excess ^{234}Th closely tracks the thickness of the high-porosity surface layer. Sediment below this layer was shellier and more compact. The shallow penetration of excess ^{234}Th indicates that only the surface layer is mixed

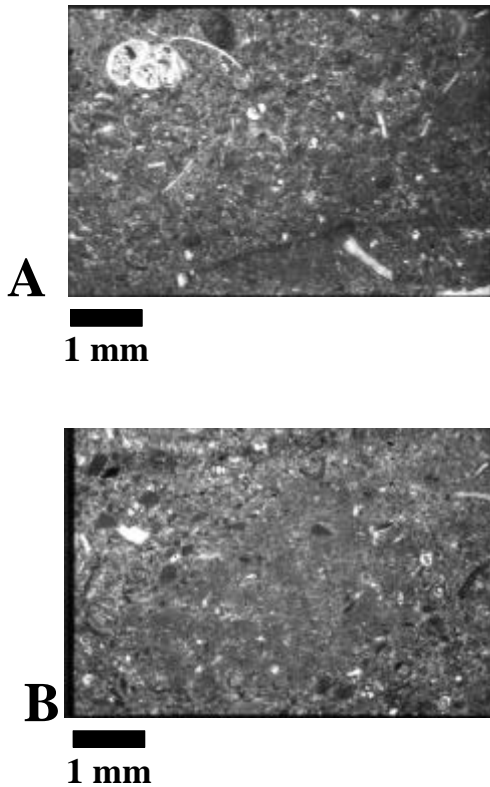


Figure 7. Thin-sections from core 20 (Fig. 2). A) 0-4 mm depth (core top). Skeletal fragments and fecal pellets in micritic matrix. Faint graded bedding (downward coarsening) is visible in the upper 2-3 mm. B) 40-44 mm depth. Unlined burrow infilled with fine sediment, typical of burrows that produce faint mottling in the surface layer.

on time scales comparable to several half-lives of ^{234}Th (2-3 months), and complete mixing of deeper sediment occurs over much longer periods.

^{210}Pb activities have been determined for 9 cores from Southeast Channel, including replicates from two stations. The general shape of all profiles is similar (Fig. 8). The upper ~15 cm is characterized by a steep gradient from surface values of 3 dpm g^{-1} to deeper activities of just over 2 dpm g^{-1} , with occasional spikes of higher activity. Below 15 cm, the gradient displays uniform exponential decay to supported activities of 0.45 dpm g^{-1} .

Mixing coefficients (D_b) calculated from these profiles range from $75 \pm 54 \text{ cm}^2 \text{ yr}^{-1}$ for the steep upper gradient to $2.1 \pm 0.4 \text{ cm}^2 \text{ yr}^{-1}$ for deeper gradient, if accumulation is assumed negligible. The deeper gradient translates into accumulation rates of $0.30 \pm 0.03 \text{ cm}^2 \text{ yr}^{-1}$, if the effects of bioturbation are assumed unimportant. It is likely that these ^{210}Pb profiles are influenced by both mixing and accumulation, based on distributions of deep deposit feeders observed by D'Andrea and Lopez (1997).

Accomplishments:

Observations in Eckernförde Bay and the Florida Keys allowed evaluation of the environmental processes that developed sedimentary structure.

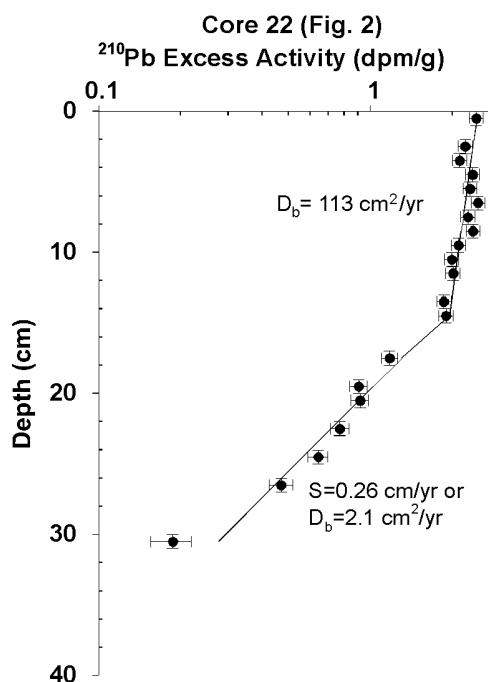


Figure 8. ^{210}Pb profile for core 22 (Fig. 2). End-member estimates for accumulation rate (S) and mixing coefficient (D_b) are shown for two distinct gradients in the profile. Calculations for S assume negligible mixing effects, and calculations for D_b assume insignificant accumulation.

Bottom shear stresses exerted in the Central Basin of Eckernförde Bay during all conditions are below critical stresses, which makes the Bay an excellent sediment trap. Sediment from both distant and local origins is reworked in the Central Basin of Eckernförde Bay by a pioneering community of benthic organisms, which is maintained by seasonal hypoxia/anoxia. The population is characterized by few species, small body sizes, young ages, and limited depth of mixing (~ 1 cm). However, the community effectively pelletizes most of the sediment reaching the seabed.

The very restricted thickness for the surface mixed layer (~ 1 cm) and the substantial sediment accumulation rates (mean of 0.39 cm y^{-1} for the Central Basin) give sediment a short exposure to modern oceanographic processes before being buried. These conditions allow for partial preservation of sediment deposited as storm layers, thus forming laminations of un-pelletized sediment. These laminations separate thick beds of pelletized sediment deposited during fair weather or as thin storm layers (i.e., < 1 cm thick). In general, the oceanographic processes in Eckernförde Bay allow for preservation of a high-resolution record of environmental processes. For example, changes recorded for the past half century indicate that slower sediment accumulation rates previously characterized some portions of the study area.

Sediment is supplied to Southeast Channel of the Dry Tortugas in roughly equal proportions from (1) erosion of nearby reefs, and (2) from *Halimeda* production in shallow-water seagrass beds to the north. Fine sediment (silt and clay-sized) is advected to the seabed of Southeast Channel by a combination of tidal and storm-driven currents, which produce a net flow to the SSW. Southward-diverging isobaths induce flow deceleration, producing conditions favorable to long-term accumulation. Accumulation rates of $0.10\text{-}0.32 \text{ cm y}^{-1}$ are estimated from ^{210}Pb profiles.

Once deposited, sediment in Southeast Channel is subjected to bioturbation by a two-tiered benthic community. Bioturbation by the surface tier (0-5 cm) is biodiffusive ($D_b = \sim 9 \text{ cm}^2 \text{ yr}^{-1}$) and produces mm-scale mottling, mixing this zone over periods of weeks to months. Other structure includes biodeposited fecal mounds of deep deposit feeders, and physical stratification in thin (1-5 cm) layers of fine sediment deposited from decelerating flow. Below ~5 cm, the dominant post-depositional process is bioadvective mixing by a deep-deposit-feeding community of callianassid shrimp and large capitellid polychaetes. The upper 10-15 cm is mixed completely every 6-21 years. Bioturbation below this depth is slower.

Even though the study area has been hit by 10 major hurricanes in the last 120 years (winds $> 190 \text{ km h}^{-1}$), sediments accumulated in Southeast Channel during this period are characterized entirely by biogenic sedimentary fabric produced by the deep callianassid/capitellid community. Bioturbation is thus capable of erasing the stratigraphic signature of the most extreme sediment transport events over decadal time scales.

Funding Profile (based on fiscal year 1 October-30 September):

Approved:

<u>1993</u>	<u>1994</u>	<u>1995</u>	<u>1996</u>	<u>1997</u>	<u>Total</u>
\$157,253	\$143,568	\$176,685	157,776	133,786	\$769,068

Received:

\$157,000	\$107,929	\$142,760	\$97,056	\$53,426	\$558,171
-----------	-----------	-----------	----------	----------	-----------

Peer Reviewed Publications:

Bentley, S.J. and Nittrouer, C.A., 1996. Environmental influences on the formation of sedimentary fabric in a fine-grained carbonate-shelf environment: Dry Tortugas, Florida Keys. *Geo-Marine Letters* 17: 268-275.

Bentley, S.J. and Nittrouer, C.A., submitted. Production and accumulation of bioclastic muds in a carbonate-platform setting: Dry Tortugas, Florida. *Journal of Sedimentary Research*.

Bentley, S.J. and Nittrouer, C.A., submitted. Physical and biological influences on the formation of sedimentary fabric in a fjord-like depositional environment: Eckernförde Bay, southwestern Baltic Sea. *Palaaios*.

Bentley, S.J., Nittrouer, C.A. and Sommerfield, C.K., 1996. Development of sedimentary strata in Eckernförde Bay, southwestern Baltic Sea. *Geo-Marine Letters* 16: 148-154.

D'Andrea, A.F. and Lopez, G.R., submitted. Deposit feeder fecal pellets as tracers of sedimentary movement in Eckernförde Bay, Germany. *Journal of Marine Research*.

D'Andrea, A.F., Lopez, G.R. and Craig, N.I., 1996. Benthic macrofauna and bioturbation in Eckernförde Bay, southwestern Baltic Sea. *Geo-Marine Letters* 16: 155-159.

Nittrouer, C.A., Lopez, G.R., Wright, L.D., Bentley, S.J., D'Andrea, A.F., Friedrichs, C.T., Craig, N.I. and Sommerfield, C.K., in press. Oceanographic processes and the preservation of sedimentary structure in Eckernförde Bay, Baltic Sea. *Continental Shelf Research*.

Symposium Proceedings:

Bentley, S.J. and Nittrouer, C.A., 1997. Constraints on rates of sediment mixing and accumulation, Southeast Channel, Dry Tortugas. In: Dawn Lavoie (ed.), Proceedings, CBBL/NRL Key West Campaign Workshop, February 1997, Stennis Space Center, Mississippi. Report number NRL/MR/7431-97-8044.

Bentley, S.J., Nittrouer, C.A. and Lopez, G.R., 1995. Measurement of progressive bioturbation in event layers: Eckernförde Bay. In: Thomas Wever (ed.), Proceedings, CBBL/NRL Workshop on Modeling Methane-rich Sediments of Eckernförde Bay. Eckernförde, Germany, July 1995.

D'Andrea, A.F., Lopez, G.R., Nittrouer, C.A. and Wright, L.D., 1995. Fecal pellets of *Abra alba* as tracers of sediment movement in Eckernförde Bay. In: Thomas Wever (ed.), Proceedings, CBBL/NRL Workshop on Modeling Methane-rich Sediments of Eckernförde Bay. Eckernförde, Germany, July 1995.

Lopez, G.R., D'Andrea, A.F., Craig, N.I., Bentley, S.J. and Nittrouer, C.A., 1995. Benthic macrofauna and bioturbation in Eckernförde Bay, southwestern Baltic Sea. In: Thomas Wever (ed.), Proceedings, CBBL/NRL Workshop on Modeling Methane-rich Sediments of Eckernförde Bay. Eckernförde, Germany, July 1995.

Lopez, G.R. and D'Andrea, A.F., 1997. Regional comparison of benthic assemblages in the Lower Florida Keys. In: Dawn Lavoie (ed.), Proceedings, CBBL/NRL Key West Campaign Workshop, February 1997, Stennis Space Center, Mississippi. Report number NRL/MR/7431-97-8044.

Nittrouer, C.A., Bentley, S.J., Lopez, G.R. and Wright, L.D., 1995. Observations of sedimentary character and their relationship to environmental processes in Eckernförde Bay. In: Thomas Wever (ed.), Proceedings, CBBL/NRL Workshop on Modeling Methane-rich Sediments of Eckernförde Bay. Eckernförde, Germany, July 1995.

Published Abstracts:

Bentley, S.J. and Nittrouer, C.A., 1997. The fate of *Halimeda*-rich sediments in a carbonate-mud depositional environment: Dry Tortugas, Florida. Geological Society of America Annual Meeting, Salt Lake City, October 20, 1997.

D'Andrea, A.F., Lopez, G.R. and Craig, N.I., 1995. Benthic macrofauna and bioturbation in Eckernförde Bay, southwestern Baltic Sea. Proceedings, Annual Benthic Ecology Meeting, New Brunswick, New Jersey.

D'Andrea, A.F. and Lopez, G.R., 1996. Deposit feeder fecal pellets as tracers of sediment movement in Eckernförde Bay, Germany. Annual Benthic Ecology Meeting, Columbia, South Carolina.

Lopez, G.R., 1994. Benthic faunal distribution and bioturbation in Eckernförde Bay. 1994 Ocean Sciences Meeting, EOS, 75, 180.

Nittrouer, C.A., Sommerfield, C.K. and Bentley, S.J., 1994. Formation of sedimentary strata in Eckernförde Bay. 1994 Ocean Sciences Meeting, EOS, 75: 180.

Dissertations

Bentley, S. J., 1998. Emplacement and evolution of sedimentary fabric: physical and biological controls in three contrasting depositional environments. Ph.D. dissertation, Marine Sciences Research Center, State University of New York, Stony Brook. Professor Charles A. Nittrouer, advisor.

Contact Micromechanics for Constitutive Acoustic Modeling of Marine Sediments

M. H. SADD

Professor of Mechanical Engineering & Applied Mechanics
Department of Mechanical Engineering & Applied Mechanics
University of Rhode Island
Kingston, RI 02281, USA.

JACK DVORKIN

Petrophysical Consulting Inc.
730 Glenmere Way
Redwood City, CA 94062, USA.

Abstract:

Contact micromechanical models are developed for geoacoustic wave propagation applications in particulate marine sediments. The modeling includes particulate, cementation and pore fluid microstructures which have been shown to strongly affect the acoustic properties of such materials. The principal modeling issue is related to the determination of energy transfer through interparticle contact cement or matrix material. Such material may be elastic (e.g., calcite), or viscoelastic (e.g., clay, silt). Both contact mechanisms are explicitly considered at the particulate scale through the analytical development of new particle contact relations. These resulting solutions are incorporated into a numerical discrete element method (DEM) modeling scheme in order to simulate acoustic wave propagation in model materials. Several DEM simulations have been carried out for both regular and random two-dimensional assemblies of spherical particles with several types of cementation. Simulation results yield information on the wave speed and amplitude attenuation as functions of the microstructural variables including both particulate and cementation properties.

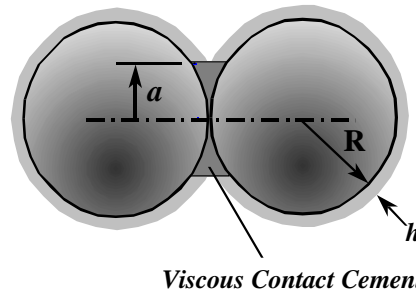
Objectives:

As clearly demonstrated at the URI Workshop in November 1995, marine sediments have extremely complicated microstructure which requires rigorous constitutive modeling. Observations indicate that the CBBL Panama City site sediments are primarily composed of cohesionless particulate materials including sands and shell fragments. The Key West site sediments are fine grained calcareous materials, and some preliminary strength and consolidation tests indicate the presence of cementation. Our overall objective is to create constitutive models for cohesionless and cemented materials such as those found at these two CBBL sites. Our concrete technical objective is to quantify the effects of two contact mechanisms on the acoustic properties of such sediments. One mechanism is related to stress transfer through interparticle elastic contact cement (e.g., calcite). The other mechanism is squirt flow (fluid squirting from the contacts during wave propagation). The fluid (e.g., clay, silt, organic matter) filling the contacts between the grains may have viscosity significantly exceeding that of sea water. The two micromechanical mechanisms are incorporated into a macroscopic constitutive model by using the numerical discrete element method.

Approach:

Particulate materials transmit mechanical signals primarily through interparticle contact, and thus the acoustic response of such materials is strongly dependent upon the stiffness of the grain-to-grain contacts. Many marine materials of this type (Lavoie, 1997) also contain additional matter between the grains such as clay suspensions or biogenic deposits, and we refer to this material as cementation. This additional material affects the intergranular contact response, producing elastic and/or viscoelastic reinforcement behaviors, thereby resulting in a frequency dependent micromechanical stiffness. The study first developed a solution to the normal contact response between two spherical particles including the effect of interparticle viscoelastic cementation. Modeling work for elastic cement had been previously developed (Dvorkin, et al., 1994). The current focus is on the viscous, time dependent behavior, and the developed solution is interpreted as a micromechanical constitutive contact law. This law was then incorporated into a discrete element numerical code to simulate the dynamic behavior of aggregate assemblies of specific particulate material systems. The discrete element method has been successfully applied to granular mechanics problems for many years, and previous work (Tai and Sadd, 1997, Sadd et al., 1997) included applications to uncemented problems. Numerical results yield information on the wave

speed and amplitude
amplitude dynamic P-wave
model materials of
cementation. This
thought of as a meso-
whereby micromechanical
sufficiently large number of
averages of particular wave
characteristics will be



attenuation of small
signals moving through
particular fabric and
modeling scheme may be
domain approach,
modeling is applied to a
particles such that
propagational
meaningful.

Micromechanical

The technical approach combination of the theory viscoelasticity, and hydrodynamics. The grains are assumed elastic, while the cement may be elastic or liquid. We solve for the normal and tangential contact stiffnesses of a two-grain cemented system, where the grains are circular or spherical. In the liquid cement case, the contact stiffnesses have imaginary parts that are used to compute attenuation.

In principle, the scheme of solving such problems is as follows. First, we use theory of elasticity to link the displacements of the grain surface to the contact stresses. Next we link stresses to displacements in the cement layer. Here we assume that this layer acts as an elastic foundation, or has the hydrodynamic properties of a thin layer of viscous compressible liquid. Finally, these two sets of equations are linked together through a displacement compatibility condition. The result is a complicated integro-differential equation. We simplify this equation by approximating it by simple analytical formulas that can be easily used in the numerical DEM routine.

Using these new contact solutions in our existing discrete element numerical routines, meso-domain simulations are conducted on model granular sediments to obtain effective velocities and attenuation. Computer generated sediment models with a variety of fabric and cementation are constructed using our previous algorithms. A DEM model was also developed from SEM photographic data from an actual Key West sample. We explore the effects of fabric (packing geometry), material properties (elastic moduli and viscosity), and amounts of cementation and saturation. This work provides linkages with the experimental activities at the URI Marine Geomechanics Lab.

Contact Solution

The contact solution developed is to quantitatively describe the squirt flow of viscous cement and understand how it effects the stiffness of the sediment microstructural frame. The problem is modeled by two spherical grains enveloped by a viscous fluid which represents the interstitial cement material (Figure 1). The solution focuses on the normal contact response (stiffness), while the interparticle shear behavior is taken to be negligible. The dynamics of the viscous cement is modeled by assuming harmonic oscillations of the grain surfaces, and using an approximate Navier Stokes equation for the radial flow in the gap between the spherical particles. Details of the solution are given by Leurer and Dvorkin (1998) and the final result reduces to an integral equation which can be solved numerically. In order to incorporate these results into a discrete element code, a simplified contact solution was developed. A numerical fit to the exact solution was obtained using a simplified Maxwell and Cole-Cole viscoelastic models.

A simple numerical solution to the Maxwell model is developed using a fourth-order Runge-Kutta scheme. In this manner, the normal contact response may be calculated at specific time steps.

Modeling

here includes a
of elasticity,

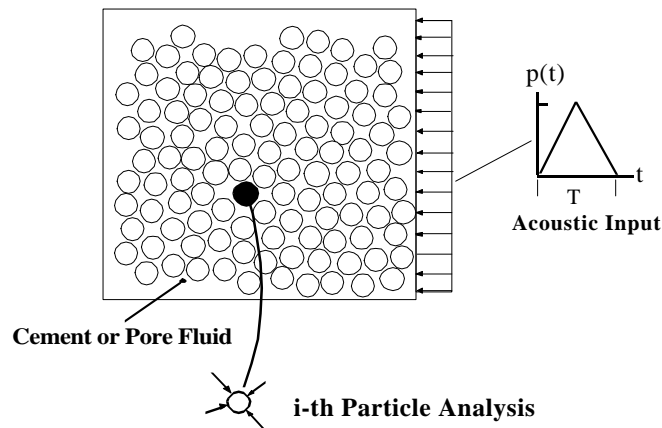
Figure 1. Basic Particulate Contact Model

Discrete Element Procedures

The computational modeling used to simulate the micromechanical wave propagation is based on the discrete element method. Originally developed by Cundall et al. (1979), the discrete element method has been successfully used to model the behavior of large assemblies of disks, spheres, blocks and particles of general shape. The technique makes simplifying constitutive assumptions for each particle (commonly assuming rigid body behavior) and then uses Newtonian mechanics to determine the translational and rotational motion of each particle in assembly system models. Particles are allowed to have contact or other forms of interaction, and interparticle forces develop as a result of particular contact stiffness and damping characteristics. The general concept of the method may be explained by considering the two-dimensional particulate assembly as shown in Figure 2.

Figure 2.
Element Modeling

Isolating
the i-th particle and
laws yields



Discrete
Scheme

attention to
applying Newton's

$$\sum_{j=1}^N F^{ij} + F^i = m_i \ddot{x}_i$$

$$\sum_{j=1}^N M^{ij} + M^i = I_i \ddot{q}_i$$

where F_{ij} are the j -contact forces on the i -th particle; F_i represents any non-contacting forces on particle i ; M_{ij} are the moments (about the particle's mass center) resulting from contact forces F_{ij} ; M_i is the resultant moment from any non-contacting forces, m is the particle mass; and I_i is the mass moment of inertia. With given contact and non-contact forces, the linear and angular accelerations of the i -th particle can thus be determined, and the velocities and displacements may be obtained through numerical integration using finite difference schemes. The new positions and velocities are used to update the previous values, and this allows new contact forces to be determined.

The DEM technique establishes a discretized time stepping numerical routine, in which granule velocities and positions are obtained through numerical integration of the computed accelerations. For applications to wave propagation, the movements of the individual particles are a result of mechanical disturbances propagating through the medium. The predicted wave speed and amplitude attenuation (intergranular contact force) will therefore be functions of the physical properties of the discrete medium, i.e., the microstructure or fabric.

Results and Accomplishments:

Squirt Flow in Marine Sediments (Viscous Cement)

We offer an exact solution to the problem of deformation of two elastic spherical particles with viscous cement at their contact. This model is intended to mimic a granular geomaterial whose grains are covered with viscous fluid of geologic or biogenic nature (e.g., marine sediment, heavy-oil sand, asphalt concrete). The solution for the normal stiffness of a two-grain combination is reduced to an ordinary integro-differential equation that has to be solved numerically. We find two approximations for the rigorous numerical solution. The simplest one, based on the Maxwell viscoelastic model, cannot accurately reproduce the relaxational behavior of the system. The second one is based on the Cole-Cole model that allows one to introduce a spectrum of relaxation times. This expression is very accurate and can be used instead of the numerical solution. The complex effective elastic moduli of the aggregate are calculated from statistical averaging for a dense random pack of identical spheres. The theoretical results match well with experimental data obtained on a glass bead pack with viscous epoxy cement.

The main part of the solution involves finding the normal stiffness of a two-grain combination. This normal stiffness is defined as the ratio of the normal contact force to the resulting increment of the relative displacement between the sphere's centers. Because the grains are not precompacted, we assume that the shear stiffness of two grains is negligible.

The expression for the normal contact stiffness is obtained, and is used in a numerical discrete element code. For the special case of a random close pack of identical spherical grains the following analytical expressions can be used to calculate the effective bulk (K_{eff}) and shear (G_{eff}) moduli of the aggregate:

$$K_{eff} = \frac{n(1-f)}{12 pR} S_n, \quad G_{eff} = \frac{3}{5} K_{eff};$$

where S_n is the normal stiffness between two grains; $n \approx 9$ is the coordination number (the average number of contacts per grain); and $f \approx 0.36$ is the aggregate's porosity. The exact solution of the problem requires numerically solving an integro-differential equation. This exact solution can be approximated by two simpler viscoelastic solutions: the Maxwell and Cole-Cole models. Maxwell's model is the simplest one. It can adequately mimic velocity-frequency dispersion present in the exact solution, but fails to precisely model the relaxation time distribution. On the other hand, the Cole-Cole model accurately reproduces the exact solution (Figure 3).

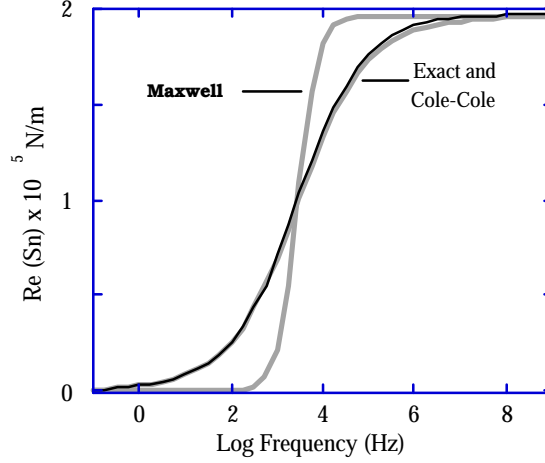


Figure 3. Two Grain Model - Real Part of Normal Stiffness Versus Frequency. Exact Solution (Thin Black Curve), Approximate Solutions (Bold Gray Curves).

Equations describing the Maxwell model are:

$$\frac{\text{Re}(S_n)}{2pRrc_0^2} = S_\infty \frac{w^2 t^2}{1 + w^2 t^2}; \quad \frac{\text{Im}(S_n)}{2pRrc_0^2} = S_\infty \frac{wt}{1 + w^2 t^2};$$

where

$$S_\infty = \tilde{A}a^2 + \tilde{B}a + \tilde{C};$$

$$\tilde{A} = 19.7472 \cdot \exp(-51.9238 \Lambda), \quad \tilde{B} = 0.795673 \cdot \Lambda^{-0.365617},$$

$$\tilde{C} = -0.00391064 \cdot \Lambda^{-0.583262}; \quad \Lambda = rc_0^2(1 - n)/(pG); \quad t = 0.8\sqrt{2}h/(a^3c_0^2).$$

Equations for the Cole-Cole (1941) model are:

$$\frac{\text{Re}(S_n)}{2pRrc_0^2} = S_\infty \left(1 - \frac{1 + \sqrt{wt/2}}{1 + \sqrt{2wt} + wt}\right); \quad \frac{\text{Im}(S_n)}{2pRrc_0^2} = S_\infty \frac{\sqrt{wt/2}}{1 + \sqrt{2wt} + wt}.$$

The modeling results have been compared to the experimentally measured P-wave velocity in a dense random pack of identical glass beads partially saturated with viscous epoxy. The match between the model and the experiment is good.

We calculated the effective P- and S-wave velocity in a quartz sand of 36% porosity where the viscosity of cement was 10^4 cPs, and the rest of the pore space was filled with water. The results are presented in Figure 4.

Velocity versus Porosity, Mineralogy, and Effective Pressure in Marine Sediments

We introduce a deterministic velocity-porosity model for marine sediments and apply it to several Key-West data sets. In the model, velocity depends on mineralogy of the sediment, effective (overburden minus hydrostatic) pressure, and porosity. The model is fully formulated in Dvorkin and Lavoie (1998). It can accurately model the experimental data (Figure 5).

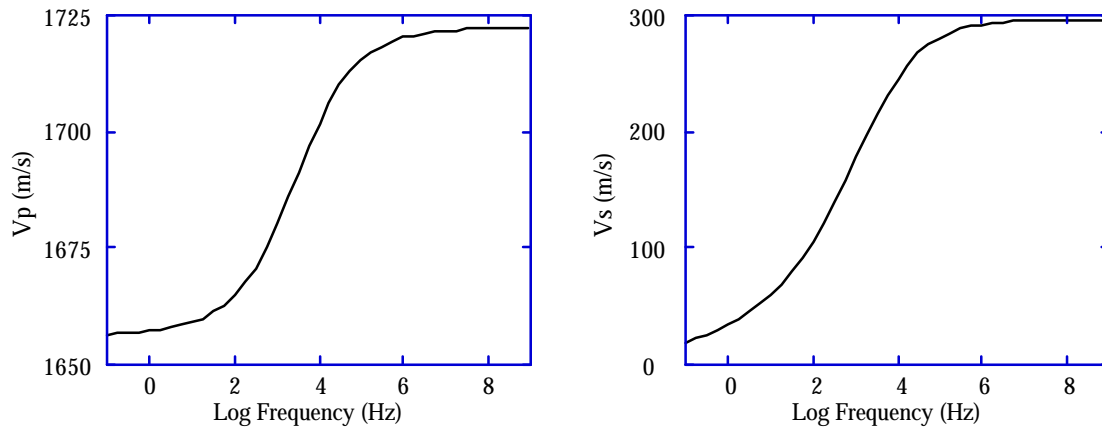


Figure 4. P- and S-wave velocity versus frequency in quartz sand.

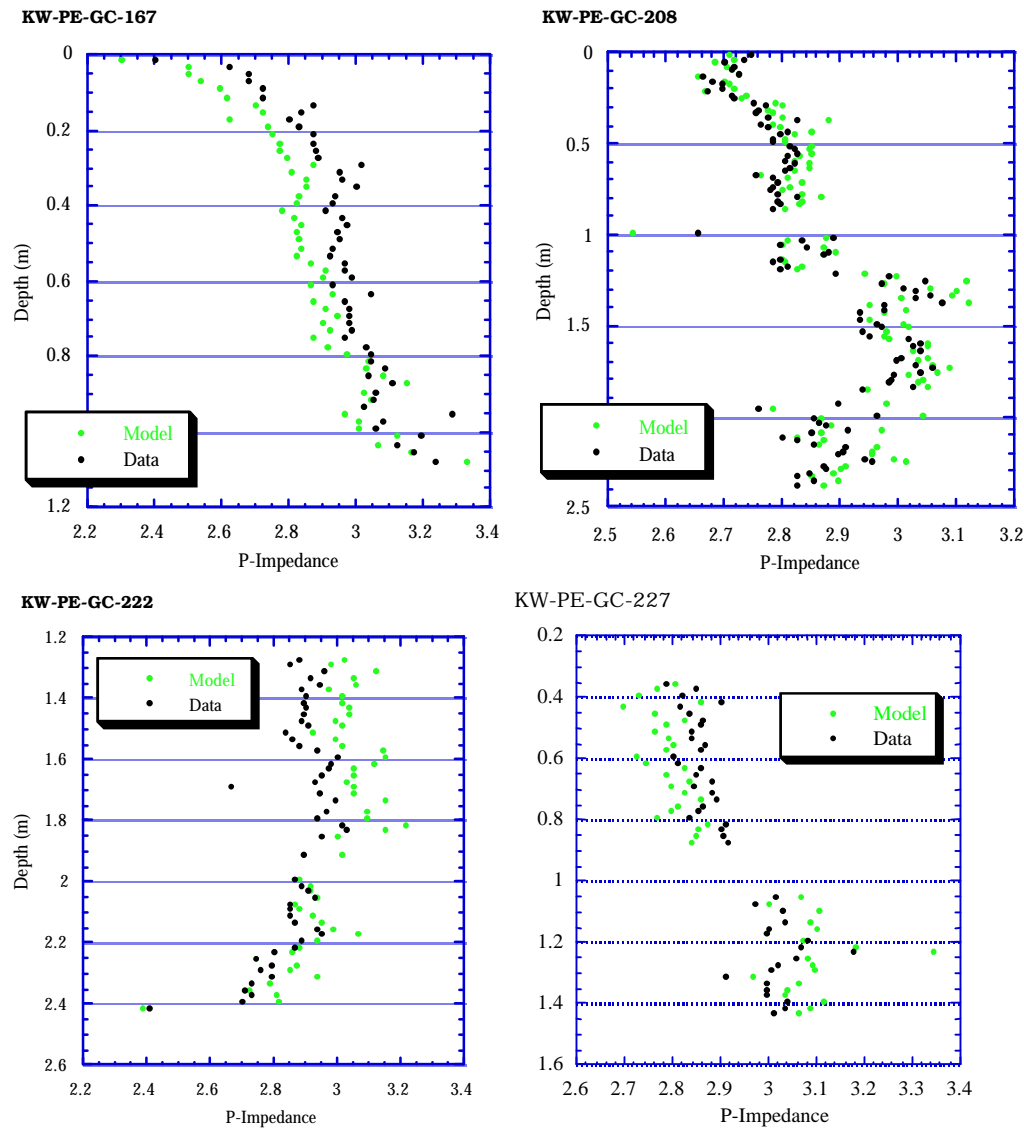


Figure 5. P-impedance (km/s g/cm^3) versus depth for four Key-West data sets. Black symbols are data; gray symbols are from the model.

Discrete Element Simulations

Discrete element simulations have been conducted on numerous model material systems including single particle chains, hexagonal closed packed assemblies (HCP) and random assemblies. The model systems were composed of spherical particles in the plane, and included variation in particle size, cementation properties and general fabric. The fabric of such materials may be measured by the angular distribution of branch vectors which connect neighboring particle mass centers. Each of the models were subjected to a triangular time dependent, planar compressional input of 10kPa along one boundary, and the resulting wave propagation was simulated. Typical results comprise average wave speed and amplitude attenuation, and it was assumed that a sufficient number of particles were included in the simulations such that these averaged values have meaning. Grain mechanical properties were chosen to model quartz, and particle sizes generally ranged between 0.1 – 1.0mm. Typical cement properties include h/R ratios between 0.05 – 0.25, and a viscosity of 5 – 50 cPs.

HCP models (typical case shown in Figure 6), included assembly systems of 502 and 1067 particles of 1.0 and 0.1mm diameter. A series of random models with both uniform and non-uniform particles have also been studied. Figure 7 illustrates one such case with uniform sized particles of 1mm diameter.

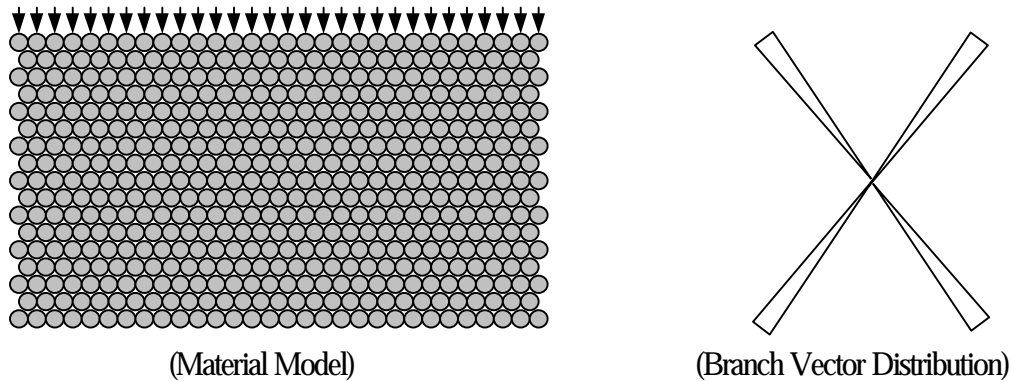


Figure 6. HCP Material Model

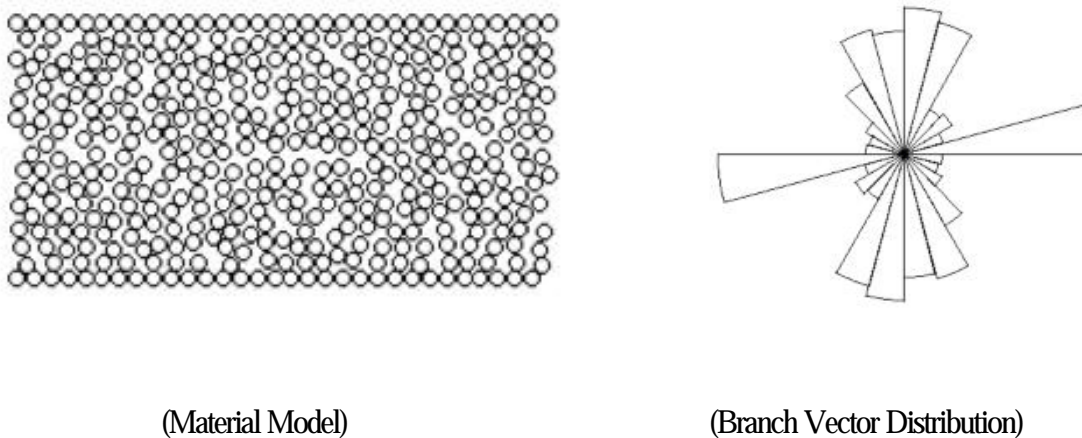
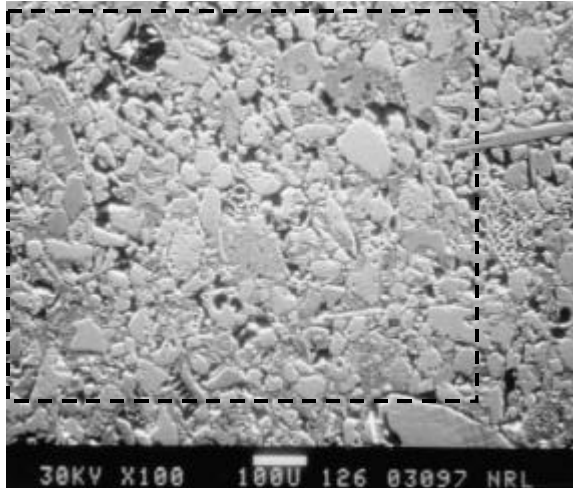


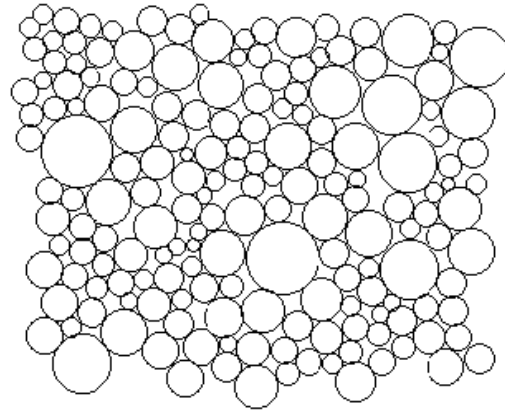
Figure 7. Random Assembly Model

A DEM simulation has also been conducted on a particular Key West Sediment sample shown in Figure 8. The SEM photograph provides fabric data to construct an approximate particulate model. This material model

was developed by placing spherical grains of proper size and location to match the larger more significant features found in the photograph. Additional particles were added on the boundaries in order to create a model of approximate rectangular shape to allow planar input loading. . The average grain size in the model was approximately 0.05mm ($\phi \cong 4.5$). This model and its fabric branch vector distribution is shown in Figure 9

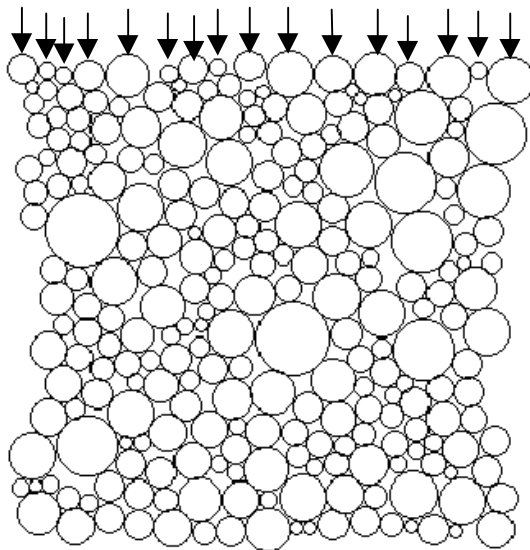


(SEM Photograph – D. Lavoie)

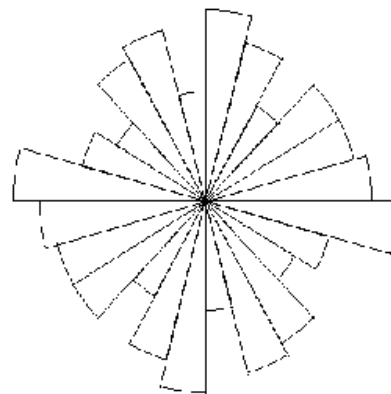


(Particulate Model)

Figure 8 . Key West Sediment Sample
(Dry Tortugas, Cone 72, 18-20cm, Post Consolidation)



(Discrete Element Model)



(Branch Vector Distribution)

Figure 9. Discrete Element Sediment Model

Results from several DEM simulations of the models in Figures 7 and 9 are summarized in Table 1. Wave speeds were determined by calculating the transit time of the averaged wave signal to propagate through the assembly model. With regard to attenuation, the wave amplitude pressure was determined by averaging the vertical interparticle contact forces across a horizontal line through the material model. Attenuation was then

calculated through the transmission loss relation $TL = 20 \log (p_{\text{input}}/p_{\text{output}})$, where the input and output pressures were determined over a contact band just inside the input and output sides of the assembly.

Table 1. Summary of DEM Simulations

HCP Model Results								
Grain Size (mm)	1.0					0.1		
Porosity, %	24					31.9		
Cementation Ratio, h/R	0.1					0.05		
Cement Bulk Modulus (Gpa)	2.25					0.25	0.4	0.6
Cement Viscosity (cPs)	10	20	30	40	50	10	10	10
Wave Speed (m/s)	682	1375	2074	2764	3240	1570	1890	2230
Attenuation (db/m)	3268	2873	2601	2371	2159	3290	3530	4090

Marine Sediment Model Results				
Grain Size (mm)	0.02-0.13mm			
Porosity, %	24-67			
Cementation Ratio, h/R	0.05			
Cement Bulk Modulus (Gpa)	0.14	0.25	0.4	0.6
Cement Viscosity (cPs)	10	10	10	10
Wave Speed (m/s)	1450	1930	2940	2940
Attenuation (db/m)	24200	23180	22400	22400

These numerical results indicate that wave speed increases with cement volume, viscosity and bulk modulus. Values of these matrix material parameters for the marine sediments under study are not well known. The particular numerical simulations produce reasonable wave speeds which compare to measured data for a cement matrix volume of $h/R \cong 0.05-0.1$, viscosity $\cong 10-20$ cPs and bulk modulus $\cong 0.25-2.25$ Gpa. Experimental data collected by our the Marine Geomechanics Lab for Dry Tortugas material indicated P-wave velocities in the range of 1450-1550m/s. Experimental studies also found that during consolidation there was an increase in the P-wave speed with confining pressure. This result could be interpreted by our micromechanical model by arguing that the consolidation would increase the effective matrix cementation density, viscosity and/or bulk modulus around the grains, and thus (according to our numerical results) produce the observed increase in the wave speed. Experimental MGL data has also indicated a decrease in wave speed with deviatoric loading, and this could be attributable to a softening of the cement/matrix material under such stress conditions.

Both the analytical modeling work and the DEM computer simulation studies have provided a better micromechanical understanding of the wave propagation processes in particulate marine sediments. Particular acoustic data has compared well with analytical model and simulation results. Details relating to the interparticle matrix material properties and its spatial distribution are not well known, and therefore additional information would be needed to more completely establish relationships between measured acoustic data and material microstructure.

References:

Cole, S., and Cole, R.H., 1941, Dispersion and absorption in dielectrics: J. Chem. Phys., 9, 341-351.

- Cundall, P.A. and Strack, O.D.L., 1979, A discrete numerical model for granular assemblies, *Geotechnique*, 29, 47-65.
- Dvorkin, J., Nur, A., and Yin, H., 1994, Effective properties of cemented granular material, *Mech. of Materials*, 12, 207-217.
- Lavoie, D., 1997, Microfabric of Dry Tortugas and Marquesas carbonate sediment, *Proceedings of the Coastal Benthic Boundary Layer Key West Workshop*, Eds. D.L. Lavoie and M. Richardson, 183-193.
- Leurer, K.C. and Dvorkin, J., 1998, Intergranular squirt flow in sand: grains with viscous cement, submitted to *Int. J. Solids and Structures*.
- Sadd, M.H., Gao, J., and Shukla, A., 1997, Numerical analysis of wave propagation through assemblies of elliptical particles, *Comp. and Geotechnics*, 20, 323-343.
- Tai, Q.M. and Sadd, M.H., 1997, A discrete element study of the relationship of fabric to wave propagational behaviors in granular materials, *Intl. Jour. Num. and Anal. Meth. Geomechanics*, 21, 295-311.
- Dvorkin, J. and Lavoie, D., 1998, Velocity-porosity model for shallow marine sediments, to be submitted to *GRL*.

Publications resulting from the effort:

- Leurer, K.C. and Dvorkin, J., 1998, Intergranular squirt flow in sand: grains with viscous cement, submitted to *Int. J. Solids and Structures*.
- Dvorkin, J. and Lavoie, D., 1998, Velocity-porosity model for shallow marine sediments, to be submitted to *GRL*.
- Sadd, M.H., Adhakari, G. and Silva, A.J., 1998, A wave propagation model for saturated granular geomaterials based on microstructural simulation, to be submitted to *J. Engineering Mechanics*.
- Sadd, M.H., Cardoso, F. and Dvorkin, J., 1998, Contact micromechanics modeling of the acoustic behavior of cemented particulate marine sediments, *Proc. 12th ASCE Engineering Mechanics Meeting*, La Jolla, CA.

The Detection of Continuous Impedance Structures Using Full Spectrum Sonar

S. SCHOCK

Associate Professor of Ocean Engineering
Department of Ocean Engineering
Florida Atlantic University
Boca Raton, FL 33431, U.S.A

Abstract:

Numerical modeling using insitu impedance data predicted that subsurface reflections have a strong frequency dependence. Chirp sonar data was collected and analyzed to determine the frequency dependence of subsurface reflectors. A new method of studying subsurface chirp data is tested on data collected at CBBL core sites. Wideband reflection data is bandpass filtered into several preset bands to provide the frequency components of subsurface reflectors. The analyses showed that the frequency response of subsurface layers can vary as much as 6 dB over a 1 octave band. Notches and peaks in the frequency response of subsurface reflectors appear to be random. Random variations in the frequency response of subsurface reflectors generate errors in impedance inversion procedures and attenuation estimation procedures. The results show that the accuracy of the acoustic property predictions improve with increased bandwidth. Increased bandwidth provides additional independent frequency bands for performing independent remote measurements of acoustic attenuation and impedance.

Based on the above studies, the chirp sonar was redesigned to provide more accurate sediment property predictions. The chirp computer system was moved into the towed vehicle. Digital telemetry over a coax cable is used to send data from the vehicle to the topside processor and to send commands from the topside unit to the towed vehicle. A two channel transmitter was added to the fish to allow the bandwidth of the system to increase to 2 octaves from 1 octave. Two receiving arrays are used to measure the reflection data over the 2 octave band. The new vehicle generates acoustic data sets that have a flat band over the range of 1 to 12 kHz. A 3 axis accelerometer and rate gyros measure fish motion and output data to the vehicle computer to allow compensation for the beam pattern as the fish pitches and rolls. These changes have made a dramatic improvement in data quality control. The expanded bandwidth and the ability to compensate for fish motion will improve the accuracy of property predictions by an order of magnitude.

In summary, this research project has shown that the frequency dependence of subsurface reflectors and vehicle motion generate large errors in impedance and attenuation prediction procedures. The solution to the problem is to improve system bandwidth to at least 2 octaves and to instrument the reflection profiler with motion

sensors. There must be at least 6 dB of attenuation across the system band to allow the attenuation to be accurately estimated. These guidelines will allow selecting the correct pulse bands for future sediment property prediction surveys. Additionally, a new multiband attenuation procedure and automatic layer detection procedure were developed for ONR using CBBL data sets.

Original Objectives:

- 1) Model the performance of normal incidence reflection profilers by using insitu impedance profiles to generate synthetic profiler data sets. The data sets will show the effect of operating frequency on the ability to detect subsurface reflectors and to measure reflection amplitude and echo phase.
- 2) Development of a multi-band reflection profiler that can detect variations in boundary layer impedance produced by a wide range of depositional processes. Make design changes to FM reflection profiler to incorporate results of the synthetic data analysis, thereby improving the performance of the chirp sonar for remotely predicting sediment properties.
- 3) Use chirp data collected at CBBL core sites to test sediment classification algorithms developed for ONR. Test and make improvements to impedance and attenuation prediction procedures as CBBL chirp and core data become available

Approach:

- 1) Generate Synthetic Acoustic Returns - Vertical impedance profiles derived from compressional wave velocity and bulk density measurements along core samples are the input to a numerical model that generates synthetic acoustic data. The model breaks the impedance profile into thin layers which are much smaller than the wavelength of the acoustic pulse. Multilayer transmission theory is used to calculate the frequency response of the seabed. The inverse Fourier transform of the frequency response is the impulse response of the seabed. The synthetic acoustic return is the transmitted pulse convolved with the seabed impulse response. Pulse bands are varied to determine which bands are the best for detecting various subsurface sediment structures.
- 2) Look at frequency dependence of subsurface reflectors - Certain sections of the impedance profiles were studied to understand the relationship between the vertical variation in impedance and the frequency response of the seabed. The frequency dependence of the sediment-water interface reflection was determined by this analysis.

Varying the pulse bands and studying the effects of impedance gradients on the reflectivity of the layer interfaces provide guidelines for selecting pulse bands that maximize reflector echo strength

3) Test sediment classification procedures on data sets - Algorithms that predict attenuation and impedance properties from FM data were tested at core sites. Variations in impedance and attenuation should compare closely with core measurements of those properties. Study differences between predicted and core measurements of acoustic properties to improve the accuracy of the remote predictions. Perform repeated predictions of acoustic properties in the vicinity of the cores to test repeatability of measurements

4) Use the results of the synthetic data and sediment property prediction studies to design a new profiler that can perform remote predictions with improved accuracy. The design is performed after identifying the causes of error in the remote prediction procedures. Projectors with overlapping bands will be used to cover the full band required for generating the frequency diversity needed for accurate property estimation. Receiving arrays are designed to limit scattering interference without making the beamwidth too narrow making the sonar measurement accuracy sensitive to vehicle motion and seabed slopes.

Results:

Impedance modeling (Schock, 1996) showed that the reflection coefficient of the sediment-water interface can vary about 6 dB over 1 octave and that variability depends on the width and shape of the transition of the impedance gradient at the sediment-water interface. Subsurface impedance changes are usually frequency dependent. Gradual changes in impedance seen in some core samples require frequencies as low as 400 Hz for reliable detection. Constructive interference from impedance gradients can cause two profilers operating in different bands to predict different sediment types. Frequency diversity (wide bandwidth) is required to solve this problem.

Impedance prediction studies

Impedance inversion procedures are affected by attenuation, scattering interference, vehicle motion and sea floor slope. If a profiler has a system beamwidth of 20 degrees, the error in the reflection coefficient measurement is 50% (6dB) when the fish pitches 10 degrees. To discard data at high pitch angles or to correct for beam pattern effects, a motion sensor is required to be mounted in the sonar vehicle. Vehicle motion accounts for most of the differences between predicted surficial impedance and the sediment impedance measured from core data at the CBBL sites.

DeBruin(1995) developed a impedance inversion procedure that searched for the best impedance profile using a genetic algorithm. The algorithm did not consistently converge to the impedance profile derived from cores. Scattering interference from volume and surface scatterers is the most likely cause of the impedance prediction errors. Widening

bandwidth would reduce the interference since scattering interference is proportional to the processed pulse length.

Attenuation property prediction

Significant progress was made in remotely predicting subsurface attenuation. The method of measuring attenuation by measuring the shift in center frequency was discarded because scattering interference and frequency dependent layer interfaces strongly influenced the center frequency of the pulse. Those random variations in center frequency prevented the accurate measurement of the center frequency as the pulse traveled through the seabed and the high frequency energy was attenuation at a high rate than the lower frequency energy.

A multiband approach was developed for ONR and tested on data sets collected under this program. The method used fuzzy multi-feature pattern recognition to find layer interfaces in a 2 step procedure. The first fuzzy logic procedure eliminated random scatterers by examining the relative position and amplitudes of adjacent echos; similar echos were grouped into layer segments. Layer segments were logically connected using a second fuzzy logic algorithm designed to handle the random variability in reflector amplitude and discontinuities in the reflection horizon. The detected layer positions are used in the multiband processing procedure.

In the multiband processing procedure, several images are formed by bandpass sampling the raw data into several bands. Each band provides a unique image. Reflector amplitudes are weaker in the higher band images. This phenomenon can be used to measure the amplitude ratio between any 2 reflectors for each frequency band. The plot of the amplitude ratio as a function of frequency band is used to measure the attenuation coefficient, the slope of the attenuation function. Figures 1 -5 show examples of how the algorithm is executed and the bands of each of the filtered data sets. Table 1 provides a summary of some of the attenuation measurements at core sites in the Baltic, Florida Bay and offshore of Panama City. Note that attenuation is approximately linear with frequency at most sites.

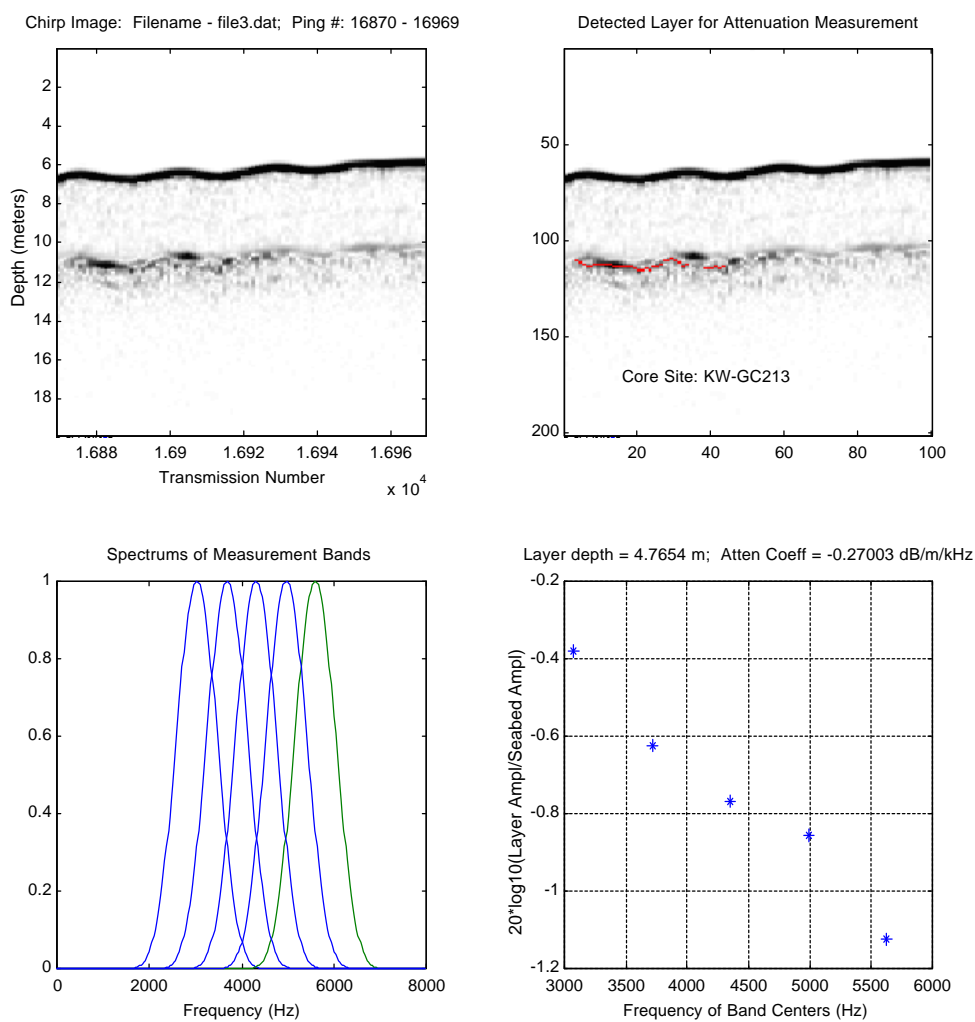


Figure 1. Remote attenuation measurement at core site GC-213 near the Dry Tortugas

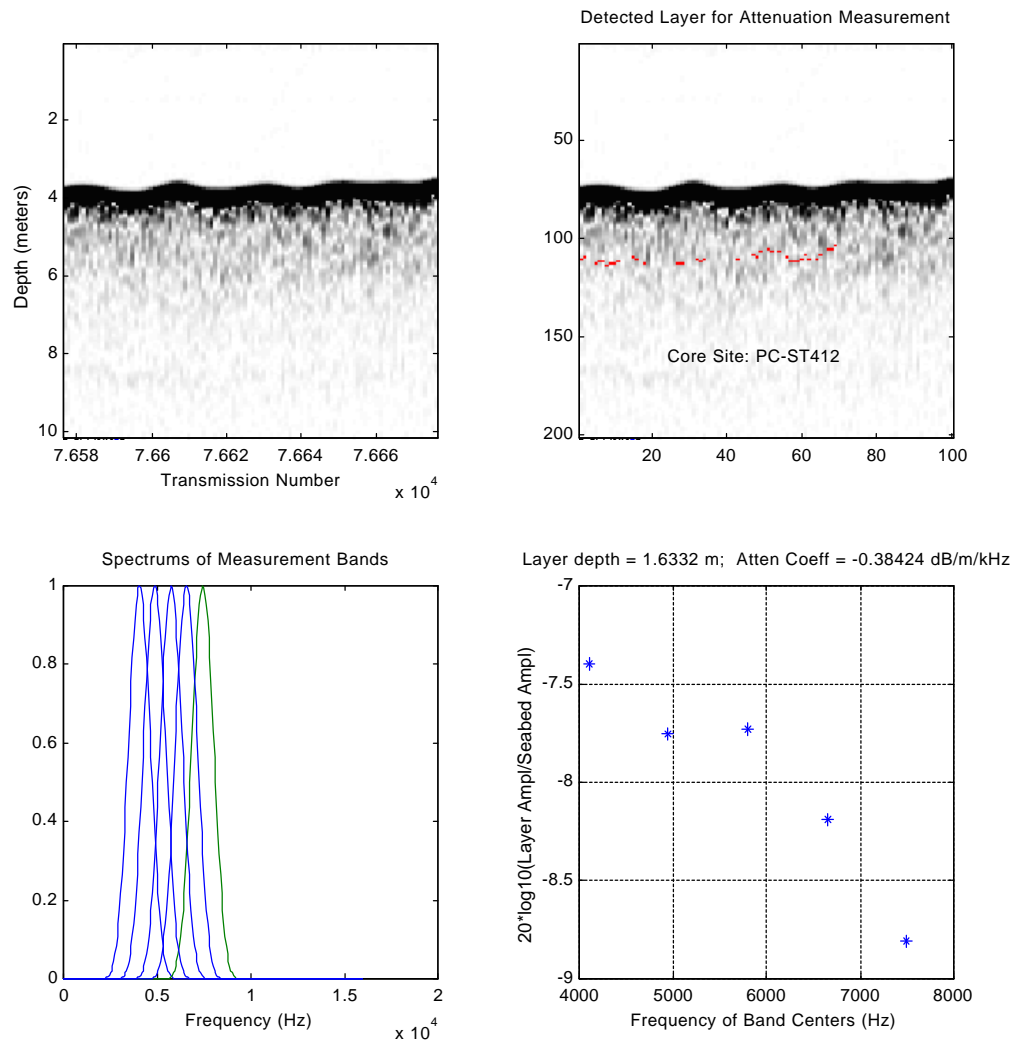


Figure 2. Remote attenuation measurement at core site ST-412 near the Panama City

New Sonar Design

The new chirp sonar design uses 2 projectors and 4 sets of receiving arrays. The receiving arrays allows the beamwidth of the system to be controlled as a function of frequency during receiver processing. The 2 projectors extends the system bandwidth to 1 to 20 kHz. The higher frequencies will improved the sensitivity of the attenuation measurement. The lower end of the band generates the long wavelengths necessary to detect gradual impedance gradients

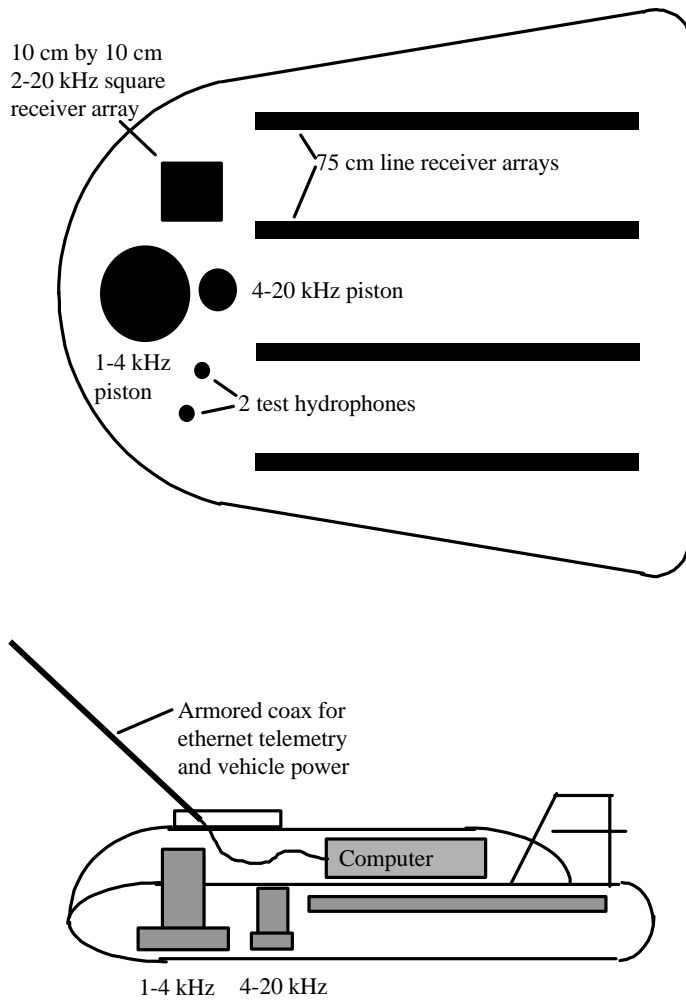


Figure 6. Configuration of acoustic transducers and arrays in redesigned towed chirp sonar

Core Sample	Tape	Tape Position	Ping Number	Latitude	Longitude	Bulk Density (g/cc)	MGS (phi)	Porosity (%)	Velocity (m/s)	Attenuation (dB/m/kHz)	Length (m)
GC147	KW-4	F21R2004	104303	24°36.562'N	82°51.566'W	1.89	5.49	50.11	1514.60	0.37	1.82
GC208	KW-4	F22R3004	110303	24°36.670'N	82°51.990'W	1.85	6.57	49.39	1630.23	0.11-0.27	2.38
GC210	KW-5	F3 R1750	17675	24°36.480'N	82°51.770'W	1.86	5.02	46.68	1634.67	0.25	1.92
GC213	KW-5	F3R1002	16923	24°36.420'N	82°51.980'W	1.88	6.15	47.66	1626.91	0.24	2.38
ST412	PC-2	F0R12008	76577	29°41.110'N	85°40.530'W	2.02		40.25	1709.98	0.37	
GU334	EB-5	F5R736	47280	54°33.397'N	10°07.507'E	1.33			1350.43	<0.1	2.15
GU335	EB-5	F3R6088	44280	54°33.415'N	10°08.482'E	1.43			1388.71	<0.1	2.15
GU336	EB-5	F3R6000	41280	54°33.422'N	10°09.592'E	1.42			1411.28	<0.1	2.10

Table 1. Summary of remote attenuation measurements at CBBL core sites

Accomplishments:

1) A new chirp sonar optimized for remote measurement of sediment properties has been developed and tested. The sonar has twice the bandwidth of previous chirp sonar. This improvement was realized by using two transmitting and two receiving channels. The sonar is instrumented with motion sensors to prevent errors associated with a narrow beamwidth and tow fish pitching and heaving. The correlation processor is performed in the fish and the digital output is sent to the topside via a coax which eliminates multiconductor cable problems.

2) A robust sediment classification procedure has been developed and tested for remotely estimating attenuation of subsurface sediments. It measures the reflector amplitude of images in different bands to estimate the slope of the attenuation function. The reflectors are found using two fuzzy logic pattern recognition procedures. The method is efficient enough to run in real time. This is a major step toward automated sediment property prediction.

Publications:

Peer Reviewed

1. "A multiband approach for remote attenuation estimation of the seabed, JASA (In prep)
2. " Remote predictions of acoustic sediment properties at CBBL sites" Marine Geology (in prep)
3. " Remote prediction of sediment properties using a wideband FM profiler" IEEE J. of Oceanic Engineering (in prep)

Proceedings:

- 1 "Analysis of wideband FM subbottomdata from Kiel Bay, Germany," S.G. Schock and L.R. LeBlanc, EOS Abstract, Jan 18, 1994 Suppl., Ocean Sciences 94, San Diego.
- 2 "Normal incidence sediment classification using wideband FM pulses in Eckernforde Bay," S.G Schock, Lester LeBlanc, Darryl DeBruin and Lachlan Munro, Proceedings of the Workshop Modelling Methane-Rich Sediments of Eckernforde Bay, 26-30 June 1995, Eckernforde, FWG-Report 22.
- 3 "Predicting vertical profiles of sediment properties from seismograms ," S. G. Schock. Oceanology International Conf. Proc., Brighton, 5-8 March 1996.
- 4 "A comparison of chirp sonar and penetrometer measurements in the Dry Tortugas, S. Schock, Proc. of CBBL Key West Workshop, Stennis Space Center, Feb 4-7, 1997.

Published Abstracts:

1. "FM sonar characteristics for normal-incidence sediment classification," S.G. Schock and L.R. LeBlanc, JASA 96(5) Pt. 2, Nov 1994, p.3222.
- 2 "Correlation of acoustic impedance and volume scattering with sediment mean grain size and bulk density, D.L. DeBruin, L.R. LeBlanc and S.G. Schock, JASA 96(5), Pt. 2, Nov 1994, p.3223.
- 3 "High resolution volume backscattering and attenuation measurements in marine sediments," Abstract, Meeting of the Acoust. Soc of Amer., June 94
- 4 "Full Spectrum sediment property predictions near the Dry Tortugas and Marquesas," S. G. Schock, L.R. LeBlanc and D. DeBruin. Abstract. 1st SEPM Congress on Sedimentary Geology, St. Pete Beach, August 13- 16, 1995.

Theses:

1. "The development and application of a numerical model for predicting the frequency response of the seabed from vertical profiles of sediment impedance" J. L. Zhang, Master's of Science Thesis, Florida Atlantic University, 1996.
2. "Sediment Classification of the Sea Floor Using the Chirp Sonar and the Biot Model" P. Beaujean, Master's of Science Thesis, Florida Atlantic University, 1996.
3. "A Neural Network Sediment Layer Tracker" V. Freyermuth, Master's of Science Thesis, Florida Atlantic University, 1998.

Dissertations:

1. "Classification of Marine Sediments Using a Fuzzy Logic Impedance Inversion Model," D. DeBruin, Ph.D. Dissertation, Florida Atlantic University, 1995.

Effects of Carbonate Dissolution and Precipitation on Sediment Physical Properties and Structure----Pore Water Flux Component

A. SHILLER

Professor of Marine Science
Department of Marine Science
University of Southern Mississippi
Stennis Space Center, MS 39529

Abstract: Our project involved providing geochemical support to the efforts to understand sediments in the lower Florida Keys. In particular we examined the issue of how biogeochemistry affects sediment structure and properties, especially with regard to precipitation and dissolution of carbonates. This work focused on collection and interpretation of sedimentary pore water data. Six box cores and three gravity cores were examined; most of these cores were from the Southeast Channel region of the Dry Tortugas. Perhaps the most surprising result was that despite vigorous oxygen consumption near the sediment-water interface, there is little change in most pore water parameters between 10 cm and 1 m below seafloor. This, and other results, can best be explained as resulting from the deep burrowing activities of Callinassid shrimp which are found in the study region. The pumping/irrigation activity of the shrimp result in rapid exchange of pore waters and bottom waters, preventing the accumulation of the by-products of organic matter diagenesis. Without a buildup of alkalinity in the pore waters, cementation is unlikely to occur. Additionally, the relatively shallow depth to basement, combined with the low sedimentary organic carbon, means that methane generation is unlikely to occur in these sediments even below the depth of irrigation.

Original Objectives: The initial objective of our work was to provide support to efforts to model carbonate dissolution/precipitation in the lower Florida Keys sediments as coordinated by Dr. Kathleen Fischer. In particular our objectives were to focus on chemical fluxes across the sediment-water interface and to examine the iron and manganese systems in the sediments. Subsequent to Dr. Fischer's departure from the program, we expanded our objectives to include a more comprehensive look at the pore water chemistry including analysis of other oxidants as well as an examination of the CO₂ system. The rationale for our work stems from the well-established idea (e.g., Froelich et al., 1979) that diagenesis of organic matter is an important driving force for changes in certain other sedimentary components. These changes in other components could well affect sedimentary structure and bulk properties. At the lower Florida Keys sites, which are dominated by carbonate sediments, the effect of diagenesis on carbonate dissolution and precipitation is the major geochemical process of interest.

Approach: Degradation of organic matter in sediments proceeds via a sequence of thermodynamically-determined reactions (e.g., Froelich et al., 1979). Initially, the organic matter is consumed by normal oxic respiration. When oxygen is used up, certain bacteria can then

mediate organic matter oxidation (and obtain energy in the process) using nitrate as the terminal electron acceptor rather than oxygen. As nitrate is used up, then manganese oxides, ferric oxides, and sulfate are all used in sequence. This diagenetic sequence is explained by thermodynamic calculations that show that the first oxidants in the sequence yield more energy per mole of oxidized organic matter than the later oxidants.

This thermodynamic sequence of reactions is commonly observed in sediments and has implications for sediment physical properties and structure. There are a number of reasons for this. First, the various oxidative pathways can generate or consume protons/alkalinity, depending on the particular oxidant involved. For instance typical aerobic respiration generates protons whereas anaerobic respiration utilizing manganese oxides consumes protons (i.e., generates alkalinity). This consumption or production of protons also means that organic matter degradation can drive carbonate dissolution or precipitation in the sediments. In nearshore carbonate sediments (where productivity and hence sedimentary diagenesis rates are high) this could be an important factor in affecting sediment physical properties and structure.

A second way in which organic diagenesis can affect the sediments relates to the production of ferrous iron (Fe^{2+}) during the use of ferric oxides to oxidize organic matter. In sulfide-rich waters (as anoxic pore waters are prone to be), the ferrous iron is precipitated as a sulfide. This produces a new phase in the sediments which, depending on its prevalence, may or may not affect sediment properties. Also, the formation of solid iron sulfide ties up dissolved sulfide, preventing it from diffusing to the oxic layer of the sediments where its oxidation would produce protons which could then result in carbonate dissolution.

A third effect of organic diagenesis on sediment properties can happen when sulfate runs out in anoxic pore waters. Organic matter diagenesis can then proceed via methane fermentation. In instances where there are very high amounts of organic matter in the sediments, this can result in the formation of methane bubbles or pockets in the sediments at fairly shallow depths. The effect on sediment physical properties and structure in such cases is quite obvious.

An additional effect of organic diagenesis relates to the release of phosphate. Under certain conditions phosphate can precipitate to form phosphatic authigenic minerals such as apatite (a calcium fluor-phosphate mineral) and vivianite (ferrous phosphate). For instance, in the shallow, anoxic carbonate sediments of Florida Bay and Bermuda, Berner (1974) reported evidence for apatite formation.

The methodology for our studies included 1) microelectrode profiling across the sediment water interface (of retrieved cores) for oxygen, pH, and resistivity, 2) collection of pore waters from box cores by utilization of whole-core squeezers, and 3) collection of pore waters from gravity cores by sectioning under N_2 and centrifugation. Pore waters were analyzed for ammonia, total CO_2 , alkalinity, sulfate, manganese, iron, fluoride, strontium, barium, rubidium, lithium, molybdenum, and uranium. Solid phase analyses of manganese were also performed. Pore water profiles were evaluated qualitatively and also quantitatively using established principles of pore water modeling (e.g., Boudreau, 1997). Five box cores were examined during the February 1995 Key West Campaign and an additional three gravity cores and one box core were examined during

the June 1997 return cruise.

Results: Figure 1 summarizes typical results from the Southeast Channel test area near the Dry Tortugas. Oxygen is rapidly consumed in the upper ~3 mm indicating the high oxygen demand of these sediments. A laboratory experiment, examining O_2 consumption in poisoned and unpoisoned sediments, indicated that most of this oxygen consumption was due to aerobic respiration. A simple diffusion model applied to the O_2 profile indicates a flux of $530 \mu\text{mol } O_2 \text{ cm}^{-2} \text{ yr}^{-1}$ into the sediments. This is quite high compared to other environments where similar measurements have been made. For example Jahnke (1990) reports an O_2 flux across Santa Monica Basin sediments of $13 \mu\text{mol } O_2 \text{ cm}^{-2} \text{ yr}^{-1}$ and Cai et al. (1995) report a flux of $58 \mu\text{mol } O_2 \text{ cm}^{-2} \text{ yr}^{-1}$ for California rise sediments. Of course, these other locations are deeper and less productive than the shallow Tortugas sediments and the differences are not unreasonable. Given the high sedimentation rate at the SE Channel site, interfacial sediments only need to be ~5% organic carbon to support the oxygen flux.

Dissolved manganese shows a maximum around 5 cm depth. Mn concentrations in the box cores never exceed a few hundred nanomolar. This is substantially lower than is commonly observed in suboxic pore waters. Part of the reason for these low values may stem from the low (~10%) terrigenous component of these sediments which results in solid phase manganese concentrations an order of magnitude lower than is typical of oxic siliciclastic sediments. Although bioturbation can increase the cycling of manganese in sub-oxic pore waters (sometimes leading to it being the dominant oxidant of organic carbon; e.g., Aller, 1990), even the most generous assumptions about Mn cycling in the Tortugas sediments indicate that this element is not an important part of organic matter diagenesis in this area. Likewise Fe and nitrate are unlikely to be important secondary oxidants of organic matter in these sediments.

Despite the lack of sulfate depletion in the pore waters, there is evidence that sulfate reduction was occurring. This evidence includes determination of trace reduced sulfur species in the pore waters (Stephens et al., 1997) as well as observation of pyrite framboids apparently forming in situ (Furukawa et al., 1997; C. Brunner, pers. comm.). Calculations demonstrate that only a little deep irrigation is required to keep pore water sulfate at seawater levels even with moderate rates of sulfate reduction. The irrigation could easily be done by the deep burrowing Callianassid shrimp in the study region (D'Andrea and Lopez, 1997).

Total CO_2 and ammonia both showed maxima around 5-10 cm depth, decreasing back to lower, more bottom water-like conditions. Even in the maximum, total CO_2 was never more than double bottom water concentrations. Likewise alkalinity showed only small changes from seawater values.

Organic carbon in the sediments was generally low, decreasing from ~0.6% in the upper 5 cm to 0.35% by ~50 cm. Low values are consistent with efficient remineralization of organic carbon during oscillating redox conditions caused by bioirrigation/bioturbation (Aller, 1994). Dissolved strontium showed a slight depletion in the box cores, compatible with uptake into minor aragonitic overgrowths. Deeper in the gravity cores, strontium increases indicating net carbonate dissolution/recrystallization.

Accomplishments: The basic accomplishment of this project has been to link benthic biological activity, sediment grain size, and pore water chemistry in a “pump-and-poop” conceptual model. The concept is developed as follows. Sediments in the Dry Tortugas region are extensively bioturbated. A simplified representation of the bioturbating community indicates a near surface community dominated by spionid polychaetes and a deep deposit-feeding community dominated by Callianassid shrimp and the large polychaete *Notomastus* (D’Andrea and Lopez, 1997). One effect of the surface deposit feeders is to convert sedimentary organic matter into feces—that is, material which is in a form to be readily utilized by the microbial community which likely dominates the sedimentary respiration. However, the most important benthic organisms (at least from the point of view of geochemistry and lithology) are the deep burrowing Callianassid shrimp. These organisms burrow deeply into the sediments (>1 m) forming large (~cm diameter) complex chambered structures. The shrimp mine fine sediments at rates up to kg/day resulting in the transport of fine materials to the surface. The mass transport rates attributable to the shrimp are enough to account for the 2 cm²/yr mixing rate for sediments below 15 cm as derived from Pb-210 profiles (Bentley and Nittrouer, 1997). The preferential mining and transport upwards of fine sediment by the Callianassid shrimp can also explain the upward fining of the sediments (C. Brunner, pers. commun.), previously attributed to an effect of rising Holocene sea-level (Mallinson et al., 1997). Furthermore, the fine-grained material should have a greater organic matter content and this, combined with the biological mixing of the sediments, could explain some of the increase in organic carbon content of sediments in the upper ~50 cm.

With regard to the geochemistry, the Callianassid shrimp are responsible for a significant pumping of bottom water through their burrow structures (~6 ml/hr/shrimp; Forster and Graf, 1995). This keeps the pore waters between ~10 and 150 cm looking more oxic than the upper 10 cm of the sediments where oxic/suboxic respiration rates are undoubtedly highest (Forster and Graf indicate an oxygenation rate of ~100 μmol O₂ m⁻² day⁻¹ shrimp⁻¹). We estimate that this pump rate would supply sulfate to the deep pore waters at a rate greater than sulfate reduction would remove it. More important, this pumping prevents the alkalinity from deviating significantly from seawater. Without the bio-irrigation alkalinity would significantly increase with depth in the pore waters due to alkalinity generation during sub-oxic and anaerobic respiration. Such an alkalinity generation is probably necessary for significant cementation to take place. The bio-irrigation, which likely results in localized oscillating redox conditions within the upper part of the sediment column, may also explain the low average organic carbon content of these sediments (Aller, 1994). Furthermore, the relatively shallow depth to basement (~3 m) combined with the low sedimentary organic carbon content and >1 m bio-irrigated region results in a lack of methane generation. Oxidation of methane would also result in alkalinity generation and probable cementation as well as the possibility of bubble generation.

A biological mystery remaining in this model relates to what the actual food of the shrimp is. That is, the sediment processing abilities of the shrimp are such that one would expect the sediments to be depleted of organic food on short order. Some process presumably must be putting organic matter back into the sediments.

The take-home message is that while one would ordinarily expect sediment geochemistry to have a significant impact on the acoustic properties of shallow marine carbonate sediments (through processes such as cementation and gas generation), the signature and effect of the geochemical processes have been substantially erased in the Dry Tortugas sediments largely through the burrowing and irrigation of the Callianassid shrimp. The presence of these shrimp in a given environment is likely to be a key biogeochemical indicator of use in predicting sediment acoustic properties.

References:

Aller, R.C. 1990. Bioturbation and manganese cycling in hemipelagic sediments. *Phil. Trans. R. Soc. Lond. A* 331: 51-68.

Aller, R.C. 1994. Bioturbation and remineralization of sedimentary organic matter: effects of redox oscillation. *Chem. Geol.* 114: 331-345.

Bentley, S.J. and C.A. Nittrouer 1997. Environmental influences on the formation of sedimentary fabric in a fine-grained carbonate-shelf environment: Dry Tortugas, Florida Keys. *Geo-Marine Lett.* 17: 268-275.

Berner, R.A. 1974. Kinetic models for the early diagenesis of nitrogen, sulfur, phosphorus, and silicon in anoxic marine sediments. In *The Sea*, Vol. 5 (E.D. Goldberg, ed.), Wiley, pp. 427-450.

Boudreau, B.P. 1997. *Diagenetic models and their interpretation*. Springer, 414 pp.

Cai, W., C.E. Reimers and T. Shaw 1995. Microelectrode studies of organic carbon degradation and calcite dissolution at a California Continental rise site. *Geochim. Cosmochim. Acta* 59: 497-511.

D'Andrea, A.F. and G.R. Lopez 1997. Benthic macrofauna in a shallow water carbonate sediment: major bioturbators at the Dry Tortugas. *Geo-Marine Lett.* 17: 276-282.

Forster, S. and G. Graf 1995. Impact of irrigation on oxygen flux into the sediment: intermittent pumping by *Callianassa subterranea* and "piston-pumping" by *Lanice conchilega*. *Marine Biology* 123: 335-346.

Froelich, P.N. et al. 1979. Early oxidation of organic matter in pelagic sediments of the eastern equatorial Atlantic: suboxic diagenesis. *Geochim. Cosmochim. Acta* 43: 1075-1090.

Furukawa, Y., D. Lavoie, K. Stephens 1997. Effect of biogeochemical diagenesis on sediment fabric in shallow marine carbonate sediments near the Dry Tortugas, Florida. *Geo-Marine Lett.* 17: 283-290.

Jahnke, R.A. 1990. Early diagenesis of biogenic debris at the seafloor, Santa Monica Basin, California. *J. Mar. Res.* 48: 413-436.

Mallinson, D., S. Locker, M. Hafen, D. Naar, A. Hine, D. Lavoie and S. Schock 1997. A high resolution geological and geophysical investigation of the Dry Tortugas carbonate depositional environment. *Geo-Marine Lett.* 17: 237-245.

Stephens, K.P., D.L. Lavoie, K.B. Briggs, Y. Furukawa, and M.D. Richardson 1997. Geotechnical and geoaoustic properties of sediments off South Florida: Boca Raton, Indian Rocks Beach, Lower Tampa Bay, and the Lower Florida Keys. NRL/MR/7431-97-8042. Naval Research Laboratory, Stennis Space Center, 303 pp.

Publications:

Published abstracts

Shiller, A.M., C.A. Brunner, Y. Furukawa, T. Hebert, and J. Yuan 1998. Early diagenesis of carbonate sediments in the Dry Tortugas and Marquesas Keys, Florida, USA. *Eos, Trans. Amer. Geophys. U.* 79 (1-suppl.): OS95.

Shiller, A.M., C.A. Brunner, Y. Furukawa, T. Hebert, and J. Yuan 1998. Early diagenesis of carbonate sediments in the Dry Tortugas and Marquesas Keys, Florida, USA. *J. Miss. Acad. Sci.* 43(1): 52.

Shiller, A.M. 1997. Evidence for phosphorite formation in sediments of the Dry Tortugas and Marquesas Keys. *J. Miss. Acad. Sci.* 42(1): 63.

Brunner, C.A., A. Reed, R. Elder, A. Falster, and A.M. Shiller, 1996. Effects of organic carbon respiration on preservation of foraminifers from the Dry Tortugas, Florida. *J. Miss. Acad. Sci.* 41(1): 54.

Shiller, A.M., T.L. Hebert, K.R. Thornton, and C.A. Brunner 1995. Sediment chemistry and pore water fluxes in the vicinity of the Dry Tortugas. *The 1st SEPM Congress on Sedimentary Geology, Congress Program and Abstracts*, v. 1, p. 113.

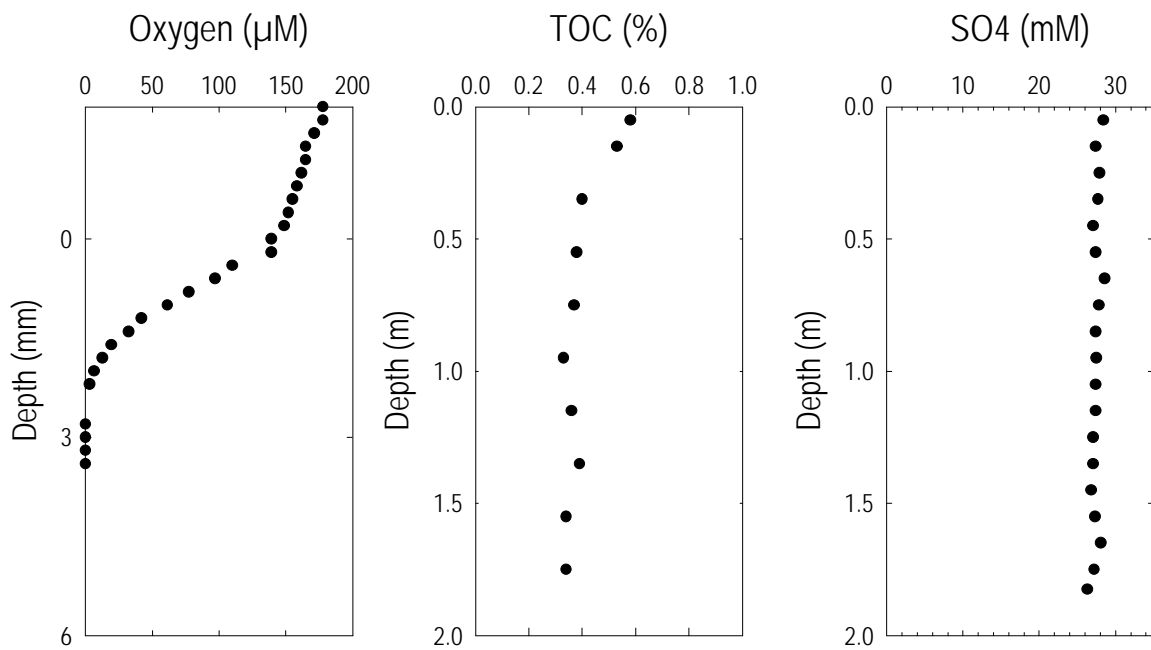


Figure 1a. Dry Tortugas Geochemistry: mm to m scale

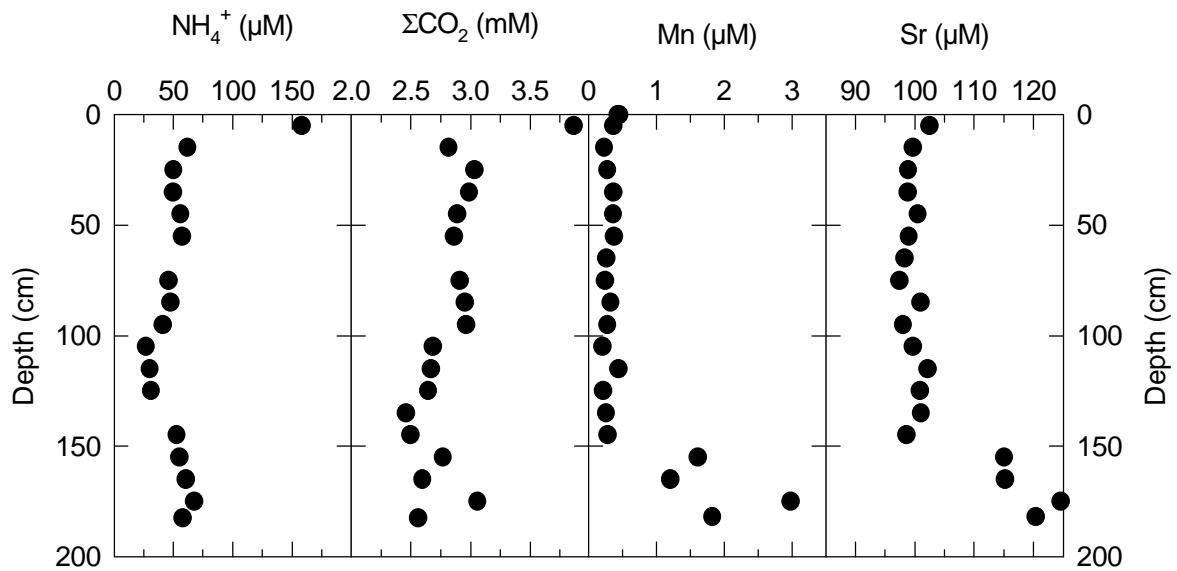


Figure 1b. Gravity core pore water results, Dry Tortugas, Southeast Channel

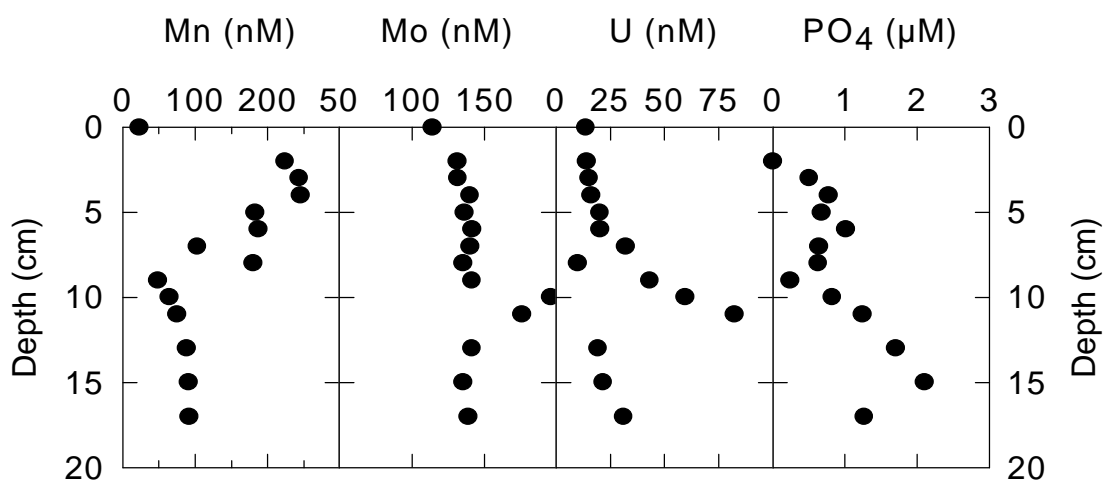


Figure 1c. Dry Tortugas Box Core Results, Southeast Channel

Title: Geomechanical and Geoacoustical Behavior of Nearshore Sediments - CBBL SRP

Principal Investigators: Armand J. Silva, George E. Veyera, Martin H. Sadd,
and Horst G. Brandes

Organization: Marine Geomechanics Laboratory, College of Engineering, University of Rhode Island

Objectives: The focus of studies conducted by the University of Rhode Island research group in support of the CBBL program was on the variability of seabed sediment microstructure, with particular attention on stress-strain behavior in relation to acoustic characteristics and stress wave propagation. In keeping with the hypothesis adopted by the overall project, the assumption was that there is a fundamental linkage between the macroscopic behavior of fine-grained sediments, including physical and mechanical and acoustic characteristics, and the microstructure of the sediment. In order to prove this hypothesis, three types of shallow-water sediments with greatly different genesis, microstructure, and environmental variables were studied in detail in order to contrast and compare the results with each other and integrate them with the findings of other researchers in the program. The overall objective was to gain a better understanding of seabed geotechnical and geoacoustic properties and behavior in relation to the processes and settings in which the sediments are found.

Approach: The behavior of a particular seabed sediment deposit is dependent on many interacting factors such as fluid properties, hydrodynamic forces, bioturbation, diagenetic alteration, and mechanical effects. The introduction of artificial disturbance caused by objects resting on or within the seabed can significantly influence behavioral properties of the sediment, mainly by changing the sediment structural configuration on scales ranging from microns to tens of centimeters. The primary assumption controlling our efforts was that there exists a fundamental linkage between the behavioral properties of fine-grained sediments and the microstructure of the sediment. The approach taken in our research program was to study contrasts over a wide range of sediment microstructures that included naturally deposited flocculated silt-clay mixtures, carbonate sediments, cohesionless sediments and completely remolded samples of these same materials. This involved extensive field research at the three CBBL SRP study sites (Eckernförde, Panama City, FL and the Lower Florida Keys) and detailed laboratory investigations at the University of Rhode Island/Marine Geomechanics Laboratory (URI/MGL). In the field, gravity and box cores were obtained, onboard geotechnical measurements and observations of some of the cores were conducted, and undisturbed and bulk subsamples were obtained for the laboratory program. The MGL research focused on determining the stress-strain behavior and geoacoustic properties of these sediments using the MGL multi-sensor core logger, triaxial acoustic-compression and consolidation-permeability testing systems. In addition, selected whole cores were also analyzed. The laboratory and field data were then integrated to assess the characteristics and variability of each sediment type studied. Where possible, correlations were also made with the findings of other researchers participating in the CBBL SRP.

Results and Accomplishments: Three very different sediment types are present in the three CBBL study sites, ranging from very high porosity, organic, soft silty clays in Eckernförde Bay, to very stiff sandy sediments at the Florida Sand Sheet site south of Panama City, Florida, and calcareous sediments at the Lower Florida Key sites. Each of these materials posed considerable challenges for both sampling and testing to assess the geotechnical and acoustic behavior in relation to the program objectives. MGL research for each of the three sites is summarized in this section.

Eckernförde Bay

The sediments of the inner portion of Eckernförde Bay, Baltic Sea, are organically rich, fine-grained, very soft, of high porosity, and contain varying amounts of methane gas. From a geotechnical point of view, these sediments are very unusual and presented substantial problems and challenges, both in field sampling and for detailed laboratory studies. For example, the undrained shear strength in the upper 50-100 cm is less than 2 kPa, porosities exceed 90% in the upper 5 cm, zones of shells occur at depth, and various amounts of gas are present.

A particular area, approximately 2.6 by 1.1 km (Fig. 1) was selected as the experimental site for the CBBL SRP (Richardson, 1994). The focus of the URI/MGL work was on the geotechnical behavior of the upper 4 to 5 meters of the seabed in the primary study site, with particular emphasis on the in situ stress state and stress-

strain-strength behavior. In addition to annual reports to the CBBL program, the results of the Eckernförde studies are contained the following publications: Silva et al, 1995; Silva et al., 1996; Brandes et al., 1996; Ag, 1994; Brogan, 1995; Ag and Silva, in press, and Silva and Brandes, in press.

The physical property data are derived from 15 cores taken on three different occasions within the study site (Fig. 1). Three types of coring gear were used to obtain samples: a 50×50×50 cm box corer, a 12.7 cm ID gravity corer supplied by German participants from the FWG (February, 1993 and July, 1994), and the URI gravity corer with an inside diameter of 10.2 cm (May, 1993).

There was distinct evidence of degassing of the February, 1993 gravity cores, manifested by voids, fractures, and a “crumbly” appearance of the sediment. Some of the gravity cores were stored at seabed pressures in special pressurized chambers and X-rayed using a Computer Aided Tomography (CAT) system to generate density images, from which in situ gas bubble concentration profiles were determined (Abegg & Anderson, 1996). Figure 2 shows an example of a 2-D image of the cross-section of a core from a pockmark (depression) region outside of the primary test site exhibiting numerous gas bubbles.

The grain size distributions show little vertical variation with a clay size fraction (2 μm or $f=9.0$) of about 55% and a silt size of 42% (Table 1). The sediment is a dark gray to black organic-rich silty clay. The organic content, determined by incineration, is relatively constant with depth with an average value of 12% by dry weight. The water contents show extreme variability within the upper 5 cm (224-668%) with an average value of about 349%. X-ray diffraction and liquid limit tests indicated only a small amount of smectite. Part, if not most of the silt fraction, consists of palletized sediments, which if further desegregated, reveals individual particles in the clay-size range (Nittrouer et al., in press).

Taken individually, all the box cores show sharp water content and density gradients in the upper 5 to 10 cm and one of the better examples of these trends is shown in Fig. 3. Also shown are the measured bulk densities, the density profile calculated from the water content profile assuming saturation with sea water, and the shear strength profile determined with a motorized miniature vane shear device. For this core, obtained in May, 1993, the agreement between measured and calculated densities is very good, indicating there was essentially no free gas in the upper 50 cm of the sediment column. However, similar data from box cores taken in February, 1993 showed a large disparity between measured and calculated densities. These trends are also apparent when data from all 11 box cores are combined (Fig. 4). Differences between measured and calculated densities are due to expansion of gas upon depressurization. The amount of gas, based on total sediment volume, ranges up to 6%. Cores collected during February, 1993 showed much higher evidence of gas expansion than cores collected during May, 1993, indicating seasonal fluctuations of in situ gas concentrations. Similar observations are reported by Wever et al. (1995).

The water content trendline shown in Fig. 4 was obtained by linear regression analysis and can be described by the following two equations:

$$w = 38.890 \ln \frac{9333}{z} \quad z = 0 - 10 \text{ cm} \quad (1)$$

$$w = 266 \quad z = 10-50 \text{ cm} \quad (2)$$

where water content, w , is in percent and depth, z , is in cm below the mudline. The trend line corresponding to Equation 1 is derived from all the box cores in the study site. The sharp gradients in water content and density are associated with the high rate of sedimentation and interparticle bonding that inhibits consolidation. It is also probable that biological reworking in the upper few centimeters further disrupts the sediment microstructure and contributes to the unusually high water contents near the surface. Since acoustic impedance is directly related to density contrasts, the upper 10 cm can be expected to significantly affect the propagation of incident acoustic energy. Also, the extremely low density sediments in the upper few centimeters could make accurate detection of the water-sediment interface problematic.

Below 50 cm, gravity cores reveal zones of variable water content and density, but the overall trend shows decreasing water content (and increasing density) with depth. The following equations characterize the trend:

$$w = 266 - 0.064 (z-50) \quad z = 50 - 300 \text{ cm} \quad (3)$$

$$w = 250 - 0.200 (z-300) \quad z = 300 - 500 \text{ cm} \quad (4)$$

The calculated saturated densities were considerably larger than the measured values below 50 cm depth. Once again, this is confirmation of the presence of gas in these sediments.

Shear strength measurements show a non-linear increase of undrained strength in the upper 50 cm (Fig. 4), which can be characterized by the following equation:

$$S_u = 0.353z^{0.382} \quad z = 0 - 50 \text{ cm} \quad (5)$$

where shear strength, S_u , is in kPa and depth, z , is in cm. Below 50 cm, the shear strength increases linearly with depth:

$$S_u = 1.573 + 0.01152(z-50) \quad z = 50 - 500 \text{ cm} \quad (6)$$

When plotted on Casagrande's plasticity chart, the Atterberg limits for the Eckernförde Bay sediments plot near the A-line (see Terzaghi and Peck, 1967), but at much higher combinations of plasticity index and liquid limit than most inorganic clays of either terrestrial or marine origin (Fig. 5). From an engineering behavior point of view, sediments plotting near the A-line are considered borderline silt-clay materials. The Atterberg limits values for Eckernförde Bay are comparable to data reported by Keller (1982) for organic-rich deposits on the Peru upper slope that have similar organic contents, in the 2% to 20% range, and to smectite-rich deep sea clays (Silva and Jordan, 1984). Since there is little evidence of smectite in the Eckernförde Bay sediments, the high Atterberg limits are attributed to the organic content.

The compressibility, permeability and stress state characteristics were determined from 21 constant-rate-of-deformation (CRD) consolidation tests conducted on undisturbed, remolded, and vertically and horizontally oriented samples collected from various box cores and gravity cores throughout the study site. All of the samples tested were very compressible, with C_c (compression index) values ranging between 2.7 and 6.8. Detailed results are given by Brandes et al. (1996) and Ag (1994). Most of the variability in compressibility occurs in the upper 50 cm, where values range between 3.1 and 6.8. This corresponds to the zone with the largest gradients in water content, density and shear strength. In the upper 50 cm, there appears to be little difference in compressibility between the vertical and horizontal directions as determined from one horizontally oriented sample, which suggests that the material has isotropic microstructure in this surficial zone.

For inorganic clays, good linear correlations have been found between the liquid limit and the compression index. However, data for our sediments indicate that the organic sediments in Eckernförde Bay are more highly compressible than published data and therefore C_c does not correlate well with the liquid limit. Microstructural studies by Lavoie et al. (1996) indicate aggregates of small clay-size particles that are linked together with each other and with larger biogenic components. It is evident that organics play an important role in controlling the entire range of sediment engineering properties and therefore can be expected to affect the mechanical and acoustical behavior of these sediments as well.

The in situ stress state is characterized by two stress measures: the preconsolidation stress, s'_c ; and the calculated existing effective overburden stress, s'_o , (assuming no excess pore pressures). Either the stress state ratio (SSR) or overconsolidation ratio (OCR) are used as a measure of the stress state:

$$SSR = OCR = \frac{s'_c}{s'_o} \quad (7)$$

The overburden stress, calculated by integrating the saturated density profile, is seen to increase non-linearly with depth (Fig. 6). The difference between s'_c and s'_o (referred to as the stress state difference, SSD) is attributed to interparticle bonds caused by physico-chemical means rather than by the removal of sediment overburden. This is known as *apparent* overconsolidation and has been observed at many deep-sea locations around the world (Silva and Jordan, 1984). The very high SSR/OCR values shown for the upper 50-100 cm in Fig. 6 are not unusual for surficial fine-grained marine sediments. The stress state approaches a normally consolidated condition (i.e. SSR = unity) at a depth of about 2.5 meters.

Permeability results on box core samples indicate an $e \log k$ relationship of the form:

$$k = \exp\left(\frac{e - 16.5}{0.79}\right) \quad (8)$$

where k is the permeability in cm/s and e is the void ratio. Since the volume of in situ free gas, when present, is typically less than 0.5% by volume at most locations, Eq. 8 can be used for depths below 50 cm as a first approximation of permeability. Using calculated in situ void ratios with Eq. 8, the in situ permeability varies significantly in the upper 10 cm, approaching a value of 10^{-5} cm/s near the surface. Below the 10-20 cm depth, permeabilities remain in the 3 to 4×10^{-6} cm/s range to a depth of 300 cm. The average coefficient of permeability of the upper 40 cm at in situ void ratios is about 4×10^{-6} cm/s.

Seven triaxial tests were conducted on samples taken from three box cores: BC-252, 238 and 225. The results show well defined peaks of maximum deviator stress at relatively low values of strain, ranging from 1.4% to 4.3% (Fig. 7). Pore pressures increased continuously in all tests, and the general shapes of the stress paths for all samples were indicative of normally consolidated behavior. When all test results are combined in a q - p plot (Fig. 7), there is some scatter about the least squares best fit line, but the average effective angle of internal friction is 22° (assuming the sediment possesses zero cohesion). Comparisons with published results for other soft marine clays suggests that, although the Baltic sediments appear to be unique in terms of organic content, microstructure, porosity, and Atterberg limits, the strength properties are related to plasticity index in ways similar to normally consolidated clays (Silva and Brandes, in press). Despite the atypical index properties of high porosity, high organic content, and high compressibility, and despite the zone of apparent overconsolidation, the sediments at the CBBL experimental site show normally consolidated behavior, but with a low friction angle.

Given the very soft nature of the sediments found at the primary study site, many applications such as penetration of objects into the seabed, will undoubtedly involve rapid shearing of the sediment. Therefore, in addition to the elasto-plastic properties previously discussed, it was also of interest to determine the viscous properties of the material. The rheological characteristics of this very soft sediment were investigated at various depths by conducting a series of stress-strain-time measurements using an 8 mm x 8 mm vane attached to a Brookfield viscometer at rates of rotation ranging from 0.5 to 100 rpm. The dependence of shear stress on the rate of rotation at four different depths is shown in Fig. 8. Overall, there is a clear trend of rapidly decreasing strength from the quasi-static state to about 20 rpm, after which the strength becomes nearly constant. This decrease in strength is indicative of shear-thinning behavior associated with non-Newtonian fluids (White, 1991). The same general behavior was present with the residual stresses (large strains) but to a lesser degree. Based on these preliminary tests, it is likely that the sediment begins to behave more like a Bingham material as it consolidates. From a practical point of view, the primary implication is that objects penetrating this type of material will encounter less resistance when traveling at higher velocities, at least within the upper 20-30 cm.

In order to quantify the amount of strength loss due to gas expansion, strength measurements were taken on large-diameter gravity cores at both in situ and sea level pressures. While at the bottom, divers decoupled the PVC barrels containing the sediment from the core head, cut the barrels into 1.0 m sections, and transferred each section into special pressure chambers. Strength measurements were taken with a Wykeham-Farrance device equipped with a sensitive torsional spring and a 25.4 x 12.5 mm vane. The difference between pressurized and unpressurized strength becomes most evident below 60 cm where gas bubbles larger than 1.0 mm are detected at concentrations up to 1.0% by volume. The maximum difference in strength appears to be about 0.5 kPa between 80 and 140 cm depth, corresponding to a 38% loss in strength due to depressurization at 60 cm and a 16% loss at 140 cm. Disruption of the sediment fabric upon depressurization resulted in undrained shear strength losses of 16% to 38% at the main study site and up to 64% at a nearby pockmark where the gas content is higher.

Following are some of the findings and conclusions of our studies with the Eckernförde Bay sediments:

- The sediment is classified as marine organic silty clay with the following average properties: 12% organic content; 23 ppt. salinity (of pore fluid); 237% liquid limit; and 163% plasticity index.
- There is a very sharp non-linear vertical gradient of water content and density in the upper 10 cm of the sediment column, with water contents exceeding 500% at the surface and decreasing to about 270% at 10 cm depth. This sharp gradient will result in a significant gradient in acoustic impedance contrast, which should be incorporated in acoustic models for the site. The overall trends within the five meter study depth are summarized in Eqs. 1-6.
- Test results on box cores as well as visual observations, show that there are significant seasonal variations in gas content in the upper 50 cm depth, with the gas content being higher in February than in May. It

is recommended that in situ densities be calculated from water contents assuming saturation and a grain density of about 2.6 gm-cm⁻³.

- Compressibility is high with compression indices, C_c , of 2.7 to 6.8 and average of 3.8. The upper 1.5 m exhibits appreciable “apparent” overconsolidation due to interparticle bonding, and the sediment column approaches a normally consolidated condition at a depth of about 2.5 m. The results show that existing correlations between C_c and liquid limit do not apply to these organic rich sediments.

- The permeability is relatively low given the high void ratios with a coefficient of permeability, k , of about 10^{-5} cm/s in the upper few centimeters ($k = 4 \times 10^{-5}$ cm/s in the upper 40 cm), and nearly constant at 3 to 4×10^{-6} cm/s to a depth of 3 meters.

- The undrained shear strength is very low near the surface (0.3 kPa), increases non-linearly with depth in the upper 50 cm to a value of 1.6 kPa, and then linearly to about 6.8 kPa at a depth of 5 m. Eqs. (5) and (6) are presented for these intervals.

- Triaxial compression tests yield a relatively low angle of internal friction of 22° and the stress strain behavior is similar to that of a normally consolidated weak clay. The average c/p' ratio for the seven CIU tests was 0.36.

- The rheological behavior of the surficial sediments in the upper 20-30 cm is indicative of shear thinning whereby both the peak and residual strengths decrease with increasing strain rate, although this effect decreases with depth and the sediment may behave more like a Bingham type material at depths below about 20-30 cm. The implication of the shear thinning phenomenon is that the resistance to dynamic penetration decreases with increasing velocity.

- There are significant strength losses due to expansion of gas upon depressurization, ranging from 16% to 38% at the main study site and 64% at a nearby “pockmark”.

Calcareous Sediments (Lower Florida Keys)

Geotechnical characteristics of carbonate sediments from three test sites near the Lower Florida Keys were investigated (Figure 9). Idealized profiles of physical properties and geotechnical behavior show that variations exists not only within each location, but between the three sites. Sediments in the Dry Tortugas and Marquesas study sites are classified as a well graded gray-white silty clayey carbonate sand with grain sizes ranging from large angular shell fragments to fine carbonate mud, while the Rebecca Shoals location is characterized as a relatively homogenous gray-white silty clay. Geotechnical behavior and acoustic characteristics are briefly discussed for each site in the following sections.

Dry Tortugas Site

Lateral / Vertical Variability: The majority of samples used for the URI/MGL testing program were taken from the “Red Box” location (Figure 10). Calcium carbonate content measurements of the Dry Tortugas sediments show an average value of 91% by weight with a specific gravity ranging from 2.73 to 2.89 (Table 2). In general, in situ void ratios from this site range from 1.0 to 1.6, corresponding to salt corrected natural water contents averaging between 35% to 100%. Little lateral or vertical variability exists, except within the surficial 25 cm. Most of the cores from the Dry Tortugas show a rapid decrease in water content from approximately 75% to 100% just below the surface to 45% at 25 cm depth (Figure 11a). Below 25 cm, there is a gradual reduction in water content to about 35% at cm depth (Silva et al, 1995). Similarly, bulk densities calculated from water content show a rapid increase near the surface to about 1.80 g/cm³ (Figure 11b) and a gradual increase below 25 cm depth. The variation of water content, w in percent, and bulk density, γ in g/cm³ with depth, z in cm, for this site may be approximated as;

$$w = 82.1 z^{-0.190} \quad z < 25 \text{ cm} \quad (9)$$

$$w = 40 - 0.0025 z \quad z > 25 \text{ cm} \quad (10)$$

and

$$\gamma = 1.57 z^{0.0459} \quad z < 25 \text{ cm} \quad (11)$$

$$\gamma = 1.83 + 5 \times 10^{-4} z \quad z > 25 \text{ cm} \quad (12)$$

Most samples from the Dry Tortugas site were determined to be non-plastic. However, samples in which limits were determined averaged 38% and 29% for the liquid and plastic limits, respectively. In general, mean grain size decreases rather significantly with depth while plasticity indices tend to increase down core.

Compressibility and Permeability: Constant rate of deformation (CRD) compressibility and permeability tests were performed on several samples from gravity core GC-313 and box core BC-245 from the Dry Tortugas site (see Figure 12a for typical results and Table 3). The consolidation data show that the sediments have very low compression indices (0.17 to 0.25). These low indices are typical of a relatively stiff material. Stress state ratios range from 0.6 to 50, implying possible cementation and/or interparticle bonding associated with surficial sediment retrieved from this study site.

In situ permeabilities interpolated from measured values ranged from 2.2×10^{-6} cm/s to 7.4×10^{-6} cm/s showing a logarithmic relationship between void ratio and permeability (Table 3, Figure 11b). Sample GC-313 (149 cm) was reconstituted to the original initial void ratio and retested. Remolding altered the sediment structure significantly as the compression index decreased from 0.21 to 0.14 and permeability decreased from 5.1×10^{-6} cm/s to 4.4×10^{-7} cm/s (Silva et al, 1996). These results imply that the remolding process tends to result in a stiffer, less permeable sediment structure; most likely due to a more even distribution of finer-grained particles.

Stress-Strain-Strength Behavior: Isotropically consolidated undrained (CIU) strength tests were conducted on seventeen undisturbed and remolded samples from Dry Tortugas box cores BC-284 and BC-324 (Table 4, Figure 13). The strength behavior of these sediments is typical of uncemented calcareous sediments and loose sands (Pizzimenti and Silva, 1997). During shear, the initial strength response is stiff with initially large excess pore pressures decreasing toward zero at large axial strains and deviatoric stresses continually increasing with loading. These results indicate no signs of brittle behavior characteristic of cemented calcareous sediments. Failure normally occurred for most specimens at axial strains of approximately 10% and the resulting friction angles averaged between 37° to 39° for both undisturbed and remolded samples (Figure 13). Comparisons between undisturbed and remolded sediment deviatoric stress responses during uniaxial loading imply possible particle interlocking associated with this angular sediment, with remolded stress-strain behavior showing a stress relaxation after the initial stiff response. This is most likely a result of particle rearrangement due to a looser fabric and sediment structure for the remolded condition. Conversely, deviatoric stress responses of undisturbed samples do not show stress relaxation and suggest a restriction of particle mobility and a relatively rigid structure. Initial tangent moduli were determined from stress-strain data using the hyperbolic method (Pizzimenti, 1996; Pizzimenti and Silva, 1997). In general, moduli ranged from 130 kPa to 1.9×10^4 kPa over a consolidation stress range of 1 to 34 kPa. Other values are shown in Table 4.

Geoacoustic Characteristics: Geoacoustic properties of sediment from the Dry Tortugas site were determined using URI/MGL's Multi Sensor Core Logger (MSCL) and the triaxial-acoustic cell. Most cores demonstrated a correlation between bulk density and acoustic response. In other words, an increase in density generally corresponded to an increase in compressional wave velocity and impedance, and a decrease in attenuation (Figure 14). In general, density increased with depth for each core; with the most prominent increase occurring in the upper 20 cm. Compressional wave velocities obtained from the MSCL averaged between 1475 m/s to 1650 m/s as determined from selected gravity cores.

In general, it was found that an increase in effective confining stress and decrease in void ratio corresponds to a linear increase in compressional wave and a logarithmic increase in shear wave velocities during isotropic consolidation. (Table 5, Figures 15 and 16). Surficial Dry Tortugas samples shown in Figures 15 and 16 are BC-318 and 245. Velocities averaged between 1435 m/s to 1460 m/s and 21 to 157 m/s over an effective stress range of 1 to 39 kPa for the compressional and shear waves, respectively (Sykora, 1998). These values actually compare reasonably well with MSCL results in the upper few centimeters of the sediment column (1475 m/s). The slight disparity of compressional wave speeds between the MSCL and triaxial measurements has not as yet been determined. However, triaxial-acoustic tests conducted on clean 20/30 Ottawa sand consistently compared well with published values, verifying proper functioning of the acoustic transducers. Wave velocities and density data were used to calculate Young's and shear moduli over a similar stress range; Young's modulus averaged between 2.3×10^6 kPa to 2.5×10^6 kPa, while shear modulus ranged between 8.3×10^2 kPa to 4.7×10^4 kPa (Table 5).

Low shear wave results during isotropic consolidation from a remolded (RM) sample in which the material was mechanically reworked to break possible cementation bonds imply that interparticle bonds tend to facilitate shear wave propagation (Figure 16). Similarly, shear wave velocity results during undrained uniaxial loading imply cementation. There was an interesting trend of changing shear wave velocity during the application of vertical deviatoric loading at constant void ratio (i.e. undrained conditions). As shown in Figure 17, the

velocity decreased significantly from about 170 m/s to about 120 m/s when the failure condition was reached. This velocity trend basically follows the curve back along the consolidation phase. However, after failure and increase in effective stress, the regain in shear wave velocity is much less than observed during consolidation. Evidently the destruction of bonds associated with shearing results in a decrease in interparticle interaction and physical coupling. As a result, shear wave velocities are significantly lowered after failure over the same stress range (Sykora, 1998).

Low compressional wave velocities associated with shelly samples from the Dry Tortugas site indicate a significant influence of material properties on wave propagation (Figure 15). In particular, samples with a higher percentage of shell fragments (BC-245-U 13 cm, BC-245-U 16 cm and BC-318-U 14 cm) exhibit significantly lower compressional wave velocities compared to finer grained Rebecca Shoals samples (GC-326-U). In support of this, results from a reconstituted sample (BC-245-RC 16 cm) in which shell fragments > 0.85 mm (No. 20 US Standard Sieve) were removed show a significant increase in compressional wave velocity as compared to the respective undisturbed sample BC-245-U 16 cm with shell material (Figure 15). To further study this affect, a series of Ottawa 20/30 sand samples were tested with varying percentages (7%, 17% and 27%) of shell material by mass (Figure 18). Results indicate a decrease in compressional wave velocity with increasing shell material.

Marquesas Site

Lateral and Vertical Variability: Sediment from the Marquesas site exhibited similar physical properties and stress strain behavior as the Dry Tortugas location. Calcium carbonate content measurements averaged about 87% and remained relatively constant down core. Water contents are near 45% in most of the cores from the Marquesas site, although significant variability exists with depth in individual cores (ranging from 72% to 35%). Considering bulk densities obtained using measured water contents, the Marquesas cores have lower bulk densities (around 1.80 g/cm³ below the top 25 cm) compared to the Dry Tortugas site. Most of these cores show significant fine scale (1 cm intervals) as well as large scale (on the order of 100 cm depth) variations, some of which are presumably related to the abundance of pockets of shelly material present in the cores. The variation of water content, w in percent, and bulk density, γ in g/cm³, with depth, z in cm, for this site may be approximated as:

$$w = 74.9 z^{-0.157} \quad z < 25 \text{ cm} \quad (13)$$

$$w = 45 \% \quad z > 25 \text{ cm} \quad (14)$$

and

$$g = 1.59 z^{0.0046} \quad z < 25 \text{ cm} \quad (15)$$

$$g = 1.80 \quad (\text{g/cm}^3) \quad z > 25 \text{ cm} \quad (16)$$

Measured specific gravities for Marquesas cores ranged from 2.75 to 2.89 (Table 2). Results from Atterberg limit tests indicate average liquid and plastic limits are 41% and 28%, respectively, with two samples exhibiting non-plastic behavior. In general, mean grain size decreases rather significantly with depth with an average value of 0.19 mm in surficial samples to 0.008 mm in samples in excess of 2 m.

Compressibility and Permeability: Constant rate of deformation (CRD) compressibility and permeability tests were conducted on several samples from the Marquesas site (Table 3, Figure 19). Compression indices between 0.22 to 0.25 indicate a relatively stiff material. The SSR/OCR values range from 4.3 in surficial samples to 0.8 in samples in excess of 2 m implying possible light cementation and/or interparticle bonding associated with surficial sediments from this study site. In situ permeabilities range from 7.1×10^{-7} cm/s to 1.9×10^{-6} cm/s showing a logarithmic relationship between void ratio and permeability.

Geoacoustic Characteristics: Core logger results show a correlation between bulk density (determined from water content measurements and gamma ray values) and acoustic parameters; an increase in density generally corresponds to an increase in compressional wave velocity and impedance and a decrease in attenuation (Figure 20). Compressional wave velocities averaged between 1450 m/s to 1590 m/s for all cores. In general, density increased with depth; with the most prominent increase in the upper 20 cm of the sediment column.

Rebecca Shoals Site

Vertical Variability: The Rebecca Shoals gravity core (GC-326) differs rather significantly in material and physical properties compared to the Dry Tortugas and Marquesas locations, with this material exhibiting properties similar to a relatively homogenous clayey silt with very little shell material. However, since the clay fraction is not comprised of clay minerals, this sediment is not clearly defined as a clay, but rather a carbonate

mud. Average grain size range from 0.05 mm in surficial samples to 0.003 mm, Table 2, generally decreasing with depth. The sediment exhibits an average liquid limit of 48% and plastic limit of 27%. In general, plasticity increases with sediment depth. These values are consistent with low to medium plasticity associated with inorganic clayey silt. Specific gravities ranged from 2.71 to 2.83 with calcium carbonate contents averaging 86%. The water content profile was a little unusual (Figure 22), decreasing from 75% to about 45% in the upper 30 cm and then increasing to about 60% at 130 cm depth. There are a few zones of higher and lower water contents that should result in acoustic reflectors. The average bulk density of this particular core was 1.80 g/cm³.

Compressibility and Permeability: Constant rate of deformation (CRD) compressibility and permeability tests were conducted on several samples from the Rebecca Shoals gravity core (Table 3 and Figure 21). In situ permeabilities ranged from 5.9×10^{-6} cm/s to 5.6×10^{-7} cm/s for the depth interval from 12 cm to 290 cm. Compression indices are relatively low, averaging between 0.16 to 0.40. Similar to the Marquesas site, light cementation may be a factor affecting deformation behavior; stress state ratios were about 7.5 in surficial samples and 0.7 in samples in excess of 2 m depth.

Geoacoustic Characteristics: MSCL results show compressional wave velocities averaged between 1500 m/s to 1570 m/s, with the highest values in the upper 50 cm (Figure 22). An increase in density generally corresponds to an increase in compressional wave velocity and impedance and a decrease in attenuation.

Compressional wave velocities obtained during isotropic consolidation from the triaxial-acoustic cell averaged between 1452 to 1480 m/s, while shear wave speeds ranged between 40 to 128 m/s over an effective stress range of 1 to 39 kPa (Figure 15 and 16). Young's and shear moduli calculated from triaxial wave speed measurements ranged from 2.4×10^6 kPa to 2.6×10^6 kPa and 3.8×10^3 kPa to 3.1×10^4 kPa, respectively (Table 5).

Similar to Dry Tortugas samples, shear wave velocity during undrained uniaxial loading imply some degree of cementation; two shear wave velocities are possible at one given effective confining stress depending upon loading status, one before failure and one during friction angle mobilization (Figure 17). During yield mobilization, the material exhibits fewer interparticle contact points possibly due to destruction of cementation bonds associated with shearing. As a result, shear wave velocities are significantly lowered after failure over the same stress range (Sykora, 1998). It is of interest that the shear wave can be used to estimate the effective stress at which failure occurs, noted by the "v" in the plot labeled as "failure" in Figure 17.

Relatively high compressional wave velocities associated with samples from the Rebecca Shoals site also indicates that material properties significantly influence P-wave propagation; the Rebecca Shoals material consistently exhibited higher wave velocities during isotropic consolidation as compared to the shellier material from the Dry Tortugas site. These results imply that shelly well graded Dry Tortugas material tends to dampen compressional wave velocities compared to a more homogenous Rebecca Shoals sediment. (Figure 15a).

Comparisons/Contrasts

Variations in sediment properties and geotechnical behavior exist between the three CBBL Lower Florida Keys study sites. Water contents were noted to decrease from 75% to 100% at the surface to between 35% to 45% below 25 cm at the Marquesas and Dry Tortugas sites. However, water contents in the Rebecca Shoals area were significantly higher at greater depths; decreasing from 75% at the surface to between 45% to 65% below 25 cm. Corresponding bulk densities were lower (averaging 1.8 g/cm³) at the Marquesas and Rebecca Shoals sites, compared to Tortugas (about 1.9 g/cm³) below 25 cm depth. The Dry Tortugas and Marquesas sites with the coarser grained material exhibited lower plastic and liquid limits compared to the finer grained material from the Rebecca Shoals site.

The full set of consolidation test results (Silva et al, 1996) indicate that the compressibilities of the Marquesas and Rebecca Shoals sediments are higher than the Dry Tortugas sediments (Table 3). Also, the compression indices increase somewhat with depth at the Marquesas and Rebecca Shoals sites and decrease with depth at the Dry Tortugas site. Apparently, the mechanisms of sediment deformation for core GC-178 (Marquesas) and core GC-326 (Rebecca Shoals) which have a higher clay content are quite different from the sediments from core GC-313 (Dry Tortugas) which has a higher coarse fraction that includes more shell fragments.

Generally speaking, density calculations from water content correlated well with densities obtained using the core logger. In addition, trends in compressional wave velocities correlated well with density and water content data for all sites. In particular, the Marquesas and Rebecca Shoals site with lower densities (averaging 1.8 g/cm³) and higher water content (75% to 45%) exhibited lower compressional wave velocities (1450 m/s to 1590 m/s) compared to the Dry Tortugas site which showed higher compressional wave velocities (1475 m/s to 1650 m/s) with higher densities and lower water content (based on MSCL results).

CRD tests on core GC-178 from the Marquesas site indicate significant apparent overconsolidation ($SSR > 4$) in the surficial sediments (upper 50 cm). Similar trends were seen in core GC-326 from the Rebecca Shoals area as well. The transition from apparent overconsolidation in the surficial layers to a normally consolidated state with depth is typical of other clayey marine sedimentary regimes indicating interparticle bonding and probably some cementation in the surficial sediments (Silva and Jordan, 1984). Samples from the Dry Tortugas site indicate significantly higher SSR ratios of up to 50 in the surficial sediments. This is supported by triaxial-acoustic data obtained from box cores in that higher shear wave velocities during consolidation were associated with undisturbed sediment as opposed to remolded sediment in which interparticle bonds were broken. Similarly, moduli results for the undisturbed coarse grained shelly material from the Dry Tortugas site exhibit a stiffer shear response relative to the Rebecca Shoals site, indicating a greater degree of interparticle locking associated with Dry Tortugas material.

Panama City, FL

Personnel from the University of Rhode Island, Marine Geomechanics Laboratory (URI/MGL) participated in the research cruise south of Panama City, Florida. The primary objective of this effort was to obtain core and grab samples for characterization of sediments at this site. The URI/MGL Large-diameter Gravity Corer (LGC) was used to obtain undisturbed samples and the TAMU team obtained the grab samples and vibracores.

A total of fourteen whole cores were recovered, ranging in length from 10 cm to 51.5 cm with eight being shipped to the URI/MGL. The sands were generally difficult to sample and it was not possible to obtain cores of any great length.

A laboratory testing program was undertaken to determine grain size distributions, water content profiles and stress-strain-strength behavior of recovered samples. Strength testing was done using both the triaxial compression and direct shear systems.

Grain Size: In situ sediments were typically well-graded dense sands containing varying amounts and sizes of shells and shell fragments. In general, the upper 10 cm (approximately) consisted of brown or gray well graded medium or coarse sand. Below this depth, the material was typically gray medium to coarse sand grading to fine gray sand. The sediments are generally classified as a well graded coarse to fine sand. The average grain size across all eight cores tested was 0.56 mm with about 3% being less than 0.075 mm. Visual inspections revealed that sediments consisted of quartz sand grains with varying amounts of shell and coral fragments. Core 623-PC-GC had the coarsest sediments and widest variation of grain size distributions with depth. All of the other cores showed little variation in grain size distribution with depth and generally had medium to fine sediments.

Water Content and Density: Water content measurements were obtained on samples from eight cores. The largest variations of water contents (as high as 15%) were in the upper 5 cm of the cores. Below this depth the variations were about 8-10%. Overall, water contents ranged from 8.4% to 28.9% with an average value of 20%. The bulk density for all of the cores tested showed little variation and was on the order of 2.0 g/cm^3 .

Stress-Strain-Strength: Three triaxial compression drained tests were performed on samples from core 575-PC-GC. One test was conducted on an undisturbed sample from a depth of 5-16 cm in the core and two tests were run on remolded samples from depths of 5-16 cm and 16-27 cm. The remolded samples were compacted to the same density as the undisturbed sample. Each of the samples failed in a dilative mode which is indicative of relatively dense sands. The average void ratio at failure was 0.71 and the average critical void ratio (void ratio for zero volume change during shear) was 0.77. Angles of internal friction ranged from 44° to 51° with an average of 47° . Figure 22 shows the stress paths for the samples during testing and a summary of pertinent results is given in Table 6.

Micromechanical Modeling

A computational modeling scheme has been developed to simulate geoaoustic wave propagation in saturated granular sediments. The primary focus of the study was to investigate microstructural or fabric effects and to relate such features with wave propagational behaviors. The modeling procedure used an interparticle contact law developed from a simplified elastohydrodynamic solution for two circular disks interacting through a viscous fluid. This fluid contact law was incorporated into a discrete element computer code to analyze the

dynamic response of model particulate materials. Simulations were conducted on both one- and two-dimensional computer generated model material assemblies with regular and random packings.

Specific results for the wave speed and amplitude attenuation (as measured by the intergranular contact force) were determined, and these wave propagational characteristics are shown to be functions of the physical microstructural properties of the discrete medium. It was found that the presence of pore fluid affected wave propagation, and this may be related to the fluid viscosity and initial interparticle liquid gap spacing. Only slight viscosity effects were found on wave attenuation, while a small increase in transmitted wave velocity was observed with increasing pore fluid viscosity. However, it has been pointed out that trapped or bound pore-fluid may behave as having a higher apparent viscosity than free fluid, and thus viscosity may produce more significant effects than observed here. The dimension of the initial fluid gap between particles had more sizable effects on wave propagation. Wave speed was found to be inversely related to the gap size, and attenuation increased with particle spacing dimension.

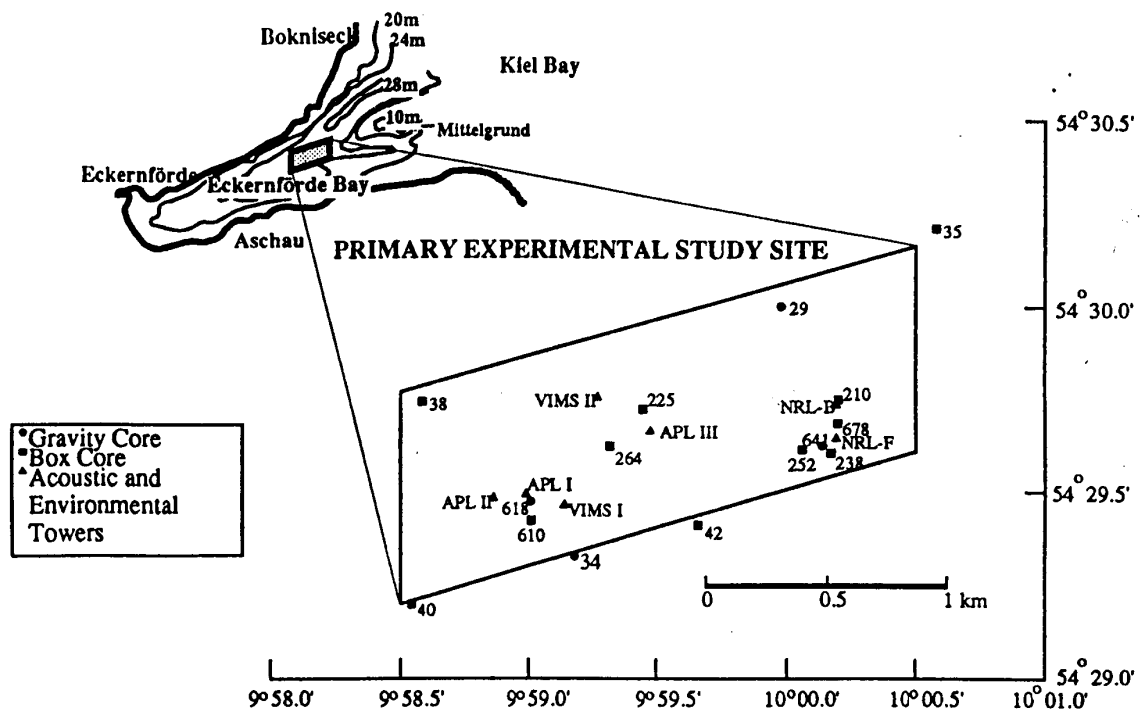


Figure 1. CBBL Experiment Site and Core Locations in Eckernförde Bay

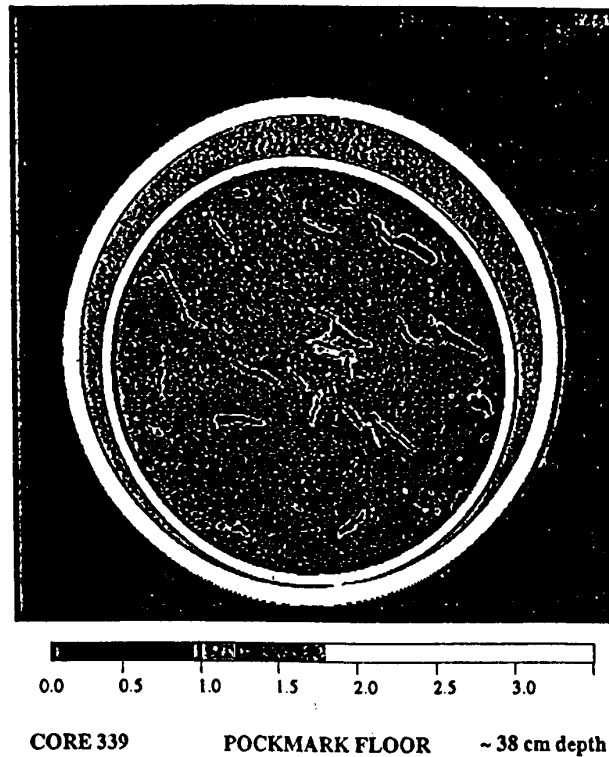


Figure 2. CAT X-ray image from pockmark, at 38 cm depth, 4.5% gas (courtesy of A. Anderson)

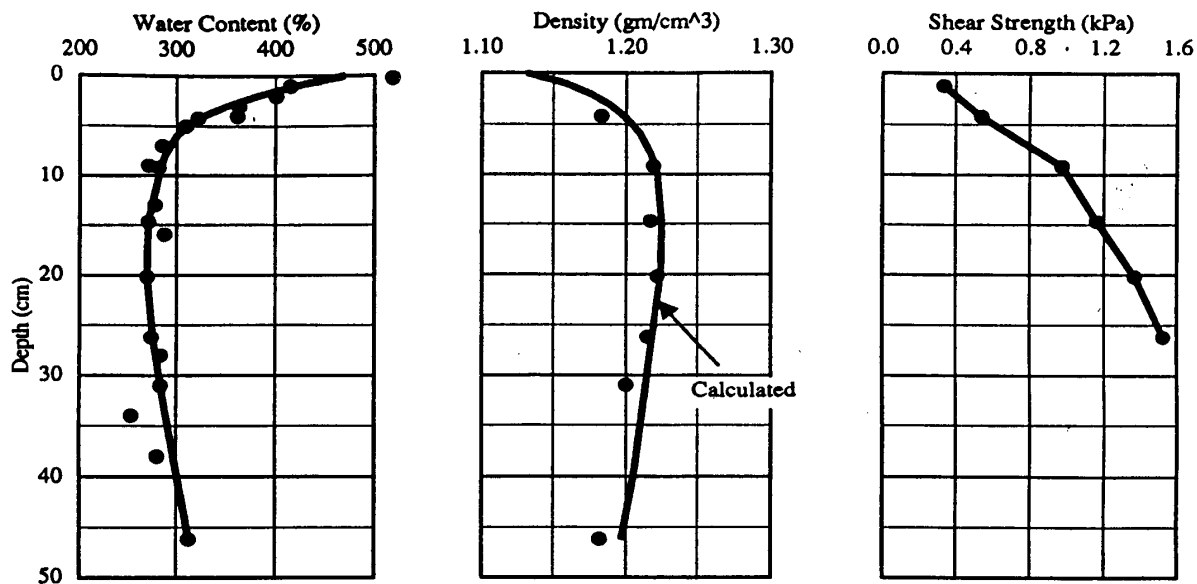


Figure 3. Geotechnical Profiles for Core BC-238, May 1993 Cruise

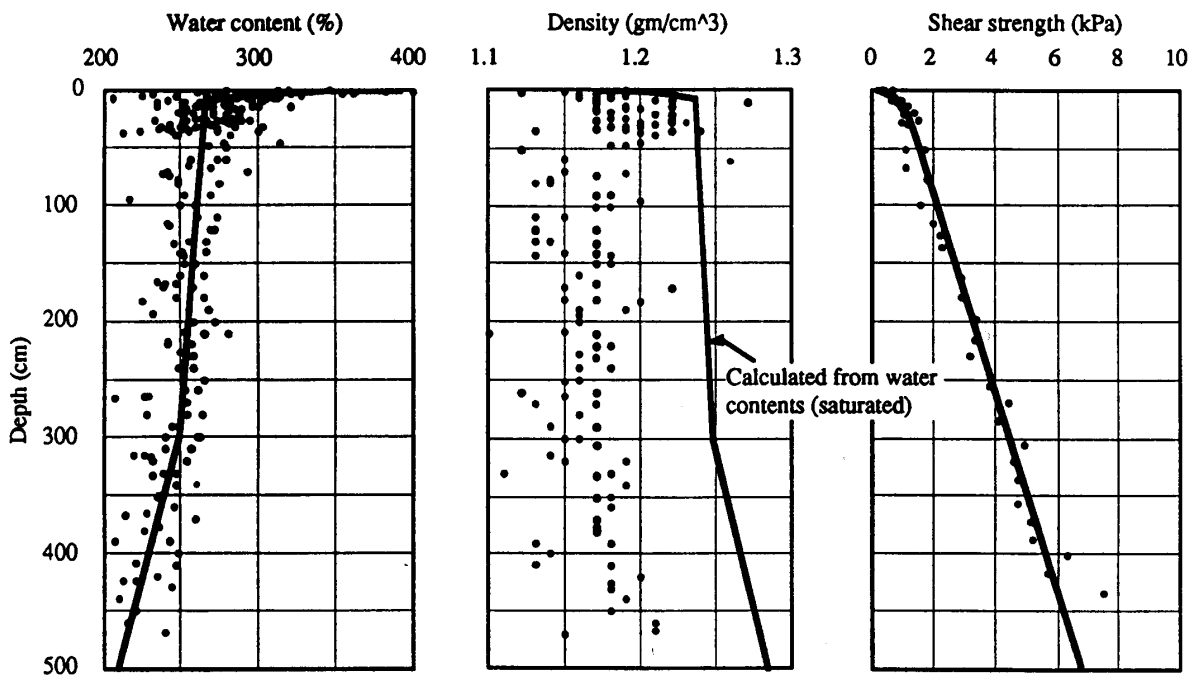


Figure 4. Geotechnical Profiles, Upper 5m, All Cores

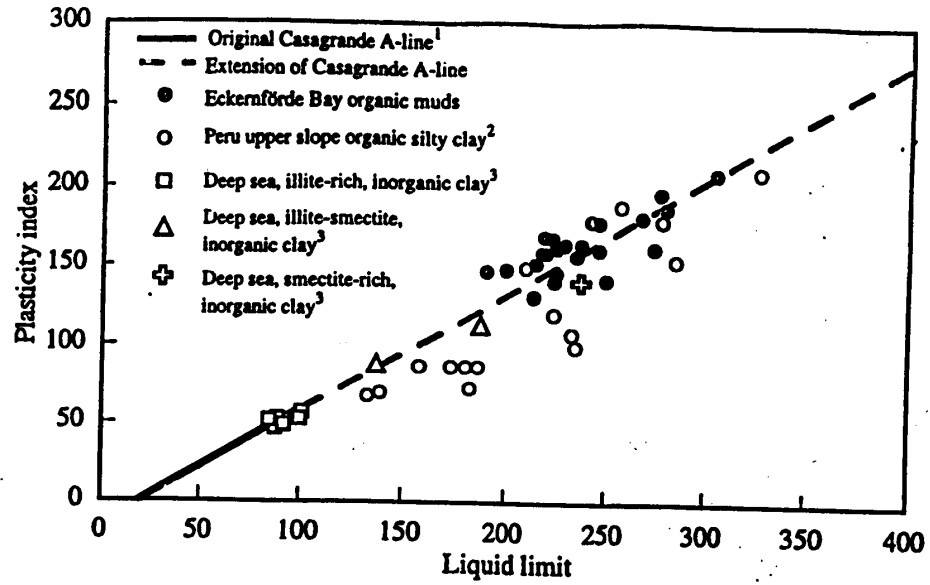


Figure 5: Plasticity of Eckernförde Bay sediments compare with A-line and other ocean sediments

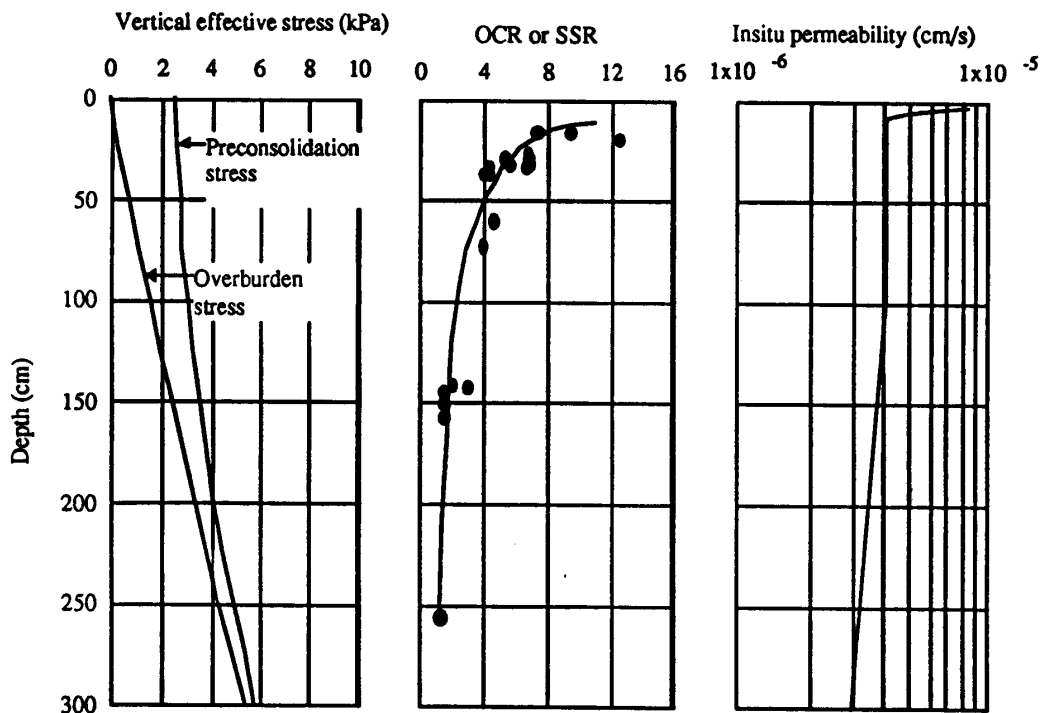


Figure 6. Summary of In Situ Stresses, Consolidation State and Permeability

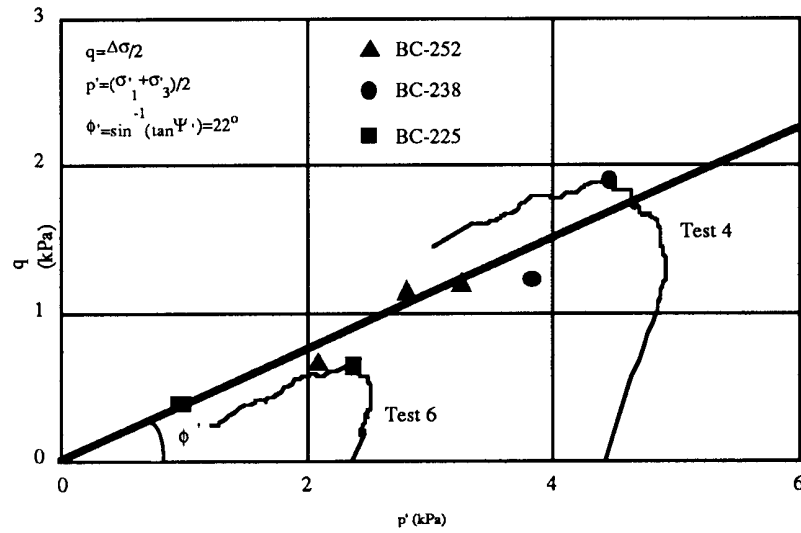


Figure 7. Stress Paths for CIU Triaxial Stress-Strain-Strength Tests

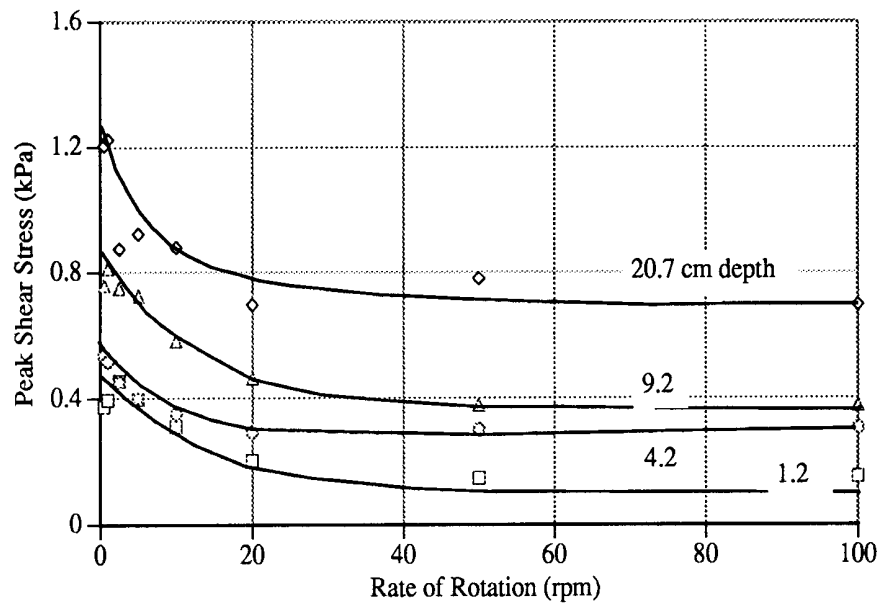


Figure 8. Rheological Test Results for Strain Rate Tests; Peak Shear Stress Behavior

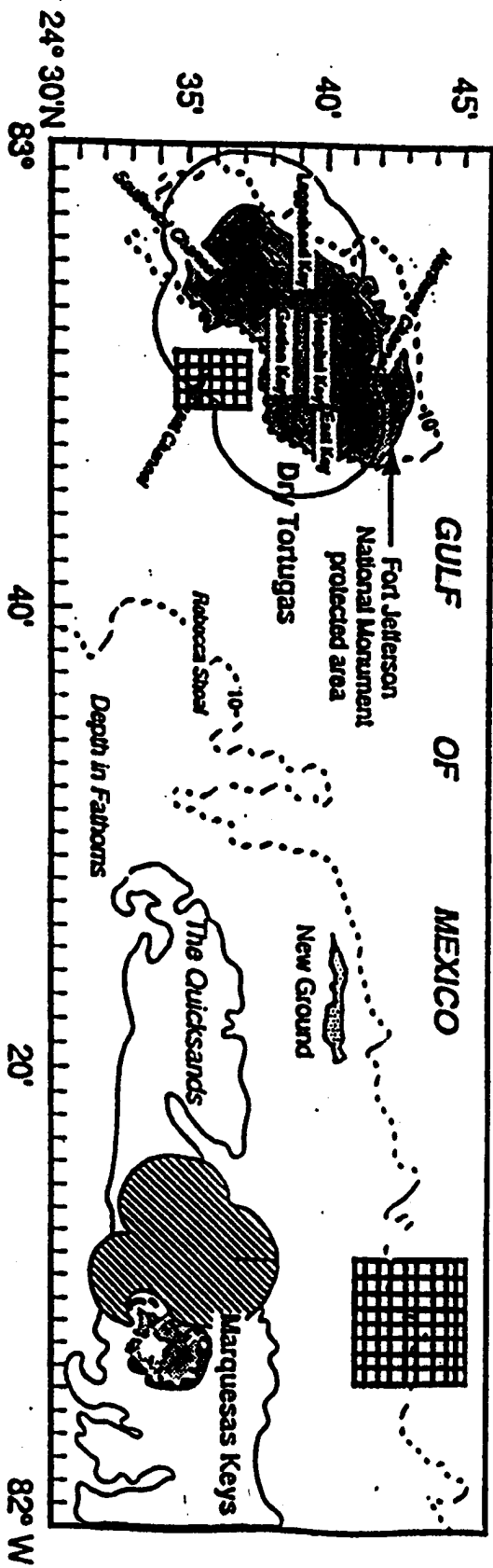


Figure 9: CBBLSRP Key West Study Site Locations

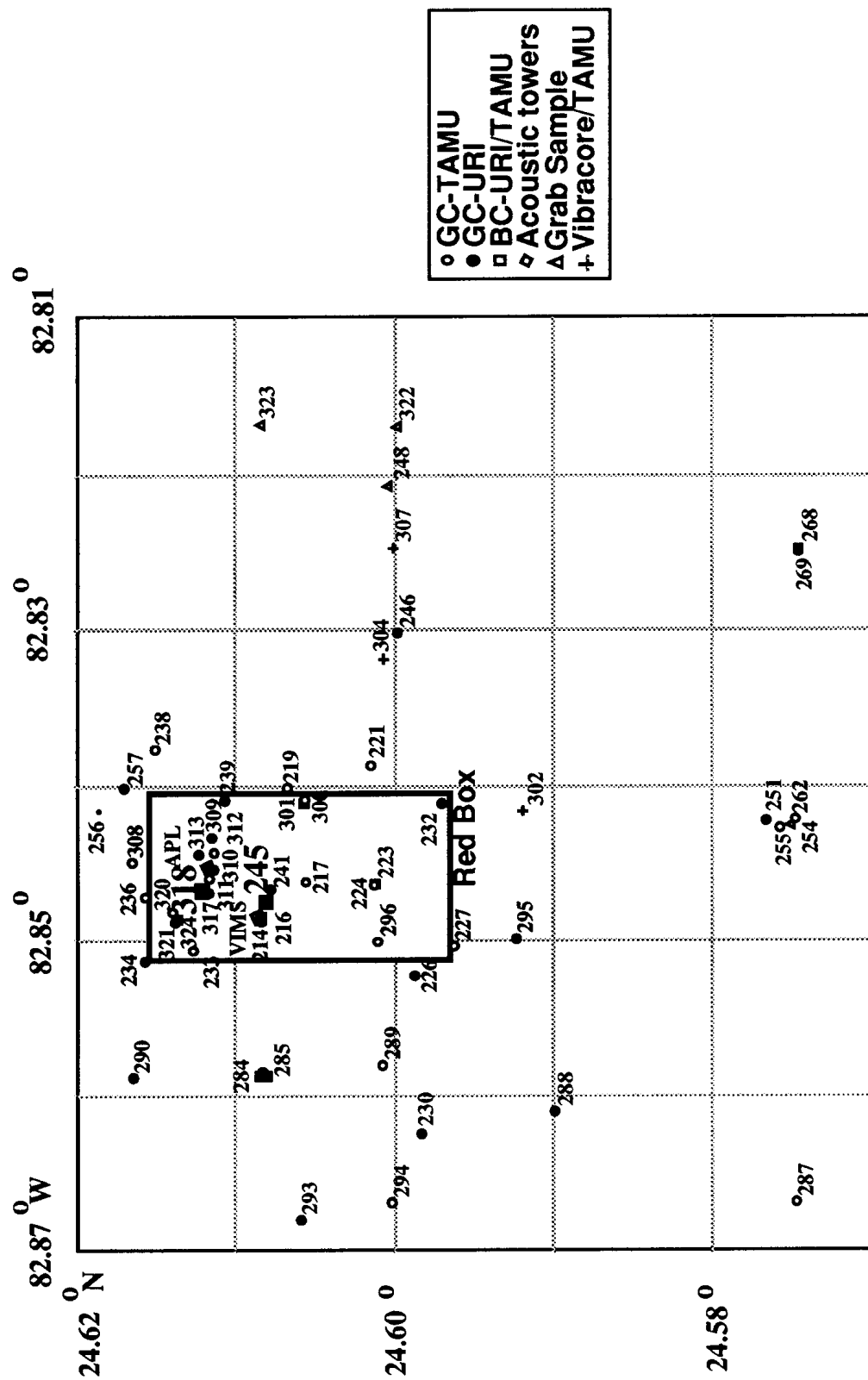


Figure 10. Core Locations in the Dry Tortugas Area

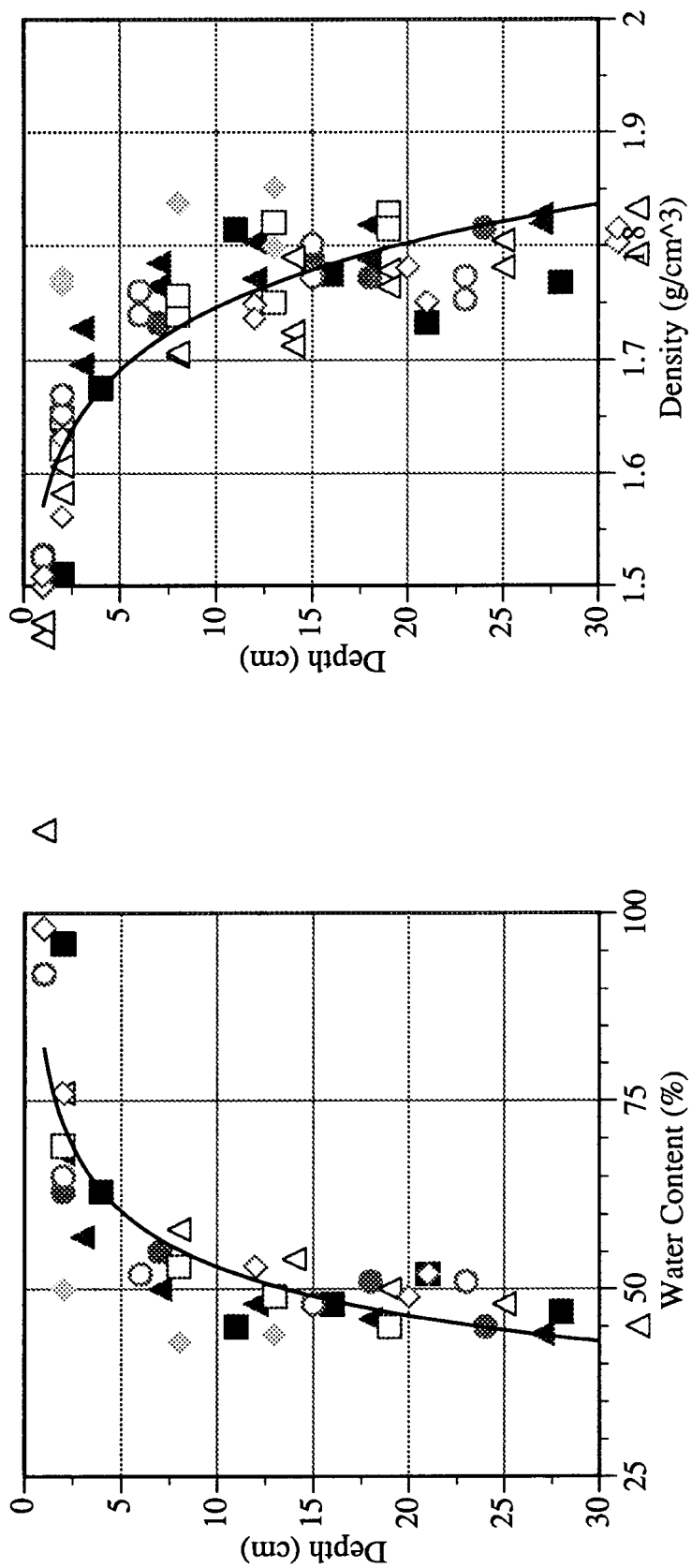
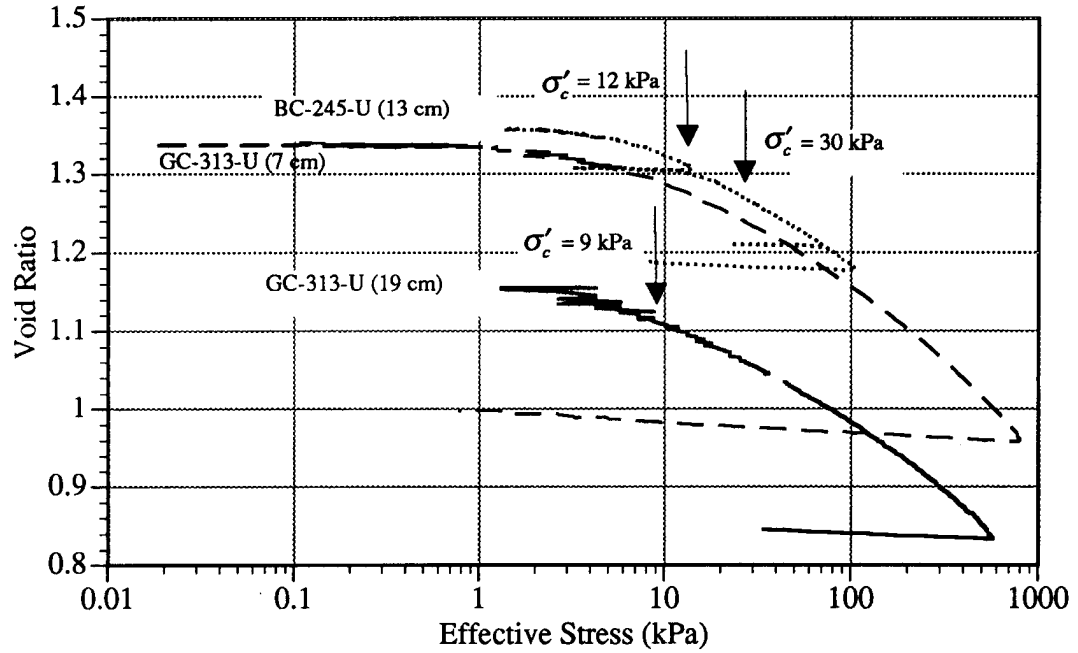
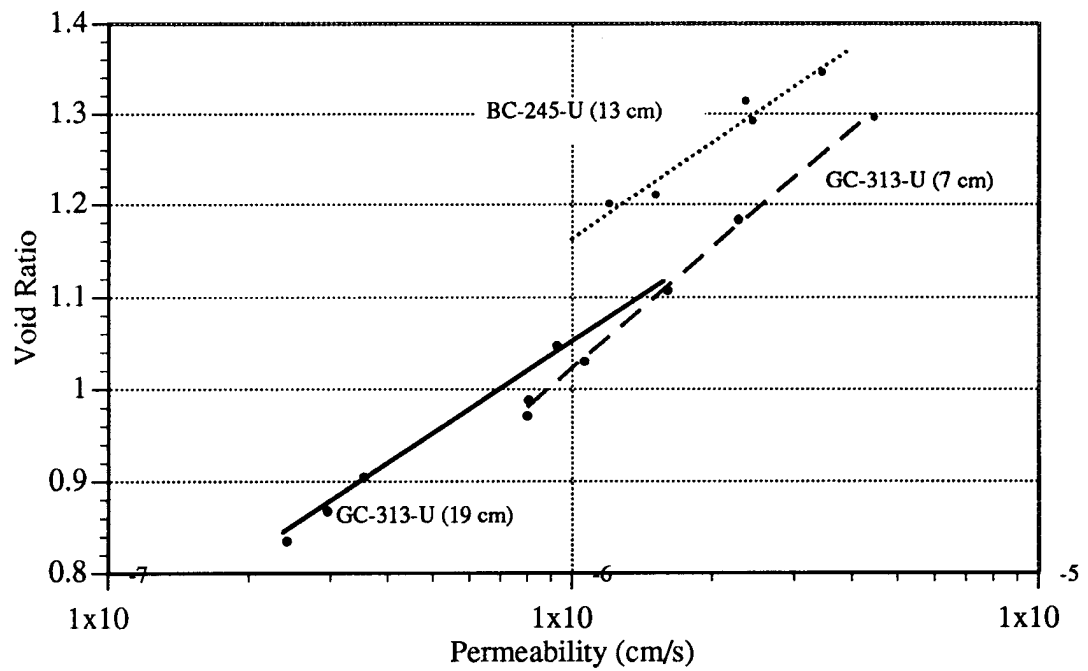


Figure 11. (a) Water Content Profiles and (b) Density Profiles from Dry Tortugas Box Cores



(a) Consolidation Results



(b) Permeability Results

Figure 12. Consolidation and Permeability Results from Constant Rate of Deformation Tests on Dry Tortugas Sediment

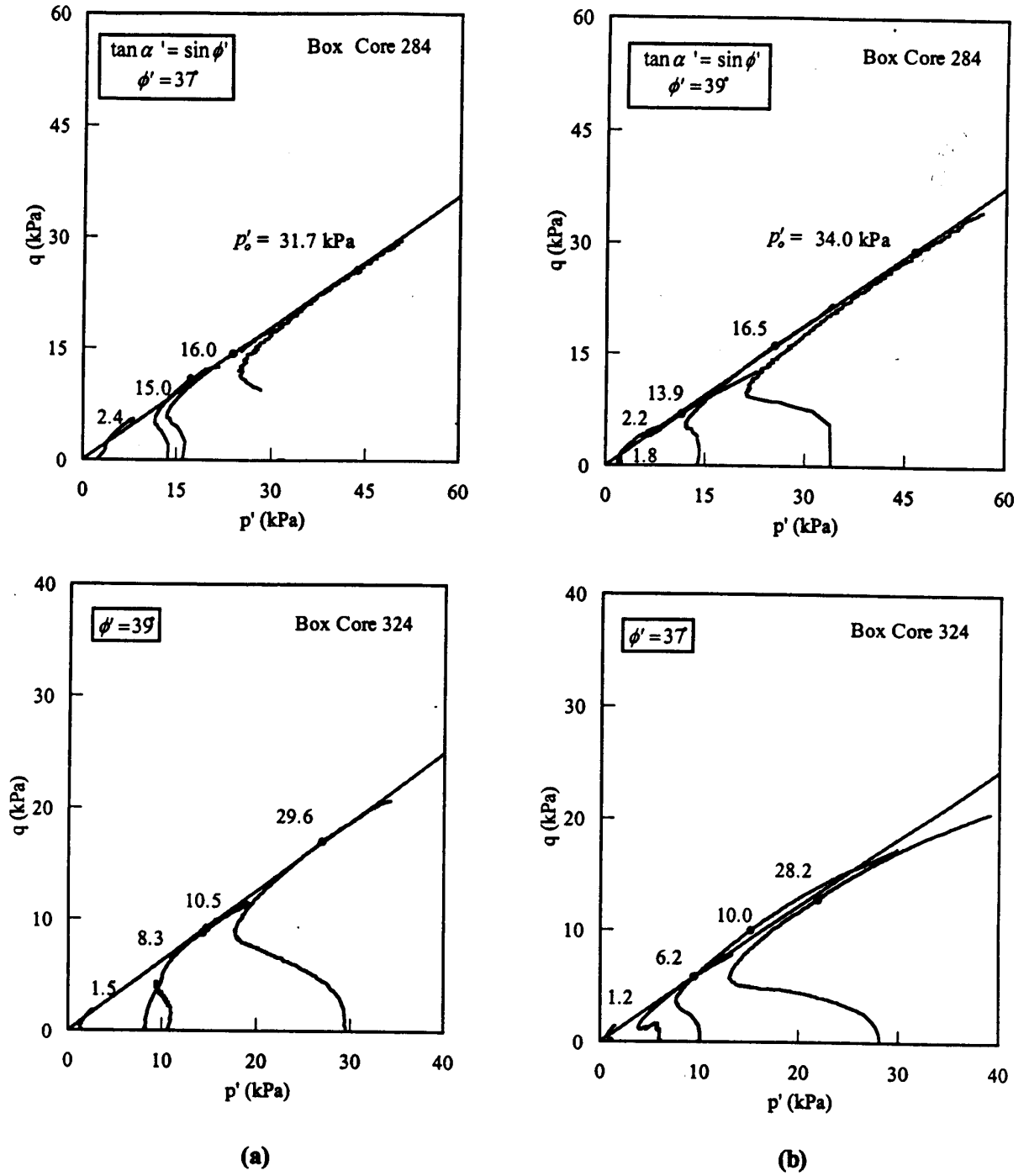


Figure 13. Failure Envelopes of (a) Undisturbed and (b) Remolded Samples from Dry Tortugas Box Cores 284 and 324

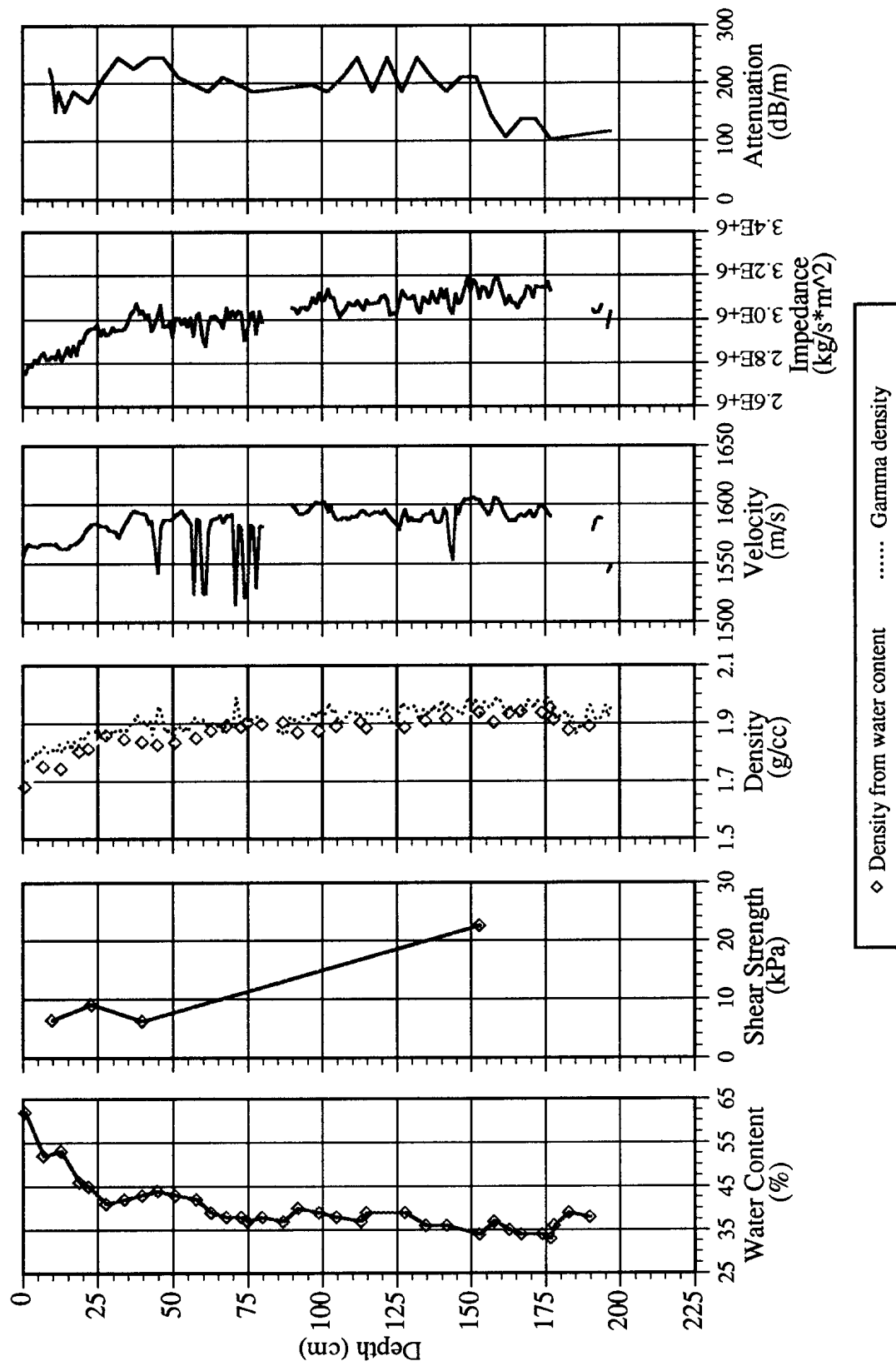


Figure 14. Typical Physical and Acoustic Profiles of Dry Tortgas Sediment

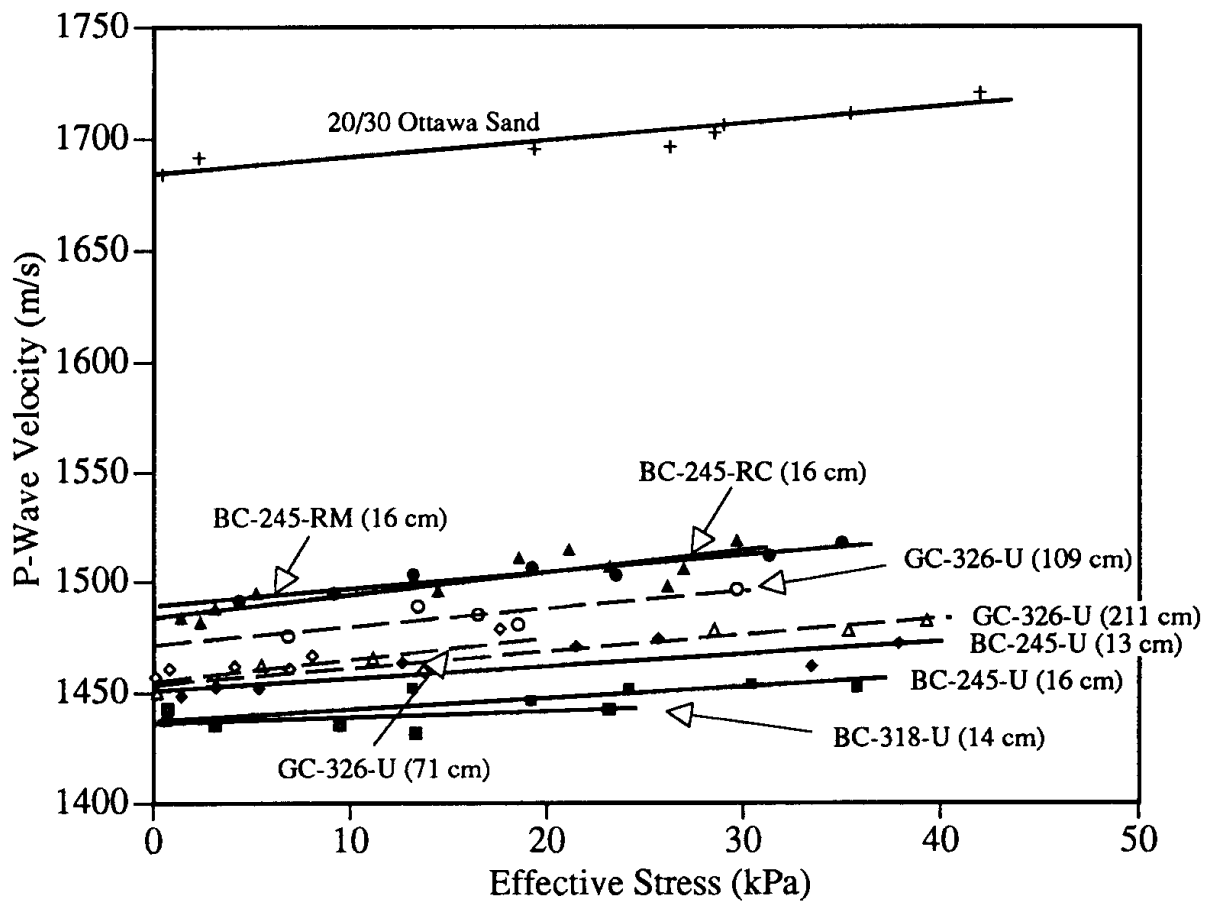


Figure 15. Compressional Wave Results During Consolidation of Key West Samples (see Table 5 for explanation of symbols)

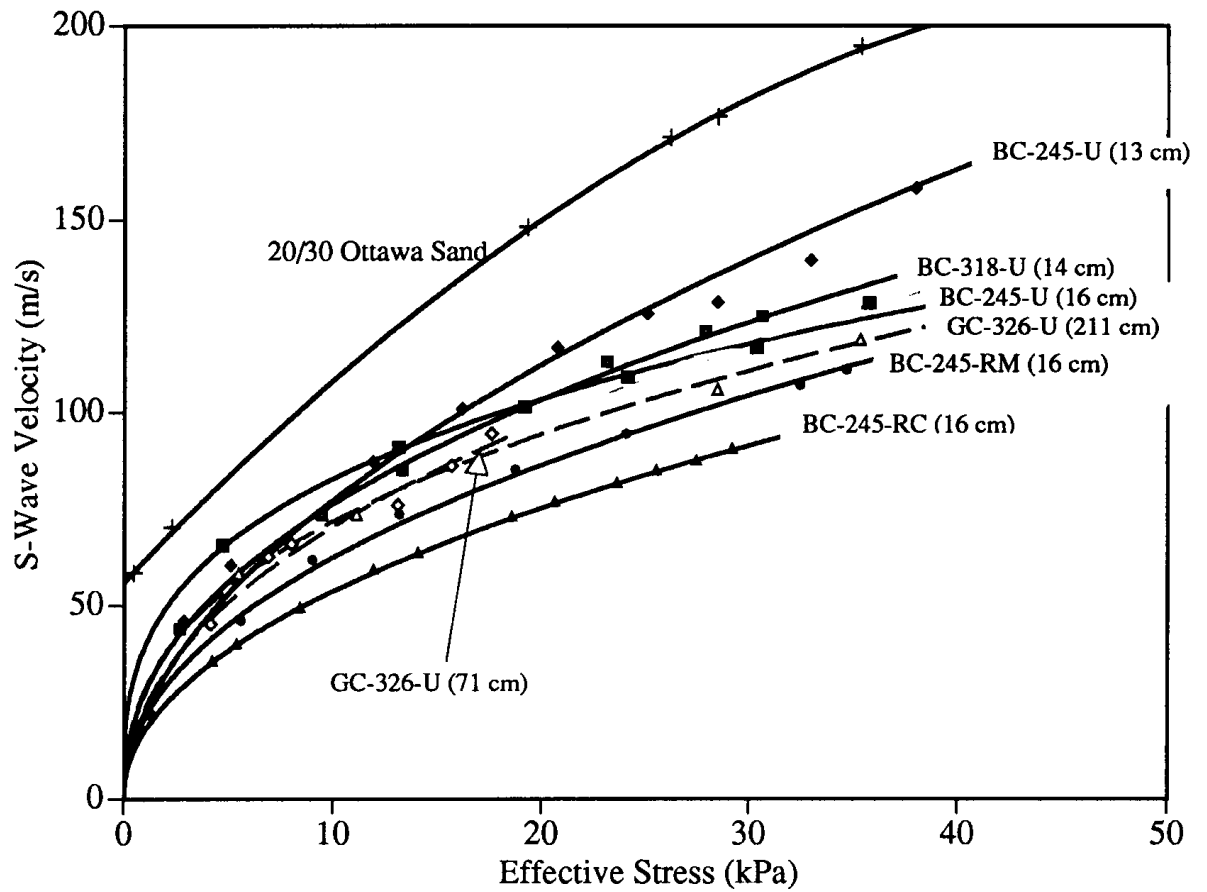


Figure 16. Shear Wave Results During Consolidation of Key West Samples
(see Table 5 for explanation of symbols)

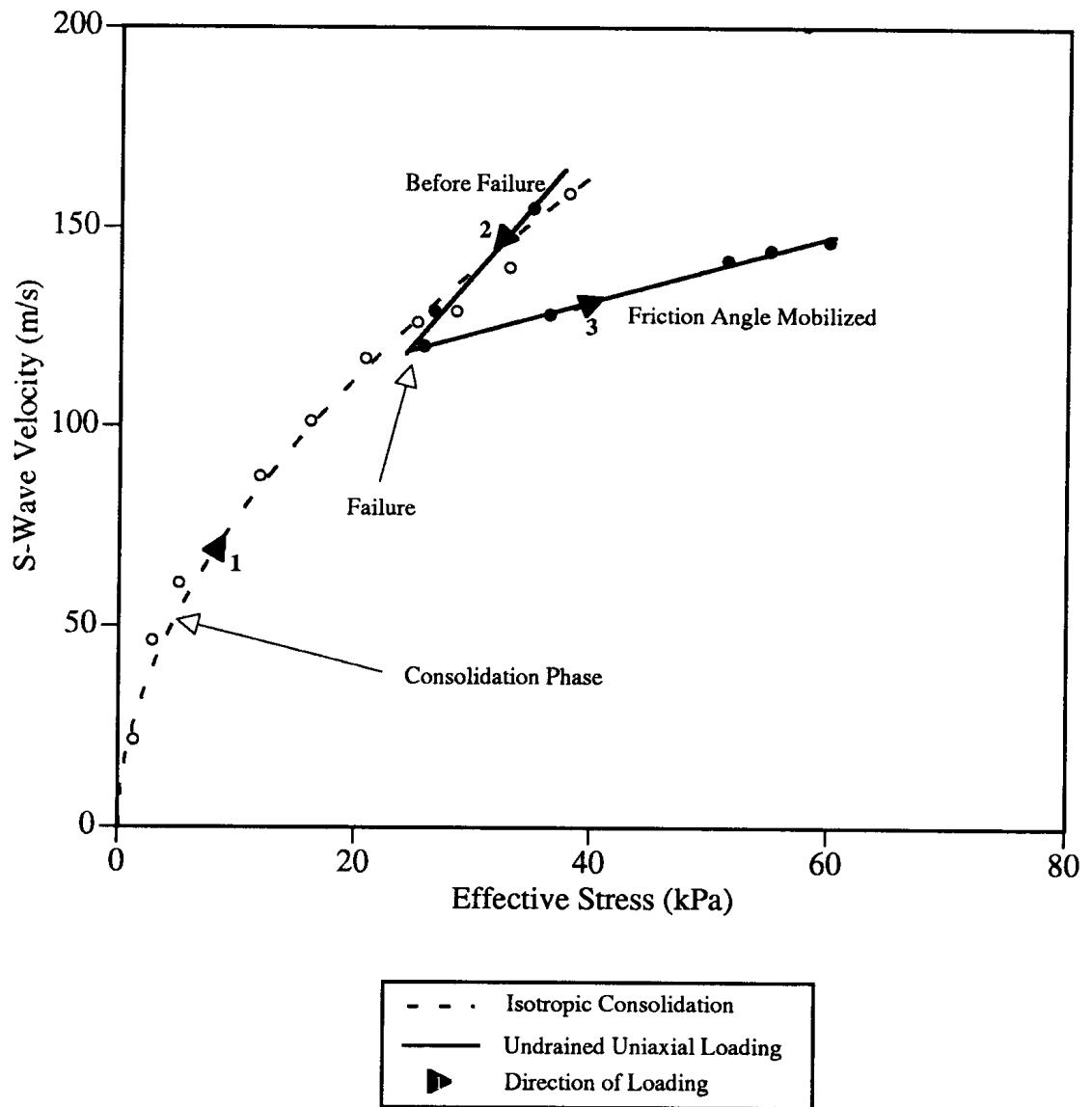


Figure 17. Shear Wave Results During Consolidation and Undrained Uniaxial Loading of Key West Sample BC-245-U (13 cm)

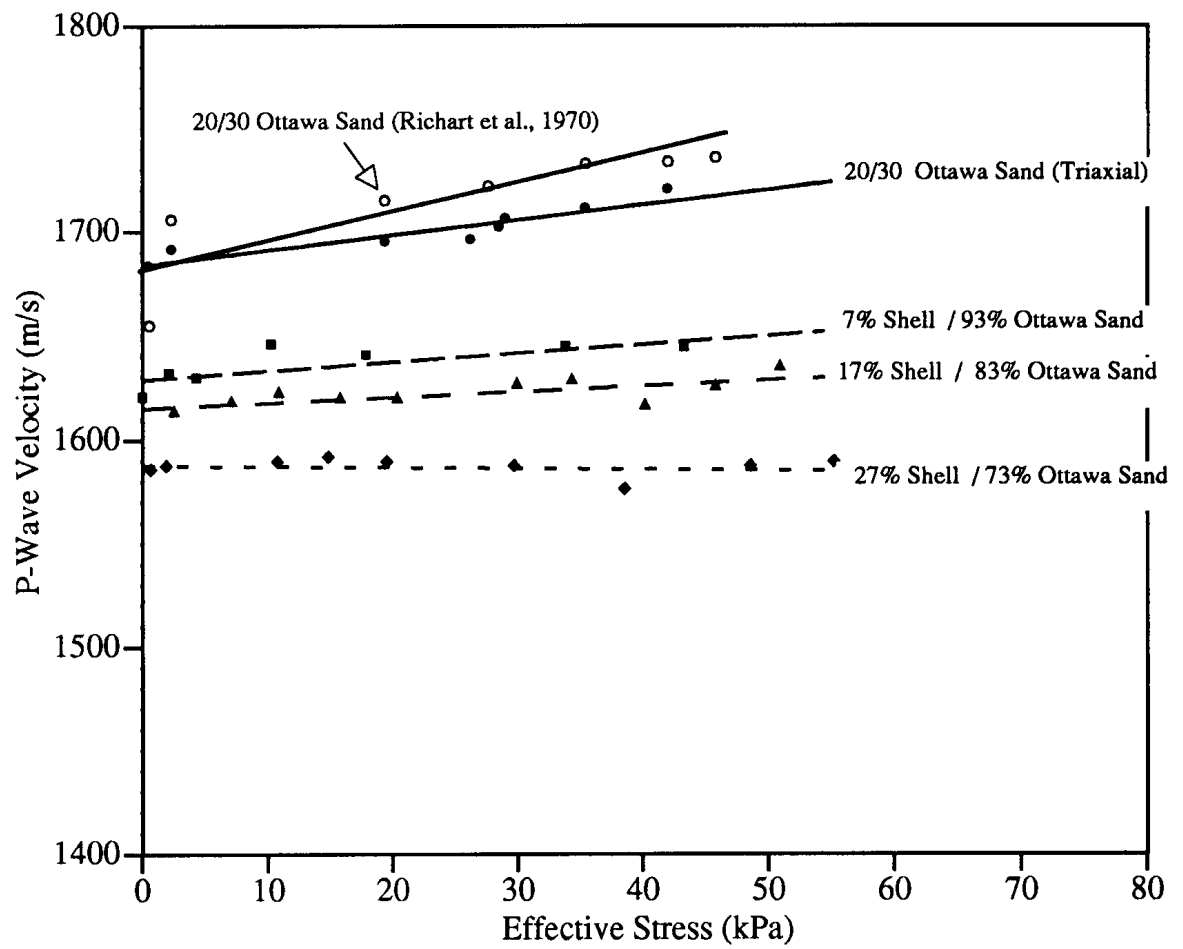


Figure 18. Compressional Wave Results During Consolidation of Sand-Shell Mixture Samples

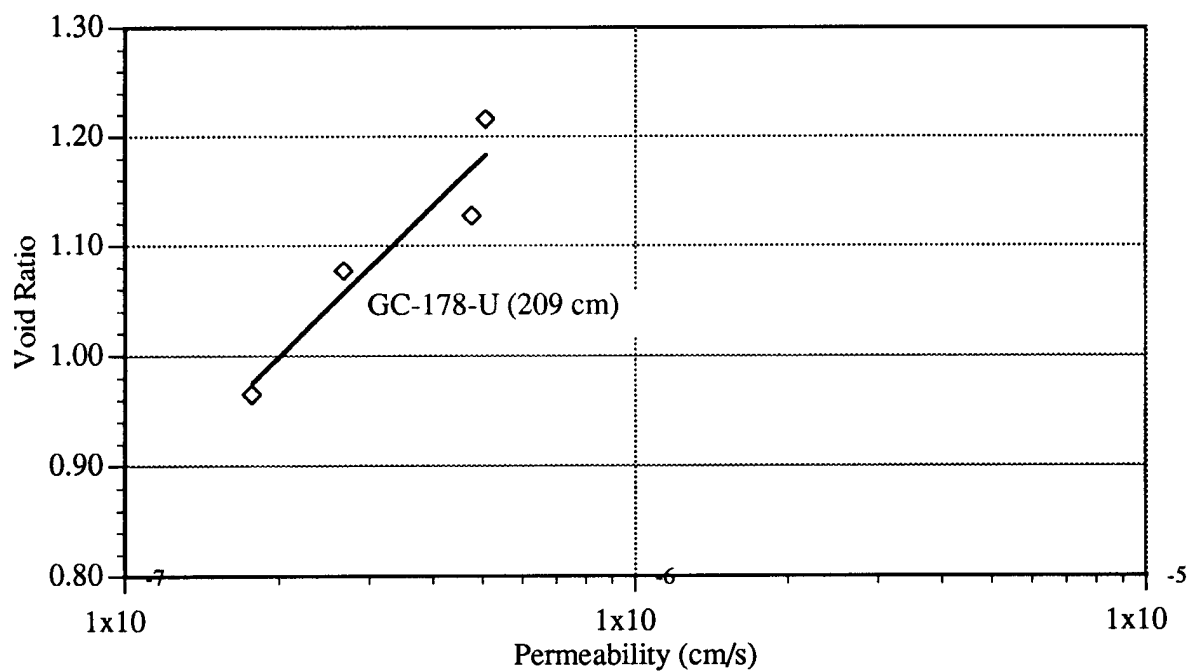
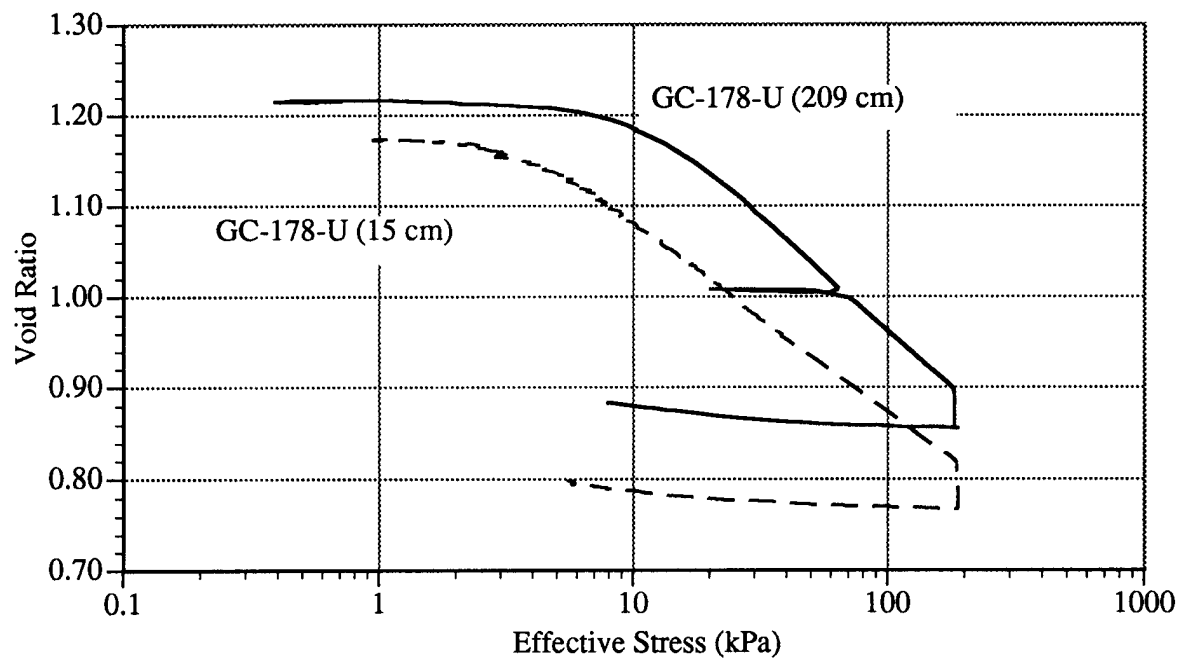


Figure 19. Consolidation and Permeability Results from Contant Rate of Deformation Tests on Marquesas Sediment

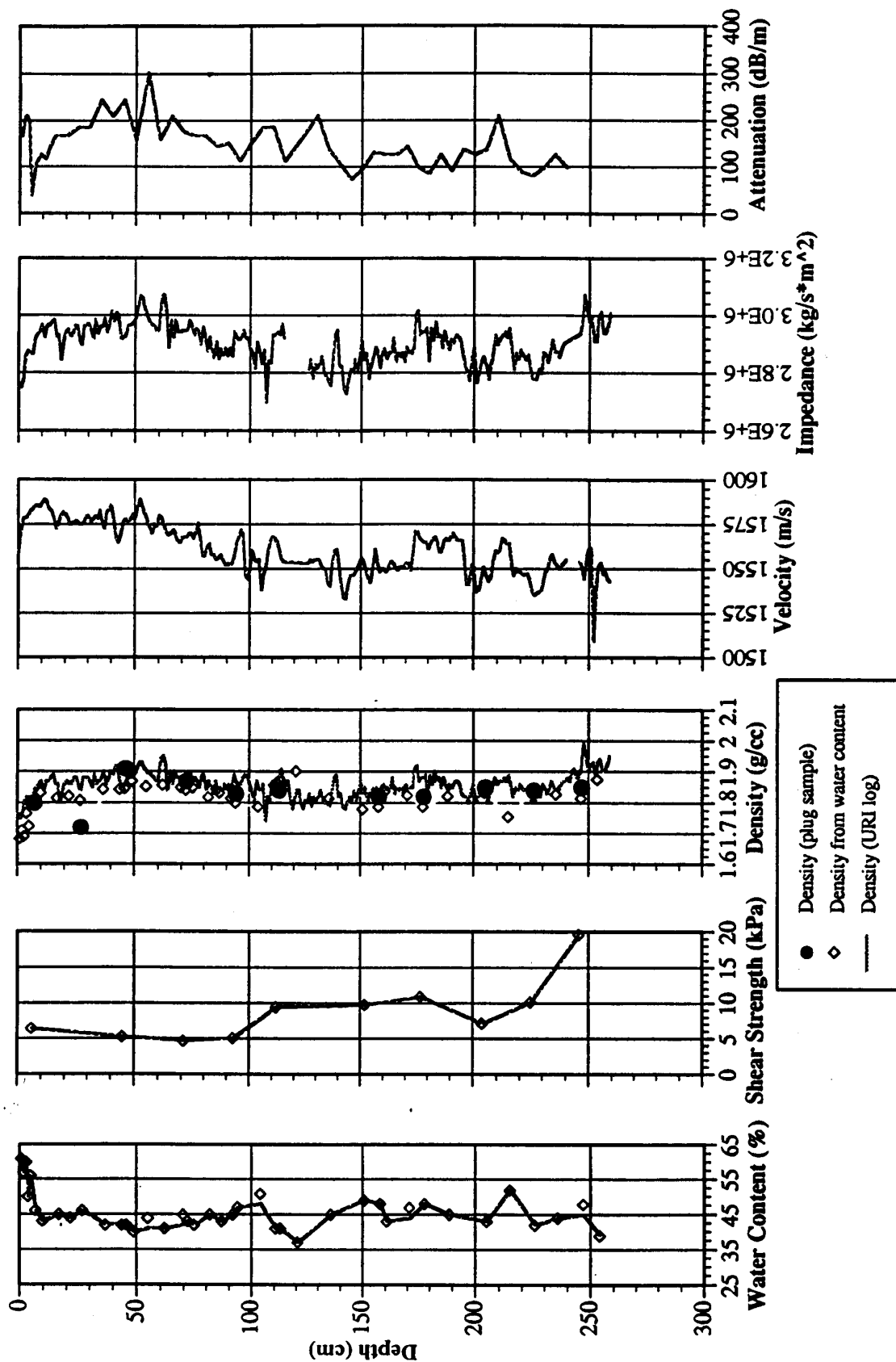
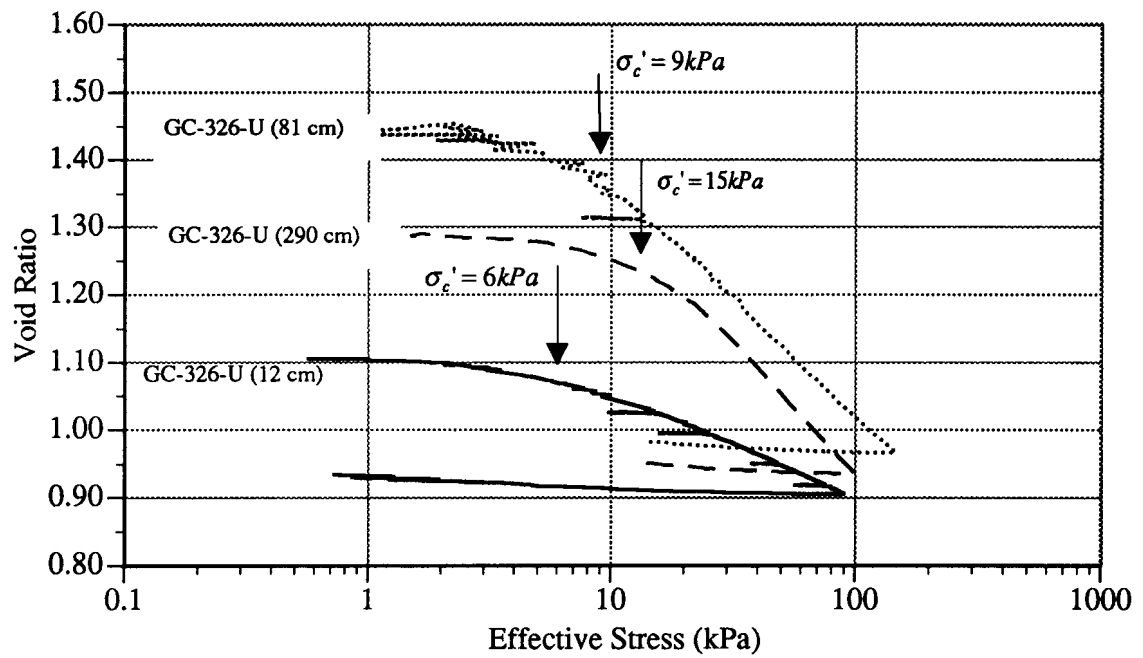
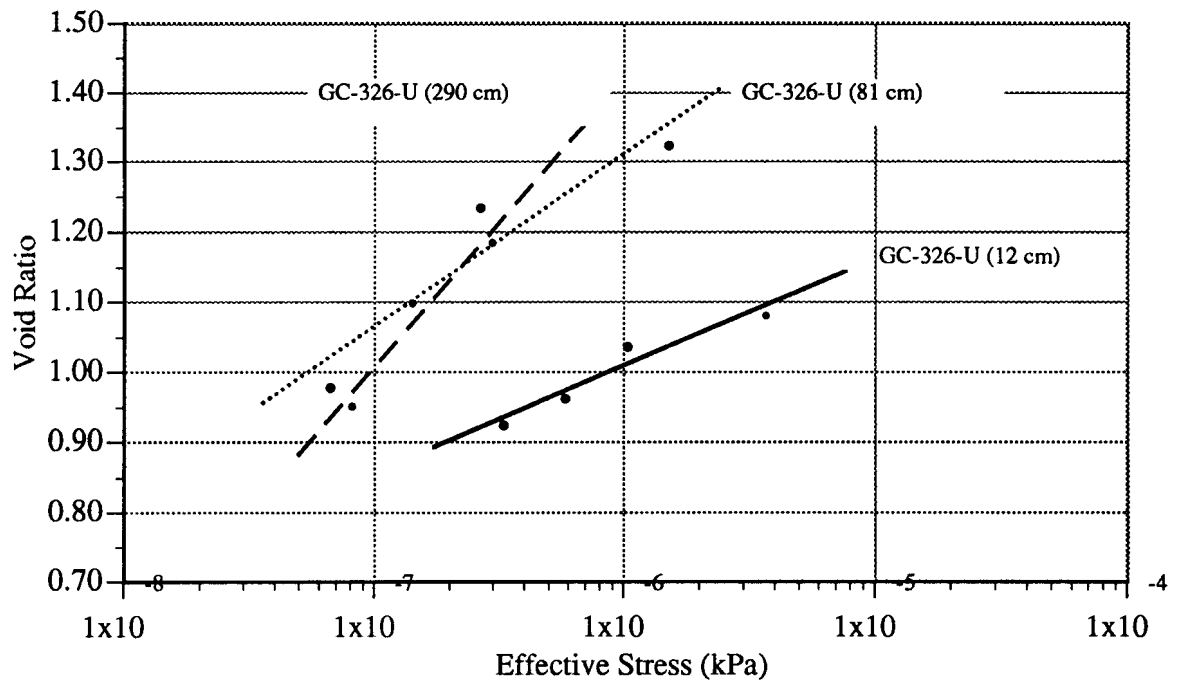


Figure 20. Typical Physical and Acoustic Profiles of Marquesas Sediment



(a) Consolidation Results



(b) Permeability Results

Figure 21. Consolidation and Permeability Results from Constant Rate of Deformation Tests Conducted on Rebecca Shoals Sediment

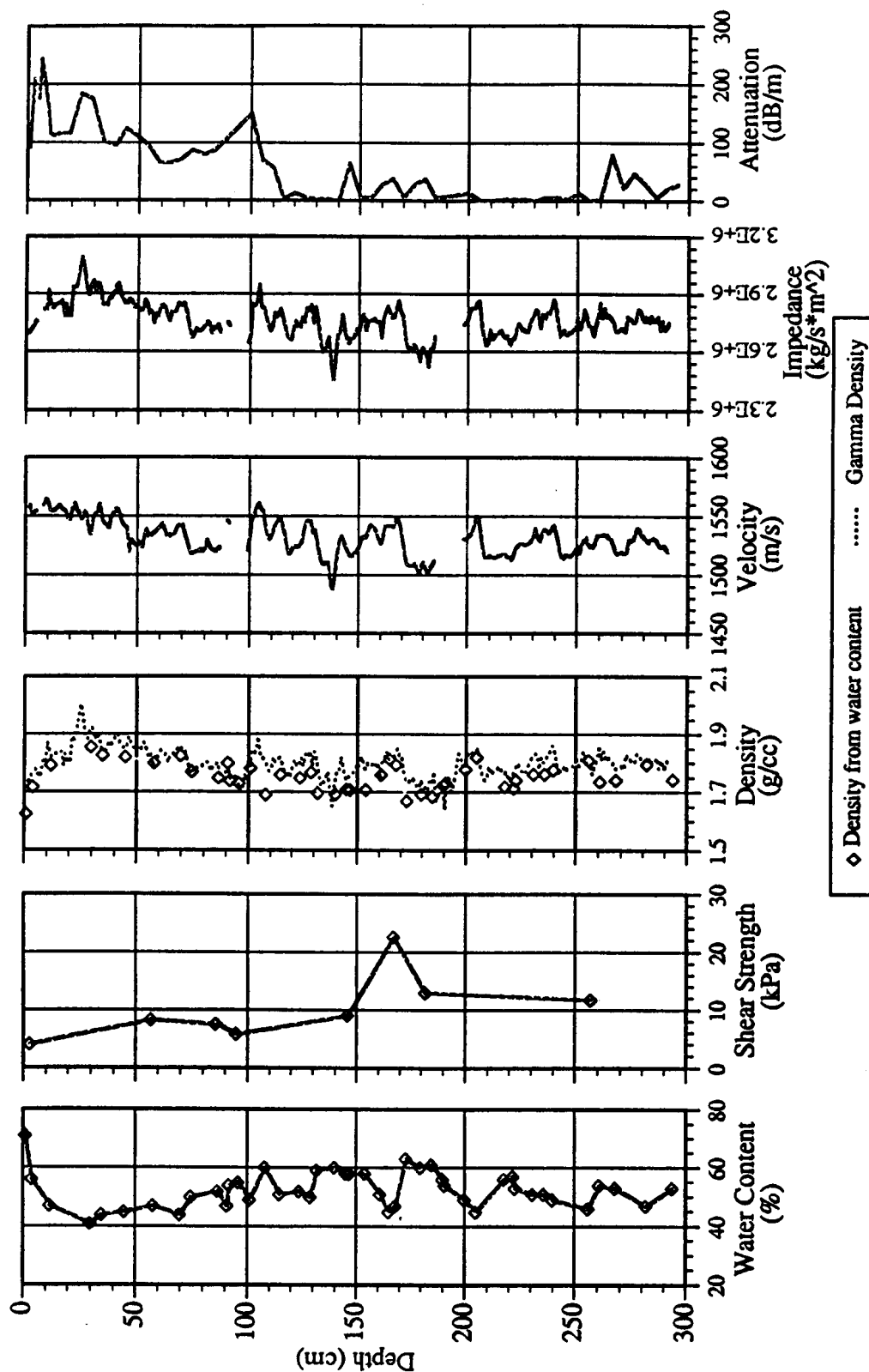


Figure 22. Typical Physical and Acoustic Core Profiles of Rebecca Shoals Sediment

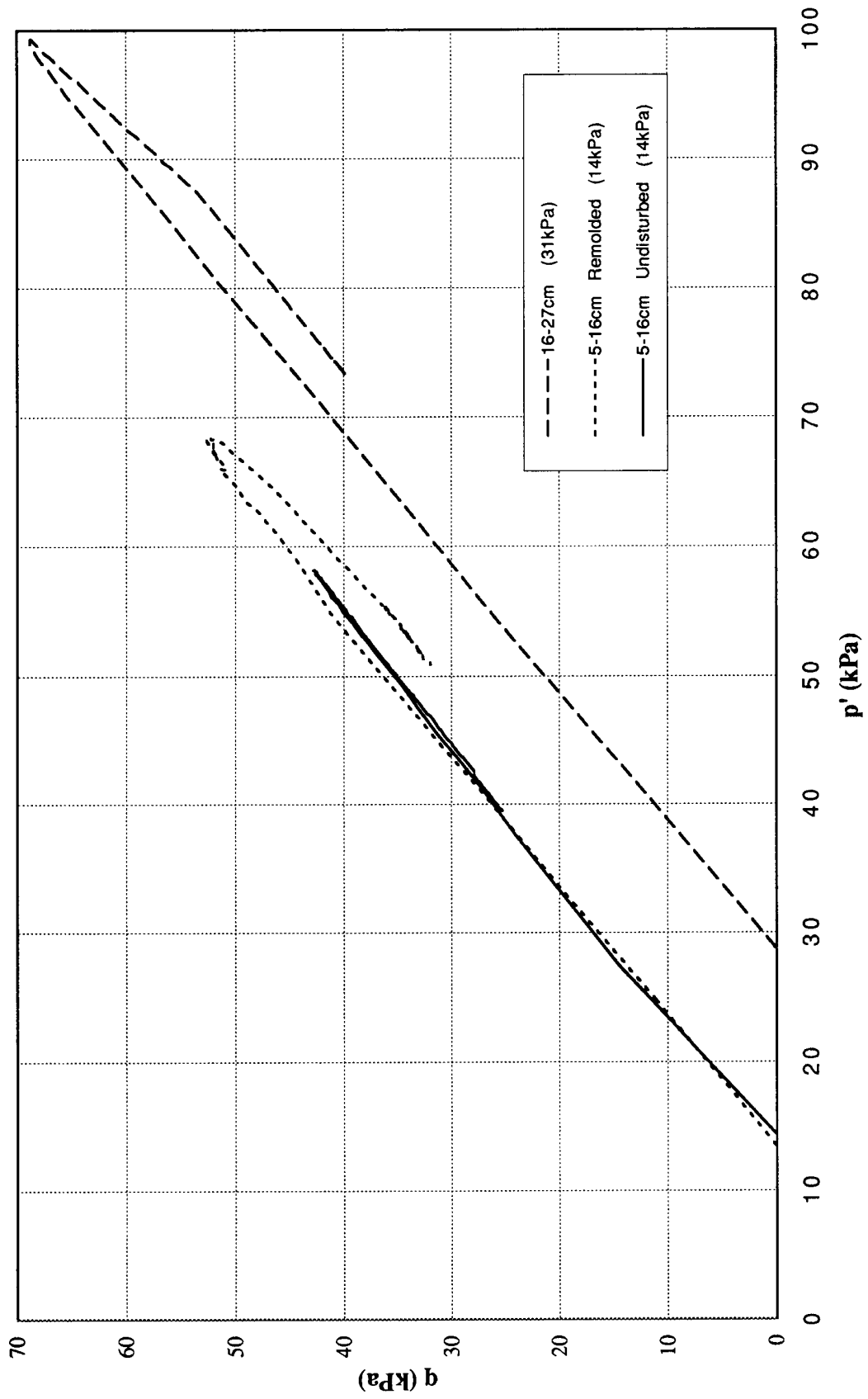


Figure 23 . CID Triaxial Test Effective Stress Path Results for Core 575-PC-GC, Panama City, FL Site.

References:

- Abegg F. & A. Anderson (1996). The acoustic turbid layer in muddy sediments." Eckernförde Bay, W. Baltic Sea: Methane concentr., saturated and bubble charact. *Marine Geology*.
- Ag, A. and Silva, (1998). "Consolidation and Permeability Behavior of High Porosity Baltic Seabed Sediments", *Geotechnical Testing Journal*. In press.
- Ag, A. (1994). Consolidation and permeability behavior of high porosity Baltic seabed sediments. *MS Thesis*, University of Rhode Island.
- Brandes, H.G., Silva, A.J., Ag, A. and Veyera, G.E. (1996). "Consolidation and permeability characteristics of high porosity surficial sediments in Eckernförde Bay." *Geomarine Letters*, 16(3):175-181.
- Brandes, H.G., Veyera, G.E. and Silva, A.J. (1994). "Rheological Characteristics of High Porosity Surficial Sediments at the CBBL/SRP Baltic Sea Site," *Abstract presented at Ocean Sciences Meeting*, San Diego, CA, Trans, AGU, Vol. 75
- Brogan, D. (1995) "The Strength Behavior of Baltic Sea Sediments." *MS Thesis*, Department of Ocean Engineering, University of Rhode Island.
- Keller, G.H. (1982) "Organic matter and the geotechnical properties of submarine sediments." *Geomarine Letters*, 2:191-198
- Lavoie, D.M, Lavoie, D.L., Pittenger, H.A. and Bennett, R.H. (1996) "Bulk sediment properties interpreted in light of qualitative and quantitative microfabric analysis." *Geomarine Letters*, 16(3):226-231.
- Nittrouer, C.A., Lopez, G.R., Wright, L.D., Bentley, S.J., D'Andrea, A.F., Friedrichs, C.T., Craig, N.I. and Sommerfield, C.K. "Oceanographic processes and the preservation of sedimentary structure in Eckernförde Bay, Baltic Sea." *Continental Shelf Research*, in press.
- Pizzimenti P. and Silva, A. (1997). "Stress-Strain Behavior of Surficial Carbonate Sediments from Key West, Florida.", *Marine Georesources and Geotechnology*, 15:335-362.
- Pizzimenti, P. (1996). "Stress-Strain Behavior of Surficial Carbonate Sediments from Key West, Florida." *MS Thesis*, University of Rhode Island.
- Richardson, M.D. (1994) "Investigating the coastal benthic boundary layer." *EOS*, Transactions, American Geophysical Union, 75(17):201, 205, 206.
- Silva, A.J. and Brandes, H.G (1998). "Geotechnical Properties and Behavior of High-Porosity, Organic-Rich Sediments in Eckernförde Bay, Germany," *Special Issue of Continental Shelf Research on CBBL/Baltic*, in press.
- Silva, A.J. and Brandes, H.G. (1997). "Geotechnical properties of organic gassy sediments from Eckernförde Bay." *Proceedings, XIV International Conference on Soil Mechanics & Foundation Engineering* in Hamburg.
- Silva, A.J., Brandes, H.G. and Veyera, G.E. (1996). "Geotechnical characterization of surficial high-porosity sediments in Eckernförde Bay." *Geomarine Letters*, 16(3):167-174.
- Silva, A.J., Sadd, M.H, Veyera, G.E. and Brandes, H.G. (1995). "Variability of Seabed Sediment Microstructure and Stress-Strain Behavior in Relation to Acoustic Characteristics", technical Report on research project sponsored by Naval Research Laboratory, Stennis Space Center. 3rd Year Report, December, 1995.
- Silva, A.J., Sadd, M.H, Veyera, G.E. and Brandes, H.G. (1996) "Variability of Seabed Sediment Microstructure and Stress-Strain Behavior in Relation to Acoustic Characteristics", technical Report on research project sponsored by Naval Research Laboratory, Stennis Space Center. 4th Year Report, November, 1996.
- Silva, A.J. and Jordan, S.A. (1984). "Consolidation properties and stress history of some deep sea sediments." In: Dennes B. (Ed.), *Seabed Mechanics, Proceedings IUTAM and IUGG symposium*, 25-40.
- Sykora, G.F. (1998). "Acoustic Characteristics in Relation to Stress-Strain Behavior of Calcareous Sediments from Key West, Florida." *MS Thesis*, Department of Ocean Engineering, University of Rhode Island.
- Terzaghi, K. and Peck, R.B. (1967). *Soil mechanics in engineering practice*. New York: John Wiley & Sons.
- Wever, T. F., Fiedler, H. M. and Stender, I. (1995) "The acoustic turbidity horizon: its variation in depth and time." In: T.F. Wever (Ed.), *Proceedings of the Workshop: Modelling Methane-Rich Sediments of Eckernförde Bay, FWG Report 22*, 30-34.
- White, F.M. (1991). *Viscous Fluid Flow*. New York: McGraw-Hill, 2nd Ed., 614 pp.

Funding Profile:

The following table shows the breakdown of project funds as requested in the original proposal from URI/MGL and the actual funds received on a yearly basis.

	Original Budget	Actual Amount Received
Year 1 (1993)	\$186,489	\$228,000
Year 2 (1994)	\$191,620	\$182,250
Year 3 (1995)	\$179,444	\$194,800
Year 4 (1996)	\$179,425	\$62,711
Year 5 (1997)	\$191,597	\$87,784
TOTALS:	\$928,575	\$755,545

Experimental and Theoretical Studies of Near-bottom Sediments to Determine
Geoacoustic and Geotechnical Properties

R. D. STOLL¹, R. FLOOD² and E. O. BAUTISTA³

¹Professor Emeritus of Civil Engineering and Special Research Scientist
Lamont-Doherty Earth Observatory of Columbia University, Palisades, New York 10964

²Associate Professor of Marine Geology
State University of New York, Marine Sciences Research Center, Stony Brook, New York 11794

³Lamont-Doherty Earth Observatory of Columbia University, Palisades, New York 10964

Abstract:

In a program designed to develop methods for predicting and measuring certain geoacoustic and geotechnical properties of the sediments immediately beneath the sea floor, several new tools were developed to measure *in situ* properties such as undrained shear strength, shear wave velocity and angle of internal friction. These tools include a motorized penetrometer designed to measure quasistatic cone penetration resistance up to depths of two meters into the bottom, a Love wave source and linear receiving array to measure shear wave velocity, and a 22-caliber source and array designed to generate Scholte waves with higher dominant frequency than conventional airgun sources. Using data obtained with this equipment as well as from other CBBL investigators, dynamic shear moduli derived from measurements of shear wave velocity were correlated with cone penetration resistance and the results were found to be consistent with results obtained by geotechnical engineers for many different clay soils. This result suggests that their regression equation may also be used for marine sediments of the type tested in the current program. In addition to the above work, the Biot-Stoll model was used to establish a baseline geoacoustic model for the soft, gassy soils of Eckernförde Bay which constitutes the starting point for studies of the perturbing effects of free gas bubbles and other scatterers in the sediment.

Objectives:

The main objective of our work in this program was to develop methods for predicting and measuring certain geoacoustic and geotechnical properties of the sediments immediately beneath the sea floor. In particular we focused on *in situ* shear strength and shear wave velocity and how they are related. The shear strength, which is a large-strain parameter usually expressed as undrained shear strength, s_u , in fine-grained sediments or angle of internal friction in coarser granular sediments, plays a fundamental role in determining the penetration and stability of mines deployed on the seafloor. On the other hand, the shear wave velocity is a small strain parameter which has been studied extensively in recent years because of its importance in the determination of bottom loss in long-range propagation in shallow water. It is also an important input parameter in all comprehensive seafloor geoacoustic models [Stoll, 1989].

A second objective of our work was to develop a baseline model for soft sediment that would match the response measured by various investigators in both the low and high frequency

ranges and thus would be a unified starting point for studies of the effects of free gas and other discontinuities.

Approach:

During the first two years of the CBBL program several new tools were developed to measure the properties mentioned above. These include a torsional wave source which generates Love waves in the sediment near the sea floor and a quasistatic cone penetrometer designed to measure shear strength. In addition, a p-sv wave source, which utilizes 22-caliber blank cartridges, was developed to generate low amplitude pulses with a somewhat higher dominant frequency than conventional airguns. These new tools are described in detail in [Stoll et al, 1994]. A photograph of the Love wave generator and the quasistatic cone penetrometer mounted on a self-righting sled is shown in Figs. 1.

In addition to the design and construction of new tools for *insitu* measurements, new computer programs for inverting the field data were developed. These include a program for analyzing the dispersion of Love waves generated by the torsional wave source mentioned above. This analysis determines velocity of horizontally polarized shear waves as a function of depth for the first several meters of sediment below the sea floor [Bautista and Stoll, 1995].

The equipment and techniques developed during the CBBL program were used in a number of field experiments:

1. Baltic Sea at Eckernförde, Germany in cooperation with FWG, May 1993.
2. Gulf of La Spezia, near SACLANT Undersea Research Center, La Spezia, Italy, May 1993.
3. Gulf of Mexico, near Panama City, Florida, August 1993.
4. Baltic Sea at Eckernförde, Germany in cooperation with FWG, June 1995.



Fig. 1 Torsional source and cone penetrometer mounted on self-righting sled.

The 1993 work in Eckernförde and the Gulf of Mexico was supported by the CBBL program whereas the work in Italy and the 1995 work in Germany were supported by ONR (U.S. Liaison Officer to SACLANT Center) and SACLANT Center.

Results:

As mentioned above, several new field techniques were developed to study *insitu* properties of the sediment immediately below the bottom. Development and testing of much of the necessary equipment was carried out during the first two years of the CBBL program.

Unfortunately, cutbacks in funding during subsequent years did not permit utilization of the new equipment to the fullest extent since we were unable to participate in the Key West or California experiments. As a result only a limited amount of field data was obtained, mainly from the 1993 and 1995 work in Eckernförde and the experiments in the Gulf of Mexico. One of our main objectives was to see if *insitu* shear strength, or alternatively, quasistatic cone resistance, Q_c , could be correlated with dynamic shear modulus G_{\max} or shear wave velocity. A plot of G_{\max} versus Q_c is shown in Fig. 2. In this figure, some of the values of shear modulus are based on measurements by Richardson et al [personal communication] using the ISSAMS probes and some were made with our shear wave source. From this preliminary figure it appears that there is a definite correlation between these two dissimilar properties (i.e., one small strain anelastic and the other large strain, plastic) and we hope to expand our data base relating to these two parameters in the future.

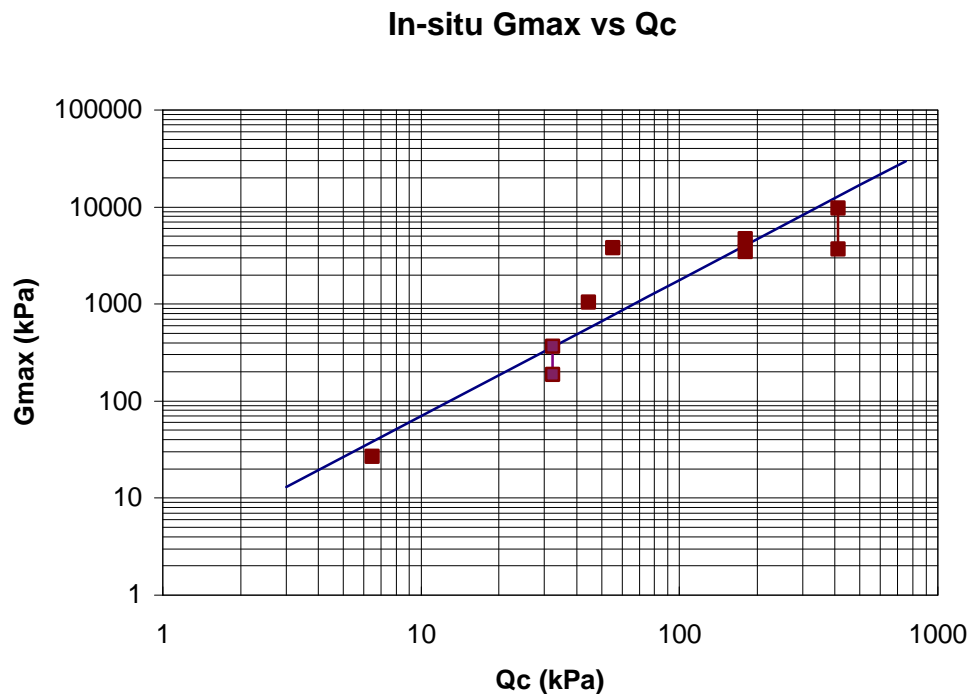


Fig. 2. Shear modulus calculated from shear wave velocity versus quasistatic cone penetration resistance. The solid line which has the equation $G_{\max} = 2.87 Q_c^{1.335}$ is based on a regression analysis of 481 tests on 31 clay soils located worldwide [Rix and Mayne, 1993]

One of the more important uses of the data collected during the CBBL program is the benchmarking or “ground truthing” of models that are used to predict velocity and attenuation in the near-bottom sediments. Measurements by various participants in the program resulted in some data taken at high frequencies using pulse propagation techniques whereas other data was obtained at low frequencies typical of interface wave experiments. Data from both kinds of measurement were used as input in constructing a “baseline” model using the Biot theory, which is valid over a wide frequency range [Stoll, 1998] and serves as a starting point for studies of the effects of discontinuities in the structure of a sediment. In another paper [Stoll, 1997], an

operator proposed by Biot, that results in a response like that of a harmonic oscillator, was incorporated into the baseline model to show the effects of bubble resonance for the case where free gas exists as bubbles in the pore spaces.

Accomplishments:

The main accomplishments of our work include the development of new field methods to measure shear wave velocity and attenuation and to measure *insitu* shear strength. Since the shear wave measurements are made at low frequencies they provide information that cannot be obtained with pulse measurements using probes of the type used on the ISSAMS apparatus or the acoustic lance used by others in the CBBL program. Moreover by measuring both velocity and strength *insitu* on undisturbed sediment, we have been able to obtain a correlation that would be questionable if it had been done on laboratory specimens which are subject to sampling disturbance and changed environmental conditions.

Our application of the Biot model to the CBBL data for the soft sediments of Eckernförde Bay showed how the theory may be used to bridge the gap between high and low frequency data in building a unified baseline model. It also highlighted the fact that more data on the low frequency dilatational response (velocity and attenuation) are needed to fully define the “best” model.

In addition to measuring shear strength for correlation with other sediment properties as described above, the cone penetrometer developed early in the CBBL program has been used to measure penetration resistance as a function of depth for a variety of different purposes ranging from the measurement of sand-cap thickness over dredge spoil areas to the establishment of “ground truth” in the development of a dynamic seafloor penetrometer. Improved versions of the penetrometer have been built as permanent equipment for the Naval Research Lab (for installation on their ISSAMS system) and for SACLANT Undersea Research Center.

Finally, an important spinoff of our CBBL work should be mentioned. Several versions of the quasistatic cone penetrometer developed in 1993 have been used to provide “ground truth” in the development of an expendable bottom penetrometer (XBP) that can be launched from a moving ship and is used to assess the penetration resistance of the seafloor to determine the potential for mine burial. The XBP is similar in shape and size to a standard bathythermograph (XBT) and uses the same double-spool, fine-wire system for data transmission. However in the XBP, the thermistor used to measure temperature in the XBT is replaced by an accelerometer which measures deceleration as the probe penetrates the seafloor. The record of deceleration is then inverted to obtain cone resistance or shear strength as a function of depth as well as information pertaining to the dynamic shear modulus of the sediment. To date over 500 XBPs have been deployed in areas where the sediment varied from soft mud to compact sand and a U.S. patent has been obtained for the system [Stoll and Akal, 1997]. Without the aid of the cone penetrometers developed under the CBBL program, it would have been impossible to evaluate the performance of these probes and to create a comprehensive data base relating probe signature to sediment properties.

References

Stoll, R. D. (1989) *Sediment Acoustics*, (Springer-Verlag, Berlin)

- Stoll, R. D., Bautista, E. O. and Flood, R. (1994) "New tools for studying seafloor geotechnical and geoacoustic properties," J. Acoust. Soc. Am., **96**, 2937-2944.
- Bautista, E. O. and Stoll, R. D. (1995) "Remote determination of *insitu* sediment properties using Love waves," J. Acoust. Soc. Am., **98**, 1090-1096.
- Mayne, P. W. and Rix, G. L. (1993) " G_{\max} - q_c relationships for clays," Geotechnical Testing Jour., **16**, 54-60.
- Stoll, R. D. and Bautista, E. O. (1998) "Using the Biot theory to establish a baseline geoacoustic model for seafloor sediments," Continental Shelf Res. (in press)
- Stoll, R. D. and Bautista, E. O. (1997) "Geoacoustic modeling of the seabed at higher frequencies," in *High Frequency Acoustics in Shallow Water*, edited by Pace et al, NATO, Saclant Undersea Research Center, La Spezia, Italy, 517-524.
- Stoll, R. D. and Akal, T. (1997) "Probe for evaluating seafloor geoacoustic and geotechnical properties," U. S. Patent No. 5,681,982 issued Oct. 28, 1997.

Publications:

Peer reviewed

- Stoll, R. D., Bautista, E. and Flood, R. (1994) "New tools for studying seafloor geotechnical and geoacoustic properties," J. Acoust. Soc. Am., **96**, 2937-2944.
- Bautista, E. O. and Stoll, R. D. (1995) "Remote determination of *insitu* sediment parameters using Love waves," J. Acoust. Soc. Am., **98**, 1090-1096.
- Stoll, R. D. and Bautista, E. O. (1998) "Using the Biot theory to establish a baseline geoacoustic model for seafloor sediments," Continental Shelf Research, (in press).

Symposium proceedings

- Stoll, R. D. and Bautista, E. O. (1995) "Measuring near-bottom shear wave velocity using Love waves," Proc. Workshop 'Modelling Methane-Rich Sediments of Eckernförde Bay', Eckernförde, Germany, 26-30 June, 1995.

Dissertation

- Bautista, E. O. (1994) "Remote determination of *insitu* sediment properties using Love waves," Ph.D. dissertation, Columbia University.

Modeling Surficial Roughness and Sub-Bottom Inhomogeneities from Acoustic Data Analysis

Dajun TANG

Applied Physics Laboratory, University of Washington
Seattle, WA 98105

and

George V. FRISK

Woods Hole Oceanographic Institution
Woods Hole, MA 02543

Abstract: During the three years funded by the Coastal Benthic Boundary Layer (CBBL) Special Research Program, we have concentrated our work on modeling scattering of sound waves by sediment bubbles. Data sets obtained in experiments conducted at Eckernfoerde Bay, Germany, and Panama City, Florida, by Darrell R. Jackson and Kevin L. Williams of the Applied Physics Laboratory, University of Washington, provided us with the opportunity to study interactions of sediment bubbles and high-frequency acoustic scattering. In analyzing high-frequency (40 kHz) backscattered data at small grazing angles (5° - 20°), we found a layer of scatterers buried about 1 m beneath the seafloor at the Eckernfoerde site. This finding is consistent with the results of field surveys using other methods. Coring and X-ray tomography analysis conducted by other CBBL investigators revealed methane gas voids of nonspherical shapes, which are clearly the dominate scatterers at this site. To model acoustic backscattering by this buried bubble layer, we used oblate spheroids to approximate the gas voids. The density and spatial distribution of the gas voids were derived from limited core data. Proper statistical averages were taken to make model/data comparisons. The results of this single scattering model compared favorably with backscattering data at 40 kHz. Later, this model was extended to cover bistatic scattering. In particular, the azimuthal dependence of the bistatic scattering strength predicted by the model was compared with experimental data, and it was found that both the model and the measured data exhibited a mild azimuthal dependence. The best agreement between the model and the data required a 35 percent reduction in the areal bubble density used in the backscattering model/data comparison. A possible reason for this is multiple scattering effects.

Original Objectives: Our objectives in this program were integrating various acoustic data with available environmental data in order to model the scattering processes in shallow water sediments. The emphasis was placed on the analysis and modeling of scattering by gassy sediments.

Approach: Data on gassy sediments were provided by Darrell Jackson and Kevin Williams of the Applied Physics Laboratory, University of Washington. In collaboration with the APL team and various other scientists in the CBBL project, we started from simple

models. The models were compared with data, and necessary changes were made if needed. First, backscattering data were analyzed and a model was developed. Later the backscattering model was extended to cover bistatic scattering as well.

Results: The main results have been published in scientific journals and are listed in the References section. Reference 1 establishes that the backscattering at Eckernförde Bay was caused by a scattering layer about 1 m beneath the seafloor and that the scatterers were methane gas voids. The backscattering strengths at this gassy site were about 3 dB higher than those at the sandy Panama City site. Reference 2 describes the technique used to model backscattering due to such gas voids. In brief, scattering cross sections of oblate spheroids were calculated to approximate those of gas voids. Proper statistical averages were taken and model/data comparisons were made. It was found that this single scattering model compared favorably with the measured acoustic backscattering at 40 kHz. In the model, the density and spatial distribution of the gas voids are derived from limited core data. Reference 3 describes the bistatic scattering model proposed as an extension of the previously developed backscattering model. In this model, gas bubbles are again assumed to be oblate spheroids with varying aspect ratios, and a single scattering approximation is used. The model results were then compared with bistatic data acquired in Eckernförde Bay, Germany. In particular, the azimuthal dependence of the bistatic scattering strength predicted by the model was tested against experimental data, and it was found that both the modeled and the measured bistatic scattering strength exhibit a mild azimuthal dependence. The best agreement between the model and the data required a 35 percent reduction in areal bubble density relative to that used in the backscattering model/data comparison. A possible reason for this is multiple scattering effects. Reference 4 addresses a particular issue in applying interferometric technique used to locate the buried scatterers in the sediments. In that paper, numerical simulations are compared to both the Eckernförde and Panama City data sets.

Accomplishments: The study of acoustic scattering by gas bubbles buried in sediments is a relatively new area. Because gas bubbles are extremely efficient scatterers of sound, it is of great importance to understand bubble acoustics in order to obtain proper sonar predictions wherever sediment bubbles exist. However, measuring the spatial and temporal distribution of bubble clouds in sediment and measuring the shape of individual bubbles in situ are difficult. It is only recently in the CBBL program that a quantitative description of sediment bubbles has become available to provide input parameters for acoustic models. In our effort in the CBBL program, we started from encountering a new phenomenon – finding that a layer of bubbles buried relatively deep in the sediment is the dominant scatterer at the Eckernförde site. A model was developed for this backscattering and later extended to bistatic scattering. These models quantitatively predict the measured scattering strength over a wide range of grazing angles and bistatic angles. It was concluded from the model/data comparison that multiple scattering effects are important, and a new model will be needed for a more complete description of scattering by sediment bubble layers.

The following is a brief review of our accomplishments. The Benthic Acoustic Measurement System (BAMS), developed by the Applied Physics Laboratory of the University of Washington, was used for measuring high-frequency sea bottom backscattering strengths and locating sources of bottom scattering. BAMS is an interferometric system, and its operation principle is similar to that of a swath bathymetric sidescan sonar. The arrival angle of the signal backscattered from the bottom is determined by measuring the phase difference between arriving signals at two slightly separated receivers. The depth of the bottom scatterers is then estimated from the measured arrival angle of the backscattered signal and its arrival time. High-frequency (40 kHz) backscattering data were obtained at two distinct coastal sites: the gas-rich soft sediments of Eckernfoerde Bay and the sandy sediments off Panama City, FL. The phase-difference method was used to locate the scatterers for each data set, and then appropriate propagation models were used to estimate the scattering strengths. Since it is known from measurements that scattering at the sandy Panama City site is from seafloor roughness and that there is little penetration into the sediment, the Panama City data set was used as a reference. Figure 1 shows the estimated depth of scatterers at each site. It is evident that the Eckernfoerde site features a scattering layer at about 1 m beneath the seafloor. When backscattering strength is estimated according to Ref. 1 (Figure 2), the results show a rather strong scattering strength. As a matter of fact, the scattering strength at the Eckernfoerde site is 3 dB stronger than that at the Panama City site. Cores taken at the Eckernfoerde site by other CBBL scientists showed a corresponding layer of gas bubbles. The strong scattering strength extracted from the data clearly is in agreement with that finding.

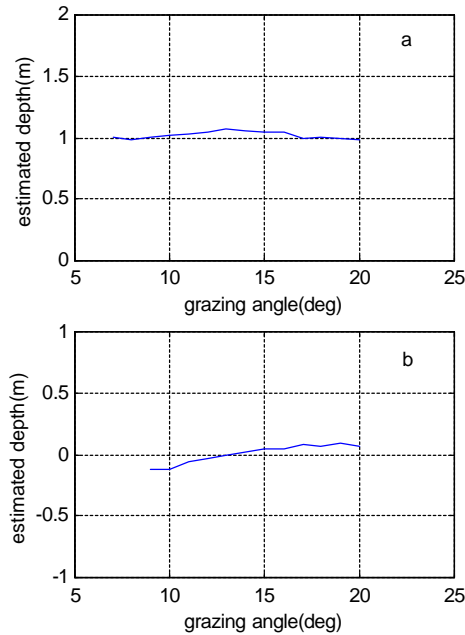


Fig. 1. Estimated average depth of bottom scatterers versus grazing angle: (a) for Eckernfoerde, (b) for Panama City.

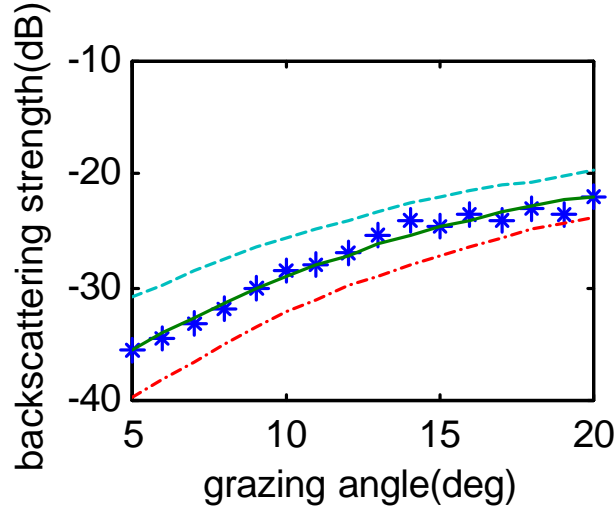


Fig. 2. Model fit to the backscattering strength data of Eckernförde Bay. The middle curve is a least-square fit and the other curves are the upper and lower bounds. For details see Ref. 1.

Based on these results we conclude the following:

- Since the Eckernförde sediment has a slower sound speed than that in the water column near the bottom, incident acoustic rays at small grazing angles will be bent to larger grazing angles while propagating in the sediment (Snell's law). Since the scatterers are buried approximately 1 m below the seafloor, the bending will shorten the distance that a ray will traverse before encountering the scatterers.
- On the basis of an attenuation measurement at 58 kHz by Richardson (reference given in Ref. 2), and assuming a linear relationship for attenuation coefficient vs. frequency over the frequency range of 40 -58 kHz, we estimated that the attenuation at 40 kHz is 2.4 dB/m. This small attenuation allows enough incident acoustic energy to reach the scatterers to result in appreciable scattered energy being measured at the receivers.
- We have estimated that the gas voids, on average, have an equivalent surface backscattering strength of -10.8 dB and that there is a weak angular dependence on grazing angle over the range of 5° - 20°.
- X-ray tomographic analysis of sediment cores by Abegg *et al.* (reference is given in Ref. 2) showed methane gas voids that tended to concentrate into thin layers approximately 10 cm thick. The layer of gas voids was about 1 m beneath the seafloor. The smallest gas bubbles that the X-ray tomographic technique can resolve are 1 mm in diameter. Larger gas voids generally had non-spherical shapes; in most cases they look like irregular shaped coins, owing to unknown sediment dynamics. In addition, the larger gas voids tended to configure themselves as coins standing on their edges. In a particular core (Core 315) taken near the site where the 40-kHz backscattering

experiment was conducted, there was a gas-rich layer at approximately 1 m beneath the seafloor that had 120 gas voids within a volume of 1200 cm^3 . The vertical span of the gas voids was less than 15 cm. Above and below this layer, few gas bubbles were present. We assume that the bubbles in this layer were the primary scatterers. Since the layer was thin, we can view it as an equivalent surface scatterer. In that case, the equivalent surface concentration of bubbles is 1.5 per cm^2 .

Based on these observations, we proposed a backscattering model in which the scatterers were oblate spheroids. Figure 3 shows the normalized bistatic scattering cross section of the spheroids.

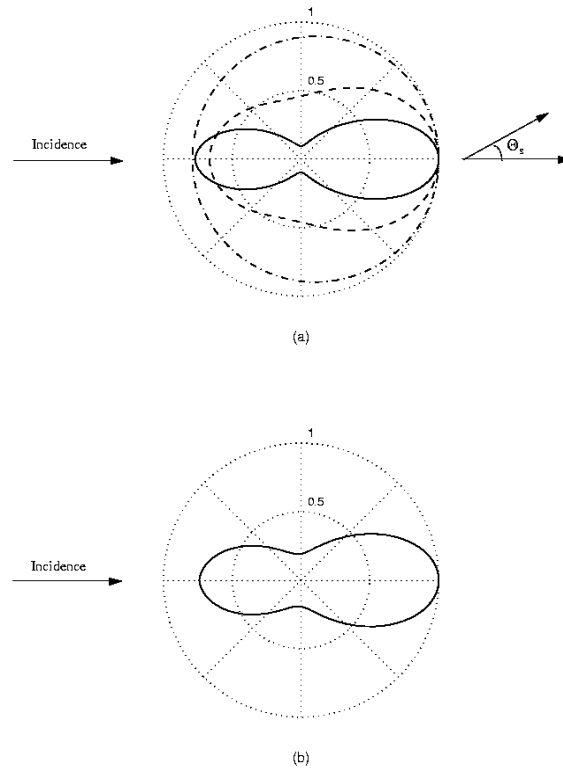


Fig. 3 Normalized bistatic scattering cross section of an oblate spheroid. In all computations, the frequency is 40 kHz, the sound speed is 1425 m/s, and the semi-minor axis of the spheroid is 1 mm, ($ka = 0.18$). (a) Scattering directivity pattern of an oblate spheroid with an aspect ratio of 1 (dash-dotted), 5 (dashed), and 10 (solid). (b) Average scattering cross section normalized over aspect ratio by using an exponential PDF. For details see Ref. 3.

In both models the measured bubble distribution is taken into account and it is assumed that small bubbles, which are not measurable, will not resonate at 40 kHz. The results of the model/data comparison of backscattering strength are given in Figure 4. The results of the model/data comparison for bistatic scattering strength are given in Figure 5.

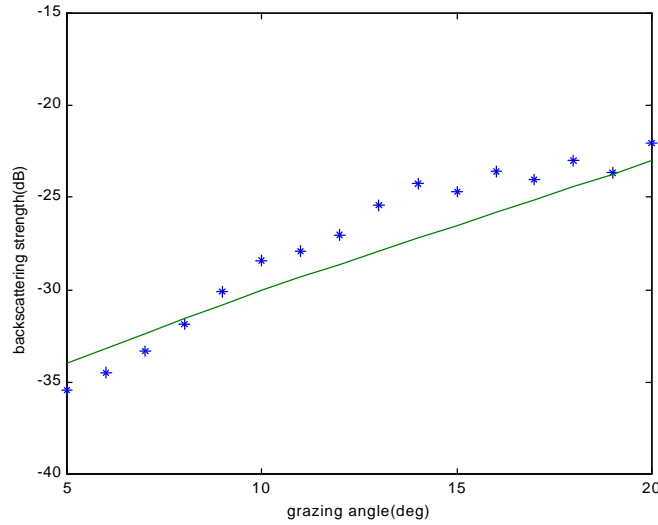


Fig. 4. Comparison of the modeled backscattering strength and measured data. Bubble density was found to be 1.4 per cm^2 . For details see Ref. 2.

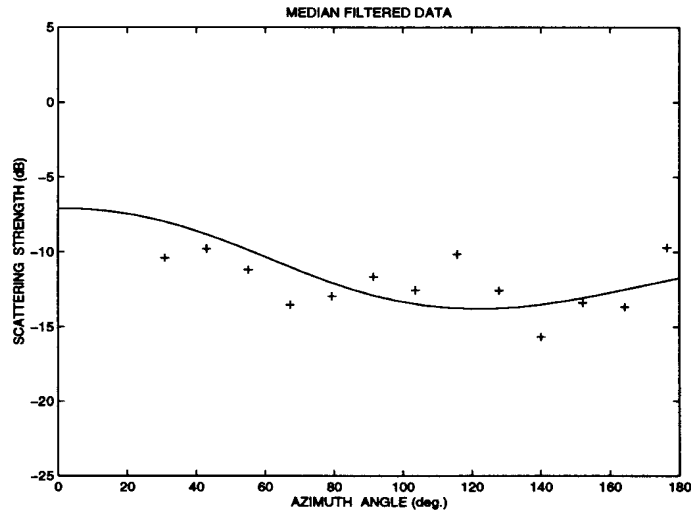


Fig. 5. Average bistatic scattering strength as a function of azimuth angle. For details see Ref. 3

In summary, we have developed a two layer, single scattering, bistatic model to simulate the scattering by nonspherical bubbles buried in an attenuating sediment. A bubble layer of a finite thickness is approximated by a bubble surface at a certain depth, i.e., all bubbles are taken to be on the surface. The bubbles are modeled as oblate spheroidal voids (pressure-release). When the results are compared with data acquired in Eckernförde Bay, Germany, there is reasonable agreement if the bubble density is reduced by 35 percent relative to that used in the backscattering model. The average scattering strength exhibits a mild azimuthal dependence: the maximum is reached in the forward direction and the minimum occurs when the transmitting and scattering directions are close to perpendicular. In contrast, backscattering strength has a medium value. The total fluctuation is about 6 dB. However, even though the single scattering theory seems quantitatively successful for the Eckernförde data in some aspects, further consideration of the amount of energy scattered indicates that it cannot be the whole story. Section II.c in Ref. 3 implies that for the Eckernförde site multiple scattering and forward scattering loss must play a role at least for some range of grazing angles in order to avoid a violation of the law of conservation of energy. A more severe criterion is set by the data of Lambert *et al.* (reference given in Ref. 3) which indicate at least qualitatively that these two scattering mechanisms are probably important even at normal incidence. This implies that multiple scattering and forward scattering loss are, in effect, being treated phenomenologically in the present single scattering model via reduction in bubble density, whereas what is probably happening is that the deeper bubbles in the bubble layer are ensouffled at a reduced sound field level. Consequently predictions of scattering back into the water column are consistent with measured results but predictions of the amount of energy in the sediment below the bubble layer violate both the conservation of energy law and the more qualitative results of Lambert *et al.* Therefore, further modeling of the Eckernförde site that incorporates multiple scattering and forward scattering loss is needed.

References/ Publications (Peer reviewed):

1. D. Tang, G. Jin, D. R. Jackson, and K. L. Williams, "Analyses of high-frequency bottom and sub-bottom backscattering for two distinct shallow water environments," J. Acoust. soc. Am. Vol. 96, 2930-2936 (1994).
2. D. Tang, "Modeling high-frequency acoustic backscattering from gas voids buried in sediments," Geo-Marine Letters, Vol. 16, 261-265 (1996).
3. D. Chu, K. L. Williams, D. Tang, and D. R. Jackson, "Modeling of bi-static scattering from sediment bubbles," J. Acoust. Soc. Am. Vol. 102, 806-814 (1997).
4. G. Jin and D. Tang, "Uncertainties of differential phase estimation associated with interferometric sonars," IEEE J. Ocean Engineering Vol. 21, 53-63 (1996).

Publications (Symposium proceedings):

5. D. Tang, C. J. Sellers, G. V. Frisk, and S. G. Schock, "Acoustic backscattering from methane gas voids buried in sediments," Proceedings of the Workshop, Modeling Methane-Rich Sediments of Eckernfoerde Bay, June 26-30 (1995).

Backscatter characteristics from different sea floor types

TH.F. WEVER, G. FECHNER, H.M. FIEDLER, I.H. STENDER

Forschungsanstalt der Bundeswehr
für Wasserschall und Geophysik
Klausdorfer Weg 2-24
24148 Kiel
Germany

Abstract

Three areas with different sea floor sediments (gassy mud, quartz sand, calcareous sand) have been investigated with a commercial side scan sonar and a digital attachment developed at FWG. The recording of the sonar data with the digital attachment of FWG enabled a digital processing of the data and the calibration with an identical procedure for comparison in terms of backscatter strength. Further sea floor information was acquired by a subbottom profiler. Mapping of the sea floor was part of the pre-site survey for JOBEX/CBBL experiments.

The results from the very soft gassy mud sea floor of Eckernförde Bay (Germany) prove an extremely low backscatter that increases as more free gas is available near the sea floor. The comparison of the quartz sand sea floor off Panama City (Florida) with the calcareous sand sea floor of the Florida Keys near the Dry Tortugas showed that backscatter from carbonate sediments is higher than from quartz sediments of the same grain size. The reason may be precipitation of soluted carbonate that 'glues grains together'.

The different results of 100 kHz side scan sonar data and the 40 kHz data of other groups in Eckernförde Bay point out the importance of sonar frequency for results from the sediment volume.

Original Objectives

Beside mapping of the areas for the selection of an homogeneous research site the side scan sonar data was to be calibrated for a direct quantitative comparison of backscatter characteristics of the different sediment types. Due to technical problems the absolute calibration of the side scan sonar with help of other, absolute backscatter measurements could not be performed. Therefore, a different approach was chosen making use of the known reflectivity/backscatter of the sea surface.

Approach

Prior to the JOBEX/CBBL (Joint High Frequency Backscatter Experiments/ Coastal Benthic Boundary Layer) experiments at the sea floor, the target areas were mapped with a commercial 100 kHz side scan sonar and a 3.5 kHz subbottom profiler. The data was combined to give a full-coverage map of backscatter variation and depths of subsurface layers (Fiedler and Stender, 1993; Davis et al., 1996; Wever et al., 1997). In addition to the commercial side scan sonar an additional system of FWG recorded and processed the raw data to allow a quantitative backscatter measurement (for details see Fechner and Waeber, 1992; Fechner et al., 1994). This data forms the basis for the quantitative comparison of different sea floor types. The full-coverage pre-site survey mapping resulted in backscatter maps of 15 km² at Eckernförde Bay, 13 km² for the Panama City (FL) sand sheet, and 81 km² off the Dry Tortugas (FL).

The lack of an absolute calibration of the side scan sonars on the basis of absolute sea floor backscatter determination prohibited a comparison of the research sites. To overcome this problem we made use of the fact that under calm conditions the sea surface is an ideal reflector with a reflection coefficient of 1 (i.e., 100%). This means, that one unknown factor in the backscatter equation (Urick, 1983) can be determined. After some physical and mathematical considerations (details are omitted here, see Stender et al., 1995, for details) the quantity describing the influence of the sea floor, the „scattering characteristic“ ($SC = 10 \log \mu$), sometimes also called „Lambert factor“, can be calculated on the basis of Lambert's rule by:

$$(1) \quad 10 \log \mu = RL + 30 \log r - 10 \log h + 2\alpha r - (SL + 10 \log A_0)$$

with RL: returned signal level in dB, h: height of the sonar above sea floor, α : absorption coefficient, r: slant range, SL: source level in dB, and A_0 : reference area. All terms of the right hand side of equation (1) can be determined by experiment with the exception of the calibration constant:

$$(2) \quad C = SL + 10 \log A_0.$$

C was to be determined at a reference location where $10 \log \mu$ was measured by other methods. This approach was not successful, therefore the following procedure was chosen as alternative.

To calibrate FWG's side scan sonar, the towfish was mounted on a tripod at 10 m below sea surface in the harbour of the Navy Yard in Kiel. On top of the tripod was a capstan that could be tilted from 0° to 90° orientation relative to the sea surface in steps of 1°. To avoid interference only one of two side scan transducers pinged. The first received signal came from the sea surface. Using all available data (amplification of the received signal, filtering, rectification, etc.) a beam pattern of the transducers and a sensitivity curve for the receivers could be determined. This was done for both transducers of the side scan fish. A detailed report about the calibration procedure with discussion of the different steps and aspects is in preparation. Although this method may have disadvantages and may not be an absolute calibration, it

allows to process all raw side scan data with the same calibration and thus compare the results from different surveys.

The physical description of the sea floor in terms of backscattering strength needs a relation to the geological properties of the sea floor. Therefore, bottom samples were taken during all side scan sonar surveys. They are described by Silva et al. (1996), Briggs and Richardson (1996), Slowey et al. (1996), Davis et al. (1996), Mallinson et al. (1997), and Stephens et al. (1997). Sediment cores taken by other groups helped to identify layers in the subbottom profiler records.

Results

The side scan data was recorded continuously. For the digital analysis, the backscatter to a distance of 60 m on both sides of the fish was registered and processed. The position was recorded every 10 s (30 s during the Panama City survey) corresponding to a distance of 20 m (60 m) at a speed of 4 kn. The data between two time marks was averaged across the whole covered area of 2,400 m² and 7,200 m², respectively. The resulting figure was plotted along the track. For each investigated area three tracks were selected for the following discussion. For brevity, maps and data are not shown. They can be found in the cited publications and reports.

1. Eckernförde Bay

Eckernförde Bay (Western Baltic) is characterised by extremely soft muddy sediments that contain free methane gas very close to the sea floor (mostly < 1 m). In some places the gas reaches the sea floor. For details about the environment see Fiedler and Stender (1993) and Wever et al. (1996). The data discussed was collected in September 1994 (Fiedler, 1994).

The southernmost track (line 15) ran along the southern border of the experimental site, the "Red Box". It started about 1 nm west of the Red Box and ended ca 1 nm east of it on the shoal Mittelgrund. Its scattering characteristic (SC) is relatively constant at -23 dB in the central basin with muddy sediments and acoustic turbidity occurring between 0.5 and 1.0 m depth. In the eastern part of the track the hard till of Mittelgrund rises to the sea floor. It correlates with an increasing SC (-20 dB).

The track along the northern boundary of the Red Box (line 12) is characterised by a SC that varies between -22 dB and -24 dB above the muddy sediments. As soon as the shoal Mittelgrund is reached, SC increases to -20 dB. Thus this track is very similar to the southern line but exhibits a higher variability of the SC in its centre.

The northernmost track (line 21) ran parallel to the coast outside the Red Box. It started above muddy sea floor with no or a deep (> 2 m) horizon of free gas. This area shows an extremely low SC of -26 dB. Along the track a general rise of the free gas to shallower levels is observed

as well as narrow spots with harder sediment and mud without free gas. Except for pockmarks where free gas is observed at the sea floor the values of SC are below -24 dB.

In general, a scattering characteristic of about -23 dB is recorded from the muddy sea floor of Eckernförde Bay with a 100 kHz system. In case of absence of free gas or free gas at greater depth below sea floor the value decreases to -26 dB.

2. Panama City

The Panama City sand sheet was selected for experiments as a representative site for quartz sand. Details about the survey, the exact location of the tracks and the sediment samples are reported by Stender et al. (1995) and Davis et al. (1996). The three tracks selected for this evaluation all run in a NW-SE direction. They are the westernmost (line 206), the easternmost (line 215) and a central (line 214) track. Roughly, fine sand dominates in the north and south of the surveyed area. Towards south a domain (width of 0.5 to > 1 km) of medium sand separates it from coarse sand. On a smaller scale 'fingers' or bands of different material complicate the situation. The side scan sonar clearly outlined these differences.

Line 206 started in the south on fine sand that rendered a SC of -19 dB. As soon as coarse sand dominates on the sea floor, SC rises to -14 dB (maximum). The decrease of grain size to medium sand reduces the SC by nearly 3 dB until the next stripe of coarse sand is crossed (-15 dB). The variable grain size domains along the line towards northwest is reflected in a SC that varies between -16 dB and -18 dB.

A very similar variability in SC is observed along the central line 214. The fine sand in the southwest yields a SC of -17 dB to -18 dB. It increases across a narrow stripe of medium sand to -14 dB. The large coarse sand sheet causes a SC of -12 dB that decreases to the northwest to -17 dB as the grain size slowly decreases again to fine sand.

Line 215 starts in the northwest above medium sand that is characterised by a SC of -16 dB. Towards southeast SC increases to -14 dB from a coarse sand. A small 'finger' of finer material (medium sand and fine sand) causes a drop of SC by 3-4 dB. At the sudden termination of the coarse sand sheet and transition to fine sand SC is reduced from -14 dB to -19 dB. Small stripes of coarser material are clearly marked in the SC data.

From this survey it is concluded that the sand grain size controls the scattering characteristic of the sea floor for 100 kHz:

- fine quartz sand: -17 to -19 dB,
- medium quartz sand: -15 to -16 dB,
- coarse quartz sand: -12 to -14 dB.

These values are only very rough estimates as they only distinguish between fine, medium, and coarse sand. The sorting or the skewness of the grain size distribution were not included. They will, however, have an influence. The inclusion of this aspect in a later, more precise evaluation will allow a better subdivision. In addition, it is planned to compare the tracks that

ran perpendicular to the ones discussed here. Especially effects that result from surface roughness are of interest. If, e.g., ripples are present they cause a higher backscatter when the lines run parallel to their crests than when the tracks are oriented perpendicularly to the crests.

3. Key West

The analysed data were collected in 1995 in a carbonate sand area. The research area included two flat sediment basins and two reefs. Both dominated the results. For detailed information about the survey see Wever (1996).

The lines were all oriented in a north-south direction. The westernmost line of this analysis (no. 58) starts in the north above a coarse silt sea floor (SC: -13 dB). The large basin with fine/medium silt shows a SC of -15 dB that increases to -14 dB in the south with presumably coarser material from the reef. Across the sand stripe north of the reef SC increases rapidly by 3 dB and at the reef is a sudden increase of SC to -7 dB to -8 dB. These values are very high and indicate that the calibration of the system is not an absolute calibration.

Line 7 near the centre of the surveyed area shows a similar distribution of SC. In the north above the sediment basin the SC has values of ca. -15 dB to -16 dB above fine/medium silt. SC increases to -13 dB as the sediment becomes coarser (sand) towards the reef. Above coarse sand SC equals -8 dB. Interestingly, this is the same value as for the reef's surface. Above the sediment basin south of the reef SC falls again to -17 dB.

Line 20 starts in the south above the southern sediment basin. The SC varies between -14 dB and -15 dB. At the reef it suddenly increases to -7 dB. The transition to coarse sand is marked by a narrow spike of decreasing SC but the sandy sediments show again the same SC as the reef. The transition to finer sediments is marked by a decrease of SC down to -11 dB. However, the northern part of the line does not run across the sediment basin and little sediment information is available from this area. The high variability of SC may be related to irregular changes of sediment grain size and surface structure.

The following SC values were observed in the Key West campaign:

- fine/medium carbonate silt: -15 to -16 dB,
- coarse carbonate silt: -13 dB,
- carbonate sand: -13 to -14 dB,
- coarse carbonate sand: -8 to -10 dB,
- reef surface: -7 to -8 dB.

The concentration of acoustic and geotechnical experiments in the north-western corner of the surveyed area caused a lack of sediment samples in its other parts. Therefore, the above mentioned correlation can only be considered a rough estimate.

Summing up all available data (despite the mentioned uncertainties) results in the following list of scattering characteristic for 100 kHz signals. The averaging over different areas (2.400 m² and 7.200 m², resp.) should also be kept in mind.

gas free/'deep'-gas mud	-26 dB
gassy mud	-23 dB
fine quartz sand	-17 to -19 dB
medium quartz sand	-15 to -16 dB
fine/medium carbonate silt	-15 to -16 dB
carbonate sand	-13 to -14 dB
coarse quartz sand	-12 to -14 dB
coarse carbonate silt	-13 dB
coarse carbonate sand	-8 to -10 dB
reef surface	-7 to -8 dB

It is interesting to note that coarse carbonate silt has approximately the same SC as coarse quartz sand. Similarly, fine/medium silt has the same SC as medium quartz sand. How far this observation is influenced by sampling and processing techniques of the grain size analysis cannot be estimated here. As a conclusion from the JOBEX/CBBL tests it can be stated that carbonate sediments cause a higher backscatter than quartz sediments of the same grain size. One possible cause for this observation can be the amalgamation of carbonate sediment grains. This can happen by carbonate that was in solution and during precipitation cements the near-surface sediments.

The influence of the surface roughness cannot be discussed in detail as no information is available from all different backscatter domains. For a discussion of the influence of surface roughness during the Key West Campaign see Wever et al. (1997).

Accomplishments

After calibration, the digital FWG attachment to the side scan sonar enabled the quantitative description and comparison of the backscatter strength of different sea floor sediments.

As expected, the least backscattered energy of the three areas investigated is recorded in the muddy areas of Eckernförde Bay. Tang et al. (1994) reported only little difference between the sandy sea floor off Panama City and the gassy mud of Eckernförde Bay. Their measurements were made at 40 kHz. The fact that a clear difference is observed on the 100 kHz side scan data underlines the frequency's important role.

The backscatter in the central basin of Eckernförde Bay is, except for a few pockmarks, relatively homogeneous. The side scan sonar survey on the Panama City quartz sand sheet showed a clear correlation of backscattering with grain size. A similar observation was made in the Dry Tortugas research site where a highly variable backscatter was observed. It could be shown that the reefs backscatter strength is 14 dB higher than that of the flat carbonate sand sediment troughs. Again, a general increase of backscatter strength is observed with increasing grain size. Interestingly, the backscatter strength of the carbonate sand and of the reef surface exhibit almost the same backscatter and could only be distinguished with the help of subbottom profiler data.

During the Panama City survey no subsurface information could be obtained with the sub-bottom profiler. The hard surface and the strong attenuation did not allow to collect subsurface information. In Eckernförde Bay, maps of depth to acoustic turbidity were prepared for different surveys and its cyclic depth change could be proven (Wever et al., 1996). In the Dry Tortugas area a map of the acoustic penetration helped to outline the extend of coarse sand and reef (Wever et al., 1997).

The variable depth of the acoustic turbidity in Eckernförde Bay was repeatedly proved with a 3.5 kHz subbottom profiler. During various surveys also the backscatter differed depending on the depth of the free methane gas bubbles (Fiedler and Stender, 1996). Not during all surveys the digital side scan processing package was employed, therefore no quantitative description of the effects is possible to date. This aspect will be considered in the future.

References

- Briggs, K.B., Richardson, M.D. (1996). Variability of in situ shear strength of gassy muds, *Geo-Marine Letters* 16, 189-195.
- Davis, K.S., Slowey, N.C., Stender, I.H., Fiedler, H.M., Bryant, W.R., Fechner, G. (1996). Acoustic backscatter and sediment textural properties of shelf sands, northeastern Gulf of Mexico, *Geo-Marine Letters* 16, 273-278.
- Fechner, G., Waeber, W. (1992). Digitale Verarbeitung von Side Scan Sonar Signalen, FWG Technischer Bericht TB 1992-15, 35 p.
- Fechner, G., Stender, I., Thiele, R. (1995). Measurement of relative bottom backscattering strength by a digital side scan sonar in Eckernförde Bay, Baltic Sea, in: *Proceedings of the Gassy Mud Workshop held at the FWG, Kiel, 11-12 July, 1994*, Th. Wever (ed.), FWG-Report 14, 95-100.
- Fiedler, H.M. (1994). Meßfahrt mit MzB(k) Mittelgrund vom 20.-29. Sept. 1994, FWG Interner Bericht IB 1994-10, 16 p.
- Fiedler, H.M., Stender, I.H. (1993). Surveying of sediment distribution and depth of the gassy absorption layer with side scan sonar and subbottom profiler at Eckernförde Bay, Baltic Sea, FWG Technical Report TB 1993-18, 18 p.
- Fiedler, H.M., Stender, I.H. (1996). Shallow gas in the seafloor of Eckernförde Bay: acoustic turbidity and related features, FWG Scientific Report FB 1996-5, 20 p.
- Mallinson, D., Locker, S., Hafen, M., Naar, D., Hine, A., Lavoie, D.L., Schock, S. (1997). A high-resolution geological and geophysical investigation of the Dry Tortugas carbonate depositional environment, *Geo-Marine Letters* 17, 237-245.
- Silva, A.J., Brandes, H.G., Veyera, G.E. (1996). Geotechnical characterization of surficial high-porosity surficial sediments in Eckernförde Bay, *Geo-Marine Letters* 16, 175-181.
- Slowey, N.C., Bryant, W.R., Lambert, D.N. (1996). Comparison of high-resolution seismic profiles and the geoacoustic properties of Eckernförde Bay sediments, *Geo-Marine Letters* 16, 240-248.

- Stephens, K.P., Fleischer, P., Lavoie, D., Brunner, C. (1997). Scale-dependent physical and geoaoustic property variability of shallow-water carbonate sediments from the Dry Tortugas, Florida, *Geo-Marine Letters* 17, 299-305.
- Stender, I.H., Fiedler, H.M., Davis, K., Fechner, G. (1995). Surveying a sandy seafloor off Panama City, Florida, Gulf of Mexico with bottom samples and side scan sonar, FWG Report 20, 15 p.
- Tang, D., Jin, G., Jackson, D.R., Williams, K. (1994). Analysis of high-frequency bottom and subbottom backscattering for two distinct shallow water sites, *Journal Acoustical Society of America* 96, 2930-2936.
- Urlick, R.J. (1983). *Principles of Underwater Sound*, McGraw-Hill, New York, 423 p.
- Wever, Th.F. (1996). Research Cruise with WFS PLANET, 1-28 February 1995 - Key West Campaign - (Cruise Report), FWG Report 27, 69 p.
- Wever, Th.F., Abegg, F., Fiedler, H.M., Fechner, G., Stender, I.H. (1996). Eigenschaften gashaltiger Sedimente der Eckernförder Bucht, FWG-Report 29, 20 p.
- Wever, Th.F., Fiedler, H.M., Fechner, G., Abegg, F., Stender, I.H. (1997). Side scan and acoustic subbottom characterization of the seafloor near the Dry Tortugas, Florida, *Geo-Marine Letters* 17, 246-252.

Publications

Peer Reviewed

- Davis, K.S., Slowey, N.C., Stender, I.H., Fiedler, H.M., Bryant, W.R., Fechner, G. (1996). Acoustic backscatter and sediment textural properties of shelf sands, northeastern Gulf of Mexico, *Geo-Marine Letters* 16, 273-278.
- Fleischer, P., Sawyer, W.B., Fiedler, H.M., Stender, I.H. (1996). Spatial and temporal variability of a coarse-sand anomaly on a sandy inner shelf, northeastern Gulf of Mexico, *Geo-Marine Letters* 16, 266-272.
- Jackson, D.R., William, K.L., Wever, Th.F., Friedrichs, C.T., Wright, L.D. (1998). Sonar observation of events in Eckernförde Bay, *Continental Shelf Research* (in press).
- Wever, Th., Fiedler, H. (1995). Variability of acoustic turbidity in Eckernförde Bay (SW Baltic Sea) related to the annual temperature cycle, *Marine Geology* 125, 21-27.
- Wever, Th.F., Fiedler, H.M., Fechner, G., Abegg, F., Stender, I.H. (1997). Side scan and acoustic subbottom characterization of the seafloor near the Dry Tortugas, Florida, *Geo-Marine Letters* 17, 246-252.
- Wever, Th., Abegg, F., Fiedler, H., Fechner, G., Stender, I. (1998). Shallow gas in the muddy sediments of Eckernförde Bay, *Continental Shelf Research* (in press).

Symposium Proceedings

- Fechner, G., Stender, I., Thiele, R. (1995). Measurement of relative bottom backscattering strength by a digital side scan sonar in Eckernförde Bay, Baltic Sea, in: *Proceedings of the Gassy Mud Workshop held at the FWG, Kiel, 11-12 July, 1994*, Th. Wever (ed.), FWG-Report 14, 95-100.

- Fiedler, H., Stender, I (1994). The absorption layer in Eckernförde Bay, in: Proceedings of the Gassy Mud Workshop held at the FWG, Kiel, 11-12 July, 1994, Th. Wever (ed.), FWG-Report 14, 19-23.
- Fiedler, H., Stender, I. (1995). The acoustic turbidity horizon in Eckernförde Bay sediments - an update, in: Proceedings of the Workshop Modelling Methane-Rich Sediments of Eckernförde Bay, Eckernförde, 26-30 June, 1995, Th. Wever (ed.), FWG-Report 22, 22-29.
- Stender, I., Fechner, G. (1995). Bottom backscattering strength measurements in Eckernförde Bay, in: Proceedings of the Workshop Modelling Methane-Rich Sediments of Eckernförde Bay, Eckernförde, 26-30 June, 1995, Th. Wever (ed.), FWG-Report 22, 84-88.
- Wever, Th. (Editor) (1994). Introduction to the Gassy Mud Workshop, in: Proceedings of the Gassy Mud Workshop held at the FWG, Kiel, 11-12 July, 1994, Th. Wever (ed.), FWG-Report 14, 1-2.
- Wever, Th. (Editor) (1995). Introduction to the Workshop Modelling Methane-Rich Sediments of Eckernförde Bay, FWG-Report 22, 1-2.
- Wever, Th., Fiedler, H., Stender, I. (1995). The acoustic turbidity horizon: its variation in depth and time, in: Proceedings of the Workshop Modelling Methane-Rich Sediments of Eckernförde Bay, Eckernförde, 26-30 June, 1995, Th. Wever (ed.), FWG-Report 22, 30-34.

Reports

- Fiedler, H.M. (1994). Meßfahrt mit MzB(k) Mittelgrund vom 20.-29. Sept. 1994, FWG Interner Bericht IB 1994-10, 16 p.
- Fiedler, H.M., Stender, I.H. (1993). Surveying of sediment distribution and depth of the gassy absorption layer with side scan sonar and subbottom profiler at Eckernförde Bay, Baltic Sea, FWG Technical Report TB 1993-18, 18 p.
- Fiedler, H.M., Stender, I.H. (1994). Verteilung gashaltiger Sedimente in der westlichen Ostsee, FWG Kurzbericht KB 1994-1, 7 p. --**Restricted**--
- Fiedler, H.M., Stender, I.H. (1996). Shallow gas in the seafloor of Eckernförde Bay: acoustic turbidity and related features, FWG Scientific Report FB 1996-5, 20 p.
- Fiedler, H.M., Wever, Th.F. (1997). Kartierung gashaltiger Sedimente in der Mecklenburger Bucht, FWG Technischer Bericht TB 1997-14, 21 p.
- Fiedler, H.M., Wever, Th.F. (1998). Test einer freifallenden Sonde zur Bestimmung der Bodenhärte mit MzB 'Mittelgrund', FWG Technischer Bericht TB 1998-4, 16 p.
- Stender, I.H. (1996). Burial of ground mines by migrating bedforms, FWG Scientific Report FB 1996-1, 19 p.
- Stender, I.H., Wever, Th.F. (1994). Zur Verbreitung meeresbodennaher gashaltiger Sedimente, FWG-Report 17, 17 p.
- Stender, I.H., Fiedler, H.M., Davis, K., Fechner, G. (1995). Surveying a sandy seafloor off Panama City, Florida, Gulf of Mexico with bottom samples and side scan sonar, FWG Report 20, 15 p.
- Tooma, S.G., Richardson, M.D., Lavoie, D.L., Lott, D., Williams, K.L., Stender, I.H. (1995). Collaborative efforts within the Key West Campaign sea test, NRL Memo Report NRL/MR/7430-95-7694, 15 p.

- Wever, Th.F. (1993). Research Cruise with WFS Planet 29.3.-6.4.1993 (Cruise Report), FWG Technischer Bericht TB 1993-5, 35 p.
- Wever, Th.F. (1994). Proceedings of the Gassy Mud Workshop held at FWG, Kiel, 11-12 July, 1994, FWG Report 14, 114 p.
- Wever, Th.F. (1994). Zur Löslichkeit von Methan in marinen Sedimenten, FWG-Report 16, 18 p.
- Wever, Th.F. (ed.) (1995). Proceedings of workshop „Modelling Methane-Rich Sediments of Eckernförde Bay“, Eckernförde, 26-30 June 1995, FWG Report 22, 247 p.
- Wever, Th.F. (1995). Gashaltige Meeresbodensedimente: Methoden und Beispiele der Kartierung, FWG Technischer Bericht TB 1995-19, 17 p.
- Wever, Th.F. (1996). Research Cruise with WFS PLANET, 1-28 February 1995 - Key West Campaign - (Cruise Report), FWG Report 27, 69 p.
- Wever, Th.F. (1996). Forschungsfahrt PLANET 4/96 (JOBEX 96-1), 18.3.-8.3.1996 (Fahrt-leiterbericht), FWG Kurzbericht KB 1996-3, 19 p.
- Wever, Th.F., Abegg, F., Fiedler, H.M., Fechner, G., Stender, I.H. (1996). Eigenschaften gashaltiger Sedimente der Eckernförder Bucht, FWG-Report 29, 20 p.
- Wever, Th.F., Milkert, D., Fiedler, H.M., Abegg, F., Stender, I.H. (1996). Die Eckernförder Bucht - Eine Übersicht, FWG-Report 30, 20 p.

Published Abstracts

- Fechner, G., Stender, I. (1994). Measurement of relative bottom backscattering strength by a digital side scan sonar, J. Acoust. Soc. Am. 96, 3222-3223.
- Fiedler, H.M., Stender, I.H. (1994). Surveying sediment distribution and depth of the gassy absorption lay with side scan sonar and subbottom profiler at Eckernförde Bay, Germany, EOS 75, 159.
- Fiedler, H.M., Wever, Th.F., Fechner, G. (1995). SSS images of the seafloor of the Dry Tortugas, SPM Congress on Sedimentary Geology, St. Petersburg, FL, 13-16 August 1995, 1:52.
- Fiedler, H.M., Th.F. Wever (1997). Vermessung von Meeresbodensedimenten mit akustischen Fernmeßmethoden, Dokumentation 12. Hydrographentag 1997, 81-84.
- Fleischer, P., Sawyer, W.B., Fiedler, H.M., Stender, I.H. (1994). Spatial and temporal complexity on a simple, sandy inner-shelf seafloor: observations with side scan sonar, EOS 75, 201.
- Martens, C., Albert, D., Fiedler, H.M., Abegg, F. (1994). Biogeochemical processes controlling gas bubble production and distribution in organic-rich sediments, J. Acoust. Soc. Am. 96, 3217.
- Stender, I.H., Fechner, G. (1994). Spatial distribution of relative backscattering strength using a digital side scan sonar at Eckernförde Bay, Germany, EOS 75, 159.
- Wever, Th.F., H.M. Fiedler (1997). Gashaltige Sedimente - Auftreten und Auswirkungen in der Eckernförder Bucht, Dokumentation 12. Hydrographentag 1997, 77-80.

‘Mobility’ of gas in muddy sediments

TH.F. WEVER, H.M. FIEDLER

Forschungsanstalt der Bundeswehr
für Wasserschall und Geophysik
Klausdorfer Weg 2-24
24148 Kiel
Germany

Abstract

The gassy sea floor of Eckernförde Bay (Germany) in the Western Baltic was repeatedly investigated with 100 kHz side scan sonar and 3.5 kHz subbottom profiler. The campaigns during different seasons revealed cyclically changing acoustic characteristics of the sea floor, both of surface backscatter and depth of acoustic turbidity. The motor for long-term changes is the annual temperature cycle. Short-term differences are expected to result from pressure changes but were not yet directly observed due to limited event-related ship availability.

The annual temperature cycle causes a depth cycle of acoustic turbidity by controlling via the solubility the amount of free methane gas in the sediment. The variable solubility results in variations of acoustic properties of the sediment. The depth of acoustic turbidity varies between a few metres and zero in the pockmarks. For reliable modelling more details are to be known, but the general description of the acoustic turbidity depth is possible.

Comparative studies were made in Mecklenburg Bay, a larger bay with muddy sea floor sediments that contain free methane gas. Observed differences (esp. the constant depth of acoustic turbidity) can be related to the protected location of Eckernförde Bay where conductive heat transport through the water is the dominant process while convection is the dominant process in Mecklenburg Bay.

Original Objectives

The first side scan sonar and subbottom profiler data were collected during the pre-site survey for JOBEX/CBBL (Joint High-Frequency Backscatter Experiments, Coastal Benthic Boundary Layer) in 1993 of Eckernförde Bay. Later side scan surveys were made to monitor possible changes of the sea floor. The central interest, however, was to calibrate the side scan sonar system with absolute backscatter measurements. This attempt did not lead to the expected results.

Already during the second campaign indications were found that the depth of the acoustic turbidity had changed (Wever, 1993). Consequently, the measurements were repeated along some key profiles whenever possible in order to monitor and possibly explain these changes (Wever and Fiedler, 1995).

The observations of an annual cycle were manifested every following year and triggered additional investigations.

In part, profiles were inspected to investigate (theoretically possible) lateral changes of the acoustic turbidity. However, the profiles did not show clear signs. Especially selected profiles at the right times have to be run in the future for answering this question (Fiedler and Wever, 1997).

Side scan sonar records showed a variable backscatter strength of trawl marks and other man-made signatures on the sea floor (Fiedler and Stender, 1996). A detailed analysis showed a correlation with the depth of the acoustic turbidity, i.e., a temperature-induced phenomenon.

Approach

In order to understand the 'ups' and 'downs' of the acoustic turbidity repeated measurements along identical profiles became the basis for this investigation. The first results have been published by Wever and Fiedler (1995). To test the hypothesis that the annual temperature cycle is the controlling factor, temperature measurements in the water column obtained during a monitoring programme of the Institute of Marine Sciences of Kiel University were used. The location for the monitoring programme is close to the CBBL research site.

Pressure variations (variations in atmospheric pressure and sea level) presumably cause short-term changes of the depth of the acoustic turbidity. No direct observation could be made with subbottom profiler. Therefore, a tower equipped with different sensors is under construction. It will be placed on the sea floor and monitor acoustic turbidity together with temperature and pressure at and in the sea floor. An indication for pressure-induced degassing of the sediments comes from the tower observations of Jackson et al. (this volume, and 1998) which are best explained by free gas bubbles moving in the water column from the sea floor to the surface.

To learn from possible similarities or differences, Mecklenburg Bay, a larger bay with gassy muddy sediments was investigated three times with acoustic systems (Fiedler and Wever, 1997). Despite a general geographic similarity, environmental conditions (influence of currents, fetch length etc) are not the same and can explain the observed differences (mainly the depth stability of the acoustic turbidity).

Results

The seasonal atmospheric temperature changes cause a variable depth of the acoustic turbidity in Eckernförde Bay by influencing the solubility of methane gas. The depth change between summer (minimum amplitude) and winter (maximum amplitude) conditions can reach 1 m.

In places the acoustic turbidity reaches the sea floor and seeps into the water column. Acoustic observations of Jackson et al. (1998) have been interpreted to be caused by gas bubbles seeping from

the sea floor. Seeping gas can cause pockmarks, i.e., crater-like morphologic structures which have been observed in Eckernförde Bay with side scan sonars.

Occasional events as the 1996 ice cover lasting until May can delay the depth cycle of acoustic turbidity which, however, will adjust within the next season.

Accomplishments

The central accomplishment of the study is a first proof of the depth variability of the acoustic turbidity with an annual cycle. Its explanation and physical description is based on a variable gas solubility according to Henry's Law. The controlling factors are mainly temperature and pressure. Of minor importance are salinity changes in the sediment.

A second accomplishment is the overall understanding of the relation between atmospheric influences (temperature and pressure) and subbottom processes. A model is under development. It has to account for local conditions such as long-term averaged atmospheric temperature amplitudes as well as short-term influences (i.e., the scale of months), short-term pressure fluctuations (on the scale of hours), water depth, currents, type of heat transport in the water, and heat conduction in the sediment. A yet unknown factor is the solution rate of methane gas after pressure increases.

References

- Fiedler, H.M., Wever, Th.F. (1997). Kartierung gashaltiger Sedimente in der Mecklenburger Bucht, FWG Technischer Bericht TB 1997-14, 21 p.
- Jackson, D.R., Williams, K.L., Wever, Th.F., Friedrichs, C.T., Wright, L.D. (1998). Sonar evidence for methane ebullition in Eckernförde Bay, Continental Shelf Research (in press).
- Wever, Th.F. (1993). Research Cruise with WFS Planet 29.3.-6.4.1993 (Cruise Report), FWG Technischer Bericht TB 1993-5, 35 p.
- Wever, Th.F., Fiedler, H.M. (1995). Variability of acoustic turbidity in Eckernförde Bay (SW Baltic Sea) related to the annual temperature cycle, Marine Geology 125, 21-27.

Publications

Peer Reviewed

- Jackson, D.R., Williams, K.L., Wever, Th.F., Friedrichs, C.T., Wright, L.D. (1998). Sonar evidence for methane ebullition in Eckernförde Bay, Continental Shelf Research (in press).
- Wever, Th., Fiedler, H. (1995). Variability of acoustic turbidity in Eckernförde Bay (SW Baltic Sea) related to the annual temperature cycle, Marine Geology 125, 21-27.

Wever, Th.F., Fiedler, H.M., Fechner, G., Abegg, F., Stender, I.H. (1997). Side scan and acoustic subbottom characterisation of the seafloor near the Dry Tortugas, Florida, *Geo-Marine Letters* 17, 246-252.

Wever, Th.F., Abegg, F., Fiedler, H.M., Fechner, G., Stender, I.H. (1998). Shallow gas in the muddy sediments of Eckernförde Bay, *Continental Shelf Research* (in press).

Symposium Proceedings

Fechner, G., Stender, I.H., Thiele, R. (1994). Measurement of relative bottom backscattering strength by a digital side scan sonar in Eckernförde Bay, Baltic Sea, in: *Proceedings of the Gassy Mud Workshop held at the FWG, Kiel, 11-12 July, 1994*, Th. Wever (ed.), FWG-Report 14, 95-100.

Fiedler, H.M., Stender, I.H. (1994). The absorption layer in Eckernförde Bay, in: *Proceedings of the Gassy Mud Workshop held at the FWG, Kiel, 11-12 July, 1994*, Th. Wever (ed.), FWG-Report 14, 19-23.

Fiedler, H.M., Stender, I.M. (1995). The acoustic turbidity horizon in Eckernförde Bay sediments - an update, in: *Proceedings of the Workshop Modelling Methane-Rich Sediments of Eckernförde Bay, Eckernförde, 26-30 June, 1995*, Th. Wever (ed.), FWG-Report 22, 22-29.

Wever, Th.F. (Editor) (1994). Introduction to the Gassy Mud Workshop, in: *Proceedings of the Gassy Mud Workshop held at the FWG, Kiel, 11-12 July, 1994*, Th. Wever (ed.), FWG-Report 14, 1-2.

Wever, Th.F. (Editor) (1995). Introduction to the Workshop Modelling Methane-Rich Sediments of Eckernförde Bay,

Wever, Th.F., Fiedler, H.M., Stender, I.H. (1995). The acoustic turbidity horizon: its variation in depth and time, in: *Proceedings of the Workshop Modelling Methane-Rich Sediments of Eckernförde Bay, Eckernförde, 26-30 June, 1995*, Th. Wever (ed.), FWG-Report 22, 30-34.

Reports

Fiedler, H.M. (1994). Meßfahrt mit MzB(k) Mittelgrund com 20.-29. Sept. 1994, FWG Interner Bericht IB 1994-10, 16 p.

Fiedler, H.M., Stender, I.H. (1993). Surveying of sediment distribution and depth of the gassy absorption layer with side scan sonar and subbottom profiler at Eckernförde Bay, Baltic Sea, FWG Technical Report TB 1993-18, 18 p.

Fiedler, H.M., Stender, I.H. (1994). Verteilung gashaltiger Sedimente in der westlichen Ostsee, FWG Kurzbericht KB 1994-1, 7 p. --Restricted--

Fiedler, H.M., Stender, I.H. (1996). Shallow gas in the seafloor of Eckernförde Bay: acoustic turbidity and related features, FWG Scientific Report FB 1996-5, 20 p.

Fiedler, H.M., Wever, Th.F. (1997). Kartierung gashaltiger Sedimente in der Mecklenburger Bucht, FWG Technischer Bericht TB 1997-14, 21 p.

Fiedler, H.M., Wever, Th.F. (1998). Test einer freifallenden Sonde zur Bestimmung der Boden Härte mit MzB 'Mittelgrund', FWG Technischer Bericht TB 1998-4, 16 p.

Stender, I.H., Wever, Th.F. (1994). Zur Verbreitung meeresbodennaher gashaltiger Sedimente, FWG-Report 17, 17 p.

- Wever, Th.F. (1993). Research Cruise with WFS Planet 29.3.-6.4.1993 (Cruise Report), FWG Technischer Bericht TB 1993-5, 35 p.
- Wever, Th.F. (1994). Zur Löslichkeit von Methan in marinen Sedimenten, FWG-Report 16, 18 p.
- Wever, Th.F. (1995). Gashaltige Meeresbodensedimente: Methoden und Beispiele der Kartierung, FWG Technischer Bericht TB 1995-19, 17 p.
- Wever, Th.F. (1996). Forschungsfahrt PLANET 4/96 (JOBEX 96-1), 18.3.-8.3.1996 (Fahrtleiterbericht), FWG Kurzbericht KB 1996-3, 19 p.
- Wever, Th.F., Abegg, F., Fiedler, H.M., Fechner, G., Stender, I.H. (1996). Eigenschaften gashaltiger Sedimente der Eckernförder Bucht, FWG-Report 29, 20 p.
- Wever, Th.F., Milkert, D., Fiedler, H.M., Abegg, F., Stender, I.H. (1996). Die Eckernförder Bucht - Eine Übersicht, FWG-Report 30, 20 p.

Published Abstracts

- Fechner, G., Stender, I.H. (1994). Measurement of relative bottom backscattering strength by a digital side scan sonar, J. Acoust. Soc. Am. 96, 3222-3223.
- Fiedler, H.M., Stender, I.H. (1994). Surveying sediment distribution and depth of the gassy absorption layer with side scan sonar and subbottom profiler at Eckernförde Bay, Germany, EOS 75, 159.
- Fiedler, H.M., Wever, Th.F. (1997). Vermessung von Meeresbodensedimenten mit akustischen Fernmeßmethoden, Dokumentation 12. Hydrographentag 1997, 81-84.
- Martens, C.M., Albert, D., Fiedler, H.M., Abegg, F. (1994). Biogeochemical processes controlling gas bubble production and distribution in organic-rich sediments, J. Acoust. Soc. Am. 96, 3217.
- Stender, I.H., Fechner, G. (1994). Spatial distribution of relative backscattering strength using a digital side scan sonar at Eckernförde Bay, Germany, EOS 75, 159.
- Wever, Th.F., Fiedler, H.M. (1997). Gashaltige Sedimente - Auftreten und Auswirkungen in der Eckernförder Bucht, Dokumentation 12. Hydrographentag 1997, 77-80.

Title: Acoustic lance: In situ Acoustic Seabed Velocity and Attenuation

Principal Investigators: R.H. Wilkens and L.N. Frazer
School of Ocean and Earth Science and Technology
University of Hawaii, 2525 Correa Road, Honolulu, 96822 HI

Other Investigators: T.J. Gorgas, S.S. Fu

Abstract

The acoustic lance is a linear array of receivers embedded in the seafloor below an acoustic source. The instrument records acoustic waveforms that are used to calculate interval velocity and attenuation in the upper several meters of the seafloor. Two deployments were successfully carried out as part of the CBBL - in the gassy sediments of Eckernförde Bay, Baltic Sea, and along slope parallel and slope normal transects of the Eel River delta, Northern California.

In and near Eckernförde Bay, the acoustic lance was deployed at 19 stations during gravity coring operations. Work centered on in situ compressional wave velocity profiles and sound signal characteristics in gassy sediments. Attenuation profiles at two non-gassy sites were analyzed, but standard attenuation calculation techniques were not applicable to the gassy sediments due to the physics of gas bubble resonance. Velocity in nongassy sediment intervals, either above gas layers or at non-gassy sites, fell within the range 1430-1465 msec⁻¹, with minimal attenuation. In gassy sections of the sediment, in situ compressional wave velocities were measured as low as 1000 msec⁻¹. Waveforms associated with gassy layers in the sediment exhibited longer codas because of scatter and/or bubble ringing. Comparison of lance data with higher frequency experiments illustrated a strong velocity dependence on frequency in the gassy layers.

During the Eel River Delta experiment a total of 17 gravity cores were recovered from the seafloor in water depths between 60 and 100 meters. During coring, simultaneous in situ acoustic data were recorded. Cores of lengths between 0.5 and 1.15 m were investigated with a standard ultrasonic table top transducer system. Results of the velocity analysis reveal maximum velocities of 1600 msec⁻¹ in the top 60 cm at 60 m water depth. At sites below 60 m water depth, in situ compressional velocities increase from 1480 msec⁻¹ in the first 0.2 m of the seafloor to ca. 1580 msec⁻¹ at 2.0 m below seafloor. In situ and laboratory compressional wave velocities are correlated positively at most at these sites. In situ and laboratory attenuation data vary between 0.1 and 1.05 dbm⁻¹kHz⁻¹. Most in situ acoustic and ultrasonic laboratory attenuation data from the Eel River study correlate with porosity. Attenuation correlated with porosity suggests a strata transition from sandy-silty to muddy-silty sediments downslope.

Original Objectives:

The original objective of the lance deployments was to take advantage of CBBL coring programs to measure in situ acoustic properties of seafloor sediments at the CBBL sites.

Approach:

The Acoustic Lance (Fu, et al., 1996) is a linear array of receivers embedded in the seafloor below an acoustic source. It provides in situ recording of waveforms above and below the sediment-seawater interface. A broad-band (5-20 kHz) acoustic source and a solid state data recording system are mounted on the weightstand of a gravity corer. An array of small hydrophones is mounted along the outside of the core. Compressional wave velocity, attenuation, and signal characteristics are extracted from the recorded waveforms. Velocity is calculated from first arrivals at known distances from the source. Attenuation is much more difficult to calculate from the acoustic waveforms. In the course of data analysis we developed

a new technique based on geophysical inverse theory and the spectral ratio technique to extract attenuation profiles from the lance signals (Frazer, et al., 1998).

Results - Eckernförde Bay

Interval velocity profiles from 19 stations in Eckernförde Bay have been published in Wilkens et al. (1995). In this final report we select typical acoustic signals from five stations (Sites 624 - 628) to characterize in situ acoustic properties in Eckernförde Bay sediments. Discussions of these sites and others are contained in Fu et al., 1996b and Wilkens and Richardson, 1998. A set of waveforms recorded at Site 626 and typical of gassy sites is shown in Figure 1. Note the abrupt loss of amplitude of the signal once the gassy layer is penetrated.

Interval compressional wave velocities at Sites 624 - 628 are shown in Figure 2. Among these 5 stations, Sites 624 and 627 are nongassy sediments, whereas the others are gassy sites. Velocity values in nongassy sediment intervals fall within the range 1430-1465 m/s (an average bottom water velocity is 1480 m/s), whether they are at nongassy sites or they overlay gassy sediments. At nongassy sites velocities are more or less constant with depth (e.g., Site 624) or have a tendency to increase slightly (e.g., Site 627). In gassy zones where signal amplitudes are strongly attenuated (Fig. 1), velocity shows large variability. Nevertheless, velocity behavior is fairly consistent: velocity increases in the uppermost parts of the gassy intervals (nongassy-gassy transition zones) and then decreases more or less rapidly in the underlying sediments, depending most likely on the vertical distribution of gas bubbles. We note here that there is no apparent evidence in the ASCS reflection profile for a gassy zone at Site 628, and yet, lance data at this site exhibit characteristics in velocity, amplitude, frequency spectra, and signal reverberation similar to gassy Sites 625 and 626.

Velocity profiles at five gassy sites in the NRL test area are shown in Figure 3. All 5 velocity profiles indicate that velocity decreases in gassy sediments. The decrease of velocity in gassy zones suggests that the gas bubble resonance frequencies are higher than the lance frequencies of 5 - 20 kHz (Anderson & Hampton, 1980). This is in contrast to higher frequency in situ and core measurements, shown as solid and open circles on Figure 3. The frequencies of these measurements, 40 kHz and 400 kHz, are greater than bubble resonance, estimated to be about 25 kHz by Wilkens and Richardson (1998).

An important waveform characteristic in Eckenförde Bay gassy sediments is the signal reverberation (ringing) caused by bubble scattering (Fig. 4). The lance signals show that even the presence of small amounts of gas in the layers overlying the gassy sediment zones (which have been regarded as nongassy sediments), acoustic reverberation is apparent. Signal spectral analysis indicates that signal energy is reduced greatly at about 7.5 kHz in gassy sediments relative to higher frequencies - the opposite of what is expected in normal attenuation. The mechanism of the energy reduction at 7.5 kHz is still unknown, but probably reflects some characteristic of the bubble size distribution. High reflectivity at the interface of gas-free and gas-bearing sediments is also clearly shown in the waveforms recorded by the lance, attesting to the reasonably abrupt nature of the gassy-non-gassy transition.

Results - Eel River Delta

During our in situ measurements on the northern California shelf a standard gravity corer with attached Lance components was deployed at 12 shelf stations downslope between 60 and 100 m water depth and along a lateral shelf transect on the 70 m contour line (Fig. 5). Our research focused on the determination of in situ compressional wave velocities and attenuation in order to enhance understanding of high-frequency sound energy propagation through the first 2 meters of seafloor on the Eel River shelf (Gorgas, et al., 1998). Velocity and attenuation data obtained from these in situ measurements were compared with laboratory ultrasonic velocity and attenuation data that were collected from cored sediments shipboard and on-shore using the methods of Richardson (1983). This suite of data was correlated with core

GRAPEdensity and porosity scan data (Boyce, 1976) in order to evaluate geoacoustic properties of the seafloor (Gorgas et al., 1998). Sites S60West, S80, and S100 were selected to be representative of the downslope transect between 60 and 100 water depth (Figs. 6a, b, c, d). Sites I70, L70, and S70 were chosen for the lateral transect along the 70 m depth contour line (Figs. 7a, b, c, d).

Downslope Properties: On the downslope transect in situ velocities range between 1450 and 1490 msec⁻¹ at the seawater-seafloor interface, and vary between 1500 and 1540 msec⁻¹ at 1.3 mbsf interval depth (Fig. 6a). At Site S100, the deepest water site (100 meter water depth), ultrasonic velocities are slightly higher (1480 to 1520 msec⁻¹) than in situ velocities (minimum 1440 msec⁻¹ to maximum 1540 msec⁻¹). In situ and ultrasonic data at Site S80 (80 meter water depth) match fairly well over a core length of ca. 85 cm (velocities vary between 1480 and 1540 msec⁻¹), whereas in situ data from S60West (one of four sites closely spaced at 60 meter water depth) do not agree well with ultrasonic velocities. Ultrasonic data at S60 West show a gradual velocity increase from the top to the bottom, a trend which can be observed in both in situ and laboratory data obtained at the deeper water stations as well. Ultrasonic velocities at Site S60W range from 1450 to 1580 msec⁻¹, whereas in situ values vary little between 1480 and 1525 msec⁻¹ from the profile's top to an interval depth of 0.65 mbsf, with a decrease in velocity to 1520 msec⁻¹ below that depth.

The S60 data (and data from Site I70 - see below) are the only sites exhibiting substantial differences between in situ and core velocity measurements. Their anomalous properties extend to density and porosity (Fig. 6b, c) and so far remain unexplained. Compressional wave velocities correlate with wet-bulk density (Fig. 6b), where highest values are observed at Site S60W (1.65 to 2.0 gcm⁻³), and lower densities at Sites S80 and S100 (1.65 to 1.8 gcm⁻³). A higher scatter in velocity and density data is seen at Site S60W compared to the deeper water stations. Porosities (Fig. 6c) agree well with densities, and show the expected inverse correlation. Minimum porosities at Site S60W are about 40%, compared to ca. 50% at Site S100. Maximum porosities are about 65% for Sites S60W and S100, and a bit lower at Station S80. Coincident with decreasing density and increasing porosities, core lengths increase from the upper to the lower shelf.

In situ attenuation profiles at Sites S60W, S80, and S100 (Fig. 6d) correlate with each other, showing a low attenuation zone at the first 0.5 mbsf core depth (0.01 to 0.1 dBm⁻¹ kHz⁻¹), followed by an increase in attenuation (up to 0.6 dBm⁻¹ kHz⁻¹) between depth intervals 0.6 to 1.2 mbsf. Ultrasonic data tend to have more uniformly high attenuation, perhaps an expression of greater scatter at higher frequencies. Ultrasonic attenuation does correlate reasonably well with ultrasonic velocities (Gorgas et al., 1998).

Lateralslope Properties: On the lateral transect in situ velocities vary between 1470 msec⁻¹ (L70) and 1520 msec⁻¹ (I70) at the seawater-seafloor interface, and between 1530 msec⁻¹ (L70, I70) and 1550 msec⁻¹ (S70) at interval depths below 0.8 mbsf (Fig. 7a). A good agreement of in situ and ultrasonic velocity data can be observed at Sites S70 and L70, but not so well at Site I70. The latter site is located furthest south, and shows a greater scatter in acoustic and bulk properties than nearby sites (Figs. 7a, b, c). Acoustic and bulk property profiles at Site I70 are most similar to data obtained at Site S60W (Figs. 6a, b, c; Figs. 7a, b, c). I70 core length was shortest, which corresponds to higher densities (2.0 gcm⁻³) at the seawater-seafloor interface (Fig. 7b).

Wet-bulk densities at adjacent Sites L70 and S70 vary between 1.6 and 1.9 gcm⁻³. Porosities match the density data as expected (Fig. 7c). The in situ attenuation profile at Site S70 (Fig. 7d) shows a trend similar to the downslope profiles (Fig. 6d) previously described (S70 is also part of the downslope section), although almost no correlation between in situ and ultrasonic data exist. Attenuation data evaluated at Site I70 (Fig. 7d) show a decrease in attenuation from the top to the bottom (0.6 to 0.2 dBm⁻¹ kHz⁻¹), with a fairly good match between in situ and laboratory data. Station L70 shows a high variation at the top interval of its profile, with values ranging from 0.2 and 0.65 dBm⁻¹ kHz⁻¹ (Fig. 7d). This

corresponds to ultrasonic data for that depth range. Below interval depth 0.4 mbsf both in situ and ultrasonic data at Site L70 show little variation, with ultrasonic data being higher than in situ data.

Systematics: Porosity has been proven to be a strong indicator of attenuation behavior in marine sediments and rocks because it reflects the number and type of interparticle contacts (Hamilton, 1972). Porosity strongly influences permeability which implies the effect of how fast the pore fluid can move within the aggregate (Biot, 1956a; 1956b). Bulk moduli of the sediment are dependent on porosity, and therefore related to the sediment's response time to a pressure disturbance, and thus indirectly to attenuation (Hamilton, 1971; Kjartansson, 1979).

A comparison between the downslope and the lateral transect with respect to attenuation versus porosity is presented in Figure 8. Gray lines on the figure represent a regression analysis according to Hamilton's empirical results (Hamilton, 1972) and his grain size 'zones' are noted. Location of the data suggest that sediments on the upper shelf (Sites S60) are dominated by a higher content of fine sand than sites further downslope (Fig. 8a), where very fine sand and silt fractions can be found. Attenuation data correlated with porosity values for downslope sites, including Sites S70 (also part of the lateralslope transect), S80, and S100 (Fig. 8a), as well as for lateral transect Sites I70, L70, and S70 (Fig. 8a, b), suggest a greater fraction of silt content in the sediments compared to those cored at Site S60. Highest in situ attenuation is reported from Sites S70 and S100, suggesting a high content of very fine sand.

Our results show the greatest change in acoustic and bulk properties in the shore-normal direction in water depths between 60 and 70 m. Compressional wave velocity decreases, coinciding with decreasing density and increasing porosity values from Site S60 to Site S100. Along the lateral transect the highest variability in acoustic and bulk properties is detected in the very south, in profiles obtained at Site I70. This leads to the conclusion that lance velocity versus depth, and attenuation versus porosity mark a transition zone of sediment distribution on the Eel River shelf, that separates the dynamic upper slope environment from the lower shelf below 70 m water depth, where calmer sedimentation conditions generate a more homogenous sediment distribution.

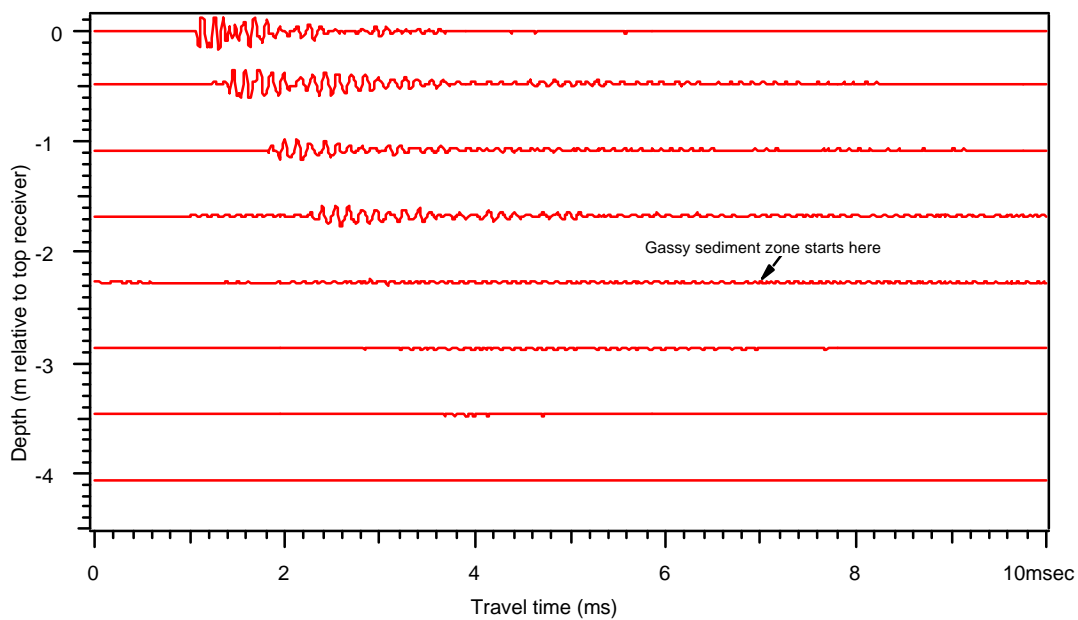


Figure 1. Typical true amplitude waveforms recorded in area of gassy sediment layer. Note the high attenuation of the signal once it enters the gassy layer.

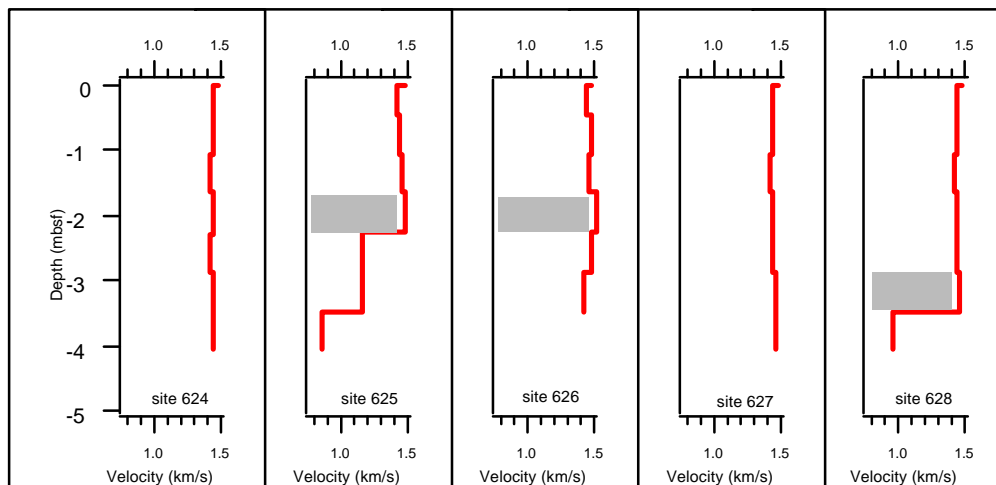


Figure 2. Compressional wave velocity-depth profiles recorded at 5 stations at the mouth of Eckernförde Bay. Gray bars indicate the top of the gassy layer. At Site 628 there was no reflector seen in sub-bottom profiling records. At Site 626 waveforms were ringing, but velocity did not decrease.

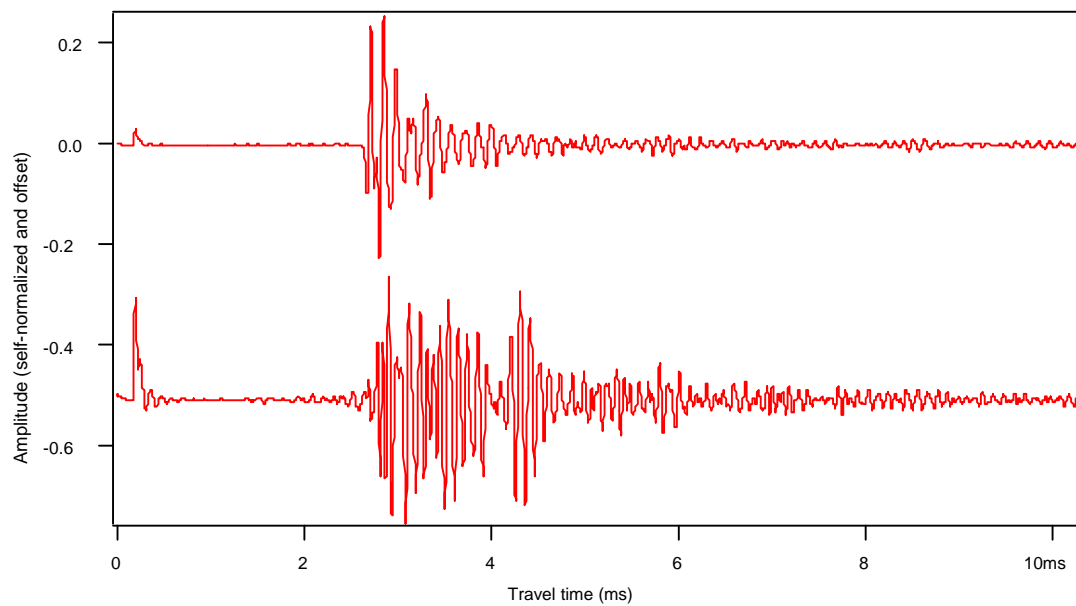


Figure 4. Waveform recorded in non-gassy sediment (top) and in gassy sediment (bottom). Gassy signals have much longer codas and exhibit more ringing.

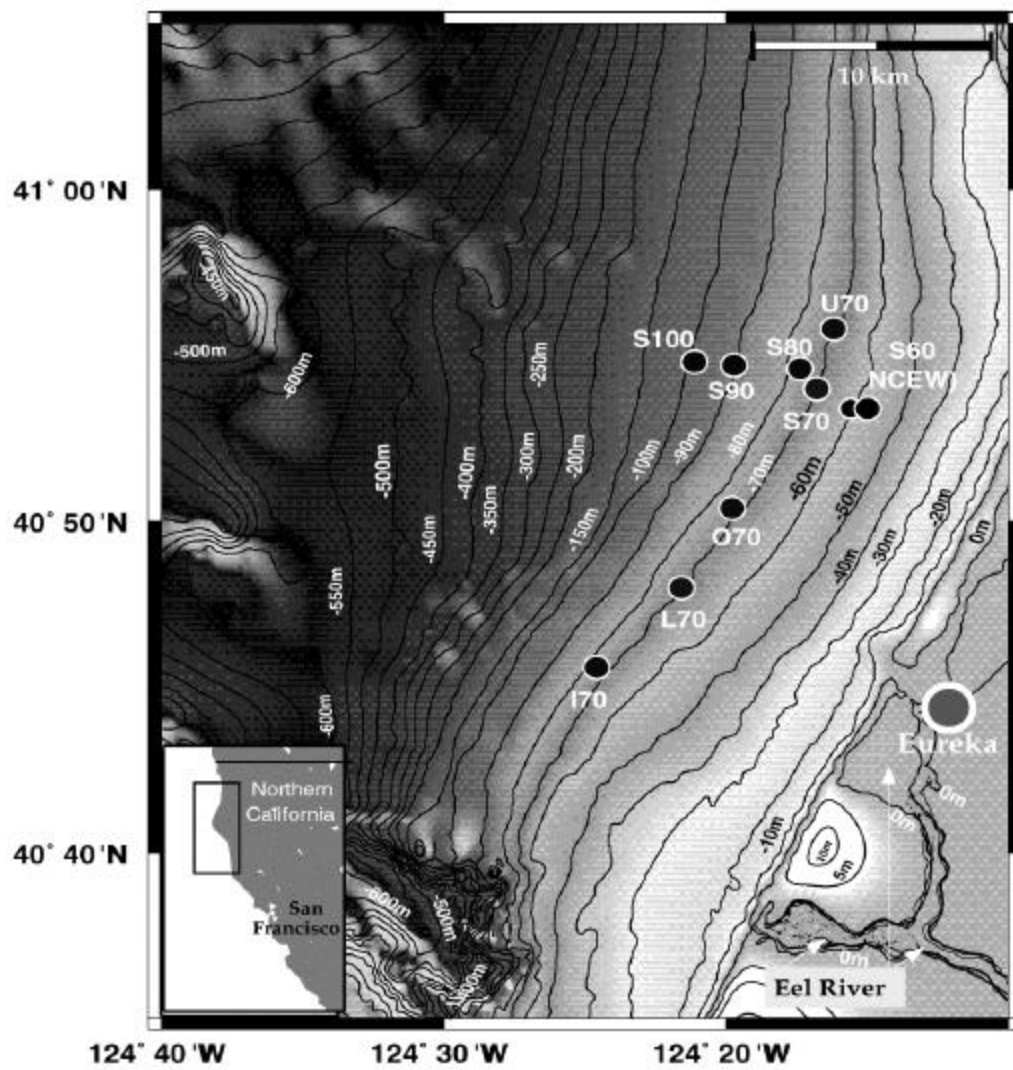


Figure 5. Map of coring and Lance deployment sites on the Eel River shelf. Numerical part of each site name indicates water depth. A transect was run along the 70m contour and normal to the shoreline along line S.

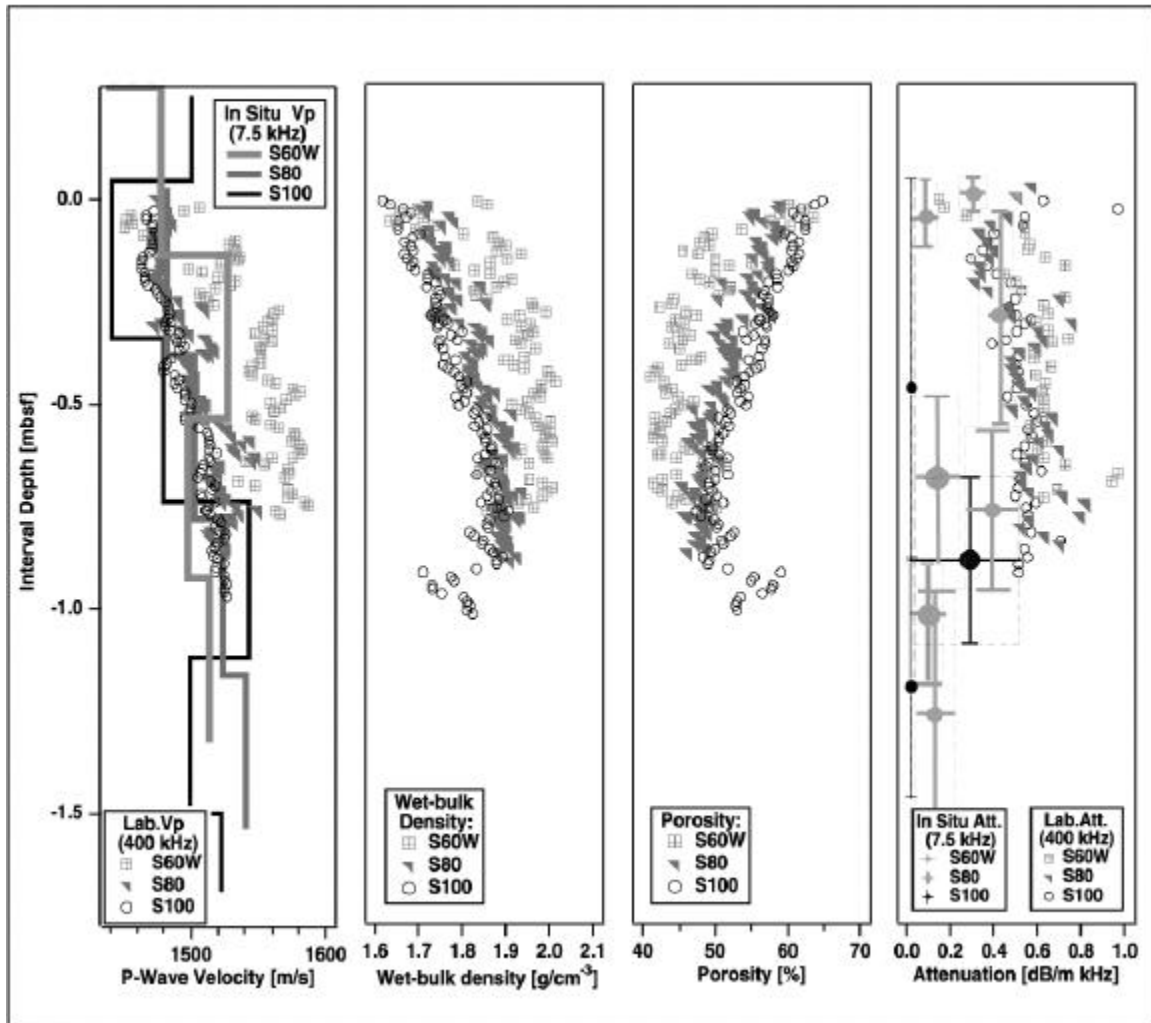


Figure 6. Representative data from the shore-normal transect. (a) In situ and laboratory velocity versus depth below seafloor, (b) laboratory measurements of core density versus depth below seafloor, (c) laboratory measurements of core porosity versus depth below seafloor, and (d) in situ and laboratory determinations of attenuation. Vertical bars on in situ attenuation data represent interval of calculation, horizontal bars represent span of 10 best fit models of data from the inversion process.

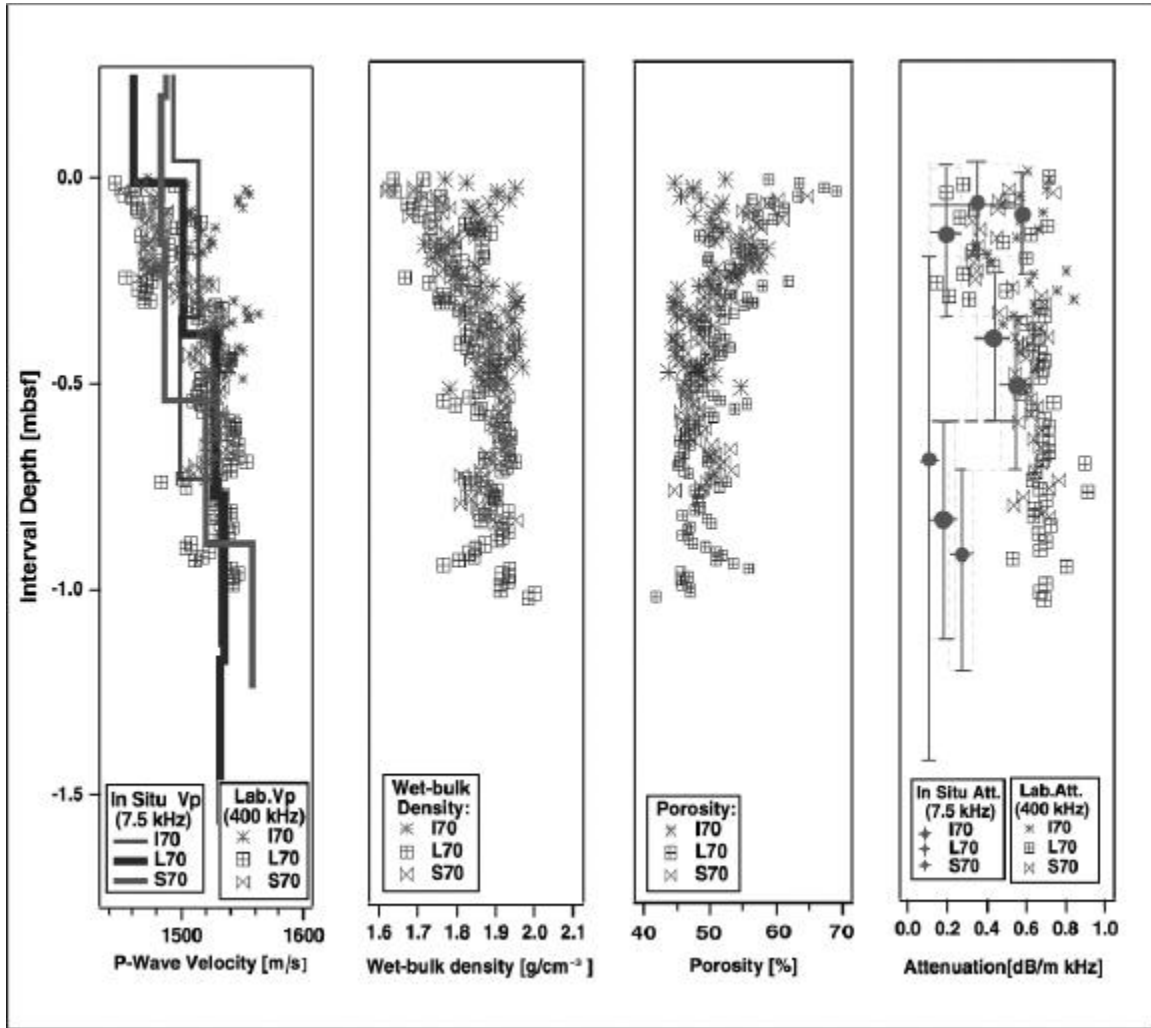


Figure 7. Representative data from the 70m depth contour transect. (a) In situ and laboratory velocity versus depth below seafloor, (b) laboratory measurements of core density versus depth below seafloor, (c) laboratory measurements of core porosity versus depth below seafloor, and (d) in situ and laboratory determinations of attenuation. Vertical bars on in situ attenuation data represent interval of calculation, horizontal bars represent span of 10 best fit models of data from the inversion process.

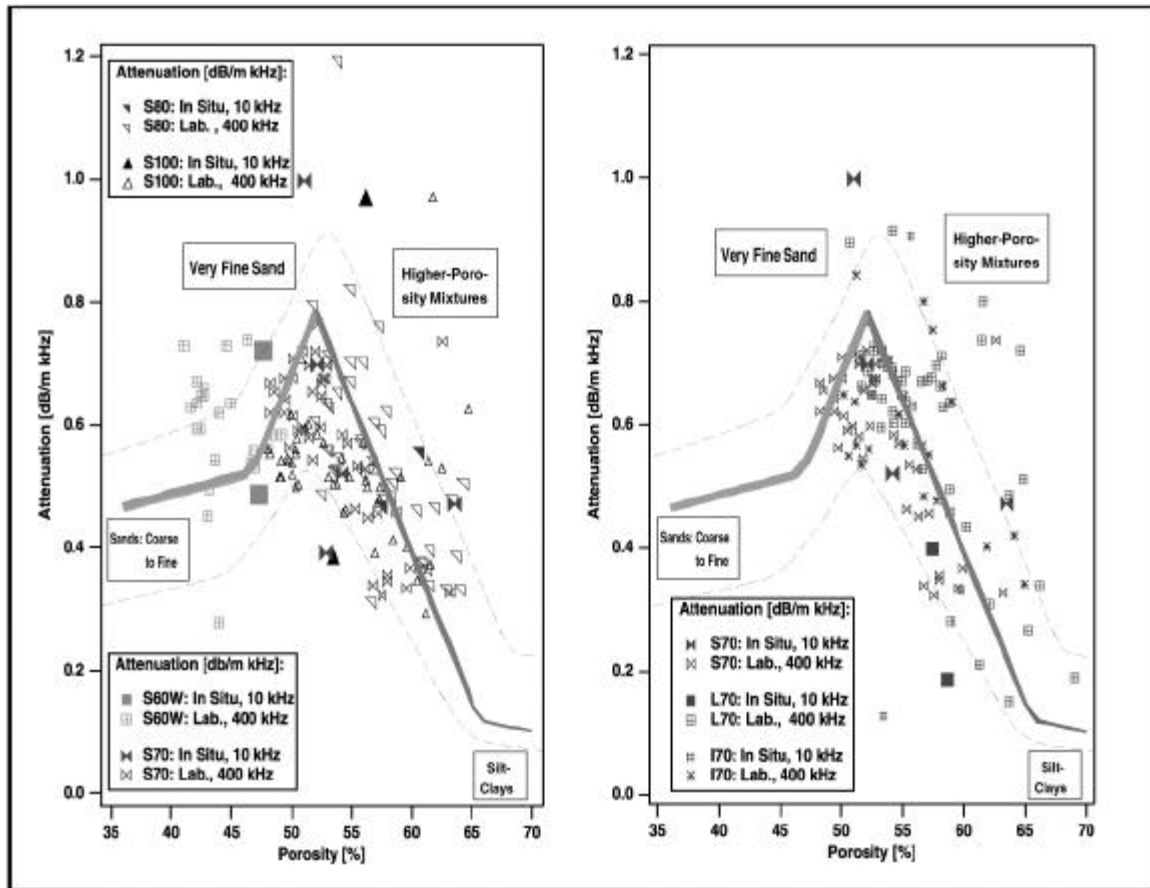


Figure 8. In situ and laboratory attenuation versus porosity. Hamilton's (1972) empirical relationships are superimposed on the data. Laboratory data are in good agreement with Hamilton's mostly laboratory results. In situ data show general agreement, but more scatter.

References

- Biot, M.A., 1956a, Theory of propagation of elastic waves in a fluid-saturated porous solid. I. Low frequency range, J. Acoust. Soc. Am., 28: 168-178.
- Biot, M.A., 1956b, Theory of propagation of elastic waves in a fluid-saturated porous solid. II. Higher frequency range, J. Acoust. Soc. Am., 28: 179-191.
- Biot, M.A., 1962, Mechanics of deformation and acoustic propagation in porous media, J. Appl. Phys., 33: 1482-1498.
- Biot, M.A., 1962, Generalized theory of acoustic propagation in porous dissipative media, J. Acoust. Soc. Am., 34: 1254-1264.
- Bouchard, R.J., Borgeld, J.C., 1988, Graded sands from the Eel River continental shelf, Northern California: storm generated deposits, Tech. Rept., TML-17, Telonicher Marine Laboratory, Humboldt State University, 36 pages.
- Boyce, R.E., 1976, Definitions and laboratory techniques of compressional sound velocity parameters and wet-water content, wet-bulk density and porosity parameters by gravimetric and gamma ray attenuation techniques, Init. Repts. DSDP, Washington (U.S. Govt. Printing Office), 33: 931-951.
- Briggs, K. & Logan, M., 1996, Eel River Study 1996 - Cruise reports For W9605A, LEG2, Naval Research Laboratory.
- Frazer, L.N., Fu, S.S., and Wilkens, R.H., 1998, Seabed sediment attenuation profiles from a moveable subbottom acoustic vertical array, J. Acoust. Soc. Amer., in press.
- Fu, S.S., Prasad, M., Wilkens, R.H. and Frazer, L.N., 1998, Hamilton parameters and acoustic properties for coral sands, Waikiki, Hawaii, Geophysics, in press.
- Fu, S.S., Wilkens, R.H. and Frazer, L.N., 1996a, Acoustic Lance: New in-situ velocity profiles, J. Acoust. Soc. Am., 99: 234-242.
- Fu, S.S., Wilkens, R.H., and Frazer, L.N., 1996b, In situ velocity profiles in gassy sediments: Kiel Bay, Geomarine Letters, 16: 249-253.
- Gorgas, T.J., Wilkens, R.H., Fu, S.S., Frazer, L.N., Richardson, M.D., Briggs, K.B., and Lee, H.J., 1998, In situ and laboratory seabed velocity and attenuation from the Eel River shelf, northern California, Continental Shelf Research, submitted.
- Hamilton, E.L., 1971, Elastic properties of marine sediments, J. Geophys. Res. 76: 579-604.
- Hamilton, E.L., 1972, Compressional wave attenuation in marine sediments, Geophysics, 37: 620-646.
- Kjartansson, E., 1979, Constant Q - Wave propagation and attenuation, J. Geophys. Res. 84: 4737-4748.
- Nitttrouer, C.A. and Kravitz, J.H., 1995, Integrated continental margin research to benefit ocean and earth sciences, EOS, Trans. Amer. Geophys. U., 76: 121, 124 and 126.

Richardson, M.D., 1983, The effects of hydrodynamic and biological processes on sediment geoacoustic properties in Long Island Sound, U.S.A., *Marine Geology*, 52: 201-226.

Richardson, M.D. & Briggs, K., 1994, Investigating the coastal benthic boundary layer, *EOS, Trans. Amer. Geophys. U.*, 75: 201, 205-206.

Richardson, M.D. & Briggs, K., 1996, In situ and laboratory geoacoustic measurements in soft mud and hard packed sand sediments: Implications for high-frequency acoustic propagation and scattering, *Geomarine Letters*, 16: 196-203.

Tarantola, L., 1987, *Inverse Problem Theory*, Elsevier Science Publishers Company Inc., New York, 630 pages.

Wilkens, R.H., 1995, In situ acoustic property profiles and signal characteristics in gassy sediments of Eckernförde Bay, in *Proceedings of the Workshop Modelling Methane-Rich Sediments of Eckernförde Bay*, 26-30 June, 1995, T.F. Wever ed., FWG, Kiel, 180-188.

Wilkens, R.H., and Richardson, M.D., 1998, In situ and laboratory measurements of the acoustic properties of gassy sediments, Eckernförde Bay, Baltic Sea, Germany. *Continental Shelf Research*, in press.

Accomplishments

Prior to deployment of the Acoustic Lance there were virtually no published in situ velocity or attenuation data for sediments at depths below seafloor greater than some 10's of centimeters. At Eckernförde Bay the lance was the only instrument that probed the entire thickness of the zone of gassy sediments, and was the only instrument that provided the frequency range to measure in situ velocities in the gassy sediments that were much less than that of water. Lance data, combined with other in situ and laboratory experiments, were crucial in determining limits on gas bubble size distribution, and have led to planning a new generation of measurements to better understand frequency dependence of acoustic properties in gassy sediments.

In much the same manner, Lance data from the Eel River delta were able to extend in situ measurements to greater depths than other systems. The comparison of in situ to laboratory velocity measurements revealed that upper slope sediments, likely coarser-grained, may behave differently at sonic and ultrasonic frequencies. Further data integration with other experiments should provide a better understanding of this phenomenon.

* Lance development was financed by the ONR ARSRP. Logistics for Eckernförde Bay travel were supplied by NSF International Programs - logistics on site were provided by M. Richardson's CBBL budget.

Publications

Peer Reviewed:

Frazer, L.N., Fu, S.S., and Wilkens, R.H., 1998, Seabed sediment attenuation profiles from a moveable subbottom acoustic vertical array, *J. Acoust. Soc. Amer.*, in press.

Fu, S.S., Prasad, M., Wilkens, R.H. and Frazer, L.N., 1998, Hamilton parameters and acoustic properties for coral sands, Waikiki, Hawaii, Geophysics, in press.

Fu, S.S., Wilkens, R.H., and Frazer, L.N., 1996b, In situ velocity profiles in gassy sediments: Kiel Bay, Geomarine Letters, 16: 249-253.

Gorgas, T.J., Wilkens, R.H., Fu, S.S., Frazer, L.N., Richardson, M.D., Briggs, K.B., and Lee, H.J., 1998, In situ and laboratory seabed velocity and attenuation from the Eel River shelf, northern California, Continental Shelf Research, submitted.

Wilkens, R.H., and Richardson, M.D., 1998, In situ and laboratory measurements of the acoustic properties of gassy sediments, Eckernförde Bay, Baltic Sea, Germany. Continental Shelf Research, in press.

Symposium Proceedings

Fu, S.S., Wilkens, R.H., and Frazer, L.N., 1997, New instrument for in situ velocity and attenuation profiles, Proceedings of the International Conference on shallow water acoustics, Beijing, China, in press.

Wilkens, R.H., 1995, In situ acoustic property profiles and signal characteristics in gassy sediments of Eckernförde Bay, in Proceedings of the Workshop Modelling Methane-Rich Sediments of Eckernförde Bay, 26-30 June, 1995, T.F. Wever ed., FWG, Kiel, 180-188.

Published Abstracts

Gorgas T., Wilkens, R. H., Fu, S. S. and Richardson, M. D., 1996, Acoustic data from the Eel River Shelf, northern California, EOS, Transactions of the American Geophysical Union, 77: F332-F333

Dissertation

Fu, S.S., 1998, The Experimental Study of In Situ Acoustic Properties in Marine Sediments, PhD Dissertation, University of Hawaii at Manoa, Honolulu, HI, pp 135.

Coastal Benthic Boundary Layer Final Report
for Grants N00014-93-1-6006 & N00014-95-1-G903

PHYSICAL TRANSPORT PROCESSES INFLUENCING SHELF SEDIMENTARY STRUCTURE

L.D. Wright and C.T. Friedrichs
Virginia Institute of Marine Science
College of William and Mary
Gloucester Point, VA 23062, U.S.A.

Abstract: Instrumented tetrapods were deployed in Eckernförde Bay, Baltic Sea, on the Shelf off Panama City, Florida, and on the Dry Tortugas Bank, Florida Keys. The purpose was to characterize physical processes most relevant to sediment erosion, transport and deposition. Results suggest that sediment transport events in Eckernförde Bay are associated with resonant internal waves. Although internal wave resonance may commonly produce velocities sufficient to advect fine sediment into Eckernförde Bay, maximum currents are constrained by the wave's phase velocity, which is only on the order of 30 cm s^{-1} . This mechanism is considered responsible for the accumulation of fines in Eckernförde Bay. Flows over the hydraulically-rough, coarse sand bed off Panama City remained too weak to entrain sediment throughout that deployment period. Bottom roughness on the Dry Tortugas Bank was dominated by shrimp burrows and worm mounds. Logarithmic velocity profiles show apparent total roughness heights ranging from 0.30 to 1.45 cm, values consistent with observed biological roughness. The bed sediments were weakly bound by an algal crust at the sediment-water interface. When this bound layer was scraped away by a mooring that was accidentally dragged, sharp-crested wave-induced ripples appeared within the resulting swath. We conclude that physically-induced roughness is biologically suppressed, but if dominant, would be significantly higher than the prevailing biological roughness.

Original Objectives: The overall objective of our study was to elucidate the temporal and spatial variability of the processes that form, modify and preserve sedimentary strata in a variety of shelf settings. In the specific case of the VIMS component of the larger multi-institutional effort, the aim was to address questions related to: (1) hydrodynamic forcings (benthic physical oceanography); (2) fluid-bed coupling through the bottom boundary layer (e.g. bed stress measurement); (3) bed micromorphodynamics and roughness variations; (4) sediment resuspension; and (5) sediment flux divergence and bed level changes. The last question (5) is relevant to explaining rates of sediment accumulation or erosion. All five of the questions are relevant to seafloor acoustic response. Our investigation was closely linked to the studies conducted by Nittrouer and Lopez (SUNY-Stony Brook) and Jackson (APL-UW).

It was emphasized in the original joint SUNY-VIMS proposal that an understanding of the formation, modification, and preservation of sedimentary structure requires interdisciplinary examination of coupled physical, biological, and sedimentological

processes. The emphasis in the VIMS study was on the physical processes as they relate to the biological and sediment processes examined by Nittrouer and Lopez. Our proposed observations were also intended to assist in the interpretation of acoustic signatures observed by Jackson and others.

Approach: Processes were measured that couple the seabed to the near-bottom hydrodynamic regime, and these observations were modeled by analytical and numerical techniques. Our aim was to explain the connection between near bottom flows, bed shear stresses, microstructure, and bottom micromorphology (ripples, "smoothness," biogenic roughness elements, etc.) over the beds of the three field sites. We made our field observations at all three sites using instrumented tetrapod systems. Details are described by Friedrichs and Wright, 1995; 1997 and Wright et al. 1997. Field measurements were made in Eckernförde Bay in April and May 1993; off Panama City, Florida in August 1993 and on the Dry Tortugas Bank in February, 1995.

a. *Bottom boundary layer instrumented system.* This system consisted of a tetrapod frame supporting a current profiling system with five 2-axis electromagnetic Marsh McBirney current sensors (3.8 cm probe diameter), a Datasonics sonar altimeter that operates at 300 kHz, and a Downing Optical Backscatterance (OBS) array with five infrared sensors used to obtain point measurements of suspended sediment concentration at approximately 5, 10, 25, 50, and 100 cm above the bed. A sample of the suspended material *in situ* was collected for calibration purposes via a sediment trap. Camera and strobe units also were mounted on the tetrapod in the Eckernförde deployments to collect time series of microtopography and water suspended flocs. Thermistors were mounted at elevations of 10 cm and 100 cm. All Onset data loggers on the tetrapod were synchronized and programmed for burst mode sampling.

b. *Shear stress and drag coefficients.* Using a theoretical model in conjunction with field data on near-bottom wave velocities and mean (current) velocity profiles, estimates of u_*c and the physical bottom roughness was obtained and related to wave-current-sediment interaction.

c. *Turbulent velocity scale.* This is affected by the presence of waves, and can be estimated. Measured vertical distribution of suspended sediment concentration may be extrapolated, using the theoretical model for suspended sediment concentration, to yield values of near bottom reference concentration for suspended sediments as a function of flow and sediment characteristics.

d. *Interrelationships between boundary layer hydrodynamics and bed micromorphology.* A combination of field observation and numerical modeling was used. The field study involved obtaining time series (at hourly intervals) of bed roughness characteristics and bed shear stress. Bed roughness was observed photographically,

acoustically and (where possible) by divers. Photographic techniques will include camera on the tetrapod and hand held video.

e. *Modeling the bottom boundary layer and sediment transport.* We applied different models to transport above and within the wave boundary layer, including effects of thermohaline stratification.

Results: Results from Eckernförde Bay suggest that sediment transport events are associated with resonant internal waves (Friedrichs and Wright, 1995). Observed turbidity events were associated with marked along-bay current oscillations, and spectral analyses of these currents are highly suggestive of baroclinic resonance. Furthermore, the peak in the current spectra is remarkably close to the previously reported 26 to 28 hour Baltic-wide seich. A one-dimensional, two-layer analytic model was developed to explain the generation of resonant internal waves within Eckernförde Bay by periodic, barotropic flows across a sill near the mouth of the bay. The analytic solution accounts for velocities much larger than those otherwise predicted by barotropic processes or by progressive internal waves, and also explains an observed sign reversal in the correlation between barotropic forcing and the internal wave response. Despite this enhancement of near-bottom currents, estimates of shear velocity suggest that bottom stress never reached the critical magnitude necessary to locally resuspend sediment and was only rarely sufficient to prevent deposition of sediment that may have been suspended elsewhere. During turbidity events, observed suspended sediment concentration did not increase with proximity to the bottom, suggesting sediment advection rather than local resuspension. Bottom photographs support this inference. Although internal wave resonance may commonly produce velocities sufficient to advect fine sediment into Eckernförde Bay, maximum currents are constrained by the wave's phase velocity, which is only on the order of 30 cm s^{-1} . Results from Eckernförde Bay also suggest fits to log profiles which neglect thermohaline stratification may lead to overestimates of bottom stress and roughness on the order of 130% and 600%, respectively (Friedrichs and Wright, 1997).

Sedimentological and geochemical evidence indicates that Eckernförde Bay is functioning as a sink for fine sediment and that sediment accumulation rates are unusually high. Furthermore, radioisotope analyses by NITTROUER *et al.* (1994) suggest minimal physical mixing of the upper part of the sediment column. For this combination of circumstances to prevail, the net flux of sediment must be into the bay, and the bed shear stresses must remain too weak to resuspend sediment. This means that near-bottom flows must be fairly delicately poised within a narrow range of velocities. Our field data show that the benthic regime is, in fact, consistent with what one would infer from the sediment record. The model proposed by Friedrichs and Wright (1995) offers an explanation for how the oceanographic regime of the Baltic Sea, the geometry of Eckernförde Bay, and time-varying stratification combine to produce the observed regime.

Additional results from Eckernförde Bay, reported by Friedrichs and Wright (1997) also provide evidence that thermohaline density stratification may significantly alter the

classic near-bottom logarithmic velocity profile in many weak to moderately energetic, partially mixed estuaries. Measurements of velocity obtained from Eckernförde Bay at four heights within one meter of the sea bed are input to theoretical models for velocity shear derived via dimensional arguments for the "overlap" layer. Salinity stratification in Eckernförde Bay is almost always present due to exchange in the adjacent Belt Sea between saltier North Sea and fresher Baltic Sea waters. As a consequence, vertical density gradients on the order of 0.01 kg/m^4 ($\sim 1/20^\circ\text{C/m}$ or $\sim 1/70$ ‰ of salinity per meter) markedly alter the velocity profile over the lowest meter of the water column when u^* is on the order of 0.5 cm/s . Formulations assuming very weak and relatively strong stratification are applied, and estimates of buoyancy frequency derived from fits to velocity profiles are compared with independent estimates of stratification. Estimates of bottom stress and roughness derived from velocity profiles are also found to be sensitive to fluid acceleration, uncertainties in instrument settling, and limitations in current meter accuracy, but, in Eckernförde Bay, these latter effects appear secondary to the impacts of thermohaline stratification. A stratification correction was derived which distinguishes quasi-logarithmic profiles from linear profiles governed by maintenance of the gradient Richardson number near a critical value.

Results from the Dry Tortugas Bank (Wright et al., 1997) add to the growing body of literature supporting the general conclusion that benthic biological processes act in complex concert with physical processes to control sediment transport and seabed micromorphology. Bottom roughness at our 26m field site was dominated by shrimp burrows and worm mounds with rms roughness amplitudes ranging from 0.47 to 1.75 cm. Logarithmic velocity profiles show apparent total roughness heights ranging from 0.30 to 1.45 cm, values consistent with observed biological roughness. The bed sediments were weakly bound by an algal crust at the sediment-water interface. When this bound layer was scraped away by a mooring that was accidentally dragged, sharp-crested wave-induced ripples appeared within the resulting swath. We conclude that physically-induced roughness is biologically suppressed, but if dominant, would be significantly higher than the prevailing biological roughness. Our results, which pertain specifically to the tropical carbonate environment of the Dry Tortugas Bank, are summarized as follows: (1) In terms of physical processes, the benthic boundary layer of the Dry Tortugas Bank is characterized by low to moderate energy with bed stresses only occasionally exceeding the threshold for sediment transport. (2) Bed micromorphology is biologically dominated which results in a low hydraulic roughness (mean apparent roughness = 0.57 cm). (3) In the absence of biological dominance of the bed, orbital ripples would be well developed and hydraulic roughness would be substantially greater than we observed. However binding of the sediment particles by an algal mat inhibits the formation of physically-induced ripples and allows biogenic roughness to prevail (Wright et al., 1997).

Accomplishments: This study has elucidated the distinguishing characteristics of bottom boundary layer processes associated with fine sediment accumulation in coastal seas and bays. In addition to the insights gained from the site-specific CBBL results described

above, the inclusion of the CBBL results among complementary results from other shelf and estuarine environments that are accumulating fine sediment support some generic implications. Table 1 shows a comparison of five soft-bottom boundary layers.

Table 1. SUMMARY OF BOTTOM BOUNDARY-LAYER CONDITIONS:
FIVE SOFT-BOTTOM ENVIRONMENTS

<i>Eckernförde</i>	<i>Dry Tortugas</i>	<i>Northern</i>	<i>Louisiana</i>	<i>Lower York R.</i>
<i>Bay, Baltic Sea</i>	<i>Bank, Fla. Keys</i>	<i>California Shelf</i>	<i>Inner Shelf</i>	<i>(Chesapeake B.)</i>
1993	1995	1996 & 1997	1992 & 1993	1995 & 1996

Depth	30 m	30 m	60 m & 70 m	15.5 m & 20.5 m	8 meters
Bed roughness	smooth	biogenic	biogenic	smooth, biogenic	smooth
Current speed *	2- 10 cm/s	5- 20 cm/s	10- 25 cm/s	5- 15 cm/s	20- 40 cm/s
Orbital speed	negligible	2- 8 cm/s	10- 30 cm/s	2- 10 cm/s	negligible
Bed stress (tot)	0.01- 0.06 Pa	0.05- 0.25 Pa	0.35-1.25 Pa	0.05- 0.35 Pa	0.02- 0.40 Pa
Bed stress (cur)	0.01- 0.06 Pa	0.01- 0.10 Pa	0.05- 0.40 Pa	0.02- 0.12 Pa	0.02- 0.40 Pa
Apparent Zo	0.1- 3.1 cm	0.01- 0.05 cm	0.8- 6.2 cm	0.2- 3.0 cm	0.1- >1.0 cm
References	Friedrichs and Wright, 1995; 1997	Wright et al 1997a	Wright et al in press	Wright et al. 1997b	Wright et al. 1997c; Kim et al. in press

With inclusion of our CBBL results, we have measured bottom-boundary-layer velocity profiles, bed stresses and suspended sediment concentration profiles in five contrasting shelf and semi-enclosed bay environments that are presently accumulating fine sediments. The sites were: 1) Eckernförde Bay, southern Baltic Sea (Friedrichs and Wright, 1995;1997); 2) the Dry Tortugas Bank, Florida Keys (Wright et al. 1997a); 3) the northern California shelf off the mouth of the Eel river (Wright et al. in press); 4) the Louisiana shelf to the west of the Mississippi River mouths (Wright et al. 1997b); and 5) the lower York River, Chesapeake Bay (Wright et al.,1997c; Kim et al. in press). Site 3) is a highly energetic open shelf regime where river sediments are deposited during flood events and frequently resuspended by moderate to high bed stresses. The other sites experience much lower bed stresses and sediments there are resuspended infrequently.

Conditions at all five sites are favorable to sediment flux convergence. Typically smooth hydraulic roughness characterized all sites. In most cases, roughness elements were biogenic. Stable near bed stratification, whether caused by salt, heat or suspended sediment, often enhanced shear over the lowest meter, causing the best-fit logarithmic velocity profile to significantly overestimate the actual magnitude of the bottom stress. The effects of stable density stratification were shown to have suppressed turbulence and reduced bed stress in several of the data sets.

Our recent field studies in regions of fine sediment accumulation have identified three basic scenarios where convergent transport processes preferentially favor the accumulation of fine sediment. First, in environments like Eckernfö́rde Bay (Friedrichs and Wright 1995, 1997) and areas of the lower Chesapeake Bay (Wright et al. 1997c), energy levels are generally low enough that mainly fine sediment is effectively transported by the active convergent transport processes. Under these low energy conditions, near-bed thermohaline stratification can often be expected because of very weak bottom stress. Second, fine sediment can accumulate in much more energetic environments if it dominates the source material. This is largely the case on the Eel River shelf off of Northern California (Wright et al. in press). Mud accumulation on the Louisiana Inner Shelf (Wright et al. 1997b) and in the York River (Wright et al. 1997c; Kim et al. in press) is favored to an intermediate degree by both of the above factors. The abundance of under-consolidated fine sediment in some energetic coastal environments presumably allows increases in stress to be accompanied by progressive increases in suspended sediment concentration within the log layer to maintain a critical balance. A general hypothesis for such energetic shelf settings is that fine sediment resuspension occurs until an "equilibrium" is reached and further resuspension is inhibited. Finally, in some coastal environments accumulating fine sediment, such as the Dry Tortugas Bank (Wright et al. 1997a), relatively energetic conditions do not disperse mud because resuspension is inhibited by the presence of biological effects such as algal mats.

References cited in this report:

- Friedrichs, C.T. and Wright, L.D. (1995) Resonant internal waves and their role in transport and accumulation of fine sediment in Eckernfö́rde Bay, Baltic Sea. *Continental Shelf Research* 15:1697-1721
- Friedrichs, C.T. and L.D. Wright, 1997, Sensitivity of bottom stress and roughness estimates to density stratification, Eckernfö́rde Bay, southern Baltic Sea, *J. Geophysical Research* 102:5721-5732.
- Kim, S.-C., C.T. Friedrichs, J.P.-Y. Maa and L.D. Wright, in review, Estimating bottom stress in a tidal boundary layer from Acoustic Doppler Velocimeter Data, submitted to *Estuaries*
- Wright, L.D., C.T. Friedrichs, and D.A. Hepworth, 1997a, Effects of benthic biology on

bottom boundary layer processes, Dry Tortugas Bank, Florida Keys. *Geo-Marine Letters* 17:291-298 (Special Issue on NRL-CBBL Dry Tortugas Results).

Wright, L.D., C.R. Sherwood, and R.W. Sternberg, 1997b, Field measurements of fairweather bottom boundary layer processes and sediment suspension on the Louisiana inner continental shelf. *Marine Geology*, 140:329-345.

Wright, L.D., L.C. Schaffner, and J. P-Y. Maa, 1997c, Biological mediation of bottom boundary layer processes and sediment suspension in the lower Chesapeake Bay. *Marine Geology*. 141:27-50

Wright, L. D., Kim, S.-C. and Friedrichs, C.T. in press, Across-shelf Variations in Bed Roughness, Bed Stress and Sediment Transport on the Northern California Shelf *Marine Geology* (Special STRATAFORM issue edited by C.A. Nittrouer).

Publications derived from this study:

Peer reviewed journal articles

Friedrichs, C.T. and Wright, L.D. (1995) Resonant internal waves and their role in transport and accumulation of fine sediment in Eckernförde Bay, Baltic Sea. *Continental Shelf Research* 15:1697-1721

Friedrichs, C.T. and L.D. Wright, 1997, Sensitivity of bottom stress and roughness estimates to density stratification, Eckernförde Bay, southern Baltic Sea, *J. Geophysical Research* 102:5721-5732.

Wright, L.D., C.T. Friedrichs, and D.A. Hepworth, 1997a, Effects of benthic biology on bottom boundary layer processes, Dry Tortugas Bank, Florida Keys. *Geo-Marine Letters* 17:291-298 (Special Issue on NRL-CBBL Dry Tortugas Results).

Nittrouer, C.A., Lopez, G.R., Wright, L.D., Bentley, S.J., D'Andrea, A.F., Friedrichs, C.T., Craig, N.I. and Sommerfield, C.K. in press, Oceanographic Processes and the Preservation of Sedimentary Structure in Eckernförde Bay, Baltic Sea, *Continental Shelf Research* (Special Issue on NRL-CBBL Eckernförde Results)

Jackson, D.R., K.L. Williams, T.F. Wever, C.T. Friedrichs, and L.D. Wright, in press, Sonar evidence of methane ebullition in Eckernförde Bay, *Continental Shelf Research* (Special Issue on NRL-CBBL Eckernförde Results).

Conference Proceedings

Friedrichs, C.T., L.D. Wright, and B.-O. Kim, 1995. Sensitivity of bottom stress measurements to stratification, fluid acceleration and instrument settling, Eckernfoerde Bay, southern Baltic Sea. Proceedings of the Workshop Modelling Methane-Rich Sediments of Eckernfoerde Bay, Eckernfoerde, Germany, 26-30 June, 1995, pp. 140-144.

Nittrouer, C.A., S.J. Bentley, G.R. Lopez, and L.D. Wright, 1995. Observations of sedimentary

character and their relationship to environmental processes in Eckernfoerde Bay.
Proceedings of the Workshop Modelling Methane-Rich Sediments of Eckernfoerde Bay,
Eckernfoerde, Germany, 26-30 June, pp. 145-148.

Wright, L.D., and C.T. Friedrichs, 1995. Physical processes responsible for the transport and accumulation of fine-grained sediment in Eckernfoerde Bay, southern Baltic Sea.
Proceedings of the Workshop Modelling Methane-Rich Sediments of Eckernfoerde Bay,
Eckernfoerde, Germany, 26-30 June, 1995, pp. 135-139.

Report

Wright, L.D., D.A. Hepworth, S.C. Kim, and R.A. Gammisch, 1996, STRATAFORM: VIMS
Cruise and Status Report, December 1995-March 1996, 15 pp. + data diskette.

Published abstracts

Wright, L.D., 1994, Benthic Transport Phenomena in Eckernförde Bay (Baltic Sea), *Abstracts
Volume, 1994 Ocean Sciences Meeting*, p. 180, San Diego, Feb 1994.
Eos, Transactions of the American Geophysical Union, 75 (3, suppl.): 180.

Richardson, M.D., K.B. Briggs, L.D. Wright and C.T. Friedrichs, 1996. The effects of biological and physical processes on near-surface sediment geoacoustic properties. Eos, Transactions, American Geophysical Union, 77, (No. 46, Suppl.): F317.

The Relationship between High-Frequency Acoustic Scattering and Seafloor Structure

LI ZHANG (*)

Center for Marine Sciences, University of Southern Mississippi, Stennis Space Center, MS
39529

*: Current Address: 4120 Sunflower Lane, Plano, TX 75024

and

RALPH R. GOODMAN

Applied Research Laboratory
Pennsylvania State University
P. O. Box 30
State College, PA 16804

Abstract:

Theoretical models are presented for high frequency acoustic backscattering from a statistically isotropic seafloor, especially applicable to continental shelves. To better describe shallow water environment, the current model includes three scattering components: two continuous scattering due to surface roughness and admittance inhomogeneity, and one discrete scattering from discrete point scatterers. The discrete scattering is introduced to simulate the appearance of high contrasts in admittance or roughness such as shells, rocks, or sediment structures created by the process of marine bioturbation in shallow-water environments.

Admittance scattering is determined by the seafloor admittance anomaly. Its angular dependence follows Lambert's law for almost all types of sediments. Roughness backscattering depends on the mean square micro-relief height and its spectral characteristics. For an exponential roughness spectrum, spectral slope controls the frequency dependence, which can be either positive or negative. A maximum in backscattering strength occurs at normal incidence when the roughness spectrum is concentrated in lower spatial frequency components. For discrete scattering, individual scatterer's target strength and the distribution of the scatterers are both important.

High frequency acoustic backscattering measurement data from shallow water areas often display big variations. Temporal and spatial fluctuations of sound speed in seawater due to the presence of dynamic oceanographic processes creating turbulence are shown to be responsible for backscattering variability. For scattering from continuously distributed scatterers, the model reveals that the standard deviation of backscattering coefficient is linearly related to the standard deviation of sound speed. Higher variability is expected if discrete scatterers exist inside the insonified area. A criterion is given to judge whether measured backscattering strength can represent seafloor backscattering when variations in sound speed in the water column are present.

Comparisons between the model and the measurements suggest that, at the West Florida Sand Sheet experiment site, scattering from discrete shells is an important and is often the dominant component of the total scattering field. Laboratory measurements show that at high frequency a shell's size determines its normal incidence target strength, that approximately can be estimated from backscattering from a same size solid sphere.

Original Objectives:

There are two objectives in the original proposal. The first is to establish, through a thorough literature review, the current state of the art on the subject of acoustic scattering from the ocean floor. The second is the development of a scattering formalism in which roughness and volume inhomogeneities are the scatterers. The purpose is to determine the strengths and limitations of acoustics for determining sediment structure. Because acoustic data show fluctuations in field measurements even with a fixed platform, the acoustic variability and its relations with seafloor structure and medium fluctuations becomes another objective of the current study. The purpose is to see if the presence of acoustic variability provides additional limitations and additional information, if any, for determining seafloor features.

Approach:

Roughness and volume inhomogeneity cause seafloor scattering. Theoretical approach of the current research follows a method developed by Morse and Ingard (1968) which is based on the Green's theorem of acoustic waves. The surface pressure and the Green's function are selected to fit the seafloor scattering problems. The contributions from the sediment volume is treated by the inhomogeneity in the surface impedance (or acoustic admittance). Both roughness and impedance inhomogeneities are regarded as continuous distributed scatterers. Their statistical characteristics will be used to estimate the acoustic scattering strength. A Gaussian type spatial autocorrelation of surface impedance inhomogeneity is used because the seafloor is assumed to be random and isotropic. Considering continental shelf environments, the roughness spectrum is assumed to be an exponential type (Briggs, 1989).

A special feature in shallow water environments is that there are, in addition to continuous irregularities, many objects on the seafloor that differ from their surroundings. These objects include shells, algae fragments, and biogenic mounds and pits. To model backscattering from such a seafloor, the concept of discrete scatterers will be introduced to describe the sharp contrasts in bottom properties such as bottom admittance and roughness. Then the total scattering is the sum of contributions from all three components: discrete scatterers and two types of continuous scatterers due to roughness and admittance inhomogeneity. To get the order of the discrete scattering, the target strengths from shallow water shells will be measured in a laboratory environment.

Sea water is more dynamic in shallow water environments. The medium variations will affect acoustic waves especially at high frequencies, so measured acoustic backscattering data show

fluctuations even the measurement system is fixed. To analyze the problem, a random distribution of sound speed in sea water is assumed to see the responses of different scattering components to such medium variations. It is expected that more acoustic variability will be observed if discrete scatterers exist.

Finally, using acoustic data to determine sediment structure should examine all aspects of the measured backscattering data, including the magnitude of acoustic backscattering strength, its angular dependence and frequency dependence, and fluctuations in acoustic data.

Results:

- A thorough literature review is conducted to present the current state of the art in the prediction of high frequency scattering from structural models of the seafloor. The review is given in Zhang's dissertation.
- A new model is presented to estimate shallow water seafloor backscattering strength. In this new model, in addition to roughness scattering, the sediment volume scattering is treated by the inhomogeneity of the surface admittance. Besides, discrete point scatterers are introduced to represent the contributions from shells, rocks, and other discrete objects in the shallow water environments. Three components' angular and frequency dependence are given.
- Fluctuations in acoustic data are analyzed. Results show that acoustic data can be used to determine sediment structure only if the magnitude of the seawater sound speed variations is less than a critical value. Because different scattering components have different responses to medium fluctuations, the acoustic variability provides additional means for sediment structure determination.
- The magnitudes of target strengths of shallow water shells are obtained through laboratory measurements. At normal incidence, the shell's target strength can be estimated by solid-sphere scattering theory.

Accomplishments:

This study provides a new theoretical model for high frequency acoustic backscattering from a statistically isotropic seafloor, especially applicable to continental shelves. In addition to surface roughness scattering and acoustic admittance inhomogeneity scattering, the present model introduces the concept of discrete point scatterers to better describe high frequency acoustic scattering patterns in shallow-water environments. Approximate formulations have been obtained to make the model suitable for different types of bottoms.

Admittance inhomogeneity scattering is determined by the admittance anomaly on seafloor. The frequency dependence of the admittance scattering is $20 \log f$. The angular dependence is controlled by the seafloor acoustic admittance and the sound speed ratio. For applications in seafloor backscattering, the simulations found Lambert's law to be a good approximation for all types of sediments commonly encountered on continental shelves. The backscattering coefficient for admittance scattering can therefore be expressed as expressed as

$$\mu_{\beta} = \frac{k^2 w^2 \langle \Delta \beta^2 \rangle \sin^2 \theta}{2 \pi^3 (1 + \beta)^4} . \quad (1)$$

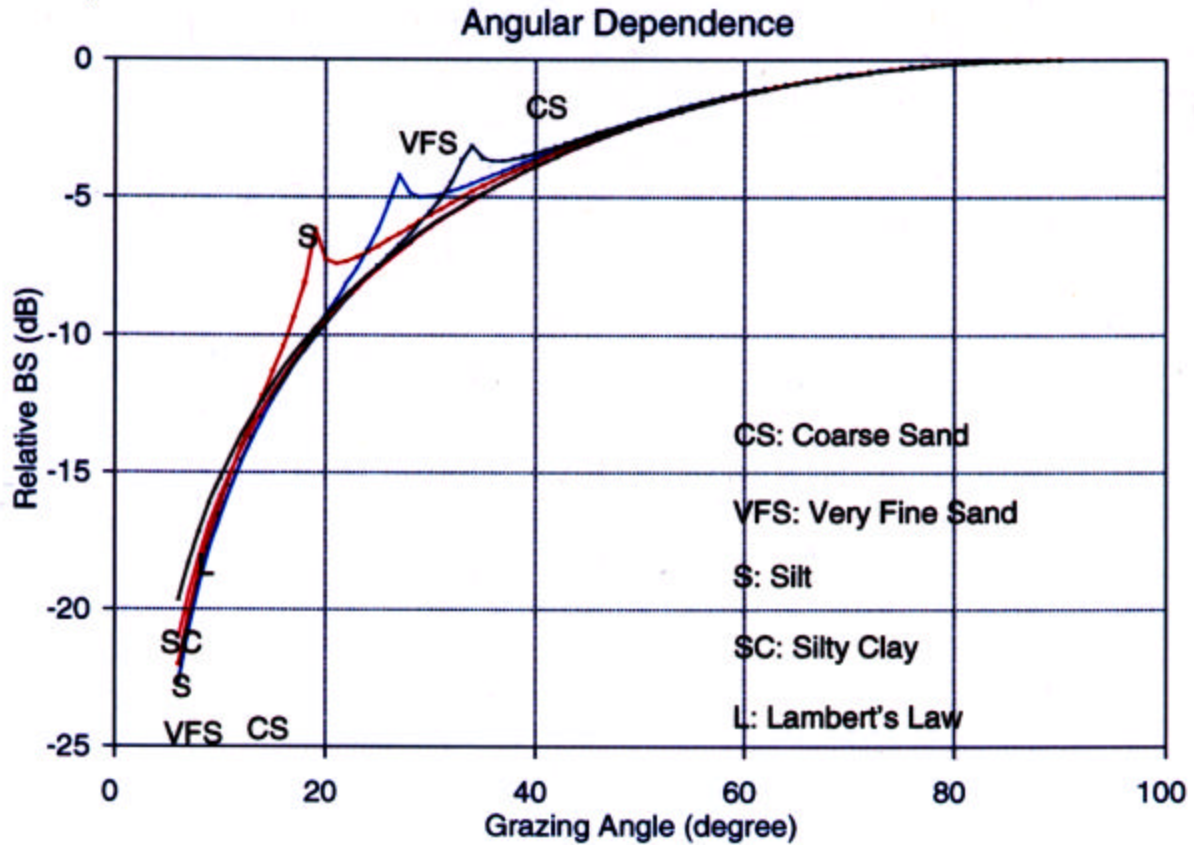


Figure 1 Angular dependence of admittance inhomogeneity scattering of different sediment types.

Figure 1 shows calculated angular dependence of backscattering strength of admittance inhomogeneity scattering from different sediment types in continental shelves.

For roughness scattering, the level of backscattering strength depends on the root mean square roughness. Its frequency dependence and angular dependence are controlled by the spectral characteristic of the roughness, namely its power spectral density function. On shallow-water continental shelves, measurements show that microtopographical roughness spectrum usually can be described by an exponential function, and the power (the slope) in roughness spectrum plays a very important role in determining the angular and frequency dependence for roughness scattering:

$$\mu_t = \frac{(b - 1) \pi^b \langle \xi^2 \rangle k^{2-b}}{D^b} (1 - \beta \frac{C_2^2}{C_1^2})^2 \frac{\sin^4 \theta \cos^{2-b} \theta}{(\sin \theta + \beta S_\theta)^4}, \quad (2)$$

where

$$S_\theta = \sqrt{\left| 1 - \frac{C_2^2}{C_1^2} \cos^2 \theta \right|}. \quad (3)$$

Depending on the value of the slope b , either negative or positive frequency dependence is possible. No frequency dependence will be found for roughness scattering when $b = 2$. The angular dependence is also affected by the slope b , especially at angles near normal incidence. A peak in angular dependence curve will occur at normal incidence if $b > 2$.

The concept of discrete scatterers is aimed at emulating the presence of shells, rocks, resultant structures created by the process of marine bioturbation, and other sharp contrasts in either surface roughness or acoustic admittance, which are not suitable for treatment as continuous scatterers. Discrete scattering is determined by each individual scatterer's target strength and the distribution of the scatterers:

$$\mu_d = \sum_{j=1}^N \sum_{l=1}^N A_{jl} e^{i2k(R_j - R_l)}. \quad (4)$$

The angular dependence and frequency dependence are dependent on corresponding features of the target strength of the discrete scatterers. More often the scattering pattern is influenced by the relative positions of the scatterers. The total scattering field is the superimposition of all scattering mechanisms:

$$\mu = \mu_p + \mu_t + \mu_d. \quad (5)$$

Dynamic oceanographic processes create turbulence in the medium, and variability in acoustic data is therefore introduced by the resultant temporal and spatial fluctuations of sound speed in seawater. The average backscattering curve can represent seafloor backscattering only when the sound speed fluctuation is less than a critical value defined as

$$\delta C_c = \frac{C_1^2}{4\pi f R}. \quad (6)$$

Otherwise, the measurement data are too variable to be used to compute the seafloor backscattering strength. For example, assuming the frequency be 50 kHz and the source-insonified area distance be 20 m, the average acoustic data can be used to calculate bottom backscattering if the range of the sound speed fluctuations in seawater is less than 0.2 m/s. This requires the magnitude of the seawater temperature oscillations be less than 0.04 °C. Fortunately, the sound speed fluctuation here is an average over the path from sound source/receiver to the insonified area, and it should be much less than the fluctuations observed at a fixed point in seawater.

It is found that different scattering mechanisms show different responses to medium fluctuations. For the two continuous scattering types, the variability of backscattering can be estimated by

$$V = 10 \log \sqrt{8} k R \frac{\sigma_c}{C_l} . \quad (7)$$

This equation is also valid for discrete scattering if the number of the scatterers is large enough. However, when there are only a few discrete scatterers inside the insonified area, using Equation (6) will underestimate the fluctuations in acoustic data. Considering the total acoustic scattering field, the total variability of backscattering is

$$V = 5 \log \frac{\sigma_p^2 + \sigma_\xi^2 + \sigma_d^2}{(\mu_p + \mu_\xi + \mu_d)^2} . \quad (8)$$

The presence of medium fluctuations decreases the quality of the acoustic data. But, on the other hand, fluctuations provide additional information on seafloor properties.

Comparisons between the model and the field backscattering measurement results from the West Florida Sand Sheet are made. Generally, models agree with data. In the experimental site, based on the analysis, discrete scatterers such as shells are shown to be important and often dominate the total scattering field.

In order to understand the shell's scattering ability, measurements on shells' target strength were performed in a laboratory environment. Measurements show that at high frequency a shell's normal incidence target strength is determined by its cross-sectional area only. The target strength approximates the solid sphere scattering theory:

$$TS = 10 \log \frac{S}{4 \pi} \text{ (dB)} . \quad (9)$$

Figure 2 shows the measured normal incidence target strength at 196 kHz.

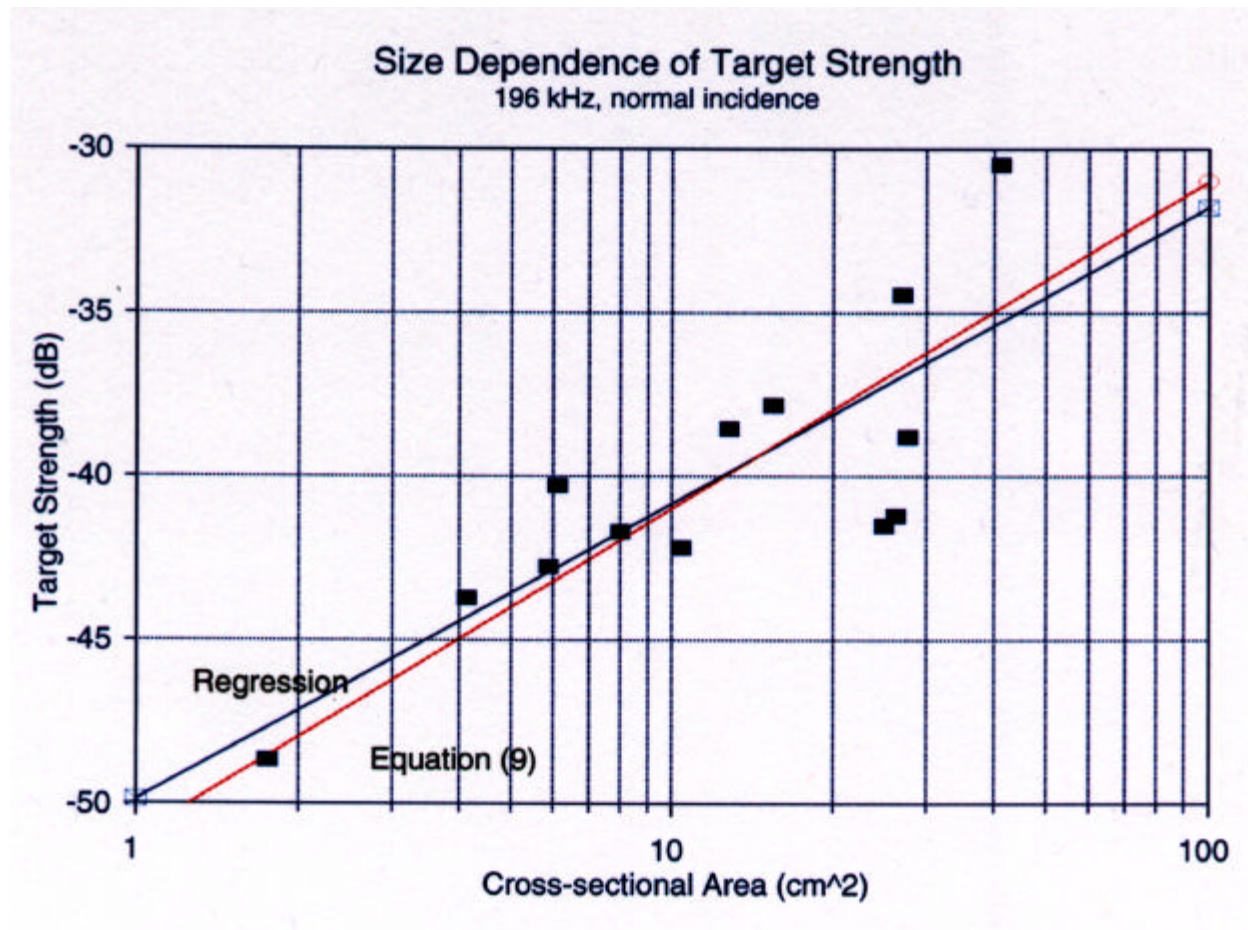


Figure 2 Measured normal incidence target strength of Panama City shells at 196 kHz.

Based on the understanding of scattering mechanisms, it is possible to use backscattering signals to sense the seafloor characteristics remotely. Such inverse problems require a synthetic analysis of all aspects of the backscattered returns including the angular dependence, the frequency dependence, and the variability of the backscattering strength.

List of Symbols Used

A_{jl}	Amplitude factor of the j th and the l th scatterer
b	Slope index of roughness spectrum
C_1	Sound speed in seawater
C_2	Sound speed in sediments
D	Path length for roughness measurements
f	Frequency

$k = \omega/C$	Wave number
R	Distance between source and observer, or distance between source/receiver and the insonified area on the seafloor
R_j	Distance of the j th scatterer
S	Cross-sectional area of a scatterer
S_θ	A function defined in Equation (3)
TS	Target strength of a scatterer
V	Variability of backscattering
w	Correlation length
β	Specific acoustic admittance
δC_c	Critical sound speed fluctuation
$\Delta\beta$	Admittance anomaly in sediments
$\langle\Delta\beta^2\rangle$	Mean-square value of admittance anomaly, i.e., $\langle(\Delta\beta)^2\rangle$
θ	Grazing angle
μ	Backscattering coefficient
μ_d	Backscattering coefficient of discrete scattering
μ_β	Backscattering coefficient of admittance scattering
μ_ξ	Backscattering coefficient of roughness scattering
ξ	Surface roughness
$\langle\xi^2\rangle$	Mean-square surface roughness
σ_c	Standard deviation of sound speed fluctuations in seawater
$\omega = 2\pi f$	Angular frequency

References:

Briggs, Kevin B. (1989). Microtopographical roughness of shallow-water continental shelves. IEEE J. Oceanic Eng. 14, 360-367.

Morse, Philip M., and Ingard, K. Uno (1968). Theoretical Acoustics (McGraw-Hill, New York).

Publications:

Reports:

Zhang, L. 1996. Preliminary Results of Target Strength Measurements for Shallow Water Shells. Technical Report, Center for Marine Science, University of Southern Mississippi, Stennis Space Center, Mississippi 39529.

Zhang, L. 1996. Estimation of Acoustic Target Strength of Shells. Technical Report, Center for Marine Science, University of Southern Mississippi, Stennis Space Center, Mississippi 39529.

Published abstract

Zhang, L., Goodman, R.R., and Stanic, S. 1994. Acoustic pulse to pulse variability due to seawater temporal temperature fluctuations. J. Acoust. Soc. Am. 96: 3286.

Dissertation

Zhang, L. 1996. High Frequency Seafloor Acoustic Backscattering with the Presence of Turbulence in Seawater. Ph.D Dissertation, University of Southern Mississippi.